申报材料目录表

姓　名	张璐	单　位 （二级单位）	林学与风景园林学院
申报专业及职称		＿＿林学＿＿专业＿＿教授＿＿职称	

序号	项目	份 数	说明
1	华南农业大学 职称评审表	1 份	统一用 A4 纸双面打印并胶装。
2	证书、证明材料	1 份	身份证、继续教育证、教师资格证、职称证书等证书、证明材料复印件，由所在单位审核签名盖章后胶装。
3	业绩成果材料	1 份	任现职以来发表的论文、论著、项目申请书、成果、奖励等所有业绩成果材料及证明的复印件（请勿用图片格式打印），由所在单位审核盖章，其中顺序请按《华南农业大学职称评审表》填写顺序依次编号，并胶装。

注：以上材料统一装在档案材料袋中，并在材料袋底部写上申请者姓名、所在单位、申报专业和申报职称。

□ 首聘

□ 博士后

□ 破格申请

□ 曾转过系列

□ 申请转系列

申报系列/类型 教师系列教学科研并重型

学科类型 自然科学类

华南农业大学
职称评审表
（2024年）

申报者单位： 华南农业大学

申报者姓名： 张璐

现职称： 生态学 **专业** 副教授 **职称**

申报职称： 林学 **专业** 教授 **职称**

华南农业大学人力资源处制

个人承诺

本人郑重承诺：本人对《华南农业大学职称评审表》所填写的内容及提交材料的真实性负责。如有虚假或不真实之处，按《华南农业大学职称评审办法》（华南农办［2022]9号)的相关规定处理。

填表人(签名)：张璐

年　　月　　日

个人情况

姓　名	张璐	工　号	30002929	性　别	女
出生年月	1973.08	政治面貌	中共党员	移动电话	13560089803
最高学历	博士研究生毕业	最高学位	理学博士学位	毕业时间	2006-06-01
所学专业	生态学	现工作岗位	教学科研	参加工作时间	1995-07-01
是否曾转系列评审	否	转系列评审前职称		转系列评审前职称取得时间	
现职称名称	副教授	取得时间	2007-12-31	现职称取得方式	评审
聘任时间	2007-12-31	累计任职年限	17	获高校教师资格时间	2007-09-13
拟申报何职称	教授	所属专业	林学		
是否首聘	否				
是否博士后	否				
是否破格申请	否				
本次是否转系列评审	否				

学习简历（从高中毕业以后填起）

入学时间	毕业时间	毕业院校	所学专业	学历	学位
1991-09-01	1995-06-01	广西农业大学	农业气象学	大学本科毕业	农学学士学位
2001-09-01	2006-06-01	华南农业大学	生态学	博士研究生毕业	理学博士学位

工作简历

开始日期	截至日期	任职单位名称	任职岗位（职务）
1995-07-01	2001-09-01	贵州农学院	教师
2006-07-01		华南农业大学	教师

继续教育情况

参加了专业技术人员公需科目、专业科目和个人选修三类科目的继续教育学习，完成学习任务。

工 作 负 面 情 况 说 明

本人负面情况申报	任职期间，是否出现下列情况：				
	负面情况	是否存在该情况	年份	处分时间	处分期限
	因师德问题受学校警告以上处分	否			
	因师德问题受学校记过以上处分	否			
	年度考核基本合格	否			
	年度考核不合格	否			
	受党纪、政纪处分	否			
	涉嫌违法违纪接受组织调查	否			
	受刑事处罚	否			
	发现并查证属实有伪造身份、学历、资历、业绩，剽窃他人成果等弄虚作假和违反学术道德行为，以及隐瞒事实真相未如实申报	否			
	指导研究生的学位论文，存在作假行为并造成严重不良影响，或在国家和省级学位论文抽检中定为“存在问题学位论文”	否			
	指导的学生参赛作品抄袭、伪造等情况	否			
	出现教学差错	否			
	出现教学事故	否			
	出现安全责任事故	否			
	其他	否			
本人对负面情况的陈述	本人签名：				
单位意见	（公章） 年 月 日				

注：1、申报人须如实填写上述各栏。若对现任职以来专业技术工作中既往过错隐瞒不报的，一经查实，按照《华南农业大学职称评审办法》（华南农办［2022]9号)的相关规定严肃处理。
2、“本人对负面情况的陈述”栏，如实填写出现负面情况的具体表述、出现原因、处理方式及本人的认识。
3、“单位意见”栏由单位针对申报人工作作风、态度、过失因果等，实事求是加具对其申报评审的意见；如有其他本人未申报的负面情况亦一并开列，并具公章。

思想政治素质和师德师风考核表

一、本人自述

本人根据《新时代高校教师职业行为十项准则》《华南农业大学教师职业道德行为负面清单》，从政治表现、道德品质、师德师风、遵纪守法等方面进行陈述。（150个字符以内）

本人在思想政治上与党中央保持高度一致，自觉爱国守法，坚持“两个确立”、做到“两个维护”。爱岗敬业，传播优秀传统文化，传递正能量；教书育人，坚持立德树人宗旨，遵循高等教育规律，因材施教，教学相长；严慈相济，诲人不倦，言行雅正；遵守学术规范，秉持公平诚信；坚守廉洁自律，履行社会责任，树立正确义利观。

本人签名：

年　月　日

二、所在系（教研室、单位）的教工党支部意见

所在系（教研室、单位）的教工党支部根据《新时代高校教师职业行为十项准则》《华南农业大学教师职业道德行为负面清单》，从政治表现、道德品质、师德师风、遵纪守法等方面考核并进行陈述。（100个字符以内）

党支部书记签名：

年　月　日

三、所在单位党组织综合意见

所在单位党组织根据《新时代高校教师职业行为十项准则》《华南农业大学教师职业道德行为负面清单》，从政治表现、道德品质、师德师风、遵纪守法等方面进行考核，提出明确考核意见。（150个字符以内）

考核结果：　合格 □　不合格 □

二级党组织负责人（签名）：　　（盖章）：

年　月　日

相关经历与培训、实践情况

表1 学生工作等相关经历情况表

项目类型	起止时间		工作经历具体描述	考核结果	备注
	自	至			
班主任	2006-09	2010-06	担任林学与风景园林学院2006级林学4班班主任。		
其他	2023-12	2027-12	担任华南农业大学林学与风景园林学院学业辅导员，围绕极小种群野生植物紫荆木拯救工作，正在指导林学专业本科生围绕紫荆木环境适应性开展科研实践活动。		学业辅导员

表2 生产实践锻炼情况表

序号	起止时间		生产实践锻炼的项目内容	生产实践锻炼的单位或地点	生产实践锻炼单位的负责人	生产实践锻炼累计时间（单位/天）	备注
	自	至					
生产实践锻炼累计时间合计（单位/天）				0			

表3 担任科技推广专家情况（研究系列推广型申报人员必填）

序号	聘任时间	名称	具体业绩表述	级别	备注

表4 社会服务工作量情况（研究系列推广型申报人员必填）

序号	年度	服务概览	年度工作量	备注
1	2023年	分别在广东云开山国家级自然保护区、华南农业大学树木园、广州市动物园、广东省高州市深镇镇耀新村、广东惠东海龟国家级自然保护区等地开展极小种群野生植物紫荆木拯救科普宣传活动。极小种群野生植物社会服务案例获广东省林业局官网和茂名网报道。	10	
2	2024年	以服务省委“百千万工程”和绿美广东生态建设为契机，实现了全国首次极小种群野生植物紫荆木野外回归云开山国家级自然保护区。极小种群野生植物社会服务案例获广东省林业局门户网站、茂名市人民政府门户网站、茂名日报、信宜共青团公众号、信宜发布报道、广东林业公众号、南岭探秘公众号等多家媒体报道和转载。	21	

社会服务工作量总计	31

表5 思想政治理论课教师研修培训情况（思想政治理论课教师填报）

序号	起止时间		培训名称	具体业绩表述	备注
	自	至			

破格条件

教学成果奖或教学类比赛情况

获奖时间	项目类型	项目名称	奖励级别	成果授予部门	本人排名	证书号	备注

主持的科研项目情况

项目类型	项目名称	项目编号	项目来源	项目分类	实到经费(万)	经费卡号	立项时间	是否结题	结题时间	课题组总人数	项目等级	备注

发表本专业论文（著）情况

论文名称	刊物名称（刊号）	发表时间（年月）	作者类型	作者排名	文献类型	论文等级	备注

注：论文附件须包含期刊封面、目录（标注出所发论文）、论文全文、封底以及检索证明。

科研平台情况

立项时间	项目名称	项目来源	总经费额（万）	进展情况	本人排名	等级	备注

科技奖励情况

获奖时间	奖励名称+等级	成果名称	成果授予部门	本人排名	项目等级	备注

应用成果情况

获得时间	类型	名称	成果授予部门	本人排名	登记号/标准编号	项目等级	备注

科技成果转化项目情况

项目名称	实到经费（万元）	经费卡号	合同签订时间	本人排名	项目等级	备注

决策咨询报告采纳实施情况

采纳 时间	采纳或实施部门	具体业绩表述	备注

教学任务

表6-A 讲授本科生课程情况-理论课程

学年学期	课程名称	授课对象	总学时	实际承担学时	是否合上课程	备注
2008-2009-2	城市生态学	全校选修	32	32	否	张璐
2009-2010-1	林业科技文献检索与论文写作	07林学1,07林学林业1	32	32	否	张璐
2009-2010-1	城市生态学	07城市规划1,07城市规划2	48	48	否	张璐
2009-2010-1	城市生态学	全校选修	32	32	否	张璐
2009-2010-2	城市生态学	全校选修	32	32	否	张璐
2009-2010-2	森林环境学	07林学1,07林学林业1	32	32	否	张璐
2010-2011-1	景观生态学	07园林1,07园林2,07园林3,07园林4	40	40	否	张璐
2010-2011-1	林业科技文献检索与论文写作	08林学1,08林学2,08林学林业1	32	32	否	张璐
2010-2011-1	城市生态学	08城市规划1,08城市规划2	48	48	否	张璐
2010-2011-2	城市生态学	全校选修	32	32	否	张璐
2010-2011-2	森林环境学	08林学1,08林学2,08林学林业1	32	32	否	张璐
2011-2012-1	景观生态学	08园林1,08园林2,08园林3	40	40	否	张璐
2011-2012-2	城市生态学	全校选修	32	32	否	张璐
2011-2012-1	林业科技文献检索与论文写作	09林学1,09林学林业1,09林学林业2,09林学生态1	24	24	否	张璐
2011-2012-2	景观生态学	09游憩生态1	40	40	否	张璐
2012-2013-1	景观生态学	09园林1,09园林2,09园林3	40	40	否	张璐
2012-2013-1	林业科技文献检索与论文写作	10城市林业1,10城市林业2,10林学1,10林学生态1	24	24	否	张璐
2012-2013-1	城市生态学	09城市规划1,09城市规划2	48	48	否	张璐
2012-2013-2	景观生态学	10游憩生态1	40	40	否	张璐
2013-2014-1	城市生态学	10城市规划1,10城市规划2,10城市规划3	32	48	否	张璐
2013-2014-2	城市生态学	全校选修	32	32	否	张璐

2013-2014-1	景观生态学	10园林1,10园林2,10园林3,10园林4	40	38	是	张璐，苏志尧
2013-2014-2	景观生态学	11游憩生态1	32	40	否	张璐
2013-2014-1	林业科技文献检索与论文写作	11城市林业1,11城市林业2,11林学1,11林学生态1	24	24	否	张璐
2014-2015-1	城市生态学	11城市规划1,11城市规划2,11城市规划3	32	48	否	张璐
2015-2016-1	景观生态学	12园林1,12园林2,12园林3,12园林4	32	32	否	张璐
2016-2017-1	景观生态学	13园林1,13园林2,13园林3,13园林4,13园林5	32	32	否	张璐
2016-2017-2	城市生态学	全校选修	32	32	否	张璐
2017-2018-2	城市生态学	15园林1—4班	32	32	否	张璐
2017-2018-2	城市生态学	全校选修	32	32	否	张璐
2018-2019-2	城市生态学	16园林1-4	32	32	否	张璐
2018-2019-2	城市生态学	17园林1-4	32	32	否	张璐
2019-2020-2	城市生态学	18园林1-4	32	32	否	张璐
2020-2021-2	城市生态学	19园林1-4	32	32	否	张璐
2021-2022-1	普通生态学	21野生动物1	32	16	是	冯志坚，张璐
2022-2023-1	城市生态学	20生态学1-2	24	24	否	张璐
2022-2023-1	普通生态学	22野生动物1	32	32	否	张璐
2023-2024-1	普通生态学	23野生动物1	32	32	否	张璐
2023-2024-1	城市生态学	21生态学1-2	24	24	否	张璐
2024-2025-1	森林生态学	23林学低碳林业1	48	48	否	张璐
总学时数	1374	**年限**	17	**年均授课学时数**		80.8

表6-B 讲授本科生课程情况-实验课程

学年学期	**课程名称**	**授课对象**		**总学时**	**实际承担学时**	**是否合上课程**	**备注**
总学时数	0	**年限**	0	**年均授课学时数**		0	

表6-C 讲授本科生课程情况-教学实习、训练类课等

学年学期	课程名称	授课对象	天数	班级数	折算学时数	备注（是否与其他教师合上）
2021-2022-1	普通生态学实习	21野生动物1	5	1	7.5	是
2022-2023-1	普通生态学实习	22野生动物1	5	1	15	否
2023-2024-1	普通生态学实习	23野生动物1	5	1	15	否

总学时数	37.5	年限	17	年均授课学时数	2.2

备注:
1.教学实习：含课程实习、生产实习、毕业实习等，每天按3学时计算；
2.参与农事训练类、通识管理训练类、工程基础训练类教学授课学时，按7学时/天/教学班计算；
3.参与军事技能训练、创新创业实践管理的教师，折算授课学时分别为32学时、7.5学时（不考虑班级数和天数因素）。

表6-D 讲授本科生课程情况-课程论文（设计）

学年学期	课程论文（设计）名称	授课对象	周数	折算学时数	是否合上课程	备注

总学时数	0	年限	0	年均授课学时数	0

注：课程论文（设计）教学时数= 周数×5

表6-E 讲授本科生课程情况- 指导毕业论文（设计）

年度	指导毕业论文（设计）	指导人数	折算学时数	备注（是否与其他教师合上）
2008年	南岭国家级自然保护区藤本植物多样性研究	1	5	否
2009年	南岭国家级自然保护区林下草本植物物种多样性、南岭山地森林群落林下植被优势物种生态位研究、城市化对广州市主干道绿化带物种多样性的影响	3	15	否
2019年	阳春百涌省级自然保护区野生植物资源现状及保护研究	1	5	否
2018年	广州城市森林冠层植物物种组成及群落结构	1	5	否
2023年	中国紫荆木属植物种子大小与幼苗生长的关系	1	5	否
2012年	乡土树种在海口市龙华区城市道路绿化中的应用研究、江门市新会区主要道路绿化带多样性研究、荔湾区主要道路绿化带树种组成及径级结构、珠江新城道路绿	5	25	否

	化带物种多样性研究、峺扈丄穴鍋匕芭｛寒癯籾珊狢せ丶	5	25	
2015年	广州市 3 条主干道绿化带物种多样性及植物配置、天河区三条道路绿化带物种多样性与植物配置研究、广州麓湖公园绿地物种组成及其植物配置研究、麓湖公园绿道物种多样性及其环境教育功能探讨、华南农业大学校园绿地物种多样性及其对校园绿化的启示	5	25	否
2011年	华南理工大学道路绿化带物种多样性的研究、广州市道路绿化带物种多样性研究、越秀公园绿地植物群落多样性研究	3	15	否
2013年	黄花岗公园绿地植物物种多样性研究、黄花岗公园绿地植物群落结构特征研究	2	10	否
2016年	广州市三条主干道绿化带物种多样性及管理措施探讨、红背桂容器苗苗木质量分级研究	2	10	否
2010年	二沙岛东面公园绿地植物群落多样性研究、城市化背景下广州道路绿化中植物多样性研究、乡土植物在华南农业大学启林区道路绿化带中的应用、华南农业大学道路绿化带乔木层优势种生态位研究、深圳排牙山次生林群落优势物种生态位研究、深圳排牙山次生林群落物种多样性研究、广州市典型居民区道路绿化带物种多样性研究、华南农业大学三校区道路绿化带物种多样性	8	40	否
2014年	惠州市惠阳区主干道绿化带物种多样性及管护情况研究、广州荔湾湖公园滨水乔木碳储量研究、华南农业大学校园绿地碳贮量研究、广州市荔湾湖公园滨水植物群落结构特征研究、荔湾湖公园滨水植物物种多样性与植物配置研究	5	25	否

2015年	广州市3条主干道绿化带物种多样性及植物配置、天河区三条道路绿化带物种多样性与植物配置研究、麓湖公园绿道物种多样性及其环境教育功能探讨、华南农业大学校园绿地物种多样性及其对校园绿化的启示	5	25	否
2016年	广州市三条主干道绿化带物种多样性及管理措施探讨、红背桂容器苗苗木质量分级研究	2	10	否
2018年	广州城市森林冠层植物物种组成及群落结构	1	5	否
2019年	阳春百涌省级自然保护区野生植物资源现状及保护研究	1	5	否
2023年	中国紫荆木属植物种子大小与幼苗生长的关系	1	5	否

总学时数	185	**年限**	17	**年均授课学时数**	10.9

注：毕业论文（设计）教学时数= 指导学生数×5

表7-A 讲授研究生课程情况表

学期学年	课程名称	授课对象	课程总学时	本人承担学时	备注
2011-2012-2	森林气象学	森林气象学1班	54	54	
2012-2013-1	森林气象学	森林气象学1班	54	54	
2012-2013-1	森林气象学	森林气象学1班	36	36	
2012-2013-1	景观生态学	景观生态学(2011风景园林深圳班）	60	60	
2012-2013-2	景观生态学	景观生态学(2012风景园林东莞班）	60	60	
2013-2014-2	景观生态学	景观生态学（13级风景园林深圳班）	60	60	
2014-2015-2	景观生态学	景观生态学（2014级风景园林东莞班）	60	60	
2015-2016-2	森林气象学	森林气象学1班	54	54	
2016-2017-1	森林气象学	森林气象学1班	32	32	
2017-2018-1	森林气象学	森林气象学1班	32	32	
2018-2019-1	森林气象学	森林气象学1班	32	32	
2019-2020-1	森林气象学	森林气象学1班	32	32	

2019-2020-2	森林生态系统理论与应用	森林生态系统理论与应用1班	48	48	
2019-2020-1	环境生态学	环境生态学1班	32	3	
2020-2021-2	森林生态系统理论与应用	森林生态系统理论与应用1班	48	48	
2020-2021-2	森林生态系统理论与应用	森林生态系统理论与应用1班	48	48	
2010-2011-1	森林气象学	森林气象学1班	54	54	
2020-2021-1	环境生态学	环境生态学1班	32	3	
2021-2022-1	环境生态研究专题	环境生态研究专题1班	32	3	
2021-2022-2	森林生态系统理论与应用	森林生态系统理论与应用1班	48	48	
2022-2023-1	环境生态研究专题	环境生态研究专题1班	32	3	
2022-2023-2	森林生态系统理论与应用	森林生态系统理论与应用1班	48	48	
2023-2024-1	环境生态研究专题	环境生态研究专题1班	32	3	
2023-2024-2	森林生态系统理论与应用	森林生态系统理论与应用1班	48	48	
2024-2025-2	森林生态系统理论与应用	森林生态系统理论与应用1班	48	48	
2024-2025-1	环境生态研究专题	环境生态研究专题1班	32	3	

总学时数	974	**年限**	17	**年均授课学时数**	57.3

注：1.表7-A以研究生院下达教学任务的课程时数为准。
2.表7-A须提供证明材料，可导出打印本表，由本人签名确认、学院（单位）审核盖章后再上传附件

表7-B 指导毕业研究生折合教学时数

毕　业　年　度			**2024年**	**2023年**	**2022年**	**2021年**	**2019年**
作为一导培养毕业全日制研究生人数	**无二导**	**博士生**					
		硕士生	2	1		1	1
	有二导	**博士生**					
		硕士生			1		
作为二导培养毕业全日制研究生人数		**博士生**					
		硕士生		1			
毕　业　年　度			**2018年**	**2017年**	**2015年**	**2014年**	

作为一导培养毕业全日制研究生人数	无二导	博士生					
		硕士生	2	1	1	1	
	有二导	博士生					
		硕士生					
作为二导培养毕业全日制研究生人数		博士生					
		硕士生					
折合学时数			220				
年均指导毕业研究生折合学时数			12.9				

备注：1.指导毕业研究生教学时数=毕业全日制硕士人数×20+毕业全日制博士人数×35；若有二位指导教师，则第一导师占三分之二，第二导师占三分之一。
2.表7-B须提供证明材料，可导出打印本表，由本人签名确认、学院（单位）审核盖章后再上传附件。

表8 指导创新创业训练项目

学年学期	指导校级以上创新创业训练项目	项目数	折算学时数	备注（是否与其他教师合上，若合上备注合上教师姓名）
2016-2017-2	指导校级创新创业项目珠三角城市森林公园近自然群落构建探索	1	5	否
2019-2020-1	校级创新创业训练计划项目冠层结构对紫荆木群落特征的影响研究	1	5	否

总学时数	10	年限	17	年均授课学时数	0.59

注：创新创业训练项目教学时数=指导项目数×5

表9-A 近五年本科生评教结果

学年学期	分数	参评人数	单位排名	排名占比	开课单位
2021-2022学年第一学期	94.17	31	162-22	13.59%	林学与风景园林学院
2019-2020学年第二学期	91.2	84	142-100	70.43%	林学与风景园林学院
2020-2021学年第二学期	91.02	81	134-92	68.66%	林学与风景园林学院
2022-2023学年第一学期	95.75	71	143-55	38.46%	林学与风景园林学院
2023-2024学年第一学期	97.145	66	142-41	28.87%	林学与风景园林学院

表9-B 近五年研究生评教结果

学年学期	分数	参评人数	单位排名	排名占比	开课单位
2019-2020春季	96.02	43	27/60		林学与风景园林学院
2020-2021春季	95.56	91	43/87		林学与风景园林学院
2020-2021春季	98.9	5	4/87		林学与风景园林学院
2020-2021秋季	93.75	6	102/110		林学与风景园林学院
2021-2022秋季	95.59	40	62/118		林学与风景园林学院
2021-2022春季	95.61	52	33/77		林学与风景园林学院
2022-2023秋季	94.68	56	87/158		林学与风景园林学院
2022-2023春季	95.19	104	62/115		林学与风景园林学院
2023-2024秋季	96.21	35	37/130		林学与风景园林学院
2023-2024春季学期	95.73	103	39/115		林学与风景园林学院
2024-2025秋季学期	95.66	35	114/162		林学与风景园林学院

表9-C 评教结果排名情况

近五年，本科评教结果在本单位排名前10%的学期	
近五年，本科评教结果在本单位排名前20%的学期	2021-2022学年第一学期
近五年，研究生评教结均在本单位排名前10%的学期	2020-2021春季
近五年，研究生评教结均在本单位排名前20%的学期	

表10 学工工作量情况统计表（仅限学生思想政治教育专业职称申报人员填报）

序号	年　度	项目清单	年度工作量	备注
年均学工工作量		0		

教研业绩

表11教学研究项目情况

序号	项目名称	项目编号	项目来源	实到经费（万元）	立项时间	是否结题	结题时间	主持人	本人排名	课题组总人数	项目级别	备注
1	PBL教学模式在林学专业课程中的创新和实践	JG08082	教改项目	0.4	2008-07-02	是	2010-12-01	张璐	1	2	校	
2	创新型《森林生态学》课程实验教学的探索与实践	JG11048	教改项目	0.3	2011-09-02	是	2013-12-01	张璐	1	3	校	

表12 以第一作者发表教改论文情况

序号	论文名称	刊物名称（刊号）	发表时间（年月）	作者排名	论文等级	备注
1	基于多样化人才培养模式实践教学改革研究——以森林生态学为例	高等农业教育	2014/05	1	C	
2	高等院校创新性实验教学的探索与实践——以“森林生态学”实验教学为例	中国林业教育	2014/05	1	普刊	

注：论文附件须包含期刊封面、目录（标注出所发论文）、论文全文、封底以及检索证明。

表13 教学成果情况

序号	获奖时间	项目类型	项目名称	奖励级别	成果授予部门	本人排名	证书号	备注

注：项目含教学成果奖、精品课程、一流课程、双语课程示范课、课程思政示范课程等。

表14 教学类比赛情况

序号	获奖时间	奖励名称	奖励级别	成果授予部门	证书号	备注

注：项目含教学比赛、青年教师教学优秀奖、教学观摩奖、十佳教师等。

表15 编写教材情况

序号	教材名称	ISBN号	出版社	出版时间	教材性质	字数（万）	排名	备注

注：教材附件须包含封面、ISBN页、目录页。

科研项目

表16-A 科研项目情况-主持的项目

序号	类型	项目名称	项目编号	项目来源	实到经费（万元）	经费卡号	立项时间	是否结题	结题时间	课题组总人数	项目等级	备注
1	纵向项目	m6A修饰在紫荆木幼苗生长与防御中的调控机制	32371742	国家自然科学基金委员会	20	B230152	2023-08-24	否	2027-12-31	1	A	
2	纵向项目	生态公益林提质增效可持续发展策略研究	2020STGYL001	广东省林业局	100	F20098	2020-05-20	是	2022-04-15	1	A	
3	纵向项目	近自然城市森林群落关键技术构建与推广	2014GA780055	科技部	0	无	2014-06-01	是	2016-01-01	3	A	经费自筹课题
4	纵向项目	极小种群野生植物紫荆木拯救项目	无	广东省林业局	50	F220329	2022-08-16	是	2024-02-20	5	B	
5	纵向项目	珍稀濒危植物观光木野外调查、繁育和救护研究	无	国家林业局	10	C16049	2016-06-07	是	2020-01-20	8	B	
6	纵向项目	珍稀濒危植物紫荆木救护、扩繁及野外回归	2130211	国家林业局	8	C15060	2015-06-18	是	2019-05-30	9	B	
7	纵向项目	粗木质残体对森林土壤表层C:N:P化学计量特征的影响机理研究	2015A030313403	广东省科技厅	10	E15199	2016-01-01	是	2018-08-01	6	B	
8	纵向项目	珠三角近自然城市森林群落构建关键技术研究	2013B020305009	广东省科技厅	8.02	E14135	2014-08-13	是	2017-04-19	7	B	

9	纵向项目	广东第一峰石坑崆CWD碳库动态及其机理研究	E10043	广东省科技厅	3	E10043	2009-02-01	是	2011-10-01	6	B	
10	纵向项目	基于比较基因组学的紫荆木救护与繁育回归	无	广东省林业局	30	F220049	2022-01-01	是	2024-02-18	1	C	
11	纵向项目	珍稀濒危植物紫荆木保护基因组学研究及应用	YSDZW2021	广东省林业局	30	F21101	2020-11-06	是	2022-05-10	13	C	
12	纵向项目	珍稀濒危植物紫荆木种子繁育关键技术研究及应用	无	广东省林业局	20	F20029	2020-01-01	是	2024-01-30	7	C	
13	纵向项目	珍稀濒危植物紫荆木野外救护和扩繁关键技术研究	2030207-2	广东省林业局	29.93	F19086	2019-03-27	是	2024-01-24	1	C	
14	纵向项目	珠三角城市森林近自然群落构建关键技术研究与示范	2019KJCX007	广东省林业局	25	F19084	2019-05-01	是	2022-05-12	10	C	
15	纵向项目	阳春百涌省级自然保护区野生植物资源调查	2130211-30299-1	广东省林业局	15	F18203	2018-07-01	是	2021-03-15	11	C	
16	纵向项目	珠三角城市森林近自然群落构建关键技术研究与示范	2017KJCX037	广东省林业局	30	F17054	2017-04-01	是	2022-05-12	10	C	
17	纵向项目	珍稀濒危植物观光木、紫荆木地理分布及保护	无	广东省林业局	10	F16020	2016-01-01	是	2017-03-24	7	C	
18	纵向项目	红背桂苗木分级与栽培技术规程	L1415761	广东省林业局	7	F14042	2014-01-15	是	2016-07-12	6	C	

表16-B 科研项目情况-主要参加的项目

序号	类型	项目名称	项目编号	项目来源	实到经费(万元)	经费卡号	立项时间	是否结题	结题时间	主持人	本人排名	课题组总人数	项目等级	备注
1	纵向项目	连南大叶茶林麝等四种珍稀濒危动植物种质资源发掘与	无	广东省林业局	140	F24011	2023-12-15	否		肖遂	3	19	A	
2	纵向项目	乡土地被植物耐荫等级测定及应用研究	2013B020305008	广东省科技厅	8	E14118	2014-08-13	是	2017-06-12	苏志尧	2	8	B	

科研成果

表17-A 以第一作者发表本专业论文（著）情况

序号	论文名称	刊物名称（刊号）	发表时间（年月）	在第一作者中的排名	文献类型	论文等级	备注
1	亚热带常绿阔叶林枯立木与冠层结构的关系	森林与环境学报	2018/01	1	期刊论文	C	
2	TOPOGRAPHIC CONTROLS ON THE DISTRIBUTION OF INDIGENOUS RHODODENDRONS IN THE SOUTHERN SLOPE OF THE NANLING MOUNTAINS, SOUTH CHINA	PAKISTAN JOURNAL OF BOTANY	2016/12	1	期刊论文	B	
3	南岭山地杜鹃花沿海拔梯度的分布及其园林应用前景	华南农业大学学报	2014/01	1	期刊论文	B	
4	南岭自然保护区常绿阔叶林枯立木数量特征分析	福建林学院学报	2012/01	1	期刊论文	C	
5	广东石坑崆森林群落优势种群生态位宽度沿海拔梯度的变化	林业科学研究	2007/10	1	期刊论文	B	

注：论文附件须包含期刊封面、目录（标注出所发论文）、论文全文、封底以及检索证明。

表17-B 以通讯作者发表本专业论文（著）情况

序号	论文名称	刊物名称（刊号）	发表时间（年月）	在通讯作者中的排名	文献类型	论文等级	备注
1	High-quality chromosome-level genomic insights into			1			

1	molecular adaptation to low-temperature stress in Madhuca longifolia in southern subtropical China	BMC Genomics	2024/09	1	Article	A	
2	Topographical Influence on Snag Distribution in a Subtropical Forest in South China	FORESTS	2023/05	1	Article	A	
3	Dynamic Transcriptomic and Metabolomic Analyses of Madhuca pasquieri (Dubard) H. J. Lam During the Post-germination Stages	FRONTIERS IN PLANT SCIENCE	2021/09	1	Article	A	
4	Single-Molecule Real-Time Sequencing of theMadhuca pasquieri(Dubard) Lam. Transcriptome Reveals the Diversity of Full-Length Transcripts	FORESTS	2020/08	1	Article	B	
5	The Composition and Diversity of Soil Bacterial and Fungal Communities Along an Urban-To-Rural Gradient in South China	FORESTS	2019/09	1	Article	B	

6	城市森林土壤微生物群落结构的季节变化	生态学杂志	2019/09	1	期刊论文	B	
7	亚热带常绿阔叶林锥和木荷枯立木点格局分析	西南林业大学学报(自然科学)	2019/01	1	期刊论文	C	
8	不同冠层结构下的植物生长型与生活型特征	中南林业科技大学学报	2018/07	1	期刊论文	C	
9	珍稀濒危植物紫荆木生态学研究进展	广西植物	2018/07	1	期刊论文	C	
10	南岭山地森林群落冠层结构对林下野生花卉的影响	西南农业学报	2015/02	1	期刊论文	B	
11	南岭山地森林群落冠层结构与立木多度的关系	中南林业科技大学学报	2014/04	1	期刊论文	B	
12	南岭国家级自然保护区森林群落枯立木分布与地形因子的相关性	福建农林大学学报	2013/06	1	期刊论文	B	

注： 1.论文附件须包含期刊封面、目录（标注出所发论文）、论文全文、封底以及检索证明。 2.“在通讯作者中的排名”，排名最后的通讯作者在此栏填1，排名倒数第2的通讯作者在此栏填2，以此类推。

表18 以第一作者发表理论文章情况

序号	文章名称	发表载体	发表版面/栏目	发表时间（年月）	发表卷期	字数（千）	备注

备注：含在《求是》《人民日报》《光明日报》《经济日报》上发表的理论文章，或在省级党报理论版上发表的理论文章，或在人民网、新华网、求是网、光明网发表的理论文章。

表19 学术专著、工具书等情况

序号	著作名称	出版社	出版时间	著作性质	字数（万）	作者排名	备注
1	不再孤独的紫荆木	中国林业出版社	2023-11-28	科普绘本	1	1	中国林业出版社第一本极小种群野生植物科普丛书。

2	东莞森林生态建设模式与评价	中国林业出版社	2008-11-18	专著	42.5	5	

注：附件须包含封面、目录页。

表20-A 科技奖励

序号	获奖时间	奖励名称+等级	成果名称	奖励授予部门	本人排名	项目等级	备注

备注：项目含《华南农业大学学术业绩评价体系》中的科技奖励和科研成果获奖。

表20-B 获得知识产权情况

序号	获得时间	知识产权类型	知识产权名称	成果授予部门	本人排名	登记号/专利号	项目等级	备注

知识产权类型选项：1.发明专利、实用新型专利、外观设计专利；2.软件著作权；3.植物新品种权；4.审定植物新品种；5.新兽药（一类、二类、三类、四类、五类）；6.其他（在备注中说明）

表20-C 标准情况

序号	获得时间	标准类型	标准名称	发布部门	本人排名	标准号	项目等级	备注
1	2017-03-10	地方标准	红背桂苗木培育与栽培技术规程	广东省质量技术监督局	1	DB44/T 1967—2017	B	
2	2014-08-18	地方标准	生态公益林样地调查技术规程	广东省质量技术监督局2014第6号（总第141号）	2	DB44/T 1389-2014	B	
3	2008-07-11	地方标准	林业生态术语	广东省质量技术监督局	3	DB44/T 552—2008	B	

表20-D 科技成果转化项目情况

序号	项目名称	实到经费（万元）	经费卡号	合同签订时间	本人排名	项目等级	备注

表20-E 决策咨询报告采纳实施

序号	采纳时间	项目类型	采纳或实施部门	具体业绩表述	备注

表20-F 科研平台

序号	立项时间	项目名称	项目来源	总经费额（万元）	进展情况	本人排名	项目等级	备注

其他

表21 指导学生参加学科竞赛

序号	获奖时间	奖励名称+等级	成果授权部门	本人在指导老师中的排名	项目等级	备注
1	2024-12-08	第三届全国林木基因组与现代种业学术研讨会研究生报告+二等奖	林木遗传育种全国重点实验室	1	其他（备注）	
2	2020-11-15	第七届全国种群生态学前沿论坛优秀青年报告奖二等奖	中国生态学会种群生态专业委员会/江苏大学	1	C	

表22 艺术类成果

序号	获得时间	项目类型	具体业绩表述	主办单位	本人排名	项目等级	备注

表23 体育类指导学生比赛获奖情况

序号	获奖时间	项目类型	获奖情况	主办单位	是否为主教练	备注

表24 个人荣誉

序号	获奖时间	项目类型	奖励名称	奖励级别	授予部门	备注
1	2010-03-31	教育教学个人荣誉	《中国林业教育》优秀作者	其他	《中国林业教育》编辑部	

备注：项目含教育教学个人荣誉、综合类个人荣誉称号、学生思政类个人荣誉等。

表25 其他业绩

序号	时间	项目名称	具体业绩表述	备注
1	2011-12-11	第九届中国林业经济论坛优秀论文二等奖	论文《基于聚类和排序的广东省自然保护区管理策略研究.》 获2011年第九届中国林业经济论坛优秀论文二等奖（排名第1）	

单位推荐意见及结果

所在学院（系、部、所）的评价意见

（对申报人的政治思想、职业道德、专业技术工作、业绩负责核实，并对其水平、能力、业绩作出客观、公正的评价。）

单位（公章）：

年　月　日

学院（教学部）推荐委员会推荐结果：

推荐委员人数	到会人数	推荐结果				备注
		同意人数		不同意人数		

评委会评前公示情况	年　月　日

<table>
<tr><td rowspan="6">职称评审委员会意见</td><td>评议组
专家数</td><td>到会人数</td><td colspan="4">表决结果</td><td>备注</td></tr>
<tr><td></td><td></td><td>同意人数</td><td></td><td>不同意人数</td><td></td><td></td></tr>
<tr><td colspan="7">学科组评审委员会结果：</td></tr>
<tr><td>高评委会
专家数</td><td>到会人数</td><td colspan="4">评审结果</td><td>备注</td></tr>
<tr><td></td><td></td><td>同意人数</td><td></td><td>不同意人数</td><td></td><td></td></tr>
<tr><td colspan="7">高评委会评审意见及结果：

评委会公章
主任委员签章：
年　月　日</td></tr>
<tr><td colspan="8">评审结果公示情况：</td></tr>
<tr><td colspan="8">职称审核确认意见：

华南农业大学（公章）
年　月　日</td></tr>
</table>

代表作鉴定意见

代表作的鉴定意见装订或在此页

（由单位负责办理，注意保密，不得将鉴定意见外泄给其本人或其他人员）

申报	系列：教师
	专业：林学
	职称：教授

证书、证明材料

（身份证、学历学位、非学历教育、职称证、任职资历、教师资格证、继续教育等一式一份，合订。）

单　位（二级单位）林学与风景园林学院

姓　名　　张璐

材料核对人：　　单位盖章：

核对时间：

华南农业大学制

说　　明

1、各类证明材料必须分类贴在方框内，如面积超出方框时，应在框内对齐。

2、凡提供的复印件，应加盖验件单位印章。

3、此件纸张规格为A4，双面印制，其结构、字体、字号不予改变。

身 份 证

粘

贴

面

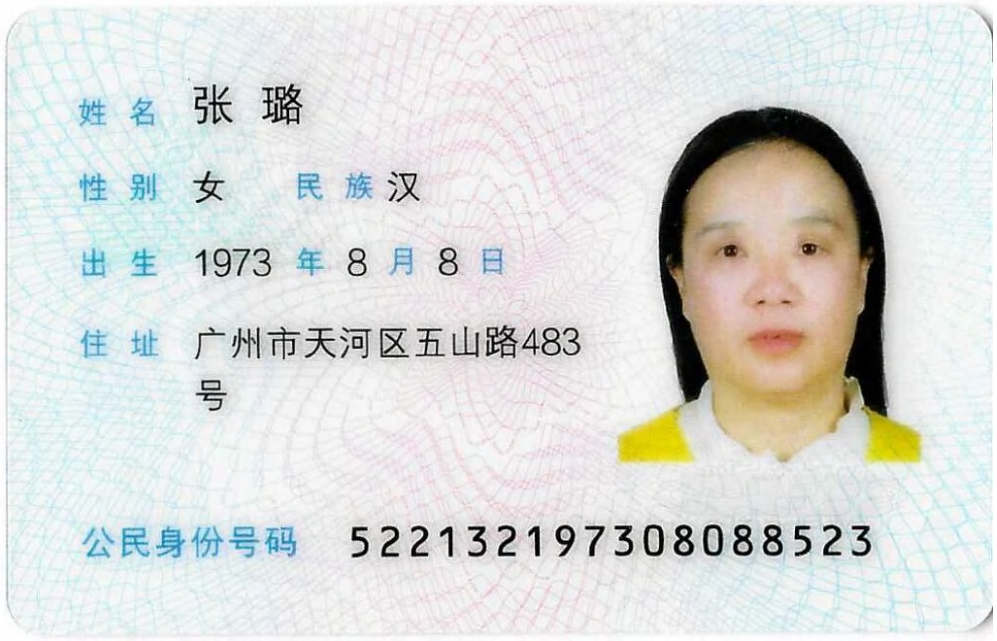
姓 名 张 璐
性 别 女 民 族 汉
出 生 1973 年 8 月 8 日
住 址 广州市天河区五山路483号
公民身份号码 522132197308088523


中华人民共和国
居民身份证
签发机关 广州市公安局天河分局
有效期限 2024.12.25-长期

学 历 、 学 位 证

粘

贴

面

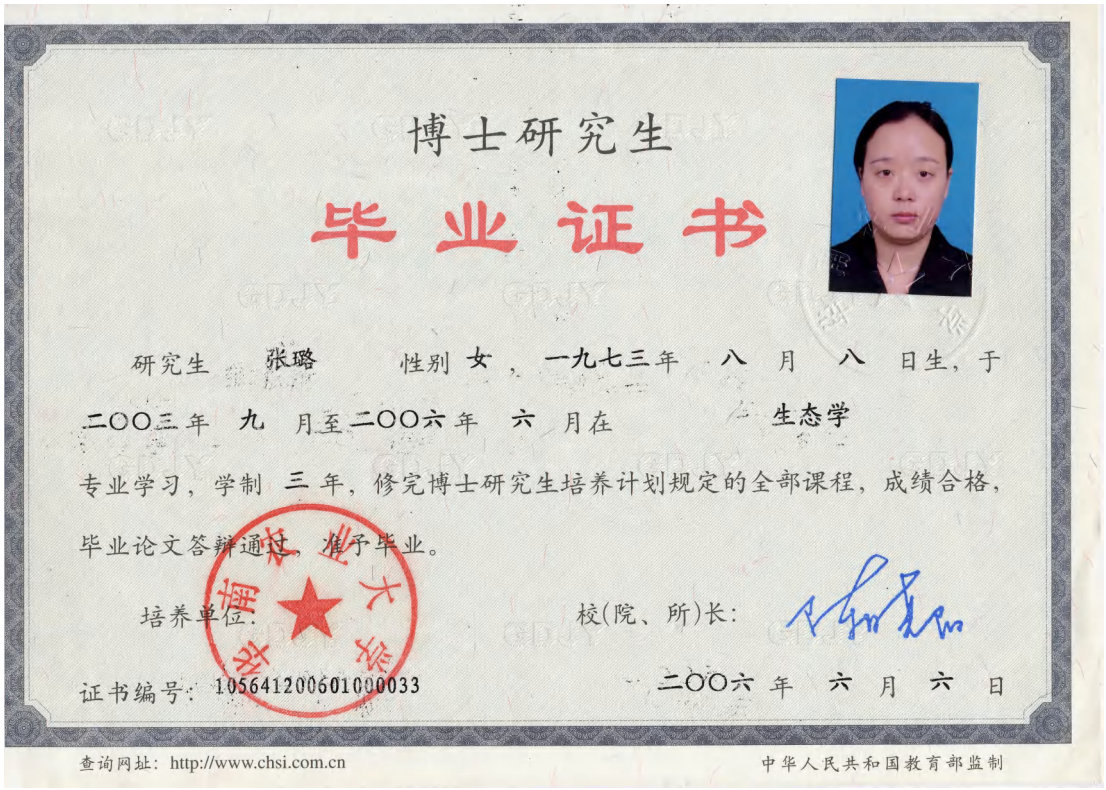

博士研究生

毕业证书

研究生 张璐 性别 女，一九七三年 八 月 八 日生，于二〇〇三年 九 月至二〇〇六年 六 月在 生态学 专业学习，学制 三 年，修完博士研究生培养计划规定的全部课程，成绩合格，毕业论文答辩通过，准予毕业。

培养单位： 校(院、所)长：

证书编号：10564120060100033 二〇〇六 年 六 月 六 日

查询网址：http://www.chsi.com.cn 中华人民共和国教育部监制

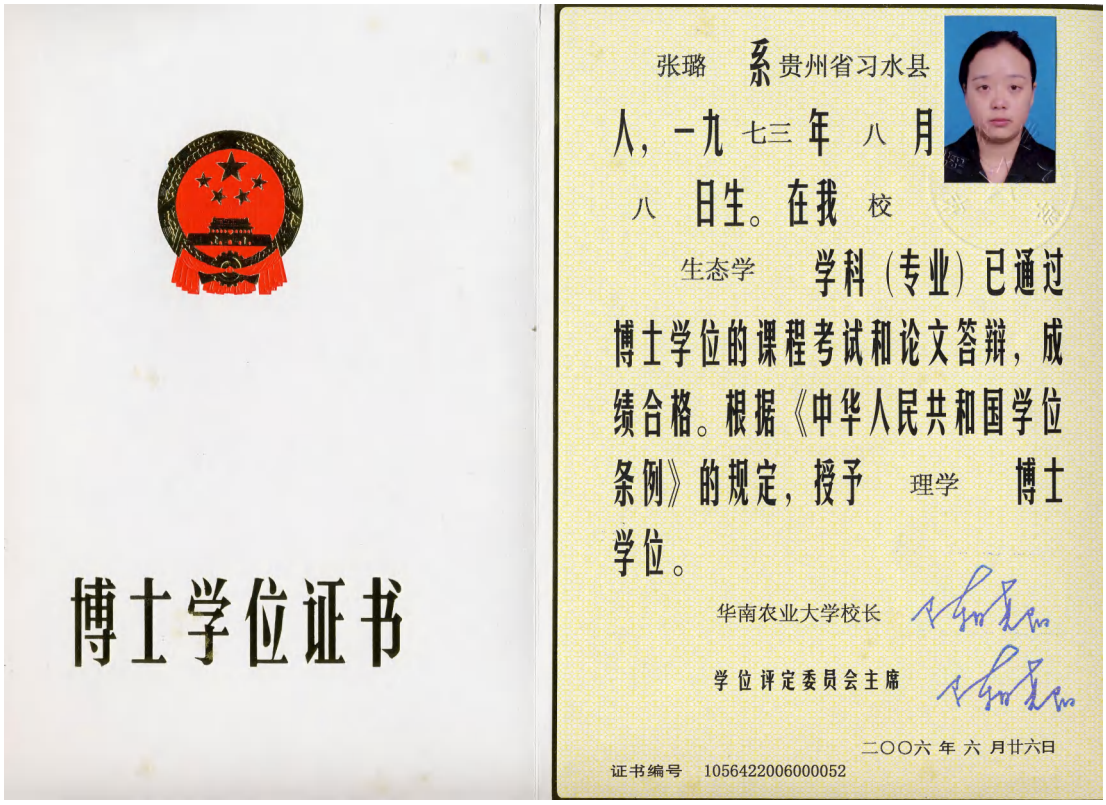

博士学位证书

张璐 系贵州省习水县人，一九七三年 八 月 八 日生。在我 校 生态学 学科（专业）已通过博士学位的课程考试和论文答辩，成绩合格。根据《中华人民共和国学位条例》的规定，授予 理学 博士学位。

华南农业大学校长

学位评定委员会主席

二〇〇六 年 六 月廿六日

证书编号 1056422006000052

职 称 证

粘

贴

面

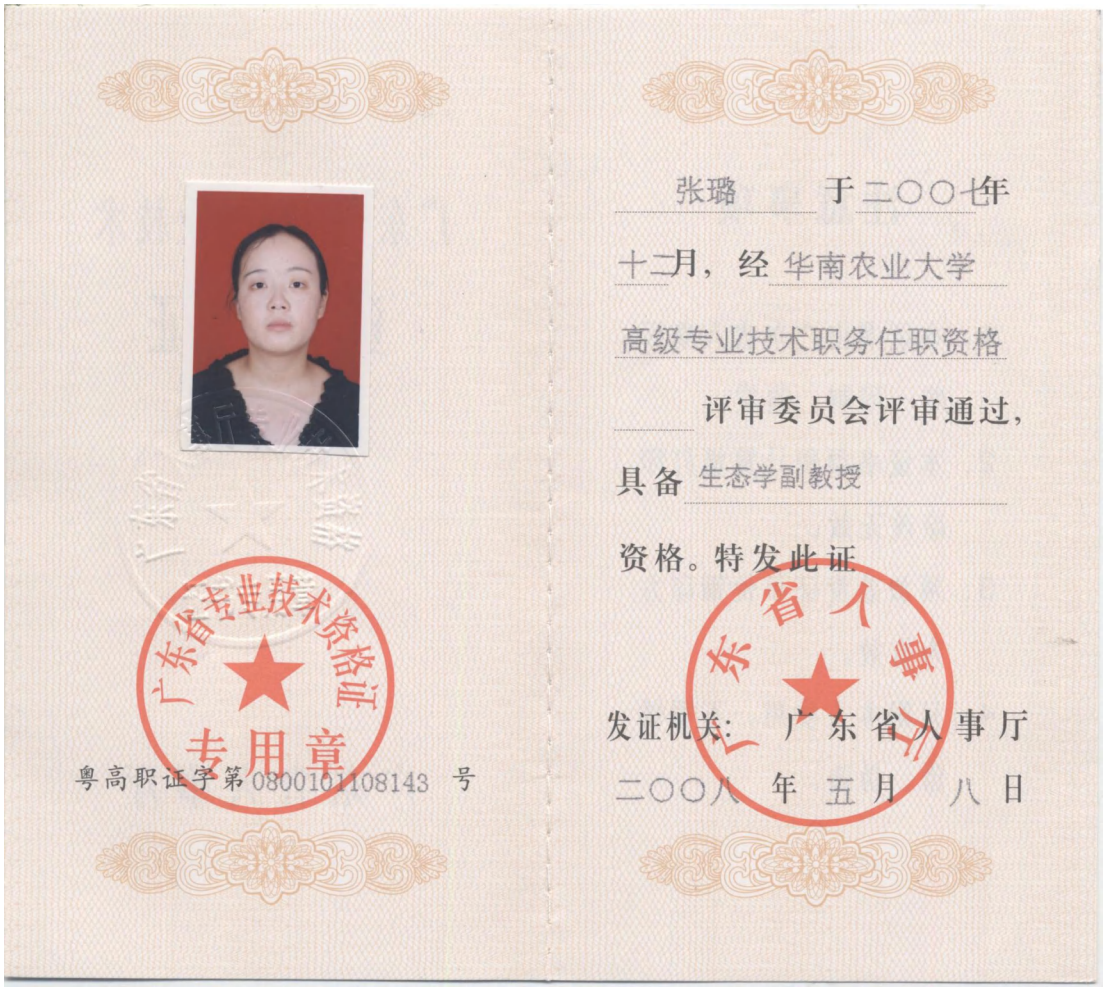
张璐 于二〇〇七年
十二月，经 华南农业大学
高级专业技术职务任职资格
评审委员会评审通过，
具备 生态学副教授
资格。特发此证
广东省专业技术资格证
专用章
粤高职证字第 08001101108143 号
广东省人事厅
发证机关：广东省人事厅
二〇〇八 年 五月 八日

继 续 教 育 证

粘

贴

面

证书编号：GD000024397958

广东省专业技术人员继续教育证书

张璐（身份证号：522132197308088523）参加专业技术人员继续教育学习，经审核，已完成2024年度高等学校教师专业系列专业技术人员继续教育学习任务，根据《广东省专业技术人员继续教育条例》，特发此证。

发证单位：

发证时间：2024年12月19日

广东省人力资源和社会保障厅制

说明：证书可凭编号在广东省人力资源和社会保障厅门户网站核实

教 师 资 格 证

粘

贴

面

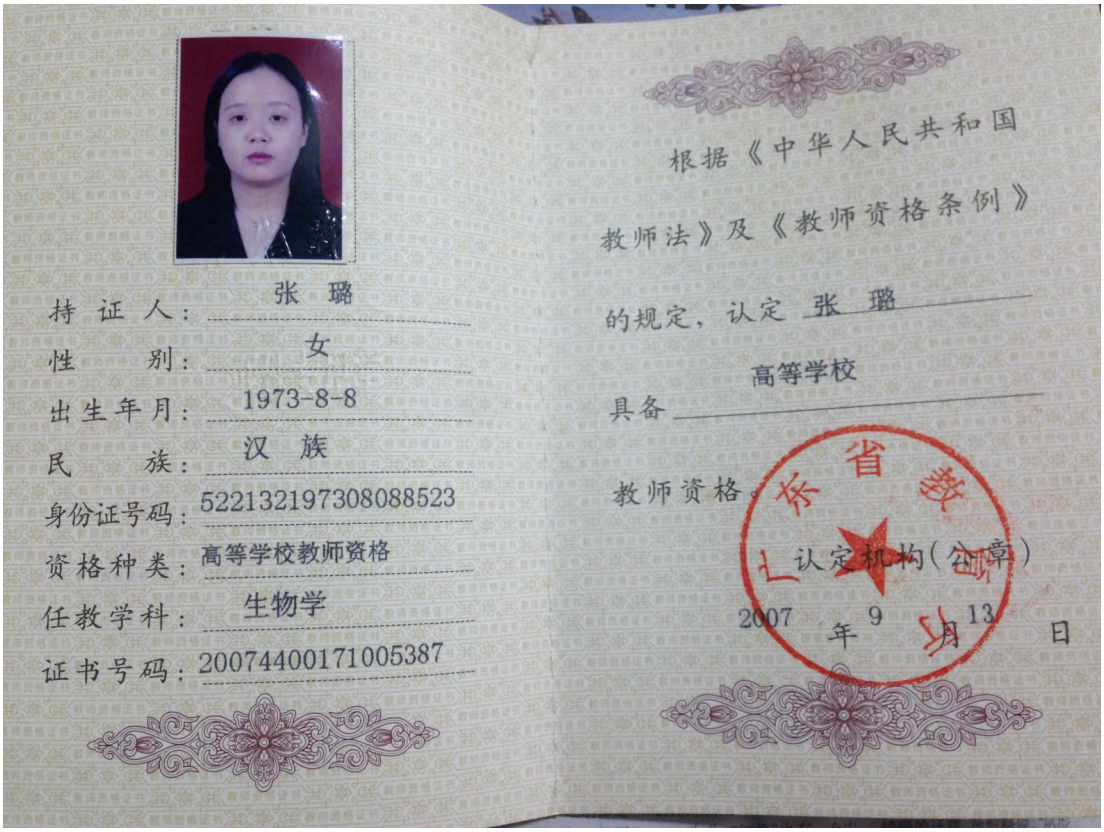
持 证 人：张 璐
性 别：女
出生年月：1973-8-8
民 族：汉 族
身份证号码：522132197308088523
资格种类：高等学校教师资格
任教学科：生物学
证书号码：20074400171005387
根据《中华人民共和国教师法》及《教师资格条例》的规定，认定 张 璐
具备 高等学校
教师资格。
认定机构（公章）
2007 年 9 月 13 日

申报	系列：教师
	专业：林学
	职称：教授

业绩成果材料

（申报人的业绩成果材料包括论文、科研项目、获奖以及其他成果等）

单　位（二级单位） 林学与风景园林学院

姓　名 **张璐**

材料核对人:　　单位盖章:

核对时间:

华南农业大学制

目　　录

一、教学研究业绩

二、科研项目

三、论文、著作等

四、科研成果

五、其他业绩

佐证材料

一、教学研究业绩

1.教学研究项目：关于 PBL 教学模式在林学专业课程中的创新和实践项目（JG08082）的立项通知

华南农业大学2008年度教育教学改革与研究立项项目一览表

序号	项目名称	项目类别	主持人	职称	经费（元）
JG08061	基因工程课程教学方法的创新与实践	一般项目	马静云	副教授	4000
JG08062	《动物繁殖学》设计性实验教学研究	一般项目	李　莉	实验师	4000
JG08063	关于我校考务管理工作存在的问题及对策研究	一般项目	崔　芸	助理研究员	4000
JG08064	基于项目的《机械CAD/CAM》双语教学改革与实践	一般项目	夏红梅	讲师	4000
JG08065	在大众教育基础上对高素质人才培养的探讨	一般项目	张国权	教授	4000
JG08066	食品专业教学与社会需求匹配研究	一般项目	鲍金勇	助教	4000
JG08067	法律英语课程教学方法改革研究	一般项目	赵蕾	讲师	4000
JG08068	专业有机化学教学内容和课程体系改革与实践	一般项目	张淑婷	副教授	4000
JG08069	国家级植物实验示范中心实验课程体系建设与创新人才培养	一般项目	郭海滨	实验师	4000
JG08070	教育技术学专业实践教学体系改革研究	一般项目	林诚彦	助教	4000
JG08071	我国观赏鱼产业与水族科学专业方向的发展	一般项目	甘　炼	讲师	4000
JG08072	高等数学案例式创新教学的研究与实践	一般项目	江雪萍	讲师	4000
JG08073	《园艺植物育种学》实验培养大学生创新能力的探索与实践	一般项目	曹必好	副教授	4000
JG08074	基于网络环境下的英美文学教学理论与实践	一般项目	郑成英	副教授	4000
JG08075	大学物理实验报告新模式探索	一般项目	李海	讲师	4000
JG08076	园艺学院学生修读辅修/双学位专业的现状分析与对策	一般项目	骆芙蓉	工程师	4000
JG08077	我校研究生培养机制改革方案的组织与实施	一般项目	孟成民		4000
JG08078	《社会调查研究方法》课程在社会工作专业人才建设中的作用研究	一般项目	马林芳	讲师	4000
JG08079	我校公共事业管理专业特色研究	一般项目	巩玉涛	讲师	4000
JG08080	自动化专业培养创新性人才办学模式的改革与研究	一般项目	邹　恩	教授	4000
JG08081	“设施农业科学与工程”多学科渗透交叉新专业人才培养模式探讨	一般项目	孙光闻	副教授	4000
JG08082	PBL教学模式在林学专业课程中的创新和实践	一般项目	张　璐	副教授	4000
JG08083	以学生为中心的艺术教育创新教学模式研究	一般项目	胡远慧	讲师	4000
JG08084	《大学生职业发展与就业指导》课程规划与建设的研究与实践	一般项目	谢珊	讲师	4000
JG08085	农业院校学生社会实践探索	一般项目	熊颜	助理研究员	4000
JG08086	学院级实验中心实验技术人员考核制度模式探讨	一般项目	刘宗莉	讲师	4000
JG08087	环境科学类专业本科生普通生态学课程实验教学的改革与实践	一般项目	廖一凌	副教授	4000
JG08088	普通高校体育教学质量管理体系优化方案的研究	一般项目	汤晓波	讲师	4000
JG08089	广东高校显微生物学虚拟实验室的构建与共享应用	一般项目	崔大方	教 授	4000
JG08090	面向艺术设计专业的《设计管理》课程教学研究与改革	一般项目	盘湘龙	助教	4000
JG08091	网络自主学习模式下互动性缺乏的弥补	一般项目	王世龙	讲师	4000
JG08092	《植物学野外实习手册》编研	一般项目	张荣京	讲师	4000
JG08093	土木工程专业基础工程类课程教学改革研究	一般项目	何春保	讲师	4000

2.教学研究项目：关于创新型《森林生态学》课程实验教学的探索与实践项目（JG11048）的立项通知

附件：

华南农业大学2011年度教育教学改革与研究立项项目一览表

编号	项目名称	项目类别	主持人	职称	经费(单位：元)
JG11037	包装工程专业包装设计类课程群建设的研究	一般项目	岳淑丽	讲师	3000
JG11038	基于良好教学效果的《高等数学》课件的设计、制作与应用研究	一般项目	曾庆茂	讲师	3000
JG11039	项目驱动下的三位一体式教学研究与实践	一般项目	江雪萍	讲师	3000
JG11040	《动物胚胎工程》课程教学改革研究与实践	一般项目	卫恒习	讲师	3000
JG11041	基于网络教学平台的精品课程《旅游学》教学改革与实践	一般项目	刘小蓓	讲师	3000
JG11042	以学生科技创新为抓手促进学风建设的探索与实践	一般项目	郭　灼	讲师	3000
JG11043	动物科学学院校企合作教育模式的探索与实践	一般项目	韩　丽	讲师	3000
JG11044	中华传统文化与物理学渗透交叉的教育问题研究	一般项目	熊万杰	讲师	3000
JG11045	适应行业发展的人才培养模式研究——以兽医行业为例	一般项目	陈晓梅	讲师	3000
JG11046	《快题设计训练》课程教学方法的创新与实践	一般项目	陈方慧	讲师	3000
JG11047	《兽医药理学》课程开放式创新性实验教学研究	一般项目	曾东平	实验师	3000
JG11048	创新型《森林生态学》课程实验教学的探索与实践	一般项目	张　璐	副教授	3000
JG11049	学科渗透交叉理念下案例式教学在统计学专业教学中的探索与实践	一般项目	李泽华	讲师	3000
JG11050	生化设计创新性综合实验教学中引入创新课题和生技大赛新体系的探讨	一般项目	巫光宏	副教授	3000
JG11051	基于 WebQuest 的 ACCESS 课程教学研究与实践	一般项目	万　华	讲师	3000
JG11052	《农产品安全检测》课程内容优化与教学实践	一般项目	钟国华	教授	3000
JG11053	互动教学方式在大学专业课程教学中的应用	一般项目	吴银宝	副教授	3000

SCAULIB202404703

检索证明

根据委托人提供的论文材料，委托人华南农业大学林学与风景园林学院 张璐 1 篇论文收录情况如下表。

序号	论文名称	发表刊物及发表的年月卷期/页码等	作者排名	论文等级	作者文中单位	收录情况	影响因子	中科院大类分区
1	基于多样化人才培养模式实践教学改革研究——以森林生态学为例	高等农业教育 出版年：2014 卷期：5 5 页码：55-57 文献号： 文献类型：	第一作者	C类	华南农业大学	北大核心	无	无

说明：论文等级和中科院大类分区按《华南农业大学学术论文评价方案（试行）》划分。

报告免责声明:如未盖章,报告无效

检索员：欧群

华南农业大学图书馆

2024-01-18

GAODENG NONGYE JIAOYU

HIGHER AGRICULTURAL EDUCATION

全国中文核心期刊
辽宁省一级期刊

高等农业教育

Higher Agricultural Education

ISSN 1002-1981
05>
9 771002 198002

2014·5

全国中文核心期刊
辽宁省一级期刊
《中国期刊网》全文收录期刊
《中国学术期刊（光盘版）》全文收录期刊
中国学术期刊综合评价数据库来源期刊
《中国核心期刊（遴选）数据库》来源期刊
中文科技期刊数据库收录期刊

目　录

MU　LU

高等农业教育（月刊）
2014 年第 5 期（总 275 期）

高等农业教育,2014-5,5:55-57
Higher Agricultural Education,2014-5,5:55-57

基于多样化人才培养模式实践教学改革研究
——以森林生态学为例

张　璐,苏志尧

(华南农业大学,广东 广州 510642)

摘要: 从探讨多样化人才培养模式的内涵入手,从课程体系、培养计划和教学管理等角度构建多样化实践教学人才培养模式,并以森林生态学课程为例,探索实施多样化实践教学模式。将验证性、综合性实验和实习、研究性实习、探索性实习与科技创新项目等有机结合,面向不同目标的学生群体,因材施教,建立验证型、综合型、研究型及探索型等多样化的实践教学模式,不断推进实践教学建设与改革。

关键词: 森林生态学; 实践教学; 多样化; 人才培养

中图分类号: G642.0　　**文献标识码:** B　　**文章编号:** 1002-1981(2014)05-0055-03

人才培养是高等学校的根本任务。人才培养模式是当前高校深化教学改革,提高人才培养质量的关键。最早使用人才培养模式概念的是原国家教委1994年启动并实施的《高等教育面向21世纪教学内容和课程体系改革计划》。原教育部副部长周远清对人才培养模式作了简明扼要的阐述,"所谓人才培养模式,实际上就是人才培养目标、培养规格和基本培养方式"[1]。目前,人才培养模式主要有狭义论、泛化论、中介论和状态论等4种观点[2]。其中,狭义论仅限与教学活动,重点探讨教学方式方法;泛化论则关注整个教育管理活动,侧重于人才培养结构和策略体系;中介论介于教学活动与整个管理活动之间,关注人才培养过程中带有方向性的管理问题;状态论没有明确地将人才培养模式限定于某一特定的教育系统范畴内,认为人才培养模式内涵即培养过程中呈现出的结构状态特征。多样化人才培养模式的内涵既体现在宏观层面,也体现在微观层面(表1)。

从宏观方面讲,教育层次要多样化[3];从微观方面讨论,同一层次的人才培养规格也要多样化,包含专业方向的多样化、知识结构多样化、能力多样化、素质多样化等。高等教育从精英走向大众化的过程,就是人才培养从精英培养走向多样化、多元化的过

表1　多样化人才培养模式内涵

培养模式	特点
专业招生培养模式	以专业教育为主的传统培养模式
学科大类培养模式	按大类招生,前期安排通识教育、学科基础知识、实践操作等基础课程,后期根据学生兴趣爱好、就业志向及人才市场需求,分别设置相应专业课程
精英实验班模式	以夯实基础、淡化专业为原则,着力促进学生知识、能力、素质协调发展和特长发挥
复合型人才培养模式	采取主辅修制、实行"双专业、双学位制",学生可辅修跨学科、跨门类的专业
产学研结合模式	通过与科研机构、企业、行业、社区的合作,使人才培养与生产实践直接结合
国际合作教育模式	通过与国外高等教育机构联合办学,互认学分,国内教育与国际交流相结合

基金项目: 广东省质量工程项目:流溪河国家森林公园大学生实践教学基地(粤教高函[2012]123号);华南农业大学教育教学改革与研究项目:创新型《森林生态学》课程实验教学的探索与实践(JG11048)。
收稿日期: 2013-07-21
作者简介: 张璐(1973-),女,林学院,副教授,博士。研究方向:森林生态学。

程[4]。通过分类培养、因材施教，实施与探索多样化人才培养模式的改革与创新，实现学生全面发展和个性发展相统一，为终身教育奠定坚实的本科基础[5]，对于提高人才培养质量，深化各项教育教学改革，起着至关重要的作用[6]。改革与创新多样化人才培养模式是世界高等教育发展的必然趋势，也是提高人才培养质量的重要保障。

一、构建多样化实践教学人才培养模式

实践教学是培养学生实践能力和创新能力的重要手段。改革与创新人才培养模式，归根结底要落实到课程体系、培养计划以及教学管理上来，这是构建多样化实践教学人才培养方案的核心内容。通过整合实验课程，完善校、院两级实验课平台建设，构建一体化、多层次、开放式的创新实验教学人才培养模式。

（一）以拓展专业内涵、拓宽专业口径为目标，构建专业课程体系

课程体系应围绕拓展专业内涵、拓宽专业面以及加强基础进行构建。设立多而灵活的实践教学课程，将理论课程和实践环节与所需知识、能力、素质一一对应，从知识结构、能力结构和素质结构三个方面整合课程体系[7]。实践教学课程体系的设计以实现学生的全面、充分和自由的发展为本位，注重学生的求同思维和求异思维统一，重视学生的全面发展和个性彰显。设置个性化的实践教学课程，构建多样化跨学科实践教学课程体系；同时强化学生个人对实践教学课程的选择自由，增加学生自主学习和操作的时间与空间，为学生充分发展个性奠定基础。

（二）以学生最优化发展为出发点，建立多样化实践教学培养计划

由于人的兴趣、爱好和特长是多样化的，实践教学应从学生的特点出发，详细分解实践教学的培养目标、实践课程学分、学期以及具体的教学安排等，因材施教，构建多样化的实践教学人才培养计划，以使每个学生的个性、专长和潜力得到最优化发展。

（三）以培养和增强学生创新能力为核心，强化实践教学管理

教学管理是为了实现教学目标，按照教学规律和特点，对教学过程的全面管理。实践教学管理要结合教学目的和学生实际，从实践教学过程、实践教学质量、实践教学评价等方面强化实践教学管理。

二、森林生态学多样化实践教学模式的探索

森林生态学是研究森林与环境相互关系的科学，是生态学的一个分支学科，也是林学的一个分支学科[8]。森林生态系统在固定大气二氧化碳方面发挥着重要作用，低碳时代赋予了森林生态学教学新思维。森林生态学课程是华南农业大学林学专业和森林资源保护与游憩专业的必修课，同时又是全校的公共选修课之一。作为一门实践性和应用性很强的学科[9]，森林生态学是林学、生态学等专业学生学习森林培育学、森林经理学、环境生态学等课程的重要基础[10]。森林生态学中的许多理论和认识都是建立在科学试验基础之上的，实践教学在森林生态学的教学中占有非常重要的地位[11]。在长期的教学实践中，森林生态学课程面向不同目标的学生群体，因材施教，不断推进多样化的实践教学模式。将验证性、综合性实验和实习、研究性实习、探索性实习与科技创新项目等有机结合，不仅在实践环节安排上体现多样性，在教学内容上也体现多样性（图1）。

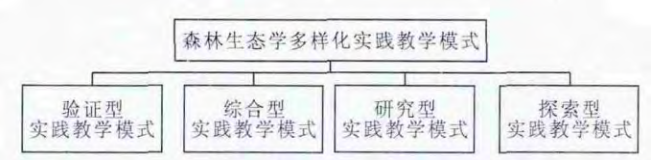

图1 森林生态学多样化实践教学模式

（一）验证型实践教学模式

华南农业大学森林生态学课程选用 Smith R L 和 Smith T M 主编的 Ecology and Field Biology 为教材蓝本，采用双语进行教学。验证型实践教学模式强调学生基本技能的培养，强化学生对专业基础知识的理解和把握，以理解基本概念和基本理论为目的，以培养学生的基本操作能力和分析能力为重点，主要在实验室完成。要求学生课后整理实验报告，系统分析实验成败的关键，提出改进意见，并通过问题讨论，加深学生对实践内容的理解和对操作技能的掌握。

（二）综合型实践教学模式

综合型实践教学模式重在强化学生综合、系统掌握课程知识的能力。为了构建内在的、系统的、科学的实践教学逻辑结构体系，从森林生态学课程特点出发并考虑学生的认知过程和规律，华南农业大学组织修订了森林生态学实验指导书，以林木资源与生态环境的相互关系为主优化森林生态学实验教学内容，密切关注森林生态学领域科学研究前沿动态，将诸如全球气候变化对森林生态系统的影响及其响应、森林与水文关系等研究引入实践教学中，综合设计与专业培养计划课程相匹配的实践教学模式。

（三）研究型实践教学模式

在森林生态学研究型实践教学过程中，注重以教

助研、以研促教，注重实践教学模式和华南农业大学优秀本科生“红满堂计划”相结合，充分发挥教师在森林生态学方面的科研优势，利用承担国家级、省部级等科研课题的条件，开放实验室，将科研项目中的有关内容与研究性实践教学相结合，让优秀本科生参与其感兴趣的科研课题。对教师而言，通过选取科研项目中的研究对象为实践教学材料，把科研内容设计成系列森林生态学实验，教学与科研结合，将研究成果和进展融入实践教学，拉近了抽象理论和实践的距离；对学生而言，学生在教师指导下进行一些与课题研究相关的实验工作。通过查阅科技文献、设计实验路线、实施实验方案、收集实验数据、阐述实验结果等，提高了学习兴趣，加深了对森林生态学课程理论的理解。另一方面，实践教学与科研项目研究相结合，可充分利用强大的本科生人力资源优势，组织学生在固定样地开展森林群落结构特征调查、群落调查和多样性指数测定等传统内容，随着时间推移，数据的不断积累，为准确分析群落的动态变化过程创造了良好的前提条件，同时也将实践教学转化为科研的一部分。

（四）探索型实践教学模式

探索型实践教学模式以国家级、省级、华南农业大学和林学院四级科技创新项目为基础，以广州市流溪河大学生实践教学基地等省级及校院级教学实习基地为依托，由教师和学生共同成立创新团队，根据科技创新项目的需要设计探索型实践项目。在探索型实践教学模式实施过程中，引入了 PBL（Problem Based Learning，探究式学习）教学模式[12]，实行“以科学问题为主导”设计实验内容的思路，提供多项综合性实习题目。指导学生对实习题目的选择以及设计和操作实验。通过学生的自主探究和合作来解决问题，从而学习隐含在问题背后的科学知识，形成解决问题的技能和自主学习的能力。这样完成一个实习内容的过程就是学生接受一次科学训练的过程，调动了学生思考问题的积极性和探索问题的主观能动性，有利于培养学生的创新精神和实践能力。

三、森林生态学多样化实践教学模式实施的效果

通过森林生态学多样化实践教学模式的实践和探索，学生的创新与实践能力显著增强，出现了多样化目标的学生群体。不少学生通过实践教学环节对森林生态学产生浓厚兴趣，立下从事森林生态学志向；一些学生参与科研创新，开展探索研究，本科毕业后继续攻读研究生，最终取得一定的成绩。

实践教学是理论联系实际的切入点，是理论过渡到实际的桥梁。以学生为本，构建多样化人才培养模式是社会经济发展对高等教育提出的要求。面向不同目标的学生群体，多样化实践教学模式使学生能够根据自身兴趣、爱好以及社会对人才的要求，自主设计发展方向，更能体现学生个体的差异和具体要求，有利于因材施教，促进个性发展。在保证基本核心的实践环节培养质量的基础上，鼓励探索，激励拔尖，从而更好地满足社会经济发展对各类人才的需求。

参考文献：

[1] 林玲. 高等院校“人才培养模式”研究述论 [J]. 四川师范大学学报：社会科学版，2008，(4)：110－117.

[2] 李亚萍，金佩华. 我国高校本科人才培养模式理论研究综述 [J]. 江苏高教，2003，(5)：103－105.

[3] 白波，张应强. 高等教育大众化与高校多样化人才培养 [J]. 黑龙江高教研究，2008，(1)：152－154.

[4] 李琼生. 多样化人才培养模式下教学管理的思考与实践——以广东工业大学为例 [J]. 广东工业大学学报：社会科学版，2011，(2)：44－47.

[5] 陈晓阳. 构建因人而异、分类培养的人才培养模式研究与实践 [J]. 高等农业教育，2013，(2)：3－6.

[6] 翟雪峰. 浅谈林业高校多样化人才培养模式的改革与创新 [J]. 国家林业局管理干部学院学报，2011，(1)：17－21.

[7] 罗三桂，蔡忠兵，李晶. 人才培养模式改革创新中的课程体系建构趋势分析 [J]. 中国大学教学，2012，(7)：30－32.

[8] 蒋有绪. 森林生态学的任务及面临的发展问题 [J]. 世界科技研究与发展，2000，(3)：1－3.

[9] 洪伟，吴承祯，刘金福，等.《森林生态学》实践基地建设的经验与启示 [J]. 福建农林大学学报：哲学社会科学版，2008，(5)：73－76.

[10] 温远光，庄嘉，招礼军，等. 森林生态学课程研究型教学模式探索 [J]. 中国科教创新导刊，2010，(8)：26－27.

[11] 许中旗，李玉灵. 森林生态学教学实习的改革与实践 [J]. 中国林业教育，2010，28 (1)：75－77.

[12] Hessami M. A.，Gani R. Using Problem－Based Learning in Mechanical Engineering Degree [M]. Campbell Town，NSW，1993：75－82.

（责任编辑与校对 孙　科）

高等农业教育 月刊

国内外发行
Public Distribution

刊号：ISSN 1002—1981
CN21—1088/G4

邮政编码：110161
Post Code:110161

2014 年 5 月出版
国内定价：10.00 元

SCAULIB202405452

检索证明

根据委托人提供的论文材料，委托人**华南农业大学林学与风景园林学院 张璐** 1 篇论文收录情况如下表。

序号	论文名称	发表刊物及发表的年月卷期/页码等	作者排名	论文等级	作者文中单位	收录情况	影响因子	中科院大类分区
1	高等院校创新性实验教学的探索与实践——以“森林生态学”实验教学为例	中国林业教育 出版年：2014 卷期：2014,32(03) 03 页码：76-78 文献号： 文献类型：期刊论文	1	普刊类	华南农业大学林学院	CNKI	无	无

说明：论文等级和中科院大类分区按《华南农业大学学术论文评价方案（试行）》划分。

报告免责声明:如未盖章,报告无效

检索员：田成

华南农业大学图书馆

2024-03-04

中国核心期刊（遴选）数据库
中国知网　华艺线上图书馆收录期刊

ISSN 1001 – 7232
CN 11 – 2729/S

中国林业教育

Forestry Education in China

3
2014年5月
第32卷　第3期
Vol.32　No.3

北京林业大学　中国林业教育学会　主办

中国林业教育

Forestry Education in China

第 32 卷 第 3 期
2014 年 5 月

目　　次

主管单位 中华人民共和国教育部
主办单位 北京林业大学 中国林业教育学会
编辑出版 《中国林业教育》编辑部
北京海淀区北京林业大学内
邮政编码 100083
电话号码 010-62338090/8397
Email: liuxiaoling@bjfu.edu.cn

主 编 宋维明
副 主 编 张铁明
责任编辑 柳小玲 王 伟 孙艳玲
印 刷 北京科信印刷有限公司
国内总发行 北京市报刊发行局
订 购 处 全国各地邮政局(所)
国内统一刊号 CN 11-2729/S

高等院校创新性实验教学的探索与实践

——以“森林生态学”实验教学为例

张 璐 苏志尧

（华南农业大学林学院，广州 510642）

摘 要：创新性实验对培养大学生专业拓展能力和就业能力具有重要的意义。针对目前高等农业院校“森林生态学”实验教学中存在的主要问题，提出“森林生态学”实验教学的改革措施：首先要优化实验教学结构体系，压缩验证性实验教学的比例，扩大研究性实验教学的比重；其次应引入PBL教学模式，以科学问题为主导，提供多项综合性实验题目，通过学生自主探究和合作来解决问题；第三要将实验教学与科研相结合，选取科研项目中的研究对象为实验材料，以教助研，以研促教。在系统培养学生的基本实验操作技能的基础上，探索并建立以问题和课题为核心的教学模式，激发学生的创新思维和创新意识，切实提高“森林生态学”实验教学的质量。

关键词：森林生态学；实验教学；结构体系；PBL教学模式；科研创新

加强实践教学环节，提升高校学生的创新精神、实践能力、社会责任感和就业能力是高校教育的重要课题[1]。“森林生态学”是研究森林与环境相互关系的科学，是生态学的一个分支学科，也是林学的一个分支学科[2]。目前，北京林业大学、南京林业大学、广西大学、福建农林大学、以及西北农林科技大学等多所高校都建有“森林生态学”国家级精品课程。作为一门实践性和应用性很强的学科[3-4]，“森林生态学”是林学、生态学等专业学生学习“森林培育学”“森林经理学”“环境生态学”等课程的重要基础[5]。实践教学在“森林生态学”的教学中占有非常重要的地位[6]，森林生态学中的许多理论和认识都是建立在科学试验基础之上的。“森林生态学”实验教学是培养森林生态学专门人才的重要手段，是“森林生态学”教学中一个不可或缺的环节。探讨“森林生态学”实验教学结构体系的更新，优化教学方法和手段，将实验教学与科研相结合，有利于培养学生的实践能力和创新能力，从而提高学生的科研素质。

一、“森林生态学”实验教学面临的问题

多年来，许多高校实验室的建设大多沿袭前苏联高等教育实验教学的模式，按课程设置将实验室依附于各个系、科和教研室。传统的“森林生态学”实验课从属于理论课程，作为验证课堂理论的方法和辅助手段，这种传统的实验教学体制重在培养学生的基础实验技能，并通过实验验证，巩固学生所学的理论知识。但这种实验教学存在着实验内容零碎、实验仪器设备使用与共享率偏低等问题，影响了实验教学质量。

（一）实验室的硬件建设落后

相对理论课而言，部分学校领导、教师和学生对实验课的重视程度不够；在无线传感技术普遍应用到森林生态研究领域的今天[7]，传统的“森林生态学”实验课教学常被认为是从属教学，经费投入不足，设备老化，教具损耗严重，实验设施不齐备，影响了实验教学的效果。

（二）验证性实验所占比例偏大

传统“森林生态学”实验课以验证性实验居多，并多停留在对一些简单指标的测定上；与现代生态学的研究内容和方法衔接较少，缺乏新意，不利于学生学习新的知识和综合素质的提高。

（三）实验教学模式单一

传统的“森林生态学”实验课教学方法基本是以灌输、模拟、验证为主，实验讲义写得很详细，学生只需按规定好的实验步骤与方法“照方抓药”，所以在整个实验教学过程中学生处于被动的学习状态，难以发挥其主观能动性和创造力。单一、落后的教学模式不利于培养学生对实验课的兴趣，使学生在实验过程中缺乏主动性、积极性和创新性。

（四）实验的学时偏少

传统的“森林生态学”实验课所占比重较小，实验学时数一般只有10学时左右，且缺乏连贯性和系统性，未能形成一个完整的“森林生态学”实验教学体系。学生在做完实验后，往往只停留在对实验现象和实验结果的表面观察上，缺乏深入比较、分析研究和对实验整体性的把握。

二、"森林生态学"创新性实验教学的实践

(一)优化实验教学体系的结构

知识的学习和创新性实验是互相促进、相互发展的[8]。在美国,各林学院开设的"森林生态学"是必修课,在三、四年级时讲授,一般为3～5个学分,课堂教学为40～50个学时,野外实习1周,两者穿插进行。在课堂讲完一个知识重点,就去野外调查、旅行实习[9]。在中国,验证性、综合性和研究性实验是各高等院校进行实验教学改革共存的3种形式。"森林生态学"是华南农业大学林学专业和森林资源保护与游憩专业的必修课,同时又是全校的公共选修课之一。课程选用Smith. R. L和Smith. T. M主编的《Ecology and Field Biology》为教材蓝本,采用双语进行教学[10]。为了构建内在的、系统的、科学的实验教学结构体系,华南农业大学林学院森林生态教研室组织修订了《森林生态学实验指导书》,以林木资源与生态环境的相互关系为主,优化了"森林生态学"的实验教学内容,密切关注了森林生态学领域科学研究的前沿动态,将诸如全球气候变化对森林生态系统的影响、森林与水文关系等研究内容引入实验教学中,保持了实验教学内容的新颖性。在传统"森林生态学"实验结构的基础上,进一步压缩了验证性实验教学比例,扩大了研究性实验教学比例,3个层次的实验按照验证性实验占20%、综合性实验占30%、研究性实验占50%的顺序循序渐进地进行,见表1。

表1　验证性、综合性和研究性实验的主要特点

	教学目标	组织形式	比例/%
验证性实验	培养学生的基本实验技能	要求学生课后整理实验报告,系统分析实验成败的关键,提出改进意见	20
综合性实验	强化学生综合运用课程知识的能力	教师提出问题,学生以团队合作的形式解决问题	30
研究性实验	培养学生解决实际问题的能力和创新能力	与教师的科研课题相结合,以学生自主学习为主导,由学生自主设计实验方案	50

(二)引入PBL教学模式

PBL又称研究式教学、问题式学习,是一种目前国际上较流行的教学模式。PBL教学模式不同于传统的以单纯的知识传授为主体的教学模式,而是一种能力培养型的教学模式。PBL教学模式把教学活动的本质看成是学生的发展过程,强调学生的主体作用,强调师生互动。教师不仅要考虑教给学生哪些知识,还应当考虑传授知识的方式,特别要注重如何帮助学生学习,给学生设置什么样的学习"场景"。其教学理念强调以问题为学习的起点,以学生的主动学习为主,注重小组的合作学习和自主学习,较少讲述性的教学。PBL基本的教学思路是提出问题—学生查找资料—分组讨论—汇报—总结和评价。

在"森林生态学"PBL实验教学过程中,笔者按照"以科学问题为主导"设计实验内容的思路,提供多项综合性实验题目,供学生参考、筛选。学生也可以根据自己的兴趣、特长确定自己的主题。以"不同取样面积对珠三角地区风景林物种多样性调查结果的影响"这一实验为例,笔者首先要求学生以小组为单位就所选题目查阅相关资料、撰写综述报告,包括是否已有类似的研究、采用过哪些研究方法、取得了什么主要结论、存在什么问题,并思考自己如何开展研究等;然后利用一定的学时在全班开展学习交流,要求每个小组利用5～8分钟的时间阐明自己的观点,教师和其他学生都可以参与讨论,确定各组的研究方案;接着安排学生在规定的时间内完成野外的调查工作,教师适时对学生进行指导,帮助学生解决外业中可能遇到的问题;在野外调查完成后,指导学生对获得的数据进行整理和分析,完成研究报告的撰写,并分小组用PPT汇报交流;最后,教师根据学生报告完成的质量及课堂讨论的态度等进行综合成绩的评定。这样完成一个实验内容的过程就是学生接受一次科学训练的过程,既锻炼了学生收集、整理和分析资料的能力,又提高了学生文字和语言的综合表达能力,更好地促进了学生对课堂知识的融合,发展和彰显了学生的个性,充分挖掘了学生的潜能,提高了学生解决问题的和自主学习的能力。

(三)将实验教学与科研相结合

学生创新能力的培养需要通过加强实验教学环节来实现[11]。教师的科研成果对学生的学习和科研活动有着巨大的激励和推动作用[12]。华南农业大学在"森林生态学"实验教学过程中,以教助研,以研促教,充分发挥教师在森林生态学方面的科研优势,选取科研项目中的研究对象为实验材料,把科研内容设计成系列森林生态学实验,让学生参与其感兴趣的科研课题。对教师而言,通过实验教学与科研的结合,将一些研究成果和进展融入实验教学,拉近了抽象理论和实际的距离;对学生而言,在教师指

导下进行一些与课题研究相关的实验工作,如查阅科技文献、设计实验路线、实施实验方案、收集实验数据、阐述实验结果等,提高了学习兴趣,加深了对"森林生态学"课程理论的理解。另一方面,实验教学与科研项目研究相结合,组织本科生在固定样地开展森林群落结构特征调查、群落调查和多样性指数测定等传统内容,随着时间推移,数据不断积累,为准确分析群落的动态变化过程创造了良好的前提条件,同时也将实验教学转化为科研的一部分。实验教学与科研相互促进,大大提高了学生的综合实验素质和科研能力。

三、"森林生态学"创新性实验教学的效果

近年来,通过对"森林生态学"实验教学内容、教学方法和教学模式的探索和实践,克服了传统实验教学中存在的诸多弊端,加强了学生综合技能的培养。一方面,从培养学生技能、创新训练的角度科学设计"森林生态学"实验课程,优化了实验教学结构体系,研究性实验所占比例得以大幅增加,调动了学生思考问题的积极性和探索问题的主动性;另一方面,改革了传统的实验教学模式,引入 PBL 教学模式,提高了学生的实践能力和创新能力,取得了较好的教学效果。此外,将实验教学与科研相结合,组织学生申报各级科技创新活动,多名学生获得国家级、省级及校院级大学生科技创新项目。

资助项目:广东省质量工程项目"流溪河国家森林公园大学生实践教学基地"(粤教高函[2012]123号);2011 年度华南农业大学教育教学改革与研究项目"创新型'森林生态学'课程实验教学的探索与实践",项目编号 JG11048。

参考文献

[1] 李雷鹏,王立峰,王强. 创新性实验对大学生就业及其潜能开发的影响[J]. 黑龙江高教研究,2012(2):127-129.

[2] 蒋有绪. 森林生态学的任务及面临的发展问题[J]. 世界科技研究与发展. 2000,22(3):1-3.

[3] 洪伟,吴承祯,刘金福,等. "森林生态学"实践基地建设的经验与启示[J]. 福建农林大学学报:哲学社会科学版,2008,11(5):73-76.

[4] WANG Q L,DENG H B. Review of forest ecology studies in China[[J]. Journal of Forestry Research,2002,13(3):231-234.

[5] 许中旗,李玉灵. "森林生态学"教学实习的改革与实践[J]. 中国林业教育,2010,28(1):75-77.

[6] 施拥军,黄坚钦,徐华潮,等. 林学专业实践教学改革探讨[J]. 中国林业教育,2008,26(4):63-66.

[7] BURGESS S S O,KRANZ M L,TURNER N E,et al. Harnessing wireless sensor technologies to advance forest ecology and agricultural research[J]. Agricultural and Forest Meteorology,2010,150(1):30-37.

[8] 孙慧珍,国庆喜,李雷鸿,等. 森林生态学实践教学方法探索——以"大学生创新性实验项目"为例[J]. 继续教育研究,2008(8):151-152.

[9] 罗菊春. 美国森林生态学教学与科研现状[J]. 北京林业大学学报,1986(3):105-110.

[10] 张璐,苏志尧. "森林生态学"双语教学的问题和对策[J]. 中国林业教育,2007,25(4):73-75.

[11] 陈桂葵,章家恩. 高等农业院校生态学专业实验教学改革的探索[J]. 安徽农业科学,2010,38(1):483-485.

[12] 吴永波. 农林院校"森林生态学"课程教学改革的探索与实践[J]. 中国林业教育,2010,28(2):43-45.

(责任编辑 王 伟)

中 国 林 业 教 育
Zhongguo Linye Jiaoyu
2014年5月 第32卷 第3期
（双月刊，1983年创刊）

主管单位 中华人民共和国教育部
主办单位 北京林业大学 中国林业教育学会
编辑出版 《中国林业教育》编辑部
北京市海淀区清华东路35号
邮政编码 100083
电话号码 010-62338090
Email: liuxiaoling@bjfu.edu.cn

主 编 宋维明
副 主 编 张铁明
责任编辑 柳小玲 王 伟 孙艳玲
印 刷 北京科信印刷有限公司
国内总发行 北京市报刊发行局
订 购 处 全国各地邮局(所)

ISSN 1001-7232
CN 11-2729/S

公开发行 邮发代号：82-201 国内定价：30.00元

ISSN 1001-7232
9 771001 723144 05>

二、科研项目

1.主持：关于国家自然科学基金面上项目“m6A 修饰在紫荆木幼苗生长与防御中的调控机制（No.32371742）”的立项通知及有关佐证材料

国家自然科学基金资助项目批准通知

（预算制项目）

张璐　先生/女士：

根据《国家自然科学基金条例》、相关项目管理办法规定和专家评审意见，国家自然科学基金委员会（以下简称自然科学基金委）决定资助您申请的项目。项目批准号：32371742，项目名称：m6A修饰在紫荆木幼苗生长与防御中的调控机制，直接费用：50.00万元，项目起止年月：2024年01月至2027年12月，有关项目的评审意见及修改意见附后。

请您尽快登录科学基金网络信息系统（https://grants.nsfc.gov.cn），**认真阅读《国家自然科学基金资助项目计划书填报说明》并按要求填写《国家自然科学基金资助项目计划书》（以下简称计划书）**。对于有修改意见的项目，请您按修改意见及时调整计划书相关内容；如您对修改意见有异议，须在电子版计划书报送截止日期前向相关科学处提出。

请您将电子版计划书通过科学基金网络信息系统（https://grants.nsfc.gov.cn）提交，由依托单位审核后提交至自然科学基金委。自然科学基金委审核未通过者，将退回的电子版计划书修改后再行提交；审核通过者，打印纸质版计划书（一式两份，双面打印）并在项目负责人承诺栏签字，由依托单位科研、财务管理等部门审核、签章并在承诺栏加盖依托单位公章，且将申请书纸质签字盖章页订在其中一份计划书之后，一并报送至自然科学基金委项目材料接收工作组。纸质版计划书应当保证与审核通过的电子版计划书内容一致。**自然科学基金委将对申请书纸质签字盖章页进行审核，对存在问题的，允许依托单位进行一次修改或补齐。**

向自然科学基金委提交电子版计划书、报送纸质版计划书并补交申请书纸质签字盖章页截止时间节点如下：

1. **2023年9月7日16点：**提交电子版计划书的截止时间；
2. **2023年9月14日16点：**提交修改后电子版计划书的截止时间；
3. **2023年9月21日：**报送纸质版计划书（一式两份，其中一份包含申请书纸质签字盖章页）的截止时间。
4. **2023年10月7日：**报送修改后的申请书纸质签字盖章页的截止时间。

请按照以上规定及时提交电子版计划书，并报送纸质版计划书和申请书纸质签字盖章页，逾期不报计划书或申请书纸质签字盖章页且未说明理由的，视为自动放弃接受资助；未按要求修改或逾期提交申请书纸质签字盖章页者，将视情况给予暂缓拨付经费等处理。

附件：项目评审意见及修改意见表

国家自然科学基金委员会

2023年8月24日

项目批准号	32371742
申请代码	C0312
归口管理部门	
依托单位代码	51064208A0499-0932

国家自然科学基金

资助项目计划书

（预算制项目）

资助类别： 面上项目

亚类说明：

附注说明：

项目名称： m6A修饰在紫荆木幼苗生长与防御中的调控机制

直接费用： 50万元　　**执行年限：** 2024.01-2027.12

负 责 人： 张璐

通讯地址： 广东省广州市天河区五山路483号华南农业大学林学与风景园林学院森林生态教研室

邮政编码： 510642　　**电　　话：** 020-85280263

电子邮件： zhanglu@scau.edu.cn

依托单位： 华南农业大学

联 系 人： 唐家林　　**电　　话：** 020-85280070

填表日期： 2023年08月25日

国家自然科学基金委员会制

Version：1.008.613

2.主持：关于广东省省级以上生态公益林效益补偿资金省统筹经费项目“生态公益林提质增效可持续发展策略研究项目（2020STGYL001）”的立项通知及有关佐证材料

广东省财政厅文件

粤财资环〔2020〕28号

广东省财政厅关于下达2020年省级以上生态公益林效益补偿资金省统筹经费的通知

省有关单位，中国科学院华南植物园，有关地级市财政局，有关财政省直管县（市）财政局：

根据《广东省林业局关于请审核下达2020年省级以上生态公益林效益补偿资金省统筹经费的函》，经研究，现将2020年省级以上生态公益林效益补偿资金省统筹经费安排给你们（具体项目、金额详见附件），并将有关事项通知如下：

一、本次下达的资金按照《广东省省级生态公益林效益补偿资金管理办法》（粤财农〔2018〕332号）的有关规定使用。请各地、各有关单位抓紧将资金安排到具体项目，切实加快预算执行，并加强资金监管，不得挤占、截留或挪用，确保专款专用。

二、此项资金支出省直部门列2020年度“农林水支出—林业和草原—森林生态效益补偿（2130209）”功能分类科目，对下转移支付列“农林水共同财政事权转移支付支出（2300252）”功能分类科目，省直部门政府预算经济分类科目列“机关商品和服务支出-其他商品和服务支出（50299）”，部门预算经济分类科目列“商品和服务支出-其他商品和服务支出（30299）”，市县部门经济分类科目按实际用途列编。年终请按要求统一编列决算。

附件：2020年省级以上生态公益林效益补偿资金省统筹经费安排表

广东省财政厅

2020年5月20日

附件

2020年省级以上生态公益林效益补偿资金省统筹经费安排表

单位：元

单位名称	单位编码	资金编码	项目名称	功能分类科目	部门经济分类科目	政府经济科目	金额	备注
合计							68,050,000.00	
各省直部门合计							28,400,000.00	
省教育厅小计	156						1,950,000.00	
华南农业大学	156003	890-2020-XMZC-2744-01-0001	生态公益林提质增效可持续发展策略研究	2130209 森林生态效益补偿			1,000,000.00	
					30299 其他商品和服务支出	50502 商品和服务支出	1,000,000.00	
惠州学院	156029	890-2020-XMZC-2748-01-0001	经树林地段种植黄玉凤花等药用植物技术研究与示范	2130209 森林生态效益补偿			500,000.00	
					30299 其他商品和服务支出	50502 商品和服务支出	500,000.00	
广东生态工程职业学院	156086	890-2020-XMZC-2745-01-0001	广东森林线虫多样性动态监测	2130209 森林生态效益补偿			450,000.00	
					30299 其他商品和服务支出	50502 商品和服务支出	450,000.00	
省林业局小计	199						25,350,000.00	
广东省林业局	199001	890-2020-XMZC-2746-01-0001	生态林业立法、普法	2130209 森林生态效益补偿			1,200,000.00	
					30299 其他商品和服务支出	50299 其他商品和服务支出	1,200,000.00	
广东省林业调查规划院	199004	890-2020-XMZC-2758-01-0001	广东省石漠化地区植被恢复评估研究	2130209 森林生态效益补偿			900,000.00	
					30299 其他商品和服务支出	50502 商品和服务支出	900,000.00	
广东省林业调查规划院	199004	890-2020-XMZC-2747-01-0001	国家储备林大径材林培育监测报告	2130209 森林生态效益补偿			400,000.00	
					30299 其他商品和服务支出	50502 商品和服务支出	400,000.00	

3.主持：关于科技部“十二五”农村领域科技计划预备项目库国家级星火计划项目“近自然城市森林群落关键技术构建与推广研究（2014GA780055）的立项通知及有关佐证材料

信息名称：	科技部星火计划办公室关于入选“十二五”农村领域科技计划预备项目库国家级星火计划项目公示的通知		
索 引 号：	306-09-2014-942	**信息类别：**	规范性文件2014
发布机构：	科技部星火计划办公室	**发文日期：**	2014年02月21日
文　　号：	国科星火办〔2014〕1号	**实施日期：**	

科技部星火计划办公室关于入选“十二五”农村领域科技计划预备项目库国家级星火计划项目公示的通知

国科星火办〔2014〕1号

各省、自治区、直辖市及计划单列市科技厅（委、局），新疆生产建设兵团科技局，有关部门科技主管单位，各有关单位：

依据《星火计划管理办法》有关规定，按照科技部农村领域科技计划管理改革相关要求，以及《科技部关于组织申报2014年度国家星火计划项目的通知》(国科发计〔2013〕553号)精神，在各有关方面的积极支持和共同努力下，2014年度国家级星火计划重点与引导项目的评审及认定工作已顺利完成。根据专家意见，并报经部领导审定，高产优质多抗玉米新品种中试与示范等339个重点项目及1013个引导项目拟入选“十二五”农村领域科技计划预备项目库（见附件），现予公示。

公示期为2014年2月24日至2014年3月3日，时间一周。任何单位或个人可在公示期内以信函或传真方式对公示内容提出书面异议。异议材料须注明真实姓名和联系方式，其真实性由提出异议的单位与个人负责。对匿名或无具体事实根据的异议，不予受理。

联系人及联系方式：

科技部农村中心星火与信息处：陈永红 于双民

电 话：010 - 68510207 68514065

科技部农村司基层科技处：秦卫东 张洪刚

电 话：010-58881412

附件：1. 拟入选“十二五”农村领域科技计划预备项目库星火计划重点项目清单

2. 拟入选“十二五”农村领域科技计划预备项目库星火计划引导项目清单

科技部星火计划办公室

2014年2月21日

华南农业大学2014、2015年度国家星火计划立项清单

序号	项目类别	项目编号	项目名称	单位名称	主持人	学院	联系电话	邮箱
1	重点	2014GA780003	华南优质高产抗病水稻及其产业化技术集成与示范应用	广东华农大种业有限公司	梁克勤	总公司	13609012777	shutaz@163.com
2	面上	2014GA780011	洗水戈宝麻叶制茶在线无损离心脱水设备应用示范	华南农业大学	徐凤英	工程	13226425786	xu_fy@scau.edu.cn
3	面上	2014GA780012	基于计算机视觉的动植物病虫害自动识别系统应用与示范	华南农业大学	陈琰	数信	13668948099	ayan0426@scau.edu.cn
4	面上	2014GA780016	手持式荔枝采摘机械的研究与开发	华南农业大学	姜焰鸣	公基中心	13416194769	jamie@scau.edu.cn
5	面上	2014GA780047	金针菇栽培环境参数自动监测服务平台应用示范	华南农业大学	万华	数信	13527723968	kycjhk@scau.edu.cn
6	面上	2014GA780048	面向农户的智能养殖技术应用与推广	华南农业大学	林丕源	数信	13650761603	pyuanlin@163.com
7	面上	2014GA780049	群养模式下母猪运动状况监测系统应用与示范	华南农业大学	刘汉兴	数信	13828442838	lhx666@scau.edu.cn
8	面上	2014GA780050	可调式水肥耦合自动灌溉系统的研究与推广应用	华南农业大学	岳学军	电子	13802969638	yuexuejun@scau.edu.cn
9	面上	2014GA780051	基于数据挖掘的龙眼病虫害远程诊断与防治专家系统	华南农业大学	杨磊	数信	15918597385	yanglei_s@scau.edu.cn
10	面上	2014GA780052	水箱养殖水下智能视频监控系统	华南农业大学	薛月菊	电子	13640839893	xueyj@scau.edu.cn
11	面上	2014GA780053	杂交兰新品种产业化示范与推广	华南农业大学	郭和蓉	林风	13580457561	guoherong@scau.edu.cn
12	面上	2014GA780054	柑小实蝇诱捕远程监测系统集成与应用示范	华南农业大学	肖德琴	数信	13794412658	deqinx@scau.edu.cn
13	面上	2014GA780055	近危[illegible]	华南农业大学	张[illegible]	林风	13560089803	zhanglu@scau.edu.cn
14	面上	2014GA780057	基于机器视觉的荔枝串与结果母枝识别系统研发与应用	华南农业大学	郭艾侠	数信	13422065370	guoaixia@scau.edu.cn
15	面上	2014GA780058	基于物联网技术的测土配方施肥决策支持研究与应用	华南农业大学	肖磊	数信	13926451632	lein_xiao@scau.edu.cn
16	面上	2014GA780061	基于视频传感器网络的果树害虫分类识别系统设计与应用	华南农业大学	潘春华	数信	13610205459	pch618163@163.com
17	面上	2014GA780062	基于国产高分卫星估算亚热带森林生物量应用示范研究	华南农业大学				
18	面上	2014GA780063	南方地区冬种马铃薯机械化收获技术推广与示范	华南农业大学	武涛	工程	13527789542	wt55pub@scau.edu.cn
19	面上	2014GA780064	农作物视觉智能传感器节点的设计与应用	华南农业大学	殷建军	数信	13560245369	jianjunyin@scau.edu.cn
20	面上	2014GA780066	RFID畜禽产品质量安全预警系统设计及应用推广	华南农业大学	杜治国	数信	18688896252	zhiguod@163.com
21	面上	2014GA780083	穗龙非洲菊新品种与栽培配套技术推广应用	华南农业大学	何少云	林风	18998339330	syhe2011@163.com
22	重点	2015GA780001	高产高抗水稻品种Y两优1173产业化技术集成与应用	华南农业大学	陈志强	航天	13802998198	zqchen@scau.edu.cn
23	重点	2015GA780002	南方蔬菜重大害虫快速监测及预警技术集成与应用示范	华南农业大学	肖德琴	数信	13794412658	deqinx@scau.edu.cn
24	重点	2015GA780005	导向农药滴灌防控柑橘黄龙病技术推广示范	华南农业大学	徐汉虹	农学	13802922918	hhxu@scau.edu.cn
25	面上	2015GA780038	多业务农情信息获取无线感知网络集成与应用	华南农业大学	肖克辉	数信	13798168148	humorxiao@163.com
26	面上	2015GA780039	轻量无人机均匀撒播技术与装备	华南农业大学	李继宇	工程	13560455485	lijiyu@scau.edu.cn

4.主持：关于广东省自然科学基金自由申请项目“粗木质残体对森林土壤表层 C:N:P 化学计量特征的影响机理研究(2015A030313403)”的立项通知及有关佐证材料

	业务类型	项目编号	项目名称	单位名称	负责人	立项年度	立项金额	科技厅下达文号	财厅下达文号	已拨付金额	任务书截止日期	状态	标记结题验收	负责人登录名
1	广东省自然科学...	2015A030313...	粗木质残体对森林土壤...	华南农业大学	张璐	2015	10.00	粤科规财字[20...		10	2018-08-01	已经通过验收		zhanglu

序号	业务类型	项目名称	立项年度	验收状态	审核意见	验收组织单位	验收结论	是否公示	任务书到期日期	查看任务书	任务书状态	操作
1	广东省自然科学基金-自由申请	粗木质残体对森林土壤表层C:N:P化学计量特征的影响机理研究	2015	项目验收_验收通过	查看	华南农业大学	-	-	2018-08-01	查看	任务书签订完成	查看 查看PDF

广东省自然科学基金项目合同书

受理编号：c15140500000116

项目编号：2015A030313403

文件编号：粤科规财字[2015]120号

2015A030313403

广东省自然科学基金项目

合同书

项目名称：粗木质残体对森林土壤表层C:N:P化学计量特征的影响机理研究

项目类别：广东省自然科学基金-自由申请

项目起止时间：2015-08-01 至 2018-08-01

管理单位（甲方）：广东省自然科学基金管理委员会

依托单位（乙方）：华南农业大学

通讯地址：广东省广州市天河区五山路483号

邮政编码：510642 单位电话：020-38632819

项目负责人：张璐 联系电话：020-85280263-601

项目联系人：张璐 联系电话：13560089803

广东省科学技术厅

二〇一四年制

广东省自然科学基金项目合同书

八、本合同签约各方

管理单位（甲方）：广东省自然科学基金管理委员会（盖章）

法定代表人（或法人代理）：（签章）

年 月 日

依托单位（乙方）：华南农业大学（盖章）

法定代表人（或法人代理）：陈晓阳（签章）

联系人（项目主管）姓名：华南农业大学科技处（签章）

Email：kjcgxk@scau.edu.cn

电话：020-85283135

开户单位名称：华南农业大学

开户银行名称：广东广州工行五山支行

开户银行帐号：3602002809000310520

2015年9月15日

联系人（课题负责人）姓名：张璐（签名）张璐

Email：zhanglu@scau.edu.cn

电话：020-85280263-601

2015年9月17日

5. 主持：关于广东省省级科技计划农业领域项目“珠三角近自然城市森林群落构建关键技术研究（2013B020305009）”的立项通知及有关佐证材料

	业务类型	项目编号	项目名称	单位名称	负责人	立项年度	立项金额	科技厅下达文号	财厅下达文号	已拨付金额	任务书截止日期	状态	标记结题验收	负责人登录名
1	农业领域科技计...	2013B020305...	珠三角近自然城市森林...	华南农业大学	张璐	2013	8.00	粤科规财字[20...			2016-12-31	已经通过验收		zhanglu

序号	业务类型	项目名称	立项年度	验收状态	审核意见	验收组织单位	验收结论	是否公示	任务书到期日期	查看任务书	任务书状态	操作
1	农业领域科技计划项目审批	珠三角近自然城市森林群落构建关键技术研究	2013	项目验收_验收通过	查看	华南农业大学	-	-	2016-12-31	查看	任务书签订完成	查看 查看PDF

广东省科技计划项目合同书

受理编号：1311150100041

项目编号：2013B020305009

文件编号：粤科规财字[2014]116号

2013B020305009

广东省省级科技计划项目

合同书

项目名称：珠三角近自然城市森林群落构建关键技术研究

计划类别：农业领域科技计划项目审批

项目起止时间：2014-09-01 至 2016-12-31

管理单位(甲方)：广东省科学技术厅

承担单位(乙方)：华南农业大学

乙方主管部门(丙方)：华南农业大学

通讯地址：广东省广州市天河区广州市天河区五山路483号

邮政编码：510642 单位电话：020-38632819

项目负责人：张璐 联系电话：020-85280263-601

项目联系人：张璐 联系电话：020-85280263-601

广东省科学技术厅
二〇一四年制

九、本合同签约各方

管理单位（甲方）： 广东省科学技术厅 （盖章）
单位地址： 广东省广州市连新路171号
法定代表人（或授权代表）： 刘家平 （签章）
联系人（经办人）姓名： 林振尧 （签章）
Email： linzl@gdstc.gov.cn
电话： 020-83163905
年 月 日

承担单位（乙方）： 华南农业大学 （签章）
二级部门： 华南农业大学林学院
单位地址： 广东省广州市天河区广州市天河区五山路483号
法定代表人（或法人代理）： 陈晓阳 （签章）
联系人（项目主管）姓名： 夏斌 （签章）
Email： kjcgzk@scau.edu.cn
电话： 020-85283435
开户单位名称： 华南农业大学
开户银行及帐号： 广东广州工行五山支行 3602002609000310520
2014 年 11 月 4 日

乙方主管部门（丙方）： 华南农业大学 （签章）
单位地址： 广东省广州市天河区广州市天河区五山路483号
法定代表人（或法人代理）： 陈晓阳 （签章）
联系人（项目主管）姓名： 夏斌 （签章）
Email： kjcgzk@scau.edu.cn
电话： 020-85283435
开户单位名称： 华南农业大学
开户银行及帐号： 广东广州工行五山支行 3602002609000310520
2014 年 11 月 14 日

6.主持：广东省自然科学基金博士研究启动项目“关于广东第一峰石坑崆CWD碳库动态及其机理研究（9451064201003716）”的立项通知及有关佐证材料

广东省自然科学基金项目
合同书

项目名称：广东第一峰石坑崆CWD碳库动态及其机理研究

下达单位（甲方）：广东省自然科学基金管理委员会办公室

承担单位（乙方）：华南农业大学

项目负责人：

邮政编码：

联系电话：

起止年月：2009年10月 至 2011年10月

广东省自然科学基金管理委员会

二00九年

六、本合同签约各方

下达单位（甲方）：广东省自然科学基金委员会办公室（盖章）

甲方法定代表人（或法人代理）：（签章）

联系人（项目主管）姓名：彭闵阳（签章）

年 月 日

承担单位（乙方）：华南农业大学（盖章）

乙方法定代表人（或法人代理）：（签章）

联系人（项目主管）姓名：陈晓（签章）

乙方开户单位名称：华南农业大学

开户银行及账号：广州 工行 五山支行 3602002809000310630

2009年6月9日

7.主持：关于广东省林业厅转下达 2016 年中央级部门预算项目支出预算经费“珍稀濒危植物观光木野外调查、繁育和救护研究（2130211）”的立项通知及有关佐证材料

广东省林业厅文件

粤林财〔2016〕24 号

广东省林业厅关于转下达 2016 年中央级部门预算项目支出预算经费的通知

各有关地级以上市林业主管部门，有关单位：

根据《国家林业局关于拨付 2016 年中央本级项目支出预算经费的通知》（林规发〔2016〕56 号），现将 2016 年中央级部门预算项目支出预算经费转下达给你们（详见附件），并就有关事项通知如下：

一、请各单位严格按照《国家林业局机关项目资金使用管理暂行办法》（林计发〔2009〕236 号）及有关规定，管好用好项目资金，不得截留、挤占和挪用，不得擅自改变项目内容和扩大资金使用范围，做到专款专用，确保资金安全有效运行。严格按照财政部《中央部门结转和结余资金管理办法》（财预〔2016〕18 号）要求，加强财政拨款结转和结余的管理。涉及政府采购的项目，应严格按照政府采购的有关规定办理。

二、加强项目资金的检查和监督，实行追踪问效，切实提高资金使用效益。请各单位于今年年底前将资金使用情况和使用成效上报我厅各相关业务处室，国家林业局和省林业厅将对项目实施和资金使用情况进行检查。

三、承担绩效评价试点项目的单位，要按照《财政支出绩效评价管理暂行办法》（财预〔2011〕285 号）和《国家林业局中央部门预算支出绩效评价管理暂行办法》（林规发〔2011〕252 号）要求，认真做好试点项目绩效目标实施、绩效监控和绩效评价工作。并按照《财政部关于推进预算绩效管理的意见》（财预〔2011〕416 号）和《财政部关于印发<预算绩效管理工作规划（2012-2015 年）>的通知》（财预〔2012〕396 号）精神，积极开展单位非试点项目的绩效自评，推动本单位全面预算绩效管理工作的开展。

附件：2016 年中央级部门预算项目资金安排表

广东省林业厅
2016 年 6 月 7 日

公开方式：不公开

抄送：国家林业局。

广东省林业厅办公室　　2016 年 6 月 8 日印

— 2 —

附件：

2016年中央级部门预算项目资金安排表

金额单位：万元

项目承担单位	项目名称	项目主要内容	金额	功能科目	备注
总计			514		
一、省级合计			347		
省林业科学研究院	小计		84		
	林业生态站等监测运行	森林病虫害生物防治重点实验室运行补助	10	2130206	
	林业生态站等监测运行	国家林业局林产品质量检验检测中心（广州）运行补助	10	2130206	
	林业生态站等监测运行	广东汕头沿海防护林生态系统国家定位观测研究站运行补助	7	2130206	
	林业生态站等监测运行	广东南岭森林生态系统国家定位观测研究站运行补助	7	2130206	
	林业生态站等监测运行	广东东江源森林生态系统国家定位观测研究站运行补助	7	2130206	
	林业生态站等监测运行	广东海丰湿地生态系统国家定位观测研究站运行补助	7	2130206	
	林业生态站等监测运行	国家林业局华南乡土树种工程技术研究中心运行补助	6	2130206	
	林产品质量安全检测	防腐木材、红木、松香等林产品检测	20	2130218	
	林业标准化	龙脑樟培育技术规程	10	2130218	
华南濒危动物研究所（广东省昆虫研究所）	小计		95		
	第二次全国重点保护野生动植物资源调查	粤东沿海山丘台地平原陆生野生动物资源调查	25	2130211	
	第二次全国重点保护野生动植物资源调查	粤西、桂东沿海台地平原-广东陆生野生动物资源调查	25	2130211	
	第二次全国重点保护野生动植物资源调查	野生动物资源调查监测及野外检查	25	2130211	
	第二次全国重点保护野生动植物资源调查	陆生野生动物资源同步调查及监测	20	2130211	
省野生动物救护中心	小计		45		
	珍稀濒危物种野外救护与人工繁育	濒危野生动植物人工繁殖示范（含华南虎野华放归基地前期评估10万元、茂名林洲顶鳄蜥救护繁育10万）	35	2130211	
	野生动物疫病监测和预警系统维护	野生动物疫源疫病监测补助	10	2130211	
华南农业大学	小计		40		
	林业标准化	丝绵木培育技术规程	10	2130218	
	林业标准化	森林防火指挥信息中心建设技术标准	10	2130218	
	林业标准化	椒树栽培技术规程	10	2130218	
	第二次全国重点保护野生动植物资源调查	珍稀濒危植物观光木野外调查、繁育和救护研究	10	2130211	
中国科学院华南植物园	第二次全国重点保护野生动植物资源调查	广东省佛山等地区第二次全国重点保护野生植物资源调查汇总、统计及总结报告	50	2130211	
广州地理研究所	第二次全国重点保护野生动植物资源调查	广东省第二次全国重点保护野生植物资源调查信息建库与统计系统建设	30	2130211	
广东内伶仃福田国家级自然保护区管理局	野生动物疫病监测和预警系统维护	野生动物疫源疫病监测补助	1	2130211	
湛江红树林国家级自然保护区管理局	野生动物疫病监测和预警系统维护	野生动物疫源疫病监测补助	1	2130211	
广东海丰公平大湖省级自然保护区管理处	野生动物疫病监测和预警系统维护	野生动物疫源疫病监测补助	1	2130211	
二、市县合计			167		
广州市	小计		12		
花都区	林业有害生物管理与预测预报补助经费	国家级林业有害生物中心测报点补助	4	2130234	
增城区	林业有害生物管理与预测预报补助经费	国家级林业有害生物中心测报点补助	4	2130234	
从化区	林业有害生物管理与预测预报补助经费	国家级林业有害生物中心测报点补助	4	2130234	
珠海市	小计		5		
市野生动植物保护管理所	野生动物疫病监测和预警系统维护	野生动物疫源疫病监测补助	1	2130211	
市森防站	林业有害生物管理与预测预报补助经费	国家级林业有害生物中心测报点补助	4	2130234	
汕头市	小计		1		
市野生动植物保护管理办公室	野生动物疫病监测和预警系统维护	野生动物疫源疫病监测补助	1	2130211	
韶关市	小计		9		
市野生动植物保护管理办公室	野生动物疫病监测和预警系统维护	野生动物疫源疫病监测补助	1	2130211	

1/2

8.主持：关于广东省林业厅转下达 2015 年中央级部门预算项目支出预算经费“珍稀濒危植物紫荆木救护、扩繁及野外回归（2130211）”的立项通知及有关佐证材料

广东省林业厅文件

粤林财〔2015〕62 号

广东省林业厅关于转下达 2015 年中央级部门预算项目支出预算经费的通知

各有关地级以上市林业主管部门，有关单位：

根据《国家林业局关于拨付 2015 年中央本级项目支出预算经费的通知》（林规发〔2015〕54 号），现将 2015 年中央级部门预算项目支出预算经费转下达给你们（详见附件），并就有关事项通知如下：

一、请各单位严格按照《国家林业局机关项目资金使用管理暂行办法》（林计发〔2009〕236 号）及有关规定，管好用好项目资金，不得截留、挤占和挪用，不得擅自改变项目内容和扩大资金使用范围，做到专款专用，确保资金安全有效运行。严格按照财政部《关于印发〈中央部门财政拨款结转和结余资金管理办法〉的通知》（财预〔2010〕7 号）要求，加强财政拨款结转和结余的管理，充分发挥财政资金的使用效益。涉及政府采购的项目，应严格按照政府采购的有关规定办理。

二、加强项目资金的检查和监督，实行追踪问效，切实提高资金使用效益。请各单位于今年年底前将资金使用情况和使用成效上报我厅各相关业务处室，国家林业局和省林业厅将对项目实施和资金使用情况进行检查。

三、承担绩效评价试点项目的单位，要按照《财政支出绩效评价管理暂行办法》（财预〔2011〕285 号）和《国家林业局中央部门预算支出绩效评价管理暂行办法》（林规发〔2011〕252 号）要求，认真做好试点项目绩效目标实施、绩效监控和绩效评价工作。并按照《财政部关于推进预算绩效管理的意见》（财预〔2011〕416 号）和《财政部关于印发〈预算绩效管理工作规划（2012-2015 年）〉的通知》（财预〔2012〕396 号）精神，积极开展单位非试点项目的绩效自评，推动本单位全面预算绩效管理工作的开展。

附件：2015 年中央级部门预算项目资金安排表

广东省林业厅

2015 年 6 月 2 日

公开方式：依申请公开

抄报：国家林业局。

广东省林业厅办公室　　2015 年 6 月 2 日印

— 2 —

附件：

2015年中央级部门预算项目资金安排表

金额单位：万元

项目承担单位	项目名称	项目主要内容	金额	功能科目	备注
总计			1567		
一、省级合计			1440		
省林业科学研究院	小计		193		
	行业专项	国外松高世代良种培育关键技术研究	3	2060302	
	行业专项	黎蒴等华南重要乡土树种良种选育研究	39	2060302	
	行业专项	新型高效绿僵菌生物杀虫剂研发	32	2060302	
	行业专项	速生型等杉木特征性状遗传解析研究	25	2060302	
	林业生态站等监测运行	森林病虫害生物防治重点实验室运行补助	10	2130206	
	林业生态站等监测运行	国家林业局林产品质量检验检测中心（广州）运行补助	10	2130206	
	林业生态站等监测运行	广东东江源森林生态系统定位观测研究站	6	2130206	
	林业生态站等监测运行	广东汕头沿海防护林森林生态系统定位观测研究站	6	2130206	
	林业生态站等监测运行	广东南岭森林生态系统定位观测研究站	6	2130206	
	林业生态站等监测运行	广东海丰湿地生态系统定位观测研究站	6	2130206	
	林业科学技术普及	森林文化普及与示范	5	2130206	
	国际先进林业科学技术引进	迎春金合欢等优良观赏金合欢种质资源引进	45	2060302	
省野生动物救护中心	小计		20		
	珍稀濒危物种野外救护与人工繁育	穿山甲收容救护及人工繁育	10	2130211	
	野生动物疫病监测和预警系统维护	重点示范站野生动物疫源疫病监测补助	10	2130211	
华南农业大学	小计		424		
	珍稀濒危物种野外救护与人工繁育	珍稀濒危植物紫荆木救护、扩繁及野外回归	8	2130211	
	行业专项	石碌含笑等珍贵木兰科树种种质资源与繁育技术研究	36	2060302	
	行业专项	油茶精深加工关键技术研究及产业化	380	2060302	
华南濒危动物研究所（广东省昆虫研究所）	小计		115		
	第二次全国重点保护野生动植物资源调查	陆生野生动物资源同步调查及野外检查	45	2130211	
	第二次全国重点保护野生动植物资源调查	南岭（No.215）陆生野生动物资源调查	25	2130211	
	第二次全国重点保护野生动植物资源调查	粤西、桂东南山地谷底-广东（No.240）陆生野生动物资源调查	20	2130211	
	野生动物疫病监测和预警系统维护	华南地区翼手目动物疫病监测与本地调查	15	2130211	
	珍稀濒危物种野外救护与人工繁育	平胸龟野外救护及生境维护	10	2130211	
中国科学院华南植物园	小计		75		
	第二次全国重点保护野生动植物资源调查	广东省第二次全国重点保护野生动植物资源调查（蕨类植物）	60	2130211	
	珍稀濒危物种野外救护与人工繁育	珍稀濒危植物坡垒、五唇兰的救护与种群扩繁	15	2130211	
省林业调查规划院	森林资源清查与动态监测	森林资源清查	250	2130208	
省森林资源管理总站	全国林地保护利用年度变更调查及林业双增指标年度考核	林地变更调查技术培训、调查、核查、统计汇总与成果编制	276	2130208	
省林业有害生物防治检疫管理办公室	林业标准化	薇甘菊检疫技术规程	8	2130218	
国家林业局林产品质量检验检测中心（广州）	林产品质量安全监测	防腐木材等林产品质量安全监测	15	2130218	
广东南岭国家级自然保护区管理局	珍稀濒危物种野外救护与人工繁育	蟒山烙铁头、短尾猴种群监测及野外巡护	8	2130211	
广东内伶仃福田国家级自然保护区管理局	野生动物疫病监测和预警系统维护	重点示范站野生动物疫源疫病监测补助	1	2130211	
广东湛江红树林国家级自然保护区管理局	野生动物疫病监测和预警系统维护	重点示范站野生动物疫源疫病监测补助	1	2130211	
广东海丰公平大湖省级自然保护区管理处	野生动物疫病监测和预警系统维护	重点示范站野生动物疫源疫病监测补助	1	2130211	
深圳市兰科植物保护研究中心（全国兰科植物种质资源保护中心）	珍稀濒危物种野外救护与人工繁育	珍稀濒危物种杏黄兜兰、斑叶构兰、五唇兰野外救护和繁育	20	2130211	
深圳市仙湖植物园管理处（全国苏铁种质资源保护中心）	珍稀濒危物种野外救护与人工繁育	中国苏铁属植物DNA条形码数据库的基础构建	25	2130211	
徐闻县神州木兰园培植中心（木兰植物保育基地）	珍稀濒危物种野外救护与人工繁育	珍稀濒危植物华盖木的繁育	8	2130211	

9.主持：关于广东省林业局转下达2022年中央预算内投资计划（林业小专项）“极小种群野生植物紫荆木拯救项目（JXZQ2022004）”的立项通知及有关佐证材料

广东省林业局

粤林函〔2022〕250号

广东省林业局关于转下达2022年草原防火等专项中央预算内投资计划的通知

有关地级以上市林业主管部门，局直属有关单位，省级有关单位

中央驻粤有关单位：

根据国家林业和草原局有关文件精神，现将国家安排我省的2022年草原防火等专项中央预算内投资计划转下达给你们，并有关事项通知如下：

一、维护计划的严肃性，严格投资方向

要认真贯彻落实中央和省关于党政机关停止新建楼堂馆所的有关规定，禁止搭车建设楼堂馆所和办公用房。要认真按照转下达的计划执行，未经国家林草局批准，不得擅自调整投资计划，变更项目建设内容，扩大或缩小建设规模。对计划执行中因建设条件发生变化确需调整计划的，应按有关规定履行审批程序，经批准后方可实施。

二、加快项目进度，尽快完成项目建设

各地各单位要迅速组织实施，加快实施进度，及时申请拨付项目建设资金，尽快形成实物工作量，及早发挥效益。营造林项目要抓紧编制作业设计，并严格按照批复的作业设计实施。市县营造林项目作业设计报所在地级以上市林业主管部门审批，项目完成后由所在地级以上市林业主管部门组织验收，并将验收批复文件抄送省林业局备案；省局直属单位营造林项目作业设计报省林业局审批，项目完成后由省林业局组织验收。造林项目全部实行“落地上图”精细化管理。

三、切实加强项目管理，确保项目建设质量

严格执行工程项目法人责任制、合同制、招投标制和监理制，按照政府采购有关规定购置仪器设备，严把项目建设质量关。严格执行国家有关资金管理法律、法规和规章制度，切实加强资金筹集、拨付、使用、管理的全程监管，任何单位和个人不准挪用、截留、串用建设资金。按照基本建设财务管理规定做好资金的核算工作，做到建设资金单独核算，专款专用，确保资金安全有效。

四、落实绩效目标，及时掌握项目进展情况

各单位指定专人负责，定期、全面、准确报告工程实施的进度、成效和存在问题，切实加强中央预算内投资绩效管理，保质保量如期完成建设任务，提高中央预算内投资效益。根据国家有关部门的要求，各单位应在每月3日前向省林业局业务主管处室报送上月投资计划执行情况表，由省林业局汇总报送国家重大建设项目库。

请各地级以上市接此通知后，于20个工作日内转下达投资计划，并将下达的明细计划及时抄报我局备案。

附件：1. 2022年草原防火等专项中央预算内投资计划表
2. 2022年草原防火等专项中央预算内投资计划执行情况表
3. 2022年草原防火等专项中央预算内投资计划绩效目标表

广东省林业局
2022年8月16日

附件

2022年中央预算内投资计划申报表（极小种群野生动植物资源拯救项目）

单位:万元

序号	项目名称	可研报告批复文号	初步设计批复文号	建设性质	建设地点（细化到县）	拟开工年份	拟建成年份	2022年投资建议计划				项目（法人）单位	项目责任人	项目责任人手机号	日常监管直接责任单位	日常监管直接责任单位监管责任人	日常监管直接责任单位监管责任人手机号	备注
								合计（万元）	中央投资（万元）	地方配套（万元）	主要建设内容							
四	林业小专项							520	520	0	极小种群野生动植物资源拯救							
3	极小种群野生动植物资源拯救项目	小计						520.00	520.00	0.00								
(1)	极小种群野生动植物资源拯救项目			新建	广东省林业科学研究院 广东省野生动物监测救护中心	2022	2022	160	160	0	开展穿山甲野外种群资源监测，研发适宜的野外种群调查与监测技术，评估穿山甲洞穴对生境的改造能力，建设穿山甲特色自然教育路径、科普宣传栏、宣传彩绘及宣传标本等，完善穿山甲野化基地自然教育设施，增强野生动物保护意识。	广东省林业科学研究院 广东省野生动物监测救护中心	窦红亮 侯方晖	15776762886 13533671161	广东省林业局	陈容斌	13660092129	
(2)				新建	广东省林业科学研究院 广东省野生动物监测救护中心 广东茂名林洲顶鳄蜥省级自然保护区管理处	2022	2022	120	120	0	建设标准繁育池、繁育场设备、场地监控设备等，构建鳄蜥面部和躯部数据库，制定人工繁育标准体系，建设鳄蜥科普宣传栏、鳄蜥模型、宣传彩绘及宣传标本等，完善鳄蜥自然教育基础设施，加强进行鳄蜥的科普宣传。	广东省林业科学研究院 广东省野生动物监测救护中心 广东茂名林洲顶鳄蜥省级自然保护区管理处	高海洋 吕春贺 陈华勇	18810008389 15602259555 13709646101	广东省林业局	陈容斌	13660092129	
(3)				新建	广东省林业科学研究院	2022	2022	60	60	0	全面调查广东含笑野生种群现状及其生境，开展抢救性保护，建设小区界桩、标识牌和视频监控系统等设施，完成迁地保护基地选址，研发实生繁育、组织培养技术，熟化综技繁育技术。	广东省林业科学研究院	徐放	13488684171	广东省林业局	陈容斌	13660092129	
(4)				新建	华南农业大学	2022	2022	60	60	0	开展紫荆木就地保护，设隔离围栏，不锈钢宣传栏。开展紫荆木迁地保护，建设在圆地1个，野外回归紫荆木，编制紫荆木保护宣传手册，开展紫荆木科普教育。	华南农业大学	张璐	13560089803	广东省林业局	陈容斌	13660092129	
(5)				新建	中国林业科学研究院热带林业研究所	2022	2022	60	60	0	开展猪血木野外监测运护，建设标桩(10)、防护栏、围栏、隔离带、宣传栏和宣传牌、苗圃基地等，购置相关野外监测、定位观测、保护仪器设备，建立猪血木护照信息档案等。	中国林业科学研究院热带林业研究所	杨锦昌	13570442890	广东省林业局	陈容斌	13660092129	
(6)				新建	中国科学院华南植物园	2022	2022	60	60	0	开展仙湖苏铁就地和迁地保护，树立保护宣传标牌，开展台山市全面调查，建立台山仙湖苏铁数据库，开展繁殖生物学研究。 建立一个仙湖苏铁苗木繁育基地。 开展仙湖苏铁野外回归示范工作。	中国科学院华南植物园	王瑞江	13556026737	广东省林业局	陈容斌	13660092129	

第 1 页，共 1 页

10.主持：关于 2023 年度广东省自然资源事务-生态林业建设专项资金“极小种群野生植物紫荆木人工培育与野生种群重建”项目的立项通知及有关佐证材料

广东省林业局文件

粤林财〔2022〕8 号

广东省林业局关于下达 2023 年度省级财政事业发展性支出项目计划的通知

局机关有关处（室），局直属有关单位，有关项目单位：

根据《广东省林业局林业项目全过程绩效管理办法（试行）》《广东省林业局关于进一步规范项目绩效管理的通知》要求，为进一步夯实项目前期准备，提高项目成熟度，确保做到预算一经批复即可执行，现将 2023 年度省级财政事业发展性支出项目计划下达给你们，并将有关事项通知如下：

一、严格论证评估重大项目

立项总额超过 500 万元的项目，项目单位须按照《广东省财政厅关于印发〈广东省省级财政绩效评估指南〉的通知》（粤财绩

4. 各二级项目绩效目标

5. 项目实施工作计划统计表及资金支出计划统计表格式

6. 广东省林业局关于进一步规范项目绩效管理的通知

广东省林业局

2022 年 10 月 24 日

（联系人：梁海燕；电话：020-81825078）

公开方式：不公开

校核：梁海燕

广东省林业局办公室　　2022 年 10 月 24 日印

附件1：

2023年度自然资源事务专项资金—生态林业建设及自然保护地体系建设（第一批）项目计划

50000

单位：万元

序号	项目单位	项目名称	立项总额	实施周期	2023年计划安排额度	政策任务	归口处室	备注
	一、生态林业建设 合计							
	156003-华南农业大学 汇总		2060.00		1540.00			
2	156003-华南农业大学	自然保护地建设与乡村振兴的融合机制及实施模式	110.00	2年实施	90.00	林业生态保护建设	保护地处	该项目共110万元，其中2023年安排90万元，2024年计划安排20万
3	156003-华南农业大学	雷州市雷高镇小微湿地保护修复试点	80.00	1年实施	80.00	林业生态保护建设	湿地处	
4	156003-华南农业大学	半野化状态下林麝养殖	50.00	1年实施	50.00	林业生态保护建设	动植物处	
5	156003-华南农业大学	广东省中华穿山甲栖息地不同类型生境白蚁分布调查	50.00	1年实施	50.00	林业生态保护建设	动植物处	
6	156003-华南农业大学	极小种群野生植物紫荆木人工培育与野生种群重建	30.00	1年实施	30.00	林业生态保护建设	动植物处	
7	156003-华南农业大学	南昆山毛叶茶种质资源的收集保存	30.00	1年实施	30.00	林业生态保护建设	动植物处	
8	156003-华南农业大学	松材线虫病疫点精准除治技术指导示范	100.00	1年实施	100.00	森林资源管护	防治检疫处	
9	156003-华南农业大学	全省林木种质资源调查（5个市）	750.00	3年实施	250.00	森林资源培育	林场种苗处	该项目共750万元，其中2022年已安排250万元，2023-2024年每年计划安排250万元。
10	156003-华南农业大学	基于高碳汇目标的造林树种筛选和林分结构研究	300.00	1年实施	300.00	森林资源培育	科技处	科研项目
11	156003-华南农业大学	紫薇属树种种质创新与产业化利用研究	150.00	1年实施	150.00	森林资源培育	科技处	科研项目
12	156003-华南农业大学	油茶新品种选育及高效开发利用关键技术研究	150.00	1年实施	150.00	森林资源培育	科技处	科研项目
13	156003-华南农业大学	广东丘陵山地“林-草-羊”生态循环种养模式构建与示范	150.00	1年实施	150.00	森林资源培育	科技处	科研项目
14	156003-华南农业大学	黄梁木抗病抗旱四倍体品种创制	50.00	1年实施	50.00	森林资源培育	科技处	科研项目
15	156003-华南农业大学	石碌含笑和乐东拟单性木兰抗逆性育种与繁育	20.00	1年实施	20.00	森林资源培育	林场种苗处	
16	156003-华南农业大学	油茶良种选育与繁育	20.00	1年实施	20.00	森林资源培育	林场种苗处	
17	156003-华南农业大学	火力楠和木荷良种选育繁育	20.00	1年实施	20.00	森林资源培育	林场种苗处	

11.主持：关于2022年度广东省自然资源事务-生态林业建设专项资金“基于比较基因组学的紫荆木救护与繁育回归”项目的立项通知及有关佐证材料

广东省林业局文件

粤林财〔2021〕6号

广东省林业局关于下达2022年度自然资源事务专项资金-生态林业建设（省级组织实施）项目计划的通知

局机关有关处（室），局直属有关单位，其他有关项目单位：

根据《广东省省级财政资金项目库管理办法（试行）》和《广东省林业局林业项目全过程绩效管理办法（试行）》，为加强项目实施前期准备工作，提高项目成熟度，加快项目资金支出进度，现将2022年度自然资源事务专项资金-生态林业建设（省级组织实施）项目计划下达给你们，并将有关事项通知如下：

一、制定资金使用计划。包括项目资金分年度使用计划和项目资金2022年度的分月资金使用计划，资金不能在2022年度完成支付的，必须填报分年度使用计划。请各项目单位于12月10日前将《项目资金使用计划表》（附件2）加盖公章后报送项目归

（一）该项目计划是2022年度自然资源事务专项资金-生态林业建设（省级组织实施）项目立项依据。

（二）涉及造林、抚育及大径材培育等年度任务的，项目年度资金须保障完成。

（三）项目年度资金必须是当年度可以支出的资金，项目资金当年度的分月资金使用计划从2022年3月份开始填报（预计省财政厅将于3月初下达资金），每月填累计额度，支出进度原则上从6月份起不得低于序时进度，并确保全年能使用完毕。

（四）项目实施计划从2022年1月份开始填报（含前期准备工作）。

（五）除特殊情况外，项目分年度资金计划期限不得超过3年。

（六）科研项目可以一次性申请。

附件：1. 2022年度自然资源事务专项资金-生态林业建设（省级组织实施）项目计划
2. 项目资金使用计划表
3. 项目绩效目标申报表
4. 项目实施计划表

广东省林业局
2021年12月3日

2022年度自然资源事务专项资金-生态林业建设（省级组织实施）项目计划

单位：万元

序号	项目单位	项目名称	业务处室	立项总金额	备注
总计				49,401.62	
	156003-华南农业大学汇总			1,805.00	
1	156003-华南农业大学	广东省自然保护区人为干扰对生态退化的影响与修复	保护地处	80.00	
2	**156003-华南农业大学**	**基于比较基因组学的紫荆木救护与繁育回归**	**动植物处**	**30.00**	
3	156003-华南农业大学	粤北珍稀和重要南药种质资源调查与遗传材料保存	动植物处	30.00	
4	156003-华南农业大学	碳中和背景下广东省典型优势树种组大径材培育关键技术体系构建与示范	科技处	300.00	科研项目，2021年已下达
5	156003-华南农业大学	广东省典型红树林与林区渔业生态模式研究及示范	科技处	150.00	科研项目
6	156003-华南农业大学	荔枝树修枝剩余物高效利用关键技术研究与示范	科技处	150.00	科研项目
7	156003-华南农业大学	木麻黄青枯病防控资源挖掘与应用研究（2022年）	科技处	75.00	科研项目
8	156003-华南农业大学	粤西地区优质高产林分碳封存潜力提升的施肥技术体系构建	科技处	50.00	科研项目
9	156003-华南农业大学	基于功能性状筛选南亚热带耐贫瘠和抗干旱性乔灌木树种	科技处	30.00	科研项目
10	156003-华南农业大学	林木种质资源调查	林场种苗处	750.00	
11	156003-华南农业大学	石碌含笑和诗琳通木兰抗逆性育种与繁育	林场种苗处	20.00	
12	156003-华南农业大学	火炬松和木荷良种选育繁育	林场种苗处	20.00	
13	156003-华南农业大学	油茶良种选育与繁育	林场种苗处	20.00	

1/2

12.主持：关于 2021 年度广东省自然资源事务-生态林业建设专项资金“珍稀濒危植物紫荆木保护基因组学研究及应用”项目的立项通知及有关佐证材料

广东省林业局办公室

粤林办函〔2020〕86 号

广东省林业局办公室关于进一步做好省级财政资金项目库管理工作的通知

局属有关预算单位，中央驻粤及省有关单位：

根据《广东省财政厅关于做好 2021 年省级财政资金项目入库储备工作的函》（粤财预〔2020〕38 号）及省财政厅有关规定，为进一步做好省级财政资金项目库管理工作，现将有关事项通知如下：

一、认真填报《省级财政资金项目绩效目标申报表》，其中项目资金总额度必须与局党组会审定的项目资金额度一致；分年度资金额度据实填报，分年度额度为各年度可以实际支出的额度，该额度将作为项目资金分年度安排的依据；项目绩效总指标值及分年度指标值将作为项目绩效评价的依据。该项工作请于 11 月 11 日分别报业务归口处室汇总审核，业务处室审核后请于 11 月 13 日前报规财处汇总，其中省属国有林场、省级以上自然保护区整合后的项目，分别报林场种苗处、保护地处汇总审核。

二、认真制定项目实施方案（作业设计）报省局审批或备案，其中由局机关本部承担的项目，由相关业务处室呈分管局领导审定；局属预算单位、中央驻粤及省有关单位承担的项目，由相关业务归口处室审批或备案；国有林场、自然保护区整合后的项目，各个子项目分别由相关业务归口处室审批或备案。该项工作须于 2021 年 1 月底之前完成。如需要招投标的请于 2021 年 2 月底完成招投标前期准备工作。

附件：1. 省级财政资金项目绩效目标申报表

2. 2021 年海洋事业费及海洋环境损失赔偿款项目入库建议表

3. 2021 年生态公益林效益补偿省统筹经费项目入库建议表

4. 2021 年生态林业建设省本级项目入库建议表（按单位）

广东省林业局办公室

2020 年 11 月 4 日

公开方式：不公开

— 2 —

2021年生态林业建设省本级项目入库建议表

单位：万元

序号	申报单位	项目名称	审核后的项目建设内容	审核后的资金额度	备注1	备注2	整合前项目个数	整合后项目个数
八十一	华南农业大学	小计		485			9	9
1	华南农业大学	粤北古驿道沿线生态修复与景观提升技术研究与示范	1.将石灰岩地区划分为6种类型，根据不同类型制定植被恢复和重建方案。 2.分析古道沿线景观效果，分类型制定景观提升计划. 3.选取代表性类型，实施植被恢复和景观提升方案，总结植被恢复和景观提升效果，为我省古驿道植被恢复和景观提升提供技术参考和示范。	100	其他			
2	华南农业大学	广东省自然保护地主要自然资源调查监测技术体系研究	针对广东省自然保护地现状，依托自然保护地优化方案和现有工作基础，广泛收集国内外自然保护地自然资源调查监测技术资料，通过现场调研、专家咨询等技术，综合各类自然保护地自然资源调查监测技术，如生态因子调查监测，野生动植物资源调查检测技术，根据自然资源的特点、调查的目的等提出广东省可操作的、具有示范性和推广性的调查监测规程、规范和标准以及相关技术指南。	50	自然保护地建设			
3	华南农业大学	珍稀濒危植物紫荆木保护基因组学研究及应用	珍稀濒危植物紫荆木保护基因组学研究及应用	30	野生动植物资源调查和监测			
4	华南农业大学	林下药用植物栽培的光环境选择及高效栽培技术研究	1、以林下仿生条件研究林下植物的生长特性、光合生理特性、药用成分等特征，研发配套的高效栽培技术并加以推广。 2、构建基于林地独特光环境与气候条件的林地筛选技术。 3、长期监测林下药用植物样地的土壤理化性质、土壤肥力及土壤微生物。 4、建立特色、优质林下种植的推广应用示范基地。 5、结合光养强化育苗技术，培育适生性强、推广性强的壮苗。	50	林业科技创新			
5	华南农业大学	广东省典型红树林与林区渔业生态模式研究及示范	待申报单位根据审核后的资金额度重新调整项目建设内容	50	林业科技创新			

1

13. 主持：关于2020年度广东省自然资源事务-生态林业建设专项资金“珍稀濒危植物紫荆木种子繁育关键技术研究及应用”项目的立项通知及有关佐证材料

广东省野生动植物保护管理项目

合 同 书

项目编号：_____

项目名称：珍稀濒危植物紫荆木种子繁育关键技术研究及应用

承担单位：华南农业大学（公章）

项目负责人：张璐　　联系电话：13560089803

项目联系人：张璐　　联系电话：13560089803

项目起止年限：2020年1月至2020年12月

广东省林业局

2020年6月

七、项目承担单位、参加单位及项目负责人、主要参加人员

项目承担单位（签章）：华南农业大学

项目负责人

姓　名	性别	年龄	职务/职称	从事专业	任务分工	所在单位	签名
张璐	女	46	副教授	生态学	主持	华南农业大学林学与风景园林学院	张璐

主要参加人员

苏志尧	男	56	教授	植物学	技术指导	华南农业大学林学与风景园林学院	
李镇魁	男	50	副教授	植物分类	物种救护	华南农业大学林学与风景园林学院	
刘效东	男	31	讲师	生态学	数据分析	华南农业大学林学与风景园林学院	
阚蕾	女	24	未取得	林业	种子萌发	华南农业大学林学与风景园林学院	阚蕾
廖绮聪	女	23	未取得	林业	幼苗培育	华南农业大学林学与风景园林学院	廖绮聪
汪书钰	女	22	未取得	林业	幼苗回归	华南农业大学林学与风景园林学院	汪书钰

九、合同签约各方
（一）项目管理部门（甲方）：广东省林业局野生动植物保护处(公章)
单位负责人（签章）： 联系人及电话：陈容斌　13660092129 2020 年　月　日
（二）项目承担单位（乙方）：华南农业大学(公章)
单位负责人（签章）： 联系人及电话：张璐　13560089803 年　月　日

2020年省级财政专项资金
项目结题报告

项目名称： 珍稀濒危植物紫荆木种子繁育关键技术研究及应用

项目编号： YSDZW202001

承担单位（盖章）： 华南农业大学

实施期限： 2020年1月-2020年12月

项目负责人： 张璐

联系电话： 13560089803

归口管理部门： 广东省林业局

2024年1月30日

14. 主持：关于2019年度省级级财政专项资金（乡村振兴战略省级财政专项资金-野生动植物保护）“珍稀濒危植物紫荆木野外救护和扩繁”项目的立项通知及有关佐证材料

广东省财政厅文件

粤财农〔2019〕70号

关于安排2019年省级涉农资金（生态林业建设类-省级组织实施项目）的通知

有关地级以上市财政局，有关省直管县（市）财政局，省直有关单位，中国科学院广州分院，国家林业局桉树研究开发中心、中国林业科学研究院热带林业研究所：

根据省林业局《关于报送2019年自然资源事务省级财政专项资金（生态林业建设）分配方案及任务清单的函》（粤林函〔2018〕774号）及《关于报送生态林业建设2019年省级涉农资金（省级组织实施项目）区域绩效目标的函》（粤林函〔2019〕74号），经研究，现将2019年省级涉农资金（生态林业建设类-省级组织实施项目）及绩效目标下达给你们（具体项目、金额、支出科目详见附件1），并将有关事项通知如下：

一、此项资金请按照《广东省人民政府关于印发广东省省级财政专项资金管理办法（试行）的通知》（粤府〔2018〕120号）及《广东省人民政府关于印发广东省涉农资金统筹整合实施方案（试行）的通知》（粤府〔2018〕123号）的有关规定使用。各市、县（市），各有关单位应抓紧将资金安排到具体项目，切实加快预算执行，并加强资金监管，不得挤占、截留或挪用，确保专款专用。市县部门经济分类科目按实际用途列编。年终请按要求统一编列决算。

二、请各地、各单位加强财政资金绩效管理，对本次下达的预算指标和任务，科学合理确定绩效目标，加强绩效目标监控和绩效评价，确保年度绩效目标如期实现。

附件：1. 2019年省级涉农资金（生态林业建设类-省级组织实施项目）安排表

2. 2019年省级涉农资金（生态林业建设类-省级组织实施项目）绩效目标表

广东省财政厅

2019年3月27日

附件1

附件1：2019年省级涉农资金（生态林业建设类-省级组织实施项目）安排表

单位：元

单位名称	单位编码	项目名称	功能分类科目	部门经济分类科目	政府经济科目	金额	备注
合计						221,280,000.00	
各省直部门合计						212,280,000.00	
广东省教育厅小计	156					6,000,000.00	
华南农业大学	156003	广东省野生兰科植物资源调查（深圳、惠州、珠海、东莞、中山、阳江、江门等地区）	2130207 森林资源管理			300,000.00	
				30299 其他商品和服务支出	50502 商品和服务支出	300,000.00	
华南农业大学	156003	珍稀濒危植物猪屎豆野外救护和扩繁关键技术研究	2130207 森林资源管理			300,000.00	
				30299 其他商品和服务支出	50502 商品和服务支出	300,000.00	
华南农业大学	156003	广东省东部野生兰科植物资源调查	2130207 森林资源管理			300,000.00	
				30299 其他商品和服务支出	50502 商品和服务支出	300,000.00	
华南农业大学	156003	林下经济立体循环高效栽培模式研究与示范	2130206 技术推广与转化			250,000.00	
				30299 其他商品和服务支出	50502 商品和服务支出	250,000.00	
华南农业大学	156003	肉桂优良品系栽培和精油生产的关键技术集成及产品开发研究	2130206 技术推广与转化			450,000.00	
				30299 其他商品和服务支出	50502 商品和服务支出	450,000.00	
华南农业大学	156003	林木饲料资源产业化利用关键技术研究	2130206 技术推广与转化			400,000.00	
				30299 其他商品和服务支出	50502 商品和服务支出	400,000.00	
华南农业大学	156003	广东适生油茶品种区域化试验与评价	2130206 技术推广与转化			450,000.00	
				30299 其他商品和服务支出	50502 商品和服务支出	450,000.00	
华南农业大学	156003	木麻黄青枯垫群体感应和群体淬灭研究与应用	2130206 技术推广与转化			400,000.00	
				30299 其他商品和服务支出	50502 商品和服务支出	400,000.00	
华南农业大学	156003	森林康养构建关键技术及其功能产品开发与示范	2130206 技术推广与转化			500,000.00	
				30299 其他商品和服务支出	50502 商品和服务支出	500,000.00	
华南农业大学	156003	黄梁木优良种源/家系定向培育及产业化开发利用	2130206 技术推广与转化			250,000.00	
				30299 其他商品和服务支出	50502 商品和服务支出	250,000.00	
华南农业大学	156003	珠三角城市森林近自然群落构建关键技术研究与示范	2130206 技术推广与转化			250,000.00	
				30299 其他商品和服务支出	50502 商品和服务支出	250,000.00	
华南农业大学	156003	松墨天牛新型引诱剂及野外应用技术研究	2130206 技术推广与转化			300,000.00	

2019 年省级财政专项资金

项目结题报告

项目名称： 珍稀濒危植物紫荆木野外救护和扩繁关键技术研究

项目编号： _____

承担单位（盖章）： 华南农业大学

实施期限： 2019 年 1 月-2019 年 12 月

项目负责人： 张璐

联系电话： 13560089803

归口管理部门： 广东省林业局

2024 年 1 月 26 日

15. 主持：关于2019年度和2017年度广东省林业科技创新项目“珠三角城市森林近自然群落构建关键技术研究与示范”项目的立项通知及有关佐证材料

广东省林业科技创新项目

合 同 书

项目编号：2017KJCX037

项目名称：珠三角城市森林近自然群落构建关键技术研究与示范

承担单位：华南农业大学（公章）

项目负责人：张璐 联系电话：020-85280263

项目联系人：张璐 联系电话：13560089803

项目起止年限：2017年4月至2020年12月

广东省林业厅

2017年4月

广东省林业科技创新项目

合 同 书

项目编号：2019KJCX007

项目名称：珠三角城市森林近自然群落构建关键技术研究与示范

承担单位：华南农业大学（公章）

项目负责人：张璐　　联系电话：020-85280263

项目联系人：张璐　　联系电话：020-85280263

项目起止年限：2019 年 5 月至 2020 年 12 月

广东省林业局

2019 年 4 月

广东省林业科技计划项目
验 收 证 书

编号：粤林科验字（2022 年）017号

项目编号：2017KJCX037、2019KJCX007

项目名称：珠三角城市森林近自然群落构建关键技术研究与示范

承担单位：华南农业大学 （盖章）

项目类别：广东省林业科技创新项目

起止时间：2017 年 4 月至 2020 年 12 月

验收时间：2022 年 5 月 12 日

广东省林业局

表 9

广东省林业科技计划项目验收审批意见

组织验收单位意见：

同意通过验收

主管领导签字：

2022 年 5 月 30 日

16. 主持：关于2018年度广东省野生动植物保护管理项目“阳春百涌省级自然保护区野生植物资源调查”项目的立项通知及有关佐证材料

广东省野生动植物保护管理项目

合 同 书

项目编号：2130211-30299-1

项目名称：阳春百涌省级自然保护区野生植物资源调查

项目承担单位：华南农业大学（公章）

项目负责人：张璐　联系电话：13560089803

项目联系人：张璐　联系电话：13560089803

项目起止年限：2018 年 7 月至 2019 年 12 月

广东省林业厅

2018 年 6 月

17. 主参：2024 年度广东省林业局资助项目“连南大叶茶林麝等四种珍稀濒危动植物种质资源发掘与保护”（排名第 3）

广东省林业科技创新项目

合 同 书

项目编号：_____

项目名称：连南大叶茶林麝等四种珍稀濒危动植物种质资源发掘与保护

承担单位：仲恺农业工学院（公章）

项目负责人：肖 遂 联系电话：13802408977

项目联系人：肖 遂 联系电话：13802408977

项目起止年限：2024.01-2024.12

广东省林业局制

18. 主参：关于广东省省级科技计划农业领域“乡土地被植物耐荫等级测定及应用研究（2013B020305008）”项目（排名第 2）

全选	序号	项目名称	评审等级	项目来源	合同经费/实到经费	立项时间	开始时间	结题时间	负责人	本人排名	课题组总人数	是否结题
☐	16	乡土地被植物耐荫等级测定及应用研究	B	广东省科技厅	8.0	2014-08-13	2014-01-01	2016-12-31	苏志尧	2	8	是

受理编号：1311150100040

项目编号：2013B020305008

文件编号：粤科规财字[2014]116号

2013B020305008

广东省省级科技计划项目

合同书

项目名称：乡土地被植物耐荫等级测定及应用研究

计划类别：农业领域科技计划项目审批

项目起止时间：2014-01-01 至 2016-12-31

管理单位（甲方）：广东省科学技术厅

承担单位（乙方）：华南农业大学

乙方主管部门（丙方）：华南农业大学

通讯地址：广东省广州市天河区广州市天河区五山路483号

邮政编码：510642 单位电话：020-38632819

项目负责人：苏志尧 联系电话：020-38294891

项目联系人：苏志尧 联系电话：13560395892

广东省科学技术厅
二〇一四年制

六、人员信息

项目负责人情况

姓名	年龄	性别	职称	职务	学历	在项目中承担的任务	所在单位	签名
苏志尧	51	男	教授	副院长	博士	主持	华南农业大学	

主要研究开发人员

姓名	年龄	性别	职称	职务	学历	在项目中承担的任务	所在单位	签名
张璐	41	女	副教授	教师	博士	指示种分析	华南农业大学	
李镇魁	46	男	副教授	教师	博士	物种鉴定	华南农业大学	
柯娴氧	28	女	博士生	学生	本科	叶光合特性研 究	华南农业大学	
胡碗秋	24	女	硕士生	学生	本科	叶形态生理指标测定	华南农业大学	
徐明锋	26	男	硕士生	学生	本科	林分因子调查	华南农业大学	
李佩瑗	26	女	硕士生	学生	本科	数据初步处理	华南农业大学	
李文斌	24	男	硕士生	学生	本科	半球面影像拍摄及分析	华南农业大学	

三、论文、著作等

1.检索证明

1.1.一作检索证明

SCAULIB202404740

检索证明

根据委托人提供的论文材料，委托人**华南农业大学林学与风景园林学院 张璐** 16 篇论文收录情况如下表。

序号	论文名称	发表刊物及发表的年月卷期/页码等	作者排名	论文等级	作者文中单位	收录情况	影响因子	中科院大类分区
1	亚热带常绿阔叶林枯立木与冠层结构的关系	森林与环境学报 出版年：2018 卷期：38 1 页码：64-70 文献号： 文献类型：J	第一作者	C 类	华南农业大学林学与风景园林学院	北大核心	无	无
2	TOPOGRAPHIC CONTROLS ON THE DISTRIBUTION OF INDIGENOUS RHODODENDRONS IN THE SOUTHERN SLOPE OF THE NANLING MOUNTAINS, SOUTH CHINA	PAKISTAN JOURNAL OF BOTANY 出版年：2016 卷期：48 6 页码：2367-2374 文献号： 文献类型：Article	第一作者	B 类	College of Forestry and Landscape Architecture, South China Agricultural University	SCI	IF2-year=0.69 IF5-year=0.817 （2016）	生物 4 区 Top 期刊：否 （2016）
3	南岭山地杜鹃花沿海拔梯度的分布及其园林应用前景	华南农业大学学报 出版年：2014 卷期：35 2 页码：73-77	第一作者	B 类	华南农业大学林学院	北大核心	无	无

		文献号： 文献类型：J						
4	南岭自然保护区常绿阔叶林枯立木数量特征分析	福建林学院学报 出版年：2011 卷期：32 1 页码：64-69 文献号： 文献类型：J	第一作者	C 类	华南农业大学林学院	北大核心	无	无
5	广东石坑崆森林群落优势种群生态位宽度沿海拔梯度的变化	林业科学研究 出版年：2007 卷期：20 5 页码：598-603 文献号：1001- 1498(2007) 05-0598- 06 文献类型：J	第一作者	B 类	华南农业大学林学院	北大核心	无	无
6	Topographical Influence on Snag Distribution in a Subtropical Forest in South China	FORESTS 出版年：2023 卷期：14 5 页码：- 文献号：997 文献类型：Article	通讯作者	A 类	College of Forestry and Landscape Architecture, South China Agricultural University	SCI	IF2-year=2.9 IF5-year=3.0 （2022）	农林科学 2 区 Top 期刊：否 （2023）

三、论文、著作等

1.检索证明

1.2.通讯作者检索证明

SCAULIB202412710

检索证明

根据委托人提供的论文材料，委托人**华南农业大学林学与风景园林学院 张璐** 1篇论文收录情况如下表。

序号	论文名称	发表刊物及发表的年月卷期/页码等	作者排名	论文等级	作者文中单位	收录情况	影响因子	中科院大类分区
1	High-quality chromosome-level genomic insights into molecular adaptation to low-temperature stress in Madhuca longifolia in southern subtropical China	BMC GENOMICS 出版年：2024 出版日期：SEP 18 卷期：25 1 页码：- 文献号：877 文献类型：Article	通讯作者	A 类	华南农业大学林学与风景园林学院	SCI	IF2-year=3.5 IF5-year=4.1 （2023）	生物学 2 区 Top 期刊：是 （2023）

说明：论文等级和中科院大类分区按《华南农业大学学术论文评价方案（试行）》划分。

报告免责声明:如未盖章,报告无效

检索员：尹银怀

华南农业大学图书馆

2024-09-29

SCAULIB202404740

检索证明

根据委托人提供的论文材料，委托人**华南农业大学林学与风景园林学院 张璐** 16 篇论文收录情况如下表。

序号	论文名称	发表刊物及发表的年月卷期/页码等	作者排名	论文等级	作者文中单位	收录情况	影响因子	中科院大类分区
1	亚热带常绿阔叶林枯立木与冠层结构的关系	森林与环境学报 出版年：2018 卷期：38 1 页码：64-70 文献号： 文献类型：J	第一作者	C 类	华南农业大学林学与风景园林学院	北大核心	无	无
2	TOPOGRAPHIC CONTROLS ON THE DISTRIBUTION OF INDIGENOUS RHODODENDRONS IN THE SOUTHERN SLOPE OF THE NANLING MOUNTAINS, SOUTH CHINA	PAKISTAN JOURNAL OF BOTANY 出版年：2016 卷期：48 6 页码：2367-2374 文献号： 文献类型：Article	第一作者	B 类	College of Forestry and Landscape Architecture, South China Agricultural University	SCI	IF2-year=0.69 IF5-year=0.817 （2016）	生物 4 区 Top 期刊：否 （2016）
3	南岭山地杜鹃花沿海拔梯度的分布及其园林应用前景	华南农业大学学报 出版年：2014 卷期：35 2 页码：73-77	第一作者	B 类	华南农业大学林学院	北大核心	无	无

		文献号： 文献类型：J						
4	南岭自然保护区常绿阔叶林枯立木数量特征分析	福建林学院学报 出版年：2011 卷期：32 1 页码：64-69 文献号： 文献类型：J	第一作者	C 类	华南农业大学林学院	北大核心	无	无
5	广东石坑崆森林群落优势种群生态位宽度沿海拔梯度的变化	林业科学研究 出版年：2007 卷期：20 5 页码：598-603 文献号：1001- 1498(2007) 05-0598- 06 文献类型：J	第一作者	B 类	华南农业大学林学院	北大核心	无	无
6	Topographical Influence on Snag Distribution in a Subtropical Forest in South China	FORESTS 出版年：2023 卷期：14 5 页码：- 文献号：997 文献类型：Article	通讯作者	A 类	College of Forestry and Landscape Architecture, South China Agricultural University	SCI	IF2-year=2.9 IF5-year=3.0 （2022）	农林科学 2 区 Top 期刊：否 （2023）

7	Dynamic Transcriptomic and Metabolomic Analyses of Madhuca pasquieri (Dubard) H. J. Lam During the Post-germination Stages	FRONTIERS IN PLANT SCIENCE 出版年：2021 卷期：12 页码：- 文献号：731203 文献类型：Article	通讯作者	A 类	College of Forestry and Landscape Architecture, South China Agricultural University	SCI	IF2-year=6.627 IF5-year=7.255 （2021）	生物学 2 区 Top 期刊：是 （2021）
8	Single-Molecule Real-Time Sequencing of theMadhuca pasquieri(Dubard) Lam. Transcriptome Reveals the Diversity of Full-Length Transcripts	FORESTS 出版年：2020 卷期：11 8 页码：- 文献号：866 文献类型：Article	通讯作者	B 类	College of Forestry and Landscape Architecture, South China Agricultural University	SCI	IF2-year=2.634 IF5-year=2.804 （2020）	农林科学 3 区 Top 期刊：否 （2020）
9	The Composition and Diversity of Soil Bacterial and Fungal Communities Along an Urban-To-Rural Gradient in South China	FORESTS 出版年：2019 卷期：10 9 页码：- 文献号：797 文献类型：Article	通讯作者	B 类	College of Forestry and Landscape Architecture, South China Agricultural University	SCI	IF2-year=2.221 IF5-year=2.484 （2019）	农林科学 3 区 Top 期刊：否 （2019）

10	城市森林土壤微生物群落结构的季节变化	生态学杂志 出版年：2019 卷期：38 11 页码：3306-3312 文献号： 文献类型：J	通讯作者	B 类	华南农业大学林学与风景园林学院	北大核心	无	无
11	亚热带常绿阔叶林锥和木荷枯立木点格局分析	西南林业大学学报 出版年：2019 卷期：39 1 页码：132-138 文献号： 文献类型：J	通讯作者	C 类	华南农业大学林学与风景园林学院	北大核心	无	无
12	不同冠层结构下的植物生长型与生活型特征	中南林业科技大学学报 出版年：2018 卷期：38 7 页码：37-44 文献号： 文献类型：J	通讯作者	C 类	华南农业大学林学与风景园林学院	北大核心	无	无
13	珍稀濒危植物紫荆木生态学研究进展	广西植物 出版年：2018 卷期：38 7 页码：866-875 文献号： 文献类型：J	通讯作者	C 类	华南农业大学林学与风景园林学院	北大核心	无	无

14	南岭山地森林群落冠层结构对林下野生花卉的影响	西南农业学报 出版年：2015 卷期：28 2 页码：833-838 文献号： 文献类型：J	通讯作者	B 类	华南农业大学林学院	北大核心	无	无
15	南岭山地森林群落冠层结构与立木多度的关系	中南林业科技大学学报 出版年：2014 卷期：34 5 页码：59-65 文献号： 文献类型：J	通讯作者	B 类	华南农业大学林学院	北大核心	无	无
16	南岭国家级自然保护区森林群落枯立木分布与地形因子的相关性	福建农林大学学报 出版年：2013 卷期：42 6 页码：531-537 文献号： 文献类型：J	通讯作者	B 类	华南农业大学林学院	北大核心	无	无

说明：论文等级和 中科院大类分区按《华南农业大学学术论文评价方案（试行）》划分。

报告免责声明:如未盖章,报告无效

检索员：田成

华南农业大学图书馆

2024-01-22

2.以第一作者发表本专业论文情况

ISSN 2096-0018
CN 35-1327/S

2016中国高校百佳科技期刊

森林与环境学报

JOURNAL OF FOREST AND ENVIRONMENT

（原刊名：福建林学院学报）

主　　办　中国林学会
Chinese Society of Forestry
Sponsored by　福建农林大学
Fujian Agriculture and Forestry University

ISSN 2096-0018
01>
9 772096 001186

第38卷　第1期　Vol.38　No.1
2018年1月　Jan.15, 2018
中国·福州　Fuzhou, China

森 林 与 环 境 学 报
Senlin yu Huanjing Xuebao

第38卷 第1期　　2018年1月15日

中国高校百佳科技期刊、中文核心期刊、中国科技核心期刊、
中国科学引文数据库(CSCD)来源期刊、RCCSE中国核心学术期刊

目　次

期刊基本参数：CN 35-1327/S * 1960 * q * A4 * 128 * zh * P * ¥20.00 * 1000 * 20 * 2018-01

森 林 与 环 境 学 报

Senlin yu Huanjing Xuebao

第 38 卷 第 1 期　　2018 年 1 月 15 日

中国高校百佳科技期刊、中文核心期刊、中国科技核心期刊、
中国科学引文数据库(CSCD)来源期刊、RCCSE 中国核心学术期刊

目　次

期刊基本参数：CN 35-1327/S * 1960 * q * A4 * 128 * zh * P * ¥20.00 * 1000 * 20 * 2018-01

DOI：10.13324/j.cnki.jfcf.2018.01.011

亚热带常绿阔叶林枯立木与冠层结构的关系

张 璐，敬小丽，苏志尧，蔡琳颖，张星元
(华南农业大学林学与风景园林学院，广东 广州 510642)

摘要： 冠层结构影响着林下光环境的变化进而影响林木的生长。以亚热带常绿阔叶林 10 hm^2 固定样地内枯立木为研究对象，运用样方调查法和半球面影像技术，量化枯立木多度、胸径、分布与冠层结构的关系。结果表明，样地内枯立木以小树为主，胸径和树高均偏小；枯立木多度随林冠开度、林下总光照、林下散射光和林下直射光的增加而减小；而枯立木胸径随林冠开度、林下总光照和林下直射光的增加而增大；林下光照在枯立木的形成中发挥重要的作用。枯立木集中分布在林下光照较弱且林冠开度较小的区域，枯立木的多度和胸径受林下直射光影响较大，而枯立木的分布则主要受到了林下散射光和总光照的影响。

关键词： 枯立木；林下光照；半球面影像；典范对应分析；林冠层
中图分类号： X821 **文献标识码：** A **文章编号：** 2096-0018(2018)01-0064-07

Relationship between distribution of snags and canopy structure of subtropical evergreen broad-leaved forest

ZHANG Lu，JING Xiaoli，SU Zhiyao，CAI Linying，ZHANG Xingyuan
(College of Forestry and Landscape Architecture，South China Agricultural University，Guangzhou，Guangdong 510642，China)

Abstract: Forest canopy structure effects understory environment factors and then affects tree growing. Base on plot survey and hemispherical photography technology，the abundance，diameter at breast height(DBH)，distribution of snag and its controlling factors were studied to explore the formation and maintenance mechanism of community biodiversity of subtropical evergreen broad-leaved forest in the 10 hm^2 permanent plot. The result showed that the snags mainly consist of small trees which the DBH and height were relatively small. Abundance of snags decreased with increasing canopy openness(CO)，transmitted total light(Ttot)，transmitted diffused light(Tdif) and transmitted direct light(Tdir) while DBH of snags increased with increasing CO，Ttot，and Tdir. Understory light played an important role in the formation of snags. The snags prefer to cluster together under the habitat with weak understory light and small CO. The abundance and DBH of snags were affected by Tdir while the distribution of snags were closely related to Tdif and Ttot.

Key words: snag; understory light; hemispherical photography; canonical correspondence analysis; canopy layer

枯立木是森林群落的重要组成部分[1]，在森林生态系统中的生物地球化学循环、碳库贮存以及为其他有机体提供生境等环节中扮演着重要的角色，对森林的结构和更新有着不可忽视的作用。近年来，随着全球的气候变化及有关生物多样性的研究深入，枯立木以其多种重要的生态功能越来越受到生态学家的重视[2]。

冠层是森林与外界接触最直接的界面，与外界环境的相互作用最活跃[3]。冠层不仅保持着较高的生物多样性[4]，冠层对照射进森林的光照具有吸收、反射和折射的作用，改变了林下光照环境[5]，从而对林下植被的生长与更新产生影响。此外，冠层茂密的枝叶还产生了遮荫效应，阻挡了部分太阳辐射，调节着林内的温度，不同的冠层结构下分布着耐荫性不同的林下植被。冠层结构的变化影响着林下光环境的变化从而影响林木的生长。文中旨在从冠层结构，尤其是林下光照条件角度探讨枯立木多度、胸径及分布与冠层结构的关系，以期为进一步探讨亚热带常绿阔叶林生物多样性的形成与群落维持机制提供科学依据。

1 试验地概况

研究地点设在广东省河源市东源县康禾自然保护区，位于北纬 23°44′~23°53′，东经 115°04′~115°09′。该

收稿日期：2017-06-22 修回日期：2017-09-18
基金项目：广东省自然科学基金项目(2015A030313403)；广东省省级林业发展及保护专项资金林业科技创新项目(2017KJCX037)。
第一作者简介：张璐(1973-)，女，副教授，博士，从事森林生态学研究。Email：zhanglu@scau.edu.cn。

区年平均气温 21.1 ℃，年平均降水量 2 142.6 mm，成土母岩为花岗岩和砂岩，土壤以赤红壤为主，其次有山地红壤、山地黄壤。试验地群落为次生常绿阔叶林，群落优势种为米槠［*Castanopsis carlesii* (Hemsl.) Hay.］、木荷(*Schima superba* Gardn. et Champ.)、红背锥(*Castanopsis fargesii* Franch.)、杉木［*Cunninghamia lanceolata* (Lamb.) Hook.］、鼠刺(*Itea chinensis* Hook. et Arn.)等亚热带地带性树种[6]。

2　研究方法

2.1　样地设置与样方调查

在线路踏查的基础上，参照热带森林科学中心建立大样地的技术规范，选择亚热带常绿阔叶林典型群落设置 10 hm^2固定样地，利用全站仪(Nikon DTM-310，日本)将整个样地分为 250 个 20 m × 20 m 的大样方，每个大样方再分为 4 个 10 m × 10 m 的小样方。在每个小样方内按逆时针的顺序调查，记录胸径≥2 cm，树高≥1.3 m 的枯立木[7]种名、树高、胸径、分枝高，并编号，同时标注其在样方中的位置，对于难以辨认物种的个体，根据与其丛生的个体、根部的萌生枝等情况确定其种名，实在无法辨认的统一命名为未知种。

2.2　半球面影像的拍摄

在阴天或无风天的日出或日落时，用数码相机(Nikon 4500 CoolPix，泰国)外接鱼眼镜头转换器(Nikkor FC-E8，泰国，广角 183°，正投影)用三角架置于离地面 1.2～1.5m 处，镜头朝上，保持水平，用指南针确定方向使记录的照片顶部与磁北方向重合，用相机内置的 Fisheye1 模式在每个小样方中心拍摄半球面林冠影像。所有照片都用高分辨率(2272 × 1704 像素)获取，以 JPEG 图像格式保存(压缩比例 1∶4)，共计拍摄 1 000 张半球面林冠影像。

2.3　数据分析

由于所获得的半球面影像有相对统一的亮度和对比度，用 Sidelook 软件检测出正确的阈值，在 GLA2.0 软件中设定该阈值以便于正确地区分出照片中的天空和林冠。采用图像处理软件分析林冠影像，并利用 GLA2.0 软件计算并输出冠层结构参数：林冠开度(canopy openness，CO)、叶面积指数(leaf area index，LAI)、林下直射光(transmitted direct light，Tdir)、林下散射光(transmitted diffused light，Tdif)和林下总光照(transmitted total light，Ttot)。重要值(importance value，IV)运用公式 $IV = A_R + F_R + P_R$ 测算。式中：A_R 为相对多度；F_R 为相对频度；P_R 为相对优势度。

利用 Statistica 8.0 软件对叶面积指数、林下直射光、林下散射光和林下总光照等冠层结构参数与枯立木的多度和胸径的差异性进行 Kruskal-Wallis 检验，并对差异显著的进一步进行多重比较。构建了 2 个数据库，一个是以样方枯立木多度构建的物种数据库(主数据库)，另一个是以样方 5 个冠层参数构建数据库(次数据库)。利用 CANOCO 4.5 软件对群落整体枯立木分布与冠层结构的关系进行典范对应分析。

3　结果与分析

3.1　枯立木的数量特征

基于 10 hm^2样地调查，共记录了枯立木 1 480 株，其中已知种 1 080 株，未知种 400 株。已知种共有 63 种，分属 54 属，33 科，其中裸子植物 3 科 3 属 3 种，被子植物 30 科 51 属 60 种。枯立木中常绿树占多数，有 47 种，占枯立木总数的 74.6%；而落叶树仅有 16 种，占枯立木总数的 25.4%。从科水平上看，群落中的枯立木以樟科(Lauraceae)占优势，有 6 属 8 种；其次为山茶科(Theaceae)和壳斗科(Fagaceae)，分别有 4 属 5 种和 1 属 4 种；豆科(Leguminosae)、夹竹桃科(Apocynaceae)和茜草科(Rubiaceae)均为 3 属 3 种。在种水平上，锥(*Castanopsis chinensis* Hance)最多，重要值为 52.58，其次为木荷和杉木(表 1)。数量群落中小树和幼苗死亡较多，样地内的枯立木胸径和树高均偏小，平均胸径和平均树高分别仅为(6.06±0.17) cm 和(4.93±0.09) m。

表 1 亚热带常绿阔叶林枯立木优势种数量特征

Table 1 Quantitative characteristic of dominant species of snags in subtropical evergreen broad-leaved forest

种名 Species	胸径 DBH/cm	树高 Height/m	多度 Abundance	出现样方数 Number of plot	重要值 Important value
锥 *Castanopsis chinensis*	8.80±0.43	5.78±0.24	277	195	52.58
木荷 *Schima superba*	9.08±1.67	4.40±0.31	72	58	17.05
杉木 *Cunninghamia lanceolata*	7.07±0.54	6.19±0.39	82	57	16.55
黄樟 *Cinnamomum porrectum* (Roxb.) Kosterm.	6.33±0.70	5.63±0.41	63	54	14.04
马尾松 *Pinus massoniana* Lamb.	15.55±3.55	8.82±1.26	11	9	11.74
山乌桕 *Sapium discolor* (Champ. ex Benth.) Muell. Arg	15.46±4.31	9.96±1.44	8	8	11.22
华润楠 *Machilus chinensis* (Champ. ex Benth.) Hemsl.	5.16±0.48	4.57±0.32	53	41	10.98
油茶 *Camellia oleifera* Abel.	2.50±0.06	2.88±0.15	68	30	10.22
酸枣 *Ziziphus jujube* Mill	15.60	24.00	1	1	9.89
红背锥 *Castanopsis fargesii*	9.27±1.68	6.19±0.69	35	22	9.35
其他已知种	4.45±0.37	3.18±0.09	410	342	136.38
未知种	5.07±0.28	3.66±0.18	400	233	–

3.2 枯立木多度与冠层结构的关系

枯立木多度随林冠开度、林下总光照、林下散射光和林下直射光的增加而减少。Kruskal-Wallis 检验分析揭示，枯立木多度与林冠开度、林下总光照、林下散射光和林下直射光各参数的差异均达到显著性水平($P<0.05$)。多重比较结果进一步揭示，枯立木多度在林下直射光分组变量间差异显著，在林冠开度、林下散射光和总光照分组变量间没有显著性差异(图 1)。究其原因，可能是直射光到达冠层后一部分被反射和散射，到达林下的比例较少，而散射光却能大部分到达林下，冠层和林下的直射光差异较大，从而导致枯立木多度在林下光照组间的差异性显著水平不同。总体而言，枯立木多度与林下光照的关系密切，弱光照条件下枯立木数量较多。

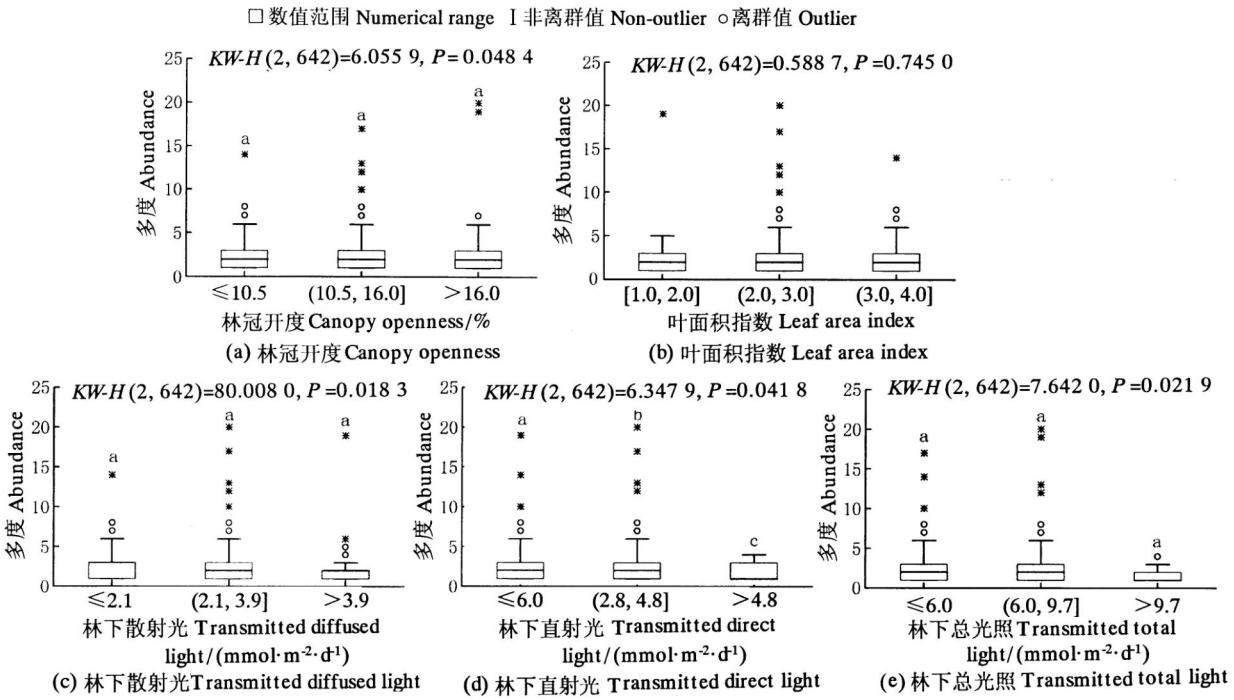

注：图中不同字母表示差异显著($P<0.05$)。Note: different small letters indicate significant difference at 0.05 level.

图 1 不同冠层结构参数的枯立木多度

Figure 1 Snag abundance in different canopy structure parameters

3.3 枯立木胸径与冠层结构的关系

与枯立木多度相反，枯立木胸径随林冠开度、林下总光照和林下直射光的增加而增大，但随林下散射光的增加先减小后增大，随叶面积指数的增加而减小。Kruskal-Wallis 检验结果表明，除林冠开度外，

枯立木胸径与叶面积指数、林下总光照、林下散射光和林下直射光各参数的差异均达到显著性水平($P<0.05$) 。多重比较结果进一步揭示，枯立木胸径在叶面积指数、林下总光照、林下直射光两两分组变量间有极显著差异($P<0.01$) (图 2) ，表明枯立木胸径受叶面积指数、林下直射光、总光照的影响较大。

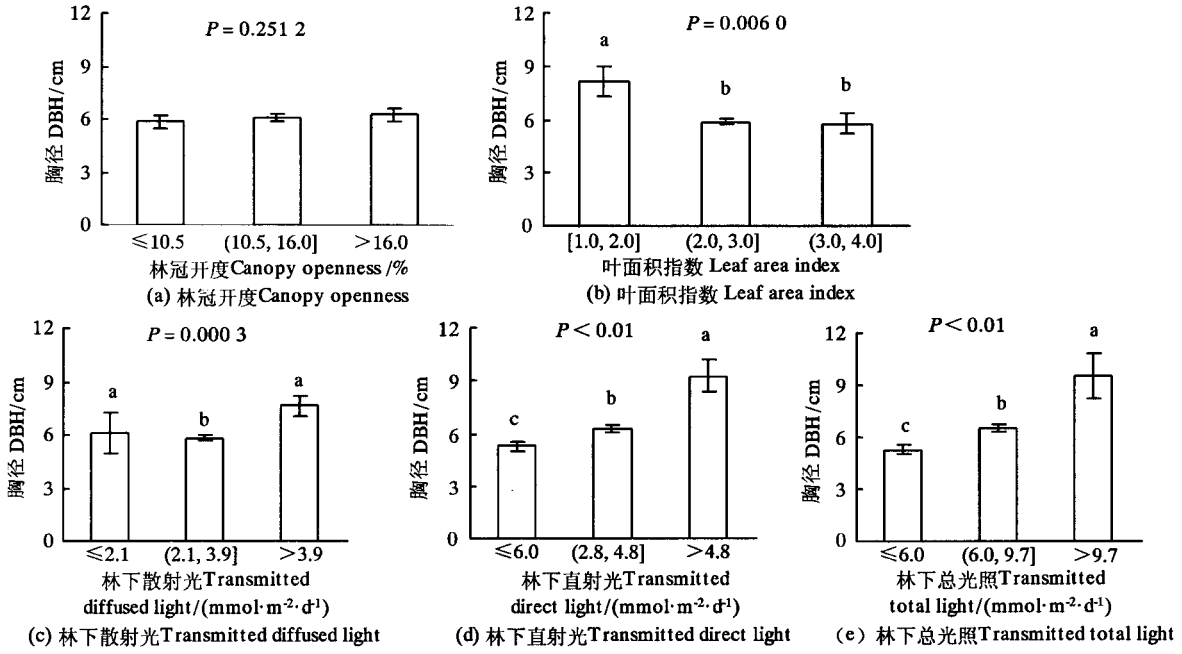

注：图中不同字母表示差异显著($P<0.05$) 。Note: different small letters meant significant difference at 0.05 level.

图 2　不同冠层结构参数的枯立木胸径

Figure 2　Diameter at breast height of snag in different canopy structure parameters

3.4　枯立木分布与冠层结构的关系

对枯立木分布与冠层结构的关系进行典范对应分析，蒙特卡罗检验结果表明排序结果可信($P<0.05$) (表 2) 。冠层结构各参数与 4 个排序轴均有一定的相关性($P<0.05$) 。

表 2　各排序轴的加权相关矩阵

Table 2 Weighted correlation matrix of axis

参数 Paramter	排序轴 1Axis 1	排序轴 2Axis 2	排序轴 3Axis 3	排序轴 4Axis 4
特征值 Eigenvalue	0.163	0.089	0.046	0.035
物种-环境关系 Species-environment correlation	0.513	0.379	0.286	0.248
物种数据的变量累积百分比 Cumulative percentage variance of species data	0.5	0.8	1.0	1.1
物种-环境关系的变量累积百分比 Cumulative percentage variance of species-environment relation	48.9	75.5	89.4	100.0
所有典范特征值之和 Sum of all canonical eigenvalues		30.999		
所有特征值之和 Sum of all eigenvalues		0.333		
第一典范轴 P 值 P-value of first canonical axis		0.024		
所有典范轴 P 值 P-value of all canonical axes		0.020		

典范对应分析二维排序(图 3) 揭示，林下光照条件对枯立木分布的影响较大，其次为叶面积指数，林冠开度的影响最弱。图 3 中实心三角形代表枯立木种类，不同字母组成代表不同树种，带有箭头的连线代表冠层结构参数，箭头所指的方向代表该冠层结构参数的变化趋势，箭头长度代表冠层结构参数与枯立木种类相关性的大小，箭头连线与排序轴的夹角表示冠层结构参数与排序轴的相关性的大小，夹角越大说明相关性越大。在林下光照越强的区域，枯立木的分布越少，表明在光照越弱的地方，立木的死亡可能与弱光照有关。锥(CACH) 、山乌桕(SADI) 、藤黄檀(DAHA) 、变叶榕(FIVA) 及红锥(CAHY) 等物种的枯立木集中分布在林下光照较弱且林冠开度较小的区域。究其原因，可能是这些物种作为亚热

带常绿阔叶林的优势种或共优种，喜欢光照充足的生境，对弱光照比较敏感，光照越小越不利于其生长。如锥是康禾自然保护区亚热带常绿阔叶林群落的优势种，又多分布在林下光照较弱的区域，所以枯立木中锥的个体数最多，出现的频率也最大，这也合理解释了为什么样地中枯立木的物种组成以锥占绝对优势地位。而同为优势种的厚壳桂(CRCH)、天料木(HOCO)等喜光植物在样地中仅出现了1株枯立木，可能与其活立木多分布在样地中林下光照较强和林冠开度较大的区域有关，说明充足的光照条件对喜光植物的生长有利。

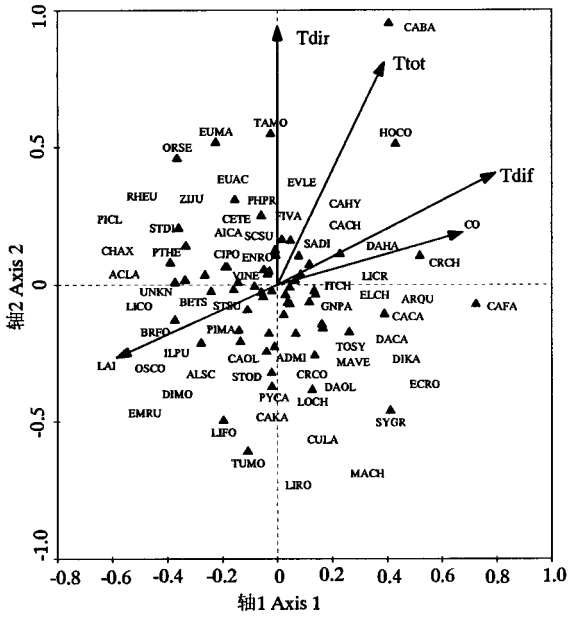

注：ACLA.阔叶猕猴桃 *Actinidia latifolia*(Gardn. & Champ.) Merr.；GNPA.小叶买麻藤 *Gnetum parvifolium*(Warb.) C. Y. Cheng ex Chun；ADMI.杨桐 *Adinandra millettii*(Hook. et Arn.) Benth. et Hook. f. ex Hance；HOCO.天料木 *Homalium cochinchinense*(Lour.) Druce；AICA.香楠 *Aidia canthioides*(Champ. ex Benth.) Masam.；ILPU.毛冬青 *Ilex pubescens* Hook. et Arn.；ALSC.鸭脚木 *Alstonia scholaris*(L.) R. Br.；ITCH.鼠刺 *Itea chinensis* Hook. et Arn.；ARQU.罗伞树 *Ardisia quinquegona* Bl.；IXCH.粘木 *Ixonanthes chinensis* Champ.；BETS.网脉琼楠 *Beilschmiedia tsangii* Merr.；LICO.香叶树 *Lindera communis* Hemsl.；BRFO.大叶土密树 *Bridelia fordii* Hemsl.；LICR.豹皮樟 *Litsea coreana* Levl.；CABA.脚骨脆 *Casearia balansae* Gagn.；LIFO.枫香树 *Liquidambar formosana* Hance；CACA.山核桃 *Carya cathayensis* Sarg.，Pl. Wils.；LIRO.豺皮樟 *Litsea rotundifolia* Hemsl.；CACH.锥 *Castanopsis chinensis* Hance；LOCH.繼木 *Loropetalum chinense*(R. Br.) Oliver；CAFA.红背锥 *Castanopsis fargesii* Franch；MACH.华润楠 *Machilus chinensis*(Champ. ex Benth.) Hemsl.；CAHY.红锥 *Castanopsis hystrix* Miq.；MAVE.绒毛润楠 *Machilus velutina* Champ. ex Benth.；CAKA.吊皮锥 *Castanopsis kawakamii* Hay.；ORSE.软荚红豆 *Ormosia semicastrata* Hance；CAOL.油茶 *Camellia oleifera* Abel.；OSCO.宁波木犀 *Osmanthus cooperi* Hemsl.；CETE.水杨梅 *Cephalanthus tetrandrus*(Roxb.) Ridsd. et Bakh. f.；PHPR.桃叶石楠 *Photinia prunifolia*(Hook. et Arn.) Lindl.；CHAX.南酸枣 *Choerospondias axillaris*(Roxb.) Burtt et Hill.；PICL.猴耳环 *Pithecellobium clypearia*(Jack) Benth.；CIPO.黄樟 *Cinnamomum porrectum*(Roxb.) Kosterm.；PIMA.马尾松 *Pinus massoniana* Lamb.；CRCH.厚壳桂 *Cryptocarya chinensis*(Hance) Hemsl.；PTHE.翻白叶树 *Pterospermum heterophyllum* Hance；CRCO.黄牛木 *Cratoxylum cochinchinense*(Lour.) Bl.；PYCA.豆梨 *Pyrus calleryana* Dcne. var. calleryana；CULA.杉木 *Cunninghamia lanceolata*(Lamb.) Hook.；RHEU.华丽杜鹃 *Rhododendron eudoxum* Balf. f. et Forrest；DACA.牛耳枫 *Daphniphyllum calycinum* Benth.；SADI.山乌桕 *Sapium discolor*(Champ. ex Benth.) Muell. Arg.；DAHA.藤黄檀 *Dalbergia hancei* Benth.；SCSU.木荷 *Schima superba* Gardn. et Champ.；DAOL.虎皮楠 *Daphniphyllum oldhami*(Hemsl.) Rosenth.；STDI.羊角拗 *Strophanthus divaricatus*(Lour.) Hook. et Arn.；DIKA.柿 *Diospyros kaki* Thunb.；STOD.芬芳安息香 *Styrax odoratissimus* Champ.；DIMO.罗浮柿 *Diospyros morrisiana* Hance；STSU.栓叶安息香 *Styrax suberifolius* Hook. et Arn.；ECRO.酸叶胶藤 *Ecdysanthera rosea* Hook. et Arn.；SYGR.轮叶蒲桃 *Syzygium grijsii*(Hance) Merr. et Perry；ELCH.中华杜英 *Elaeocarpus chinensis*(Gardn. et Chanp.) Hook. f. ex Benth.；TAMO.白花苦灯笼 *Tarenna mollissima*(Hook. et Arn.) Rob.；EMRU.网脉酸藤子 *Embelia rudis* Hand. -Mazz；TOSY.木蜡树 *Toxicodendron sylvestre*(Sieb. et Zucc.) O. Kuntze；ENRO.黄杞 *Engelhardtia roxburghiana* Wall.，Pl. As. Rar.；TUMO.山香圆 *Turpinia Montana*(Bl.) Kurz. var. montana；EUAC.尾叶柃 *Eurya acuminatissima* Merr. et Chun；VINE.牡荆 *Vitex negundo* L.；EVLE.三極苦 *Evodia lepta*(Spreng.) Merr.；ZIJU.酸枣 *Ziziphus jujube* Mill.；FIVA.变叶榕 *Ficus variolosa* Lindl. ex Benth.。

图3 枯立木与冠层结构参数的典范对应分析

Figure 3 Canonical correspondence analysis between snags and canopy structure parameters

4 讨论与结论

4.1 枯立木数量特征的影响因素

死亡是林木生长发育过程中的正常现象，发生在林木个体发育的各个阶段，导致其死亡的原因也多

种多样，如病虫害、大风、火烧、人为干扰和纬度差异等[8]。枯立木对群落生境有明显的指示作用[9]，而环境因子也影响着植物的数量与分布[10]，对环境因子的竞争也是立木死亡的重要原因，同种的不同个体之间和不同物种之间的竞争都会使立木死亡，产生枯立木。研究表明，林木间相互争夺营养空间，会导致林冠上层高大的植株得到较多的养分而生长较好，而林冠下层的植株生长迟缓甚至死亡[11]。林分密度过大也会导致林木个体间对资源的激烈竞争，形成枯立木。文中枯立木密度为 148 株·hm^{-2}，与其他研究地点相比较高，如华北土石山区天然次生林 4 hm^2样地的枯立木密度为 79.25 株·hm^{-2}[12]、云南哀牢山国家级自然保护区的核心区 4 hm^2样地的枯立木密度为 68.5 株·hm^{-2}[13]。有研究[14]指出，人为采伐以及人类可接近的程度对枯立木密度的影响也很大。文中研究地点位于生活区附近，在调查期间常有附近居民上山采伐，但枯立木密度仍偏高，这可能与枯立木起测径阶为 2 cm 有关。此外，枯立木物种共有 63 种，以樟科、山茶科和壳斗科最占优势，这 3 科植物均是我国南方森林中的重要类群，不少种为次生林的建群种或优势种[15]。样地中的枯立木以锥、木荷和杉木的多度和频度最占优势，鼎湖山季风常绿阔叶林 1 hm^2永久性样地内粗木质残体的研究结果也显示，样地中的粗木质残体以锥、木荷、肖蒲桃［*Acmena acuminatissima* (Blume) Merr. et Perry］的多度占优势[16]，说明在亚热带常绿阔叶林中，锥和木荷为常见的枯立木物种。但这并非可以直接推断这两个种容易形成枯立木，确定该种是否容易形成枯立木应由其枯立木数量与该树种总数的比例大小来定，比例较大的树种容易形成枯立木，关于枯立木形成还需进一步研究。

4.2　枯立木胸径变化及其与冠层结构的关系

文中样地内枯立木以小树为主，胸径集中在 2～10 cm 的小径级，这与其他地区的枯立木特征相同，如游惠明等[17]对天宝岩国家级自然保护区长苞铁杉林内粗木质残体的研究也发现区内的粗木质残体主要集中在 0～20 cm 的小径级和 0～5 m 的高度级；大兴安岭薛类-兴安落叶松林的中龄林中没有发现粗木质残体，近熟林中也仅调查到直径为 10～20 cm 的粗木质残体，过熟林中未见胸径>30 cm 的枯立木[18]，但是样地内 20～30 cm 以及≥ 30 cm 等大径级的枯立木仍然存在，样地中枯立木的龄级组成较完整。虽然国外对枯立木的胸径限定较高，但研究结果仍显示枯立木集中在小径级[19]。此外，随着径级的增加，样地枯立木的数量逐渐减少，也与很多其他地区的枯立木径级特征相似。大兴安岭杜香-兴安落叶松林粗木质残体的研究也发现随径级增加，各个年龄林分中粗木质残体比例逐渐降低[20]；鼎湖山自然保护区内典型南亚热带森林生态系统的粗木质残体研究结果也表明枯立木的数量均随径级的增加而减少[21]。研究揭示，枯立木与林下光照的关系密切，弱光照条件下枯立木数量较多，强光照条件下枯立木胸径较大。林下直射光对枯立木多度的影响较大，叶面积指数越大，枯立木胸径越大，但枯立木多度却变少了。枯立木胸径与叶面积指数、林下直射光、总光照的关系密切。大树对环境的适应性较强，对不良环境的抵抗力较强，而小树处在生长旺盛阶段，需要充足的光照和水分等条件，对不适环境的抵抗力较弱，样地冠层越郁闭，林下光照越弱，小树生长所需的光照越得不到满足，导致林木在幼苗和小树阶段相对死亡越多。

参考文献

[1] COUSINS S J M，BATTLES J J，SANDERS J E，*et al*. Decay patterns and carbon density of standing dead trees in California mixed conifer forests [J]. Forest Ecology and Management，2015，353：136-147.

[2] ONODERA K，TOKUDA S. Do larger snags stand longer? —snag longevity in mixed conifer-hardwood forests in Hokkaido，Japan [J]. Annals of Forest Science，2015，72(5)：621-629.

[3] 沈浩，蔡佳宁，李萌姣，等. 中国森林冠层生物多样性监测 [J]. 生物多样性，2017，25(3)：229-236.

[4] OZANNE C M P，ANHUF D，BOULTER S L，*et al*. Biodiversity meets the atmosphere：a global view of forest canopies [J]. Science，2003，301(5630)：183-186.

[5] 区余端，苏志尧. 粤北山地常绿阔叶林自然干扰后冠层结构与林下光照动态 [J]. 生态学报，2012，32(18)：5 637-5 645.

[6] 胡砚秋，柯娴氧，徐明锋，等. 亚热带森林群落草本植物对林下光环境的响应 [J]. 中南林业科技大学学报，2016，36(8)：72-76.

[7] IWASHITA D K，LITTON C M，GIARDINA C P. Coarse woody debris carbon storage across a mean annual temperature gradient in tropical montane wet forest [J]. Forest Ecology and Management，2013，291：336-343.

[8] VÁZQUEZ L，RENTON K. High density of tree-cavities and snags in tropical dry forest of western Mexico raises questions for a latitudinal gradient [J]. PLoS One，2015，10(1)：e0116745.

[9] 张璐，贺立静，区余端，等. 南岭自然保护区常绿阔叶林枯立木数量特征分析 [J]. 福建林学院学报，2012，32(1)：64-69.

[10] TUOMISTO H，RUOKOLAINEN K，YLI-HALLA M. Dispersal，environment，and floristic variation of western Amazonian forests [J]. Science，2003，299(5 604)：241-244.

[11] 洪滔，吴承祯，胡喜生. 安曹下杉木丰产林不同阶段生长比较研究 [J]. 福建林学院学报，2008，28(1)：19-22.

[12] 安云，丁国栋，高广磊，等. 华北土石山区天然次生林枯立木数量特征与分布格局 [J]. 水土保持通报，2012，32(4)：246-250.

[13] 张树斌，郑征. 哀牢山中山湿性常绿阔叶林枯立木数量及分配规律 [J]. 东北林业大学学报，2009，37(2)：3-5，13.

[14] HOLLENBECK J P，BATE L J，SAAB V A，*et al*. Snag distributions in relation to human access in ponderosa pine forests [J]. Wildlife Society Bulletin，2013，37(2)：256-266.

[15] 方燕鸿. 武夷山米槠、甜槠常绿阔叶林的物种组成及多样性分析 [J]. 生物多样性，2005，13(2)：148-155.

[16] 杨方方，李跃林. 鼎湖山粗死木质残体生物量特征 [J]. 应用与环境生物学报，2011，17(5)：750-752.

[17] 游惠明，何东进，洪伟，等. 海拔对天宝岩长苞铁杉林粗死木质残体分布的影响 [J]. 福建农林大学学报(自然科学版)，2011，40(4)：365-369.

[18] 张秋良，王飞，李小梅，等. 藓类-兴安落叶松林木质物残体贮量及组成 [J]. 生态环境学报，2013，22(3)：437-442.

[19] PESSOA S D V A，ARAUJO D S D D. Tree community dynamics in a submontane forest in southeastern Brazil：growth，recruitment，mortality and changes in species composition over a seven-year period [J]. Acta Botanica Brasilica，2014，28(2)：190-197.

[20] 王飞，张秋良，王冰，等. 不同年龄杜香-兴安落叶松林粗木质残体贮量及特征 [J]. 生态学杂志，2012，31(12)：2 981-2 989.

[21] 唐旭利，周国逸. 南亚热带典型森林演替类型粗死木质残体贮量及其对碳循环的潜在影响 [J]. 植物生态学报，2005，29(4)：559-568.

(责任编辑：江 英)

《森林与环境学报》第一届编辑委员会名单

森林与环境学报(Senlin yu Huanjing Xuebao)
(季刊 1960年创刊)
第38卷　第1期　2018年1月15日

Journal of Forest and Environment
(Quarterly, Started in 1960)
Volume 38　Number 1　Jan. 15, 2018

主管单位 福　建　农　林　大　学
主办单位 中国林学会　福建农林大学
编辑出版 森林与环境学报编辑部
(福州金山，邮政编码 350002)
网　　址 http: //fjlxyxb.paperopen.com/
主　　编 尹伟伦
执行主编 洪　伟
常务副主编 周新年　肖文发
印　　刷 福建东南彩色印刷有限公司
(福州金山，邮政编码 350008)
发行范围 公开发行
国内发行 福建省邮政报刊发行局
订　　阅 全国各地邮局（所）
国外发行 中国国际图书贸易集团有限公司

Supervised by Fujian Agriculture and Forestry University
Sponsored by Chinese Society of Forestry
Fujian Agriculture and Forestry University
Edited and Published by Editorial Department of
Journal of Forest and Environment
(Jinshan, Fuzhou, Fujian 350002, China)
Website http: //fjlxyxb.paperopen.com/
Editor-in-Chief YIN Weilun
Executive Editor-in-Chief HONG Wei
Executive Deputy Editor-in-Chief ZHOU Xinnian XIAO Wenfa
Printed by Fujian Southeast Colour Printing Co. Ltd.
Issued in Public
Distributed by Fujian Provincial Postal Distribution Bureau
of Newspapers and Periodicals
Distributed abroad by
China International Book Trading Corporation

ISSN 2096-0018
CN 35-1327/S

国外发行代号：Q7690　　国内邮发代号：34-62　　国内定价：20.00元

Pak. J. Bot., 48(6): 2367-2374, 2016.

TOPOGRAPHIC CONTROLS ON THE DISTRIBUTION OF INDIGENOUS RHODODENDRONS IN THE SOUTHERN SLOPE OF THE NANLING MOUNTAINS, SOUTH CHINA

LU ZHANG*, DING MA, XIAO-LI JING AND ZHI-YAO SU

College of Forestry and Landscape Architecture, South China Agricultural University, Guangzhou 510642, China
**Corresponding author's e-mail: zhanglu@scau.edu.cn*

Abstract

Rhododendrons, one of the traditional flowering plants in China and overseas, are famous for their beautiful flowers. However, only a few indigenous Rhododendron plants are used for landscaping in China. To determine the ecological role of distribution of Rhododendrons, and analyse whether and how major topographic factors influence the distribution and growth of indigenous Rhododendrons, a total of one hundred and two plots (10 m × 10 m, 100 m^2) were laid out in the southern slope of the Nanling Mountains, South China (700–1900 m a.s.l.). We found that the topography affecting the Rhododendron species, i.e., *Rhododendron simiarum, R. cavaleriei, R. bachii, R. championae, R. kwangtungense R. fortune, R. chunii*., and there are different patterns among species. The richness and abundance of the seven indigenous Rhododendrons depaned on topographical gradient, greater higher elevation, intermediate slope steepness, convex slopes and shady aspect. By contrast, sunny habitats and habitat at low positions in the slope had fewer rhododendron plants. Non–parametric Kruskal–Wallis test and canonical correspondence analysis showed that altitude, position in the slope, slope shape and slope aspect had significant effects on the total abundance of Rhododendrons (p<0.05) compared with slope steepness. Indicator species analysis identified were indicative of altitude (four species), slope aspect (one species), position in the slope (one species), and slope shape (two species), respectively. The spatial heterogeneity of indigenous Rhododendron plants to topographic factors has significant implications for species conservation and potential for use in landscaping.

Key words: Indigenous Rhododendrons, Indicator species, Topographic, Landscaping.

Introduction

Determination of the environmental gradients that influence species richness, composition and biomass of plant communities is one of the most important issues in ecology (Körner, 2007). Topography is one of the most important factors affecting the tree growth performance (Sattler *et al.,* 2014) and distribution of trees in mountainous forests (Enoki, 2003), which also has been proven to be a strong regional predictor of above ground biomass accumulation in tropical forests (Alves *et al.,* 2010). The availability of accurate topographic information at different spatial scales is a limiting factor for relating to forest productivity (Laamrani *et al.,* 2014), and as a driver of cryptic speciation (Britton *et al.,* 2014).

Ericaceae are widely distributed in temperate and subarctic regions, also at high elevations in tropical regions. There were 22 genera and 826 species (524 endemic) have been found in China (Fang, 2005). The genus Rhododendron is the largest genus of Ericaceae that are widely spread in Asia, Europe, and North America. Sino-Himalaya Region is the largest centre of distribution for modern Rhododendron (Min & Fang, 1979). George Forrest collected large numbers of living and herbarium specimens of hitherto unknown species in Yunnan, China, to introduce to the western world (Geng, 2010). The genetic relationships among Rhododendron species were partially related to their taxonomic position, geographic distribution and morphological classification (Zhao *et al.,* 2015). Tree Rhododendron adapts to a wide range of habitats with different environmental conditions (Ranjitkar *et al.,* 2013). However, Rhododendron plants, are also serious invasive alien plants, can inhibit forest regeneration in several systems worldwide (Wurzburger & Hendrick, 2007). Using invasive shrub rhododendron as a case study, Harris *et al.,* (2011) integrated information on both the demographics and spatial dynamics within an individual–based, spatially–explicit model to investigate the invasion potential of shrub Rhododendrons in different habitats. Moreover, Rhododendron toxins was degraded during composting (Hough *et al.,* 2010). Rhododendrons are increasingly recognized as a keystone element in the Himalayan region, which provides the ecological stability, associated niche and community continuum (Singh *et al.,* 2009). Biodiversity conservation was recognised as a globally serious subject at the United Nations Conference on Environment and Development Earth Summit in June 1992 in Rio de Janeiro, Brazil (Hsu *et al.,* 2013). Biodiversity has become a major concern in landscape planning in the recent years (Morimoto & Yoshida, 2005). Hybrid Rhododendron plants, such as *Rhododendron pulchrum*, *Rhododendron pulchrum* var. *phoeniceum*, and *Rhododendron simsii,* are widely applied in parks, residential areas and street–side green spaces in China, with versatile application patterns presenting excellent landscape effects. However, indigenous Rhododendron plants are seldom applied in landscaping in China.

The spatial distribution of high–elevation tropical forest patches is controlled by landscape–scale topographic characters (Coblentz & Keating, 2008). Topography can significantly alter microclimates and resource availability (Simonson *et al.,* 2014). Moreover, community–scale topographic factors, which also have great impact on species composition and diversity patterns of forest communities (Palmer & Dixon, 1990), significantly influence the distribution of understory species in the Nanling Mountains, with the magnitude of influence in the following order: elevation > slope aspect > slope steepness

(Ou *et al.,* 2009). The distribution of species play a key ecological role in forest communities. Understanding the relationship between topographic factors and species patterns is important for forest conservation and sustainable management.

In this study, we analyzed the ecological relationships between the distribution of Rhododendron plants and five topographic factors in the southern slope of the Nanling Mountains. The objectives of this study were to: 1) to reveal whether the topography affect the richness and abundance of Rhododendron species; 2) to ascertain the major topographic factors influence the distribution of indigenous Rhododendron; and 3) to determine whether the abundance of each species of Rhododendron vary in topographical gradient or not?.

Materials and Methods

Study area: The Nanling mountain (24º37′–24º57′N, 112º30′–113º04′E) range is located in southern China, straddling from west to east across the borders of Guangxi, Guangdong, Hunan, and Jiangxi provinces for more than 1000 km. It is a natural dividing line in southern China that separates the Yangtze River from the Zhujiang River. The Nanling National Nature Reserve, the largest Nature Reserve in Guangdong province (58400 ha), is located in the southern slope of the Nanling Mountains, with rugged topography and altitude ranging from 300 m to 1902 m at the summit of Shikengkong in Ruyang. On the average, annual temperature is 17.7 ℃, annual relative humidity is 84%, and annual precipitation is 1705 mm mainly occurring between March and August. The Nanling Mountains are the refugium of ancient tropical flora and the origin and key belts of temperate and subtropical plants in East Asia. A huge reservoir of biodiversity exists in the Nanling Mountains, with a record of 3760 vascular plant species (including subspecies levels), belonging to 268 families and 1306 genera (Xing, 2012).

Sampling design and plant census: Community monitoring plots were set along the elevation gradient based on the relative distribution of the indigenous Rhododendron plants in the southern slope of the Nanling Mountains. We studied the Rhododendron community in 102 plots (10 m × 10 m, 100 m^2) which were set along thirteen 120 m transects (700–1900 m a.s.l.) (Fig. 1). The total inventoried area was 1.02 ha. The plots were distributed over a 120 × 1200 m^2 area (≈14.4 ha). We identified all indigenous Rhododendron species in each sample plot using the available literature (Fang, 2005), and counted the number of stems, height, percentage cover or diameter at breast height (DBH) of all individuals including seedlings, juveniles and adults (Hao *et al.,* 2002).

We recorded the topographic factors on each plot. Slope steepness and slope aspect were measured using a professional forest compass (DQL-1, Harbin Optical Instrument Factory, China), whereas position in the slope and slope shape were determined by visual estimation. According to a general classification system from gentle to very steep, the slope degree of the sample plots ranged from 6.0° to 59.8° and were classified into five slope steepness groups. Where as slope aspect was initially divided into eight groups from the starting point of due north, namely, north aspect (338°–22°), northeast aspect (23°–67°), east aspect (68°–112°), southeast aspect (113°–157°), south aspect (158°–202°), southwest aspect (203°–247°), northwest aspect (248°–292°) and west aspect (293°–337°) in a clockwise direction (Olivero & Hix, 1998). As shown in Table 1, slope aspect was divided into sunny slope, semi–sunny slope, semi–shady slope and shady slope. The sunny slopes are south aspect, south west aspect and south east aspect, semi-sunny slopes are east aspect and west aspect, semi-shady are northwest aspect and northeast aspect, shady slopes are north aspect, respectively.

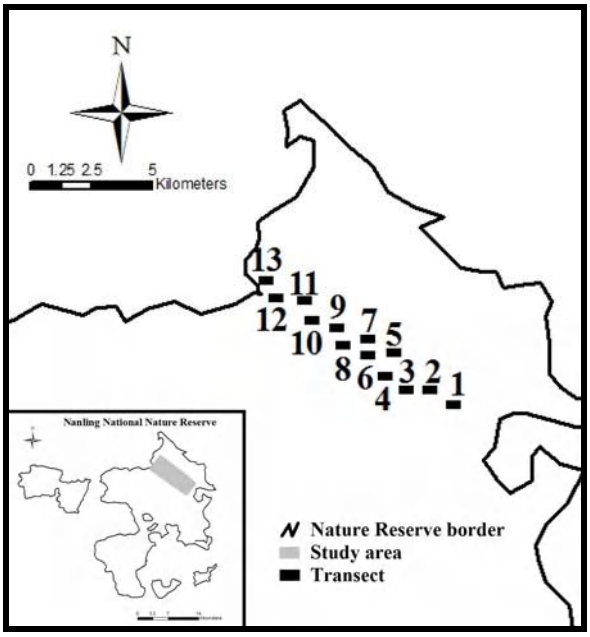

Fig. 1. Nanling National Nature Reserve. The light grey shaded rectangle on the inset indicates the location of the study area, and the black shaded rectangle indicates the location of transects.

Statistical data analysis: Two datasets were constructed based on data collected from the 102 plots. The first dataset consisted of Rhododendron plants. The second dataset comprised a quantitative environmental data matrix, including five topographical factors, (i.e. altitude, slope steepness, slope aspect, position in the slope and slope shape). Non–parametric Kruskal–Wallis test were used to analyse the differences in Rhododendron plant distribution between groups. Kruskal–Wallis test was carried out using Statistica version 8.0. All tests were performed at $p<0.05$. Canonical correspondence analysis (CCA) was performed to investigate the relationships between Rhododendron plants distribution and topographical factors. A Monte Carlo permutation test based on 999 random permutations was conducted to test the significance of the eigenvalue of the first canonical axis. CCA was carried out using CANOCO 4.5. Indicator species of indigenous Rhododendron in the Nanling Mountains were sieved using indicator species analysis (ISA). It was computed using the Dufrene and Legendre method to calculates the IV values (Su *et al.,* 2012).

Table 1. Measurements and variables of the study.

Measurement and variable	Variable coding
Altitude	1 = 700–900 m, 2 = 1000–1200 m, 3 = 1300–1600 m, 4 = 1700–1900 m
Slope steepness	1 =5.0°–15.0°, 2 =15.1°–25.0°, 3 =25.1°–35.0°, 4 =35.1°–45.0°, 5 =45.1°–59.8°
Slope aspect	1 = Sunny, 2 = Semi–sunny, 3 = Semi–shady, 4 = Shady
Position in the slope	1 = Upper, 1 = Middle, 1 = Lower
Slope shape	1 = Convex, 1 = Flat, 1 = Concave

Table 2. Number of stems in plots of seven indigenous Rhododendrons, and mean (± S.E.) of average basal area and average height of these species at the southern slope of the Nanling Mountains in South China.

Species	No. of stems	No. of plots	Average basal area (cm^2)	Average height (m)
Rhododendron simiarum Hance	205	24	44.7±3.2	3.7±0.1
Rhododendron cavaleriei Levl.	173	42	39.6±3.1	6.5±0.2
Rhododendron bachii Levl.	154	35	24.1±2.5	5.7±0.2
Rhododendron championae Hook.	57	26	67.5±10.7	5.7±0.4
Rhododendron kwangtungense Merr. et Chun	27	5	23.5±3.4	6.1±0.3
Rhododendron fortunei Lindl.	13	5	9.7±1.0	2.4±0.1
Rhododendron chunii Fang	3	3	35.2±4.8	4.7±0.7

Results

Species composition and distribution: In our 102 plots, we found 1,149 Rhododendron individuals, including 632 stems (Diameter at Breast Height, DBH> 3 cm), belonging to seven species (Table 2). *Rhododendron simiarum* had the highest abundance, whereas *Rhododendron cavaleriei, Rhododendron bachii* and *Rhododendron championae* were more widely distributed. All the Rhododendron plants in our plots were perennial evergreen woody plants, shrubs or small trees, in which the tallest tree (*R. championae)* was 16 m, whereas the shortest tree (*R. fortunei)* was only 1.8 m. In terms of the average height of rhododendron individuals, *R. cavaleriei* was the highest, whereas *R. fortunei* was the shortest. Regarding average basal area, *R. championae* was the biggest, whereas *R. fortunei* was the smallest. Basal area had significantly positive correlations with tree height (r = 0.4012, $p<0.001$). The species richness and abundance of Rhododendrons were greater in higher elevations, whereas fewer individuals were found at lower elevations (Fig. 2a). Moreover, species richness and abundance of Rhododendrons peaked at intermediate slope steepness (Fig. 2b). By contrast, sunny habitat and habitat at lower position in the slope and concave slope had fewer rhododendron individuals (Figs. 2c, 2d and 2e).

Relationship between topographic and Rhododendrons: Our study revealed that the total abundance of Rhododendrons was affected by altitude, position in the slope, slope shape, slope aspect, but not by slope steepness. Altitude had a significant effect on the total abundance of Rhododendrons. Total abundance was increased with elevation (Kruskal–Wallis test, $p<0.001$) (Fig. 3a). Multiple comparisons showed that the total abundance of Rhododendrons at 700–900-m was significantly lower than that at higher elevation. Similarly, the position in the slope had significant effect on the total abundance as well (Kruskal–Wallis test, $p<0.001$). Plots at the upper and middle positions in the slope had the higher total abundance than plots at lower position in the slope (Fig. 3b). Besides, slope shape had a significant effect on the total abundance of rhododendron (Kruskal–Wallis test, $p<0.001$), in which the concave slope had significantly lower total abundance as compared to convex slope and flat slope (Fig. 3c). In general, slope aspect had a significant effect on the total abundance of Rhododendrons (Kruskal–Wallis test, $p<0.001$). Plots at the sunny aspect had the lowest total abundance than plots at semi-sunny aspect and shady aspect (Fig. 3d). However, slope steepness did not significantly affect the total abundance of rhododendron in our plots (KW–H (4, 102) = 7.3135, $P = 0.1202$ for steepness).

In this study, the CCA results show the relationship between the abundance of seven rhododendron species and topographical variables ($p<0.001$) (Fig. 4). A Monte Carlo test based on 999 permutations found four significant canonical axes ($p<0.001$), in which the aggregate explained 24.8% variance in the species data and 99.6% variance of the species–environmental relation (Table 3). The first canonical axis had an eigenvalue of 0.636, and represented the topography–stand structure gradient. This canonical axis was significantly negatively correlated with altitude (r = –0.3185, $p<0.05$), and significantly positively correlated with slope steepness (r = 0.3123, $p<0.05$) and slope aspect (r = 0.2770, $p<0.05$). The second canonical axis had an eigenvalue of 0.402 and was significantly negatively associated with slope shape (r = –0.6499, $p<0.01$), altitude (r = –0.6129, $p<0.01$), and position in the slope (r = –0.5431, $p<0.01$) (Table 3).

ISA identified that indicator species that were indicative of altitude (four species), slope aspect (one species), position in the slope (one species), and slope shape (two species), respectively (Table 4). No indicator species was found for slope steepness ($p>0.05$). *R. kwangtungense* was indicative of middle–elevation, shade–tolerant slope aspect and flat slope shape. Similarly, the strongest indicator species of high elevation, *R. championae*, grew well in the concave slope. *R. fortunei* was an indicator species of the upper position in the slope (Table 4; Fig. 4).

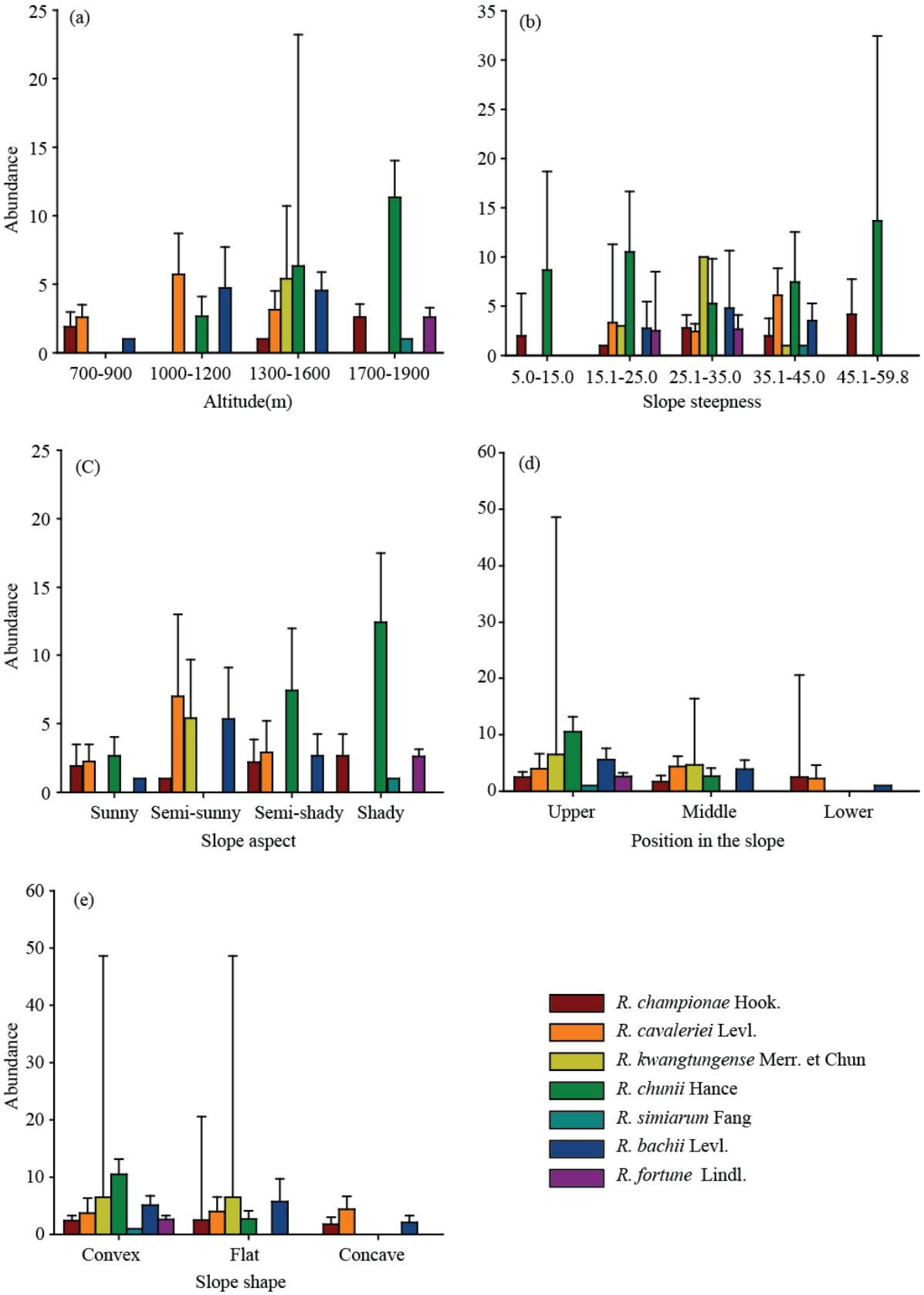

Fig. 2. Relationship between abundance of Rhododendrons and altitude (a), slope steepness (b), slope aspect (c), position in the slope (d), slope shape (e) in the Nanling Mountains, South China. The error bars represent the standard error.

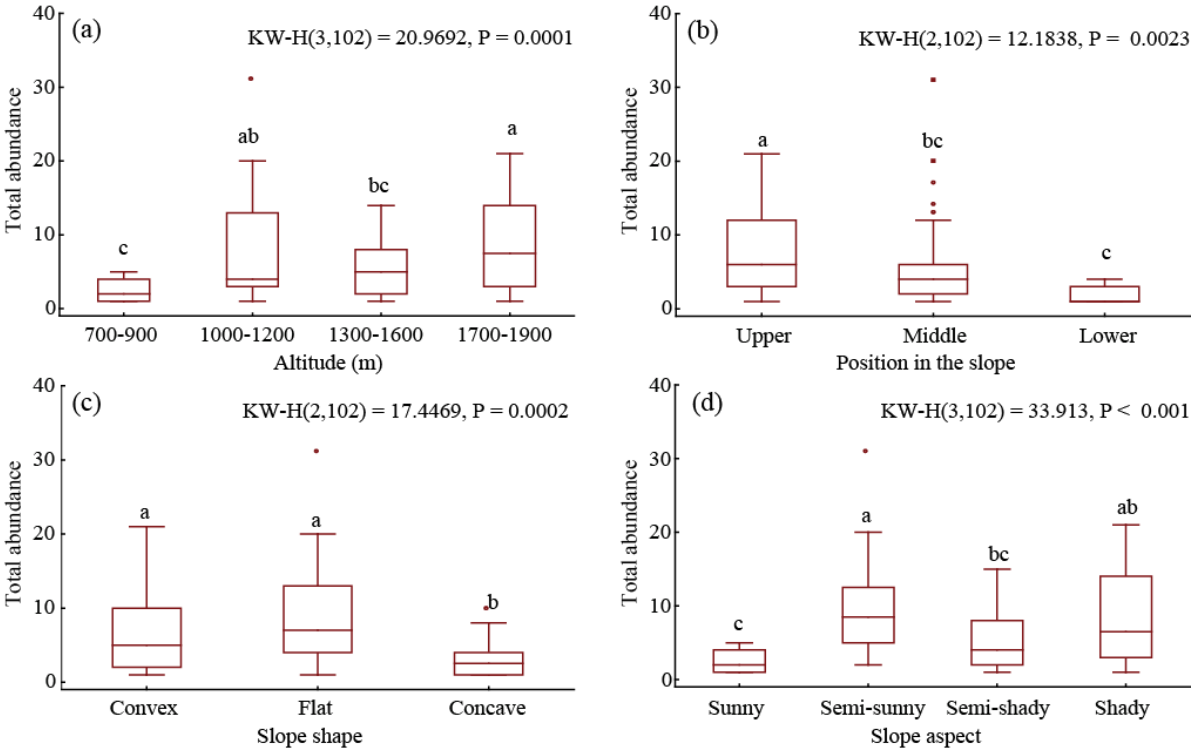

Fig. 3. Boxplots showing the Kruskal–Wallis test results for total abundance of Rhododendrons and altitude(a), position in the slope(b), slope shape (c), slope aspect(d) in the southern slope of the Nanling Mountains, South China. Different letters (a and b) in the graph show significant differences at the level of 0.05. The total abundance of Rhododendrons in our plots did not differ significantly with changes in slope steepness (p>0.05). The horizontal line in each box indicates the median, and the box endpoints indicate the 25th and 75th percentile values. The whiskers represent the non–outlier range. The circles and asterisks indicate the outliers and extreme values of rhododendron abundance, respectively.

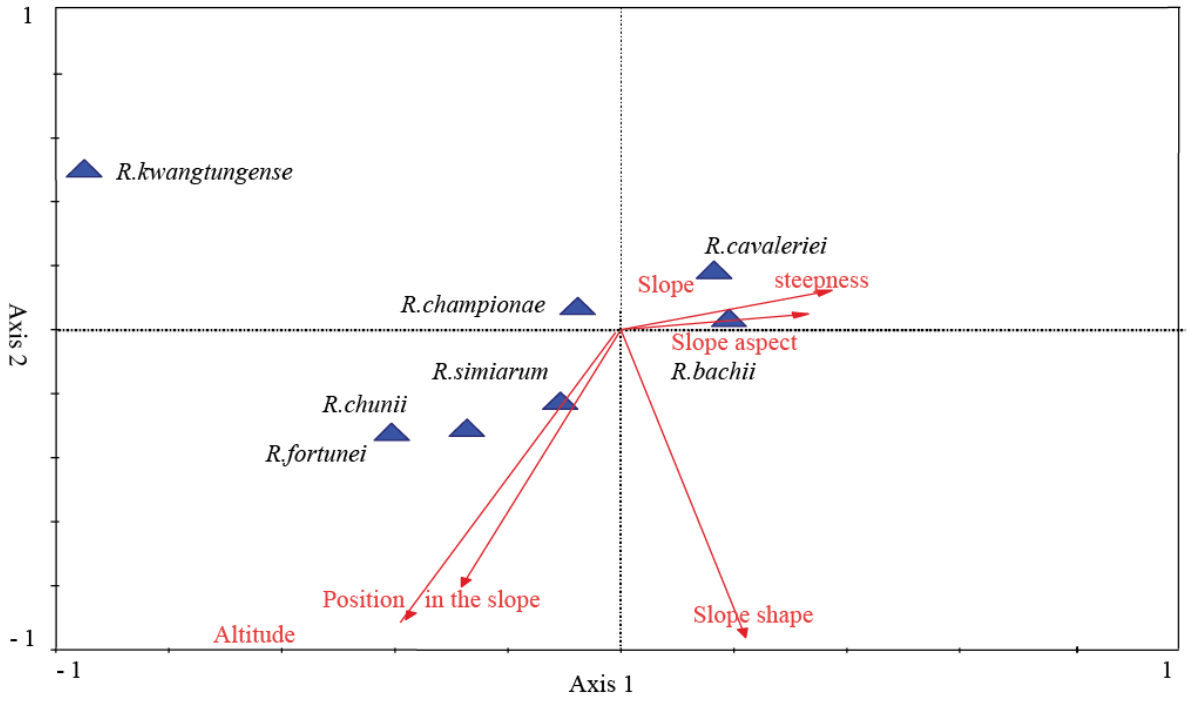

Fig. 4. Two–dimensional ordination diagram of canonical correspondence analysis (CCA) for seven species of Rhododendrons on 102 plots as constrained by five topographic variables in a subtropical mountain in Nanling, South China. The arrows represent the environmental variables. The length of an arrow indicates the strength of the correlation between the variable and axis.

Table 3. Summary and weighted correlation matrix of canonical correspondence analysis (CCA) for Rhododendrons in the southern slope of the Nanling Mountains, South China.

Attribute	Axis			
	1	2	3	4
Eigenvalue	0.636	0.402	0.035	0.012
Species–environment correlations	0.835	0.676	0.233	0.117
Cumulative % variance of species data	14.5	23.7	24.5	24.8
of species–environment relation	58.4	95,4	98.6	99.6
Intra–set correlations				
Altitude	–0.3185*	–0.6129**	0.0230	–0.0025
Slope steepness	0.3123*	0.0830	0.0280	–0.0884
Slope aspect	0.2770*	0.0338	–0.2101	–0.0115
Position in the slope	–0.2358	–0.5431*	0.0442	–0.0461
Slope shape	0.1850	–0.6499**	0.0271	–0.0050

Values at each treatment group followed by different letters are significantly different (*p<0.05, **p<0.01)

Table 4. Indicator Species Analysis (ISA) for Rhododendrons in the southern slope of the Nanling Mountains, South China based on topographic grouping variables. The topographic indicator species, *Rhododendron kwangtungense, Rhododendron championae, Rhododendron chunii* and *Rhododendron fortunei* were identified indicative of altitude, slope aspect, position in the slope and slope shape, respectively.

Grouping variable		Species name	IV	*P*
Altitude (m)	1300–1600	*Rhododendron kwangtungense*	14.3	0.0210
	1700–1900	*Rhododendron championae*	31.0	0.0010
	1700–1900	*Rhododendron chunii*	16.7	0.0090
	1700–1900	*Rhododendron fortunei*	20.8	0.0020
Slope aspect	Shady	*Rhododendron kwangtungense*	13.7	0.0210
Position in the slope	Upper	*Rhododendron fortunei*	11.4	0.0480
Slope shape	Concave	*Rhododendron championae*	22.4	0.0320
	Flat	*Rhododendron kwangtungense*	20.0	0.0020

No indicator species was found to be indicative of slope steepness (p>0.05)

Discussions

Topographic influence of rhododendron plants: Altitudinal belts are one of the most basic methods used in mountain vegetation research (Beals, 1969). Altitudinal effect on the composition and richness of montane plant assemblages are complex and involve different factors, including temperature, air pressure and precipitation (Krömer *et al.,* 2013). Biodiversity encompasses multiple levels of biological organisation. In different levels, species richness along the elevation gradient exhibits different distribution patterns (Mahdavi *et al.,* 2013; Ghazal, 2015). A consistent 'altitude concept' in comparative ecology is necessary, such as multivariate analysis of data from altitudinal gradients replicated across various regions contrasting in moisture regimes can assist in separating moisture from thermal effects (Körner, 2007). Studies pointed out that species richness peaks at lower and intermediate altitudes (Hao *et al.,* 2002). Our study demonstrated that species richness and abundance of rhododendron plants were greater in habitats of higher elevation, intermediate slope steepness, convex slopes, and shady aspect. By contrast, sunny habitats and habitat at lower positions in the slope had fewer rhododendron individuals. Among seven indigenous Rhododendrons in our study, *R. kwangtungense* was indicative of middle–elevations, shade–tolerant slope aspect and flat slope shape. *R. championae*, the strongest indicator species of high elevation, was also an indicator species of concave slope. *R. fortunei* was an indicator species of the upper position in the slope. Species used in vegetation restoration should be carefully selected based on local environmental characteristics (Zhang, 2013). This research can lead to a predictive understanding and potential management strategies for indigenous Rhododendrons in community–scale.

The ecological role of distribution of Rhododendrons: An earlier study found that elevation and slope aspect were important controls of palm species distribution in the Andes of north–western Ecuador, while small–scale topography was of little importance (Svenning *et al.,* 2009). Topographic gradient includes complex variables such as water, nutrients and disturbances. Species distributed on steep and concave slopes regenerate depending on disturbances such as landslides on unstable topography, whereas species distributed on ridges and upper slopes regenerate depending on the canopy gap. The total abundance of Rhododendrons was high on upper positions and convex slopes in the present study. Altitude, position in the slope and slope shape had greater impacts on the distribution patterns of rhododendron plants than slope steepness and slope

aspect. This study revealed that a community could be affected simultaneously by several topographic factors. Therefore interactions and compensations among topographic factors should be considered when assessing the effects of a single topographic factor on the spatial patterns of rhododendron plants. This finding was probably due to the fact that ridges or upper positions of gentle slopes are relatively stable in terms of soil surface disturbance, as demonstrated previously by Tsujino *et al*. (2009), who explained the large basal area found on this type of topography.

Conclusion

This study demonstrated that the topography affecting the richness and abundance of indigenous Rhododendrons. Altitude, position in the slope, slope shape and slope aspect had greater impacts on the distribution patterns of rhododendron plants than slope steepness. The richness and abundance of seven indigenous Rhododendrons varying in topographical gradient, and there are different patterns among species. *R. kwangtungense* was indicative of middle–elevations, shade–tolerant slope aspect and flat slope shape. *R. championae*, the strongest indicator species of high elevation, was also an indicator species of concave slope. *R. fortunei* was an indicator species of the upper position in the slope. The spatial heterogeneity of indigenous rhododendron plants distribution to topographic factors in the southern slope of the Nanling Mountains reflected their bioclimatic adaptation and phenology, indicating significant implications for species conservation and potentials for use in landscaping.

Acknowledgments

This study was supported by Guangdong Natural Science Foundation (Grant No. 2015A030313403) and the Science and Technology Planning Program of Guangdong Province (Grant No. 2013B020305009). The authors would like to thank for assistance in field plant identification.

References

Alves, L.F., S.A. Vieira, M.A. Scaranello, P.B. Camargo, F.A.M. Santos, C.A. Joly and L.A. Martinelli. 2010. Forest structure and live aboveground biomass variation along an elevational gradient of tropical Atlantic moist forest, Brazil. *For. Ecol. Manage.,* 260: 679-691.

Beals, E.W. 1969. Vegetation change along altitudinal gradients. *Sci.,* 5: 981-985.

Britton, M.N., T.A. Hedderson and V.G. Anthony. 2014. Topography as a driver of cryptic speciation in the high-elevation cape sedge *Tetraria triangularis* (Boeck.) C. B. Clarke (Cyperaceae: Schoeneae). *Mol. Phylogenet. Evol.,* 77: 96-109.

Coblentz, D. and P.L. Keating. 2008. Topographic controls on the distribution of tree islands in the high Andes of south-western Ecuador. *J. Biogeogr.,* 35(11): 2026-2038.

Enoki, T. 2003. Microtopography and distribution of canopy trees in a subtropical evergreen broad-leaved forest in the northern part of Okinawa Island, Japan. *Ecol. Res.,* 18(2): 103-113.

Fang, M.Y. 2005. Ericaceae. In: *Flora of China.* (Ed.): P.H. Raven, Science Press and Missouri Botanical Garden Press. Beijing and St. Louis, pp. 242-517.

Ghazal, A.M.F. 2015. Vegetation patterns and plant communities distribution along an altitudinal gradient at Asir mountain, southwest Saudi Arabia. *Pak. J. Bot.,* 47(4): 1377-1389.

Geng, Y.Y. 2010. Catalogue of Rhododendrons collected by George Forrest in China. *Guihaia,* 30(1): 13-25, 32 [In Chinese].

Hao, Z.Q., D.Y. Yu, J. Ye and P. Jiang. 2002. The estimation of species richness at different altitudes on the northern slope of Changbai Mountain. *J. Forest. Res.,* 13(3): 191-195.

Harris, C.M., H.L. Stanford, C. Edwards, J.M.J. Travis and K.J. Park. 2011. Integrating demographic data and a mechanistic dispersal model to predict invasion spread of Rhododendron ponticum in different habitats. *Ecol. Inform.,* 6(3-4): 187-195.

Hough, R.L., C. Crews, D. White, M. Driffield, C.D. Campbell and C. Maltin. 2010. Degradation of yew, ragwort and rhododendron toxins during composting. *Sci. Total. Environ.,* 408(19): 4128-4137.

Hsu, A., A. Lloyd and J.W. Emerson. 2013. What progress have we made since Rio? Results from the 2012 Environmental Performance Index (EPI) and Pilot Trend EPI. *Environ. Sci. Policy.,* 33: 171-185.

Körner, C. 2007. The use of 'altitude' in ecological research. *Trends Ecol. Evol.,* 22(11): 569-574.

Krömer, T., A. Acebey, J. Kluge and M. Kessler. 2013. Effects of altitude and climate in determining elevational plant species richness patterns: A case study from Los Tuxtlas, Mexico. *Flora*, 208(3): 197-210.

Laamrani, A., O. Valeria, Y. Bergeron, N. Fenton, L.Z. Cheng and K. Anyomi. 2014. Effects of topography and thickness of organic layer on productivity of black spruce boreal forests of the Canadian Clay Belt region. *For. Ecol. Manage.,* 330: 144-157.

Mahdavi, P., H. Akhani and E.Van der Maarel. 2013. Species diversity and life-form patterns in steppe vegetation along a 3000 m altitudinal gradient in the Alborz Mountains, Iran. *Folia Geobot.,* 48(1): 7-22.

Min, T.L. and R.Z. Fang. 1979. On the origin and geographic distribution of genus Rhododendron. *Acta Bot. Yunnan*, 1(2): 121-127. [In Chinese].

Morimoto, J. and H. Yoshida. 2005. Dynamic changes of native Rhododendron colonies in the urban fringe of Kyoto city in Japan: detecting the long-term dynamism for conservation of secondary nature. *Landscape Urban Plan.,* 70 (3-4): 195-204.

Olivero, A.M. and D.M. Hix. 1998. Influence of aspect and stand age on ground flora of southeastern Ohio forest ecosystems. *Plant Ecol.,* 139: 177-187.

Ou, Y.D., H.N. Wang, L. Zhang and Z.Y. Su. 2009. Topographic correlates of understory plant species distribution in Nanling National Nature Reserve. Guangdong. *J. Wuhan Bot. Res.,* 27(1): 41-46. [In Chinese].

Palmer, M.W. and P.M. Dixon. 1990. Small-scale environmental heterogeneity and the analysis of species distributions along gradients. *J. Veg. Sci.,* 1: 57-65.

Ranjitkar, S., E. Luedeling, K.K. Shrestha, K.Y. Guan and J.C. Xu. 2013. Flowering phenology of tree rhododendron along an elevation gradient in two sites in the Eastern Himalayas. *Int. J. Biometeorol.,* 57: 225-240.

Sattler, D., L.T. Murray, A. Kirchner and A. Lindner. 2014. Influence of soil and topography on aboveground biomass accumulation and carbon stocks of afforested pastures in South East Brazil. *Ecol. Eng.,* 73: 126-131.

Simonson, W.D., H.D. Allen and D.A. Coomes. 2014. Overstorey and topographic effects on understories: Evidence for linkage from cork oak (Quercus suber) forests in southern Spain. *For. Ecol. Manage.,* 328: 35-44.

Singh, K.K., L.K. Rai and B. Gurung. 2009. Conservation of Rhododendrons in Sikkim Himalaya: An Overview. *World J. Agri. Sci.,* 5(3): 284-296.

Su, Z.Y., X.D. Ke and S.J. Zhang. 2012. Vascular plants as indicators of organic carbon gradient in subtropical forested soils. *Pol. J. Environ. Stud.* , 21(5): 1393-1398.

Svenning, J., D. Harlev, M.M. Sørensen and H. Balslev. 2009. Topographic and spatial controls of palm species distributions in a montane rain forest, southern Ecuador. *Biodivers. Conserv.,* 18: 219-228.

Tsujino, R., H. Takafumi, N. Agetsuma and T. Yumoto. 2009. Variation in tree growth, mortality and recruitment among topographic positions in a warm temperate forest. *J. Veg. Sci.,* 17(3): 281 - 290.

Wurzburger, N. and R.L. Hendrick. 2007. Rhododendron thickets alter N cycling and soil extracellular enzyme activities in southern Appalachian hardwood forests. *Pedobiologia*, 50(6): 563-576.

Xing, F.W. 2012. Inventory of plant species diversity in Nanling Mountains., (Ed.): H. F. Chen, 1-2. Wuhan: Huazhong University of Science and Technology Press. [In Chinese].

Zhang, H.N. 2013. Effects of topographical and edaphic factors on the distribution of plant communities in two subtropical karst forests, southwestern China. *J. Mt. Sci.,* 10 (1): 95-104.

Zhao, B., J.J. Xu and X.Z. Zheng. 2015. Genetic relationship among nine rhododendron species in Qinling mountains, china using amplified fragment length polymorphism markers. *Pak. J. Bot.,* 47(3): 1069-1074.

(Received for publication 15 December 2015)

華南農業大學学报

JOURNAL OF SOUTH CHINA AGRICULTURAL UNIVERSITY

ISSN 1001-411X
CODEN HNDXBH
中国·广州
GUANGZHOU CHINA

全国中文核心期刊

2014

3月 第35卷 第2期
Mar. Vol.35 No.2

华南农业大学学报

第 35 卷　第 2 期　2014 年 3 月

目　　次

期刊基本参数：CN44-1110/S＊1959＊b＊A4＊116＊zh＋en＊P＊￥15.00＊1600＊22＊2014-03　　**封面设计**：林　敏

网络出版时间：2014-01-03 08:32
网络出版地址：http://www.cnki.net/kcms/detail/44.1110.S.20140103.0832.031.html
华南农业大学学报 2014,35(2):73-77
Journal of South China Agricultural University
http://xuebao.scau.edu.cn
doi:10.7671/j.issn.1001-411X.2014.02.014

张 璐,敬小丽,苏志尧,等:南岭山地杜鹃花沿海拔梯度的分布及其园林应用前景[J].华南农业大学学报,2014,35(1):73-77.

南岭山地杜鹃花沿海拔梯度的分布及其园林应用前景

张 璐,敬小丽,苏志尧,杜伟静
(华南农业大学 林学院,广东 广州 510642)

摘要:【目的】从植物资源利用的角度,定量研究南岭山地杜鹃花沿海拔梯度的分布,以期为城乡园林绿化推荐可供引种的潜在杜鹃花种类.【方法】在南岭山地海拔700~1 900 m范围内,采用样方法设置样地,运用相关分析和双向指示种分析(TWINSPAN)探讨南岭山地垂直带谱上的杜鹃花分异特征.【结果和结论】基于15 600 m^2样方数据,南岭山地共有杜鹃花属植物7种,皆为小径阶的常绿灌木或小乔木;TWINSPAN将7种杜鹃花分为3大类,第1大类由刺毛杜鹃 *Rhododendron championae*、猴头杜鹃 *R. simiarum* 和龙山杜鹃 *R. chunii* 组成,第2大类由多花杜鹃 *R. cavaleriei*、广东杜鹃 *R. kwangtungense* 和腺萼马银花 *R. bachii* 组成,云锦杜鹃 *R. fortunei* 自成第3大类,分类结果反映出南岭山地杜鹃花属沿海拔梯度的变化,揭示采用数量分类方法能够根据植被组成反映环境特点的生态原理;垂直带谱上,多花杜鹃分布最为广泛,其次为腺萼马银花,刺毛杜鹃和猴头杜鹃出现在多个海拔段.

关键词:垂直带谱;杜鹃花;园林绿化;南岭
中图分类号:S718.5 **文献标志码**:A **文章编号**:1001-411X(2014)02-0073-05

Rhododendron plants in Nanling mountains along an altitudinal gradient and the prospect of landscape greening

ZHANG Lu, JING Xiaoli, SU Zhiyao, DU Weijing
(College of Forestry, South China Agricultural University, Guangzhou 510642, China)

Abstract:【Objective】The objective was to determine the altitudinal pattern of *Rhododendron* plant distribution and the potential of using indigenous *Rhododendron* plant resource in landscape greening. 【Method】The continuous transect sampling method was employed and a total area of 15 600 m^2 was surveyed. A horizontal transect (10 m×120 m) was placed at an 100 m altitudinal interval from 700 m to 1 900 m a. s. l., representing the altitudinal range of *Rhododendron* in Nanling mountains of north Guangdong. The contiguous grid quadrat sampling method was used for plant census in each transect, which consisted of 12 quadrats (10 m×10 m). Correlation analysis and two-way indicator species analysis (TWINSPAN) were used to analyze the altitudinal patterns of *Rhododendron* species.【Result and conclusion】Seven *Rhododendron* species were found in the 15 600 m^2 plot, all of which were perennial evergreen woody shrubs or small trees. These *Rhododendron* species were divided into three categories by TWINSPAN. The first category was *R. championae*, *R. simiarum* and *R. chunii*; the second was *R. cavaleriei*, *R. kwangtungense* and *R. bachii*, and the third was *R. fortunei*. These TWINSPAN results indicated that environmental factors influenced the distribution and ecological characteristics of *Rhododendron* species. The most widely distributed species in an altitudinal spectrum is *R. cavaleriei*, followed by *R. bachii* and

收稿日期:2013-05-30 **优先出版时间**:
优先出版网址:
作者简介:张 璐(1973—),女,副教授,博士,E-mail:zhanglu@scau.edu.cn
基金项目:广东省自然科学基金(9451064201003716)

R. championae. The altitudinal patterns of these native *Rhododendron* species reflect their bioclimatic adaptation and phenology, which have potentials for use in landscape greening.

Key words: altitudinal spetrum; *Rhododendron*; landscape greening; Nanling mountains

杜鹃花是杜鹃花科 Ericaceae 杜鹃花属 *Rhododendron* 植物的统称,是世界四大著名花卉之一,也是我国十大传统名花和三大野生园艺植物的来源之一[1],自古以来被誉为花中"西施"[2]. 杜鹃花具有树形优美,花叶形态多样,色彩艳丽多变,花期长,适应性强等特点,是优质园林绿化资源,具有极高的观赏价值和经济价值. 杜鹃花属是杜鹃花科中最大的属,全世界约有 960 种,广泛分布于欧洲、亚洲、北美洲,主产东亚和东南亚. 中国拥有极其丰富的野生杜鹃花资源,约有杜鹃花 542 种,除新疆、宁夏外,各地均有,以云南、贵州、四川 3 省的山地最为丰富,为杜鹃花属植物的发源地及世界分布中心[3-4]. 华南的杜鹃花种类也有上百种,其中粤北占 24.5%,乳源县又占粤北的 80%[5]. 有研究指出,在山地垂直带中,杜鹃花组成了位于树线以上的杜鹃林、杜鹃矮林或灌丛植被带. 在森林中杜鹃也占有重要的地位,常组成优势的灌木层,或作为主要成分混生于森林中,是森林生态系统中的重要组成成分. 在 100 多年前,杜鹃花就已被种到英国,用于园林观赏. 目前,中国杜鹃花及其杂交后代已遍布世界各地. 尤其在欧洲,至今还没有一种观赏植物能代替中国常绿杜鹃花的地位. 但是,我国野生杜鹃资源在园林绿化上的应用相对滞后,野生杜鹃花的利用目前仍然处于直接从自然界获取的初期阶段,乡土野生杜鹃在园林绿化上应用少之又少. 许多珍贵品种,至今仍埋没山野,任其自生自灭,开发、保存、利用杜鹃花属植物资源已迫在眉睫. 因此,笔者基于样方调查数据,从杜鹃花资源利用的角度,定量研究垂直带谱上杜鹃花的分布,以期为城乡园林绿化推荐可供引种的潜在杜鹃花种类.

1 研究区域概况

南岭山地包括江西、湖南与广东、广西交界以及广西东北部山地. 南岭山地的中部,自西向东由越城岭、都庞岭、萌诸岭、骑田岭和大庾岭等五岭组成. 本研究地点设置在位于南岭山地中部的广东南岭国家级自然保护区内. 地貌以中山山地为主,山脉多为西北－东南走向,海拔千米以上的山峰有 30 多座. 成土母岩主要有花岗岩、砂页岩、变质岩等. 气候属典型的亚热带温湿气候,中山兼具亚热带季风气候特征,因地势高又具山地气候特色. 年均气温 17.7 ℃,年均降水量 1 705 mm,多集中于 8 月,年日照约 1 234 h,年相对湿度 84%. 水平地带性土壤为红壤,分布的土壤类型随海拔高度的不同而异[6]. 作为一块古陆,南岭在地史时期是古热带植物区系的避难所,也是近代东亚温带、亚热带植物的发源地和核心地带[7],具有丰富的物种资源,分布着广东省内最为典型的森林垂直带谱,地带性植被为常绿阔叶林,从山脚到山顶,植被类型依次为常绿阔叶林、常绿落叶阔叶混交林、针阔叶混交林、山顶矮林和山顶灌草丛.

2 研究方法

2.1 取样方法

在线路勘察的基础上,在广东第 1 峰石坑崆海拔 700 ~ 1 900 m 范围内,采用样方法设置 13 条水平样带,每条样带由 12 个 10 m × 10 m 的样方组成,共计调查了 15 600 m^2. 在每个 10 m × 10 m 样方单元内进行每木调查,并记录样方内所有维管束植物. 另外,在每个样方单元的四角和中心布设 5 个 2 m × 2 m 小样方,在每个 2 m × 2 m 小样方中进行林下植物调查,记录植物种名、株数和盖度.

2.2 数据分析

利用 13 条样带的乔木层样方物种多度矩阵信息,在软件 PC-ORD 6.0 的双向指示种分析(Two-way indicator species analysis, TWINSPAN)模块下,对南岭山地不同海拔梯度上杜鹃花属乔木层植物群落进行聚类分析.

3 结果与分析

3.1 杜鹃花属植物数量特征沿海拔梯度的变化

基于 15 600 m^2 样方数据,从海拔 700 ~ 1 900 m,共有杜鹃花属植物 7 种,分别为刺毛杜鹃 *Rhododendron championae*、广东杜鹃 *R. kwangtungense*、多花杜鹃 *R. cavaleriei*、猴头杜鹃 *R. simiarum*、龙山杜鹃 *R. chunii*、云锦杜鹃 *R. fortunei* 和腺萼马银花 *R. bachii*. 7 种杜鹃花皆为多年生常绿木本植物,灌木或小乔木,分布在海拔 900 m 的刺毛杜鹃最高达 16 m. 以胸径(DBH)大于 3 cm 的立木计算,南岭山地杜鹃花属植物以小径阶和低矮树为主(表 1),胸径 < 10 cm 的立木占全部立木数的 85.1%,占胸高

断面积总和的 50.7%. 同时,1 m≤树高 <5 m 的立木占总立木数的 49.2 %,多分布在海拔 1 200 ~ 1 900 m的山地. 其中,分布于 1 700 ~1 900 m 山地矮林中的杜鹃花高度普遍低于 5 m,云锦杜鹃平均树高仅为 2.4 m. 树高≥10 m 仅占总立木数的 5.1 %,均分布在 900 ~1 500 m 的海拔段. 5 m≤树高 <10 m 的立木,除了 1 900 m 外,各海拔段皆有分布.

南岭山地杜鹃花属植物物种丰富度和多度皆以 1 200 ~1 800 m 的海拔段较高(图 1). 各海拔段分布 1 ~4 种杜鹃花不等,多数海拔段分布 2 种. 海拔 1 300 m 分布刺毛杜鹃、多花杜鹃、广东杜鹃、腺萼马银花等 4 种,而海拔 1 900 m 仅分布云锦杜鹃 1 种.

表 1　杜鹃花属径阶和树高分布

Tab. 1　Diameter and height distribution of *Rhododendron*

径阶/cm	立木数/株	胸高断面积/cm^2	树高/m	立木数/株	胸高断面积/cm^2
3≤DBH <5	274	3 038.34	1≤*H* <5	311	9 313.90
5≤DBH <10	264	9 337.58	5≤*H* <10	289	12 008.52
10≤DBH <20	90	10 748.07	*H*≥10	32	3 106.27
DBH≥20	4	1 304.68			

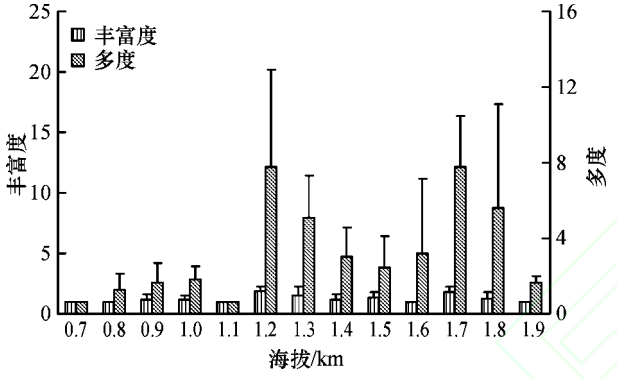

图 1　物种丰富度和多度沿海拔梯度的变化

Fig. 1　Species richness and abundance along an altitudinal gradient

3.2　垂直带谱上的杜鹃花分异特征

双向指示种分析(TWINSPAN)通常针对群落类型分类,本研究利用物种多度的信息,利用 TWINSPAN 在操作上具有同时划分样方和物种的性质,既实现了植被等级的划分,同时还完成了分类和分级的任务. TWINSPAN 将 7 种杜鹃花分为 3 大类. 第 1 大类由刺毛杜鹃、猴头杜鹃和龙山杜鹃组成,第 2 大类由多花杜鹃、广东杜鹃和腺萼马银花组成,云锦杜鹃自成第 3 大类(图 2). 第 1 大类中的刺毛杜鹃和猴头杜鹃在垂直带谱上分布较广,3 种杜鹃花在 1 800 m 海拔段都有分布;第 2 大类杜鹃花主要集中在中低海拔有分布,都只出现在 1 600 m 以下;而第 3 大类云锦杜鹃只出现在最高海拔段 1 900 m. 相关分析揭示南岭山地杜鹃花属植物与海拔呈显著线性正相关(r = 0.311 3, P = 0.001 4),TWINSPAN 的分类结果反映出南岭山地杜鹃花属 7 种杜鹃花沿海拔梯度分布,揭示采用数量分类方法能够根据植被组成反映环境特点的生态原理,快速提取指示种,使复杂的植被分类变得简捷化,得到比较客观、合理的分类结果.

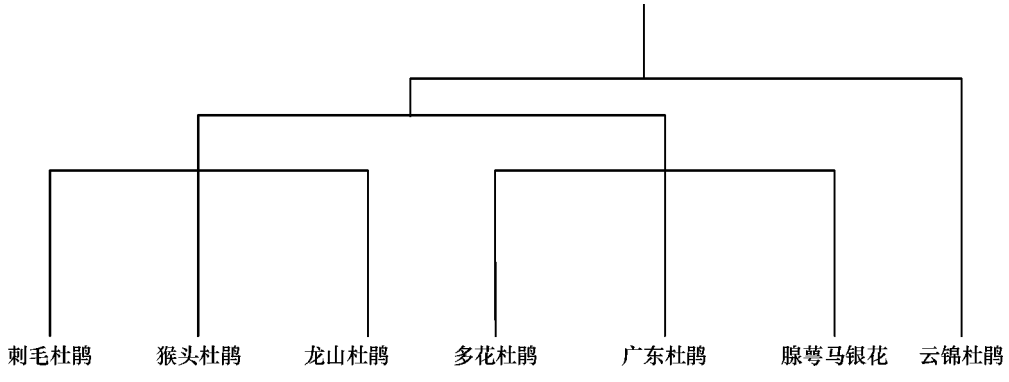

图 2　7 种杜鹃花的 TWINSPAN 分类

Fig. 2　TWINSPAN classification of seven species of *Rhododendron*

3.3　7 种杜鹃花沿海拔梯度的分布

南岭山地 7 种杜鹃花中,多花杜鹃分布最为广泛,海拔 700 ~1 500 m 都有分布,腺萼马银花在 700 ~ 1 600 m 的海拔段也多有出现,而广东杜鹃、龙山杜鹃和云锦杜鹃分布较窄,只分别出现在1 300、1 800和 1 900 m(图 3). 7 种杜鹃花中,猴头杜鹃数量最多

(199 株),占总立木数(633 株)的 31.4%;其次为多花杜鹃和腺萼马银花,分别占 27.3% 和 24.5%;龙山杜鹃数量最少,不足 10 株,云锦杜鹃也仅有 13 株.

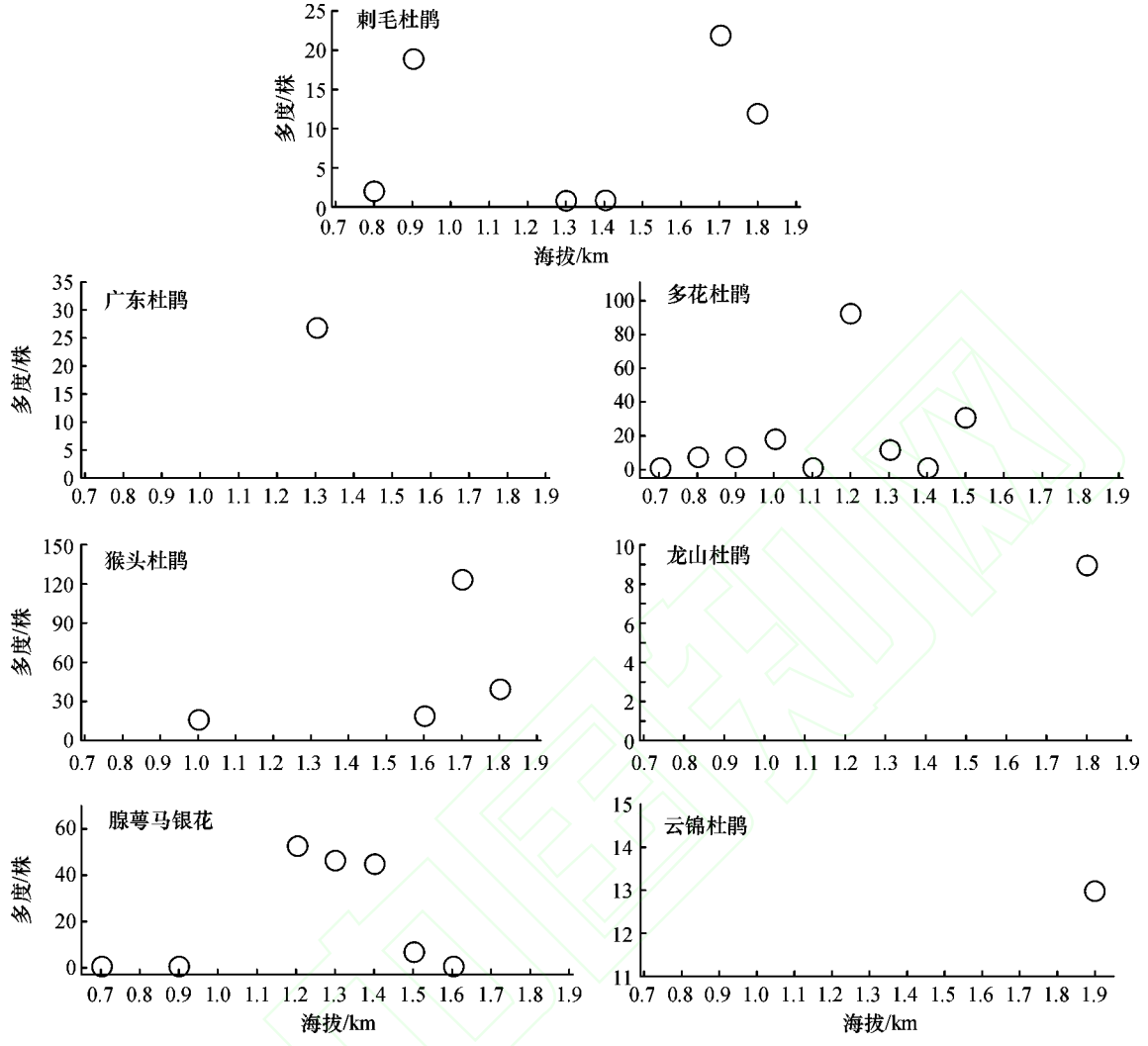

图 3 7 种杜鹃花多度沿海拔梯度的变化

Fig. 3 Abundance of seven species of *Rhododendron* along an altitudinal gradient

4 讨论

基于 15 600 m^2 样方数据,南岭山地共有杜鹃花属植物 7 种,皆为常绿灌木或小乔木,物种丰富度和多度呈现中间膨胀趋势. 垂直带谱上,多花杜鹃分布最为广泛,其次为腺萼马银花和刺毛杜鹃. 根据 TWINSPAN 分析,南岭山地杜鹃花属 7 种杜鹃花沿海拔梯度分为 3 个类型. 第 1 大类中的刺毛杜鹃和猴头杜鹃在南岭山地适应性较强,数量较多,长势良好;第 2 大类中的多花杜鹃和腺萼马银花在多个样带均有出现,但可能受光照、温度等条件限制,故和广东杜鹃一样,主要分布在中低海拔段;而自成一类的云锦杜鹃,树形低矮,分枝较多,叶厚革质,喜光,是典型的高山木本花卉. 在南岭杜鹃花垂直带谱中,云锦杜鹃仅分布在最高海拔段 1 900 m.

有研究表明,海拔是影响物种丰富度格局的决定性因素之一,物种丰富度与海拔梯度呈现负相关,或者物种丰富度随海拔的升高没有明显变化,或者表现为单调下降[8]、先下降后升高以及先升高后降低[9-10]. 不同分类群植物的物种丰富度随海拔升高的变化趋势是不同的[11],树种的再生能力随海拔升高而降低[12]. 杜鹃花喜疏松、酸性土壤,喜光但怕强光,杜鹃枝生长平均温度一般在 15 ℃左右,20 ~ 26 ℃时枝条快速生长,在 29 ℃以上进入休眠期,15 ℃以下开花时间延长至 50 d 以上[13]. 最近,针对树形杜鹃 *R. arboreum* 的研究指出,在全球变暖的大背景下,冬春气温的升高和高温对开花效应的影响将会促使杜鹃花分布范围扩大[14],有利于杜鹃花的引种驯化. 在垂直梯度上,随海拔的增加,杜鹃花的始花期和末花期相应延后[15].

广东省有 40 余种野生杜鹃花,虽然成功引种部分种类[16],但总体而言野生杜鹃花园林应用并不多. 目前城市绿化中最常用的种类是杂交种锦绣杜鹃 *R. pulchrum* 和凤凰杜鹃 *R. pulchrum* var. *phoeniceum*,偶见映山红 *R. simsii*[17]. 本研究结果揭示,南岭山地杜鹃花属植物物种丰富度和多度呈现中间膨胀趋势,前人的研究也支持物种丰富度中段膨胀模式[18-20]. 南岭山地杜鹃花主要分布在中、高海拔的针阔混交林、常绿落叶阔叶混交林和山顶矮林,但在水平地带性植被常绿阔叶林也有分布. 董安强等[21]对南岭秤架猴头杜鹃群落调查研究揭示,猴头杜鹃是该群落的绝对优势种,但处于衰退阶段. 在城市园林绿化应用中,杜鹃花是一个创新资源,在城市绿地系统生物多样性中有着重要地位[22]. 在南岭山地较高海拔段出现的猴头杜鹃在华南植物园的引种试验中能开花结果[16],说明在较高海拔山地分布的杜鹃花也能够成功引种驯化. 本研究结果表明,TWINSPAN 划分的第 2 大类多花杜鹃、广东杜鹃和腺萼马银花在南岭山地较低海拔段多有分布. 在线路勘察时发现,刺毛杜鹃在海拔 300 m 的常绿阔叶林林下也有较多分布,是除多花杜鹃和腺萼马银花外,在垂直带谱上分布较广的物种. 多花杜鹃、腺萼马银花和刺毛杜鹃等乡土杜鹃花在城市园林绿化中具有较大应用潜力.

参考文献:

[1] 程会凤, 沈守云, 詹文. 中国杜鹃属植物种质资源异地保存库建设及其园林应用[J]. 现代农业科技,2009(7): 66-68.

[2] 张华, 谢利娟, 白宇清, 等. 3 种杜鹃光合特性的比较[J]. 东北林业大学学报,2012, 40 (5): 59-61.

[3] 中科院中国植物志编辑委员会. 中国植物志: 第一卷[M]. 北京: 科学出版社, 1999: 57.

[4] 耿兴敏, 祝遵凌, 李敏, 等. 杜鹃花属植物扦插繁殖研究进展[J]. 中国野生植物资源,2011, 30(6):1-6.

[5] 郑文澄. 乳源县境内的杜鹃花[J]. 广东园林,1992(1):37-38.

[6] 庞雄飞. 广东南岭国家级自然保护区生物多样性研究[C]. 广州: 广东科技出版社, 2003:1-5.

[7] 陈林, 龚粤宁, 谢国光, 等. 广东南岭国家级自然保护区珍稀濒危植物及其保护[J]. 植物科学学报,2012, 30(3): 277-284.

[8] MAHDAVI P, AKHANI H, VAN DER MAAREL E. Species diversity and life-form patterns in steppe vegetation along a 3 000 m altitudinal gradient in the alborz mountains, Iran[J]. Folia Geobot, 2013,48(1): 7-22.

[9] LIEBERMAN D, LIEBERMAN M, PERALTA R, et al. Tropical forest structure and composition on a largescale altitudinal gradient in Costa Rica[J]. J Ecol, 1996,84(2):137-152.

[10] LOMOLINO M V. Elevation gradients of species density: Historical and prospective views[J]. Global Ecol Biogeogr, 2001,10(1):3-13.

[11] KESSLER M. Elevational gradients in species richness and endemism of selected plant groups in the central Bolivian Andes[J]. Plant Ecol, 2000, 149, 181-193.

[12] MAJILA B S, KALA C P. Forest structure and regeneration along the altitudinal gradient in the Binsar Wildlife Sanctuary, Uttarakhand Himalaya, India[J]. Russ J Ecol, 2010,41 (1):75-83.

[13] 张敬丽,赵海洲,吴雅文, 等. 杜鹃属植物在昆明市园林绿化中的应用研究[J]. 安徽农业科学,2012, 40(29): 14341-14344.

[14] RANJITKAR S, LUEDELING E, SHRESTHA K, et al. Flowering phenology of tree rhododendron along an elevation gradient in two sites in the Eastern Himalayas[J]. Int J Biometeorol,2013, 57(2): 225-240.

[15] RAWAT D S. Flowering phenology on altitudinal gradient in the Himalaya[J]. Curr Sci, 2012,103 (11):1281-1284.

[16] 许明英,李跃林,任海. 杜鹃花在华南植物园引种栽培的初步研究[J]. 福建林业科技, 2004, 31 (1): 53-56.

[17] 何卓彦,庄雪影. 杜鹃花属植物在广州园林绿地中的应用[J]. 广东园林,2009,31(1): 64-68.

[18] RAHBEK C. The role of spatial scale and the perception of large-scale species richness patterns[J]. Ecol Lett, 2005,8(2): 224-239.

[19] ZHAO Changming, CHEN Weilie, TIAN Ziqiang, et al. Altitudinal pattern of plant species diversity in Shennongjia Mountains, Central China[J]. J Integrat Plant Biol, 2005,47(12):143-449.

[20] DESALEGN W, BEIERKUHNLEIN C. Plant species and growth form richness along altitudinal gradients in the southwest Ethiopian highlands[J]. J Veg Sci, 2010,21(4): 617-626.

[21] 董安强, 梁耀, 胡明锋. 广东南岭国家级自然保护区南华杜鹃群落学研究[J]. 安徽农业科学, 2012, 40(21): 10929-10933.

[22] 张永辉,姜卫兵,翁忙玲. 杜鹃花的文化意蕴及其在园林绿化中的应用[J]. 中国农学通报,2007, 23 (9): 376-380.

【责任编辑　李晓卉】

華南農業大學学报

JOURNAL OF SOUTH CHINA AGRICULTURAL UNIVERSITY

华南农业大学学报

Huanan Nongye Daxue Xuebao

（双月刊，1959 年创刊，1980 年复刊）

第 35 卷　第 2 期　2014 年 3 月

Journal of South China Agricultural University

(Bimonthly, Started 1959, Resumed 1980)

Vol.35 No.2 Mar. 2014

主管单位：华南农业大学

主办单位：华南农业大学

主　　编：陈晓阳

编辑出版：华南农业大学学报编辑部

（广州五山，邮政编码: 510642）

网　　址：http://xuebao.scau.edu.cn

电子邮箱：journal@scau.edu.cn

电　　话：(020)85280069/38746672

印刷单位：暨南大学印刷厂

发行订购：华南农业大学学报编辑部

国外发行：中国国际图书贸易总公司

（中国国际书店）北京399信箱

Responsible Institution: South China Agricultural University

Sponsor: South China Agricultural University

Chief Editor: CHEN Xiaoyang

Edited and Published by Editorial Department, Journal of South China Agricultural University

Address: Wushan, Guangzhou, 510642, China

Website: http://xuebao.scau.edu.cn

E-mail: journal@scau.edu.cn

Tel: (86-20)85280069/38746672

Distributed by China International Book Trading Corporation(P.O.Box 399 Beijing, China)

国内外公开发行

国内定价：15.00 元/册

刊号：ISSN 1001-411X / CN 44-1110/S

ISSN 1001-411X

03>

9 771001 411140

中文核心期刊

ISSN 1001-389X
CN 35-1095/N

福建林学院学报

JOURNAL OF FUJIAN COLLEGE OF FORESTRY

福建农林大学 主办

SPONSORED BY
FUJIAN AGRICULTURE AND FORESTRY UNIVERSITY

ISSN 1001-389X
9 771001 389128 01>

第32卷 第1期 Vol. 32 No. 1
2012年1月 Jan., 2012
中国·福州 Fuzhou, China

福 建 林 学 院 学 报

Fujian Linxueyuan Xuebao

第32卷 第1期　　2012年1月15日

目　次

期刊基本参数：CN 35－1095/N＊1960＊q＊A4＊96＊zh＊P＊￥10.00＊1000＊20＊2012－01

主　编　洪　伟　　本期责任编辑　江　英

南岭自然保护区常绿阔叶林枯立木数量特征分析

张 璐[1,2],贺立静[1,3],区余端[1],苏志尧[1,2]
(1.华南农业大学林学院,广东 广州 510642;2.农业部生态农业重点开放实验室,
广东 广州 510642;3.琼州学院生物科学与技术学院,海南 三亚 572022)

摘要: 采用典型取样法,对南岭国家级自然保护区常绿阔叶林枯立木数量特征进行了研究。结果表明:(1)南岭国家级自然保护区0.9 hm^2的常绿阔叶林样地共有枯立木59株,27种,分属于16科23属。优势科为山茶科、壳斗科、大戟科和樟科。白锥、马尾松、红背锥、黄樟、青檀的重要值之和占样地枯立木总重要值的60%以上。(2)不同保护条件下,南岭国家级自然保护区常绿阔叶林枯立木数量特征表现不一,并非保护程度越高枯立木数量优势越明显。受保护条件最弱的试验区枯立木丰富度、多度、总胸高断面积和径级结构都最小,保护条件较好的缓冲区和核心区枯立木径阶分配比较均匀,但缓冲区枯立木的总胸高断面积却比核心区的多。(3)多响应置换过程分析和指示种分析揭示,枯立木对群落生境有明显的指示作用。不同保护条件下有不同的枯立木指示种($P<0.05$)。

关键词: 枯立木;物种组成;数量特征;径级结构;南岭自然保护区
中图分类号: S762.1 **文献标识码:** A **文章编号:** 1001-389X(2012)01-0064-06

Quantitative characters of standing dead trees of the evergreen broadleaved forest in Nanling National Nature Reserve, Guangdong, China

ZHANG Lu[1,2], HE Li-jing[1,3], OU Yu-duan[1], SU Zhi-yao[1,2]
(1. College o f Forestry, South China Agriculture University, Guangzhou, Guangdong 510642, China;
2. Key Laboratory of Ecological Agriculture of Ministry of Agriculture, Guangzhou, Guangdong 510642, China;
3. College of Bioscience and Biotechnology, Qiongzhou University, Sanya, Hainan 572022, China)

Abstract: Using the classic survey method, quantitative characters of standing dead trees of 3 forest communities under different protection regimes i. e., the experimental area, the buffer area and core area, respectively, each represented by 30 plots, in Nanling National Nature Reserve in Guangdong Province were studied. The results showed that: (1) 57 stems, 29 species in 23 genera and 15 families of standing dead trees were found in the 0.9 hm^2 plot. Dominant families of the flora were Theaceae, Fagaceae, Euphorbiaceae, Lauraceae. The total of important value of *Castanopsis fabric* Hance, *Pinus massoniana* Lamb., *Castanopsis fargesii* Franch., *Cinnamomum parthenoxylon* (Roxb.) Kost., *Pteroceltis tatarinowii* Maxim. account for more than 60% of the whole important value. (2) There was significant difference in quantitative characters of standing dead trees under different protection conditions. It is difficult to conclude that quantitative characters of standing dead trees with higher protection are better. The experimental area with the least protection, had the least species richness, abundance, total basal area, and size-class structure of standing dead trees than the other two. The buffer area and core area with higher protection had uniform size-class structure of standing dead trees, while the total basal area of standing dead trees of buffer area was more than that of core area. (3) The analysis of multi-response permutation procedures (MRPP) and indicator species analysis (ISA) identified that standing dead trees had a significant influence on the community habitat. There were different indicator species under different protection conditions.

Key words: standing dead trees; species composition; quantitative characters; size-class structure; Nanling National Nature Reserve

南岭山地是我国生物多样性保护的关键性地区和开展生态系统就地保护的重要基地[1],至今仍保存着大面积原生性较强的天然常绿阔叶林[2]。关于南岭国家级自然保护区的植物资源[3]、种间关系[4]、生活型[5]、群落特征[6]、物种多样性[7]、植被与地形相关性[8]已有大量的研究,但是南岭国家级自然保护区常绿阔叶林枯立木的数量特征尚未见报道。

收稿日期:2011-08-20 修回日期:2011-09-20
基金项目:广东省自然科学基金资助项目(9451064201003716);广东省林业科技创新专项(2010KJCX012-02);华南农业大学校长科学基金资助项目(2009K026)。
作者简介:张璐(1973-),女,副教授,博士,从事森林生态研究。通讯作者苏志尧(1963-)男,教授,博士生导师,从事森林生态和碳汇研究。E-mail: zysu@scau.edu.cn。

枯立木是森林生态系统中粗木质残体(coarse woody debris, CWD) 的重要组成部分[9] ,是组成森林生态系统食物网结构、空间结构的重要单元,也是联系森林生态系统养分循环、碳库贮存、群落更新以及为其它有机体提供生境等主要功能的载体和纽带[10-11] 。在枯立木众多生态功能中,最为突出的是为其它生物提供生境以维持生物多样性[12] 和延续生物地球化学过程[13] 。枯立木深刻影响着森林生态系统中的野生物种和生态进程[14] ,研究森林生态系统中枯立木的物种组成,是评价森林生态系统物种更替的有效方法[15] 。枯立木的体积常被认为对森林生物多样性有指示作用[16] 。

1　材料与方法

1.1　研究地概况

研究地设在广东南岭国家级自然保护区内,北纬 24°37′-24°57′,东经 112°30′-113°04′,区内总面积 58 368.4 hm^2,是广东省目前陆地森林面积最大的国家级自然保护区。该区属亚热带季风气候区,海拔 500 m,年平均气温 17.4 ℃,最冷月(1 月份) 平均气温 7.1 ℃,最热月(7 月份) 平均气温 26.2 ℃,年平均降水量 2 108.4 mm[17] 。区内地形复杂,山峰陡峭,坡度一般在 25°-55°之间,属中山地形,山脉多为西北—东南走向,主要由花岗岩、变质岩和砂岩组成。水平地带性土壤为红壤,分布的土壤随海拔高度的不同而异。该区森林覆盖率达 97%,地带性植被为常绿阔叶林,从山脚到山顶,植被类型依次为常绿阔叶林、常绿落叶阔叶混交林、针阔叶混交林、山顶矮林和山顶灌草丛[18] 。南岭国家级自然保护区常绿阔叶林群落外貌终年常绿,结构较复杂,物种组成丰富,区系成分以泛热带分布为主。组成种类以青冈[*Cyclobalanopsis glauca* (Thunb.) Oerst.]、红背锥(*Castanopsis fargesii* Franch.) 、白锥(*Castanopsis fabric* Hance) 、甜锥[*Castanopsis eyrei* (Champ.) Tutch.]等壳斗科(Fagaceae) 常绿树种占优势。此外,山茶科(Theaceae) 、大戟科(Euphorbiaceae) 、榆科(Ulmaceae) 、五列木科(Pentaphylacace) 等常绿树种如疏齿木荷(*Schima remotiserrata* Chang) 、毛果巴豆(*Croton lachnocarpus* Benth.) 、米碎花(*Eurya chinensis* R. Br.) 、青檀(*Pteroceltis tatarinowii* Maxim.) 、五列木(*Pentaphylax euryoides* Gardn. et Champ.) 也很常见。

1.2　研究方法

以线路调查为基础,采用典型取样技术,选择南岭国家级自然保护区内 3 个不同保护条件的山地常绿阔叶林作为调查点——乳源大桥镇石回寨(试验区,海拔 370 m) 、保护区管理局后山五里坑(缓冲区,海拔 600 m) 、南岭小黄山(核心区,海拔 1 300 m) 。在 3 个调查点中以相邻格子样方法分别设置 30 个 10 m×10 m的样方,取样总面积为 0.9 hm^2。在每个样方内进行每木调查,测定胸径(*DBH*) ≥3 cm 所有立木的胸径、树高、冠幅和林分郁闭度。枯立木要求 *DBH*≥5 cm,高度不低于 2 m[19] 。根据与枯立木丛生的个体、根部萌枝、树形或木质等特征确定枯立木的树种。在每个样方的四角和中心设置 5 个 2 m×2 m 的小样方,记录植物种名、株数和盖度,灌木和草本植物仅记录种类和数量。

1.3　数据统计分析

1.3.1　重要值测算　根据调查样地枯立木的胸径、树高、冠幅等数据,用多元统计分析软件 PC-ORD 4.0 测算枯立木的重要值。

1.3.2　多响应置换过程分析　采用检验 2 组或更多实体间差异性的非参数程序多响应置换过程分析(multi-response permutation procedures, MRPP) 法进行样地枯立木分布和不同保护条件间差异性检验。用 Sorensen 距离系数来计算距离矩阵。

1.3.3　指示种分析　采用指示种分析(indicator species analysis, ISA) 检测和描述样地枯立木对不同保护条件下的指示作用,并用蒙特卡罗检验来决定指示值(indicator value, *IV*) 的统计显著性。

MRPP 和 ISA 均在多元统计分析软件 PC-ORD 4.0 上运行。

2　结果与分析

2.1　枯立木的物种组成

南岭国家级自然保护区 0.9 hm^2 的常绿阔叶林样地共有枯立木 59 株,27 种,分属于 16 科 23 属(表 1) 。树种组成以壳斗科的白锥、红背锥,松科(Pinaceae) 的马尾松(*Pinus massoniana* Lamb.) ,榆科的

青檀,樟科(Lauraceae)的黄樟[*Cinnamomum parthenoxylon* (Roxb.) Kost]为主。其中,山茶科是第一大科,4属4种,其次依次为大戟科(3属3种),樟科(3属3种),金缕梅科(Hamamelidaceae)(2属2种),其余皆为单科单属。27个物种中,白锥的个体数最多(15株),出现在9个样方,重要值最大,为28.07%,其次是马尾松、红背锥、黄樟、青檀,重要值分别为12.27、9.24、5.79、5.11,排在前5位的物种重要值之和占样地枯立木总重要值的60%以上。

表1 南岭自然保护区常绿阔叶林枯立木的物种组成

Table 1 Species composition of standing dead trees of the evergreen broadleaved forest in Nanling National Nature Reserve

科名	种名	出现的样方数	株数	平均胸径/cm	重要值/%
大戟科(Euphorbiaceae)	毛果巴豆(*Croton lachnocarpus* Benth.)	2	2	5.1	2.55
	圆叶乌桕(*Sapium rotundifolium* Hemsl.)	1	1	3.3	1.25
	白楸[*Mallotus paniculatus* (Lam.) Muell.-Arg.]	1	1	3.0	1.25
壳斗科(Fagaceae)	白锥(*Castanopsis fabric* Hance)	9	15	19.7	28.07
	红背锥(*Castanopsis fargesii* Franch.)	3	3	24.5	9.24
	钩锥(*Castanopsis tibetana* Hance)	1	1	41.9	3.98
	甜锥[*Castanopsis eyrei* (Champ.) Tutch.]	1	1	11.7	1.45
松科(Pinaceae)	马尾松(*Pinus massoniana* Lamb.)	6	8	12.9	12.27
山茶科(Theaceae)	折柄茶(*Hartia sinensis* Dunn)	2	3	7.7	3.31
	疏齿木荷(*Schima remotiserrata* Chang)	2	2	4.8	2.54
	二列叶柃(*Eurya distichaophylla* Hemsl.)	1	1	4.3	1.26
	油茶(*Camellia oleifera* Abel.)	1	1	8.0	1.33
榆科(Ulmaceae)	青檀(*Pteroceltis tatarinowii* Maxim.)	4	4	5.1	5.11
樟科(Lauraceae)	黄樟[*Cinnamomum parthenoxylon* (Roxb.) Kost. I	3	3	18.7	5.79
	山苍子[*Litsea cubeba* (Lour.) Pers.]	1	1	3.0	1.25
	中华楠[*Machilus chinensis* (Champ. ex Benth.) Hemsl.]	1	1	7.8	1.33
金缕梅科(Hamamelidaceae)	大果马蹄荷[*Exbucklandia tonkinensis* (Lec.) Steenis]	1	1	6.3	1.29
	大叶蚊母树(*Distylium macrophyllum* Chang)	1	1	6.8	1.30
大风子科(Flacourtiaceae)	柞木[*Xylosma congestum* (Lour.) Merr.]	1	1	7.3	1.31
杜鹃花科(Ericaceae)	羊角杜鹃(*Rhododendron moulmainense* Hook.)	1	1	36.6	1.25
含羞草科(Mimosaceae)	山合欢[*Albizia kalkora* (Roxb.) Prain)	1	1	29.7	3.32
壳斗科(Fagaceae)	青冈[*Cyclobalanopsis glauca* (Thunb.) Oerst.]	1	1	6.0	1.25
五列木科(Pentaphylacace)	五列木(*Pentaphylax euryoides* Gardn. et Champ.)	1	1	12.1	1.46
杨梅科(Myricaceae)	杨梅[*Myrica rubra* (Lour.) Sieb. Et]	1	1	29.7	2.61
芸香科(Rutaceae)	小叶黄皮[*Clausena anisum-olens* (Blanco) Merr]	1	1	3.8	1.25
紫金牛科(Myrsinaceae)	密花树[*Rapanea neriifolia* (Sieb. et Zucc.) Mez]	1	1	6.0	1.29
交让木科(Daphniphyllaceae)	虎皮楠[*Daphniphyllum oldhamii* (Hemsl.) Rosenth.]	1	1	17.0	1.68

2.2 林分枯立木数量特征

试验区常绿阔叶林枯立木的丰富度和多度皆为最少的,仅有枯立木7种11株,出现在30个调查样方中的8个样方,且枯立木总胸高断面积仅为0.024 m^2(表2)。缓冲区和核心区常绿阔叶林枯立木分别出现在30个样方中的比例为40%和50%,枯立木丰富度相差不大,缓冲区常绿阔叶林枯立木的个体多度(19株)少于核心区常绿阔叶林枯立木的个体多度(29株),但缓冲区常绿阔叶林枯立木的总胸高断面积却比核心区常绿阔叶林枯立木的总胸高断面积多0.233 m^2。赖树雄等[6]对这3个调查点常绿阔叶林活立木结构研究指出,试验区常绿阔叶林的丰富度和平均胸径都最小,缓冲区常绿阔叶林的平均立木胸径占优势,而核心区常绿阔叶林在丰富度上表现出优势。本研究揭示,试验区枯立木丰富度、多度、总胸高断面积皆最低,缓冲区枯立木的总胸高断面积最大,核心区枯立木的丰富度和多度最大。究其原因,可能在于试验区人类活动较为频繁,而缓冲区常绿阔叶林群落有较多个体长成大树,如壳斗科的红背锥、钩锥、白锥等的枯立木胸径也较大,红背锥枯立木的胸径甚至达到了58.4 cm,故缓冲区枯立木丰富度和多度虽然没有核心区的大,但缓冲区枯立木的总胸高断面积最大。

2.3 枯立木径级结构

枯立木以小径级为主。5 cm≤*DBH*<10 cm、10 cm≤*DBH*<20 cm,20 cm≤*DBH*<30 cm、30 cm≤

DBH < 40 cm和 *DBH*≥40 cm 五个径级的枯立木分别为 35 株、11 株、6 株、3 株和 4 株,分别占枯立木总数的59.3%、18.6%、10.2%、5.1%和 6.8%(表 3)。

表 2　南岭自然保护区常绿阔叶林枯立木数量特征

Table 2　Quantitative characters of standing dead trees of the evergreen broadleaved forest in Nanling National Nature Reserve

样地	海拔/m	枯立木			活立木		
		丰富度	多度	总胸高断面积/m^2	丰富度	多度	总胸高断面积/m^2
试验区	370	7	11	0.024	31	1 050	3.719
缓冲区	600	10	19	0.942	51	473	9.901
核心区	1 300	11	29	0.709	63	861	10.451

表 3　南岭自然保护区常绿阔叶林枯立木径级结构

Table 3　Size-class structure of standing dead trees of the evergreen broadleaved forest in Nanling National Nature Reserve

样地	5 cm≤*DBH* < 10 cm	10 cm≤*DBH* < 20 cm	20 cm≤*DBH* < 30 cm	30 cm≤*DBH* < 40 cm	*DBH*≥40 cm
试验区	11	0	0	0	0
缓冲区	5	6	3	3	2
核心区	19	5	3	0	2
合计	35	11	6	3	4

不同保护条件对枯立木的径级大小影响不同。试验区临近村落,受到人为干扰较大,森林群落次生性较强,11 株枯立木径阶都小于 10 cm。缓冲区和核心区的常绿阔叶林保护得较好,缓冲区枯立木径阶分配比较均匀,5 个径阶皆有枯立木,表现为随胸径增大,枯立木个体数显著减少的趋势。核心区枯立木在 30 cm≤*DBH* < 40 cm 缺失,径阶分配也是以小径级的为主,3 cm≤*DBH* < 10 cm 的枯立木占整个核心区枯立木数的 65.5%。

2.4　枯立木对群落生境的指示作用

采用 MRPP 比较样地枯立木组成的差异。MRPP 是一个用于检验 2 组或更多实体间差异性的非参数程序,在生态群落研究中备受推崇。MRPP 提供检验统计量(test statistic, *T*)、一致性统计量(agreement statistic, *A*)和 *P* 值。*T* 是描述组间分离的检验统计量,*T* 负得越多,组间分离越强。*A* 是与随机预测值相比较,描述组内同质性的一致性统计量。多响应置换过程分析揭示(表 4),不同保护条件下常绿阔叶林对枯立木分布的影响具有统计学意义。试验区、缓冲区和核心区常绿阔叶林枯立木组间分离较强($T = -6.204\ 9$),组内一致性大于偶然预测值($A = 0.131\ 7$),表明试验区、缓冲区和核心区常绿阔叶林枯立木物种组成存在极显著差异。试验区、缓冲区和核心区常绿阔叶林枯立木的两两配对检验结果揭示常绿阔叶林枯立木物种组成两两之间均存在显著差异。

表 4　样地枯立木组成的多响应置换过程分析

Table 4　MRPP for species compositions among different transects

组别	预测值	观测值	方差	偏度	*T*	*P*	*A*
群落	0.500 0	0.434 1	0.000 0	−0.597 4	−6.204 9	<0.000 1	0.131 7
各群落配对比较							
试验区与缓冲区					−4.440 1	0.000 9	0.071 1
试验区与核心区					−5.772 0	0.000 3	0.088 9
缓冲区与核心区					−3.883 7	0.003 1	0.046 4

其中,试验区与核心区常绿阔叶林枯立木的组间分离最强,组内一致性最好($A = 0.088\ 9$, $P < 0.000\ 1$),枯立木物种组成差异最显著。缓冲区与核心区常绿阔叶林枯立木的组间分离最弱,组内一致性最差($A = 0.046\ 4$, $P < 0.000\ 1$),枯立木物种组成差异最不显著。

进一步采用 ISA 检测和描述枯立木与不同保护

表 5　南岭自然保护区常绿阔叶林枯立木指示种分析

Table 5　Indicator species analysis of standing dead trees of the evergreen broadleaved forest in Nanling National Nature Reserve

物种	分组	指示值	*P* 值
青檀	1	50	0.001
马尾松	3	40	0.014
红背锥	2	25	0.039
黄樟	2	25	0.043

条件下常绿阔叶林的关系。ISA 所用的 IV 值结合了组中物种的相对多度(relative abundance, RA) 和相对频度(relative frequency, RF) 的信息,即 $IV=100(RA\times RF)$;南岭国家级自然保护区常绿阔叶林枯立木指示种分析揭示: 不同保护条件下常绿阔叶林有不同的指示种。试验区枯立木的指示种是青檀,缓冲区的是红背锥和黄樟,核心区的是马尾松。其中,只有分布于试验区的唯一指示种青檀的 IV 值≥50($P<0.05$) 。究其原因,在于试验区的青檀、缓冲区的红背锥和黄樟,以及核心区的马尾松都是各区相对多度和相对频度最大或次大的。试验区枯立木青檀多达 4 株; 缓冲区和核心区枯立木物种较为丰富,分布也较均匀,红背锥和黄樟各为 3 株,马尾松 8 株分别是缓冲区和核心区除白锥外相对多度和相对频度最大的。白锥虽然在 0.9 hm^2 样地中个体数最多(15 株) ,但在缓冲区和核心区都有出现,故不能作为以分区为分组标准的指示种。

3 讨论

3.1 干扰强度与枯立木数量特征的关系

本研究揭示,南岭国家级自然保护区保护等级最低的试验区枯立木在丰富度、多度、总胸高断面积、以及平均立木胸径都比保护等级较高的缓冲区和核心区小。但并非保护程度愈高,群落枯立木在丰富度、多度、总胸高断面积、以及平均立木胸径等优势愈明显。赖树雄等[6]对该区森林群落活立木的研究也得出,频繁的人类活动对群落的丰富度、结构和区系成分的负面影响是明显的,但并非保护程度越高,群落的组成和结构越好。Connell[20]提出中等程度的干扰能维持较高的生物多样性的假说,但有人认为很难将这个假说一般化。因为所研究的群落类型,方法和尺度不同,所得出的结果不一定支持中等干扰假说。如何应用干扰来维持森林较高的多样性,是当前研究的一个新的热点,同时也为森林的经营和管理提供了信息帮助[21]。但是,如何保护和什么样的保护等级才能使生物多样性保持最高,一直未有一致的看法。进一步研究不同保护等级对常绿阔叶林枯立木组成、结构和多样性的影响对于常绿阔叶林保护具有积极的意义。

3.2 海拔梯度对枯立木的影响

由于海拔梯度包含了温度、水分、风力、光照和土壤等多种环境因子的综合影响,随着海拔的升高,生物群落表现出明显的垂直地带性分布规律。有研究指出,海拔因子是研究常绿阔叶林物种多样性、植被变化、群落结构和区系组成的重要因素[22]。不同分类群植物的物种丰富度随海拔升高的变化趋势不同[23],表现为单调下降、先下降后升高、或先升高后降低。本研究揭示,随着海拔的增加,该常绿阔叶林群落活立木和枯立木的物种丰富度也有所增加。究其原因,可能在于本研究试验区位于低海拔地带、缓冲区位于中海拔地带、核心区位于高海拔地带,海拔梯度对立木物种丰富度的影响比不上干扰的影响,故表现出受人为活动影响最大的低海拔试验区立木物种丰富度最小。

4 结论

南岭国家级自然保护区 0.9 hm^2 的常绿阔叶林样地共有枯立木 59 株,27 种,分属于 16 科 23 属。不同保护条件下,南岭国家级自然保护区常绿阔叶林枯立木的丰富度、多度、总胸高断面积、以及径级结构皆以试验区的最少,而缓冲区和核心区常绿阔叶林枯立木丰富度相差不大,但缓冲区森林群落枯立木的总胸高断面积却比核心区森林群落枯立木的总胸高断面积多。受保护条件较弱的试验区枯立木径阶都小于 10 cm,保护条件较好的缓冲区和核心区枯立木径阶分配比较均匀,表现为随胸径增大,枯立木个体数显著减少的趋势。多响应置换过程分析和指示种分析揭示,枯立木对群落生境有明显的指示作用。不同保护条件下有不同的枯立木指示种($P<0.05$) ,但只有试验区常绿阔叶林具有显著指示种青檀($IV\geq 50$) 。

参考文献

[1] 庞雄飞,庄雪影,田明义,等. 南岭和岭南——生物多样性特丰产地 [C] //庞雄飞. 广东南岭国家级自然保护区生物多样性研究. 广州: 广东科技出版社,2003: 28 – 64.

[2] 广东省科学家南岭森林生态考察团. 广东省南岭森林生态考察报告 [J] . 生态科学,1993(1) : 3 – 13.

[3] 李镇魁. 广东南岭国家级自然保护区珍稀濒危植物调查 [J] . 亚热带植物资源,2001,30(3) : 28 – 32.

[4] 张璐,苏志尧,陈北光. 中国特有植物华南五针松群落的种间关系研究 [J] . 生态学报,2006,26(4) : 1 063 – 1 072.

[5] 张璐. 苏志尧. 陈北光. 等. 广东石坑崆森林群落优势种群生态位宽度沿海拔梯度的变化 [J] . 林业科学研究,2007,20

(5):598 – 603.

[6] 赖树雄,区余端,苏志尧,等. 南岭国家级自然保护区不同保护条件下林分的组成和立木结构 [J]. 热带亚热带植物学报,2008,16(4):315 – 320.

[7] 田怀珍,邢福武. 南岭国家级自然保护区兰科植物物种多样性的海拔梯度格局 [J]. 生物多样性,2008,16(1):75 – 82.

[8] 区余端,王华南,张璐,等. 南岭国家级自然保护区林下植物分布的地形相关性 [J]. 武汉植物学研究,2009,27(1):41 – 46.

[9] Webster C R, Jenkins M A. Coarse woody debris dynamics in the southern Appalachians as affected by topographic position and anthropogenic disturbance history [J]. Forest Ecology and Management, 2005,217:319 – 330.

[10] Beets P N, Hood I A, Kimberley M O, et al. Coarse woody debris decay rates for seven indigenous tree species in the central North Island of New Zealand [J]. Forest Ecology and Management, 2008,256:548 – 557.

[11] Woodall C W, Liknes G C. Relationships between forest fine and coarse woody debris carbon stocks across latitudinal gradients in the United States as an indicator of climate change effects [J]. Ecological Indicators, 2008,8:686 – 690.

[12] Pesonen A, Leino O, Maltamo M, et al. Comparison of field sampling methods for assessing coarse woody debris and use of airborne laser scanning as auxiliary information [J]. Forest Ecology and Management, 2009,257:1 532 – 1 541.

[13] Bowman J C, Sleep D, Forbes G J, et al. The association of small mammals with coarse woody debris at log and stand scales [J]. Forest Ecology and Management, 2000,129:119 – 124.

[14] Stephens S L, Fry D L, Franco-Vizca´no E, et al. Coarse woody debris and canopy cover in an old-growth Jeffrey pine-mixed conifer forest from the Sierra San Pedro Martir, Mexico [J]. Forest Ecology and Management, 2007,240:87 – 95.

[15] Woodall C W, Nagel L M. Coarse woody type: a new method for analyzing coarse woody debris and forest change [J]. Forest Ecology and Management, 2006,227:115 – 121.

[16] Brin A, Meredieu C, Piou D, et al. Changes in quantitative patterns of dead wood in maritime pine plantations over time [J]. Forest Ecology and Management, 2008,256:913 – 921.

[17] 黄少敏,龙志强,张金泉. 广东南岭自然保护区地貌 [C] // 庞雄飞. 广东南岭国家级自然保护区生物多样性研究. 广州:广东科技出版社,2003:14 – 27.

[18] 中国植被编辑委员会. 中国植被 [M]. 北京:科学出版社,1980:1 – 87.

[19] 张树斌,郑征. 哀牢山中山湿性常绿阔叶林枯立木数量及分配规律 [J]. 东北林业大学学报,2009,37(2):3 – 5,13.

[20] Connell J H. Diversity in tropical rain forest and coral reefs [J]. Science, 1978,199:1 302 – 1 310.

[21] Odion C D, Sarr A D. Managing disturbance regimes to maintain biological diversity in forested ecosystems of the Pacific Northwest [J]. Forest Ecology and Management, 2007,246:57 – 65.

[22] Beals E W. Vegetation change along altitudinal gradients [J]. Science, 1969,165:981 – 985.

[23] El-Keblawy A, Ksiksi T. Artificial forests as conservation sites for the native flora of the UAE [J]. Forest Ecology and Management, 2005,213:288 – 296.

(责任编辑:江　英)

- 第三届中国高校优秀科技期刊
- 中国科技核心期刊
- RCCSE中国核心学术期刊
- 《国际农业与生物科学中心数据库（CABI）》收录期刊
- 《联合国粮食与农业组织国际农业科技情报系统数据库（AGRIS）》收录期刊
- 《中国科学引文数据库》来源期刊
- 《中国期刊全文数据库》收录期刊
- 《中国学术期刊综合评价数据库》来源期刊
- 《中国生物学文摘》收录期刊
- 《中国核心期刊（遴选）数据库》收录期刊

福建林学院学报

（季刊 1960年创刊）

第32卷 第1期 2012年1月15日

JOURNAL OF FUJIAN COLLEGE OF FORESTRY

(Quarterly, Started in 1960)

Volume 32 Number 1 January 15, 2012

主管单位 福建农林大学

主办单位 福建农林大学

编辑出版 《福建林学院学报》编辑部
（福州金山，邮政编码 350002）
E-mail: fjlb@chinajournal.net.cn

主　　编 洪　伟

副 主 编 尤民生 林思祖 卢凤美(常务)

印刷装订 福建农林大学印刷厂
（福州金山，邮政编码 350002）

发行范围 公开发行

国内发行 福州市报刊发行局

国外发行 中国国际贸易总公司
（北京399信箱，邮政编码 100044）

Sponsored by
Fujian Agriculture and Forestry University

Edited and Published by Editorial Department of Fujian College of Forestry
(Jinshan, Fuzhou, Fujian 350002, China)
E-mail: fjlb@chinajournal.net.cn

Chief Editor: Hong Wei

Deputy Chief Editor: You Minsheng, Lin Sizu, Lu Fengmei

Printed by Printing House of FAFU

Issued in Public

Distributed by Fuzhou Bureau for Distribution of Newspapers and Journals

Distributed abroad by
China International Book Trading Corporation
(P. O. Box 399, Beijing 100044, China)

ISSN 1001-389X
CN 35-1095/N

国外发行代号:Q7690　　国内邮发代号:34-90　　国内定价:10.00元

中文核心科技期刊
中国自然科学核心期刊
中国科学引文数据库来源期刊

ISSN 1001-1498
CODEN LKYAEB

林业科学研究

FOREST RESEARCH

第 20 卷 第 5 期 VOL. 20 NO. 5

2007 5

10>
771001 149005

中 国 林 业 科 学 研 究 院
THE CHINESE ACADEMY OF FORESTRY

林业科学研究　　第 20 卷　　第 5 期
Linye Kexue Yanjiu　　（双　月　刊）　　2007 年 10 月

目　次

期刊基本参数：CN 11-1221/S * 1988 * b * 16 * 148 * zh * P * ¥8.00 * 1500 * 26 * 2007-10

林业科学研究 2007,20(5):598～603
Forest Research

文章编号:1001-1498(2007)05-0598-06

广东石坑崆森林群落优势种群生态位宽度沿海拔梯度的变化

张 璐, 苏志尧*, 陈北光, 李镇魁

(华南农业大学林学院,广东 广州 510642)

摘要:在石坑崆从海拔300 m到海拔1 900 m的范围内,海拔每升高100 m设置一条水平样带,共计调查了17条样带,样地面积20 400 m^2。运用典范对应分析(CCA)和方差分析研究森林群落优势种群生态位随海拔梯度的变化。结果表明:(1)石坑崆森林群落优势种群皆表现出在腐殖质层厚度这一资源位上的生态位宽度最大,在坡度资源位上的生态位宽度最小的趋势;(2)单因素方差分析和Tukey's HSD多重比较进一步表明,常绿阔叶林优势种群5个资源位上的生态位宽度不存在显著差异($P > 0.05$),而针阔混交林和山地阔叶矮林的生态位宽度则存在显著差异($P < 0.001$);(3)优势种群生态位宽度的典范对应分析表明,坡向和枯枝落叶层厚度与石坑崆森林群落第一和第二排序轴的相关性较强,不同优势种群的生态位宽度在不同资源位上表现不一。典范对应分析与生态位宽度结合能较好地反映石坑崆森林群落优势种群生态位宽度与环境因子的关系。

关键词:生态位宽度;典范对应分析;海拔梯度;森林群落;南岭国家级自然保护区

中图分类号:S718.5 **文献标识码**:A

Variations in Niche Breadth of Dominant Plant Populations along an Altitudinal Gradient in Shikengkong of Guangdong Province

ZHANG Lu, SU Zhi-yao, CHEN Bei-guang, LI Zhen-kui

(College of Forestry, South China Agricultural University, Guangzhou 510642, Guangdong, China)

Abstract: A horizontal transect (10 m × 120 m) was placed at 100 m altitudinal interval from an elevation of 300 m to 1 900 m a. s. l. in Shikengkong. Canonical Correspondence Analysis (CCA) and One-way ANOVA were used to detect altitudinal patterns of niche and its environmental correlates. The results were as follows: 1) Dominant plant populations had the biggest niche breadth with thickness of humus layer as the resource state, which had the smallest niche breadth with slope as the resource state in Shikengkong; 2) One-way ANOVA and Tukey's HSD showed niche breadth of dominant populations did not change significantly in the evergreen broad-leaved forest ($P > 0.05$), while niche breadth of dominant populations in the coniferous and broad-leaved mixed forest and the montane broad-leaved and elfin forest change significantly ($P < 0.001$); 3) Canonical Correspondence Analysis indicated that aspect and litterfall were correlated with CCA axes 1 and axes 2. Dominant populations had different niche breadth as different resource states. Compared with niche breadth, CCA could indicate niche and its environmental correlates in Shikengkong.

Key words: niche breadth; Canonical Correspondence Analysis; altitudinal gradient; forest community; Nanling National Nature Reserve

收稿日期: 2006-12-26

基金项目: 香港嘉道理农场暨植物园资助项目(4400G04001);广东省科技项目(2002C20703)

作者简介: 张璐(1973—),女,博士,主要从事森林生态学研究. E-mail:zhanglu@scau.edu.cn

*通讯作者:苏志尧(1963—),男,博士,教授. E-mail:zysu@scau.edu.cn

生态位是生态学理论中一个应用广泛但定义繁多的概念[1]。生态位与种间竞争有关,同资源的利用密不可分[2]。通过植物利用资源的状况可以反映种群间相互关系。广东石坑崆保存着大面积的原生林和原生性较强的天然常绿阔叶林,是广东省目前保存得较好、面积较大的自然生态系统和物种宝库[3]。测度石坑崆森林群落生态位宽度随海拔梯度的变化,不仅可以揭示森林群落优势种群在森林中的生态适应幅度,还可以明确不同植物种群对生态条件要求的相似性程度,为森林环境资源的有效利用提供科学依据。

1　研究区域概况

研究地点设置在位于广东南岭国家级自然保护区及其周边地区广东乳源县大桥镇。南岭国家级自然保护区(112°30′～113°04′ E,24°37′～24°57′ N)总面积58 368.4 hm^2,是广东省目前陆地森林面积最大的国家级自然保护区。该区属于亚热带季风气候区,年平均气温17.4 ℃,最冷月(1月)平均气温7.1 ℃,最热月(7月)平均气温26.2 ℃,年均降水量2 108.4 mm[4]。在地质构造上属华南褶皱带的一部分,地貌以中山山地为主,石坑崆(1 902 m)坐落其间。水平地带性土壤为红壤[5],森林覆盖率达97 %[6]。

2　研究方法

2.1　野外取样

从海拔300 m到海拔1 900 m,海拔每升高100 m设置一条水平样带,共17条样带。样带长120 m,宽10 m,分为12个10 m×10 m的样方单元。共计调查了20 400 m^2。在每个10 m×10 m样方单元内进行每木调查,测定胸径≥3 cm的所有立木的种名、胸径、树高、冠幅和枝下高,并记录样方内所有维管束植物。另外,在每个样方单元四角和中心布设5个2 m×2 m小样方,在每个2 m×2 m小样方中进行:①林下植物调查,记录植物种名、株数和盖度;②更新频度调查,记录乔木树种在主林层、演替层和更新层的株数和高度。分别用手持式GPS、气压式海拔表、坡度计、郁闭度测定仪等实测样方的地理坐标、海拔、坡度、坡向、林冠郁闭度、土壤腐殖质层厚度和枯枝落叶层厚度等环境因子。

2.2　数据分析

利用17条样带的乔木层样方物种重要值矩阵信息,对石坑崆森林群落乔木层的植物群落,按照Flexible Beta.分组方法进行聚类分析。以环境变量中的坡度、坡向、腐殖质层厚度、枯枝落叶层厚度和林冠郁闭度为一维资源位状态,以个体多度为生态位计测的资源状态指标[7],计测各样带森林群落中6个优势种群在5个资源位以及整个群落优势种群的生态位宽度。坡度以5°为单位划分等级,坡向以每45°为一个区间划分等级,腐殖质层厚度、枯枝落叶层厚度和林冠郁闭度以实测数据为计测等级。利用物种与样方数据进行典范对应分析(Canonical Correspondence Analysis, CCA),分析各样带优势种群与环境因子的关系,并在CCA图中标示各优势种群的生态位宽度。

聚类分析和典范对应分析在软件PC-ORD[8]中完成,单因素方差分析及多重比较在软件Statistica[9]中完成。

3　结果与分析

3.1　森林群落聚类分析

乔木层是森林生态系统的主要成分,其组成成分决定了林下植物层的组成和结构。聚类分析结果表明,当Bray-Curtis距离系数为3.9时,石坑崆森林群落可分为常绿阔叶林、针阔混交林和山地阔叶矮林等植被类型(图1)。其中,常绿阔叶林包括样带1(海拔300 m)、样带2(海拔400 m)、样带3(海拔500 m)、样带4(海拔600 m)、样带5(海拔700 m)、样带6(海拔800 m)、样带7(海拔900 m)和样带9(海拔1 100 m)的森林群落。该类型森林群落主要分布在低海拔地段,乔木层主要以金缕梅科(Hamamelidaceae)占优势,优势种有檵木[*Loropetalum chinense* (R. Br.) Oliv.]、木果马蹄荷[*Exbucklandia tonkinensis* (Lec.) Steenis]、枫香(*Liquidambar formosana* Hance)等;针阔混交林包括样带8(海拔1 000 m)、样带10(海拔1 200 m)、样带11(海拔1 300 m)、样带12(海拔1 400 m)、样带13(海拔1 500 m)以及样带14(海拔1 600 m)的森林群落。该类型森林群落乔木层皆主要以松科(Pinaceae)的华南五针松(*Pinus kwangtungensis* Chun ex Tsiang)和五列木科(Pentaphylacaceae)的五列木(*Pentaphylax euryoides* Gardn. et Champ.)为优势种,二者在各样带的重要值都在30以上。华南五针松在样带14(海拔1 600 m)的重要值更是达到了92;山地阔叶矮林则包括了样带15(海拔1 700 m)、样带16(海拔1 800 m)以及样带17(海拔1 900 m)的森林群落。该类型由于主要分布在较高海拔地段,群落结

构相对简单，立木主要以山茶科(Theaceae)、杜鹃花科(Ericaceae)以及壳斗科(Fagaceae)的种类为主。如样带15(海拔1 700 m)以猴头杜鹃(*Rhododendron simiarum* Hance)的重要值最大(64)，样带16(海拔1 800 m)则以青冈[*Cyclobalanopsis glauca* (Thunb.) Oerst.]的重要值最大(47)，疏齿木荷(*Schima remotiserrata* H. T. Chang)在样带17(海拔1 900 m)的森林群落重要值也达到48。森林群落基本按照海拔从低到高组合，聚类分析结果反映出石坑崆森林群落沿海拔梯度的分布。

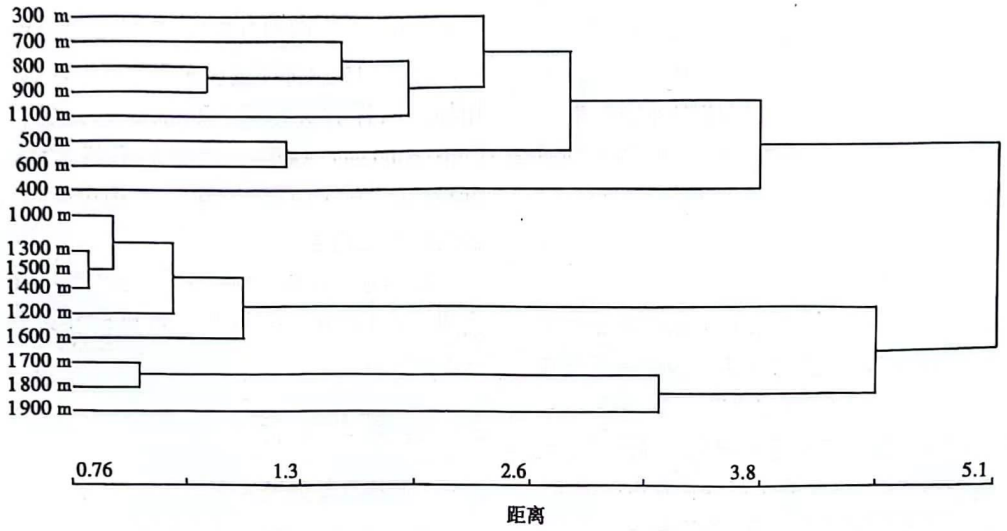

图1 广东石坑崆森林群落聚类分析

3.2 森林群落优势种群的生态位宽度

石坑崆森林群落优势种群在5个资源位上的生态位宽度见图2。从图2中可以看出，无论是常绿阔叶林、针阔混交林还是山地阔叶矮林，皆表现出优势种群在腐殖质层厚度这一资源位上的生态位宽度最大，在坡度资源位上的生态位宽度最小的趋势。

单因素方差分析和Tukey's HSD多重比较进一步指出，在显著水平 $\alpha=0.05$ 时，常绿阔叶林优势种群5个资源位上的生态位宽度不存在显著差异[$F(4,25)=2.446, P>0.05$]。而针阔混交林5个资源位上的生态位宽度差异显著[$F(4,25)=46.826, P<0.001$]。其中，坡度资源位上的生态位宽度与其他4个资源位上的生态位宽度差异尤为显著。与针阔混交林相似，山地阔叶矮林在5个资源位上的生态位宽度也存在显著差异[$F(4,25)=12.568, P<0.001$]。同样表现为坡度资源位上的生态位宽度与其他4个资源位上的生态位宽度差异显著，且坡向资源位与林冠郁闭度资源位上的生态位宽度之间差异不显著。但在针阔混交林不存在显著差异的腐殖质层厚度和枯枝落叶层厚度资源位上的生态位宽度，在山地阔叶矮林中却表现出显著差异。究其原因，可能与森林群落所分布的海拔高度有关。不同生境类型的森林群落优势种群生态位宽度表现不一，反映出环境因子影响森林群落优势种群的生态位宽度。

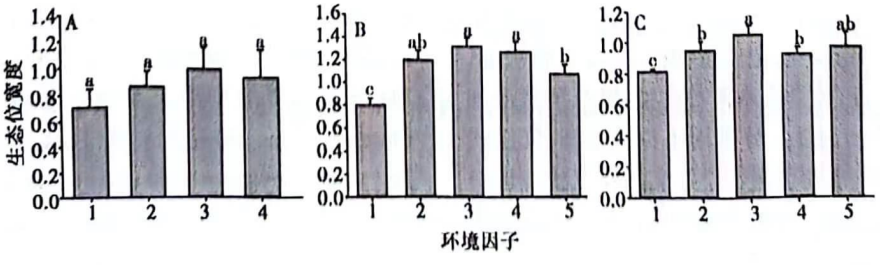

图2 广东石坑崆森林群落优势种群生态位宽度(均值±标准差，$n=6$)

注：1，2，3，4和5分别表示坡度、坡向、腐殖质层厚度、枯枝落叶层厚度和郁闭度；

A，B，C分别表示常绿阔叶林、针阔混交林、山地阔叶矮林。同一小写字母表示差异不显著。

3.3　优势种群生态位宽度的典范对应分析

石坑崆森林群落优势种群的生态位宽度的典范对应分析(CCA)见图 3 ～ 5。其中实心圆点代表优势种群,实线长度表示环境因子与乔木种类的相关性大小,实心圆点与实线的相对位置解释了乔木种类与环境因子的相关性,数值为各优势种群的总体生态位宽度。

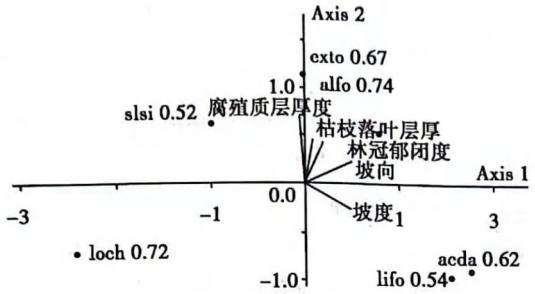

图 3　常绿阔叶林优势种群生态位宽度的典范对应分析

注:种群编码分别为 acda:青榨槭(*Acer davidii* Franch.);alfo:拟赤杨[*Alniphyllum fortunei*(Hemsl.) Makino];exto:大果马蹄荷[*Exbucklandia tonkinensis*(Lec.)Steenis];lifo:枫香(*Liquidambar formosana* Hance);loch:椎木[*Loropetalum chinense*(R. Br.)Oliv.];slsi:猴欢喜[*Sloanea sinensis*(Hance) Hemsl.]

常绿阔叶林典范对应分析(CCA)3 个排序轴的特征根值分别为 0.691、0.402 和 0.087,群落与环境因子 3 个排序轴的相关系数各为 0.871、0.729 和 0.398,且特征根和优势种群与环境因子的相关系数都通过蒙特卡罗检验($P<0.05$),说明排序效果理想。5 个环境因子与第一和第二排序轴均有不同程度的相关性。其中,坡度和坡向与第一排序轴的正相关性较强,相关系数 $r>0.87$,腐殖质层厚度与第二排序轴也有较强正相关性($r=0.91$)。优势种群拟赤杨在总体、腐殖质层厚度和枯枝落叶层厚度资源位上的生态位宽度是常绿阔叶林群落优势种群中最大的。而优势种群大果马蹄荷在坡向和林冠郁闭度资源位上的生态位宽度最大。优势种群猴欢喜在坡度资源位上的生态位宽度最大,但在总体资源位上的生态位宽度却最小。

针阔混交林典范对应分析(CCA)3 个排序轴的特征根值分别为 0.182,0.045 和 0.013,群落与环境因子 3 个排序轴的相关系数各为 0.717,0.696 和 0.520。坡度、坡向、腐殖质层厚度和枯枝落叶层厚度等环境因子与第一和第二排序轴的相关性较强。优势种群五列木在总体及 5 个资源位上的生态位宽度都是最大的,而优势种群疏齿木荷在总体、坡向、枯枝落叶层厚度以及林冠郁闭度等资源位上的生态位宽度都是最小的。

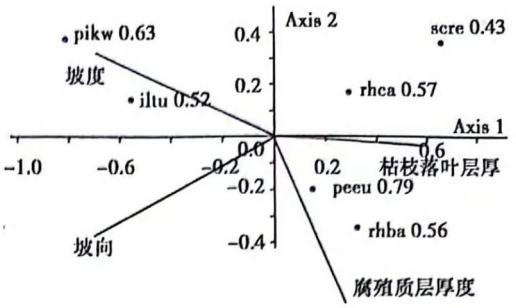

图 4　针阔混交林优势种群生态位宽度的典范对应分析

注:种群编码分别为 iltu:罗浮冬青(*Ilex tutcheri* Merr.);peeu:五列木(*Pentaphylax euryoides* Gardn. et Champ.);pikw:华南五针松(*Pinus kwangtungensis* Chun ex Tsiang);rhba:石壁杜鹃(*Rhododendron bachii* Lévl.);rhca:羊角杜鹃(*Rhododendron cavaleriei* Lévl.);scre:疏齿木荷(*Schima remotiserrata* H. T. Chang)。

山地阔叶矮林典范对应分析(CCA)3 个排序轴的特征根值分别为 0.218,0.095 和 0.065。林冠郁闭度与第一排序轴负相关性较强($r=-0.623$),坡向与第一排序轴有较强的正相关($r=0.341$)。与第二排序轴正相关较强的是枯枝落叶层厚度($r=0.476$),负相关较强的是坡向($r=-0.393$)。优势种群猴头杜鹃在总体资源位上生态位宽度最大,但在腐殖质层厚度和枯枝落叶层厚度资源位上的生态位宽度却是最小的。优势种群青冈在坡向和腐殖质层厚度资源位上的生态位宽度最大。甜槠[*Castanopsis eyeri*(Champ. ex Benth.)Tutch.]在林冠郁闭度资源位上的生态位宽度最大,但在坡度资源位上却最小。南亚新木姜[*Neolitsea zeylanica*(Ness.) Merr.]在总体和坡向资源位上的生态位宽度最小,但在坡度资源位上却是 6 个优势种群中最大的。

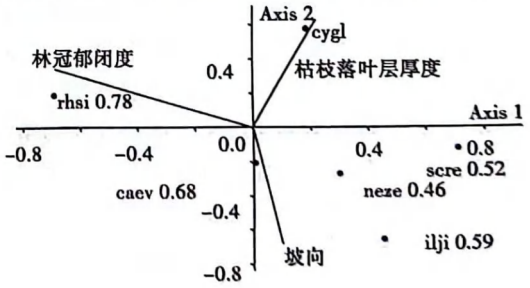

图 5　山地阔叶矮林森林群落优势种群生态位宽度的典范对应分析

注:种群编码分别为 caey:甜槠[*Castanopsis eyeri*(Champ. ex Benth.) Tutch.];cygl:青冈[*Cyclobalanopsis glauca*(Thunb.) Oerst.];ilji:假地枫皮(*Illicium jiadifengpi* B. N. Chang);neze:南亚新木姜[*Neolitsea zeylanica*(Ness.) Merr.];rhsi:猴头杜鹃(*Rhododendron simiarum* Hance);scre:疏齿木荷(*Schima remotiserrata* H. T. Chang)

4 结论与讨论

4.1 小结

石坑崆森林群落优势种群均在腐殖质层厚度这一资源位上的生态位宽度最大，在坡度资源位上的生态位宽度最小。单因素方差分析和 Tukey's HSD 多重比较揭示，常绿阔叶林优势种群 5 个资源位上的生态位宽度不存在显著差异($P>0.05$)，而针阔混交林和山地阔叶矮林群落的生态位宽度则存在显著差异($P<0.001$)。优势种群生态位宽度的典范对应分析表明，坡向和枯枝落叶层厚度与森林群落的第一和第二排序轴的相关性较强，不同优势种群的生态位宽度在不同资源位上表现不一。

4.2 讨论

4.2.1 *生态位宽度的计测* 目前在植物生态位宽度的测定中，有采用 1973 年 Whittaker 依据群落梯度分析中物种间的关系计算生态距离[10]。也有直接依据群落梯度差异，如以样方[11]、群落类型[12]、不同林层[7]等为一维资源位状态，以个体多度、重要值、胸高断面积等为生态位计测的资源状态指标计算生态位宽度。还有以环境梯度为一维资源位状态推算生态位宽度[13]。其中，有以海拔梯度为一维资源位状态[14]，也有根据植物群落下的土壤理化属性指标来建立环境梯度[15]，还有将地形特征加以分解定义，并以此环境梯度一维资源位状态推算生态位宽度[16]。以上种种方法中，第一种和第二种方法都仅仅依据植物群落本身的梯度推算生态位宽度，难免失之偏颇。第三种方法中的土壤理化属性具有极复杂的空间异质性和垂直层次上的分异，且变化的尺度难以测度。依据样方中个别土样反映整个样方的土壤属性，其结果存在着很大的不确定性。而作为环境状况的一种综合反映，地形体现了异质的环境梯度空间的直观梯度特征。在分析景观尺度上物种的生态位宽度时，借助于地形因子指标是一个有效的途径[16]。因此，本研究尝试以环境变量中的坡度、坡向、腐殖质层厚度、枯枝落叶层厚度和林冠郁闭度作为一维资源位状态，以个体多度为生态位计测的资源状态指标，计测各样带森林群落中 4 个优势种群在 5 个资源位以及整个群落优势种群的生态位宽度，分析石坑崆森林群落生态位沿海拔梯度的变化规律。

4.2.2 *生态位宽度的表达* 通常以矩阵形式来表示生态位宽度，也有学者[17]应用极点排序和图论聚类分析中的最小生成树法来表达。典范对应分析能够在同一排序图上展示植物种类与环境因子的关系，是当今生态学应用最广泛的直接梯度排序方法[18,19]。本文首次将典范对应分析与生态位宽度结合起来，较好地反映了石坑崆森林群落优势种群生态位宽度与环境因子的关系。

4.2.3 *生态位宽度沿海拔梯度变化规律探讨* 石坑崆森林群落 DBH≥3 cm 的优势种群没有一个连续出现在从海拔 300 m 到海拔 1 900 m 的样带中。优势种群五列木连续在海拔 1 000 m 到海拔 1 600 m 出现，但主要在海拔 1 300 m 和海拔 1 400 m 占优势地位，其总体及各资源位上均拥有较大的生态位宽度。其他优势种群，如黎蒴[*Castanopsis fissa* (Champ. ex Benth.) Rehd. et Wils.]在海拔 300 m，拟赤杨在海拔 800 m，华南五针松在海拔 1 500 m 和海拔 1 600 m，猴头杜鹃在海拔 1 700 m，假地枫皮在海拔 1 800 m 分别占优势地位，表现出较大的生态位宽度。王伯荪等[20]对海南岛热带山地雨林的研究也指出，五列木在山地雨林中垂直分布幅度最大，在霸王岭连续从海拔 750 m 一直分布到海拔 1 500 m，在五指山也从海拔 800 m 到 1 500 m。Stevens[21]认为分布在高海拔的物种需要更宽的生态位，从而导致分布在高海拔的物种数量减少，但本研究未能证实这一点。本研究表现出较大的生态位宽度的优势种群能够在多个样带连续出现，这也许从一个侧面解释了种群垂直分布的内在原因。

参考文献：

[1] 尚玉昌. 现代生态学中的生态位理论[J]. 生态学进展，1988，5(2)：77～84

[2] Silvertown J W. Plants in limestone pavements: tests of species interaction and niche separation [J]. J Ecol, 1983, 71:819～828

[3] 广东省科学家南岭森林生态考察团. 广东省南岭森林生态考察报告[J]. 生态科学，1993，(1)：3～13

[4] 黄少敏，龙志强，张金泉. 广东南岭自然保护区地貌[A]. 见：庞雄飞. 广东南岭国家级自然保护区生物多样性研究[C]. 广州：广东科技出版社，2003：14～27

[5] 张金泉. 广东省自然保护区[M]. 广州：广东省旅游出版社，1997：255～258

[6] 中国植被编辑委员会. 中国植被[M]. 北京：科学出版社，1980

[7] 苏志尧，吴大荣，陈北光. 粤北天然林优势种群生态位研究[J]. 应用生态学报，2003，14(1)：25～29

[8] McCune B, Mefford M J. PC-ORD. Multivariate Analysis of Ecological Data, Version 4.20 [CP/DK]. Gleneden Beach: MjM Software Design, 1999

[9] Statsoft Inc. STATISTICA for Windows (Computer Program Manual)

[CP/DK]. Tulsa: Statsoft, Inc. 1997

[10] 王刚,赵松岭,张鹏云,等. 关于生态位定义的探讨及生态位重叠计测公式改进的研究[J]. 生态学报, 1984, 4 (2): 119～127

[11] 李意德. 海南岛尖峰岭热带山地雨林主要种群生态位特征研究[J]. 林业科学研究, 1994, 71 (1): 78～85

[12] 杨远兵,刘玉成,钟章成. 重庆缙云山不同龄级植物种群生态位宽度研究[J]. 西南师范大学学报, 2001, 26 (1): 51～56

[13] 张远东,潘晓玲,顾峰雪,等. 阜康荒漠植被灌木与半灌木种群生态位的研究[J]. 植物生态学报, 2001, 25 (6): 741～745

[14] 郑元润. 大青沟森林植物群落主要木本植物生态位研究[J]. 植物生态学报, 1999, 23 (5): 475～479

[15] 刘加珍,陈亚宁,张元明. 塔里木河中游植物种群在四种环境梯度上的生态位特征[J]. 应用生态学报, 2004, 15 (4): 549～555

[16] 沈泽昊,方精云. 基于种群分布地形格局的两种水青冈生态位比较研究[J]. 植物生态学报, 2001, 25 (4): 392～398

[17] 郭水良. 浙江金华北山木本植物种群生态位研究[J]. 植物研究, 1998, 18 (3): 311～320

[18] Palmer M W. Putting things in even better order: the advantages of canonical correspondence analysis [J]. Ecology, 1993, 74:2 215～2 230

[19] Makarenkov V, Legendre P. Nonlinear redundancy analysis and canonical correspondence analysis based on polynomial regression [J]. Ecology, 2001, 83:1 146～1 161

[20] 王伯荪,张炜银,张军丽. 海南岛热带山地雨林种类组成的局域分布与垂直分布[J]. 应用生态学报, 2001, 12(5): 641～647

[21] Stevens G C. The elevational gradient in altitudinal range: an extension of Rapoport's latitudinal rule to altitude[J]. American Naturalist, 1992, 140:893～911

林业科学研究

LINYE KEXUE YANJIU

（双月刊，1988年创刊）

2007年10月　第20卷　第5期

FOREST RESEARCH

（Bimonthly, Started in 1988）

Vol. 20　No. 5　Oct. 2007

主　　管：国家林业局科技司

主　　办：中国林业科学研究院

主　　编：盛炜彤

编辑出版：《林业科学研究》编辑部

（北京万寿山后中国林科院，100091）

印　　刷：北京北林印刷厂

国内发行：中国林业科学研究院林业研究所

订 购 处：《林业科学研究》编辑部

国外发行：中国国际图书贸易总公司

（北京399信箱）

电子信箱：xumq@caf.ac.cn

电话：010-62889680. 62872015（传真）

Sponsored by Chinese Academy of Forestry

Chief Editor: SHENG Wei-tong

Edited & Published by the Editorial Department of Forest Research

（The Chinese Academy of Forestry, Wanshoushan, Beijing 100091, China）

Distributed by

Domestic: Research Institute of Forestry, CAF

Foreign: China International Book Trading Corporation (P. O. Box 399, Beijing, China)

E-mail: xumq@caf.ac.cn

Telephone: 86-10-62889680. 62872015 (Fax)

ISSN 1001-1498

CN 11-1221/S

国外代号：BM 4102

公　开　发　行

国内定价：8.00元

3.以通讯作者发表本专业论文情况

BMC Genomics

RESEARCH Open Access

High-quality chromosome-level genomic insights into molecular adaptation to low-temperature stress in *Madhuca longifolia* in southern subtropical China

Shuyu Wang[1], Haoyou Lin[1], Shuiyun Ye[1], Zhengli Jiao[2], Zhipeng Chen[1], Yifei Ma[1] and Lu Zhang[1*]

Abstract

Background *Madhuca longifolia*, the energy-producing and medicinal tropical tree originally from southern India, faces difficulties in adapting to the low temperatures of late autumn and early winter in subtropical southern China, impacting its usability. Therefore, understanding the molecular mechanisms controlling the ability of this species to adapt to environmental challenges is essential for optimising horticulture efforts. Accordingly, this study aimed to elucidate the molecular responses of *M. longifolia* to low-temperature stress through genomic and transcriptomic analyses to inform strategies for its effective cultivation and utilisation in colder climates.

Results Herein, the high-quality reference genome and genomic assembly for *M. longifolia* are presented for the first time. Using Illumina sequencing, Hi-C technology, and PacBio HiFi sequencing, we assembled a chromosome-level genome approximately 737.92 Mb in size, investigated its genomic features, and conducted an evolutionary analysis of the genus *Madhuca*. Additionally, using transcriptome sequencing, we identified 17,941 differentially expressed genes related to low-temperature response. Through bioinformatics analysis of the *WRKY* gene family, 15 genes crucial for *M. longifolia* low-temperature resistance were identified.

Conclusions This research not only lays the groundwork for the successful ecological adaptation and cultivation of *M. longifolia* in China's southern subtropical regions but also offers valuable insights for the genetic enhancement of cold tolerance in tropical species, contributing to their sustainable horticulture and broader industrial, medicinal, and agricultural use.

Keywords Whole genome, Transcriptome, *WRKY*, Tropical tree species

*Correspondence:
Lu Zhang
zhanglu@scau.edu.cn
[1]College of Forestry and Landscape Architecture, South China Agricultural University, Guangzhou, Guangdong 510642, China
[2]School of Life Sciences, Guangzhou University, Guangzhou 510006, China

Background

Ecological adaptation is a key mechanism for species to cope with environmental changes. Understanding the molecular mechanisms involved in adaptation is crucial for cultivating and utilising individual species. Temperature is an abiotic factor that considerably affects plant growth, development, and physiological activities. To mitigate the damage resulting from low temperatures, plants have developed cold acclimation mechanisms that involve a complex set of physiological and biochemical responses to environmental factors [1].

Madhuca longifolia (J. Koenig ex L.) J. F. Macbr, called 'Mahua' in India, is a broadleaf evergreen tree species originating from southern India and Burma and belonging to the family Sapotaceae. The species produces edible fruit and is a source of hardwood. *M. longifolia* is considered a panacea in Indian traditional medicine, with its leaves, flowers, seeds, and bark utilised as medicines [2–5]. Moreover, studies of *M. longifolia* suggest promising roles in food processing, renewable energy, urban greening and other fields. The flowers of the tree are universally utilised for food, feed, and fuel [6]. Its seed oil is a promising non-edible oil that can be employed to improve the quality of bitumen [7]. *M. longifolia* provides a solution for the three major "Fs", namely food, forage and fuel [8]. This plant can be considered an effective agent against oral diseases like dental caries [9]. A nano-composite material prepared from the seed extract of *M. longifolia* has a remarkable insecticidal effect on vector larvae and can be used to control mosquitos and other major vectors as an eco-friendly substitute for modern chemical synthetic insecticides [10]. Furthermore, the bark fibre of *M. longifolia* has robust tensile strength, light weight, and good thermal steadiness and is appropriate for manufacturing biodegradable materials for sporting goods, automotive body panels, wallboards, partitions, and non-structural lightweight components in the construction industry [11]. The tree has a strong tolerance to air pollution and can help in its alleviation through its high capacity for absorbing greenhouse gases and other air pollutants. It is one of the most promising street trees for urban greening in the humid tropics [12].

Valued for its industrial and medicinal uses, *M. longifolia* was introduced to China in 1964, where it has shown potential for anti-typhoon forest development in Hainan province [13]. However, climatic differences can lead to unforeseeable outcomes when attempting to acclimatise woody species to locations beyond their native habitat [14]. In China, *M. longifolia* faces challenges in temperature acclimatisation, with low temperatures causing growth stagnation and mortality in seedlings. Our team's previous research found that after the introduction of *M. longifolia* to the southern subtropics in China, there is a risk of the air temperature plummeting to around 10 ℃ during the cold snap in late autumn and early winter when the buds emerge from the soil. Once this happens, even if the air temperature rises after a few days, it will cause harm to the young buds, showing that the young buds and young leaves lose water and wilt, leading to their growth stagnation, and even causing their death in serious cases. To date, there have been no reports on the temperature adaptation of *M. longifolia* after its introduction to South China, and there are very few studies on its genomics, and information on ploidy, chromosome number and genome size is unknown. This absence of whole-genome data has limited research on its phylogenetic origin and evolutionary history and hindered attempts to improve breeding, ecological adaptation, and related biological aspects.

Plant genome sequencing serves as a highly useful tool for studying the molecular mechanisms underlying plant adaptation and determining the impacts of environmental stressors on the evolution, growth, and development of plants as well as allowing for the domestication of useful traits [15]. For example, by sequencing and screening possible genes linked with flowering, growth, and responses to osmotic pressure and temperature stress, Sork et al. [16] revealed important insights into the spatial selection of climate-related genes within natural populations of *Quercus lobata*, highlighting potential environmental adaptation mechanisms of the species. Similarly, the construction of a high-quality reference genome for *Corylus heterophylla* elucidated the molecular mechanisms underlying its response to environmental stress and informed genetic guidelines for optimised breeding [17].

In addition to genome sequencing, RNA-sequencing (RNA-seq) is an important tool for analysing differential gene expression with the transcriptome and understanding genome function, precisely determining gene expression and supporting precise bioinformatic analyses [18, 19]. Transcriptome analyses have been conducted to screen plant genomes for functional genes regarding low-temperature stress resistance and to obtain high-throughput expression data for these key genes. For instance, a transcriptome analysis of cold-tolerant *Zea mays* under cold stress yielded 43 million high-quality sequences, from which a weighted gene co-expression network analysis recognised *Zm00001d037590* and *Zm00001d012321* as the most likely key genes concerning cold hardiness at the seedling stage [20]. Similarly, transcriptome sequencing analysis of *Eremochloa ophiuroides* showed that the expression of genes encoding AUX_IAA as well as *WRKY* and heat shock factor (HSF) transcription factors (TFs) increased with different low-temperature stress treatments [21]. A transcriptome and weighted gene co-expression network analysis of *Ilex dabieshanensis* after cryogenic treatments of different

durations revealed 5,750 differentially expressed genes (DEGs), among which the hub genes for stress response to low temperature were *evm.TU.CHR1.1507* and *1821* and *evm.TU.CHR2.210*, *244*, and *89* [22].

TFs assume an essential role in governing the transduction of signals and the management of gene expression in response to environmental stress. Identification of TFs is infuenced by the annotation quality of genome [23]. The developments of whole genome sequencing in walnut and woody species have revealed evidence of cold and chilling stress and the genome-wide identification of gene families related to stress studies [24]. The *WRKY* gene family is specific to algae and higher plants and greatly affects many plant life processes, particularly in response to biological stress [25, 26]. In *Oryza sativa*, *OsWRKY71* acts as a beneficial controller of responses to low-temperature stress, enhancing the photosynthesis and survival of plants [27]. In contrast, in *Arabidopsis thaliana*, *AtWRKY34* negatively influences plant growth in cold temperatures [28]. In *Musa acuminata* fruits, four *MaWRKY*s enhance low-temperature resistance through an abscisic acid (ABA)-mediated signalling pathway [29]. Based on these examples, studying the *WRKY* gene family through transcriptome analysis is a particularly effective method for studying plant stress resistance at the molecular level. Despite their value, genomic and transcriptomic analyses have not yet been used to elucidate the molecular mechanisms underlying low-temperature stress responses in *M. longifolia.*

The present study aimed to identify the key genes controlling the low-temperature response of *M. longifolia* through transcriptome and whole-genome sequencing. The results could provide a theoretical basis for the comprehensive cultivation and utilisation of this species in subtropical China and a reference for future ecological studies of *Madhuca*-related species.

Methods

A comprehensive methodology was employed to explore the genomic and transcriptomic responses of *M. longifolia* to low-temperature stress. The approach included the cultivation of *M. longifolia* from seeds, isolation of genomic DNA for sequencing and assembly, and genome annotation to identify coding and non-coding regions. A phylogenetic analysis was conducted to place *M. longifolia* in its evolutionary context. Transcriptome sequencing of seedlings under low-temperature conditions was performed to analyse gene expression changes, focusing particularly on the *WRKY* gene family owing to its role in stress response. Quantitative real-time PCR (qPCR) was utilised to verify key findings obtained from RNA-seq. This methodology aimed to elucidate the molecular mechanisms underpinning *M. longifolia*'s adaptation to low temperatures.

Sample collection, genomic DNA extraction and chromosome counts

The mature seeds of *M. longifolia* that had fallen to the ground were collected at South China National Botanical Garden, Tianhe District, Guangzhou, Guangdong, China (113°21′50″E, 23°11′7.3″N). *Madhuca longifolia* seeds were germinated on wet paper towels and then transplanted to peat soil for cultivation after the embryonic roots emerged. The cultivation site was outside the College of Forestry and Landscape Architecture, South China Agricultural University, Tianhe District, Guangzhou City, Guangdong Province, China (113°21′20″E, 23°9′44″N). From among the artificially grown seedlings, we randomly selected a well-grown, healthy, and pest-free specimen and collected its healthy mature leaves for DNA collection. Genomic DNA extraction was conducted utilising cetyltrimethylammonium bromide (CTAB) method. The leaves were grinded into fine powder by liquid nitrogen and then transfer approximately 100 mg to a pre-cooled 2 mL centrifuge tube. After mixing with 1 mL pre-warmed CTAB extract and 20 μL β-Mercaptoethanol, the samples were incubated in a 65 ℃ constant temperature water bath for 1 h, and the samples were mixed upside down several times during the water bath. Then the samples were cooled to room temperature and centrifuged at room temperature, 12,000 rpm for 10 min. The supernatant was mixed with an equal volume of chloroform: isoamyl alcohol (24:1) and centrifuged at room temperature for 10 min at 12,000 rpm. Then the supernatant was mixed with an equal volume of phenol: chloroform: isoamyl alcohol (25:24:1) and centrifuged at room temperature for 10 min at 12,000 rpm. The supernatant was again aspirated and mixed with an equal volume of chloroform: isoamyl alcohol (24:1) and centrifuged at room temperature and 12,000 rpm for 10 min. The nucleic acid was precipitated with isopropanol, washed with 75% ethanol and dissolved in 50 μL ddH_2O. DNA quality was confirmed using NanoDrop and Qubit spectrophotometers (Thermo Fisher Scientific, Waltham, MA, USA). Lastly, 1% agarose gel electrophoresis was employed for testing the sample DNA integrity. The seedlings of 10-month-old *M. longifolia* were selected for chromosome counts. At approximately 9:00 am when the meristems of the plant root tips were flourishing, a 1–2 cm section was excised from the root tips using a blade. The apical materials were treated with 0.002 mol/L quinolin-8-ol solution for 1.5 h. The plant material was rinsed twice with distilled water, transferred to Carnot's fixative for 24 h, and then washed twice with water for 20 min each. Then 2.5% cellulase and 2.0% pectinase solution were added and treated for 2.5 h at 37 ℃. After removing the enzyme solution, the sample was rinsed with distilled water for 2–3 times and let stand in the water for more than 40 min. The treated

root tip was placed on a glass slide and the root cap and elongation area were excised, leaving only the meristems. Finally, the prepared specimen was stained in basic fuchsin dye solution for 10–15 min, and then dried for chromosome counting in root tip cells. The micrographs were taken with an CX33 microscope camera system (Olympus).

Genome sequencing and assembly

Quality-checked genomic DNA was interrupted with Yeasen enzyme digestion kit (Hieff NGS® OnePot TM II DNA Library Prep Kit for MGI®). A total of 1 μg of genomic DNA, 10 μL of Smearase® Mix, and ddH_2O was added to the PCR system to a total volume of 60 μL. The PCR programme was 4 ℃ for 1 min, 30 ℃ for 15 min, 72 ℃ for 20 min and 4 ℃ hold. Then, the NEBNext Ultra DNA Library Prep Kit library (New England Biolabs, Ipswich, MA, USA) was adopted for repairing ends and adding A-tails and Illumina sequencing connectors. DNA fragments of 300–400 bp in length were concentrated by PCR; an AMPure XP system (Beckman Coulter, Brea, CA, USA) was used for PCR product purification. The library was assayed using an Agilent 2100 Bioanalyzer (Agilent, Santa Clara, CA, USA), and qPCR was used for quantification, followed by sequencing using a NovaSeq 6000 sequencer (Illumina, San Diego, CA, USA) according to the PE 150 sequencing strategy. Initial data were filtered using the Illumina platform with fastp (version 0.18.0) [30] for the eradication of reads with ≥10% unknown nucleotides (N), 50% reads with a 20 base-Phred quality score, and those containing connectors. Next, we performed k-mer analysis using high-quality reads. Jellyfish (version 2.2.6) [31] was employed to predict the genomic features (size, heterozygosity rate, and repeat content) according to k-mer (k=21) distributions. Jellyfish used default parameters.

Genomic DNA was processed into fragments of 8–10 kb in length utilising the G-tube method (Covaris, Woburn, MA, USA), followed by DNA fragment end repair. Exonuclease III and IV digestions were performed to remove DNA with gaps or not joined to the ring junction and to remove the junction dimer. To improve sequencing quality and obtain longer average insert fragments, the library was fragmented using the BluePippin Nucleic Acid Fragment Recovery System (Sage Science, Beverly, MA, USA) to remove short fragments of library molecules. After library construction, the Qubit instrument was used for quality assurance. An Agilent 2100 system was employed to evaluate the size of the insert, followed by sequencing using the PacBio platform. To guarantee the reliability and accuracy of the follow-up analysis, the subreads obtained from the raw sequencing reads after removing sequence junctions were considered clean data, and the length distribution of the subreads was used as the main content to evaluate the sequencing effect. Because of the long length and minimal error rate of the PacBio HiFi data, Hifiasm (version 0.15.1-r334) [32] was utilised to splice and assemble the triple sequencing data. The initial genomic assembly integrity assessment was performed using the core eukaryotic gene mapping approach (CEGMA) and benchmarking universal single-copy orthologs (BUSCO) approaches.

Chromosome-level assembly with Hi-C data and evaluation

Filtered reads were compared with the preliminary sequencing results obtained from the assembly of HiFi utilising the MEM algorithm with the Burrows–Wheeler Aligner (version 0.7.12) [33], and a scaffold was established according to interactions between sequences. Scaffolds were sorted and oriented to acquire the ultimate quasi-chromosome-level genome. Hi-C data were analysed using LACHSIS (version 2014-09-12.12) [34], ALLHIC (version 0.9.8) [35] and 3D-DNA (version 180114) [36]. The construction of interaction matrices, calibration of chromosome-constructed genomes, and evaluation of results were performed via ICE software [37]. BUSCO (version 4) was applied for sequence integrity evaluations [38].

Genome annotation

Repeated sequence annotation

In order to use homology to identify genomic repetitive sequences, we matched the genomic sequences with existing databases of repetitive sequences. Homology alignment of the genome sequences and repeats from the Repbase library (version 19.05, http://www.girinst.org/repbase) was performed through ProteinMask and RepeatMasker (version open-4.05) [39], and detected repeat sequences were annotated. Multiple copies of genomic repeated sequences were detected by cross-matching sequences. Using the amino acid sequences of plants in the uniprot library/closely related species as homologous proteins, the genomes aligned by spaln were obtained as a result of homology prediction (spaln: -XQ90 -Q7 -O0 -LS -ya0 -yX2 -d spaln). The Augustus was trained using RNAseq+homology prediction results as a training set (etraining: default parameter). Evidence-based *de novo* prediction was performed using Augustus (augustus: --UTR=off --alternatives-from-evidence=true --allow_hinted_splicesites=atac, gcag --softmasking=1 --gff3=on).

First, we used PILER (version 1.0) [40], RepeatModeler (version 2.0.1) [41], and RepeatScout (version 1.05) [42] to retrieve multiple copies of sequences in the genome through internal alignment of the genome and established a repeat library *de novo*. We removed redundant repeats established from scratch and filtered out

misidentifications, thus establishing a repeat sequence library for *M. longifolia*. We used the obtained repeat sequence library as a reference and again used RepeatMasker to recognise the genomic repeat regions through homologous alignment. LTR_FINDER (version 1.0.7) [43] was utilised to scan and extract the sequences of long terminal repeat (LTR) transposons in the genome, and RepeatMasker was used to annotate their position information. TRF software (version 4.04) [44] was employed to locate simple sequences in tandem.

Coding gene annotation

Protein-coding gene prediction in *M. longifolia* was conducted using a joint strategy including homology, RNA-seq, and methods based on *de novo* prediction. Employing hidden Markov models, the entire genome's coding genes were predicted using Augustus (version 2.7) [45]. Augustus was trained with default parameters using RNAseq and homologous prediction results as a training set. We compared the known homologous species' coding protein sequences with the novel species' genome sequence. Afterward, the new species' related gene region was determined via clustering algorithms like solar and GeneWise for the purpose of homology prediction (MAKER, version 2.2.1) [46]. The EST/cDNA sequence and the genome were compared. Using EVM (version r2012-06-25) [47] and MAKER, gene sets estimated through diverse approaches were combined into a non-redundant and more comprehensive gene set. The parameters used for EVM are: EVidenceModeler: --search_long_introns 25,000 -w weight.txt (weight.txt: stringtie2: 4, scallop2: 1, psiclass: 1, bloomT: 2, bloomP: 2, hom: 1, augustus: 6). By means of manual integration, the final dependable gene set was derived. Transcription set data assembled by Tophat (version 2.0.8b) alignment and Cufflinks (version 2.2.1) were also employed to supplement and complete the final gene set (including supplementing variable shear and UTR information).

BLAST (version 2.2.29+) [48] was adopted to annotate the predicted gene protein sequences based on the Gene Ontology (GO), RefSeq Non-Redundant Protein (NR), Clusters of Orthologous Groups of Proteins (COG), SwissProt, and Kyoto Encyclopedia of Genes and Genomes (KEGG) databases. An alignment array was used as a function of the target array. Because of the large number of possible matching results per sequence during the alignment process, matches were filtered using a threshold value of $\leq 1\times10^{-5}$ to ensure that further analyses were biologically meaningful. The 20 highest-scoring sequences were chosen from each sequence's comparison results and used as alignment results.

Non-coding RNA annotation

tRNAscan-SE software (version 1.3.1) [49] was utilised to search for genomic transfer RNA (tRNA) sequences according to tRNA structural features. The reference sequence was selected from the ribosomal RNA (rRNA) sequences of closely related species using BLASTN (version 2.6.0+) [50] alignment because rRNA is highly conserved. Using the Rfam 11.0 covariance model, we predicted the sequence information for small nuclear RNA (snRNA) and microRNA (miRNA).

Species evolution and phylogenetic analysis

In total, 14 species were employed to construct a phylogenetic tree: *Amborella trichopoda*, *Rhododendron simsii*, *Camellia sinensis*, *Vitis vinifera*, *Populus trichocarpa*, *Theobroma cacao*, *Juglans regia*, *Gossypium hirsutum*, *Actinidia chinensis*, *Z. mays*, *O. sativa*, *A. thaliana*, *M. pasquieri* (unpublished), and *M. longifolia* (Table S1). Divergence time was estimated according to the following methods: orthogroups were detected via OrthoMCL [51] with the DIAMOND [52] aligner. For each single-copy orthogroup, protein sequence alignment was conducted via MUSCLE (http://www.drive5.com/muscle/) [53], with all alignments combined into a supergene. This was used to establish a maximum-likelihood phylogenetic tree through RAxML under the GTR+F+R4 model containing 1000 bootstrap replicates, and maximum-likelihood evolutionary trees were constructed via IQ-tree [54]. Subsequently, the mcmctree functionality [55] in the PAML package (version 4.9) [56] was applied to predict the inter-species differentiation time, referring to other species' known differentiation times in the TimeTree database (http://www.timetree.org).

Based on evolutionary trees with varying times and gene family clustering results, we utilised birth rate and mortality models to estimate the number of ancestral gene family members per branch using CAFÉ software (version 4.0) [57]. We predicted expanded and contracted gene families in *M. longifolia*, as compared to their ancestral state. *P*-values <0.05 across the family were considered to determine significance. Expanded/contracted gene families in *M. longifolia* underwent GO and KEGG enrichment analyses. Genome-wide replication event analysis was performed for *M. longifolia*, *M. pasquieri*, *R. simsii*, *C. sinensis*, and *V. vinifera* genomes using the synonymous mutation rate (Ks) method.

Low-temperature experiment, RNA-seq, and transcriptome sequencing

Young leaves of *M. longifolia* are susceptible to chilling injury in winter during sudden temperature drops, which may cause wilting of the leaves and hinder seedling growth. We collected naturally dropped *M. longifolia* seeds from the same plant that provided the leaves

for DNA isolation. Seeds were germinated on wet paper towels; seedlings were then planted in peat soil for cultivation after the embryonic roots grew, using the same cultivation site noted in Sect. 2.1. A batch of uniformly grown specimens (age: 9 months) was selected from among these seedlings and transferred to an intelligent artificial climate chamber (5 °C, 65% humidity, 12 h photoperiod, 17,600 lx), and young leaves were collected after 0 (control check, CK), 1 (D1), 3 (D3), 5 (D5), and 7 (D7) days of exposure for RNA extraction (Figure S1). Three biological replicates per group were used. A TRIzol kit (Invitrogen, Carlsbad, CA, USA) was utilised to isolate total RNA. The Agilent 2100 Bioanalyzer was employed to determine the RNA quality, which was then confirmed via RNAse-free agarose gel electrophoresis. Subsequently, oligo (dT) beads were used to enrich mRNA. Short fragments were generated from the enriched mRNA using a fragmentation buffer. Reverse transcription was carried out utilising the NEBNext Ultra RNA Library Prep Kit for Illumina (NEB #7530; New England Biolabs) to obtained cDNA. An Illumina Novaseq6000 by Gene Denovo Biotechnology Co. (Guangzhou, China) was utilised to sequence the obtained cDNA library.

Comparative transcriptome analysis of leaves after varying low-temperature exposure durations

Reads were fast filtered using fastp (version 0.18.0) to acquire extremely high-quality reads [30]. Reads from raw RNA were filtered and truncated to produce desired reads. Fastp (v 0.18.0) has parameters -a AGATCGGAAG AGC -q 20 -u 50 -n 15 -l 50. The purpose of this step is: (1) Remove reads containing adapter; (2) Remove reads with N ratio greater than 10%; (3) Remove reads with all A bases; (4) Remove low-quality reads (the number of bases with quality value Q≤20 accounts for more than 50% of the whole read). After establishing the reference indicator of the *M. longifolia* genome, the clean paired-end reads were aligned to this reference genome using HISAT2 (version 2.4) [58]. The parameter is set to "-rna-strandness RF" and the rest of the parameters are default. For each sample, read mapping and assembly was conducted via StringTie v1.3.1 following published protocols [59, 60]. To quantify the expression and variation of each transcription area, reads were normalised via fragments per kilobase of transcript per million mapped reads calculation using RSEM software [61]. The input data for the gene differential expression analysis were the read counts data obtained from the gene expression level analysis, which were analysed using the edgeR [62] software. The analysis was divided into three parts: (1) normalisation of the read counts; (2) calculation of the probability of hypothesis *P*-value according to the model.

DESeq2 [63] software was adopted to perform inter-group analysis of differentially expressed RNA. All DEGs were aligned with GO terms and KEGG pathways, and each term's gene count was computed. Hypergeometric testing was performed to detect GO terms remarkably enriched in the DEG in comparison with the genomic context, and KOBAS software [64] was employed to quantify significant KEGG pathway enrichment of the DEGs. *P*-values were quantified using hypothesis testing and corrected by FDR. Pathways with a *Q*-value≤0.05 were defined as significantly enriched among DEGs.

Identification, alignment, and phylogenetic analysis of *WRKY* gene family

Using blastp (parameter settings: e-value 10^{-5} and identity 50%), the protein sequences of *M. longifolia* were contrasted with the *WRKY* protein family of *A. thaliana* to identify genomic *WRKY* gene family members. Using the hmmsearch programme in hmmer 3.3.1 [65] under default parameters, the corresponding gene family members among *M. longifolia* protein sequences were determined according to the *WRKY* gene family structural domains. The members obtained from these two steps are merged as the result of the final *WRKY* gene family, where if the IDs of the genes obtained from the two steps are the same, they are retained only once. Using genome sequencing and chromosomal information of the *WRKY* genes of *M. longifolia*, chromosomal localisation analysis was performed utilising MG2C (http://mg2c.iask.in/mg2c_v2.0/) to precisely localise each *WRKY* member and facilitate gene homology analysis over evolutionary history. Based on the *A. thaliana* and *M. longifolia* *WRKY* gene family members, neighbour-joining tree construction with MUSCLE multiple sequence alignment (default parameters) was performed using MEGA11.0.8 [66] (parameters: Poisson model, partial deletion 80%, and 1000 bootstraps). Conserved motif analysis was carried out utilising the Multiple Em for Motif Elicitation (MEME) suite (version 5.3.0) [67] (parameter settings: repetition count: any; maximum motif count: 20; and optimal width per motif: 6–100 residues), and motif functional analysis was conducted as per the NCBI Conserved Domains Database (http://www.ncbi.nlm.nih.gov/Structure/cdd/cdd.shtml).

Validation of key gene expression patterns via real-time fluorescence reverse transcription qPCR (RT-qPCR)

RT-qPCR was performed to verify RNA-seq findings. Fifteen genes were chosen for expression analysis at 1D, 3D, 5D and 7D using mikado Chr 09G46 as the internal reference gene, which encoding ubiquitin-coupled enzyme. Each set of experiments consisted of 3 biological replicates. Primer Premier 5.0 (Premier Biosoft International, Palo Alto, CA, USA) was utilised to design primers (Table S2). Total RNA was isolated from each sample using TRIzol reagent [68], and reverse transcription was

performed on a T100 Thermal Cycler (Bio-Rad, Hercules, CA, USA) to acquire template cDNA. qPCR was carried out on a TianLong 988 Real-Time PCR System (Tianlong Technologies, Xi'an, China) with ChamQ SYBR qPCR Master Mix (Vazyme, Nanjing, China) using the following programme: 90 s denaturation at 95 °C, and 40 amplification cycles were conducted of 95 °C for 5 s, 60 °C for 15 s, and 72 °C for 20 s. Each sample underwent three rounds of testing. Relative expression was computed using the $2^{-\Delta\Delta Ct}$ method [69].

Results

Madhuca longifolia genome size prediction and assembly

Altogether, 31.23 Gb (42.27×) PacBio long reads and 26.79 Gb (36.26×) Illumina short paired-end reads were obtained (Table S3). Using the valid *M. longifolia* genome data obtained from Illumina sequencing, a total of 22,037,014,232 k-mers with a main peak k-mer depth of 31.82 were identified (Table S4). A clear heterozygosity peak appeared approximately halfway to the major k-mer distribution curve peak (Figure S2), indicating a high heterozygosity rate. Through further calculation and correction, the genome size was calculated as 646.92 Mb, with a 1.48% heterozygosity ratio and a 38.75% repeat sequence ratio.

Based on preliminary genome assembly and correction, the genome of *M. longifolia* contained 340 contigs, and the genome scale was 739.00 Mb with the GC content of 33.76%. Contig N50 was 56.71 Mb long, with the longest assembled contig size being 76.57 Mb (Table 1). Chromosome counts showed that *M. longifolia* was diploid (2n = 24, Figure S3). Contigs obtained from preliminary Hi-C assembly were clustered into 12 pseudochromosomes (Fig. 1A, Table S5). The Hi-C interaction heat map showed a well-organised diagonal pattern of intrachromosomal interactions, indicating a satisfactory genome assembly (Fig. 1B). The ultimate assembled genome dimension was 737.92 Mb in size, and contig N50 and scaffold N50 had lengths of 56.71 Mb and 60.05 Mb, respectively. The longest assembled contig and scaffold sizes were 76.63 Mb and 84.26 Mb, respectively, with a GC content of 33.74% (Table 1).

Illumina data were re-matched to the initially assembled *M. longifolia* genome to assess assembly integrity and accuracy, and the Illumina reads showed 98.62% alignment and 99.81% coverage (Tables S6 and S7). CEGMA assessment showed a detection rate of 234/248 (94.35%) for core eukaryotic genes (Table S8). The BUSCO evaluation results indicated that 1,571 of 1,614 direct homologous single-copy genes (97.34%) were observed in the *M. longifolia* genome (Table S9). The final assembly outcomes were also evaluated using the BUSCO software and yielded 1,535 single-copy genes, representing 95.11% of the gene counts (Table S10). This indicated that the final assembled genome of *M. longifolia* had good integrity and high quality.

Table 1 Statistics of *Madhuca longifolia* genome assembly

PacBio assembly		
Statistics	Contig length (bp)	Number
Max	76,565,288	1
N10	76,565,288	1
N20	72,498,706	2
N30	60,044,954	4
N40	57,664,288	5
N50	56,707,685	6
N60	51,577,671	8
N70	51,515,675	9
N80	41,195,910	11
N90	30,563,916	13
Total length	738,965,282	340
GC rate (%)	33.7631	-
Hi-C assembly		
Statistics	Scaffold	Contig
Total number	329	331
Total length (bp)	737,923,470	737,921,470
Gap (N) (bp)	2,000	0
Average length (bp)	2,242,928.48	2,229,370
N50 length (bp)	60,054,753	56,707,731
N90 length (bp)	41,669,588	30,985,487
Maximum length (bp)	84,256,480	76,625,452
Minimum length (bp)	13,157	13,157
GC content (%)	33.74	33.74

Genome annotation

A total of 1,294 rRNA, 2,043 tRNA, 264 miRNA, and 287 snRNA sequences were obtained by annotating the non-coding RNAs of the *M. longifolia* genome. The average length for these four RNA types was 2,581.70 bp, 74.54 bp, 133.95 bp, and 123.97 bp, respectively (Table S11). The genome contained 486.30 Mb of repeated sequences, occupying 65.90% of the total genome. Among the detected transposable elements, which are important components of repeated sequences, the LTR transposon class was predominant at 69.16 Mb in size and occupying 9.36% of the genome. The next most common class was the long interspersed nuclear element class, with a dimension of 18.03 Mb, occupying 2.44% of the genome. Among the DNA transposons, the highest proportion of genomes was in the Helitron class (62.31%), followed by miniature inverted-repeat transposable elements (1.63%) (Table S12). Structural annotation of genomic coding genes yielded 46,610 coding genes. The mean gene length of the *M. longifolia* genome was 5,561.26 bp, with the N50 gene being 9,993 bp in length. The average mRNA length was 1,625.14 bp. The mean coding sequence was 1,154.17 bp long. The mean exon length was 272.37 bp, and the mean count of exons in each gene was 5.78 (Table

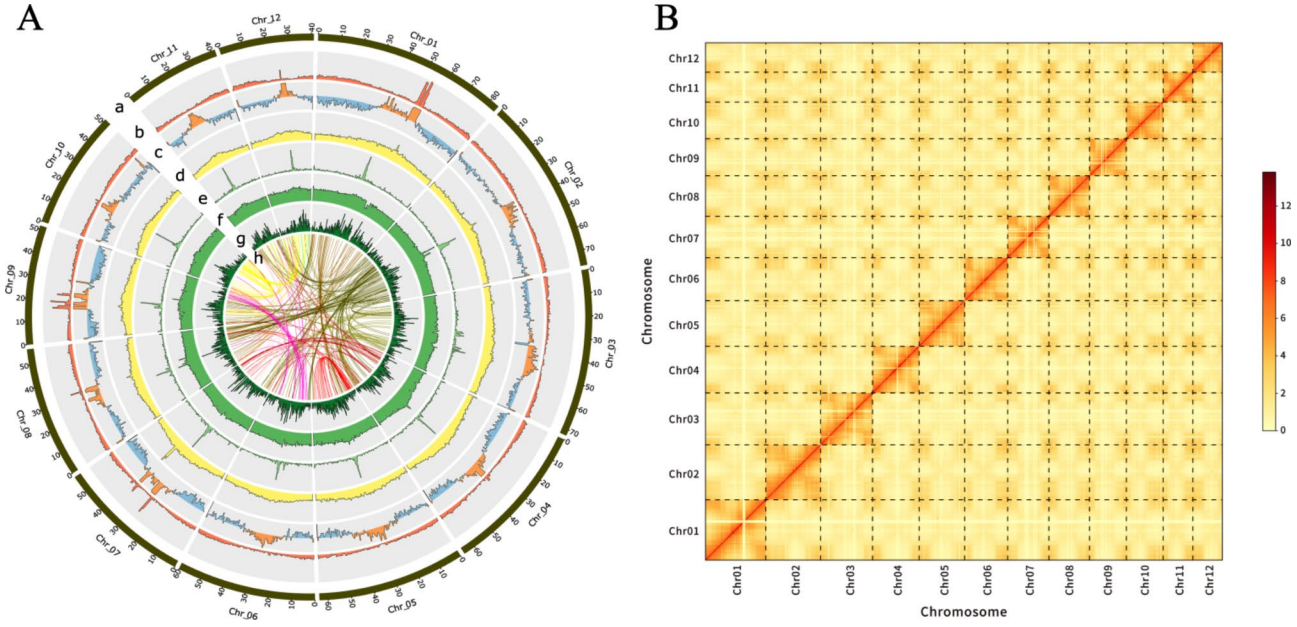

Fig. 1 Chromosomal features and Hi-C map of the *Madhuca longifolia* genome (**A**) Landscape of the *M. longifolia* genome. Inwards from the outside: Chromosome (a), Gene density (b), GC distribution density (c), Transposon distribution density (d), LINE distribution density (e), Illumina short read distribution density (f), LTR copy distribution density (g), Schematic of major inter-chromosomal relationships in the *M. longifolia* genome (h). (**B**) Heat map of the Hi-C interaction density between 12 pseudochromosomes in *M. longifolia*
LTR, long terminal repeat; LINE, long interspersed nuclear element

S13 and S14). BUSCO assessment (Table S15) showed 96.47% completeness, indicating excellent annotation of the encoded genes. Among the genes with coded proteins, 34,927 were annotated against the NR database (75% coverage), 24,100 for SwissProt (52%), 26,665 for GO (57%), 20,243 for COG (43%), and 34,162 for KEGG (73%; Table S16).

Evolution of gene families

The *M. longifolia* genome contained 15,545 gene families consisting of 26,724 genes. Table S17 shows the clustered gene families in the remaining 13 analysed species. A total of 10,517 genes were identified and shared by *M. longifolia*, *M. pasquieri*, *R. simsii*, *V. vinifera*, and *A. chinensis* (Fig. 2A). Forty-one single-copy gene families were shared among all species. Homologous single-copy gene sequence comparison and maximum-likelihood tree construction showed that *M. longifolia* and *M. pasquieri* diverged at 15–75 mya, slightly later than *O. sativa* and *Z. mays* (Fig. 2B). The gene family expansion/contraction analysis for *M. longifolia* revealed that 632 gene families underwent expansion and 161 experienced contraction (Fig. 2B). Among the expanded gene families, 2,669 genes were annotated with GO terms, with 1,540 genes enriched in biological process terms, 313 in cellular component terms, and 815 in molecular function terms (Figure S4). Altogether, 749 genes were enriched in 91 KEGG pathways (Figure S5). Genes that underwent expansion were significantly enriched in metabolic, glutathione metabolism, RNA polymerase, and oxidative phosphorylation pathways.

Whole-genome duplication

The results of the covariance analysis showed a 2:1 syntenic depth rate between *M. longifolia* and *V. vinifera* and a 2:2 syntenic depth rate between *M. pasquieri* and *R. simsii* (Fig. 2C). The *V. vinifera* genome did not exhibit the whole-genome doubling (WGD) followed by whole-genome tripling common to core dicotyledons [70], whereas this was the case in *R. simsii* [71]. Ks distribution mapping for *M. longifolia*, *M. pasquieri*, *V. vinifera*, *C. sinensis*, and *R. simsii* highlighted a shared peak at ~1.5 Ks representing a genome-wide triploidisation event (γ event) common to core dicots, after which *M. longifolia* experienced another, more recent WGD event (Fig. 2D).

Comparative transcriptome analysis of young leaves under different low-temperature treatment durations

Across all pairwise comparisons of seedlings from the CK, 1D, 3D, 5D, and 7D groups, 17,941 DEGs were recognised, with 3,382 overlapping DEGs (Fig. 3A). The D7 group showed the highest number of DEGs (14,291) against the CK group, of which 4,765 were upregulated and 9,526 were downregulated. The fewest DEGs (5,945) were found between CK and D1, of which 3,237 were upregulated and 2,708 were downregulated in the D1 group. Altogether, 13,116 DEGs were detected between the CK and D3 groups, where 4,512 were upregulated

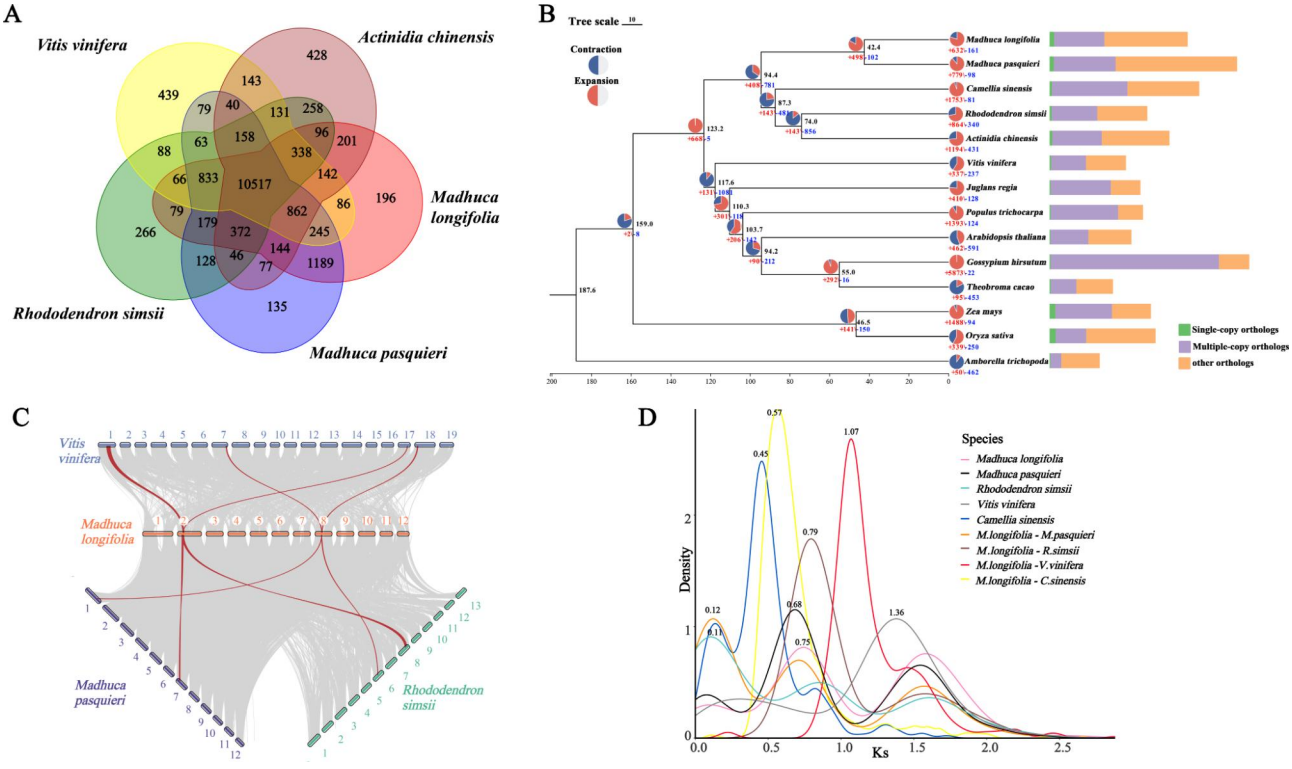

Fig. 2 Comparative genomic analysis of *Madhuca longifolia* with other plants (**A**) Venn diagram of unique and common gene families in *M. longifolia*, *M. pasquieri*, *Rhododendron simsii*, *Vitis vinifera*, and *Actinidia chinensis*. (**B**) Phylogenetic analysis of the *M. longifolia* genome based on phylogenetic relationships with 14 species. Node labels denote node ages. Gene family expansion or contraction is presented in the pie chart. Numbers of gene family cluster classes in each species are presented in the histogram. (**C**) Phylogenetic relationships of *M. longifolia* and other species (*V. vinifera*, *M. pasquieri*, and *R. simsii*). (**D**) Distribution of synonymous substitution rates (Ks) for homologous genomes used for intrachromosomal comparisons. The Ks value peaks (Ks = 0.7 and 1.5) indicate the occurrence of a recent WGD and an ancient WGD, respectively, in the *M. longifolia* genome
WGD, whole-genome doubling

and 8,604 were downregulated in the D3 group; 13,988 DEGs were found between the CK and D5 groups, of which 4,629 were upregulated and 9,359 were downregulated in the D5 group (Fig. 3B). Based on GO annotation with hypergeometric tests, DEGs were predominantly enriched in the organonitrogen compound metabolic process (GO:1901564), ion binding (GO:0043167), and catalytic complex (GO:1902494) GO terms (Figure S6). KEGG analysis showed that DEGs between CK and D1, CK and D3, CK and D5, and CK and D7 were enriched in 129, 135, 138, and 137 pathways, respectively (Figure S7). Further trend analysis showed that DEGs were clustered into 20 profiles. Among these, 15,993 DEGs were clustered into five profiles at $P<0.05$ (downregulation mode, profile 0; upregulation mode, profile 19; upregulation then stable then downregulation, profile 18; upregulation then downregulation then stable, profile 12; and stable then downregulation then upregulation, profile 8) (Fig. 3C). Profile 0 contained 9,391 DEGs that were downregulated in the 1D, 3D, 5D, and 7D groups compared to levels in the CK group. Profile 19 contained 2,941 DEGs that were upregulated in these groups.

Identification of the *WRKY* gene family

Altogether, 94 *WRKY* putative genes were identified in the genome of *M. longifolia*. Chromosomal localisation analysis revealed that these genes were distributed on 12 chromosomes, with each chromosome containing 14, 15, 4, 6, 12, 7, 6, 8, 5, 6, 7, and 4 *MlWRKY*s, respectively (Fig. 4A and Table S18). Phylogenetic analyses of *WRKY* gene families for *M. longifolia* and *A. thaliana* revealed three principal families (groups I–III), among which group II was subdivided into five subfamilies: II-a to II-e (Fig. 4B). *WRKY* gene family groups I, II, and III respectively contained 15, 58, and 21 genes, and group II subfamilies IIa, IIb, IIc, IId, and IIe respectively contained 4, 11, 25, 8, and 10 genes (Table S19). Utilising the MEME Suite, 20 conserved amino acid sequences corresponding to members of the *M. longifolia*'s *WRKY* gene family were found. Four conserved sequences with characteristic *WRKY* structural domains were identified (Figure S8). Genes containing four *WRKY* structural domain sequences (motifs 1, 2, 3, and 5) were all located in group I. Of 94 *MlWRKY*s, only 14 (*MlWRKY*1, *MlWRKY*2, *MlWRKY*3, *MlWRKY*6, *MlWRKY*14, *MlWRKY*20, *MlWRKY*24, *MlWRKY*25, *MlWRKY*31, *MlWRKY*37,

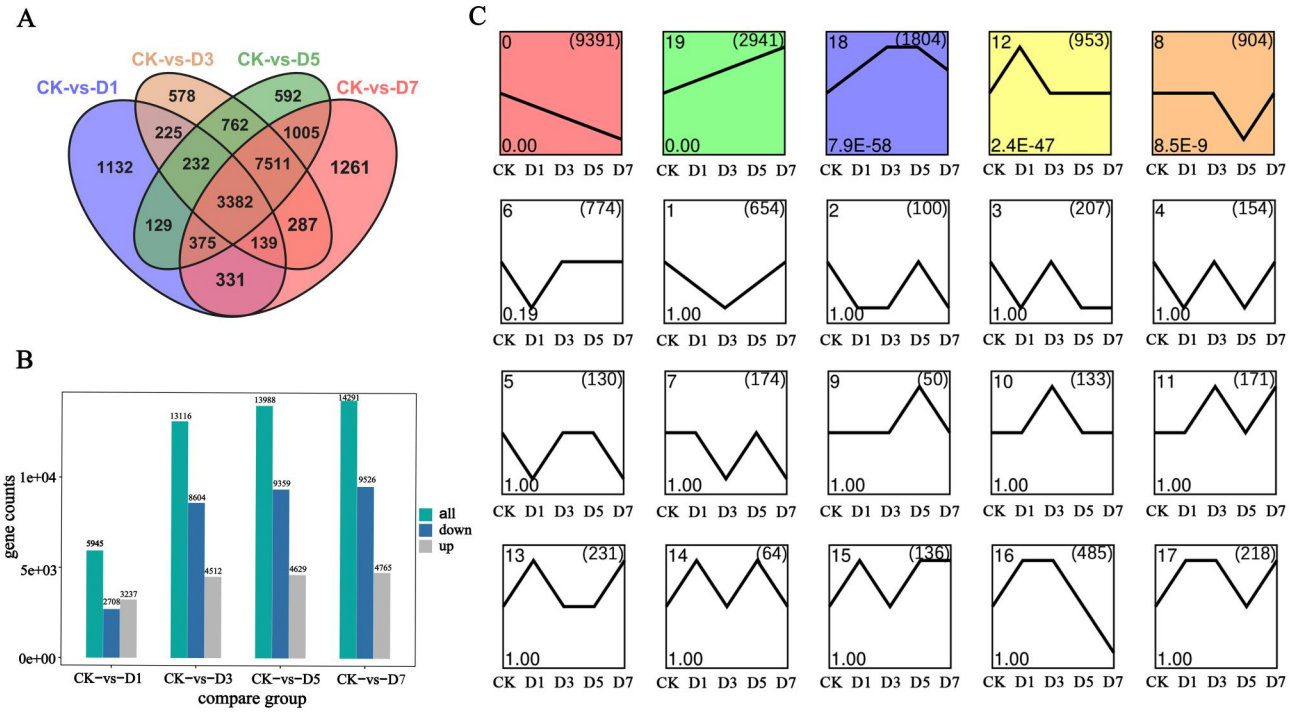

Fig. 3 Low-temperature transcriptome analysis of *Madhuca longifolia* (**A**) Venn diagram of the number of DEGs under different durations of low-temperature stress: 0 days versus 1 day (CK-vs-D1), 0 days versus 3 days (CK-vs-D3), 0 days versus 5 days (CK-vs-D5), and 0 days versus 7 days (CK-vs-D7). (**B**) Number of up- and downregulated DEGs in the four comparisons shown in A. (**C**) Total trend of all expression changes in DEGs under low-temperature stress in *M. longifolia*. For each profile, the number in the lower left corner denotes the *P*-value, the number in the upper left corner symbolises the profile ID, the number in parentheses in the upper right corner indicates the number of genes assigned to that profile, and the coloured profile represents instances of $P < 0.05$

DEG, differentially expressed gene; CK, blank control group with 0 days of low-temperature treatment; D1, D3, D5 and D7, control groups with 1, 3, 5, 7 days of low-temperature treatment

*MlWRKY*47, *MlWRKY*84, *MlWRKY*88, and *MlWRKY*89) contained either motif 1 or motif 2 but not both, whereas each of the other genes contained both motifs, which were closely related (Figure S9).

The transcriptome trend analysis revealed that of the 94 *WRKY* genes identified in the *M. longifolia* genome with differential expression under low-temperature stress, 17 upregulated *MlWRKY*s corresponded to profile 19 and 15 downregulated *MlWRKY*s represented profile 0. Based on this result, a gene expression heat map was plotted via the TBtools software [72] (Figure S10). The top eight differentially expressed *MlWRKY*s in profile 19 and the equivalent top seven in profile 0 were identified as genes likely to be tightly linked with the response to low-temperature stress in *M. longifolia* (Table S20). These 15 differentially expressed *MlWRKY*s (*MLWRKY81*, *MLWRKY21*, *MLWRKY52*, *MLWRKY74*, *MLWRKY99*, *MLWRKY46*, *MLWRKY54*, *MLWRKY5*, *MLWRKY59*, *MLWRKY90*, *MLWRKY13*, *MLWRKY48*, *MLWRKY28*, *MLWRKY97*, and *MLWRKY76*) were selected and validated via qRT-PCR, and their expression in the transcriptome was largely consistent with the fluorescence quantification of expression in different samples (Fig. 4C), further supporting the credibility of the RNA-seq data.

Discussion

In this study, Illumina sequencing, PacBio HiFi sequencing, and Hi-C technology were incorporated to sequence and assemble the complete *M. longifolia* genome to obtain a high-quality chromosome-level reference genome. This is the first complete chromosome-level reference genome for the genus *Madhuca* and provides considerable genomic data for investigations of other species in the genus. The *M. longifolia* genome also provides a basis for future research on molecular breeding, phylogeny, and resistance mechanisms. The size of the assembled genome is approximately 737.92 Mb, with contig N50 (56.71 Mb) and scaffold N50 (60.05 Mb) both notably larger than contig N50 (2.2 Mb) and scaffold N50 (36 Mb) of the closely related species *R. simsii* [71]. In this study, 65.90% of the total genome of *M. longifolia* was represented by duplicated sequences, a considerably larger percentage than in *R. simsii* (47.48%) and *R. delavayi* (51.77%) [71]. This indicates that *M. longifolia* could have undergone greater sequence differentiation and genome expansion than these species. Altogether, 46,610

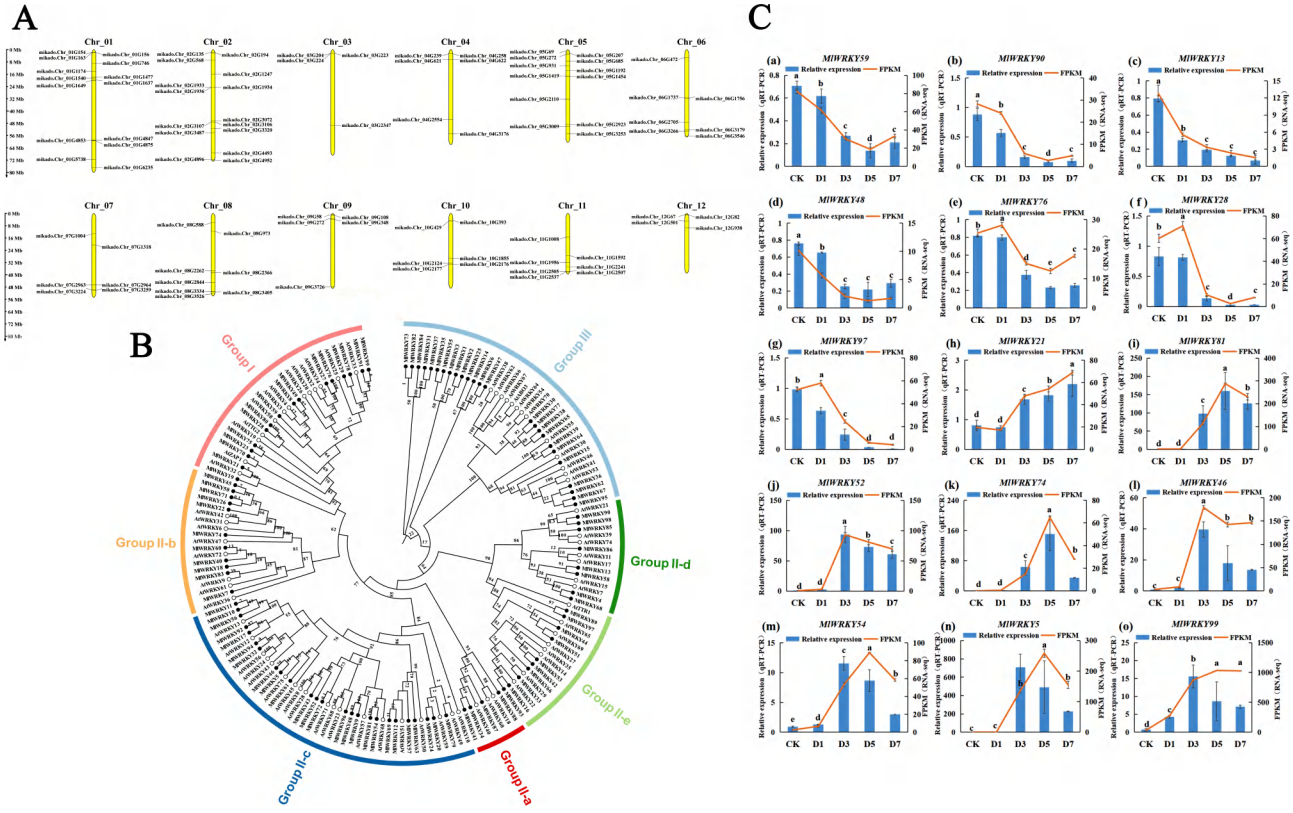

Fig. 4 Analysis of the *WRKY* gene family and RT-qPCR validation of key *WRKY* genes for low-temperature response in *Madhuca longifolia* (**A**) Chromosomal localisation of 94 *WRKY* genes on *M. longifolia* chromosomes. (**B**) Phylogeny of the *WRKY* gene family in *M. longifolia* and *Arabidopsis thaliana*. (**C**) RT-qPCR validation of 15 *MIWRKY* genes in response to low-temperature stress in *M. longifolia*. In (c), panels (a)–(g) show *WRKY* genes consistently downregulated in profile 0. Panels (h)–(o) show *WRKY* genes consistently upregulated in profile 19

coding genes corresponded to known functional annotations for *M. longifolia*, close to the count for the closely related species *A. chinensis* (40,464) [73] but markedly higher than that for *R. simsii* (32,999).

Adaptive evolution is a key strategy for the survival of all species. Understanding the molecular mechanisms controlling adaptive evolution helps us to comprehend the development of adaptive characteristics and the correlations that support species diversification, phenotype convergence, and interspecific interactions. It may also provide valuable knowledge of the formation and sustainability of biodiversity [74]. Gene family expansion significantly affects species differentiation. We found that 632 gene families in *M. longifolia* have expanded during its evolutionary history and exhibit enrichment in oxidative phosphorylation, glutathione metabolism, and RNA polymerase pathways. These gene families may have been associated with resistance to environmental stress during the species' evolutionary history. The natural habitat of *M. longifolia* is southern India and Myanmar, where it is warm throughout the year and hot in the summer. It can therefore be assumed that *M. longifolia* has gradually evolved to become more tolerant to hot environments and less adaptable to low temperatures. This may be one of the reasons for the poor overwintering adaptability of the species during cold waves in winter after its introduction to southern China.

The divergence time of *A. chinensis* and *R. simsii* in the present study was approximately 74.0 Ma, which is almost identical to the previously reported divergence time of 74.78 Ma. In contrast, the differentiation time of 87.3 Ma for *A. chinensis* and *C. sinensis* was greater than that of 60.95–76.84 Ma reported in other studies [73]. This may be due to the use of genomes from more species in this investigation, particularly the inclusion of genomic data from the Sapotaceae family, which is closely related to the Actinidiaceae and Theaceae families. Genome-wide replication events are important drivers of species evolution and can lead to changes in plant genome size and gene number [75, 76]. *M. longifolia* exhibited covariate relationships of 2:1, 2:2, and 2:2 with *V. vinifera*, *M. pasquieri*, and *R. simsii*, respectively. Both *M. longifolia* and *M. pasquieri* have 12 pseudochromosomes, whereas the closely related species *Synsepalum dulcificum* [77] and *R. simsii* have 13 pseudochromosomes. Therefore, the evolution of the chromosomes of *M. longifolia* is of great importance to the Sapotaceae and Ericales. *M. longifolia* and *M. pasquieri* peaked at Ks=0.75 and

Ks=0.68, respectively, while *S. dulcificum* of the same family peaked at Ks=0.56. Given *M. longifolia*'s evolutionary position in the phylogenetic tree, we speculate that this WGD event was not unique to the Sapotaceae family. It has been reported that *C. sinensis* underwent only one WGD event following a whole-genome tripling event, and that this was the same WGD event shared by *A. chinensis*, *C. sinensis*, *R. simsii*, and *Diospyros kaki* [78], which may also be shared with other species in the family. However, because of the lack of genomic studies on *M. longifolia*, the neutral mutation rate of the tightly related species *A. chinensis* was utilised to calculate the timing of the WGD event in this analysis. This may have led to less accurate results and could be corrected in conjunction with more relevant subsequent research results.

Low temperatures are a key factor limiting the large-scale cultivation of high-quality tropical trees in China. Low-temperature stress often results in the severe dehydration of plant cells, leading to tissue injury, stunted growth, and wilting. Various physiological, molecular, and metabolic responses driven by multiple pathways occur when plants resist the adverse effects of low temperatures [79, 80]. We found that the total number of DEGs between the low-temperature groups and the CK group gradually rose with an increasing duration of seedling exposure to stress. More genes were downregulated than upregulated on days 3, 5, and 7 of low-temperature treatment but not on day 1, when the count of upregulated genes surpassed that of downregulated genes. Enrichment analyses of several groups of DEGs using the GO and KEGG databases demonstrated that DEGs were remarkably enriched in membrane pathways (GO:0016020) on D1 as compared to CK. One of the key mechanisms for adapting to low-temperature stress involves modifying the plasma membrane's function and composition [81]. As the low-temperature treatment duration escalated, the DEGs in plant tissues became remarkably enriched in pathways related to stress response. Examples of other pathways associated with membranes included the integral component (GO:0005887) and the obsolete intrinsic component of the plasma membrane (GO:0031226). The enrichment analysis results in this study are highly similar to previously reported enrichment pathways of DEGs in *Kandelia obovata* during cold acclimation in coastal environments [82].

When exposed to abiotic stress factors, some *WRKY* TFs quickly promote signal transduction and lead to differential gene expression [83]. The *WRKY* expression modes and functional identification are identified through transcriptome analysis and RT-qPCR. The ongoing expansion of plant genome and transcriptome databases has led to the detection of a rising number of *WRKY* genes, e.g., 82 in *Solanum tuberosum* [84] and 95 in *Daucus carota* [85]. A previous study predicted 96 *WRKY* TFs in the genome of *M. pasquieri* [86]; herein, 94 *MlWRKYs* were recognised for the first time in the *M. longifolia* genome. The *WRKY* gene count in both species was very similar, which may be related to their close affinity. *WRKY* genes in *M. longifolia* were nonuniformly distributed across the species' 12 chromosomes. Phylogenetic analysis allowed the classification of these genes into three groups, of which group II was subdivided into five subgroups (II-a to II-e). This clustering result is accordant with that found in a prior study [87]. Subgroup II-c had the largest number of members (25), whereas II-a had only four *MlWRKY* members; this distribution is similar to the clustering results of *WRKY* subgroups in *S. lycopersicum* [88] and *Manihot esculenta* [89].

Various investigations have indicated that *WRKY* genes influence many plants' responses to low-temperature stress. The *WRKY71* protein is localised in the nucleus of *Fragaria×ananassa* seedlings and plays a role in responses to abiotic stressors such as cold, salt, and low phosphate levels [90]. *BcWRKY46* in *Brassica campestris* is triggered by low-temperature stress and ABA to improve plant resistance through the activation of relevant genes in ABA signalling pathways [91]. In the present study, 15 key *MlWRKYs* were found to respond to low temperatures, all of which were enriched in GO terms related to the control of transcription and transcription with a DNA template (GO:0006355), DNA binding specific to sequences (GO:0043565), and transcription factor activity binding to DNA (GO:0003700) (Table S20). These genes may be key regulators of related pathways that rapidly respond to low-temperature stress, regulating the expression of related genes and altering metabolite synthesis and secretion, among other responses.

Despite our valuable findings, the study has some limitations. First, the transcriptome samples we used were leaf sections that were not further disassembled for sequencing to analyse the differential expression among different tissues; therefore, it remains unclear whether there are differences in the expression modes of *MlWRKY*s in distinct tissues under low-temperature stress. Further, it is unknown how these *WRKY* gene family members respond to low-temperature signals and regulate gene expression. Further experiments are needed to validate the functions of these genes and investigate their specific roles in the complicated molecular mechanisms related to the low-temperature response of *M. longifolia*. Moreover, there is a lack of metabolomic data related to *M. longifolia* under low-temperature stress, limiting our analysis of differential metabolites and core metabolic pathways. In the future, further combinations of genomic, transcriptomic, metabolomic, proteomic and other multi-omics data can be used to establish a gene–metabolite regulatory network, mine additional

hub genes, and clarify the related regulatory relationships. Finally, although RT-qPCR verified recognised hub gene expression, insufficient direct molecular experiments were performed to functionally verify them. As a next step, a genetic transformation system of *M. longifolia* needs to be established to facilitate the verification of gene functions. Combined with multi-omics association analysis and molecular biology techniques, we plan to explore the principal target genes and pathways related to low-temperature stress responses and clarify the existence of any interactions between these, so as to analyse the molecular mechanism of these responses in depth.

Conclusions

In this study, high-quality chromosome-level genome assembly was performed for *M. longifolia*, and key genes controlling low-temperature responses were identified for the first time based on genomic and transcriptomic data. The genomic data and comparative genomic analyses provide valuable references for further studies on the adaptive evolution of *M. longifolia* and related species. The derived transcriptome information constitutes a basis for further elucidating the adaptive mechanisms of *M. longifolia* to unfavourable low-temperature environmental conditions and for optimising the molecular breeding and cultivation of other high-quality tropical woody plants. Future studies can use our genome assembly, annotation, and transcriptome data to enhance the ecological adaptability and exploitability of valuable tropical trees to different environments following their introduction.

Supplementary Information

The online version contains supplementary material available at https://doi.org/10.1186/s12864-024-10769-2.

Supplementary Material 1

Supplementary Material 2

Acknowledgements

The authors appreciate Gene Denovo Biotechnology Co. (China)'s support on the project and particularly Zhiyuan Yang for her technical guidance and assistance.

Author contributions

ZL secured funding and managed the project, which reviewed and edited this article. WSY prepared the experimental materials and completed the resource survey, data collation and visualization, and was a major contributor in writing the manuscript. LHY was involved in the experiments and the data analysis. YSY assisted in the preparation of experimental materials and software analysis. JZL participated in the revision and editing of the experiment and writing. CZP and MYF assisted in the software analysis and data visualization process. All the authors read and approved the final manuscript.

Funding

This work was funded by the National Natural Science Foundation of China [No. 32371742], the Wildlife Conservation and Management Projects of Guangdong Forestry Administration (2022 and 2023), and the Forestry Department of Guangdong Province, China, for non-commercial ecological forest research [No. 2020STGYL0019].

Data availability

The whole-genome sequence data used in this paper have been stored in the Genome Warehouse in the National Genomics Data Center, Beijing Institute of Genomics, Chinese Academy of Sciences/China National Center for Bioinformation, under accession number GWHDTZT00000000. The data are accessible to the public at https://ngdc.cncb.ac.cn/gwh.

Declarations

Ethics approval and consent to participate

Not applicable.

Consent for publication

Not applicable.

Competing interests

The authors declare no competing interests.

Received: 18 February 2024 / Accepted: 4 September 2024
Published online: 18 September 2024

References

1. Chinnusamy V, Zhu J, Zhu JK. Cold stress regulation of gene expression in plants. Trends Plant Sci. 2007;12:444–51.
2. Akshatha KN, Mahadeva Murthy S, Lakshmidevi N. Ethnomedical uses of *Madhuca longifolia*-A review. Int J Life Sci Pharm Res. 2013;3:44–53.
3. Sharma M, Yadav S, Ganesh N, Srivastava MM, Srivastava S. Biofabrication and characterization of flavonoid-loaded ag, au, Au-Ag bimetallic nanoparticles using seed extract of the plant *Madhuca longifolia* for the enhancement in wound healing bio-efficacy. Prog Biomater. 2019;8:51–63.
4. Pinakin DJ, Kumar V, Kumar S, Kaur S, Prasad R, Sharma BR. Influence of pre-drying treatments on physico-chemical and phytochemical potential of dried mahua flowers. Plant Foods Hum Nutr. 2020;75:576–82.
5. Simon JP, Evan Prince S. Ameliorative activity of aqueous leaf extract from *Madhuca longifolia* against diclofenac-administered toxicity on rat stomach and intestine. J Histotechnol. 2021;44:114–26.
6. Pinakin DJ, Kumar V, Suri S, Sharma R, Kaushal M. Nutraceutical potential of tree flowers: a comprehensive review on biochemical profile, health benefits, and utilization. Food Res Int. 2020;127:108724.
7. Pradhan SK, Sahoo UC. Evaluation of recycled asphalt mixtures rejuvenated with *Madhuca longifolia* (Mahua) oil. Int J Pavement Res Technol. 2021;14:43–53.
8. Asanthi H, Yasasvi J, Ashoka G, et al. Nutritional, functional properties and applications of Mee (*Madhuca longifolia*) seed fat. Agronomy. 2023;13:2445.
9. Fatma A, Ahuja V, Ahuja A, et al. Evaluation of antibacterial activity of *Madhuca longifolia* (Mahua) stem extract against *Streptococcus mutans*: an in vitro study. Cureus. 2024;16(1):e52210.
10. Vinotha V, Vaseeharan B. Bio-fabricated zinc oxide and cry protein nanocomposites: synthesis, characterization, potentiality against Zika, malaria and West Nile virus vector's larvae and their impact on non-target organisms. Int J Biol Macromol. 2023;224:699–712.
11. Gopinath R, Billigraham P, Sathishkumar TP. Characterization studies on novel cellulosic fiber obtained from the bark of *Madhuca longifolia* tree. J Nat Fibers. 2022;19:14880–97.
12. Bandara WART, Dissanayake CTM. Most tolerant roadside tree species for urban settings in humid tropics based on Air Pollution Tolerance Index. Urban Clim. 2021;37:100848.
13. Hou Q, Li Y, Kang W, Zhou T, Liu J, Luo J et al. Selection of tree species for anti-typhoon shelter forests of tropical coastal city in Hainan. J Cent S Univ Technol. 2011;31:184 – 91, 240.
14. Ebrahimi A, Lawson SS, McKenna JR, Jacobs DF. Morpho-physiological and genomic evaluation of Juglans species reveals regional maladaptation to cold stress. Front Plant Sci. 2020;11:229.
15. Shang J, Tian J, Cheng H, Yan Q, Li L, Jamal A, et al. The chromosome-level wintersweet (*Chimonanthus praecox*) genome provides insights into floral scent biosynthesis and flowering in winter. Genome Biol. 2020;21:200.

16. Sork VL, Squire K, Gugger PF, Steele SE, Levy ED, Eckert AJ. Landscape genomic analysis of candidate genes for climate adaptation in a California endemic oak, *Quercus lobata*. Am J Bot. 2016;103:33–46.
17. Zhao T, Ma W, Yang Z, Liang L, Chen X, Wang G, et al. A chromosome-level reference genome of the hazelnut. Corylus heterophylla Fisch GigaScience. 2021;10:giab027.
18. Simon SA, Zhai J, Nandety RS, McCormick KP, Zeng J, Mejia D, et al. Short-read sequencing technologies for transcriptional analyses. Annu Rev Plant Biol. 2009;60:305–33.
19. Wang Z, Gerstein M, Snyder M. RNA-Seq: a revolutionary tool for transcriptomics. Nat Rev Genet. 2009;10:57–63.
20. He RY, Yang T, Zheng JJ, Pan ZY, Chen Y, Zhou Y, et al. QTL mapping and a transcriptome integrative analysis uncover the candidate genes that control the cold tolerance of maize introgression lines at the seedling stage. Int J Mol Sci. 2023;24:2629.
21. Liu Y, Xiong Y, Zhao J, Bai S, Li D, Chen L, et al. Molecular mechanism of cold tolerance of centipedegrass based on the transcriptome. Int J Mol Sci. 2023;24:1265.
22. Li H, Zhou T, Chong X, Lu X, Li Y, Zheng B, et al. Transcriptome and expression analysis of genes related to regulatory mechanisms in Holly (*Ilex dabieshanensis*) under cold stress. Forests. 2022;13:2150.
23. Song S, Ma D, Xu C, et al. In silico analysis of NAC gene family in the mangrove plant *Avicennia marina* provides clues for adaptation to intertidal habitats. Plant Mol Biol. 2023;111:393–413.
24. Zhou H, M J, Liu H, et al. Genome-wide identification of the CBF gene family and ICE transcription factors in walnuts and expression profiles under cold conditions. Int J Mol Sci. 2024;25:25.
25. Zhang Y, Wang L. The *WRKY* transcription factor superfamily: its origin in eukaryotes and expansion in plants. BMC Evol Biol. 2005;5:1.
26. Pandey SP, Somssich IE. The role of *WRKY* transcription factors in plant immunity. Plant Physiol. 2009;150:1648–55.
27. Kim C, Vo KTX, Nguyen CD, Jeong D, Lee S, Kumar M, et al. Functional analysis of a cold-responsive rice *WRKY* gene, *OsWRKY71*. Plant Biotechnol Rep. 2016;10:13–23.
28. Zou C, Jiang W, Yu D. Male gametophyte-specific *WRKY34* transcription factor mediates cold sensitivity of mature pollen in *Arabidopsis*. J Exp Bot. 2010;61:3901–14.
29. Luo DL, Ba LJ, Shan W, Kuang JF, Lu WJ, Chen JY. Involvement of *WRKY* transcription factors in abscisic-acid-induced cold tolerance of banana fruit. J Agric Food Chem. 2017;65:3627–35.
30. Chen S, Zhou Y, Chen Y, Gu J. Fastp: an ultra-fast all-in-one FASTQ preprocessor. Bioinformatics. 2018;34:i884–90.
31. Marçais G, Kingsford C. A fast, lock-free approach for efficient parallel counting of occurrences of k-mers. Bioinformatics. 2011;27:764–70.
32. Cheng H, Concepcion GT, Feng X, Zhang H, Li H. Haplotype-resolved de novo assembly using phased assembly graphs with hifiasm. Nat Methods. 2021;18:170–5.
33. Li H, Durbin R. Fast and accurate short read alignment with Burrows-Wheeler transform. Bioinformatics. 2009;25:1754–60.
34. Burton JN, Adey A, Patwardhan RP, Qiu R, Kitzman JO, Shendure J. Chromosome-scale scaffolding of de novo genome assemblies based on chromatin interactions. Nat Biotechnol. 2013;31:1119–25.
35. Zhang X, Zhang S, Zhao Q, Ming R, Tang H. Assembly of allele-aware, chromosomal-scale autopolyploid genomes based on Hi-C data. Nat Plants. 2019;5:833–45.
36. Dudchenko O, Batra SS, Omer AD, Nyquist SK, Hoeger M, Durand NC, et al. De novo assembly of the *Aedes aegypti* genome using Hi-C yields chromosome-length scaffolds. Science. 2017;356:92–5.
37. Imakaev M, Fudenberg G, McCord RP, Naumova N, Goloborodko A, Lajoie BR, et al. Iterative correction of Hi-C data reveals hallmarks of chromosome organization. Nat Methods. 2012;9:999–1003.
38. Simão FA, Waterhouse RM, Ioannidis P, Kriventseva EV, Zdobnov EM. BUSCO: assessing genome assembly and annotation completeness with single-copy orthologs. Bioinformatics. 2015;31:3210–2.
39. Tarailo-Graovac M, Chen N. Using RepeatMasker to identify repetitive elements in genomic sequences. Curr Protoc Bioinformatics. 2009, Chap. 4;Chapter:4.10.1–4.10.14.
40. Edgar RC, Myers EW. PILER: identification and classification of genomic repeats. Bioinformatics. 2005;21(Suppl 1):i152–8.
41. Bao Z, Eddy SR. Automated de novo identification of repeat sequence families in sequenced genomes. Genome Res. 2002;12:1269–76.
42. Price AL, Jones NC, Pevzner PA. De novo identification of repeat families in large genomes. Bioinformatics. 2005;21(Suppl 1):i351–8.
43. Xu Z, Wang H. LTR_FINDER: an efficient tool for the prediction of full-length LTR retrotransposons. Nucleic Acids Res. 2007;35:W265–8.
44. Benson G. Tandem repeats finder: a program to analyze DNA sequences. Nucleic Acids Res. 1999;27:573–80.
45. Stanke M, Tzvetkova A, Morgenstern B. AUGUSTUS at EGASP: using EST, protein and genomic alignments for improved gene prediction in the human genome. Genome Biol. 2006;7(Suppl 1):S111–8.
46. Campbell MS, Law M, Holt C, Stein JC, Moghe GD, Hufnagel DE, et al. MAKER-P: a tool kit for the rapid creation, management, and quality control of plant genome annotations. Plant Physiol. 2014;164:513–24.
47. Haas BJ, Salzberg SL, Zhu W, et al. Automated eukaryotic gene structure annotation using EVidenceModeler and the program to assemble spliced alignments. Genome Biol. 2008;9:R7.
48. Conesa A, Götz S, García-Gómez JM, Terol J, Talón M, Robles M. Blast2GO: a universal tool for annotation, visualization and analysis in functional genomics research. Bioinformatics. 2005;21:3674–6.
49. Kollmar M, TRNAscan, -SE. Searching for tRNA genes in genomic sequences. London: Springer; 2019. pp. 1–14.
50. Altschul SF, Gish W, Miller W, Myers EW, Lipman DJ. Basic local alignment search tool. J Mol Biol. 1990;215:403–10.
51. Li L, Stoeckert CJ, Roos DS. OrthoMCL: identification of ortholog groups for eukaryotic genomes. Genome Res. 2003;13:2178–89.
52. Buchfink B, Xie C, Huson DH. Fast and sensitive protein alignment using DIAMOND. Nat Methods. 2015;12:59–60.
53. Edgar RC. MUSCLE: multiple sequence alignment with high accuracy and high throughput. Nucleic Acids Res. 2004;32:1792–7.
54. Nguyen LT, Schmidt HA, von Haeseler A, Minh BQ. IQ-TREE: a fast and effective stochastic algorithm for estimating maximum-likelihood phylogenies. Mol Biol Evol. 2015;32:268–74.
55. Yang Z. PAML: a program package for phylogenetic analysis by maximum likelihood. Comput Appl Biosci. 1997;13:555–6.
56. Yang Z. PAML 4: phylogenetic analysis by maximum likelihood. Mol Biol Evol. 2007;24:1586–91.
57. De Bie T, Cristianini N, Demuth JP, Hahn MW. CAFE: a computational tool for the study of gene family evolution. Bioinformatics. 2006;22:1269–71.
58. Kim D, Langmead B, Salzberg SL. HISAT: a fast spliced aligner with low memory requirements. Nat Methods. 2015;12:357–60.
59. Pertea M, Pertea GM, Antonescu CM, Chang TC, Mendell JT, Salzberg SL. StringTie enables improved reconstruction of a transcriptome from RNA-seq reads. Nat Biotechnol. 2015;33:290–5.
60. Pertea M, Kim D, Pertea GM, Leek JT, Salzberg SL. Transcript-level expression analysis of RNA-seq experiments with HISAT, StringTie and Ballgown. Nat Protoc. 2016;11:1650–67.
61. Li B, Dewey CN. RSEM: accurate transcript quantification from RNA-Seq data with or without a reference genome. BMC Bioinformatics. 2011;12:323.
62. Robinson MD, McCarthy DJ, Smyth GK. edgeR: a Bioconductor package for differential expression analysis of digital gene expression data. Bioinformatics. 2010;26(1):139–40.
63. Love MI, Huber W, Anders S. Moderated estimation of Fold change and dispersion for RNA-seq data with DESeq2. Genome Biol. 2014;15:550.
64. Xie C, Mao X, Huang J, Ding Y, Wu J, Dong S, et al. KOBAS 2.0: a web server for annotation and identification of enriched pathways and diseases. Nucleic Acids Res. 2011;39Suppl2:W316–22.
65. Eddy SR. Profile hidden Markov models. Bioinformatics. 1998;14:755–63.
66. Kumar S, Tamura K, Nei M. MEGA: molecular evolutionary genetics analysis software for microcomputers. Comput Appl Biosci. 1994;10:189–91.
67. Bailey TL, Johnson J, Grant CE, Noble WS. The MEME suite. Nucleic Acids Res. 2015;43:W39–49.
68. Rio DC, Ares MJ, Hannon GJ, Nilsen TW. Purification of RNA using trizol (TRI reagent). Cold Spring Harb Protoc. 2010;2010:pdb.prot5439.
69. Livak KJ, Schmittgen TD. Analysis of relative gene expression data using real-time quantitative PCR and the 2-ΔΔCT method. Methods. 2001;25:402–8.
70. Jaillon O, Aury JM, Noel B, Policriti A, Clepet C, Casagrande A, et al. The grapevine genome sequence suggests ancestral hexaploidization in major angiosperm phyla. Nature. 2007;449:463–7.
71. Yang FS, Nie S, Liu H, Shi TL, Tian XC, Zhou SS, et al. Chromosome-level genome assembly of a parent species of widely cultivated azaleas. Nat Commun. 2020;11:5269.

72. Chen C, Chen H, Zhang Y, Thomas HR, Frank MH, He Y, et al. TBtools: an integrative toolkit developed for interactive analyses of big biological data. Mol Plant. 2020;13:1194–202.
73. Wu H, Ma T, Kang M, Ai F, Zhang J, Dong G, et al. A high-quality *Actinidia chinensis* (kiwifruit) genome. Hortic Res. 2019;6:117.
74. Hu Y, Wang X, Xu Y, Yang H, Tong Z, Tian R, et al. Molecular mechanisms of adaptive evolution in wild animals and plants. Sci China Life Sci. 2023;66:453–95.
75. Soltis PS, Soltis DE. Ancient WGD events as drivers of key innovations in angiosperms. Curr Opin Plant Biol. 2016;30:159–65.
76. Wu S, Han B, Jiao Y. Genetic contribution of paleopolyploidy to adaptive evolution in angiosperms. Mol Plant. 2020;13:59–71.
77. Yang Z, Liu Z, Xu H, Chen Y, Du P, Li P, et al. The chromosome-level genome of miracle fruit (*Synsepalum dulcificum*) provides new insights into the evolution and function of miraculin. Front Plant Sci. 2021;12:804662.
78. Wang Y, Chen F, Ma Y, Zhang T, Sun P, Lan M, et al. An ancient whole-genome duplication event and its contribution to flavor compounds in the tea plant (*Camellia sinensis*). Hortic Res. 2021;8:176.
79. Thomashow MF. Role of cold-responsive genes in plant freezing tolerance. Plant Physiol. 1998;118:1–8.
80. Thomashow MF. Molecular basis of plant cold acclimation: insights gained from studying the CBF cold response pathway. Plant Physiol. 2010;154:571–7.
81. Barrero-Sicilia C, Silvestre S, Haslam RP, Michaelson LV. Lipid remodelling: unravelling the response to cold stress in *Arabidopsis* and its extremophile relative *Eutrema salsugineum*. Plant Sci. 2017;263:194–200.
82. Su W, Ye C, Zhang Y, Hao S, Li QQ. Identification of putative key genes for coastal environments and cold adaptation in mangrove *Kandelia obovata* through transcriptome analysis. Sci Total Environ. 2019;681:191–201.
83. Jiang Y, Deyholos MK. Functional characterization of *Arabidopsis* NaCl-inducible *WRKY25* and *WRKY33* transcription factors in abiotic stresses. Plant Mol Biol. 2009;69:91–105.
84. Liu Q, Liu Y, Xin Z, Zhang D, Ge B, Yang R, et al. Genome-wide identification and characterization of the *WRKY* gene family in potato (*Solanum tuberosum*). Biochem Syst Ecol. 2017;71:212–8.
85. Li MY, Xu ZS, Tian C, Huang Y, Wang F, Xiong AS. Genomic identification of *WRKY* transcription factors in carrot (*Daucus carota*) and analysis of evolution and homologous groups for plants. Sci Rep. 2016;6:23101.
86. Kan L, Liao Q, Su Z, Tan Y, Wang S, Zhang L. Single-molecule real-time sequencing of the *Madhuca pasquieri* (Dubard) Lam. Transcriptome reveals the diversity of full-length transcripts. Forests. 2020;11:866.
87. Eulgem T, Rushton PJ, Robatzek S, Somssich IE. The *WRKY* superfamily of plant transcription factors. Trends Plant Sci. 2000;5:199–206.
88. Huang S, Gao Y, Liu J, Peng X, Niu X, Fei Z, et al. Genome-wide analysis of *WRKY* transcription factors in *Solanum lycopersicum*. Mol Genet Genomics. 2012;287:495–513.
89. Wei Y, Shi H, Xia Z, Tie W, Ding Z, Yan Y, et al. Genome-wide identification and expression analysis of the *WRKY* gene family in cassava. Front Plant Sci. 2016;7:25.
90. Yue M, Jiang L, Zhang N, Zhang L, Liu Y, Wang Y, et al. Importance of *FaWRKY71* in strawberry (*Fragaria* × *ananassa*) fruit ripening. Int J Mol Sci. 2022;23:12483.
91. Wang F, Hou X, Tang J, Wang Z, Wang S, Jiang F, et al. A novel cold-inducible gene from pak-choi (*Brassica campestris* ssp. *chinensis*), *BcWRKY46*, enhances the cold, salt and dehydration stress tolerance in transgenic tobacco. Mol Biol Rep. 2012;39:4553–64.

Publisher's note

forests

MDPI

Article

Topographical Influence on Snag Distribution in a Subtropical Forest in South China

Yifei Ma, Zhipeng Chen, Shuyu Wang, Haoyou Lin, Lei Kan, Weijing Du, Zhiyao Su and Lu Zhang *

College of Forestry and Landscape Architecture, South China Agricultural University, Guangzhou 510642, China; mayf@stu.scau.edu.cn (Y.M.); hnnyczp@stu.scau.edu.cn (Z.C.); wshuyu@stu.scau.edu.cn (S.W.); llucky@stu.scau.edu.cn (H.L.); kanlei5523@stu.scau.edu.cn (L.K.); gdduweijing@163.com (W.D.); zysu@scau.edu.cn (Z.S.)

* Correspondence: zhanglu@scau.edu.cn; Tel.: +86-135-6008-9803

Abstract: Snags are highly important for many wildlife species and ecological processes. In this study, we analyzed the relationship between snags and topographic factors in a secondary forest plot in South China. Data on 544 snags were collected and recorded from 236 subplots in a permanent plot (400 subplots). The frequency of *Castanopsis carlesii* and *Schima superba* was higher than that of other species. The snags derived mostly from saplings and small trees, and the presence of snags decreased as the DBH and height increased after 25 years of logging. The snags displayed an aggregated spatial pattern distribution, which was strongly correlated with elevation, slope steepness, and slope aspect ($p < 0.05$), as revealed by canonical correspondence analysis (CCA); however, the response of snags varied with topographic factors. Our results demonstrate that topography is an important factor that affects the snag spatial distribution in the subtropical secondary forest. These results will further improve our understanding of forest dynamics and provide guidance for forest management and biodiversity conservation.

Keywords: standing dead trees; elevation; slope steepness; slope aspect; canonical correspondence analysis

Citation: Ma, Y.; Chen, Z.; Wang, S.; Lin, H.; Kan, L.; Du, W.; Su, Z.; Zhang, L. Topographical Influence on Snag Distribution in a Subtropical Forest in South China. *Forests* **2023**, *14*, 997. https://doi.org/10.3390/f14050997

Academic Editor: Takuo Nagaike

Received: 23 March 2023
Revised: 9 May 2023
Accepted: 10 May 2023
Published: 11 May 2023

1. Introduction

Climate change not only increases the risk of species extinction [1], but also affects the structural diversity of woody plants [2] and induces tree mortality, which is often exacerbated towards the warm or dry limits of the species ranges [3,4]. Snags (standing dead trees) are an important component of forest ecosystems, representing a significant part of dead wood [5,6] and the most common result of tree mortality within forests [7]. Big snags are vital to biodiversity and the cycling of nutrients in forest ecosystems [8,9], where they play a particularly important role in carbon and nitrogen cycling [10–12]. Moreover, snags with larger diameters provide nests, perches, roost sites, foraging substrates, song posts, and escape cover for organisms such as amphibians, arthropods, birds, and small mammals [13–16]. When they fall, snags also offer germination and growth substrates for lichens, various types of fungi, and bryophytes [17,18].

Tree mortality is a critical process in forest dynamics [19] and can influence community composition and species coexistence [20]. Snags represent the most common result of tree mortality in forests, so the analysis of snags can reveal characteristics of tree mortality and disturbance events in forest systems [7]. Tree mortality is generally affected by many factors, including biotic and abiotic variables [4]. Topography (i.e., elevation, slope, aspect, and convexity) is among the most important habitat factors [20,21], and by altering the patterns of precipitation, temperature, solar radiation, and relative humidity, topography can influence local and regional microclimates [22]. Moreover, topography can contribute to the accumulation and export of soil nutrients [23], as well as regulate the redistribution of seeds, water, and materials, thereby indirectly affecting plant distribution [24].

Thermal energy distribution is primarily affected by spatial heterogeneity under different topographic conditions at the forest stand level [25]. Due to the numerous functions of snags in terrestrial systems, understanding the topographical factors that influence snag quantity and spatial patterns in subtropical forests is highly important. Although the relationships between living woody vegetation and topographic gradients have been fairly well established in the region, little is known about how topographic factors affect the spatial distribution of snags. Landscape position was strongly correlated with the accumulation of coarse woody debris in an old-growth deciduous forest on the Cumberland Plateau in southeastern Kentucky [26]. Similarly, a complex relationship between coarse woody debris loads and topographic position was revealed in southern Ohio [27]. Topography is a common factor that influences the abundance of snags and dead woody material in mountainous areas [28]. In addition, terrain-related difficulties (such as distance to roads and watercourse density) positively affected coarse woody debris [29]. However, few studies have investigated the effects of topographic factors on snag quantity and quality. The objectives of this study were (1) to determine the quantitative characteristics of snags after logging in a subtropical secondary forest in South China, and (2) to identify the major topographic factors that influence the distribution and growth of snags.

2. Materials and Methods

2.1. Study Site

This study was conducted in a permanent plot in the Kanghe Provincial Natural Reserve, a secondary forest in eastern Dongyuan County in Guangdong Province (23°44′ N–23°53′ N, 114°04′ E–115°09′ E) in South China. The reserve covers an area of 6484.8 ha and was established in 2001 for the conservation of an ecosystem dominated by evergreen broadleaved forest. The reserve is within the subtropical monsoon climate region. The mean annual precipitation is 1567–2142 mm; the wettest months are April–June. The mean annual temperature is 20.7 °C, and the annual temperature ranges from −4.5 °C to 39.3 °C. The mean annual relative humidity is 77%. A four-hectare permanent sampling plot was established at an elevation of 204–372 m (Figure 1). The soil in this region is classified as krasnozem soil according to the national standards of China. The zonal vegetation is evergreen broadleaved forest; however, the woody plants with a diameter at breast height (DBH) >12 cm underwent selective logging in the Kanghe Mountains in 1993. The permanent plot was a secondary forest of natural restoration.

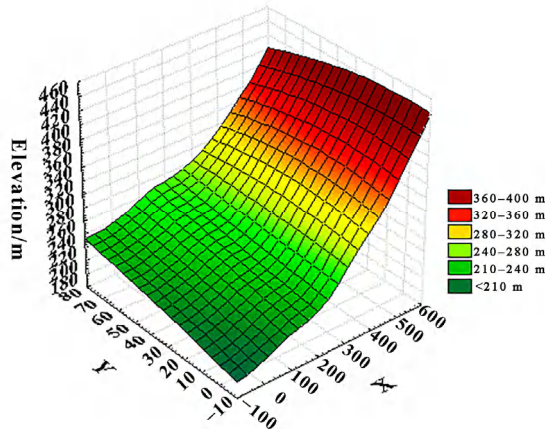

Figure 1. Topographic map of the permanent plot in a secondary forest in South China. The topographic map was generated from the survey data of the plot using the software Statistica (Version 8.0) (Statsoft, Inc., Tulsa, OK, USA). The *X* axis represents the northwest-to-southeast direction; the *Y* axis represents the northeast-to-southwest direction.

2.2. Field Surveys

A total of 400 10 m × 10 m square subplots were established. In each subplot, all individual snags whose DBH ≥ 2.5 cm and whose height ≥ 1 m were sampled. The species of each snag was identified, and their heights (measured to the nearest 0.1 m) and DBH (measured to the nearest 0.1 cm) were measured and recorded.

2.3. Topographic Factors

We recorded topographic factors in each subplot. The elevation, slope aspect, and slope steepness were measured using a total station (Nikon DTM-310, Tokyo, Japan). Slope steepness was classified in accordance with a general classification system—from gentle to very steep. The slope steepness of the four-hectare sample plot ranged from 15.2° to 47.6°, and therefore was classified into three groups: 15–25°, 25–35°, and 35–50°. The elevation ranged from 204 m to 372 m and was classified into four groups: 200–250 m, 250–300 m, 300–350 m, and 350–400 m. Aspect-related thermal gradients shape forest habitats that exhibit heterogeneous energy distributions, thus driving plant structural diversity patterns. The slope aspect of the four-hectare sample plot ranged from 9.8° to 356.6°; from the starting point due north and moving in a clockwise direction, the classifications included the north aspect (338–22°), northeast aspect (23–67°), east aspect (68–112°), southeast aspect (113–157°), south aspect (158–202°), southwest aspect (203–247°), west aspect (248–292°), and northwest aspect (293–337°). The above eight aspects were further divided into four groups: sunny slopes include south aspects, southwest aspects and southeast aspects; semi-sunny slopes include east aspects and west aspects; semi-shady slopes include northwest aspects and northeast aspects; and shady slopes include north aspects [30].

2.4. Analytical Methods

Species abundance, basal area, and density of snags were measured in each subplot. Frequency refers to the percentage of a species among the snags in a sample. Snag diameters were classified into five groups: 2.5–10 cm, 10–20 cm, 20–30 cm, 30–40 cm, and ≥40 cm [31]. Similarly, snag heights were classified into five groups: 1–5 m, 5–10 m, 10–15 m, 15–20 m, and ≥20 m.

The index of dispersion I was used to characterize the spatial patterns of snags. When $I \approx 0$, the snags are distributed regularly. Values of $I = 1$ indicate a random spatial pattern, and values of I greater than 1 present an aggregated spatial pattern [32].

$$I = \frac{S^2}{\overline{m}^2}$$

We used a multivariate approach to investigate the relationships between snag distribution and topographic factors. A preliminary detrended correspondence analysis (DCA) was performed to assess the gradient length of the species data for each of the three structural layers. The DCA revealed the presence of large (unimodal) gradients (>4 standard deviations). Hence, to assess the relationships between snag abundance and several topographic factors, we used canonical correspondence analysis (CCA), which is a direct gradient analysis technique that is constrained by a set of a priori environmental characteristics that are hypothesized to influence species distribution patterns. A Monte Carlo permutation test based on 9999 random permutations was performed to test the significance of the eigenvalue of the first canonical axis. Inter-set correlations from the ordination analysis were used to assess the importance of the topographic factors. The CCA was carried out using CANOCO software (version 4.5). A nonparametric Kruskal–Wallis test was used to test the differences in snag distributions between each group of topographic factors. The Kruskal–Wallis test was performed using Statistica software (version 8.0, StatSoft, Inc.). All tests were performed at a significance level of $p < 0.05$.

3. Results

3.1. Snag Species Composition and Quantitative Characteristics

Data on 544 snags were collected and recorded from 236 subplots in the permanent plot. Forty-four snag species were identified. The overall snags density was 230.5 ± 10.4 snags/ha. *Castanopsis carlesii* was the most abundant species (90 snags (16.5%) in 53 subplots), followed by *Schima superba* (30 snags (5.5%) in 21 subplots) and *Camellia oleifera* (27 snags (4.9%) in 17 subplots). The frequency of each species was calculated as the proportion of subplots in which the species was found, with frequencies of 13.3% (53/400 × 100), 5.3% (21/400 × 100), and 4.3% (17/400 × 100) for *Castanopsis carlesii*, *Schima superba*, and *Camellia oleifera*, respectively. *Schefflera octophylla* presented the largest basal area (2.66 ± 1.13 m^2/ha), followed by *Schima superba* (1.73 ± 0.40 m^2/ha) and *Castanopsis carlesii* (1.50 ± 0.19 m^2/ha). The frequency of *Castanopsis carlesii* and *Schima superba* was much greater than that of the other species. The number of snags, accounting for 3.0% of all standing trees, as well as the quantity characteristic of standing trees in the secondary forest plot, is shown in Table 1.

Table 1. Quantity characteristic of dominant snags of a secondary forest plot in South China.

Species	Abundance	Frequency (%)	Average DBH Mean ± SE (cm)	Max DBH (cm)	Average Height Mean ± SE (m)	Max Height (m)
Castanopsis carlesii	90	13.3	11.9 ± 0.8	30.3	5.1 ± 0.5	20.2
Schima superba	30	5.3	12.0 ± 1.6	31.8	3.0 ± 0.5	13.1
Camellia oleifera	27	4.3	3.0 ± 0.1	4.5	3.2 ± 0.2	5.7
Machilus chinensis	23	3.8	7.4 ± 0.9	16.5	6.0 ± 0.8	15.6
Cunninghamia lanceolata	23	4	8.3 ± 1.1	21.5	6.1 ± 0.8	15.4
All snags	544	59	7.6 ± 0.3	43.5	4.8 ± 0.1	20.2

The snag abundance and richness decreased rapidly as both the snag DBH and height increased. This suggests that tree mortality decreases as tree size increases. The abundance decreased from 408 in the first DBH class to 2 in the ≥40 cm DBH class, indicating a typical reverse-J size distribution (Figure 2A). The most striking feature in Figure 2 is that the abundance and richness strongly decreased from the 2.5–10 cm diameter class. The abundance and richness both strongly significantly differed among the five diameter classes ($p < 0.01$). The DBH of the snags ranged from 2.5 to 43.5 cm, and the snags of the smallest diameter class (2.5–10 cm) greatly outnumbered those of the other larger-diameter classes. It reflects the reality that trees occupy more space as they grow; hence, plots of a given size will support fewer trees if trees are large compared to when they are small.

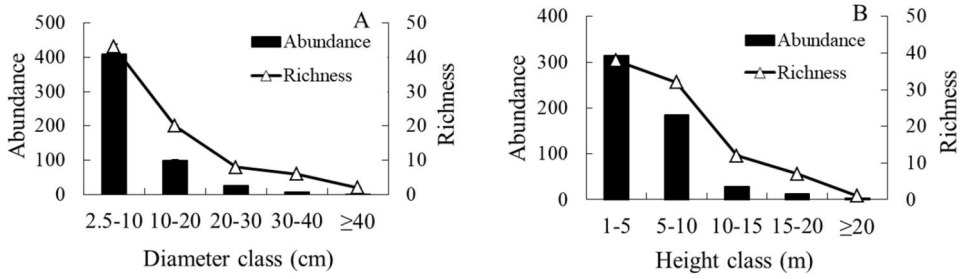

Figure 2. Distribution of snag abundance and richness across diameter (**A**) and height classes (**B**). The diameter and height are both divided into five classes.

The smallest-diameter class (2.5–10 cm) constituted 75.0% of the snags and constituted the most abundant group in our study. We recorded only 10 snags whose DBH was greater than 30 cm; of those snags, only two (0.4%) had a DBH greater than 40 cm, and snags with a DBH ≥ 20 cm constituted only 6.6%. Only two large snags were in the last DBH class, indicating that large snags rarely form. These results indicate that there is a higher mortality among smaller trees and saplings within the community. The abundance decreased from 314 in the

first height class to 3 in the ≥20 m height class (Figure 2B), indicating a typical reverse-J size distribution. Both the abundance and richness significantly differed among the five height classes (Kruskal–Wallis test, $p < 0.01$ and $p < 0.05$, respectively). The snag abundance decreased as the height increased (Figure 2B). Snags ≤ 10 m in height predominated and constituted 91.7% of the total snag population. We recorded 26 snags that were taller than 15 m and only 3 snags (0.6%) that were taller than 20 m. The results of our study indicated that the snags mostly consisted of individuals with a DBH ≤ 20 cm and a height ≤ 10 m.

3.2. Snag Spatial Distribution Associated with Topographic Factors

The index of dispersion ($I = 1.1 > 1$) showed that snags were distributed in an aggregated spatial pattern in the sample plots. Of the 400 subplots, 164 contained no snags (41.0%), and approximately 1/5th of the subplots contained one snag (22.0%). Two and three snags were recorded in 16% and 11% of the subplots, respectively.

The results of a CCA (Figure 3) demonstrated that snag patterns were associated with the three measured topographic factors ($p < 0.01$). The Monte Carlo test (9999 permutations) revealed four significant canonical axes ($p < 0.01$), which in aggregate explained 6.5% of the variance in species data and 100.0% of the variance in the species–environment relationship (Table 2).

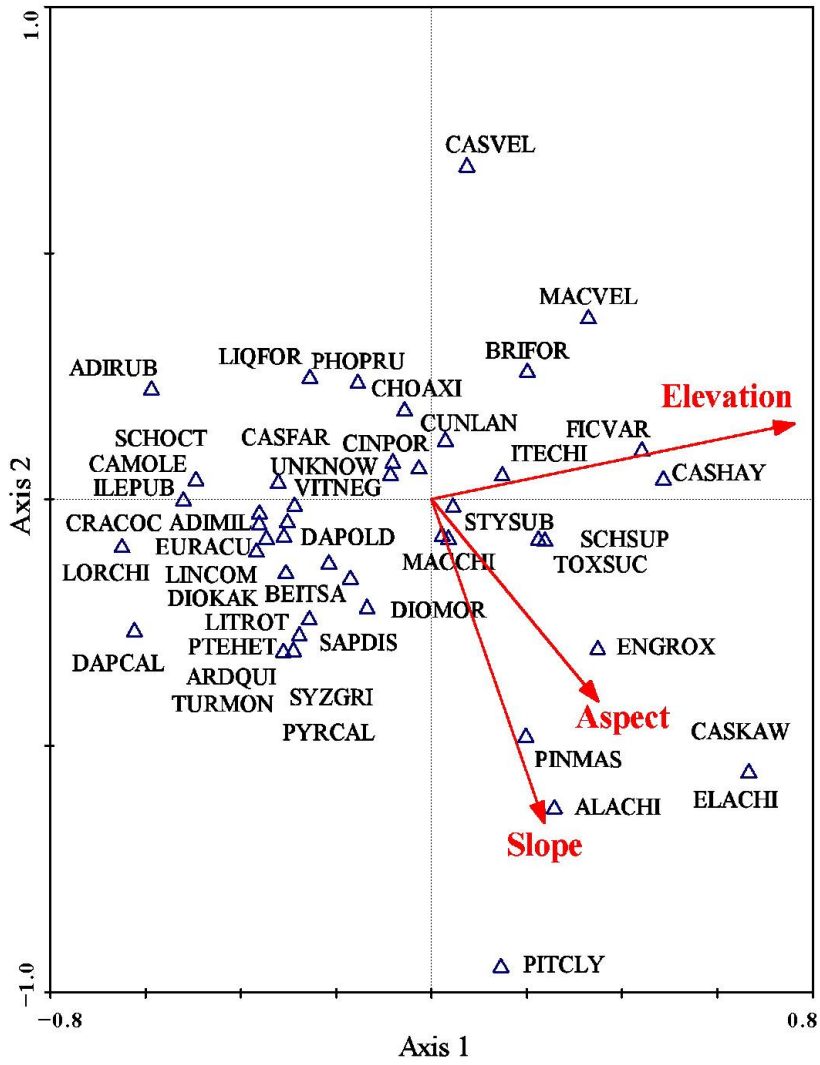

Figure 3. Two-dimensional ordination diagram of the canonical correspondence analysis (CCA) of 45 snag species recorded in 236 plots as constrained by three topographic factors in a secondary forest in South China. Topographic factors are represented by arrows. The length of an arrow indicates the strength of the correlation between the variable and the axis. Snags species are represented by species

codes: *Castanopsis carlesii* (CASCAR), *Schima superba* (SCHSUP), *Camellia oleifera* (CAMOLE), *Machilus chinensis* (MACCHI), *Cunninghamia lanceolata* (CUNLAN), *Cratoxylum cochinchinense* (CRACOC), *Cinnamomum porrectum* (CINPOR), *Pterospermum heterophyllum* (PTEHET), *Itea chinensis* (ITECHI), *Schefflera octophylla* (SCHOCT), *Adinandra millettii* (ADIMIL), unknown (UNKNOW), *Styrax suberifolius* (STYSUB), *Engelhardia roxburghiana* (ENGROX), *Beilschmiedia tsangii* (BEITSA), *Diospyros morrisiana* (DIOMOR), *Photinia prunifolia* (PHOPRU), *Sapium discolour* (SAPDIS), *Liquidambar formosana* (LIQFOR), *Litsea rotundifolia* (LITROT), *Castanopsis fargesii* (CASFAR), *Lindera communis* (LINCOM), *Loropetalum chinense* (LORCHI), *Ardisia quinquegona* (ARDQUI), *Machilus velutina* (MACVEL), *Pinus massoniana* (PINMAS), *Pyrus calleryana* (PYRCAL), *Adina rubella* (ADIRUB), *Bridelia fordii* (BRIFOR), *Choerospondias axillaris* (CHOAXI), *Diospyros kaki* (DIOKAK), *Elaeocarpus chinensis* (ELACHI), *Syzygium grijsii* (SYZGRI), *Toxicodendron succedaneum* (TOXSUC), *Alangium chinense* (ALACHI), *Casearia velutina* (CASVEL), *Castanopsis kawakamii* (CASKAW), *Daphniphyllum calycinum* (DAPCAL), *Daphniphyllum oldhamii* (DAPOLD), *Eurya acuminata* (EURACU), *Ficus variolosa* (FICVAR), *Ilex pubescens* (ILEPUB), *Pithecellobium clypearia* (PITCLY), *Vitex negundo* (VITNEG), *Turpinia montana* (TURMON).

Table 2. Eigenvalues and correlation coefficients for snag abundance and topographic factors (elevation, slope steepness, and slope aspect). * Level of statistical significance: * $p < 0.05$, ** $p < 0.01$.

Attribute	Axes			
	1	2	3	4
Eigenvalues	0.397	0.110	0.090	1.000
Species–environment correlations	0.72	0.41	0.38	0.0
Cumulative % variance of species data	1.6	2.1	2.4	6.5
Cumulative % variance of species–environment relation	66.5	85.0	100.0	0.0
Slope steepness	0.30	−0.70 *	0.65 *	0.00
Elevation	0.98 **	0.16	0.11	0.00
Slope aspect	0.45 *	−0.43 *	−0.78 *	0.00

With an eigenvalue of 0.397, the first canonical axis of the CCA explained the most variance in the data. Axis 1 represents the species–environment; strongly positive correlations (r = 0.718) occurred, and the axis explained 66.5% of the species–environment relation. The first axis was strongly significantly correlated with elevation (r = 0.98, $p < 0.01$) and slope aspect (r = 0.45, $p < 0.05$). The second canonical axis had an eigenvalue of 0.110 and was significantly correlated with slope steepness (r = −0.70, $p < 0.01$) and slope aspect (r = −0.43, $p < 0.05$). The examination of the inter-set correlation (correlations between species axes and environmental variables) and intra-set correlation (correlations between environmental axes and environmental variables) values revealed that both species axis 1 and environmental axis 1 presented the strongest correlations with elevation (r = 0.73 and 0.98, respectively, $p < 0.01$). Slope steepness and slope aspect were strongly correlated with environmental axis 2 (r = −0.70, $p < 0.01$ and −0.43, $p < 0.05$, respectively) and environmental axis 3 (r = 0.65 and −0.78, respectively, $p < 0.01$). The species distributions in multidimensional space are consistent with the biological characteristics and habitat affinities of individual species. For example, heliophyte species such as *Castanopsis carlesii* and *Castanopsis kawakamii* are on the right side of the CCA biplot (sunny aspects and high elevation).

3.3. Relationships between Snags and Topographic Factors

Both the DBH (Kruskal–Wallis test, $p < 0.001$) and height (Kruskal–Wallis test, $p < 0.001$) of snags largely varied across the elevation gradient (Figure 4). The mean diameter of snags increased from 4.6 ± 0.3 cm to 11.2 ± 0.9 cm as the elevation increased.

The maximum diameter of snags reached 43.5 cm at an elevation of 250–300 m. The average height of snags at an elevation of 250–300 m was significantly higher than that at other elevations. The maximum height of snags reached 20 m.

The DBH largely varied across slope aspect (Kruskal–Wallis test, $p < 0.001$); however, no significant differences between height and slope aspect were observed (Kruskal–Wallis

test, $p > 0.05$). The DBH and height of snags decreased from shady to sunny aspects, which indicated that, in more mesic plots, snags are much larger and taller.

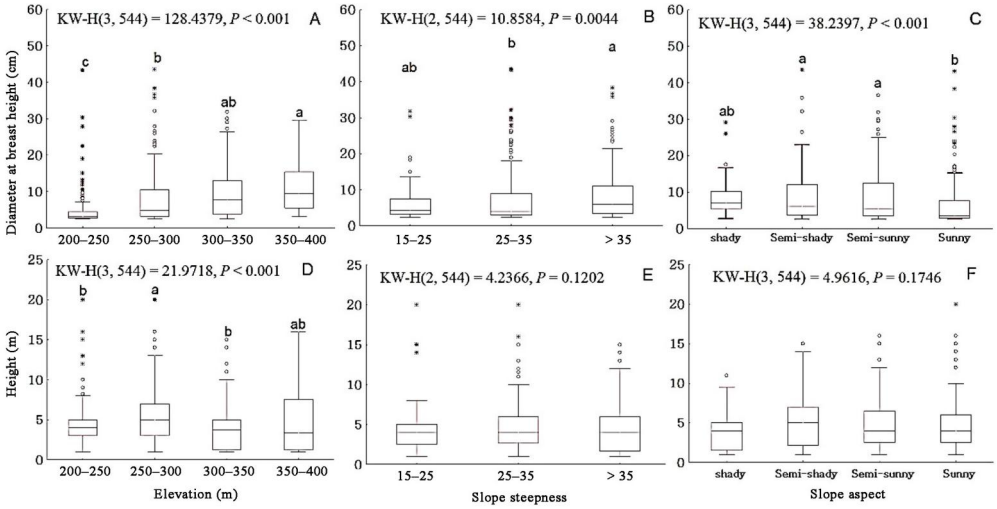

Figure 4. Response of snags to an elevation gradient according to (**A**) diameter at breast height (DBH) and (**D**) height; to slope steepness according to (**B**) DBH and (**E**) height; and to slope aspect according to (**C**) DBH and (**F**) height. The box plots show the Kruskal–Wallis test results. The horizontal line and small box within each box indicates the median, the box endpoints indicate the 25th and 75th percentile values, and the whiskers represent the non-outlier range; the circles and asterisks indicate the outliers and extreme values of the DBH and height of the snags. Different letters (a, b, c) in the figures represent significant differences between groups ($p < 0.05$).

Similarly, the DBH largely varied across slope steepness (Kruskal–Wallis test, $p < 0.05$); however, no significant differences between height and slope steepness were observed (Kruskal–Wallis test, $p > 0.05$). The DBH and height of snags at a 35–45° slope steepness were greater than those at other slope steepness degrees.

4. Discussion

Based on the assumption that trees gain and use the same amount of energy, studies have suggested that tree mortality decreases as tree size increases, and compared with small trees, large trees have an advantage in terms of resource competition [33]. Our research shows that tree mortality tends to decline as tree size increases. However, other studies have reported that, for very large trees, tree mortality is not negatively associated with tree size [34,35]. Among the recorded snags, only 10 (1.8%) had a DBH greater than 30 cm, which supports the conclusion that the size of snags is considerably low in old-growth forests [6]. This phenomenon may be due to differences in climate, site productivity, tree species composition, and disturbance regimes compared to other regions. For instance, the Kanghe Mountains have experienced selective logging, while other regions, such as the Ailao Mountains, have experienced little anthropogenic disturbance. Additionally, topography differs between these regions, with the Kanghe Mountains featuring more undulating terrain and various slope aspects.

The study revealed that topographical heterogeneity, which leads to habitat heterogeneity, was the predominant mechanism generating the spatial distribution of most analyzed species [36]. Snags have shown a consistent aggregated distribution at 0–30-m scales in subtropical mountain forests [20]. Our results also revealed that the spatial pattern of snags was aggregated in the secondary forest of the Kanghe Mountains. Different dead trees showed different spatial patterns: small dead trees presented an aggregated distribution, and large dead trees presented a random distribution [37,38]. The clustered pattern of small snags (DBH $\leq$ 15 cm) may be explained by the clustered pattern of tree regeneration, and competitive exclusion was the main cause of tree mortality in subcanopy

trees. However, the random pattern of large snags may be a consequence of continuous individual tree mortality caused by aging.

The future global extinction risk from climate change is predicted not only to increase but to accelerate as global temperatures increase. Topography-associated thermal gradients predict warming effects on woody plant structural diversity [2]. Other studies have reported a high density of snags at high elevations [39], which contrasts with our results, indicating that snag density decreases as elevation increases.

Our results showed that elevation is an important factor that limits snag distribution in the secondary forest ecosystems of the Kanghe Mountains, which agrees well with many other studies [18,40–43]. The average DBH and basal area decreased as elevation decreased, which may be due to competition for limited resources. The average height of snags at low elevations was small, possibly because a greater number of species can adapt to low elevations. Competition for limited resources at low elevations limits the growth of individual trees, so the DBH and height of snags remain small.

Our results showed that the abundance of snags was lower on shady slopes than on sunny slopes in the secondary forest of the Kanghe Mountains in South China. However, along the gradient of shady slopes (cold slopes) to warmer slopes, mature trees had significantly fewer stems. Deadwood volume depends on terrain and slope gradient [21]. Aspect-related thermal gradients shape forest habitats that exhibit heterogeneous energy distributions. The energetic equivalence rule supports the hypothesis that elevated temperatures increase the standing stock of species, as these temperatures accelerate the biochemical reactions that govern speciation rates [44].

Light conditions were relatively more abundant on the sunny slopes than on the shady slopes, leading to more intense competition and higher individual mortality in the former; woody plant diversity patterns on small scales is potentially associated with the topographic heterogeneity of energy distribution [45]. Slope aspect and slope steepness represent the horizontal and vertical dimensions of topographic factors, respectively. Temperature clearly changes along the vertical gradient, and vegetation type subsequently exhibits a distinct vertical zonality. Given the multiple functions that snags play in terrestrial systems, knowledge of the factors that affect the distribution of snags is highly important [19,41,46]. An understanding of snag spatial distribution and dynamics, which requires the identification of the factors that influence snag quantity and quality, is difficult to achieve given the numerous factors that simultaneously influence snag distribution.

5. Conclusions

The results of the present study suggest that snags display an aggregated spatial pattern distribution in the subtropical secondary forest in South China, which strongly correlates with elevation, slope steepness, and slope aspect. The snags responded differently to different topographic factors. The number of snags decreased as the elevation increased and tended to increase from shady to sunny slope aspects after logging. However, the DBH of snags showed an opposite trend. Moreover, the snags were tallest at medium elevations and along the steepest slopes. Elevation is an important factor that influences the distribution and growth of snags.

Author Contributions: Conceptualization, L.Z.; Data curation, Y.M., Z.C., S.W., H.L., L.K. and W.D.; Formal analysis, Y.M. and Z.C.; Funding acquisition, L.Z.; Investigation, Y.M., Z.C., S.W., H.L., L.K. and W.D.; Methodology, Y.M. and L.Z.; Project administration, L.Z.; Software, Y.M., Z.C. and S.W.; Writing—original draft, Y.M.; Writing—review and editing, Z.S. and L.Z. All authors have read and agreed to the published version of the manuscript.

Funding: This study was supported by the Forestry Department of Guangdong Province, China, for noncommercial ecological forest research (Grant No: 2020STGYL001) and the Wildlife Conservation and Management Projects of Guangdong Forestry Administration (2022).

Data Availability Statement: Not applicable.

Conflicts of Interest: The authors declare no conflict of interest.

References

1. Urban, M.C. Accelerating extinction risk from climate change. *Science* **2015**, *348*, 571–573. [CrossRef] [PubMed]
2. He, S.; Zhong, Y.; Sun, Y.; Su, Z.; Jia, X.; Hu, Y.; Zhou, Q. Topography-associated thermal gradient predicts warming effects on woody plant structural diversity in a subtropical forest. *Sci. Rep.* **2017**, *7*, 40387. [CrossRef] [PubMed]
3. Taccoen, A.; Piedallu, C.; Seynave, I.; Gégout-Petit, A.; Gégout, J. Climate change-induced background tree mortality is exacerbated towards the warm limits of the species ranges. *Ann. For. Sci.* **2022**, *79*, 23. [CrossRef]
4. Stovall, A.; Shugart, H.; Yang, X. Tree height explains mortality risk during an intense drought. *Nat. Commun.* **2019**, *10*, 4385. [CrossRef]
5. Klockow, P.A.; Putman, E.B.; Vogel, J.G.; Moore, G.W.; Edgar, C.B.; Popescu, S.C. Allometry and structural volume change of standing dead southern pine trees using non-destructive terrestrial LiDAR. *Remote Sens. Environ.* **2020**, *241*, 111729. [CrossRef]
6. Bölöni, J.; Ódor, P.; Ádám, R.; Keeton, W.S.; Aszalós, R. Quantity and dynamics of dead wood in managed and unmanaged dry-mesic oak forests in the Hungarian Carpathians. *For. Ecol. Manag.* **2017**, *399*, 120–131. [CrossRef]
7. Ganey, J.L.; Vojta, S.C. Tree mortality in drought-stressed mixed-conifer and ponderosa pine forests, Arizona, USA. *For. Ecol. Manag.* **2011**, *261*, 162–168. [CrossRef]
8. Garber, S.M.; Brown, J.P.; Wilson, D.S.; Maguire, D.A.; Heath, L.S. Snag longevity under alternative silvicultural regimes in mixed-species forests of central Maine. *Can. J. For. Res.* **2005**, *35*, 787–796. [CrossRef]
9. Oberle, B.; Ogle, K.; Zanne, A.E.; Woodall, C.W. When a tree falls: Controls on wood decay predict standing dead tree fall and new risks in changing forests. *PLoS ONE* **2018**, *13*, e196712. [CrossRef]
10. Ohtsuka, T.; Shizu, Y.; Hirota, M.; Yashiro, Y.; Jia, S.G.; Iimura, Y.; Koizumi, H. Role of coarse woody debris in the carbon cycle of Takayama forest. *Ecol. Res.* **2014**, *29*, 91–101. [CrossRef]
11. Romashkin, I.; Shorohova, E.; Kapitsa, E.; Galibina, N.; Nikerova, K. Carbon and nitrogen dynamics along the log bark decomposition continuum in a mesic old-growth boreal forest. *Eur. J. For. Res.* **2018**, *137*, 643–657. [CrossRef]
12. Harmon, M.E.; Fasth, B.; Woodall, C.W.; Sexton, J. Carbon concentration of standing and downed woody detritus: Effects of tree taxa, decay class, position, and tissue type. *For. Ecol. Manag.* **2013**, *291*, 259–267. [CrossRef]
13. Ibarra, J.T.; Novoa, F.J.; Jaillard, H.; Altamirano, T.A. Large trees and decay: Suppliers of a keystone resource for cavity-using wildlife in old-growth and secondary Andean temperate forests. *Austral. Ecol.* **2020**, *45*, 1135–1144. [CrossRef]
14. Kilgo, J.C.; Vukovich, M.A. Can snag creation benefit a primary cavity nester: Response to an experimental pulse in snag abundance. *Biol. Conserv.* **2014**, *171*, 21–28. [CrossRef]
15. Lešo, P.; Kropil, R.; Kajtoch, Ł. Effects of forest management on bird assemblages in oak-dominated stands of the Western Carpathians—Refuges for rare species. *For. Ecol. Manag.* **2019**, *453*, 117620. [CrossRef]
16. Parisi, F.; Frate, L.; Lombardi, F.; Tognetti, R.; Campanaro, A.; Biscaccianti, A.B.; Marchetti, M. Diversity patterns of Coleoptera and saproxylic communities in unmanaged forests of Mediterranean mountains. *Ecol. Indic.* **2020**, *110*, 105873. [CrossRef]
17. Nascimbene, J.; Dainese, M.; Sitzia, T. Contrasting responses of epiphytic and dead wood-dwelling lichen diversity to forest management abandonment in silver fir mature woodlands. *For. Ecol. Manag.* **2013**, *289*, 325–332. [CrossRef]
18. Chmura, D.; Żarnowiec, J.; Staniaszek-Kik, M. Altitude is a better predictor of the habitat requirements of epixylic bryophytes and lichens than the presence of coarse woody debris in mountain forests: A study in Poland. *Ann. For. Sci.* **2022**, *79*, 7. [CrossRef]
19. Sylvain, J.; Drolet, G.; Brown, N. Mapping dead forest cover using a deep convolutional neural network and digital aerial photography. *ISPRS J. Photogramm.* **2019**, *156*, 14–26. [CrossRef]
20. Wu, H.; Franklin, S.B.; Liu, J.; Lu, Z. Relative importance of density dependence and topography on tree mortality in a subtropical mountain forest. *For. Ecol. Manag.* **2017**, *384*, 169–179. [CrossRef]
21. Bujoczek, L.; Bujoczek, M.; Zięba, S. How much, why and where? Deadwood in forest ecosystems: The case of Poland. *Ecol. Indic.* **2021**, *121*, 107027. [CrossRef]
22. Berry, Z.C.; Gotsch, S.G.; Holwerda, F.; Muñoz-Villers, L.E.; Asbjornsen, H. Slope position influences vegetation-atmosphere interactions in a tropical montane cloud forest. *Agric. For. Meteorol.* **2016**, *221*, 207–218. [CrossRef]
23. Suleymanov, A.; Abakumov, E.; Suleymanov, R.; Gabbasova, I.; Komissarov, M. The Soil Nutrient Digital Mapping for Precision Agriculture Cases in the Trans-Ural Steppe Zone of Russia Using Topographic Attributes. *ISPRS Int. J. Geo-Inf.* **2021**, *10*, 243. [CrossRef]
24. Liu, X.; Zhang, W.; Yang, F.; Zhou, X.; Liu, Z.; Qu, F.; Lian, S.; Wang, C.; Tang, X. Changes in vegetation-environment relationships over long-term natural restoration process in Middle Taihang Mountain of North China. *Ecol. Eng.* **2012**, *49*, 193–200. [CrossRef]
25. Lippok, D.; Beck, S.G.; Renison, D.; Hensen, I.; Apaza, A.E.; Schleuning, M. Topography and edge effects are more important than elevation as drivers of vegetation patterns in a neotropical montane forest. *J. Veg. Sci.* **2014**, *25*, 724–733. [CrossRef]
26. Muller, R.N. Landscape patterns of change in coarse woody debris accumulation in an old-growth deciduous forest on the Cumberland Plateau, southeastern Kentucky. *Can. J. For. Res.* **2003**, *33*, 763–769. [CrossRef]
27. Rubino, D.L.; McCarthy, B.C. Evaluation of coarse woody debris and forest vegetation across topographic gradients in a southern Ohio forest. *For. Ecol. Manag.* **2003**, *183*, 221–238. [CrossRef]
28. Kennedy, R.S.H.; Spies, T.A.; Gregory, M.J. Relationships of dead wood patterns with biophysical characteristics and ownership according to scale in Coastal Oregon, USA. *Landsc. Ecol.* **2008**, *23*, 55–68. [CrossRef]
29. Kapusta, P.; Kurek, P.; Piechnik, Ł.; Szarek-Łukaszewska, G.; Zielonka, T.; Żywiec, M.; Holeksa, J. Natural and human-related determinants of dead wood quantity and quality in a managed European lowland temperate forest. *For. Ecol. Manag.* **2020**, *459*, 117845. [CrossRef]
30. Zhang, L.; Ma, D.; Jing, X.L.; Su, Z.Y. Topographic controls on the distribution of indigenous rhododendrons in the southern slope of the Nanling mountains, South China. *Pak. J. Bot.* **2016**, *48*, 2367–2374.

31. Sweeney, O.F.M.; Martin, R.D.; Irwin, S.; Kelly, T.C.; O'Halloran, J.; Wilson, M.W.; McEvoy, P.M. A lack of large-diameter logs and snags characterises dead wood patterns in Irish forests. *For. Ecol. Manag.* **2010**, *259*, 2056–2064. [CrossRef]
32. Taylor, L.R. Aggregation, Variance and the Mean. *Nature* **1961**, *189*, 732–735. [CrossRef]
33. Limin, A.; Slik, F.; Sukri, R.S.; Chen, S.B.; Ahmad, J.A. Large tree species composition, not growth rates, is affected by topography in a Bornean tropical forest. *Biotropica* **2021**, *53*, 1290–1300. [CrossRef]
34. Coomes, D.A.; Allen, R.B. Mortality and tree-size distributions in natural mixed-age forests. *J. Ecol.* **2007**, *95*, 27–40. [CrossRef]
35. Bennett, A.C.; McDowell, N.G.; Allen, C.D.; Anderson-Teixeira, K.J. Larger trees suffer most during drought in forests worldwide. *Nat. Plants* **2015**, *1*, 15139. [CrossRef]
36. Silveira, A.P.; Martins, F.R.; Menezes, B.S.; Araújo, F.S. Is the spatial pattern of a tree population in a seasonally dry tropical climate explained by density-dependent mortality? *Austral. Ecol.* **2018**, *43*, 191–202. [CrossRef]
37. Chen, K.; Zhang, H.; Zhang, B.; He, Y. Spatial distribution and associations of dead woods in natural spruce-fir secondary forests. *J. Appl. Ecol.* **2021**, *32*, 2745–2754. [CrossRef]
38. Von Oheimb, G.; Westphal, C.; Härdtle, W. Diversity and spatio-temporal dynamics of dead wood in a temperate near-natural beech forest (*Fagus sylvatica*). *Eur. J. For. Res.* **2007**, *126*, 359–370. [CrossRef]
39. Castagneri, D.; Garbarino, M.; Berretti, R.; Motta, R. Site and stand effects on coarse woody debris in montane mixed forests of Eastern Italian Alps. *For. Ecol. Manag.* **2010**, *260*, 1592–1598. [CrossRef]
40. Sefidi, K.; Esfandiary Darabad, F.; Azaryan, M. Effect of topography on tree species composition and volume of coarse woody debris in an Oriental beech (*Fagus orientalis* Lipsky) old growth forests, northern Iran. *iForest—Biogeosci. For.* **2016**, *9*, 658–665. [CrossRef]
41. Liu, X.; Frey, J.; Denter, M.; Zielewska-Büttner, K.; Still, N.; Koch, B. Mapping standing dead trees in temperate montane forests using a pixel- and object-based image fusion method and stereo WorldView-3 imagery. *Ecol. Indic.* **2021**, *133*, 108438. [CrossRef]
42. Stadelmann, G.; Bugmann, H.; Wermelinger, B.; Bigler, C. Spatial interactions between storm damage and subsequent infestations by the European spruce bark beetle. *For. Ecol. Manag.* **2014**, *318*, 167–174. [CrossRef]
43. Stritih, A.; Senf, C.; Seidl, R.; Grêt-Regamey, A.; Bebi, P. The impact of land-use legacies and recent management on natural disturbance susceptibility in mountain forests. *For. Ecol. Manag.* **2021**, *484*, 118950. [CrossRef]
44. Allen, A.P.; Brown, J.H.; Gillooly, J.F. Global biodiversity, biochemical kinetics, and the energetic-equivalence rule. *Science* **2002**, *297*, 1545–1548. [CrossRef] [PubMed]
45. Carlucci, M.B.; Bastazini, V.A.G.; Hofmann, G.S.; de Macedo, J.H.; Iob, G.; Duarte, L.D.S.; Hartz, S.M.; Müller, S.C. Taxonomic and functional diversity of woody plant communities on opposing slopes of inselbergs in southern Brazil. *Plant Ecol. Divers.* **2015**, *8*, 187–197. [CrossRef]
46. Harmon, M.E.; Franklin, J.F.; Swanson, F.J.; Sollins, P.; Gregory, S.V.; Lattin, J.D.; Anderson, N.H.; Cline, S.P.; Aumen, N.G.; Sedell, J.R.; et al. *Ecology of Coarse Woody Debris in Temperate Ecosystems*; Academic Press: Cambridge, MA, USA, 1986; pp. 59–234.

frontiers in Plant Science

ORIGINAL RESEARCH
published: 30 September 2021
doi: 10.3389/fpls.2021.731203

Dynamic Transcriptomic and Metabolomic Analyses of *Madhuca pasquieri* (Dubard) H. J. Lam During the Post-germination Stages

*Lei Kan, Qicong Liao, Zhipeng Chen, Shuyu Wang, Yifei Ma, Zhiyao Su and Lu Zhang**

College of Forestry and Landscape Architecture, South China Agricultural University, Guangzhou, China

The wild population of *Madhuca pasquieri* (Dubard) H. J. Lam is currently dwindling; its understory seedlings are rare, and there is a lack of molecular studies, which impedes the conservation of this species. This study exploited second-generation sequencing and widely targeted metabolomics analysis to uncover the dynamic changes in differentially expressed genes (DEGs) and differentially accumulated metabolites (DAMs) in five post-germination stages of *M. pasquieri* whole organism. Notably, the weighted gene co-expression network analysis (WGCNA), transcriptome, and metabolome association analyses all indicated significant enrichment of the flavonoid biosynthesis pathway in stage 4 (two-leaf), and an upregulation of the genes encoding flavonol biosynthesis in this stage. In stage 5 (nine-leaf), the flavonols were significantly accumulated, indicating that the changes in metabolites were driven at the transcript level. According to the significant changes in gene expression encoding auxin transport carriers and their correlation with flavonols during stage 5, the flavonols were speculated to have a direct inhibitory effect on the expression of PIN4 encoding gene, which may inhibit the process of polar auxin transport. The results provided important insights into the molecular network relationships between the transcription and metabolism of this rare and endangered species during the post-germination stages and explained the reasons for the slow growth of its seedlings at the molecular level.

Keywords: *Madhuca pasquieri* (Dubard) H. J. Lam, post-germination stages, transcriptomics, widely-targeted metabolomics, flavonols biosynthesis, polar auxin transport

OPEN ACCESS

Edited by:
Jinling Huang,
East Carolina University, United States

Reviewed by:
Amit Rai,
Chiba University, Japan
Atsushi Fukushima,
RIKEN, Japan
Xuebin Zhang,
Henan University, China

****Correspondence:***
Lu Zhang
zhanglu@scau.edu.cn

Specialty section:
This article was submitted to Plant Development and EvoDevo, a section of the journal Frontiers in Plant Science

Received: *26 June 2021*
Accepted: *24 August 2021*
Published: *30 September 2021*

Citation:
Kan L, Liao Q, Chen Z, Wang S, Ma Y, Su Z and Zhang L (2021) Dynamic Transcriptomic and Metabolomic Analyses of Madhuca pasquieri (Dubard) H. J. Lam During the Post-germination Stages. Front. Plant Sci. 12:731203. doi: 10.3389/fpls.2021.731203

INTRODUCTION

Seed germination is the start of the plant life cycle (Bewley, 1997), and the development after germination has a straightforward influence on plant survival (Li et al., 2005). Under the influence of environment, during post-germination, the growth is complicated by various morphological (Romero-Rodriguez et al., 2018), physiological (Qu et al., 2019a), and biochemical changes (Wang et al., 2020). Extensive studies have been conducted on both physiological and morphological levels of post-germination in herbaceous plants, such as maize (*Zea mays*) (Anzala et al., 2006), soybean (*Glycine max* L.) (Gronwald et al., 2009), rice (*Oryza sativa* L.) (Ho et al., 2013), and wheat (*Triticum aestivum* L.) (Sun et al., 2020).

According to the International Union for the Conservation of Nature (IUCN) Red List, *Madhuca pasquieri* (Dubard) H. J. Lam is regarded as a vulnerable (VU) species in the Sapotaceae family. In China, it has been recorded as a national key protected wild plant (II) of tiny population. These trees mainly grow in mixed forests or mountain forest edges below the height of 1,100 m in southern China and northern Vietnam (Flora of China (FOC), 2021). *Madhuca pasquieri* is not only a rare woody oil tree but also a precious timber species. The current research on *M. pasquieri* mainly focuses on *in-situ, ex-situ* protection, chemical composition, and artificial cultivation, and is still in the primary stage. Based on the previous investigation of the authors on the population of this species, we found that its native habitat was seriously fragmented; its seedlings in the understory were very rare, and were difficult to regenerate. We also found that the growth of *M. pasquieri* was very slow during the artificial cultivation in the post-germination stages. Although in the previous study, PacBio combined with an Illumina platform was used to obtain reference sequence through full-length transcriptome sequencing of *M. pasquieri* (Kan et al., 2020), there is still a lack of research on the growth of *M. pasquieri* in post-germination stages at the molecular level.

"Omics" methods have been used in recent years to obtain knowledge of the alterations of metabolites, proteins, and gene transcripts (Wedow et al., 2019). Gene expression can be detected with transcriptome methods, whereas functional changes caused by these genes or proteins can be investigated by metabolomics (Yuan et al., 2018), which is an effective way to analyze the complicated process of post-germination growth. Multi-omics analysis has been a powerful method to identify correlations between genes and metabolites (Saito, 2013). Using transcriptome and integrated metabolome to study the biological process of poplar (*Poplar simonii* × *Poplar nigra*) post-germination growth, it was found that cell wall, amino acid metabolism, and transport-related pathways were obviously enriched during cotyledon expansion, while primary metabolic processes were not (Qu et al., 2019b). Combined transcriptome and metabolome analyses were performed on mung bean (*Vigna radiata*) and seedlings at three time points: 6 h, 3 days, and 6 days (seed germination, hypocotyl elongation, and epicotyl elongation). A lot of transcript changes occurred between samples from seed germination and hypocotyl elongation, including starch and sucrose metabolism, glycolysis, plant hormone regulation, and amino acid synthesis. Additionally, the alterations in metabolites were also detected, including carbohydrates and amino acids, indicating it was driven by the altered genes expressions (Wang et al., 2020). In another poplar study, it was found that during the growth process from the early seed germination stage to the post-germination stage, genes related to CHO metabolism were activated first, followed by gene expression related to lipid metabolism, and then protein metabolism, and changes in metabolites further verified the sequence of these biological events (Qu et al., 2019a). Widely targeted metabolomics is a new method that can accurately detect hundreds of target metabolites, and is broadly used in plants, e.g., *Arabidopsis* (*Arabidopsis thaliana*) (Sawada et al., 2017), rice (Yang et al., 2019b), and apple (*Malus domestica*) (Xu et al., 2020). Moreover, it has proven that the combination analysis of metabolome and transcriptome data can effectively reveal the biosynthetic mechanisms of the main metabolic pathway of post-germination growth in plants (Yang et al., 2020). Therefore, the combination of widely targeted metabolomics and transcriptomics is very necessary for the in-depth understanding of the post-germination growth of *M. pasquieri*. The integration of modern omics techniques provides a comprehensive perspective to better understand the biological processes of post-germination events in plants at the molecular level.

Investigating the molecular mechanism of slow growth in the post-germination of *M. pasquieri* could clearly elucidate the reasons why this species is endangered. Seed germination, by definition, begins when mature dry seeds absorb water, and ends when the radicle protrudes through the seed envelope (Bewley, 1997). With the development of the tree growth, we divided and defined it as five stages, namely stages 1–15: the seed germination stage, which is the last stage of germination, subsequent hypocotyl elongation stage, epicotyl elongation stage, two-leaf stage, and nine-leaf stage. Using Illumina RNA-seq and ultra-performance liquid chromatography-tandem mass spectrometry (UPLC-MS/MS) technologies, we obtained transcriptome and metabolome data from the five post-germination stages in the whole organism of *M. pasquieri*. Weighted gene co-expression network analysis (WGCNA) was performed to identify stage-specific gene clusters, network modules, and module key genes of differentially expressed genes (DEGs) between each stage. Then, combined with the metabolome data, an association analysis was performed to a construct transcript-metabolite correlation network, and the flavonol synthesis pathway and polar auxin transport process were further analyzed. From the perspective of transcription and metabolism, this study explored the reasons for the slow growth of *M. pasquieri* post-germination, which provided new insight for the in-depth analysis of post-germination growth and functions of *M. pasquieri*, and a molecular basis for the protection of this species in the future.

MATERIALS AND METHODS

Plant Materials

Madhuca pasquieri was grown in an artificial climate chamber (RXZ-500C-LED; Ningbo Jiangnan Instrument Factory, Zhejiang, China), at a temperature of 25°C, humidity of 60–80%, and a light cycle of 14/10 h (day/night), 17,600 lx, at the South China Agricultural University. *Madhuca pasquieri* plants were selected based on the five developmental stages from the same batch of light matrix culture in the artificial climate chamber (seed germination, hypocotyl elongation, epicotyl elongation, two-leaf, and nine-leaf stages; **Figure 1**) during post-germination growth, with three biological replicates per stage. The collected whole organism samples were snap-frozen in liquid nitrogen and stored at −80°C until use.

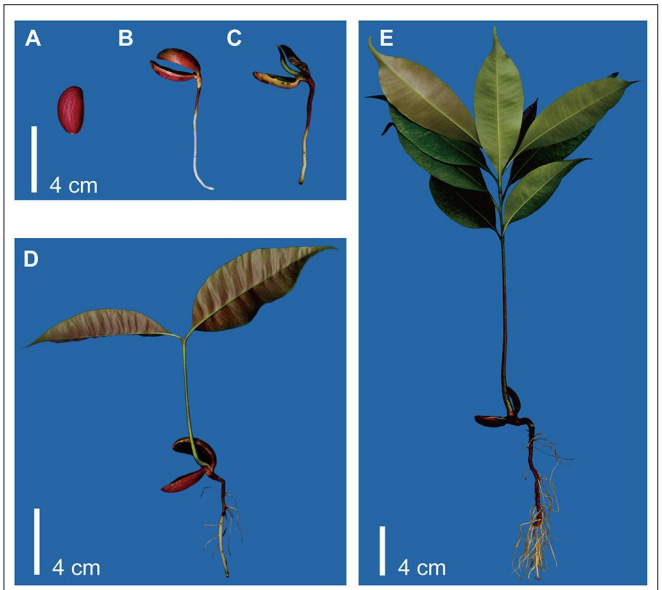

FIGURE 1 | Schematic representation of the experimental setup. **(A)** Stage 1: seed germination. **(B)** Stage 2: hypocotyl elongation. **(C)** Stage 3: epicotyl elongation. **(D)** Stage 4: two-leaf stage. **(E)** Stage 5: nine-leaf stage.

Widely Targeted Metabolome Detection and Data Analysis

The freeze-dried whole organism samples from the five developmental stages, with three biological replicates per stage, were crushed using a mixer mill (MM 400; RETSCH, Haan, Germany) with a zirconia bead for 1.5 min at 30 Hz. Then, 100 mg powder of homogenized tissue was extracted overnight at 4°C with 1 ml 70% aqueous methanol (Merck, Darmstadt, Germany; www.merckchemicals.com) containing 0.1 mg/l lidocaine for the internal standard. Following centrifugation at 10,000 g for 10 min, the supernatant was absorbed and filtrated (SCAA-104, 0.22 μm pore size; ANPEL, Shanghai, China; www.anpel.com.cn/) before liquid chromatography-tandem mass spectrometry (LC-MS/MS) analysis. Quality control (QC) samples were mixed by all the samples to detect the reproducibility of the whole experiment. The repeatability of metabolite extraction and detection was judged by the overlapping analysis of the total ion current (TIC) in the different QC samples (**Supplementary Figure 1**). The TIC curves overlapped during metabolite detection, and the retention times and peak intensities were consistent, indicating that the signals of the identical sample were stable at a different detection time.

The compounds extracted were analyzed using an LC-ESI-MS/MS system [UPLC, Shim-pack UFLC Shimadzu CBM30A system; Shimadzu, Kyoto, Japan; http://www.shimadzu.com.cn/; MS/MS (6500 Q TRAP; Applied Biosystems, Waltham, MA, United States; http://www.appliedbiosystems.com.cn/) (Chen et al., 2013). Data filtering, peak detection, alignment, and calculations were performed using the Analyst 1.6.1 (AB SCIEX, USA) software. The metabolites were identified by searching the internal and public databases MassBank (Horai et al., 2010), KNApSAcK (Nakamura et al., 2013), HMDB (Wishart et al., 2013), MoTo DB (Grennan, 2009), and METLIN (Zhu et al., 2013)), and comparing the m/z values, RT, and fragmentation patterns with the standards. The standards were divided into two levels. The standard of Level A was that the m/Z and RT were consistent with the database substances, and the matching score of the secondary mass spectrometry was more than 90. Level B meant that the matching score of the secondary mass spectrometry was between 60 and 90 when the above parameters were checked with the database. Both levels were for known substances and were scored using MasterView Software.

Metabolite abundances were quantified using the peak areas. To preliminarily visualize the differences between different groups, an unsupervised dimensionality reduction method principal component analysis (PCA) was performed in all the samples using R package models (http://www.r-project.org/). Partial least squares discriminant analysis (PLS-DA) is a supervised dimensionality reduction method in which class memberships are coded in the matrix form into Y to better distinguish the metabolomics profile of two groups by screening variables correlated to class memberships. Orthogonal least partial squares discriminant analysis (OPLS-DA) is derived from PLS-DA. Compared with PLS-DA, OPLS-DA is a combination of orthogonal signal correction (OSC) and PLS-DA (Westerhuis et al., 2008). The data obtained from the metabolite profiling were normalized for the PCA and OPLS-DA. The differentially accumulated metabolites (DAMs) were identified using a combination of variable importance in the projection (VIP) score of the OPLS model and Student's *t*-test. Those with a *P*-value of *t*-test < 0.05 and VIP ≥ 1 were considered as differential metabolites between the two groups.

Transcriptome Profiling and Analysis

Whole organisms of *M. pasquieri* plants sampled at five developmental stages, with three biological replicates per stage, were used for the Illumina RNA sequencing. After the total RNA was extracted, the eukaryotic mRNA with a poly-A tail was enriched with Oligo (dT) beads, and then the enriched mRNA was fragmented into short fragments by ultrasonic waves and reverse-transcribed into cDNA using random primers. The second-strand cDNA was synthesized with DNA polymerase I, RNase H, dNTP, and a buffer (New England Biolabs, Ipswich, MA, United States). Next, the cDNA fragments were purified using a QiaQuick PCR extraction kit (Qiagen, Düsseldorf, Germany) and end-repaired, the poly-A was added, and the fragments were then ligated to the Illumina sequencing adapters. The ligation products were size-selected by agarose gel electrophoresis, amplified by PCR, and sequenced using Illumina HiSeq™ 4000 by Gene Denovo Biotechnology Company (Guangzhou, China).

Reads obtained from the sequencing machines included raw reads containing adapters or low-quality bases, which affect subsequent assembly and analysis. Thus, fastp (version 0.18.0) was applied to obtain high-quality clean reads by further filtering according to the following rules (Chen et al., 2018): (1) removal of reads containing adapters; (2) removal of reads containing more than 10% of unknown nucleotides (N); (3) removal of

reads containing all A bases; (4) removal of low-quality reads containing more than 50% low-quality (Q-value $\leq$ 20) bases. The high-quality clean reads were mapped to the ribosomal RNA (rRNA) to identify the residual rRNA reads. The rRNA-removed reads were used for further analysis.

The rRNA-removed high-quality clean reads were mapped to the reference transcriptome of *M. pasquieri* (SRP267710, https://www.ncbi.nlm.nih.gov/sra/15293472) using a short reads alignment tool, Bowtie2 (Johns Hopkins University, Baltimore, Maryland, United States) (Li et al., 2009) by default parameters, and mapping ratio was calculated.

$$\textbf{Mapping ratio} = \left(\textbf{Unique mapped reads number} + \textbf{Multiple mapped reads numbers}\right) / \textbf{All read number}$$

Principal component analysis was also performed with R package models (http://www.r-project.org/) in this study. To identify DEGs across the groups, the edgeR package (http://www.r-project.org/) was used. The DEGs were identified with a fold change $\geq$2 and a false discovery rate (FDR) $<$0.05 by comparison. The fragments per kilobase of transcript per million mapped (FPKM) reads of each gene were calculated and used to quantify the expression level of the annotated genes.

Gene Ontology (GO) Enrichment Analysis

Gene Ontology enrichment analysis provides all GO terms that are significantly enriched in DEGs compared with the genome background and filters of the DEGs that correspond to biological functions. First, the GOseq R package was applied to perform GO enrichment analysis, and all the DEGs were mapped to GO terms in the Gene Ontology database (http://www.geneontology.org/), gene numbers were calculated for every term, significantly enriched GO terms in DEGs compared with the genome background were defined by Wallenius' non-central hypergeometric distributions (Young et al., 2010). GO categories with FDR $q \leq 0.05$ were considered to be significantly enriched.

Kyoto Encyclopedia of Genes and Genomes (KEGG) Pathway Analysis

The Kyoto Encyclopedia of Genes and Genomes (KEGG, https://www.kegg.jp/kegg/) is the major public pathway-related database that links genomic or transcriptomic contents of genes to chemical structures of endogenous molecules (Kanehisa et al., 2008), thus providing a method to perform integration analysis of genes and metabolites. All the differentially expressed genes and metabolites in the study were mapped to the KEGG pathway database, and KOBAS 2.0 with hypergeometric tests was used to perform the KEGG enrichment analysis (Xie et al., 2011). The significance of KEGG pathway enrichment was determined with FDR $q \leq 0.05$. Pathways meeting this condition were defined as significantly enriched in DEGs or DAMs.

Weighted Gene Co-expression Network Analysis (WGCNA)

Co-expression networks were constructed using the WGCNA (v1.47) package in R (Langfelder and Horvath, 2008). Genes that were not expressed in more than half of the samples were filtered. After the filtration of low-expression genes, the gene expression values were imported into WGCNA to construct co-expression modules using the automatic network construction function blockwiseModules with default settings, except that the power is 7, mergeCutHeight power is 0.2, and minModuleSize power is 50. Genes were clustered into 15 correlated modules. Module eigengene (ME) values were calculated for each module and used to test for association with each stage. Networks were visualized using Cytoscape v.3.7.1 (Shannon et al., 2003).

Transcriptome and Metabolome Correlation Network

Pearson's correlation coefficients were calculated based on the gene expression level (FPKM) of the transcriptome and the relative content of metabolites to obtain the correlation between metabolome and transcriptome data. Gene and metabolite pairs were ranked in the descending order of absolute correlation coefficients.

Real-Time Quantitative Polymerase Chain Reaction (RT-qPCR)

The same RNA samples used in RNA-Seq were used in a real-time quantitative polymerase chain reaction (RT-qPCR). According to the instructions of the reverse transcription kit (R223; Vazyme Biotech, Nanjing, China), a 20-μl reaction system was established with 50 ng−2 μg total RNA and was incubated at 50°C for 50 min and 95°C for 5 min to obtain cDNAs. The cDNAs were then loaded in a 96-well plate for qRT-PCR analysis using StepOnePlus (ABI, CA, United States) with an RT-PCR reagent (Q341; Vazyme Biotech, Nanjing, China). The 20-μl reaction system consisted of 10 μl of 2 × ChamQ SYBR qPCR Master Mix (Vazyme Biotech, Nanjing, China), 0.4 μl of a PCR forward primer (10 μM), 0.4 μl of a PCR reverse primer (10 μM), 4 μl of a cDNA template, and 5.2 μl of ddH_2O. PCR conditions were as follows: 95°C for 90 s, 40 cycles of 95°C for 5 s, 60°C for 15 s, and 72°C for 20 s. Relative gene expression levels were analyzed according to the $2^{-\Delta\Delta Ct}$ method. Product specificity and reaction efficiencies were verified for each primer pair. The primer pairs are listed in **Supplementary Table 1**.

RESULTS

Metabolite Analysis

In the definition of the traditional seed germination stage, the termination of germination is the protuberance of the radicle through the seed envelope, so in this study, we define this stage as stage 1 (seed germination). According to the post-germination stages, hypocotyl elongation, epicotyl elongation, two-leaf stage, and nine-leaf stage were defined as stages 2 to 5, respectively. First, we prepared the whole organism samples at five stages of *M. pasquieri,* as shown in **Figure 1**.

The dynamic metabolite changes in the five different stages of *M. pasquieri* were evaluated by UPLC-MS/MS. By qualification control and repeatability analysis, we showed the stability of the instruments and ensured the reliability and repeatability of the metabonomic data. PCA was performed to show the overall metabolic differences between inner and inter-group variations.

As shown in **Figure 2A**, the samples from stage 1 and stage 5 gathered into a distinct cluster, respectively, while the samples from stages 2, 3, and 4 had an obvious overlap. However, OPLS-DA showed that there was still a clear separation between any two comparison stages (**Supplementary Figure 2**). These results indicated that the data were reproducible enough to be used in subsequent analyses.

In the available data, there were 497 metabolites that had been identified in the five development stages of *M. pasquieri* with three biological replicates in each stage (**Supplementary Table 2**). Of the 497 metabolites, phenolic acids (16.5%), amino acids and derivatives (15.3%), organic acids (7.8%), nucleotides and derivatives (7.6%), flavonols (6.4%), and saccharides and alcohols (5.6%) accounted for a large proportion (**Figure 2B**). DAMs were identified according to the standard of VIP $\geq$ 1 of OPLS-DA and $P < 0.05$ of *t*-test between each pairwise comparison. In total, 51, 57, 65, and 80 DAMs were identified (**Table 1**). For stage 1 vs. stage 2, 24 DAMs were upregulated and 27 were downregulated, and most of the upregulated DAMs were lipids, tannins, and flavonoids; the downregulated DAMs were mainly amino acids and derivatives. For stage 1 vs. stage 3, 30 DAMs were upregulated and 27 were downregulated; the upregulated DAMs were mainly tannins, flavonoids, and terpenoids, and the downregulated DAMs were mainly amino acids and derivatives. Of the 65 DAMs in stage 1 vs. stage 4, 38 and 27 DAMs were upregulated and downregulated, respectively. Among them, the upregulated DAMs were mainly flavonoids and phenolic acids, and the downregulated DAMs were mainly amino acids and derivatives. Of the 80 DAMs in stage 1 vs. stage 5, 36, and 44 DAMs were upregulated and downregulated, respectively. Among them, most of the upregulated DAMs were flavonoids, phenolic acids, and lipids; the downregulated DAMs were also mainly amino acids and derivatives (**Supplementary Table 3**). The DAM accumulation patterns in the different groups were also evaluated by hierarchical cluster analysis (**Supplementary Figure 3**).

Of these DAMs, amino acids and derivatives (37.25%), flavonoids (19.61%), organic acids (7.84%), tannins (7.84%), lipids (5.88%), nucleotides and derivatives (5.88%), and phenolic acids (5.88%) had a relatively large proportion in stage 2 compared with stage 1 (**Figure 3A**). Amino acids and derivatives (35.09%), flavonoids (19.30%), tannins (10.53%), organic acids (8.77%), and terpenoids (7.02%) were differentially accumulated in stages 1 and 3 (**Figure 3B**). Of the DAMs in stage 1 vs. stage 5, amino acids and derivatives (30%), flavonoids (25%), phenolic acids (12.5%), and other metabolites (10%) had the highest representation (**Figure 3D**). Interestingly, flavonoids (29.23%), amino acids and derivatives (26.15%), phenolic acids (12.31%), organic acids (10.77%), and alkaloids (6.15%) accounted for a large proportion in stages 1 and 4 (**Figure 3C**). To explore the functions of post-germination-related metabolites, the DAMs in stage 1 vs. stage 2, stage 1 vs. stage 3, stage 1 vs. stage 4, and stage 1 vs. stage 5 were functionally annotated using the KEGG database. For stage 1 vs. stage 2, the terms "aminoacyl-tRNA biosynthesis," "glucosinolate biosynthesis," and "biosynthesis of amino acids" were dominantly enriched (**Supplementary Figure 4A**). The terms "aminoacyl-tRNA biosynthesis," "valine, leucine, and isoleucine degradation" and "alanine, aspartate, and glutamate metabolism" were enriched in stage 1 vs. stage 3 (**Supplementary Figure 4B**). However, only the term "valine, leucine, and isoleucine degradation" was significantly enriched in stage 1 vs. stage 4 (**Supplementary Figure 4C**). Meanwhile, for stage 1 vs. stage 5, the DAMs were strongly related to the terms "aminoacyl-tRNA biosynthesis," "cyanoamino acid metabolism," and "ABC transporters" (**Supplementary Figure 4D**).

Global Analysis of RNA-seq Data and WGCNA

Subsequently, we performed RNA-Seq to detect transcriptome differences among the post-germination stages of *M. pasquieri*. For each stage of the samples, an average of 45.6 million raw reads per library was detected (**Table 2**). All the reads in this study were mapped to the *M. pasquieri* reference transcriptome after mapping to the ribosome (Kan et al., 2020). In 15 libraries, approximately 54.23–68.65% of all the reads could be mapped on the reference transcriptome. Finally, a total of 22,685 genes, which correspond to 89.53% of the 25,339 genes predicted in the *M. pasquieri* transcriptome (Kan et al., 2020), were found to be expressed during the post-germination stages (**Table 2**). The PCA showed that the contribution rate of the first two primary components was 73.1%, and that the clustering of the samples in stage 1 and stage 5 was obvious, while the samples in the other three stages were relatively scattered and partially overlapped (**Supplementary Figure 5**). However, the overall grouping trend was consistent with the PCA result of the metabolome samples. In this study, we set FDR < 0.05 and $|\log2FC| > 1$ (FC: fold change) as cut-off for screening DEGs. Here, 1,987 DEGs (1,433 up, 554 down) between stages 1 and 2 were detected; 3,176 DEGs (2,244 up, 932 down) between stages 1 and 3 were detected; 3,800 DEGs (2,727 up, 1,073 down) between stages 1 and 4 were detected; 4,365 DEGs (3,286 up, 1,079 down) between stages 1 and 5 were detected. The number of genes with significantly changed expression during *M. pasquieri* post-germination increased gradually, as shown in **Figure 4A**. A total of 5,894 DEGs were detected in the post-germination stages (stages 2–5) compared with the seed germination stage (stage 1), 1,280 DEGs were identified differentially expressed between stage 1 and the other development stages; 179, 255, 483, and 1,280 DEGs were specifically expressed in stages 2–5, respectively (**Figure 4B**). To classify the genes involved in the different development stages, KEGG pathway and GO enrichment analyses were performed for DEGs in stage 1 vs. stage 2, stage 1 vs. stage 3, stage 1 vs. stage 4, and stage 1 vs. stage 5. The terms "metabolic pathways" (ko01100), "biosynthesis of secondary metabolites" (ko01110), and "photosynthesis—antenna proteins" (ko00196) were all significantly enriched in each of the four other stages compared with stage 1 (**Supplementary Figure 6**). The GO analysis indicated that the DEGs of the different stages in biological process were mainly enriched for terms "metabolic process"

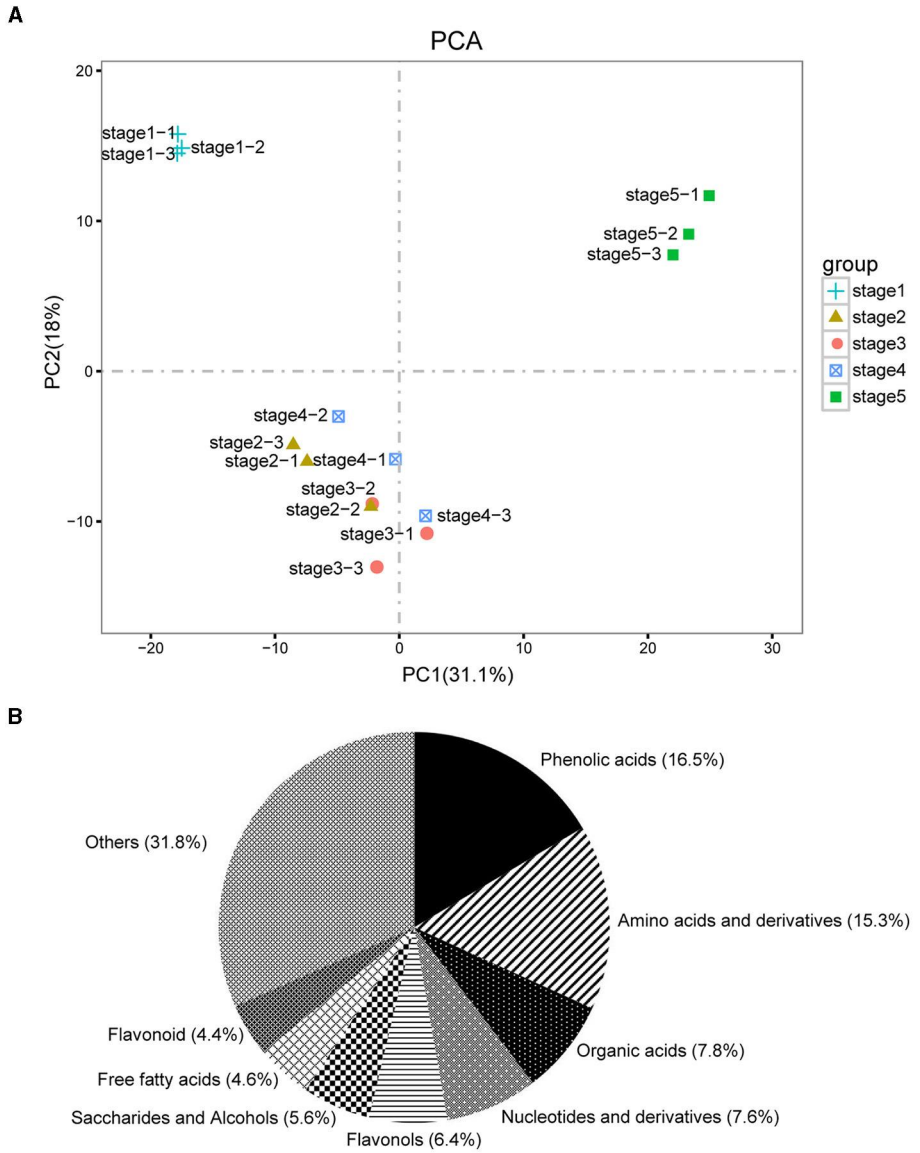

FIGURE 2 | Overall qualitative and quantitative analyses of the metabolomics data. **(A)** Principal component analysis (PCA) of the five development stage samples and quality control samples (mixed); the x-axis represents the first principal component, and the y-axis represents the second principal component. **(B)** Component analysis of the identified metabolites. The top eight metabolites are shown beside the graph.

(GO:0008152), "cellular process" (GO:0009987), and "single-organism process" (GO:0044699). For cellular component, the DEGs were mainly involved in "cell" (GO:0005623) and "cell part" (GO:0044464) in each stage compared with stage 1. The DEGs involved in molecular function mainly composed of "catalytic activity" (GO:0003824), "binding" (GO:0005488), and "transporter activity" (GO:0005215) in the different stages (**Supplementary Table 4**).

We performed WGCNA to find the co-expression network of genes specifically expressed in the *M. pasquieri* post-germination stages from a comprehensive network perspective. The co-expression network was constructed with all the DEGs at different stages. The genes with similar expression patterns were clustered into the same modules, and different modules were distinguished by color, as shown in **Figure 5A**. Finally, 14 different merged modules were identified, and the subsequent analysis was carried out according to the merged modules. According to correlation analysis, these modules corresponded to a specific distribution pattern in the post-germination stages (**Figure 5B**). Compared with other modules, such as grey 60, the genes of this module displayed the highest correlation with stage 4 ($p = 0.004$, $r = 0.69$), while the genes in the purple module showed the highest correlation with stage 5 ($p = 3 \times 10^6$, $r = 0.91$). The genes in the pink, magenta, and light-yellow modules

TABLE 1 | Summary of differentially accumulated metabolites (DAMs) between stage 1 and the other groups (stages 2–5).

Group Name	Number Up-regulated	Number Down-regulated	Number of differential metabolites
Stage 1 vs. stage 2	24	27	51
Stage 1 vs. stage 3	30	27	57
Stage 1 vs. stage 4	38	27	65
Stage 1 vs. stage 5	36	44	80

Stage 1, seed germination; stage 2, hypocotyl elongation; stage 3, epicotyl elongation; stage 4, two-leaf stage; stage 5, nine-leaf stage.

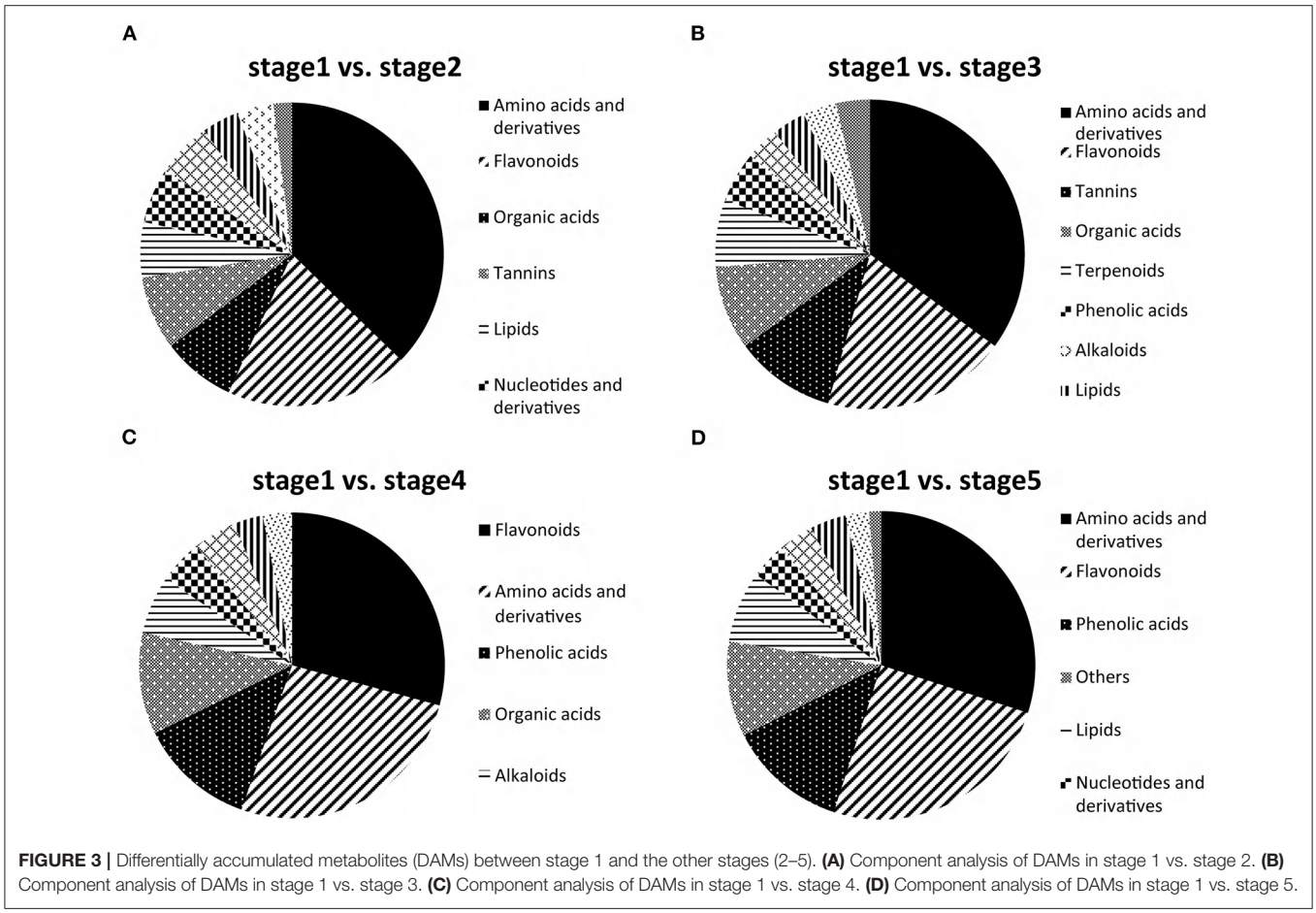

FIGURE 3 | Differentially accumulated metabolites (DAMs) between stage 1 and the other stages (2–5). **(A)** Component analysis of DAMs in stage 1 vs. stage 2. **(B)** Component analysis of DAMs in stage 1 vs. stage 3. **(C)** Component analysis of DAMs in stage 1 vs. stage 4. **(D)** Component analysis of DAMs in stage 1 vs. stage 5.

were most associated with stages 1 ($p = 6 \times 10^6$, $r = 0.9$), 2 ($p = 0.04$, $r = 0.53$), and 3 ($p = 0.02$, $r = 0.58$), respectively.

The ME values are the principal component of a gene module, which represents the gene expression profile of each module. The eigengene expression profiles of 11 modules were analyzed, as shown in **Figure 5C**. MEs of the pink, green-yellow, and light cyan modules had higher expression levels during stage 1, whereas MEs of the magenta and grey 60 modules were expressed at higher levels during stages 2 stage 4. MEs of the light yellow and tan modules had the highest expression during stage 3. During stage 5, MEs of the dark red, purple, light green, and red modules were expressed at higher levels.

The categories of enriched pathways and their mobilization trends in each module were determined for the purpose of understanding the changes of biological processes in different modules. By comparing the number of background genes, genes in the magenta module were significantly enriched in six categories: "glycolysis/gluconeogenesis," "glutathione metabolism," "nicotinate and nicotinamide metabolism," "biosynthesis of secondary metabolites," "phenylpropanoid biosynthesis," and "alpha-Linolenic acid metabolism." The light yellow module was significantly correlated with stage 3, with "RNA polymerase," "tropane, piperidine, and pyridine alkaloid biosynthesis," and "pyrimidine metabolism" being significantly enriched. The purple module was significantly associated with stage 5, with 13 significantly enriched categories identified (**Supplementary Table 5**). The number of enriched categories varied in the other modules.

TABLE 2 | Statistics of ribonucleic acid sequencing (RNA-Seq) reads obtained from the 15 samples and mapping to the *Madhuca pasquieri* (Dubard) H. J. Lam reference transcriptome.

Sample	Low quality(%)	All reads number (%)	Mapped reads (%)	Genes number (%)
Stage 1-1	181244 (0.20%)	42154302 (93.50%)	26796006 (63.57%)	17575 (69.36%)
Stage 1-2	155184 (0.19%)	38114744 (95.12%)	23373476 (61.32%)	17498 (69.06%)
Stage 1-3	162132 (0.21%)	36015022 (91.84%)	22075196 (61.29%)	17432 (68.80%)
Stage 2-1	231632 (0.23%)	48029318 (95.71%)	32195188 (67.03%)	18274 (72.12%)
Stage 2-2	220308 (0.27%)	38762952 (93.73%)	24676470 (63.66%)	18563 (73.26%)
Stage 2-3	201792 (0.19%)	49637142 (94.76%)	34075820 (68.65%)	18376 (72.52%)
Stage 3-1	152348 (0.19%)	39303962 (97.36%)	21313352 (54.23%)	18289 (72.18%)
Stage 3-2	257772 (0.29%)	42831964 (96.82%)	28085726 (65.57%)	18286 (72.17%)
Stage 3-3	179708 (0.21%)	41001822 (97.70%)	26498838 (64.63%)	18066 (71.30%)
Stage 4-1	191608 (0.22%)	41645196 (96.09%)	25515568 (61.27%)	18112 (71.48%)
Stage 4-2	181812 (0.18%)	47917986 (95.97%)	31312242 (65.35%)	18339 (72.37%)
Stage 4-3	279144 (0.32%)	41537518 (95.34%)	25755626 (62.01%)	18354 (72.43%)
Stage 5-1	185552 (0.20%)	42246108 (93.45%)	26543010 (62.83%)	18781 (74.12%)
Stage 5-2	214664 (0.20%)	52505450 (96.79%)	33765504 (64.31%)	19303 (76.18%)
Stage 5-3	193572 (0.19%)	49037022 (95.64%)	31349528 (63.93%)	19252 (75.98%)

All read numbers: Unmapped read numbers of rRNA.
Mapped reads: Mapped read numbers of reference genes (ratio = mapped read/all read number).
Gene number: Number of genes expressed in each sample (ratio = gene number/total reference gene number).

Among the 14 modules, we found that the number of flavonoids accounted for the largest proportion among the DAMs in this stage from the metabolome results; thus, the following main analysis was performed on the grey 60 module. "Flavonoid biosynthesis," "biosynthesis of secondary metabolites" and "phenylalanine metabolism" were significantly enriched in grey 60 module genes (**Figure 6A**), which further proved that "flavonoid biosynthesis" was active in stage 4. WGCNA is also available for constructing gene co-expression networks, where each node represents a gene, and the connecting lines between nodes are called edges, which represent the co-expression of related genes. The node with the highest connectivity, named hub gene, may play a vital role in the different modules. The grey 60 module network is shown in **Figure 6B**, and the top 10 hub genes are identified by red triangles, among which Isoform0005812, Isoform0003985, and Isoform0006467 were assigned to "flavonoid biosynthesis" (ko00941) (**Supplementary Table 6**). This indicated that hub genes were mainly involved in "flavonoid biosynthesis," except for "metabolic pathways" and "biosynthesis of secondary metabolites."

Transcript-Metabolite Correlation Network

To simulate the regulatory properties of DAMs and DEGs, a subnetwork was constructed for the top 10 hub genes to determine transcript-metabolite correlations. Pearson's correlation tests were carried out between relative quantitative changes of metabolites and related transcripts, and we set correlation coefficient > 0.8 as cut-off in the analysis. Meanwhile, the pathways involved in DAMs and DEGs were shown by the pie chart; it can be found that except for "metabolic pathways," DAMs and DEGs were most involved in "flavonoid biosynthesis" (**Figure 7**). Not only that, in these DAMs, four flavonols and three flavonoids were found. These results indicated that the top 10 hub genes were highly correlated with their corresponding metabolites involved in "flavonoid biosynthesis," and many flavonols were identified in this process, which reconfirmed the large accumulation of flavonols and their special importance during stage 4. The authenticity and accuracy of the metabolic analysis were validated by transcriptome data.

Flavonol Biosynthesis Pathway

The flavonol biosynthesis pathway involves three pathways: "phenylpropanoid biosynthesis," "flavonoid biosynthesis," and "flavone and flavonol biosynthesis." As shown in **Figure 8**, after a series of conversions, phenylalanine is converted to *p*-Coumaroyl coenzyme A (CoA) through a series of enzymes in the "phenylpropanoid biosynthesis" pathway. Since then, many genes and metabolites of the latter two pathways were upregulated in stage 4, such as chalcone synthase (CHS, five DEGs), chalcone isomerase (CHI, three DEGs), naringenin 3-dioxygenase (F3H, four DEGs), flavonol synthase (FLS, three DEGs), flavonoid 3′,5′-hydroxylase (F3′5′H, 2 DEGs), and flavonoid 3′-monooxygenase (F3′M, 1 DEG).

Most of these genes were significantly upregulated in stage 4 (**Figure 8**). The expression levels of two CHS genes, Isoform0003264, and Isoform0003528, were 2.54 and 2.44, respectively, times higher in stage 4 than in stage 3, indicating the high accumulation of naringenin chalcone in stage 4. Naringenin was produced from naringenin chalcone, catalyzed by CHI (Isoform0010762 and Isoform0015047; 3.91- and 2.88-fold upregulation in stage 4; however, Isoform0013593 downregulated by about one time but upregulated again in stage 5), and naringenin was not upregulated in stage 4, but was significantly accumulated in stage 5. Naringenin 3-dioxygenase catalyzes the conversion of naringenin into dihydrokaempferol, and its encoding gene F3H, Isoform0003066, Isoform0004496,

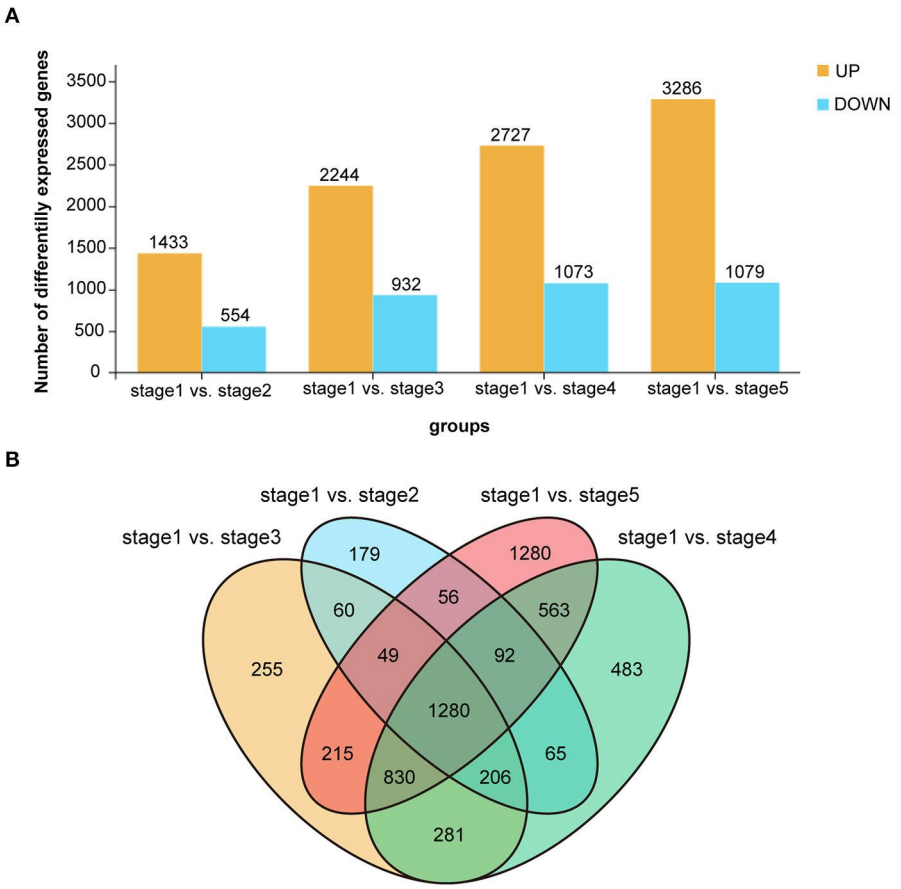

FIGURE 4 | Differentially expressed genes (DEGs) of *Madhuca pasquieri* (Dubard) H. J. Lam during the post-germination stages. **(A)** Summary of the number of significantly changed transcripts between successive stages during *M. pasquieri* post-germination stages. **(B)** Venn diagram showing the overlap of DEGs during *M. pasquieri* post-germination stages.

Isoform0005727, and Isoform0013502 were upregulated 1.24, 1.89, 3.73, and 2.67 times in stage 4, respectively. The content of dihydrokaempferol was significantly accumulated in stage 5; the upregulation was not significant in stage 4. FLS catalyzes the conversion of dihydrokaempferol into kaempferol, and two genes (Isoform0005532 and Isoform0006515) were upregulated in stage 4; however, the content of kaempferol was also significantly increased in stage 5. Meanwhile, F3′5′H and F3′M can catalyze the conversion of dihydrokaempferol and kaempferol into dihydroquercetin and quercetin, respectively. In stage 4, there were two F3′5′H genes (Isoform0022755 and Isoform0025197) and one F3′M gene (Isoform0022617) that were up-regulated. Quercetin can also be obtained by the FLS catalytic conversion of dihydroquercetin, and quercetin can be further catalyzed by F3′5′H to myricetin.

Plant Hormone Signal Transduction Pathway

Plant hormones, such as auxin, gibberellin (GA), cytokinine, and abscisic acid (ABA), are closely related to post-germination growth. However, 349 genes were found and involved in the "plant hormone signal transduction" pathway; but only one metabolite, salicylic acid, was found in the whole pathway (**Supplementary Figure 7**). In order to study the genes related to plant hormones further, 86 DEGs were selected from the 349 genes, and their expression levels were analyzed with a heatmap. As shown in **Figure 9**, there are 30 auxin-related DEGs, of which most auxin transporter protein 1 (AUX1) genes are upregulated in stages 3–5; the expression of transport inhibitor response1 (TIR1) genes is upregulated in stages 2-4; most of the auxin/indole-3-acetic acid (AUX/IAA) and auxin response factor (ARF) genes are upregulated in stage 5; most of the gretchenhagen 3 (GH3) and small auxin-upregulated RNA (SAUR) genes are upregulated in the first two stages. Only three DEGs were associated with GA, namely, GA-insensitive dwarf mutant 1 (GID1), GA-insensitive dwarf mutant 2 (GID2), and DELLA. Among them, GID1 was upregulated in stages 2 and 4, GID2 was upregulated in stages 1 and 3, and DELLA was upregulated in stages 4 and 5. There were 15 ABA-related DEGs, among which all pyrabactin resistance/PYR-like (PYR/PYL) genes were upregulated in stage 5; however, most of the protein phosphatase 2C (PP2C), sucrose non-fermenting 1-related protein kinases subfamily 2 (SnRK2), and ABRE-binding factor (ABF) genes were upregulated in

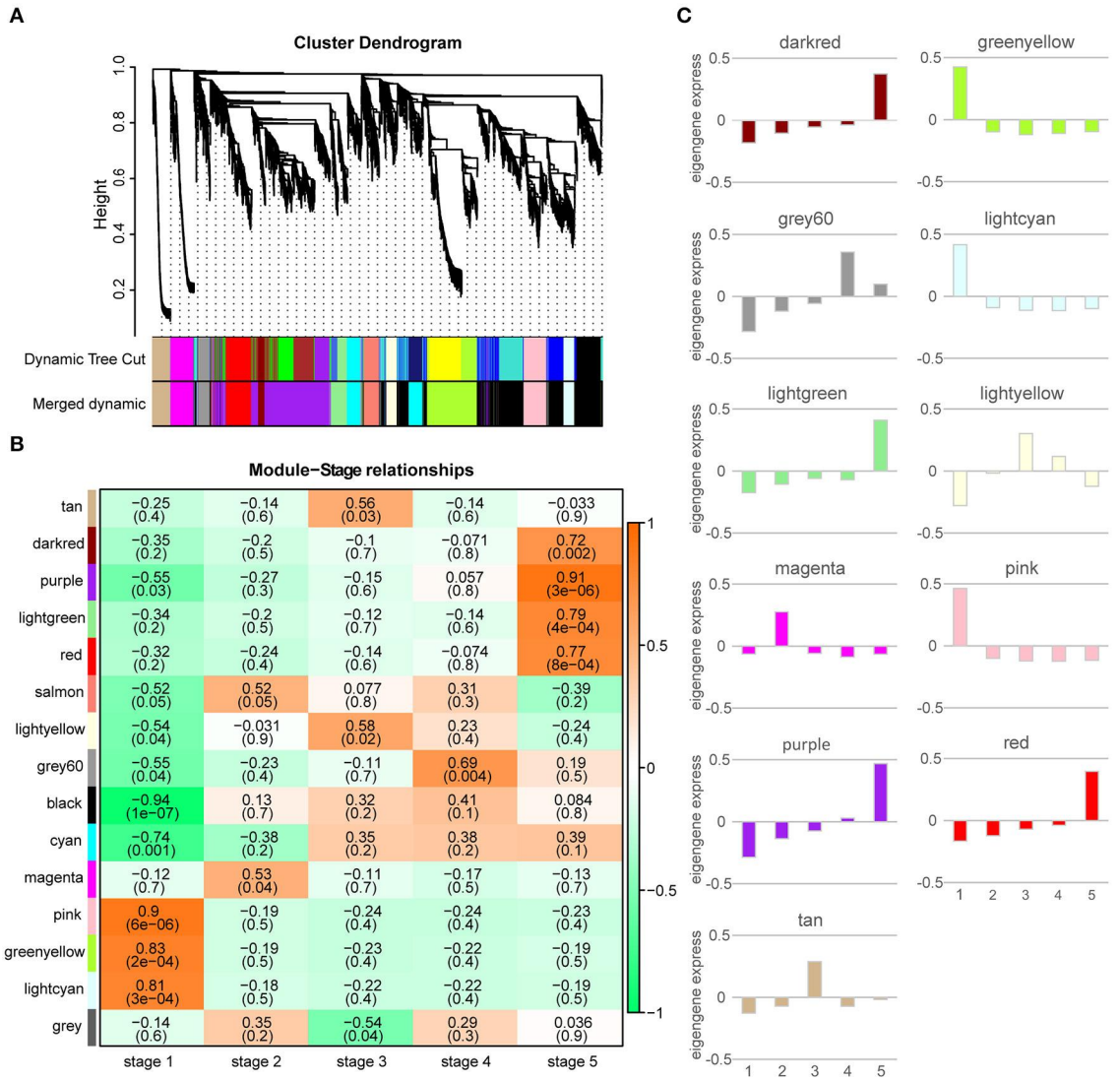

FIGURE 5 | Weighted gene co-expression network analysis (WGCNA) of the significantly changed transcripts. **(A)** Hierarchical cluster tree showing co-expression modules and merged modules identified by the WGCNA. Each leaf in the tree is one gene. The dynamic tree cut were modules divided according to the clustering results, and merged dynamic were modules that were merged with a similar representation pattern based on module similarity. The major tree branches constitute 15 merged modules labeled with different colors. **(B)** Module-stage relationships. Each row corresponds to a module, and each column represents a specific stage. The color of each cell at the row-column intersection indicates the correlation coefficient between a module and a stage. A high degree of correlation between a specific module and stage is indicated by red. **(C)** Eigengene expression profile of each module. The y-axis indicates the value of the module eigengene; the x-axis indicates the sampled post-germination stage (1–5).

the first three stages. Most ethylene-related DEGs, such as ethylene receptor (ETR), mitogen-activated protein kinase 6 (MPK6), ethylene insensitive3 (EIN3), EIN3-binding F-BOX1 and 2 (EBF1/2), and ethylene-responsive transcription factors 1 and 2 (ERF1/2), were upregulated in stages 1 and 2. Most of the brassinosteroid insensitive 1-associated receptor kinase 1 (BAK1), brassinosteroid-insensitive 1 (BRI1), xyloglucosyl transferase TCH4 (TCH4), and cyclin D3 (CYCD3) genes related to brassinosteroid, and jasmonic acid resistant1 (JAR1), jasmonate ZIM domain-containing protein (JAZ), and transcription factor MYC2 (MYC2) genes related to jasmonic acid were upregulated in stage 5. However, DEGs related to salicylic acid, transcription factor TGA (TGA) and pathogenesis-related protein 1 (PR-1), were upregulated in the different stages. The cytokinine-related genes changed indistinctively in stages 1–5, so they were not included in this analysis.

Flavonol Affects Polar Auxin Transport

In all, the 349 genes were upregulated and involved in the "plant hormone signal transduction" pathway; however, only one metabolite, salicylic acid, was found in the whole pathway (**Supplementary Figure 7**). In many previous studies, flavonols,

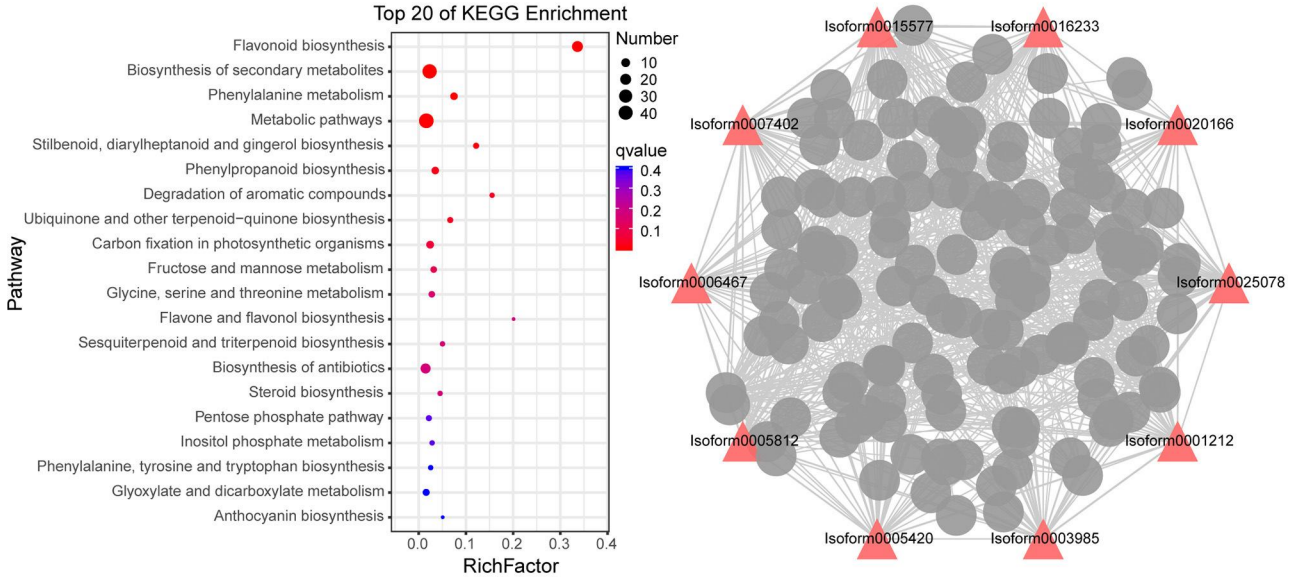

FIGURE 6 | Co-expression network analysis of grey 60 module. **(A)** Enriched Kyoto Encyclopedia of Genes and Genomes (KEGG pathways) of the grey 60 module genes. **(B)** Correlation network of genes in the grey 60 module (stage 4). *q*-value is a *P*-value that has been adjusted for the false discovery rate (FDR). A lower *q*-value indicates that a lower percentage of significant results will be false positives. Rich factor represents the degree of enrichment of genes under the designated pathway term, the greater the value of the rich factor, the greater the degree of pathway enrichment. Red triangles indicate the top 10 hub genes, the wider the edge, the greater the weight between the two genes.

a flavonoid subgroup, have been found to significantly affect the polar transport of auxin and can be used as plant transport inhibitors (Buer et al., 2010). Polar auxin transport carrier was mainly completed by the influx carrier Auxin1/Like-AUX1 (AUX/LAX), efflux carrier ATP-binding cassette subfamily Bs/P-glycoprotein (ABCBs/PGP), and the pin-formed (PIN) protein family (Teale and Palme, 2018). The gene expression levels of the above five encoding proteins at each stage were analyzed, and no gene encoding PGP was found in *M. pasquieri* transcripts in all the stages. Five genes were encoding AUX, among which Isoform0006674 and Isoform0007151 were significantly down- and upregulated in stage 4, respectively, while the other genes had no significant changes (**Figure 10A**). Among the six genes encoding LAX, Isoform0008732, Isoform0010377, Isoform0018938, and Isoform0002221 are all downregulated in stage 4 and upregulated in stage 5 (**Figure 10B**). Seven and 13 genes were found encoding PIN and ABCB, respectively, but only one gene (Isoform0013295) was found encoding pin-formed protein4 (PIN4), and two genes were found encoding ATP-binding cassette subfamily B1 (ABCB1, Isoform0001269, and Isoform0019016). Among them, no significant expression difference of Isoform0013295 in each stage had been found. The expression level of Isoform0001269 was downregulated in stages 4 and 5, but not significantly, while Isoform0019016 had a higher expression in stage 4 (**Figures 10C,D**).

To further investigate the relationship between flavonols and gene expression of these polar auxin transport carriers, a correlation heatmap was constructed (**Figure 10E**). The result showed that the contents of kaempferol (mws1068) and myricetin (mws0032) were negatively and significantly correlated with the expression level of the PIN4 encoding gene (Isoform0013295), respectively, while kaempferol was positively and significantly associated with the expression levels of four genes encoding LAX (Isoform0008732, Isoform0010377, Isoform0018938, and Isoform0002221), respectively. Additionally, there was no obvious correlation between the content of myricetin and the expression levels of genes encoding LAX, or between the contents of kaempferol and myricetin and the expression levels of ABCB1 encoding genes.

Validating Gene Expression Patterns by RT-qPCR

To identify the actual expression patterns of key DEGs involved in the flavonol biosynthesis pathway and polar auxin transport, RT-qPCR was performed to validate the seven DEGs encoding CHS (1), CHI (2), F3H (1), FLS (1), F3′5′H (1), and F3′M (1) from the flavonol biosynthesis pathway and eight DEGs encoding LAX (3), AUX (1), ABCB (2), and PIN (2) belong to the polar auxin transport carriers in the five post-germination stages of *M. pasquieri*. The results of the RT-qPCR were consistent with the RNA-Seq data (**Figure 11A**) and indicated that the qRT-PCR and RNA-Seq data were highly correlated and presented consistency in the upregulation and downregulation of DEG expression ($r^2 = 0.8846$) (**Figure 11B**). These results indicated that the RNA-Seq data were reliable.

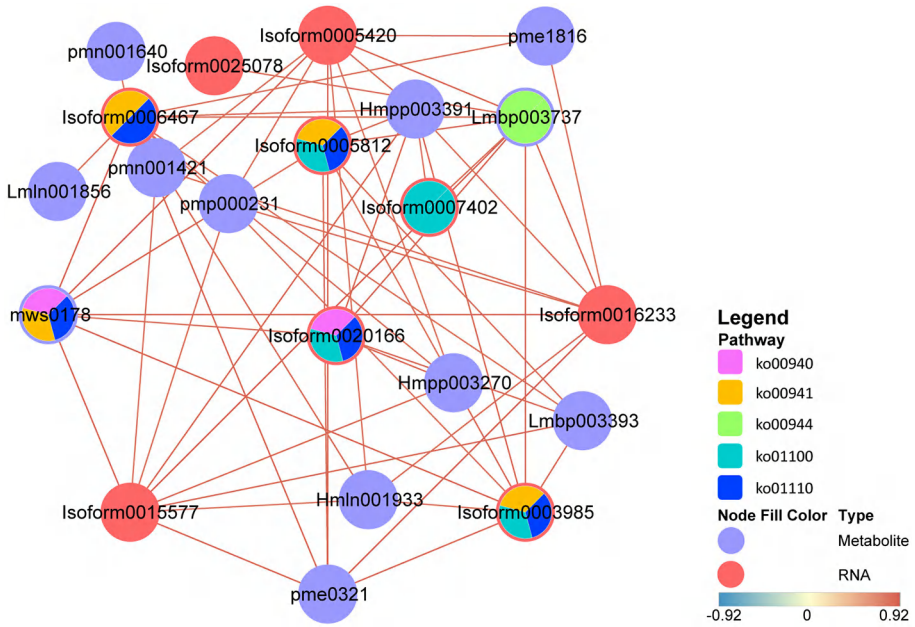

FIGURE 7 | Transcript-metabolite Pearson's correlation network representing DAMs and DEGs involved in *M. pasquieri*. The gene-metabolite pairs were connected within the network by edges. Red nodes represent genes, and purple nodes represent metabolites. The edges between nodes represent correlation. The color bar below indicates red edges represent positive correlations, and blue edges represent negative correlations. Only correlation pairs with a correlation coefficient > 0.8 were included in the network. The pie chart on the nodes shows part of pathways involved in DAM and DEG. DAMs, differentially accumulated metabolites; DEGs differentially expressed genes. Lmbp003393, quercetin-3-O-α-L-rhamnopyranoside; pme0321, kaempferol 7-O-rhamnoside; pmn001640, myricetin 3-α-L-arabinofuranoside; Lmbp003737, kaempferol-3-O-rhamnoside; Hmln001933, myricetin 3-O-galactoside; Hmpp003391, luteolin-3′-O-β-D-glucoside; Hmpp003270, luteolin-4′-O-β-D-glucoside; mws0178, chlorogenic acid; pmn001421, 3-O-(E)-p-Coumaroyl quinic acid; pmp000231, trans-3-O-p-coumaric quinic acid; pme1816, neochlorogenic acid; Lmln001856, 5,7-dihydroxy-4-oxo-2-(3,4,5-trihydroxyphenyl)-4H-chromen-3-yl-β-D-allopyranoside.

DISCUSSION

Differentially Accumulated Metabolites (DAMs) Specifically Involved in Different Post-Germination Stages

We detected a total of 497 metabolites in the five post-germination stages of *M. pasquieri*, including 34 substances and their derivatives (**Supplementary Table 2**), among which phenolic acids (82, 16.5%), amino acids and derivatives (76, 15.3%), organic acids (39, 7.8%), nucleotides and derivatives (38, 7.6%) and flavonols (32, 6.4%) accounted for the largest proportion (**Figure 2B**). However, Wang et al. (2020) only identified 57 metabolites in mung bean by untargeted metabolome analysis performing gas chromatography-mass spectrometry (GC-MS), and most of the metabolites were sugar metabolism compounds, amino acid metabolism compounds, tricarboxylic acid (TCA), and other organic acid metabolism compounds. Seven hundred thirty metabolites were detected in the germination and post-germination growth stages of the two varieties of rice by widely targeted metabolome, including 32 substances and their derivatives, among which flavone (74, 10.1%), organic acids (67, 9.2%), amino acid derivatives (60, 8.2%), nucleotide and its derivates (57, 7.8%), and flavone C-glycosides (44, 6.0%) accounted for the largest proportion (Yang et al., 2020). This indicated that the widely targeted metabolome method could identify more metabolites than the untargeted metabolome method, and the metabolites of rice were far more than that of *M. pasquieri*, which may be related to the different species and germination stages.

We found that the maximum number of DAM was observed in stage 5, which may be because the seedlings in the nine-leaf stage have begun to use photosynthesis for energy supply, participate in a variety of metabolic pathways, and are active in the synthesis and degradation of various metabolites. Interestingly, except for the highest proportion of flavonoids in the DAMs for stage 4 vs. stage 1, the DAMs of the other groups had the largest proportion of amino acids and derivatives (**Figure 3**), indicating the largest change in flavonoid substances in stage 4. In addition, the contents of organic acids, phenolic acids, tannins, and lipids also changed significantly in each stage.

In the analysis of DAMs in the five stages, it was found that compared with stage 1, most of the lipids were significantly accumulated in stages 2 and 5, the majority of tannins were significantly accumulated in stages 2 and 3, terpenoids were mainly significantly accumulated in stage 3, and most of the phenolic acids were significantly accumulated in stages 4 and 5. Most of flavonoids were increased to different degrees in the five stages (**Supplementary Table 3**). However, in a study on poplar post-germination, lipids were found decreased during the hypocotyl elongation stage and increased in the seedling stage,

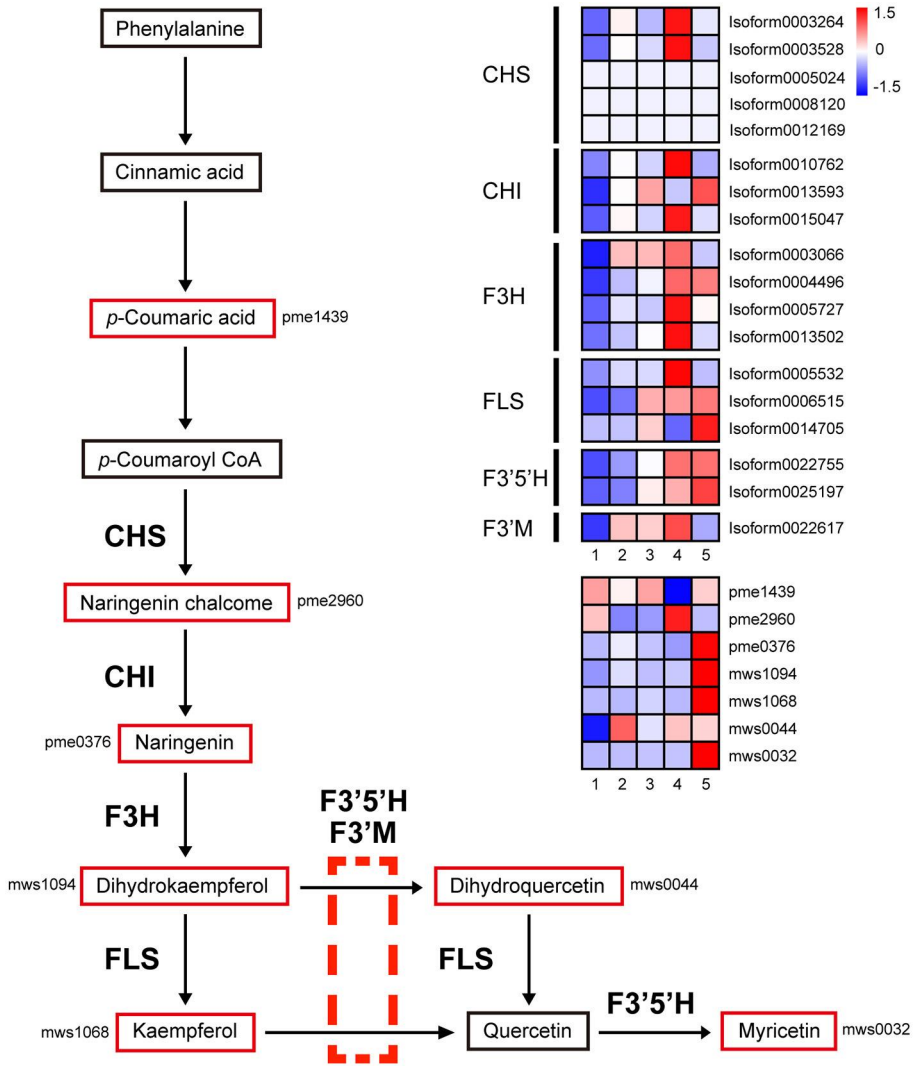

FIGURE 8 | Transcript and metabolic profiling of genes in the flavonoid and flavonol biosynthetic pathways in *M. pasquieri*. The heatmap is drawn according to the average expression levels of related biosynthetic genes and relative accumulation levels of related metabolites. A color bar is presented at the top right, and the colors from blue to red indicate low to high expression and accumulation. CHS, chalcone synthase; CHI, chalcone isomerase; F3H, naringenin 3-dioxygenase; FLS, flavonol synthase; F3′5′H, flavonoid 3′,5′-hydroxylase; F3′M, flavonoid 3′-monooxygenase.

suggesting that this may be related to the increased demand for lipids in poplar seeds (Qu et al., 2019a). This result was contrary to those of this study, which may be because of the fact that *M. pasquieri* is a woody oil tree, whose seeds have a high oil content, so its lipids metabolism was still active in stage 2. Interestingly, in both poplar and mung bean studies, amino acids and derivatives were obviously upregulated from the hypocotyl elongation stage, which may be related to the decomposition of storage proteins (Qu et al., 2019a; Wang et al., 2020). However, in this study, most of the amino acids and derivatives were significantly downregulated in stages 2–5 (**Supplementary Table 3**), which may be caused by the requirement of high levels of protein synthesis in the post-germination of *M. pasquieri*, but more in-depth studies are needed. These results indicate that although poplar and *M. pasquieri* are both woody plants, they belong to Sapotaceae and Salicaceae, respectively, and there are significant differences in the changes in metabolites in post-germination growth. In addition, most tannins were significantly upregulated in stages 2 and 3, which was consistent with the previously reported tannins in *M. pasquieri* (Kan et al., 2020), indicating that tannins had begun to accumulate in the early post-germination stage. The terpenoids accumulated significantly in stage 3 and were all triterpene (**Supplementary Table 3**). Triterpene is not only important for the formation of saponins and resins in plants; it is also related to defense function (Kemen et al., 2014), indicating that terpenoid metabolism became active in stage 3, possibly in preparation for environmental adaptation. Moreover, phenolic acids, which act as signal molecule and defense plant

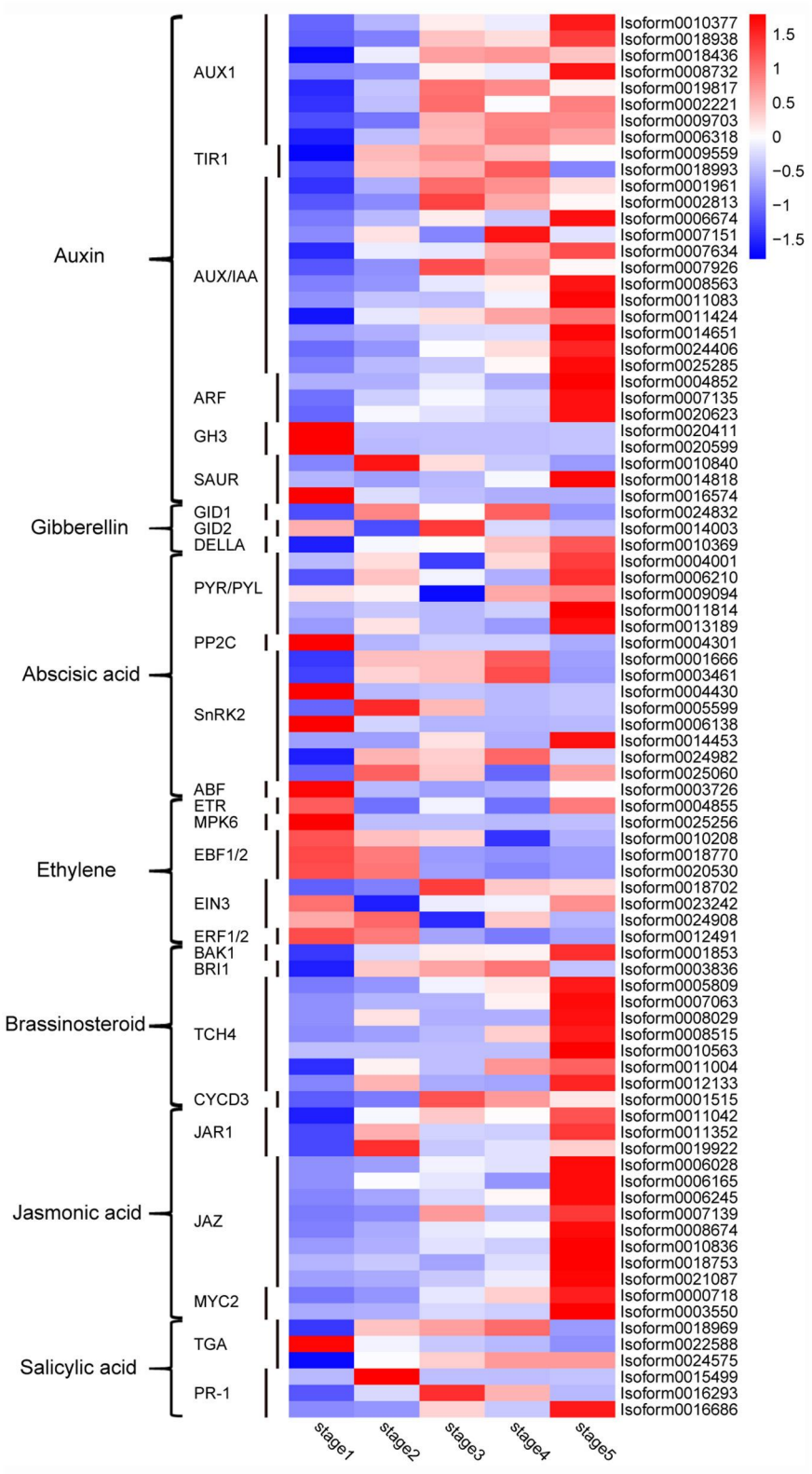

FIGURE 9 | Heatmap of expression of DEGs in the plant hormone signal transduction pathway. A color bar is presented at the top right, and the colors from blue to red indicate low to high expression. AUX1, auxin transporter protein 1; TIR1, transport inhibitor response1; AUX/IAA, auxin/indole-3-acetic acid; ARF, auxin response

(Continued)

FIGURE 9 | factor; GH3, gretchenhagen 3; SAUR, small auxin upregulated RNA; GID1, GA-insensitive dwarf mutant 1; GID2, GA-insensitive dwarf mutant 2; PYR/PYL, pyrabactin resistance/PYR-like; PP2C, protein phosphatase 2 C; SnRK2, sucrose non-fermenting 1-related protein kinases subfamily 2; ABF, ABRE-binding factor; ETR, ethylene receptor; MPK6, mitogen-activated protein kinase 6; EIN3, ethylene insensitive 3; EBF1/2, EIN3-binding F-BOX 1 and 2; ERF1/2, ethylene-responsive transcription factors 1 and 2; BAK1, brassinosteroid-insensitive 1-associated receptor kinase 1; BRI1, brassinosteroid-insensitive 1; TCH4, xyloglucosyl transferase TCH4; CYCD3, cyclin D3; JAR1, jasmonic acid-resistant 1; JAZ, jasmonate ZIM domain-containing protein; MYC2, transcription factor MYC2; TGA, transcription factor TGA; PR-1, pathogenesis-related protein 1.

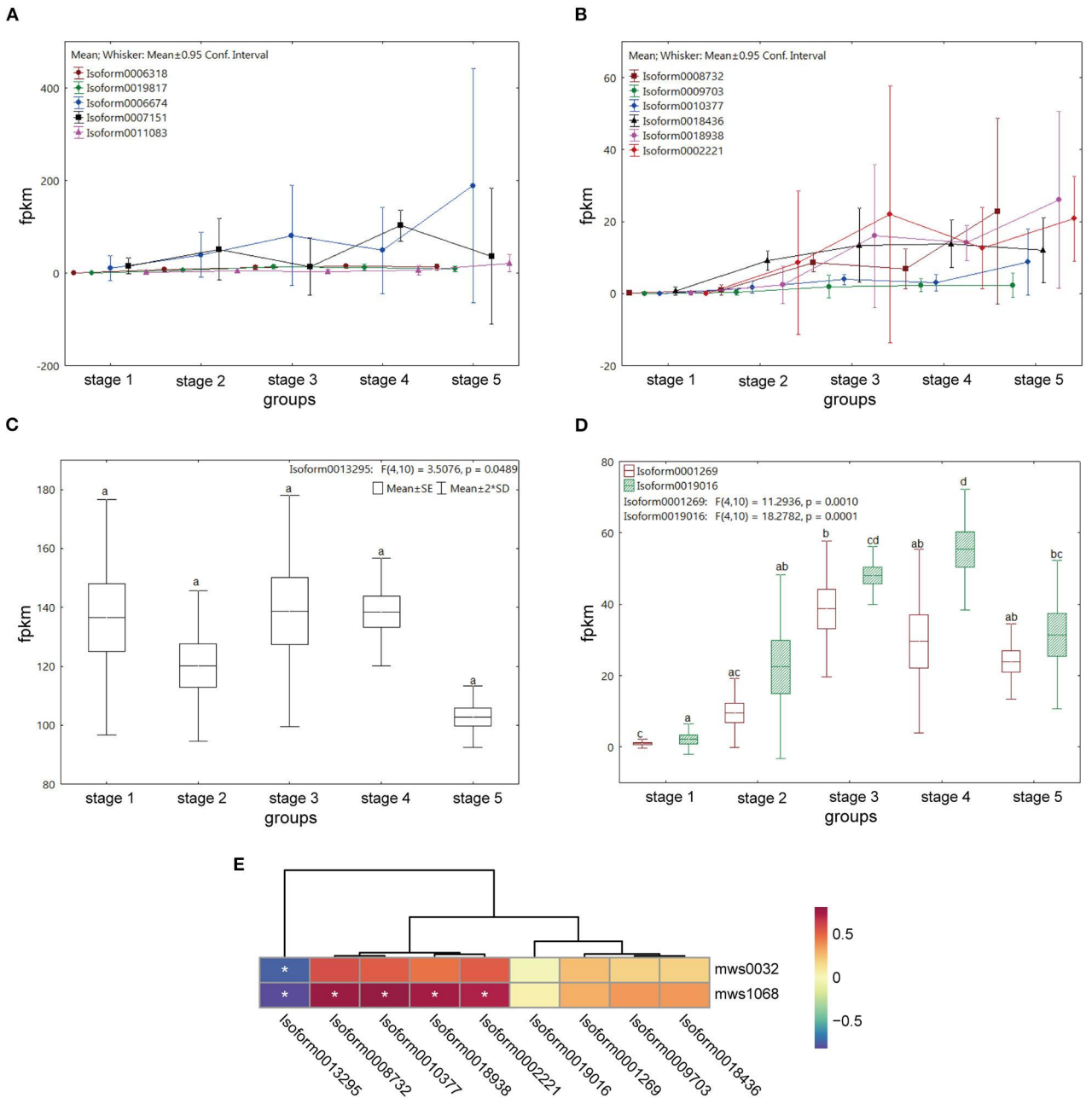

FIGURE 10 | Expression of the genes encoding polar auxin transport carriers at the five stages and its correlation with flavonol contents during stages 4 and 5 in *M. pasquieri*. **(A)** Expression of five genes encoding AUX. **(B)** Expression of six genes encoding LAX. **(C)** Expression of the gene encoding PIN4. **(D)** Expression of two genes encoding ABCB1. AUX/LAX, Auxin1/Like-AUX1; PIN4, pin-formed protein4; ABCB1, ATP-binding cassette subfamily B1. **(E)** Heatmap of correlation between genes encoding polar auxin transport carriers and flavonol contents during stages 4 and 5. In the color bar, red represents a positive correlation, and blue represents a negative correlation. $^*p < 0.05$.

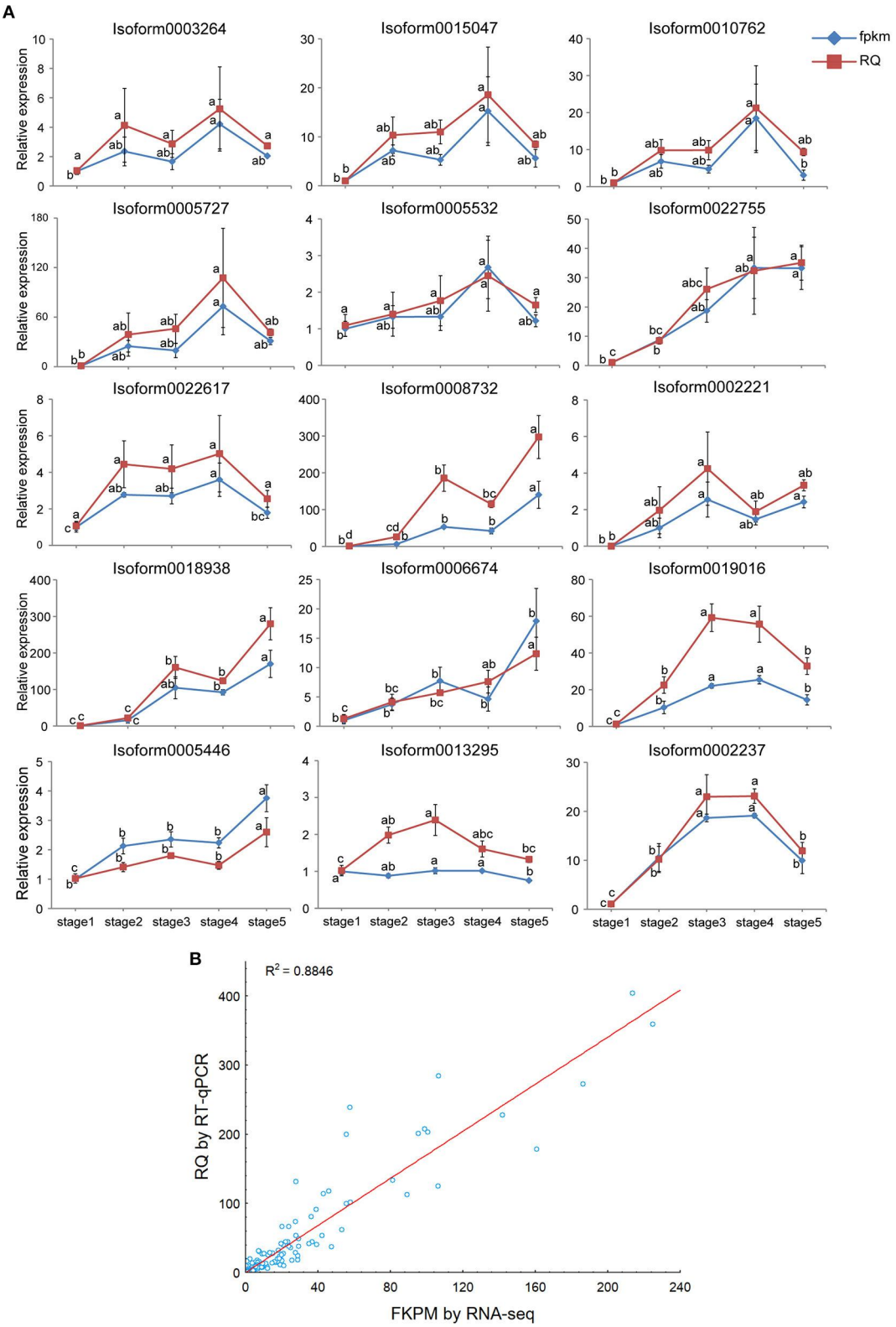

FIGURE 11 | Real-time quantitative polymerase chain reaction (RT-qPCR) validation of 15 structural genes. **(A)** Expression patterns of the 15 genes involved in the flavonol biosynthesis and polar auxin transport in five post-germination stages of *M. pasquieri* (from stages 1 to 5). Each column represents an average of three biological replicates, with standard errors indicated by vertical bars. Values with a different accompanying letter are statistically significantly different according to Duncan's multiple range test at $p < 0.05$. **(B)** Correlation of the expression levels of 15 selected genes measured by RNA-seq and RT-qPCR.

herbivores and pathogens, accumulated significantly in later two stages (Mandal et al., 2010). These indicated that secondary metabolites had been gradually active since stage 3 in *M. pasquieri*. All the DAMs that were upregulated in each stage had flavonoids, indicating that they played a vital role in the post-germination growth of *M. pasquieri*.

Transcriptome Analysis of Post-germination Stages in *M. pasquieri*

This study found that the mapped rate of transcripts from the five post-germination stages to the reference sequence of *M. pasquieri* was 68.8–76.18%, which was lower than that of other studies. For example, 78.7–83.9% of the reads were mapped on the mung bean reference genome (Wang et al., 2020). The average rates of mapped transcripts for the *indica* rice and *japonica* rice in the Nipponbare reference genome were 80.94 and 80.27%, respectively (Yang et al., 2020). This is because *M. pasquieri* lacks genomic information and only full-length transcriptome sequences are used as reference sequences, while the third-generation sequencing uses mixed samples, which may filter some low-quality reads during assembly, and the transcript length is longer, leading to a relatively lower mapped rate with the single RNA-Seq samples. Transcripts of stages 2–5 were compared with those of stage 1 to obtain DEGs for WGCNA.

Weighted gene co-expression network analysis is a biological tool that provides an effective way to analyze correlations between gene expression levels from complex RNA-Seq data at different developmental stages, treatments, and time courses (Yuan et al., 2018). The WGCNA results showed that the magenta and light yellow modules were mostly correlated with stages 2 (hypocotyl elongation) and 3 (epicotyl elongation). Genes of the magenta module were mainly enriched in "glycolysis/gluconeogenesis," "glutathione metabolism," "nicotinate and nicotinamide metabolism," "biosynthesis of secondary metabolites," and "phenylpropanoid biosynthesis" (**Supplementary Table 5**), which were consistent with the enrichment pathways of the rice hypocotyl elongation stage (Yang et al., 2020). However, in other studies, the genes during this stage were significantly enriched in starch and sucrose metabolism, glycolysis, TCA cycle, biosynthesis of amino acids, and plant hormone signal transduction pathway (Sreenivasulu et al., 2008; Wang et al., 2020), where glycolysis and TCA cycle provide the required energy for subsequent growth. The light yellow module was significantly enriched in "RNA polymerase," "tropane, piperidine, and pyridine alkaloid biosynthesis," and "pyrimidine metabolism" pathways (**Supplementary Table 5**), which was completely different from previous reports that DEGs were significantly enriched in carbohydrate synthesis, biosynthesis of amino acids, and plant hormone signal transduction during the epicotyl elongation stage in mung bean (Wang et al., 2020). This may be caused by the specific growth characteristics of woody plants and herbaceous plants, and the bias of different growth stages in post-germination, leading to different enrichment pathways. The purple module had the strongest correlation with stage 5 (nine-leaf), which was mainly enriched in photosynthesis, photosynthesis-related metabolic pathways, nitrogen metabolism, carbon metabolism, and amino acid metabolism pathways, which was consistent with previous studies (An and Lin, 2011; Qu et al., 2019b). It is worth noting that the grey 60 module had the strongest correlation with stage 4 (two-leaf), significantly enriched in secondary metabolites biosynthesis pathways, such as flavonoid biosynthesis, phenylalanine metabolism, stilbenoid, diarylheptanoid, and gingerol biosynthesis (**Supplementary Table 5**), and the key genes with the high connectivity within the module were also mainly involved in flavonoid biosynthesis (**Supplementary Table 6**). However, using the same WGCNA method, the study on poplar germination in different stages showed that the module key genes of the highest correlation with the two-leaf stage were mainly involved in CHO, cell wall, lipids metabolism, and PS (Qu et al., 2019b); this discrepancy may be the result of differences between the species being studied. We speculate that the energy reserve and secondary metabolite synthesis significantly changed in stage 2 of *M. pasquieri*, that photosynthesis significantly changed in stage 5, and that the pathway significantly enriched in stage 3 still needs to be further studied. The significant changes in secondary metabolites, such as flavonoid biosynthesis in stage 4, might be the potential reason for the slow growth of *M. pasquieri* seedlings in the early culture process.

Post-germination growth is regulated by the synergistic interaction of various endogenous plant hormones (Miransari and Smith, 2014). However, the WGCNA results showed that the genes in the modules of interest were not significantly enriched in the "plant hormone signal transduction" pathway (**Supplementary Table 5**), and that only one metabolite, salicylic acid, was detected in this pathway (**Supplementary Figure 7**). In order to further explore these results, the expression levels of plant hormone-related genes in the pathway were analyzed (**Figure 9**). Auxin is known to promote cell elongation and plays an important role in post-germination growth (Pacifici et al., 2015). Most of the DEGs related to auxin signal transduction, such as AUX1, TIR1, AUX/IAA, and ARF, were upregulated in stage 3–5, indicating that the auxin signal transduction process was active from epicotyl elongation and promoted the growth of *M. pasquieri*. GA promotes growth mainly by stimulating radicle elongation (Romero-Rodriguez et al., 2018; Song et al., 2019); we have also found that its related DEGs were upregulated in the different stages of *M. pasquieri* (**Figure 9**). In addition to inhibiting seed germination, ABA is also involved in regulating stomatal closure and reducing evapotranspiration (Jin et al., 2013). In this study, most ABA-related genes, such as PP2C, SnRK2, and ABF, were upregulated in the first three stages, while PYR/PYL genes were upregulated in stage 5, which may be related to different environmental stress conditions in the different stages. Except for auxin, GA, and ABA, other plant hormones like ethylene, brassinosteroid, jasmonic acid, and salicylic acid were also important in the growth of post-germination. Ethylene not only promotes fruit ripening and senescence, in other studies, it has also been reported to promote seed germination and growth (Wang et al., 2020). Based on the results of this study, it was found that most of the ethylene-related DEGs were upregulated in

stages 1 and 2 (**Figure 9**), which may be related to the promotion of growth in the early post-germination stages. Studies have reported that brassinosteroid mainly promotes cell division and cell elongation (Pacifici et al., 2015), and that jasmonic acid is mainly involved in stress response (Zhao et al., 2019). Most of the DEGs related to brassinosteroid and jasmonic acid were increased in stage 5 (**Figure 9**), indicating that other than growth promotion, there may have been anti-stress involved in stage 5. Salicylic acid, known for its disease resistance response, is also involved in the regulation of physiological and chemical processes in plants (Matic et al., 2016). Salicylic acid was also the only plant hormone detected in this study, and was significantly accumulated in all the stages, while its related DEGs upregulated in the different stages (**Figure 9**), indicating that salicylic acid metabolism was activated from stage 1, which may be actively involved in the regulation of disease resistance process.

Flavonol Affects Polar Auxin Transport

Flavonoids are secondary metabolites widely distributed in plants with diverse physiological functions (Taylor and Grotewold, 2005; D'Amelia et al., 2018), which play important roles such as ultraviolet photo-damage protection (Biever and Gardner, 2016), defense against pathogens and pests (Zhao et al., 2020), stress response (Gu et al., 2020), pollen and pollen tube formation (Zhang et al., 2020b), and auxin transport regulation (Ramos et al., 2016). Flavonols, a subgroup of flavonoids, regulate auxin transport and auxin-dependent physiological processes, and act as an auxin transport inhibitor (Pollastri and Tattini, 2011; Brunetti et al., 2018). Many studies have reported that flavonols, such as kaempferol, quercetin, isorhamnetin, and myricetin, are distributed in plants (Zhang et al., 2020a). In addition, naringenin, as a precursor of flavonols, has strong inhibitory effects on *Arabidopsis* seed germination and main root growth of seedlings (Hernández and Munné-Bosch, 2012). The polar auxin transport carriers are mainly completed by influx carrier AUX/LAX, efflux carrier ABCBs/PGP, and PIN protein families (Mohanta et al., 2018). However, flavonol can affect ABCBs/PGP and PIN carriers (Teale and Palme, 2018), and can also be converted to the glycosyl form under the action of UDP-glycosyltransferase to affect auxin transport carriers (Kuhn et al., 2016; Yin et al., 2017). The expression levels of pin-formed protein1 (PIN1) were found to be decreased in the *tt4* mutant (without flavonoid synthesis), which affects PINs protein aggregation and circulation, and enhances auxin transport; while the high content of quercetin and kaempferol in the *tt7* mutant (excessive accumulation of kaempferol) inhibits auxin transport (Peer et al., 2004; Buer et al., 2013).

At present, the chemosmosis hypothesis is widely accepted in the study on polar auxin transport, that is, auxin can form ionized $IAAH^+$ outside plastid (pH = 5.5), and the lipophilicity of ionized $IAAH^+$ can be diffused or form the ion with influx carrier AUX/LAX flow into the cytoplasm. After entering the cell, auxin is deionized in the neutral cytoplasm and can only be transported out of the cell by efflux carrier ABCBs/PGP and PIN, among which ABCBs are mainly responsible for long-distance non-directional transport, while PIN is mainly involved in the intercellular directional transport of auxin (Mohanta et al., 2018). There have been many reports that flavonol is considered an auxin transport inhibitor (Ramos et al., 2016; Brunetti et al., 2018). The results of this study found that most of the genes that participated in the flavonol biosynthesis pathway were obviously upregulated during stage 4, and some were upregulated during stage 5, but most of the metabolites involved in the pathway were apparently accumulated only in stage 5, such as the final flavonols, kaempferol, and myricetin (**Figure 8**). It might be that the flavonol biosynthesis pathway in stage 4 significantly enriched (**Figure 6A**), which was consistent with the WGCNA results. In this stage, most genes began to be upregulated to carry out transcription and translation and eventually become metabolites, which took some time. Therefore, most of the metabolites accumulated significantly in stage 4, indicating that the changes in the metabolites seemed to be driven by increased transcript levels. In addition, in the metabolome data, it can be found that flavonoid accounted for the largest proportion of DAMs in stage 4 (**Figure 3C**), indicating that flavonoid changed significantly in stage 4, but that it still needed a certain time for the accumulation of substances.

PGPs belong to the ABCB transporter family and can hydrolyze ATP to transport substrates (Peer and Murphy, 2007). Some studies have shown that flavonols can inhibit P-glycoproteins (PGP) transport auxin by affecting the expression pattern of the PGP gene and its subcellular localization (Lewis et al., 2007). In this study, no transcript encoding PGP was found, so it was speculated that the accumulation of flavonols may directly inhibit the expression of PGP encoding genes, which needed further studies. PIN plays an essential part in regulating auxin distribution in plants and affecting plant development (Kreček et al., 2009). Studies have shown that the PIN protein mediates auxin effluxion (Zhou and Luo, 2018; Yang et al., 2019a). Flavonols can indirectly affect the gene expression and subcellular localization of PIN1 and pin-formed protein2 (PIN2) (Peer and Murphy, 2007; Santelia et al., 2008). In a study on *Arabidopsis rol1-2* mutants, it was found that flavonols changed the polar localization of PIN2, thus affecting auxin transport (Kuhn et al., 2017). It has also been shown that a flavonol interacted with the protein complex of PIN1, making it more stable and less able to mediate cellular auxin efflux (Teale et al., 2021). Moreover, some research studies have found that flavonols directly affected PIN4 expression and subcellular localization, and changed the intercellular concentration of auxin (Peer and Murphy, 2007). In this study, seven genes encoding PIN were found, but only one gene encoding PIN4 (Isoform0013295) was downregulated in stage 5, but not significant (**Figure 10C**). Further correlation analysis revealed that the contents of kaempferol and myricetin were significantly negatively correlated with Isoform0013295 in stages 4 and 5, respectively (**Figure 10E**), which suggested that flavonols might inhibit PIN4 encoding gene expression to some extent. Some studies suggest that ATP-binding cassette subfamily B19 (ABCB19), rather than PIN1, was the target of 1-naphthylphthalamic acid (NPA)-mediated polar auxin transport inhibition, and that flavonols can compete with NPA for binding sites (Geisler et al., 2016). In addition, flavonols can bind and inhibit the transport proteins ABCB1 and ABCB19, and interfere with their interaction with

FK506-binding protein TWISTED DWARF1 (FKBP42/TWD1), thus inhibiting the transport of auxins, among which quercetin has the best effect (Muday et al., 2006; Geisler et al., 2016), but no studies have proved that flavonols directly inhibit the expression of ABCB encoding genes. A total of 13 ABCB encoding genes were found in this study, two of which were encoding ABCB1 (Isoform0001269 and Isoform0019016), but no ABCB19 encoding gene was found. Isoform0001269 was downregulated in stage 5, but not significant. Compared with stage 4, Isoform0019016 was significantly downregulated in stage 5 (**Figure 10D**). However, the correlation heatmap displayed no obvious correlation between the expression levels of these two genes and flavonols contents (**Figure 10E**), so whether flavonols directly affect the expression of ABCB encoding genes needs further experiments to be proved. There were also data supporting the interaction between PIN1 and ABCB19 in *Arabidopsis*, but PIN1 and ABCB19 were not associated at any time in terms of the ratio of the two proteins in PIN1-GFP affinity precipitates (Teale et al., 2021). Meanwhile, biochemical data indicated that ABCBs and TWD1 were targets of the flavonol inhibition of polar auxin transport, while genetic data pointed to PIN1 (Mohanta et al., 2018), indicating that the process of flavonols regulating polar auxin transport was very complex. Moreover, the effects of flavonols on polar auxin transport and PIN localization varied with tissue and cell type (Kuhn et al., 2017).

At present, although no studies have reported the effect of flavonols on influx carrier AUX/LAX, six genes encoding AUX and six genes encoding LAX were found based on the results this study. AUX encoding gene expression changed irregularly in different stages (**Figure 10A**). However, most of the genes encoding LAX (Isoform0008732, Isoform0010377, Isoform0018938, and Isoform0002221) were downregulated in stage 4 but were upregulated in stage 5 (**Figure 10B**). We speculated that flavonols may bind to LAX, and that to maintain normal auxin transport, the system may promote the expression of genes encoding LAX, leading to the increase in its expression in stage 5. The correlation heatmap also showed a significant positive correlation between kaempferol content and the expression levels of Isoform0008732, Isoform0010377, Isoform0018938, and Isoform0002221, but this process still needs further studies. Interestingly, there was no significant correlation between myricetin content and these four genes expression levels. Previous studies have reported that the impact of different flavonols on PIN binding affinity and induction of PIN subcellular localization is different; for example, compared with other flavonols, morin can relatively effectively stabilize the PIN complex (Teale et al., 2021). Based on the results of this study, it can also be speculated that compared with myricetin, kaempferol has more effective impact on LAX gene expression, and that the regulatory mechanism of this process can also become the direction of further research in the future. Meanwhile, these results indicated that a large amount of flavonols was accumulated in stage 5 of *M. pasquieri*, and that flavonols may affect the expression of polar auxin transport carriers encoding genes at the transcriptional level, which may lead to the inhibition of polar auxin transport, resulting in slow growth.

Although the effects of flavonols on auxin transport have been studied from the perspective of proteomics and metabolomics (Geisler et al., 2016; Kuhn et al., 2017), so far, few studies have combined transcriptome and metabolome to study how flavonols affect polar auxin transport in post-germination growth. This is the novelty of this study, but it does not involve proteome analysis, which leads to certain limitations of the analysis. To further explore the mechanisms by which flavonols affect polar auxin transport, genetic approaches should be used in combination with computational analyses of large datasets, such as genomes, transcriptome, proteome, and metabolome, which may help identify new regulatory and related candidate relationships. In addition, the results of this study showed that 349 genes were found involved in the plant hormone signal transduction pathway, but that only one metabolite, salicylic acid, was found in the whole pathway, and that no auxin was detected (**Supplementary Figure 7**). This may be because of the relatively low content of plant hormones, and we performed widely targeted metabolomics, so they were undetected. Therefore, in the latter study, targeted metabolome detection methods should be used to detect plant hormone substances to better study the polar auxin transport and further verify the specific reasons for the slow growth of *M. pasquieri* seedlings. Furthermore, the samples were mixed samples of the whole organism, and there was no separate sampling and sequencing for different tissues, so the expression of transcription and metabolism of each tissue could not be determined in the later analysis, which hindered the study on the effect of flavonols on polar auxin transport in different tissues. In addition, the relationship between the binding affinity of different flavonols with different auxin transport carriers, the induction of their subcellular localization, and the inhibition intensity of polar auxin transport also needs to be further studied.

In summary, this study investigated *M. pasquieri* post-germination biological processes using a combination of transcriptomic and metabolomic methods. Using the morphological differential strategy, we have addressed the combination of molecular level and morphology better. The results of WGCNA showed that the flavonoid biosynthesis pathway was significantly enriched in stage 4, and that most of the key genes within the modules were also involved in this pathway. In addition, the transcriptome and metabolome association analysis showed that the genes encoding flavonol biosynthesis were significantly upregulated in stage 4 and promoted the accumulation of flavonols in stage 5, suggesting that the changes in metabolites were driven by the level of transcript. By analyzing the expression level of the genes encoding auxin transport carriers and its association with flavonol content, it was speculated that flavonols may directly inhibit the expression of the PIN4 encoding gene and indirectly affect other genes encoding polar auxin transport carriers in *M. pasquieri*, which might also explain the slow growth of the *M. pasquieri* seedlings. This study was the first to reveal the dynamic changes in DEGs and DAMs of *M. pasquieri* in the

post-germination stages using the multi-omics method, which laid a foundation for the study on the growth and development of the seedlings of *M. pasquieri* at the molecular level and provided new insights for the protection of this rare and endangered plant.

DATA AVAILABILITY STATEMENT

The datasets presented in this study can be found in online repositories. The names of the repository/repositories and accession number(s) can be found at: https://www.ncbi.nlm.nih.gov/, BioProject ID: PRJNA639907.

AUTHOR CONTRIBUTIONS

LK and LZ designed the study. LK, QL, ZC, SW, and YM performed the experiments. LK analyzed and visualized the transcriptomic, metabolomic, and RT-qPCR data and drafted the manuscript. ZS and LZ revised the manuscript. All authors contributed to the article and approved the submitted version.

FUNDING

This study was supported by Guangdong Wildlife Conservation and Management Projects (Grant Nos: YSDZW202001 and YSDZW2021) and Forestry Department of Guangdong Province, China, for noncommercial ecological forest research (Grant No: 2020STGYL001).

ACKNOWLEDGMENTS

We thank the Guangzhou Gene Denovo Biotechnology Company for assisting with the sequencing analysis.

SUPPLEMENTARY MATERIAL

The Supplementary Material for this article can be found online at: https://www.frontiersin.org/articles/10.3389/fpls.2021.731203/full#supplementary-material

REFERENCES

An, Y.-Q., and Lin, L. (2011). Transcriptional regulatory programs underlying barley germination and regulatory functions of gibberellin and abscisic acid. *BMC Plant Biol.* 11:105. doi: 10.1186/1471-2229-11-105

Anzala, F., Morere-Le Paven, M. C., Fournier, S., Rondeau, D., and Limami, A. M. (2006). Physiological and molecular aspects of aspartate-derived amino acid metabolism during germination and post-germination growth in two maize genotypes differing in germination efficiency. *J. Exp. Bot.* 57, 645–653. doi: 10.1093/jxb/erj054

Bewley, J. D. (1997). Seed germination and dormancy. *Plant Cell* 9, 1055–1066. doi: 10.1105/tpc.9.7.1055

Biever, J. J., and Gardner, G. (2016). The relationship between multiple UV-B perception mechanisms and DNA repair pathways in plants. *Environ. Exp. Bot.* 124, 89–99. doi: 10.1016/j.envexpbot.2015.12.010

Brunetti, C., Fini, A., Sebastiani, F., Gori, A., and Tattini, M. (2018). Modulation of phytohormone signaling: a primary function of flavonoids in plant-environment interactions. *Front. Plant Sci.* 9:1042. doi: 10.3389/fpls.2018.01042

Buer, C. S., Imin, N., and Djordjevic, M. A. (2010). Flavonoids: new roles for old molecules. *J. Integr. Plant Biol.* 52, 98–111. doi: 10.1111/j.1744-7909.2010.00905.x

Buer, C. S., Kordbacheh, F., Truong, T. T., Hocart, C. H., and Djordjevic, M. A. (2013). Alteration of flavonoid accumulation patterns in *transparent testa* mutants disturbs auxin transport, gravity responses, and imparts long-term effects on root and shoot architecture. *Planta* 238, 171–189. doi: 10.1007/s00425-013-1883-3

Chen, S., Zhou, Y., Chen, Y., and Gu, J. (2018). fastp: an ultra-fast all-in-one FASTQ preprocessor. *Bioinformatics* 34, 884–890. doi: 10.1093/bioinformatics/bty560

Chen, W., Gong, L., Guo, Z., Wang, W., Zhang, H., Liu, X., et al. (2013). A novel integrated method for large-scale detection, identification, and quantification of widely targeted metabolites: application in the study of rice metabolomics. *Mol. Plant* 6, 1769–1780. doi: 10.1093/mp/sst080

D'Amelia, V., Aversano, R., Chiaiese, P., and Carputo, D. (2018). The antioxidant properties of plant flavonoids: their exploitation by molecular plant breeding. *Phytochem. Rev.* 17, 611–625. doi: 10.1007/s11101-018-9568-y

Flora of China (FOC) (2021). *Madhuca pasquieri (Dubard) H. J. Lam*. Available online at: http://www.iplant.cn/info/Madhuca%20pasquieri?t=foc (accessed August 11, 2021).

Geisler, M., Bailly, A., and Ivanchenko, M. (2016). Master and servant: regulation of auxin transporters by FKBPs and cyclophilins. *Plant Sci.* 245, 1–10. doi: 10.1016/j.plantsci.2015.12.004

Grennan, A. K. (2009). MoTo DB: a metabolic database for tomato. *Plant Physiol.* 151, 1701–1702. doi: 10.1104/pp.109.900308

Gronwald, J. W., Jung, H.-J. G., Litterer, L. A., and Somers, D. A. (2009). Comparison of post-germination mobilization of cell wall polysaccharides and non-cell wall carbohydrates in soybean (*Glycine max* L.) cotyledons. *J. Sci. Food Agr.* 89, 1981–1986. doi: 10.1002/jsfa.3665

Gu, H., Wang, Y., Xie, H., Qiu, C., Zhang, S., Xiao, J., et al. (2020). Drought stress triggers proteomic changes involving lignin, flavonoids and fatty acids in tea plants. *Sci. Rep.* 10:15504. doi: 10.1038/s41598-020-72596-1

Hernández, I., and Munné-Bosch, S. (2012). Naringenin inhibits seed germination and seedling root growth through a salicylic acid-independent mechanism in *Arabidopsis thaliana*. *Plant Physiol. Biochem.* 61, 24–28. doi: 10.1016/j.plaphy.2012.09.003

Ho, S.-L., Huang, L.-F., Lu, C.-A., He, S.-L., Wang, C.-C., Yu, S.-P., et al. (2013). Sugar starvation- and GA-inducible calcium-dependent protein kinase 1 feedback regulates GA biosynthesis and activates a 14-3-3 protein to confer drought tolerance in rice seedlings. *Plant Mol. Biol.* 81, 347–361. doi: 10.1007/s11103-012-0006-z

Horai, H., Arita, M., Kanaya, S., Nihei, Y., Ikeda, T., Suwa, K., et al. (2010). MassBank: a public repository for sharing mass spectral data for life sciences. *J. Mass Spectrom.* 45, 703–714. doi: 10.1002/jms.1777

Jin, Z., Xue, S., Luo, Y., Tian, B., Fang, H., Li, H., et al. (2013). Hydrogen sulfide interacting with abscisic acid in stomatal regulation responses to drought stress in *Arabidopsis*. *Plant Physiol. Biochem.* 62, 41–46. doi: 10.1016/j.plaphy.2012.10.017

Kan, L., Liao, Q., Su, Z., Tan, Y., Wang, S., and Zhang, L. (2020). Single-molecule real-time sequencing of the *Madhuca pasquieri* (Dubard) Lam. transcriptome reveals the diversity of full-length transcripts. *Forests* 11:866. doi: 10.3390/f11080866

Kanehisa, M., Araki, M., Goto, S., Hattori, M., Hirakawa, M., Itoh, M., et al. (2008). KEGG for linking genomes to life and the environment. *Nucleic Acids Res.* 36, 480–484. doi: 10.1093/nar/gkm882

Kemen, A. C., Honkanen, S., Melton, R. E., Findlay, K. C., Mugford, S. T., Hayashi, K., et al. (2014). Investigation of triterpene synthesis and regulation in oats reveals a role for beta-amyrin in determining root epidermal cell patterning. *Proc. Natl. Acad. Sci. U.S.A.* 111, 8679–8684. doi: 10.1073/pnas.1401553111

Kreček, P., Skupa, P., Libus, J., Naramoto, S., Tejos, R., Friml, J., et al. (2009). The PIN-FORMED (PIN) protein family of auxin transporters. *Genome Biol.* 10:249. doi: 10.1186/gb-2009-10-12-249

Kuhn, B. M., Errafi, S., Bucher, R., Dobrev, P., Geisler, M., Bigler, L., et al. (2016). 7-rhamnosylated flavonols modulate homeostasis of the plant

hormone auxin and affect plant development. *J. Biol. Chem.* 291, 5385–5395. doi: 10.1074/jbc.M115.701565

Kuhn, B. M., Nodzynski, T., Errafi, S., Bucher, R., Gupta, S., Aryal, B., et al. (2017). Flavonol-induced changes in PIN2 polarity and auxin transport in the *Arabidopsis thaliana rol1-2* mutant require phosphatase activity. *Sci. Rep.* 7:41906. doi: 10.1038/srep41906

Langfelder, P., and Horvath, S. (2008). WGCNA: an R package for weighted correlation network analysis. *BMC Bioinformatics* 9:559. doi: 10.1186/1471-2105-9-559

Lewis, D. R., Miller, N. D., Splitt, B. L., Wu, G., and Spalding, E. P. (2007). Separating the roles of acropetal and basipetal auxin transport on gravitropism with mutations in two *Arabidopsis multidrug resistance-like* ABC transporter genes. *Plant Cell* 19, 1838–1850. doi: 10.1105/tpc.107.051599

Li, F. R., Zhao, L. Y., Zhao, X. Y., Zhang, T. H., and Li, G. (2005). The relative importance of pre-and post-germination determinants for recruitment of an annual plant community on moving sandy land. *Ann. Bot.* 96, 1215–1223. doi: 10.1093/aob/mci271

Li, R., Yu, C., Li, Y., Lam, T. W., Yiu, S. M., Kristiansen, K., et al. (2009). SOAP2: an improved ultrafast tool for short read alignment. *Bioinformatics* 25, 1966–1967. doi: 10.1093/bioinformatics/btp336

Mandal, S. M., Chakraborty, D., and Dey, S. (2010). Phenolic acids act as signaling molecules in plant-microbe symbioses. *Plant Signal. Behav.* 5, 359–368. doi: 10.4161/psb.5.4.10871

Matic, S., Bagnaresi, P., Biselli, C., Orru, L., Amaral Carneiro, G., Siciliano, I., et al. (2016). Comparative transcriptome profiling of resistant and susceptible rice genotypes in response to the seedborne pathogen *Fusarium fujikuroi*. *BMC Genomics* 17:608. doi: 10.1186/s12864-016-2925-6

Miransari, M., and Smith, D. L. (2014). Plant hormones and seed germination. *Environ. Exp. Bot.* 99, 110–121. doi: 10.1016/j.envexpbot.2013.11.005

Mohanta, T. K., Bashir, T., Hashem, A., Abd_Allah, E. F., Khan, A. L., and Al-Harrasi, A. S. (2018). Molecular players of auxin transport systems: advances in genomic and molecular events. *J. Plant Interact.* 13, 483–495. doi: 10.1080/17429145.2018.1523476

Muday, G. K., Brady, S. R., Argueso, C., Deruere, J., Kieber, J. J., and DeLong, A. (2006). RCN1-regulated phosphatase activity and EIN2 modulate hypocotyl gravitropism by a mechanism that does not require ethylene signaling. *Plant Physiol.* 141, 1617–1629. doi: 10.1104/pp.106.083212

Nakamura, K., Shimura, N., Otabe, Y., Hirai-Morita, A., Nakamura, Y., Ono, N., et al. (2013). KNApSAcK-3D: a three-dimensional structure database of plant metabolites. *Plant Cell Physiol.* 54:e4. doi: 10.1093/pcp/pcs186

Pacifici, E., Polverari, L., and Sabatini, S. (2015). Plant hormone cross-talk: the pivot of root growth. *J. Exp. Bot.* 66, 1113–1121. doi: 10.1093/jxb/eru534

Peer, W. A., Bandyopadhyay, A., Blakeslee, J. J., Makam, S. N., Chen, R. J., Masson, P. H., et al. (2004). Variation in expression and protein localization of the PIN family of auxin efflux facilitator proteins in flavonoid mutants with altered auxin transport in *Arabidopsis thaliana*. *Plant Cell* 16, 1898–1911. doi: 10.1105/tpc.021501

Peer, W. A., and Murphy, A. S. (2007). Flavonoids and auxin transport: modulators or regulators? *Trends Plant Sci.* 12, 556–563. doi: 10.1016/j.tplants.2007.10.003

Pollastri, S., and Tattini, M. (2011). Flavonols: old compounds for old roles. *Ann. Bot.* 108, 1225–1233. doi: 10.1093/aob/mcr234

Qu, C., Zhao, H., Chen, J., Zuo, Z., Sun, X., Huang, J., et al. (2019a). The transcriptional events and their relationship to physiological changes during poplar seed germination and post-germination. *BMC Genomics* 20:801. doi: 10.1186/s12864-019-6180-5

Qu, C., Zuo, Z., Cao, L., Huang, J., Sun, X., Zhang, P., et al. (2019b). Comprehensive dissection of transcript and metabolite shifts during seed germination and post-germination stages in poplar. *BMC Plant Biol.* 19:279. doi: 10.1186/s12870-019-1862-3

Ramos, P., Guajardo, J., Moya-León, M. A., and Herrera, R. (2016). A differential distribution of auxin and flavonols in radiata pine stem seedlings exposed to inclination. *Tree Genet. Genomes* 12:42. doi: 10.1007/s11295-016-1003-1

Romero-Rodriguez, M. C., Archidona-Yuste, A., Abril, N., Gil-Serrano, A. M., Meijon, M., and Jorrin-Novo, J. V. (2018). Germination and early seedling development in *Quercus ilex* recalcitrant and non-dormant seeds: targeted transcriptional, hormonal, and sugar analysis. *Front. Plant Sci.* 9:1508. doi: 10.3389/fpls.2018.01508

Saito, K. (2013). Phytochemical genomics—a new trend. *Curr. Opin. Plant Biol.* 16, 1–8. doi: 10.1016/j.pbi.2013.04.001

Santelia, D., Henrichs, S., Vincenzetti, V., Sauer, M., Bigler, L., Klein, M., et al. (2008). Flavonoids redirect PIN-mediated polar auxin fluxes during root gravitropic responses. *J. Biol. Chem.* 283, 31218–31226. doi: 10.1074/jbc.M710122200

Sawada, Y., Tsukaya, H., Li, Y., Sato, M., Kawade, K., and Hirai, M. Y. (2017). A novel method for single-grain-based metabolic profiling of Arabidopsis seed. *Metabolomics* 13:75. doi: 10.1007/s11306-017-1211-1

Shannon, P., Markiel, A., Ozier, O., Baliga, N. S., Wang, J. T., Ramage, D., et al. (2003). Cytoscape: a software environment for integrated models of biomolecular interaction networks. *Genome Res.* 13, 2498–2504. doi: 10.1101/gr.1239303

Song, Q., Cheng, S., Chen, Z., Nie, G., Xu, F., Zhang, J., et al. (2019). Comparative transcriptome analysis revealing the potential mechanism of seed germination stimulated by exogenous gibberellin in *Fraxinus hupehensis*. *BMC Plant Biol.* 19:199. doi: 10.1186/s12870-019-1801-3

Sreenivasulu, N., Usadel, B., Winter, A., Radchuk, V., Scholz, U., Stein, N., et al. (2008). Barley grain maturation and germination: metabolic pathway and regulatory network commonalities and differences highlighted by new MapMan/PageMan profiling tools. *Plant Physiol.* 146, 1738–1758. doi: 10.1104/pp.107.111781

Sun, M., Tuan, P. A., Izydorczyk, M. S., and Ayele, B. T. (2020). Ethylene regulates post-germination seedling growth in wheat through spatial and temporal modulation of ABA/GA balance. *J. Exp. Bot.* 71, 1985–2004. doi: 10.1093/jxb/erz566

Taylor, L. P., and Grotewold, E. (2005). Flavonoids as developmental regulators. *Curr. Opin. Plant Biol.* 8, 317–323. doi: 10.1016/j.pbi.2005.03.005

Teale, W., and Palme, K. (2018). Naphthylphthalamic acid and the mechanism of polar auxin transport. *J. Exp. Bot.* 69, 303–312. doi: 10.1093/jxb/erx323

Teale, W. D., Pasternak, T., Dal Bosco, C., Dovzhenko, A., Kratzat, K., Bildl, W., et al. (2021). Flavonol-mediated stabilization of PIN efflux complexes regulates polar auxin transport. *EMBO J.* 40:e104416. doi: 10.15252/embj.2020104416

Wang, H., Guo, X., Li, Q., Lu, Y., Huang, W., Zhang, F., et al. (2020). Integrated transcriptomic and metabolic framework for carbon metabolism and plant hormones regulation in *Vigna radiata* during post-germination seedling growth. *Sci. Rep.* 10:3745. doi: 10.1038/s41598-020-60771-3

Wedow, J. M., Yendrek, C. R., Mello, T. R., Creste, S., Martinez, C. A., and Ainsworth, E. A. (2019). Metabolite and transcript profiling of Guinea grass (*Panicum maximum* Jacq) response to elevated [CO_2] and temperature. *Metabolomics* 15:51. doi: 10.1007/s11306-019-1511-8

Westerhuis, J. A., Hoefsloot, H. C. J., Smit, S., Vis, D. J., Smilde, A. K., van Velzen, E. J. J., et al. (2008). Assessment of PLSDA cross validation. *Metabolomics* 4, 81–89. doi: 10.1007/s11306-007-0099-6

Wishart, D. S., Jewison, T., Guo, A. C., Wilson, M., Knox, C., Liu, Y., et al. (2013). HMDB 3.0—the human metabolome database in 2013. *Nucleic Acids Res.* 41, 801–807. doi: 10.1093/nar/gks1065

Xie, C., Mao, X., Huang, J., Ding, Y., Wu, J., Dong, S., et al. (2011). KOBAS 2.0: a web server for annotation and identification of enriched pathways and diseases. *Nucleic Acids Res.* 39, 316–322. doi: 10.1093/nar/gkr483

Xu, J., Yan, J., Li, W., Wang, Q., Wang, C., Guo, J., et al. (2020). Integrative analyses of widely targeted metabolic profiling and transcriptome data reveals molecular insight into metabolomic variations during apple (*Malus domestica*) fruit development and ripening. *Int. J. Mol. Sci.* 21:4797. doi: 10.3390/ijms21134797

Yang, C., Wang, D., Zhang, C., Kong, N., Ma, H., and Chen, Q. (2019a). Comparative analysis of the PIN auxin transporter gene family in different plant species: a focus on structural and expression profiling of PINs in *Solanum tuberosum*. *Int. J. Mol. Sci.* 20:3270. doi: 10.3390/ijms20133270

Yang, J., Su, L., Li, D., Luo, L., Sun, K., Yang, M., et al. (2020). Dynamic transcriptome and metabolome analyses of two types of rice during the seed germination and young seedling growth stages. *BMC Genomics* 21:603. doi: 10.1186/s12864-020-07024-9

Yang, M., Yang, J., Su, L., Sun, K., Li, D., Liu, Y., et al. (2019b). Metabolic profile analysis and identification of key metabolites during rice seed germination under low-temperature stress. *Plant Sci.* 289:110282. doi: 10.1016/j.plantsci.2019.110282

Yin, Q., Shen, G., Chang, Z., Tang, Y., Gao, H., and Pang, Y. (2017). Involvement of three putative glucosyltransferases from the UGT72 family in flavonol

glucoside/rhamnoside biosynthesis in *Lotus japonicus* seeds. *J. Exp. Bot.* 68, 597–612. doi: 10.1093/jxb/erw420

Young, M. D., Wakefield, M. J., Smyth, G. K., and Oshlack, A. (2010). Gene ontology analysis for RNA-seq: accounting for selection bias. *Genome Biol.* 11:R14. doi: 10.1186/gb-2010-11-2-r14

Yuan, H., Zeng, X., Yang, Q., Xu, Q., Wang, Y., Jabu, D., et al. (2018). Gene coexpression network analysis combined with metabonomics reveals the resistance responses to powdery mildew in Tibetan hulless barley. *Sci. Rep.* 8:14928. doi: 10.1038/s41598-018-33113-7

Zhang, L., Zhou, W. N., Tu, Z. C., Yang, S. H., Xu, L., and Yuan, T. (2020a). Influence of hydroxyl substitution on the suppression of flavonol in harmful glycation product formation and the inhibition mechanism revealed by spectroscopy and mass spectrometry. *J. Agric. Food Chem.* 68, 8263–8273. doi: 10.1021/acs.jafc.0c03163

Zhang, Y. C., He, R. R., Lian, J. P., Zhou, Y. F., Zhang, F., Li, Q. F., et al. (2020b). OsmiR528 regulates rice-pollen intine formation by targeting an uclacyanin to influence flavonoid metabolism. *Proc. Natl. Acad. Sci. U.S.A.* 117, 727–732. doi: 10.1073/pnas.1810968117

Zhao, Q., Sun, Q., Dong, P., Ma, C., Sun, H., and Liu, C. (2019). Jasmonic acid alleviates boron toxicity in *Puccinellia tenuiflora*, a promising species for boron phytoremediation. *Plant Soil* 445, 397–407. doi: 10.1007/s11104-019-04326-0

Zhao, X., Chen, S., Wang, S., Shan, W., Wang, X., Lin, Y., et al. (2020). Defensive responses of tea plants (*Camellia sinensis*) against tea green leafhopper attack: a multi-omics study. *Front. Plant Sci.* 10:1705. doi: 10.3389/fpls.2019.01705

Zhou, J. J., and Luo, J. (2018). The PIN-FORMED auxin efflux carriers in plants. *Int. J. Mol. Sci.* 19:2759. doi: 10.3390/ijms19092759

Zhu, Z. J., Schultz, A. W., Wang, J., Johnson, C. H., Yannone, S. M., Patti, G. J., et al. (2013). Liquid chromatography quadrupole time-of-flight mass spectrometry characterization of metabolites guided by the METLIN database. *Nat. Protoc.* 8, 451–460. doi: 10.1038/nprot.2013.004

Conflict of Interest: The authors declare that the research was conducted in the absence of any commercial or financial relationships that could be construed as a potential conflict of interest.

Publisher's Note: All claims expressed in this article are solely those of the authors and do not necessarily represent those of their affiliated organizations, or those of the publisher, the editors and the reviewers. Any product that may be evaluated in this article, or claim that may be made by its manufacturer, is not guaranteed or endorsed by the publisher.

forests

MDPI

Article

Single-Molecule Real-Time Sequencing of the *Madhuca pasquieri* (Dubard) Lam. Transcriptome Reveals the Diversity of Full-Length Transcripts

Lei Kan, Qicong Liao, Zhiyao Su, Yushan Tan, Shuyu Wang and Lu Zhang *

College of Forestry and Landscape Architecture, South China Agricultural University, Guangzhou 510642, China; kanlei5523@stu.scau.edu.cn (L.K.); liaoqicong@stu.scau.edu.cn (Q.L.); zysu@scau.edu.cn (Z.S.); tanyushanscau@163.com (Y.T.); wshuyu@stu.scau.edu.cn (S.W.)

* Correspondence: zhanglu@scau.edu.cn; Tel.: +86-135-6008-9803

Received: 18 June 2020; Accepted: 6 August 2020; Published: 8 August 2020

Abstract: *Madhuca pasquieri* (Dubard) Lam. is a tree on the International Union for Conservation of Nature Red List and a national key protected wild plant (II) of China, known for its seed oil and timber. However, lacking of genomic and transcriptome data for this species hampers study of its reproduction, utilization, and conservation. Here, single-molecule long-read sequencing (PacBio) and next-generation sequencing (Illumina) were combined to obtain the transcriptome from five developmental stages of *M. pasquieri*. Overall, 25,339 transcript isoforms were detected by PacBio, including 24,492 coding sequences (CDSs), 9440 simple sequence repeats (SSRs), 149 long non-coding RNAs (lncRNAs), and 182 alternative splicing (AS) events, a majority was retained intron (RI). A further 1058 transcripts were identified as transcriptional factors (TFs) from 51 TF families. PacBio recovered more full-length transcript isoforms with a longer length, and a higher expression level, whereas larger number of transcripts (124,405) was captured in de novo from Illumina. Using Nr, Swissprot, KOG, and KEGG databases, 24,405 transcripts (96.31%) were annotated by PacBio. Functional annotation revealed a role for the auxin, abscisic acid, gibberellin, and cytokinine metabolic pathways in seed germination and post-germination. These findings support further studies on seed germination mechanism and genome of *M. pasquieri*, and better protection of this endangered species.

Keywords: *Madhuca pasquieri* (Dubard) Lam.; SMRT sequencing; Illumina; alternative splicing; lncRNA

1. Introduction

Madhuca pasquieri (Dubard) Lam., a member of the Sapotaceae family, is considered a vulnerable (VU) species on the International Union for Conservation of Nature (IUCN) Red List, and in China, is listed as a national key protected wild plant (II) and wild plant of extremely small population. This tree is endemic to southwest Guangdong, southern Guangxi, and southeast Yunnan, China, and usually grows in mixed forests or mountain forest margins at elevations below 1100 m. The oil content of *M. pasquieri* seeds can reach approximately 30%. In addition, it is a precious timber species, with a basic density of 0.711 and an air-dry density of 0.893, which is often used for its strength, wear resistance, when used for equipment or furniture, and in veneer manufacturing. The whole *M. pasquieri* plant is rich in latex; its bark contains tannin, which can be extracted for hard rubber and rubber. However, we previously showed that understory seedlings of *M. pasquieri* are rare, and its native habitat is fragmented or lost due to excessive logging and digging, which affects regeneration (including seed germination, seedling survival, and growth) of the wild *M. pasquieri* community. To date, few studies have investigated the in-situ protection, ex-situ protection,

chemical composition, and artificial cultivation of this species; however, such studies remain in the preliminary stage, and data from long-term follow-up are lacking. Moreover, a lack of genomic and high-quality transcriptome information acts as a barrier to the development of in-depth molecular studies, preventing a comprehensive exploration of the plant's value.

Knowledge on the transcriptome, which comprises all RNA transcripts produced by the genome, is vital for understanding the relationship between genotype and phenotype [1]. Next-generation high-throughput sequencing (NGS) technology, also known as second-generation sequencing, is a revolutionary tool that aims to better understand differential gene expression and regulatory mechanisms due to its lower costs and greater sequencing depth compared with first-generation Sanger sequencing technology [2]. This approach requires no strict reference genome sequence [3]; therefore, it is suitable for model species, such as *Arabidopsis* (*Arabidopsis pumila* [Steph.] N. Busch) [4] and rice (*Oryza sativa* L.) [5], or non-model species, such as sugarcane (*Saccharum officinarum L.*) [6] and *Nothapodytes nimmoniana* (Graham) Mabb [7]. Transcriptome sequences obtained by NGS have been important for capturing diversity in RNA populations at a high sequencing depth [8]. However, incomplete and low-quality transcripts are a major limitation in NGS short-read sequencing, which makes it difficult to analyze alternative splicing (AS) variants and to correct annotation [9]. Single-molecule real-time (SMRT) sequencing, developed by Pacific Biosciences (PacBio, Menlo Park, CA, USA), enables long-read or full-length (FL) transcriptomes to be obtained without assembly, permitting the collection of large-scale long-read transcripts with complete coding sequences, and the subsequent characterization of gene families [10,11]. FL transcripts can significantly improve the accuracy of genome annotation and transcriptome information [12]. Thus, the PacBio platform provides a user-friendly and accurate technique that can be used for gene annotation [13], novel gene and isoform identification [14], AS identification [15], and long non-coding RNA (lncRNA) discovery [16]. For example, RNA-Seq was able to map up to 85.94% of the castor (*Ricinus communis*) genome to the reference genome; however, using PacBio, 22.71% of the transcripts were completely or partially mapped to the reference genome, and nearly 62% of those might be new transcripts of known genes. This indicates that the information content of the genome covered by SMRT sequencing is greater than that of the known genome [11]. Using PacBio transcriptome sequencing, 30,591 transcripts were identified in ramie (*Boehmeria nivea* L. Gaud), with an average length of 2629 bp, 91.1% of which were functionally annotated. Compared with previous studies, PacBio significantly improved the length and number of annotated transcripts, further demonstrating the advantage of PacBio in transcriptome sequencing [17]. So far, no report has been found about the application of SMRT technology in a plant species from the family Sapotaceae.

Although PacBio reads are longer than Illumina reads, PacBio provides inaccurate isoforms on genes and less coverage of genes, leading to a high error rate [18]; this can be corrected using Illumina RNA-Seq reads and circular consensus sequence (CCS) reads [19]. In a study on the highly polyploid sugarcane, Illumina RNA-Seq was used to improve the PacBio transcript isoforms by short-read error correction. The results showed that the corrected PacBio dataset was more complete than the non-corrected dataset (CEGMA (Core eukaryotic genes mapping approach): 98 and 96%; BUSCO (Benchmarking universal single-copy orthologs): 90 and 87%, respectively) [20]. Recently, PacBio and Illumina have been combined to obtain comprehensive information, detect more gene isoforms, and determine functional variety on a transcriptional level. Thus, the genome database offers a scientific basis for species conservation and molecular breeding [21–24].

According to our previous investigation, we found that the seedlings of *M. pasquieri* in understory were very rare, and difficult to regenerate. Seed germination is the beginning of plant life cycle [25], and seed germination and post-germination directly affect the maintenance of the population and its quantity in time and space, which is particularly important for the protection of rare and endangered plants [26]. To evaluate seed germination and post-germination stages, and ensure wide coverage of transcript isoforms, *M. pasquieri* plants from five developmental stages, including seed germination, hypocotyl elongation, epicotyl elongation, two-leaf, and nine-leaf stages, were mixed for transcriptome

analysis by SMRT. The PacBio Sequel platform has been used to generate comprehensive full-length transcriptome of *M. pasquieri*, and combined with Illumina platform to obtain a more complete transcriptome. In this study, Illumina RNA-Seq was used to correct short-read errors on SMRT transcripts obtained from PacBio, allowing differences to be compared between the two platforms. Then, we functionally annotated the full-length transcriptomes. Isoform analysis revealed the complexity of AS in *M. pasquieri*, and lncRNAs were also identified. Thus, we systematically characterized the complexity of the *M. pasquieri* transcriptome, as well as its structure and functional annotation. This in-depth characterization will provide a valuable tool for understanding the seed germination and growth mechanism of *M. pasquieri* and for future conservation purposes. Furthermore, this transcriptome provides basic data and important references for future studies on functional gene mining and utilization, genetic resource classification and evolution, and molecular marker development to promote the efficient and sustainable exploitation of this precious biological resource.

2. Materials and Methods

2.1. Plant Materials

M. pasquieri was grown in an artificial climate chamber, with a light cycle of 14 h/10 h (day/night), 17,600 lx, temperature 25 °C, and humidity of 60%–80%, at South China Agricultural University in China. During seed germination and post-germination growth, *M. pasquieri* plants were selected based on five developmental stages from the same batch of light matrix culture in the artificial climate chamber (seed germination, hypocotyl elongation, epicotyl elongation, two-leaf, and nine-leaf stages; Figure 1), with three biological replicates per stage. Collected samples were snap frozen in liquid nitrogen and stored at −80 °C until use.

2.2. Library Construction and SMRT Sequencing

Total *M. pasquieri* plants from five developmental stages, with three biological replicates per stage, were pooled. Total RNA was extracted by grinding tissue in TRIzol reagent (Life Technologies, Carlsbad, CA, USA) on dry ice and processed following the manufacturer's protocol. RNA integrity was determined using the Agilent 2100 Bioanalyzer and agarose gel electrophoresis. RNA purity and concentration were determined via a Nanodrop micro-spectrophotometer (Thermo Fisher Scientific, Wilmington, DE, USA). mRNA was enriched by Oligo (dT) magnetic beads, and then reverse-transcribed into cDNA using the Clontech SMARTer PCR cDNA Synthesis Kit (Clontech Laboratories, CA, USA). The PCR program was optimized to determine the optimal number of amplification cycles for the downstream large-scale PCR. Then, the optimized cycle number was used to generate double-stranded cDNA. In addition, cDNA of >4 kb was selected using the BluePippin^{TM} Size Selection System (Sage Science, Beverly, MA, USA) and mixed equally with the no-size-selection cDNA. Large-scale PCR was also performed to construct the next SMRTbell library. cDNA underwent DNA-damage repair, end-repair, and was ligated to sequencing adapters. The SMRTbell template was annealed to a sequencing primer, bound to a polymerase, and sequenced on the PacBio Sequel platform using P6-C6 chemistry with 10 h movies.

2.3. Analysis of SMRT Sequencing Data

The raw sequencing reads of cDNA libraries were classified and clustered into a transcript consensus using the SMRT Link v5.0.1 pipeline supported by Pacific Biosciences. CCS reads were extracted from subreads BAM files and then were classified as FL non-chimeric, non-full-length (nFL), chimeras, or short reads based on cDNA primers and the polyA tail signal. Short reads were discarded. Subsequently, the full-length non-chimeric (FLNC) reads were clustered by Iterative Clustering for Error Correction (ICE) software to generate the cluster consensus isoforms. To improve the accuracy of PacBio reads, two strategies were employed: (1) the nFL reads were used to polish the obtained cluster consensus isoforms by Quiver software to attain FL polished high-quality consensus sequences

(accuracy ≥ 99%). (2) The LoRDEC tool (version 0.8) was used to further correct the low-quality isoforms using Illumina short reads obtained from the same samples. Then, the final transcriptome isoform sequences were filtered by removing redundant sequences using the software CD-HIT-v4.6.7 with a threshold of 0.99 identities (Figure 1).

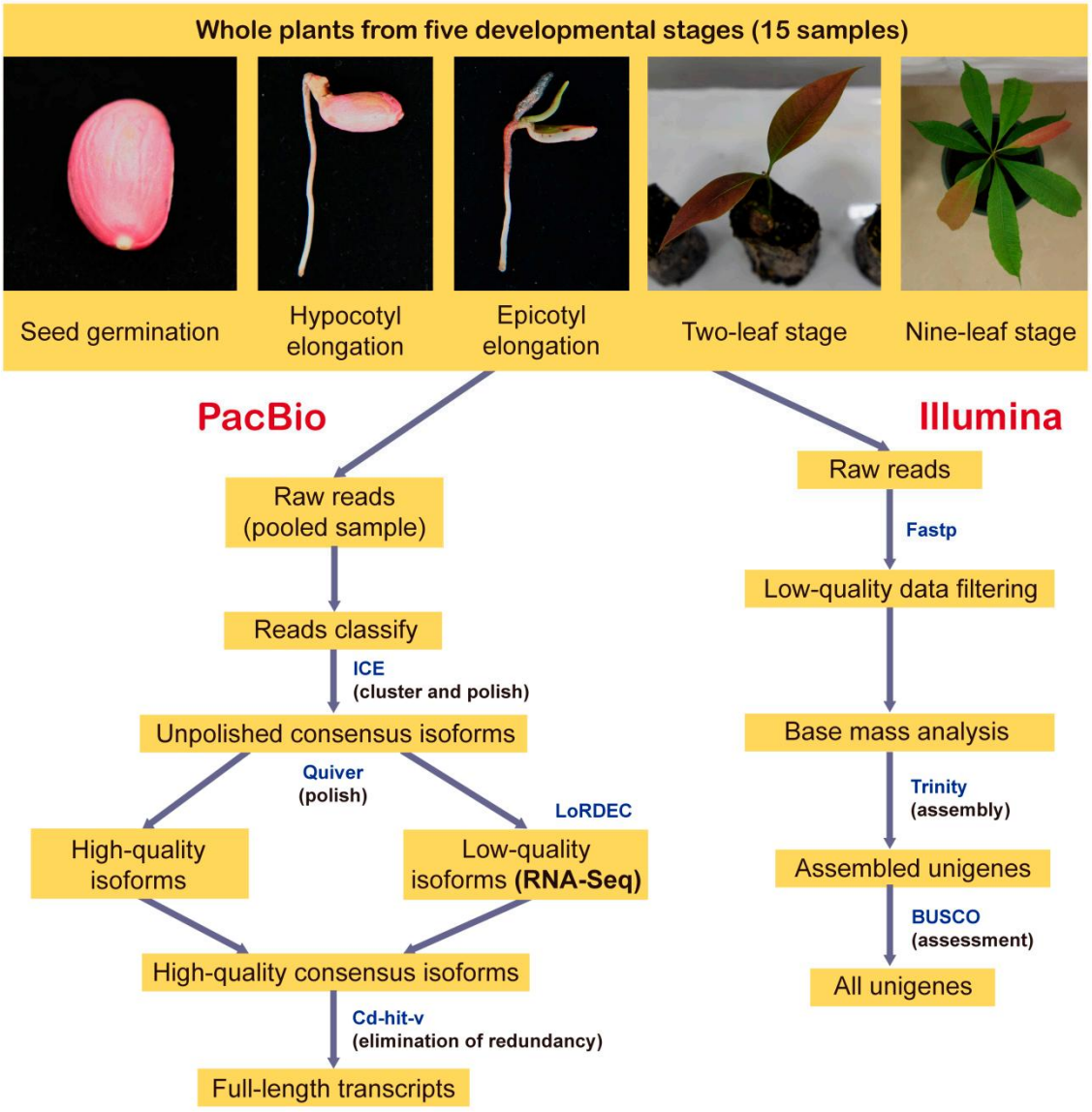

Figure 1. Images of *Madhuca pasquieri* (Dubard) Lam., which was used for sequencing, and the workflows used in this study.

2.4. Illumina RNA Sequencing and De Novo Assembly of Short Reads

M. pasquieri plants sampled at five developmental stages, with three biological replicates per stage, were each used for Illumina RNA sequencing. After total RNA was extracted, eukaryotic mRNA with a polyA tail was enriched by Oligo (dT) beads, and then the enriched mRNA was fragmented into short fragments by ultrasonic waves and reverse-transcribed into cDNA using random primers. Second-strand cDNA was synthesized by DNA polymerase I, RNase H, dNTP, and buffer (New England Biolabs, Ipswich, MA, USA). Next, the cDNA fragments were purified using a QiaQuick PCR extraction kit (Qiagen, Düsseldorf, GER) end-repaired, the polyA was added, and the fragments were then ligated to Illumina sequencing adapters. The ligation products were size-selected by agarose gel electrophoresis, amplified by PCR, and sequenced using Illumina HiSeq™

4000. SMRT sequencing and Illumina RNA sequencing were performed by Gene Denovo Biotechnology Company (Guangzhou, China).

Reads obtained from the sequencing machines included raw reads containing adapters or low-quality bases, which affect subsequent assembly and analysis. Thus, high-quality clean reads were obtained by further filtering according to the following rules: (1) removal of reads containing adapters; (2) removal of reads containing more than 10% of unknown nucleotides (N); (3) removal of reads containing all A bases; (4) removal of low-quality reads containing more than 50% low-quality (Q-value ≤ 20) bases. After filtering the data, base composition and mass distribution were analyzed to visualize data quality. The more balanced the base composition, the higher the quality, and the more accurate the subsequent analysis will be. Then, Trinity v2.8.4 software was used to assemble reads (Figure 1), and the quality of the assembly could be evaluated from the N50 value.

2.5. Evaluation of Sequencing Results

The protein sequences predicted from two sequencing results were analyzed using BUSCO v3 i to determine the completeness of the conserved content in the transcriptome. The percentage of transcripts that fully aligned (≥70%) and partially aligned to the conserved proteins, as well as the percentage missing proteins were determined and compared.

2.6. Prediction of Coding Sequences (CDSs), Simple Sequence Repeats (SSRs), and Transcription Factors (TFs)

Open reading frames (ORFs) in the isoform sequences were detected using ANGEL software in order to determine the CDSs, protein sequences, and untranslated region (UTR) sequences.

SSR prediction was analyzed using the MISA (version 1) software (http://pgrc.ipk-gatersleben.de/misa/) 64 with default parameters in the whole transcriptome. Based on the MISA results, Primer 1.1.4 was used to design primer pairs specific for the flanking regions of SSRs for subsequent validation.

Protein coding sequences of isoforms were aligned by hmmscan to Plant TFdb (http://planttfdb.cbi.pku.edu.cn/) or Animal TFdb (http://www.bioguo.org/AnimalTFdb/) to predict TF families.

2.7. Characterization of AS Events

To analyze AS events of transcript isoforms, the COding GENome reconstruction Tool (Cogent) was first used to partition transcripts into gene families based on k-mer similarity, and to reconstruct each family into a coding reference genome based on De Bruijn graph methods. Then, the SUPPA tool was used to analyze AS events of transcript isoforms. Five major types of AS events, namely A3 (alternative 3′ splice sites), A5 (alternative 5′ splice sites), AF (alternative first exon), RI (retained intron), and SE (skipping exons), were extracted from the output files and counted.

2.8. LncRNA Identification from PacBio Sequences

CNCI (version 2), CPAT, CPC (version 1), and Pfam were used to assess the protein-coding potential of transcripts without annotations by default parameters for potential lncRNAs. To better annotate lncRNAs on an evolutionary level, the software Infernal (http://eddylab.org/infernal/) was used for sequence alignment. LncRNAs were classified based on their secondary structures and sequence conservation.

2.9. Functional Annotation

Corrected isoforms were analyzed by BLAST against the NCBI non-redundant protein (Nr) database (http://www.ncbi.nlm.nih.gov), the Swiss-Prot protein database (http://www.expasy.ch/sprot), the Kyoto Encyclopedia of Genes and Genomes (KEGG) database (http://www.genome.jp/kegg), and the COG/KOG database (http://www.ncbi.nlm.nih.gov/COG) using the BLASTx program (http://www.ncbi.nlm.nih.gov/BLAST/) at an E-value threshold of 1×10^{-5} to evaluate sequence similarity with genes of other species. Gene Ontology (GO) annotation was analyzed by Blast2GO software

with Nr annotation results of isoforms. Isoforms with the top 20 highest scores, and no shorter than 33 high-scoring segment pair (HSP) hits were selected for Blast2GO analysis. Then, isoforms were functionally classified using WEGO software.

3. Results

3.1. General Properties of Single-Molecule Long-Reads

In order to obtain *M. pasquieri* transcripts that were as complete as possible, high-quality total RNA was extracted from each pooled sample representing the five different developmental stages. Because PacBio Sequel does not screen fragments, a full library of samples was built. After filtering, 22,704,140 subreads were obtained, with a mean length of 1193 bp and a N50 of 1529 bp. A total of 438,795 CCSs with an average depth of nine passes were generated from subreads after merging and correcting errors by multiple sequencing. The length distribution of CCSs was consistent with the expected size (Figure 2a). Furthermore, ICE and Quiver algorithms were used to obtain 29,003 high-quality sequences and 85 low-quality sequences. The length distribution of consensus isoforms is shown in Figure 2b.

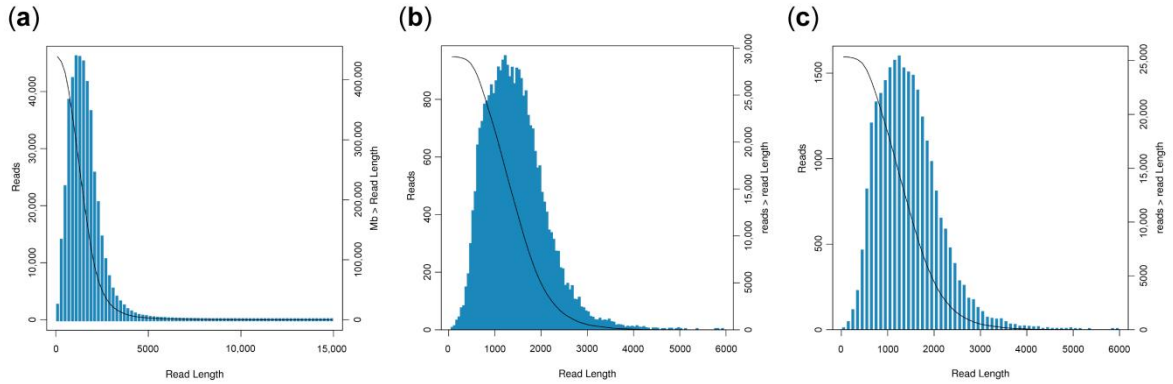

Figure 2. The length distribution of PacBio single-molecule long-read (SMRT) sequencing. (**a**) Length distribution of circular consensus sequences (CCSs). (**b**) Length distribution of consensus isoforms. (**c**) Length distribution of isoforms sequences.

3.2. Acquisition of High-Quality Sequences and Error Correction of Long Reads Using Illumina Data

The basic error rate of the SMRT sequences was 12–15%, mainly due to the insertion of extra bases. Low-quality sequences obtained on the PacBio Sequel platform were corrected using Illumina RNA-Seq transcripts and LoRDEC (version 0.8). After polishing, low-quality sequences with polish coverage (percentage of bases corrected by the second-generation data in the third-generation consistent sequence) of more than 99% were combined with the high-quality sequences obtained by Quiver polish. Finally, 29,042 sequences were obtained, with a mean length of 1438.11 bp, a N50 of 1645 bp, and GC content of 44.59% (Table S1). Then, cd-hit-v4.6.7 software was used to remove redundant sequences from the high-quality consistent sequences in the library. Local alignment was adopted, where the alignment rate was 99% for shorter sequences and the number of bases unaligned was less than 30 bp. For longer sequences, the alignment rate was 90% and the number of bases unaligned was less than 100 bp. The final set of PacBio transcript isoforms contained 25,339 sequences, with a mean length of 1436.77 bp, a N50 of 1652 bp, and GC content of 44.39% (Table S1); the length distribution of these isoforms is shown in Figure 2c. Overall, correcting errors improved transcript prediction, with more transcripts covering the full-length of known proteins, and a longer N50, which is suitable for further structural and functional analysis. To assess the completeness of our transcriptome, BUSCO was used to evaluate the sequencing results and showed that 26.81% were complete and single-copy BUSCOs, 12.22% were complete and duplicated BUSCOs, 3.54% were fragmented BUSCOs, and 57.43% were missing BUSCOs (Figure S1).

3.3. Comparison of PacBio and Illumina Transcripts and Sequencing Depth

De novo assembly has been used widely to construct transcriptomes without any reference sequence; therefore, the *M. pasquieri* transcriptome was assembled from Illumina short-reads to provide a comparative reference for the isoform transcript sequences obtained from PacBio Sequel. In this study, 15 samples were tested, generating an average of 45,627,996 raw reads. Then, fastp 0.18.0 was used to filter raw data and obtain clean reads (each sample > 99.5%, Table S2). After filtering, the base composition and mass distribution was analyzed to visualize data quality. The results showed that the Q20 and Q30 of each sample were both >90% and the GC content of each sample was >47% (Table S3), indicating the quality of data sequencing. Trinity v2.8.4 was used to assemble reads, resulting in 124,405 unigenes, with a mean length of 834 bp, a N50 of 1387 bp, and a GC content of 44.89% (Table S1). The length distribution of assembled unigenes is shown in Figure S2. BUSCO was then used to evaluate the sequencing results; there were 1035 (71.88%) complete and single-copy BUSCOs, 108 (7.5%) complete and duplicated BUSCOs, 170 (11.81%) fragmented BUSCOs, and 127 (8.82%) missing BUSCOs (Figure S1).

Compared to PacBio transcript isoforms, *de novo* assembly form Illumina detected more unigenes (124,405), as well as more annotated unigenes (66,026 *de novo* versus 24,405 PacBio) (Figure 3a and Figure S3). Of the annotated transcripts, 8.2% of the *de novo* transcript unigenes (10,140 unigenes) exhibited similarity to 61.4% of the PacBio transcript isoforms (15,564 isoforms) by BLASTN (*e*-value $\leq 1 \times 10^{-20}$, pairwise identity $\geq$ 75%, min bit score $\geq$ 100), and 114,265 (91.8%) *de novo* transcript unigenes, and 9775 (38.6%) PacBio transcript isoforms were specifically identified by each of the datasets (Figure 3b). Moreover, the *de novo* transcript unigenes from Illumina were expressed at low levels and were shorter than the PacBio transcript isoforms in SMRT (Figure 3c,d). In conclusion, these results indicated that although the SMRT sequencing depth was less than that of the Illumina platform, SMRT significantly improved the length and expression level of transcripts.

3.4. Prediction of CDSs, SSRs, and TFs

CDS is a sequence of protein products that correspond exactly to a protein codon. A total of 24,492 CDSs were predicted by PacBio Sequel, and the number and length distribution of proteins encoded by CDS regions are shown in Figure 4. Additionally, 65,297 CDSs were identified based on Illumina data; however, the mean length was less than that predicted by PacBio (Figure S4).

SSR markers can serve as useful tools for genetic diversity analysis, genetic linkage, evolutionary studies, and marker-assisted breeding in many species, especially endangered species, due to their abundance, highly polymorphic nature, co-dominant inheritance, and random distribution throughout the genome [27–30]. In this study, 9400 SSRs and 7819 SSR-containing sequences were detected across 25,339 transcripts from *M. pasquieri*. Of these, 1363 transcripts contained more than one SSR, and 1033 contained compound SSRs. Di-nucleotide repeat transcripts were the most frequent type (5269, 67.39%) with six to 30 repeats, followed by 1718 (21.97%) tri-nucleotide repeats transcripts with five to 24 repeats, 369 (4.72%) tetra-nucleotide repeats transcripts with four to eight repeats, 162 (2.07%) penta-nucleotide repeats, and 141 (1.80%) hexa-nucleotide repeats both with four to seven repeats (Figure 5a). Among the di-, tri-, and tetra-nucleotide repeats, the motifs were AC/GT, AAC/GTT, and AAAT/TTTA, respectively. Detailed information is shown in Figure 5b. A total of 18,070 SSRs and 15,444 SSR-containing sequences were detected across 124,405 unigenes. Di-nucleotide repeat unigenes were also the most frequent type (11,633), followed by 5105 tri-nucleotide repeats unigenes, 1081 tetra-nucleotide repeats unigenes, 451 penta-nucleotide repeats unigenes, and 326 hexa-nucleotide repeats unigenes (Table S4). In the di-, tri-, tetra- and penta-nucleotide repeats, the motif was AG/CT, AAG/CTT, AAAT/ATTT, and AAACC/GGTTT, respectively (Figure S5).

TFs play important roles in the regulation of plant growth and development [31]. We compared the predicted protein sequences with the corresponding TF database (plant TFdb/animal TFdb) for hmmscan. A total of 1058 transcripts were identified as TFs and classified into 51 TF families. The top 10 TF families were ERF (121, 11.44%), WRKY (96, 9.07%), GRAS (87, 8.22%), NAC (71, 6.71%),

bHLH (70, 6.62%), C3H (68, 6.43%), bZIP (49, 4.63%), C2H2 (46, 4.35%), MYB_related (45, 4.25%), and TALE (38, 3.59%) (Table 1). Conversely, among the *de novo* transcript unigenes, we identified 2048 TFs from 57 TF families, among which HB-PHD, SRS, SAP, STAT, LFY and HRT-like families were specific. And C2H2 (241, 11.77%), bHLH (172, 8.40%), ERF (154, 7.52%), bZIP (141, 6.88%), MYB (124, 6.05%), NAC (99, 4.83%), GRAS (88, 4.30%), WRKY (83, 4.05%), MYB_related (82, 4.00%), and C3H (72, 3.52%) were the top 10 TF families (Table 1).

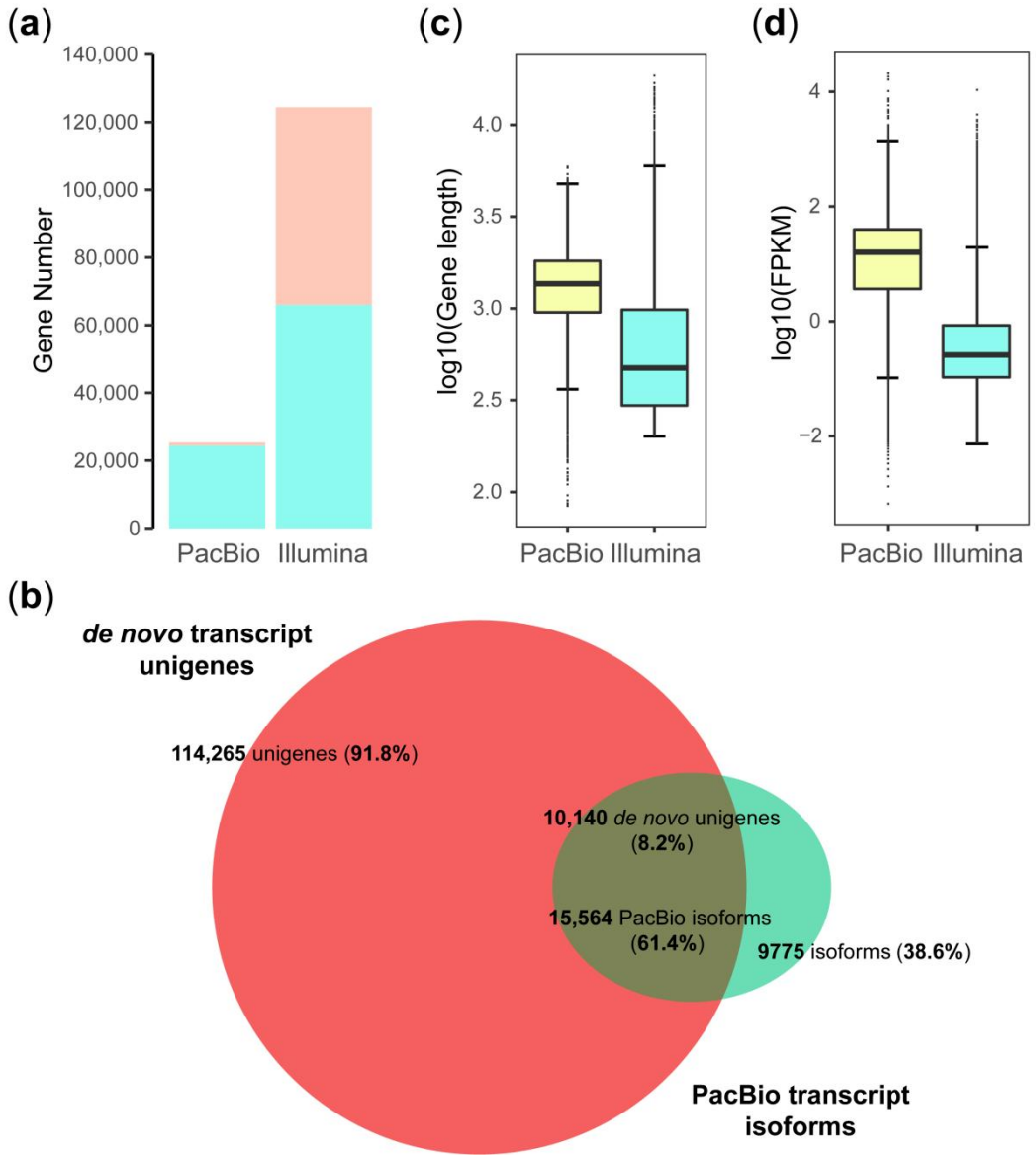

Figure 3. Comparison of PacBio and Illumina data. (**a**) The number of transcripts detected by PacBio and Illumina. (**b**) Comparison between the *M. pasquieri* PacBio transcript isoforms and *de novo* transcript unigenes. (**c**) Boxplot showing the length of transcript isoforms in PacBio and transcript unigenes in Illumina. (**d**) Boxplot showing the expression level of transcript isoforms in PacBio and transcript unigenes in Illumina.

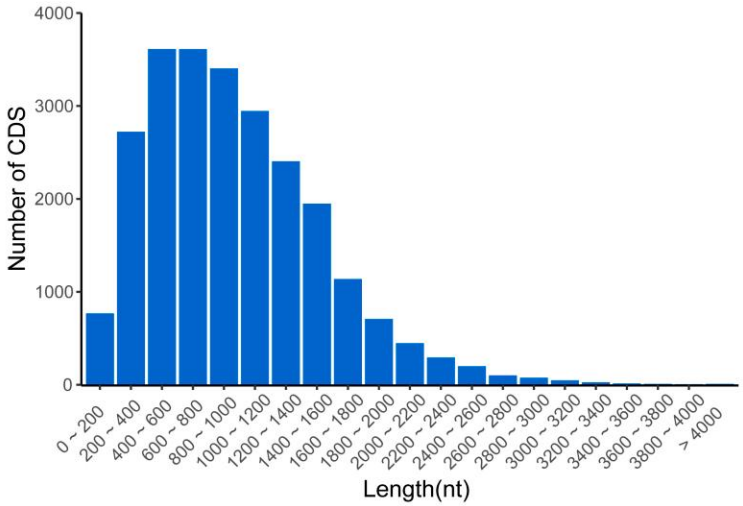

Figure 4. The length distribution of coding sequences (CDSs).

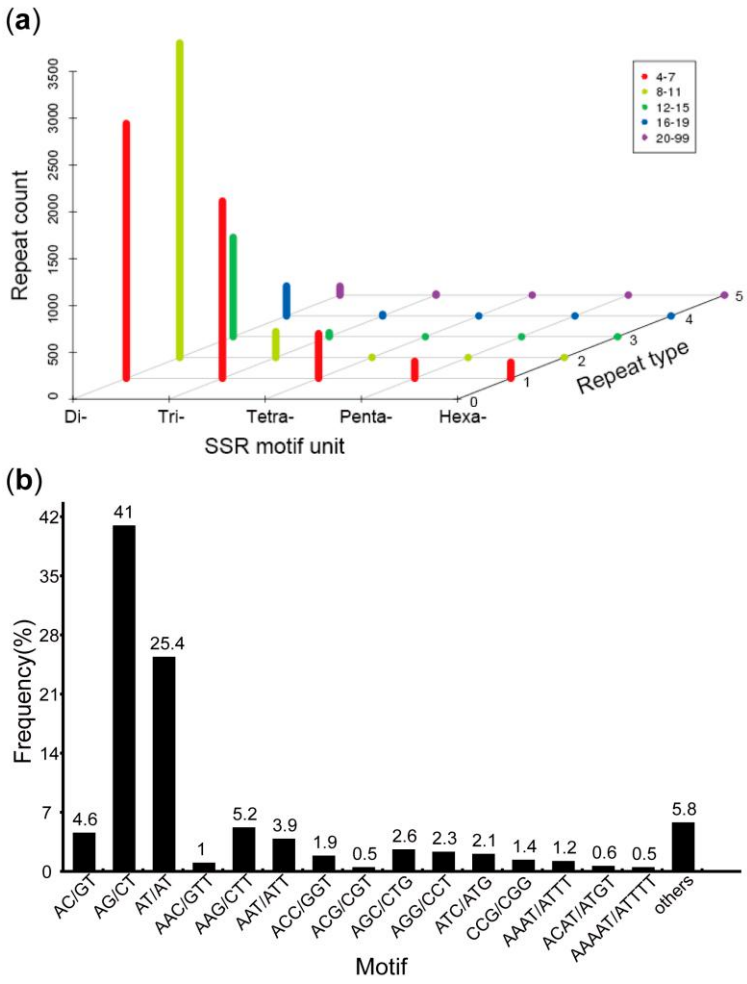

Figure 5. Distribution of simple sequence repeat (SSR) nucleotide classes among different nucleotide types in the transcriptome of *M. pasquieri*. (**a**) Distribution statistics for six types of SSRs from *M. pasquieri*. (**b**) The proportion of SSRs of different types of tandem repeat elements in total SSRs.

Table 1. Statistics for the transcriptional factor (TF) family predicted by Illumina and PacBio in *M. pasquieri*.

Family	PacBio	Illumina	Family	PacBio	Illumina	Family	PacBio	Illumina
ERF	121	154	TCP	13	28	ARR-B	2	8
WRKY	96	83	BBR-BPC	12	9	CPP	2	11
GRAS	87	88	ARF	11	24	LSD	2	8
NAC	71	99	B3	11	37	M-type	2	22
bHLH	70	172	BES1	11	10	S1Fa-like	2	6
C3H	68	72	DBB	10	13	YABBY	2	9
bZIP	49	141	Dof	9	42	CAMTA	1	7
C2H2	46	241	GeBP	9	6	E2F/DP	1	7
MYB_related	45	82	CO-like	6	12	GRF	1	11
TALE	38	29	ZF-HD	6	22	HB-other	1	11
MYB	28	124	FAR1	5	38	Whirly	1	3
EIL	27	6	LBD	5	32	HB-PHD	0	2
HD-ZIP	25	55	NF-YA	5	11	HRT-like	0	1
Trihelix	25	47	NF-YB	5	30	LFY	0	1
GATA	23	48	SBP	5	22	SAP	0	2
Nin-like	19	13	AP2	4	20	SRS	0	8
G2-like	18	40	RAV	4	2	STAT	0	1
HSF	17	32	WOX	4	5			
NF-YC	14	18	NF-X1	3	2			
MIKC	13	20	VOZ	3	1			

3.5. AS Events Detected from PacBio Sequel

Using the results obtained from PacBio transcript isoforms, 182 AS events were identified, including 42 (23.08%) A3, 33 (18.13%) A5, 18 (9.89%) AF, 82 (45.05%) RI, and seven (3.85%) SE, among which RI was the main AS event (Figure 6a,b). The AS events in our study largely enriched the transcript information for *M. pasquieri*. Due to the lack of a genome database, splice isoforms of unannotated genes remain unknown. Results from the PacBio analysis indicated that only a single isoform was detected in 109 (2.44%) genes, and two or more isoforms were found in 4353 genes (97.55%) (Figure 6c). Ten; and more than ten splice isoforms were detected in 204 (4.57%) genes. For example, 16 different COGENT000951 isoforms were identified in this study and were predicted to be associated with metabolic pathways, biosynthesis of secondary metabolites, and phenylpropanoid biosynthesis; sequencing results are shown in Figure 6d (example of A3). Additionally, 11 different COGENT002109 isoforms were identified, and the results are shown in Figure 6e, which were predicted to be associated with plant hormone signal transduction (an example of RI).

3.6. LncRNA Detected from PacBio Sequel

Four computational approaches (CNCI, CPAT, CPC, and Pfam) were combined to predict lncRNAs from putative protein-coding RNAs among the unknown transcripts. From the four different analyses, 779, 264, 866, and 933 transcripts longer than 200 nt were selected as lncRNAs, among which 149 common lncRNAs were predicted for subsequent analysis (Figure 7a). Some of these lncRNAs were up to 4000nt long (Figure 7b).

3.7. Functional Annotation of Transcripts

All 25,339 transcripts (corrected isoforms) were functionally annotated by searching Nr, Swissprot, KOG, and KEGG databases, and 24,405 transcripts (96.31%) were annotated in PacBio. Of these, 24,358 transcripts were annotated in the Nr database, 21,059 were annotated in the Swissprot database, 16,957 were annotated in the KOG database, and 13,185 were annotated in the KEGG database (Figure 8a and Figure S3). A total of 934 transcripts did not return any matches and may reflect novel transcripts in the *M. pasquieri* transcriptome. Homologous species were analyzed by comparing the transcript sequences with those in the Nr database, and the results showed that the highest numbers of

transcripts were found in *Vitis vinifera* (3484, 14.30%), *Theobroma cacao* (1432, 5.88%), *Sesamum indicum* (1182, 4.85%), *Juglans regia* (1182, 4.85%), *Nelumbo nucifera* (1063, 4.36%), *Cephalotus follicularis* (895, 3.67%), *Ziziphus jujuba* (753, 3.09%), *Camellia sinensis* (725, 2.98%), *Jatropha curcas* (664, 2.73%), and *Citrus sinensis* (535, 2.20%) (Figure 8b).

3.8. Gene Ontology (GO) Annotation

GO analysis showed that 11,810 PacBio transcript isoforms (46.61% of total set) could be divided into three groups; biological processes, molecular functions, and cellular components. Transcripts in 'biological processes' were mainly enriched for metabolic process, cellular process, single-organism process, and others (Figure 9). Transcripts involved in 'cellular components' consisted of cell, cell part, organelle, membrane, and membrane part. For the category 'molecular function', transcripts were mainly involved in catalytic activity, binding, and transporter activity. A comparison of enriched GO terms between the PacBio transcript isoforms and *de novo* transcript unigenes (which had 76,548 unigenes annotated, accounting for 61.53% of the total *de novo* set) is presented in Figure 9.

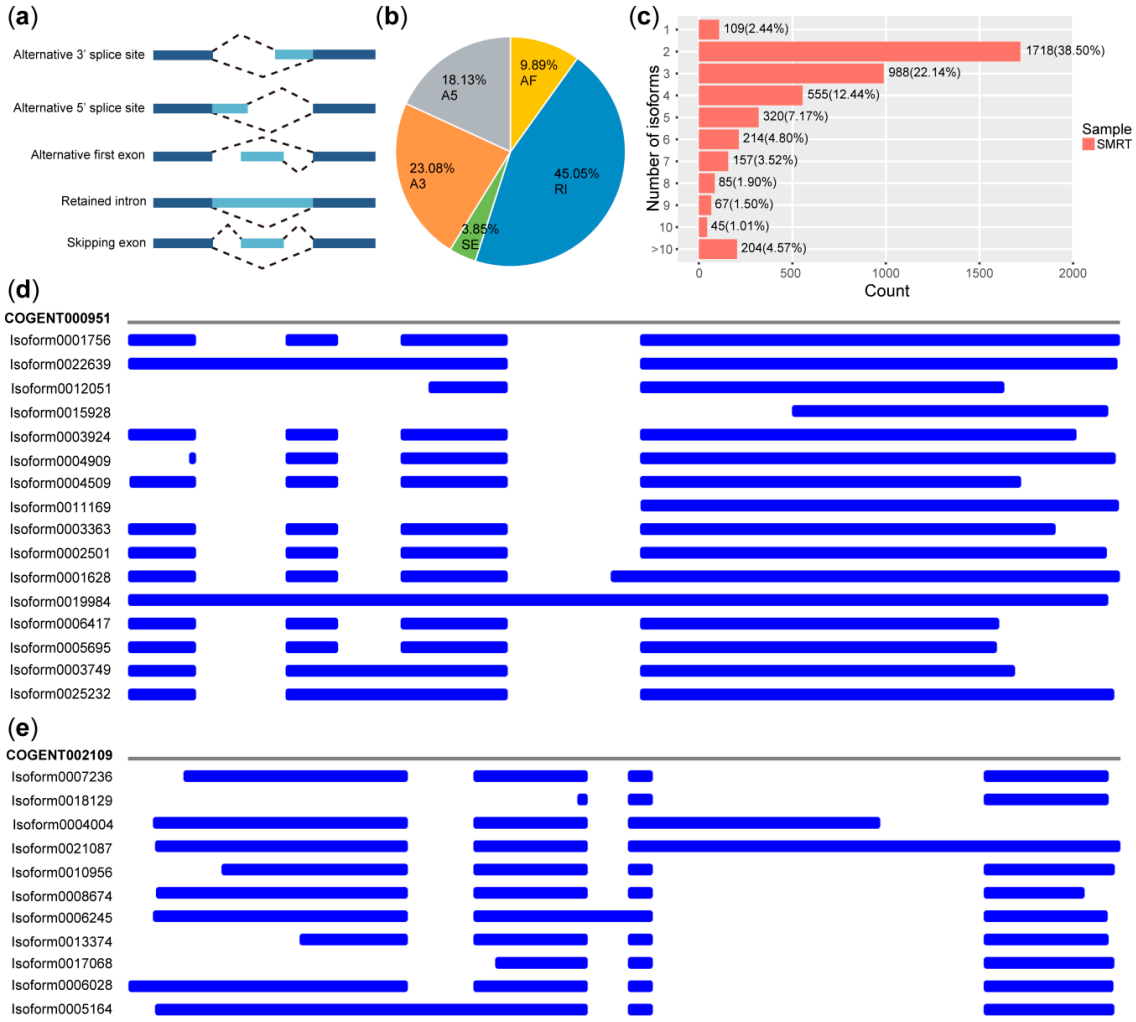

Figure 6. Analysis of alternative splicing (AS) events in the *M. pasquieri* transcriptome. (**a**) Schematic representation of five AS modes. (**b**) The number and percentage of different types of AS events detected by PacBio. A3, alternative 3′ splice site; A5, alternative 5′ splice site; AF, alternative first exon; RI, retained intron; SE, skipping exon. (**c**) Statistics for the isoforms of some genes. (**d**) Sequence analysis of different COGENT000951 isoforms. (**e**) Sequence analysis of different COGENT002109 isoforms.

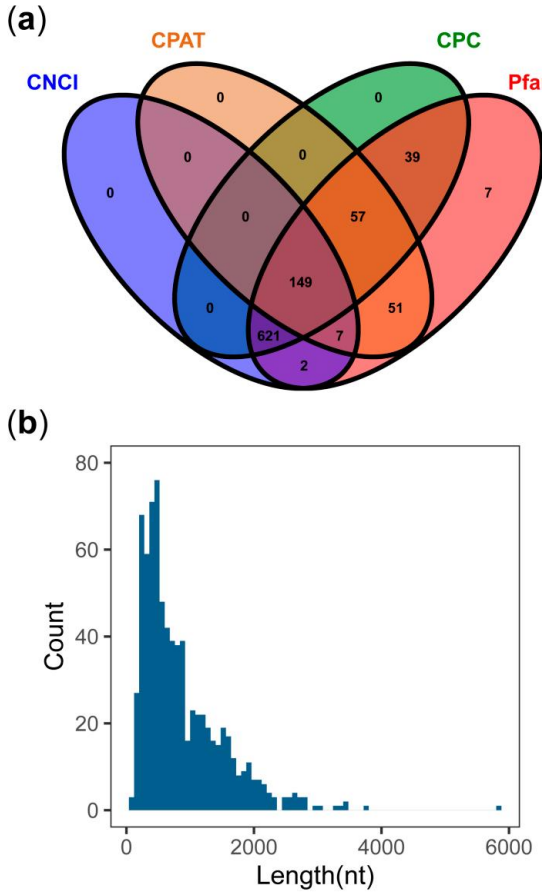

Figure 7. Identification of *M. pasquieri* long non-coding RNAs (lncRNA). (**a**) Venn diagram of lncRNAs predicted by CNCI, CPAT, CPC, and Pfam computational approaches. (**b**) Length distribution of identified lncRNAs.

3.9. Analysis of KEGG Pathways and Gene Annotation Information

KEGG pathway analysis provided additional functional information relating to the pathways associated with each transcript isoform, since one gene could be assigned to more than one GO term in the Gene Ontology annotation. The KEGG results demonstrated that 13,185 PacBio transcript isoforms (52.03% of the total) from *M. pasquieri* were annotated to 132 KEGG pathways, while 55,975 *de novo* transcript unigenes (44.99% of the total) were annotated to 136 KEGG pathways (Figure 10). The functional pathway was first assigned to five KEGG biochemical pathways, including cellular processes, environmental information processing, genetic information processing, metabolism, and organismal systems. 'Metabolism' represented the largest group in both PacBio and *de novo* transcript datasets, containing 102 and 105 pathways, respectively. With most associated with metabolic pathway (3795/7267), biosynthesis of secondary metabolites (2189/4069), biosynthesis of antibiotics (1229/0), microbial metabolism in diverse environments (1081/0), carbon metabolism (910/1504), and biosynthesis of amino acids (679/1236). Those pathways related to genetic information processing were the second largest group, including transcripts involved in protein processing in endoplasmic reticulum (715/971), ribosome (672/2321), spliceosome (509/780), and RNA transport (387/718). The third largest group comprised cellular processes, with a majority of transcripts involved in endocytosis (381/618) and phagosome (220/430). Plant hormone signal transduction (349/436) and plant-pathogen interaction (336/728) were the most in environmental information processing and organismal systems, respectively. In addition, some important pathways were also found in *M. pasquieri*, including carbon fixation in photosynthetic organisms, photosynthesis, phenylpropanoid biosynthesis, flavonoid biosynthesis, anthocyanin biosynthesis, isoflavonoid biosynthesis, flavone and

flavonol biosynthesis, terpenoid backbone biosynthesis, sesquiterpenoid and triterpenoid biosynthesis, monoterpenoid biosynthesis, and diterpenoid biosynthesis (Table S5). These results provide a valuable resource for investigating metabolic pathways in *M. pasquieri*.

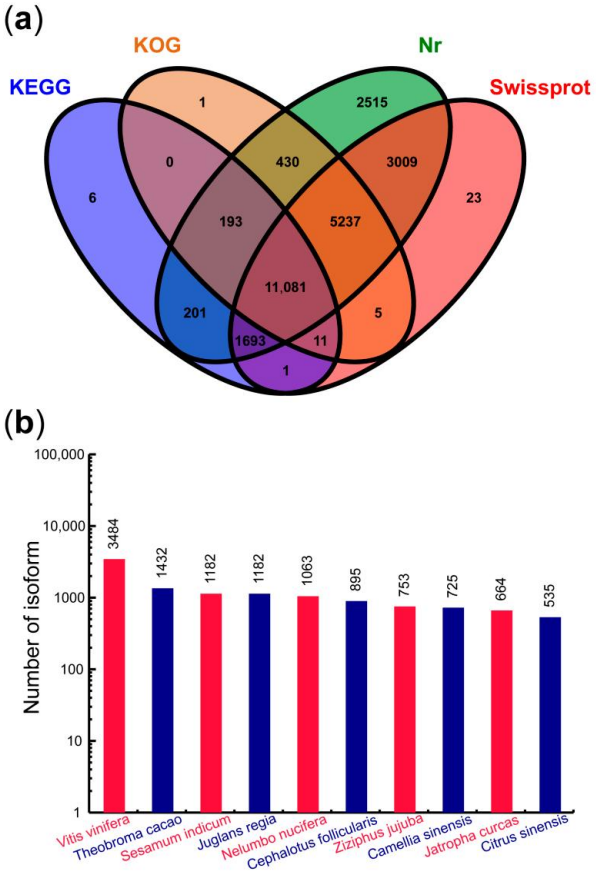

Figure 8. Functional annotation of corrected isoforms. (**a**) Venn diagram of annotated result in four different databases, Nr, Swissprot, KOG, and KEGG. (**b**) Distribution diagram showing the top ten Nr homologous species of transcripts.

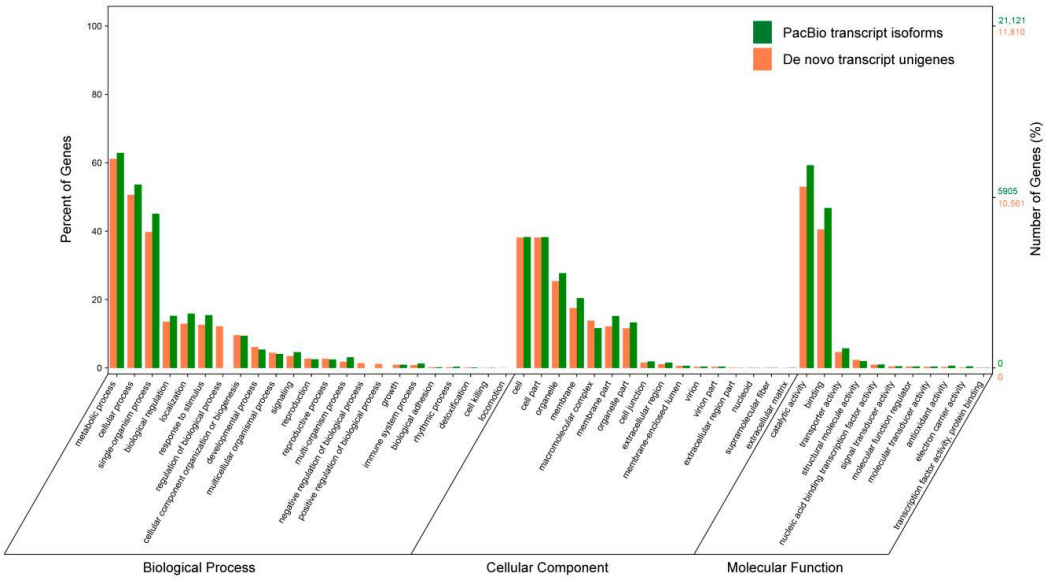

Figure 9. Gene ontology enrichment analysis of *M. pasquieri* transcript sequences.

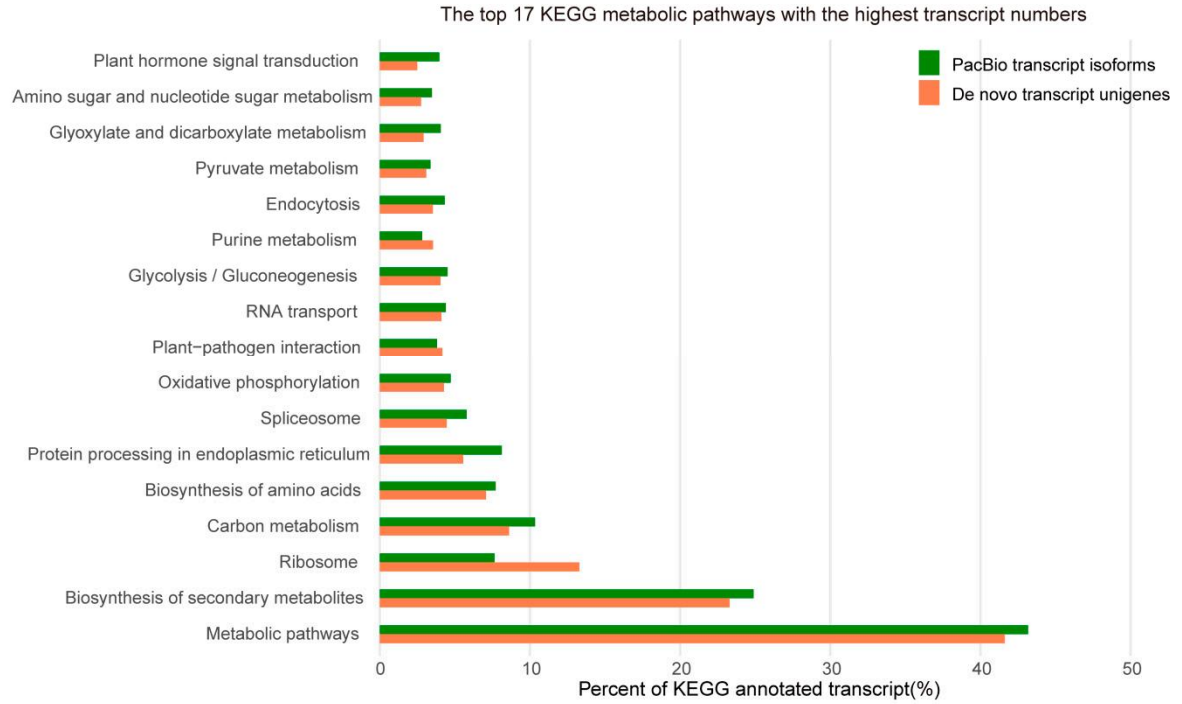

Figure 10. KEGG metabolic pathway classification of *M. pasquieri* PacBio transcript isoforms and *de novo* transcript unigenes.

Plant hormone signal transduction is important for regulating germination and growth, and 349 PacBio transcript isoforms have been shown to be involved in plant hormone signal transduction pathway (ko04075; Table S5). Auxin, gibberellin (GA), and cytokinine signal transduction pathways accelerate seed germination and plant development, while abscisic acid (ABA) signal transduction pathway plays the opposite role. In the auxin pathway, 59 transcripts were annotated as key genes, which encoded auxin transporter protein 1 (AUX1), transport inhibitor response 1 (TIR1), auxin/indole-3-acetic acid (AUX/IAA), auxin response factor (ARF), gretchen hagen 3 (GH3), and small auxin upregulated RNA (SAUR). In the GA pathway, 22 transcripts were annotated as four key genes, GA-insensitive dwarf mutant 1 (GID1), GA-insensitive dwarf mutant 2 (GID2), DELLA, and TF. In the cytokinine pathway, nine transcripts were annotated as four key genes, cytokinin response 1 (CRE1), arabidopsis histidine-containing phosphotransfer protein (AHP), type-B arabidopsis response regulators (B-ARR), and type-A arabidopsis response regulators (A-ARR). In the ABA pathway, 47 transcripts were annotated as pyrabactin resistance/PYR-like (PYR/PYL), Protein Phosphatase 2 C (PP2C), Sucrose non-fermenting 1-related protein kinases subfamily 2 (SnRK2), and ABRE-binding factor (ABF) (ko04075; Figure S6).

4. Discussion

4.1. Comparison of PacBio Transcripts and De Novo Unigenes

The *de novo* transcriptome assembly of second-generation sequencing technology has been used widely for transcriptome analysis in species without a genomic reference. Large-scale sequencing of transcriptome data by second-generation sequencing cannot generate full-length sequences or alternatively spliced forms of RNA. With the emergence of SMRT sequencing technology, full-length transcripts could be obtained without large-scale assembly. For example, *de novo* assembly from short reads only reconstructed 8% of PacBio isoforms in maize (*Zea mays*) [32]. Moreover, compared with RNA-Seq data or previously annotated references, PacBio retrieved longer transcripts, including for *Amborella trichopoda* [33], avocado (*Persea americana*) [34], and *Populus alba* var. *pyramidalis* [35]. To date, no genomic or transcriptome information for *M. pasquieri* has been reported. In this study,

five developmental stages of *M. pasquieri* were sampled to obtain more comprehensive transcript information, and 438,795 CCSs were obtained by PacBio Sequel. Due to the high error rate associated with third-generation sequencing, Illumina RNA-Seq transcripts and LoRDEC (v 0.8) were used to correct the low-quality sequences. Finally, 25,339 full-length transcripts were obtained, with a mean length of 1436.77 bp and an N50 value of 1652 bp, which will benefit further studies on *M. pasquieri*. However, these transcripts were shorter than reported in previous transcriptome studies of alfalfa (*Medicago sativa* L.) (mean length = 2551 bp, N50 = 2928 bp) [36] and *Gnetum luofuense* (mean length = 3237 bp, N50 = 3629 bp) [37], using the same technology. This result may be related to the differences in the parameters and nature characteristics of the species.

In this study, *de novo* assembly from Illumina using the same experimental material generated more transcripts (124,405 unigenes) than PacBio Sequel; however, the mean length of the transcripts was 834 bp and the N50 was 1387 bp, which were substantially shorter than those obtained by PacBio, at 1436.77 bp and 1652 bp, respectively (Table S1). The results indicate that PacBio is better able to capture long transcript sequences, similar to those reported in adlay (*Coix lacryma-jobi*) [38]. Although *de novo* assembly resulted in a higher number of transcripts and annotated transcripts (66,026), the latter accounted for only 53.07% of the total transcripts, which was much lower than the 96.31% obtained by PacBio. Notably, the annotation rate in all databases was significantly higher with PacBio sequencing data compared with Illumina data; for example, Nr, 51.19% Illumina versus 96.13% PacBio; Swissprot, 36.69% Illumina versus 83.11% PacBio; COG/KOG, 30.58% Illumina versus 66.92% PacBio; and KEGG, 44.99% Illumina versus 52.03% PacBio) (Figure 3a and Figure S3). By comparing *de novo* and PacBio transcripts, 10,140 unigenes and 15,564 isoforms were found in common by BLASTN, accounting for 8.2 and 61.4% respectively. Additionally, 91.8% (114,265) transcripts were found specifically in *de novo* assembly, and 38.6% (9775) in PacBio (Figure 3b). Thus, although *de novo* assembly can obtain a large number of transcripts and annotated transcripts, this may account for the great depth of reads used for assembly [20], while a large number of unannotated transcripts may contain many new transcripts. Therefore, although Illumina provides more transcripts and greater sequencing depth compared with PacBio Sequel, the PacBio Sequel method can detect more full-length transcripts and more accurately annotated transcripts; this is more conducive to obtaining accurate transcript information for *M. pasquieri*.

4.2. Analysis of Alternative Splicing in Transcriptomes

AS of precursor mRNAs (pre-mRNAs) during eukaryotic gene transcription may increase the number of protein isoforms produced by the removal of introns and the joining of exons [39–41]. The splicing mode of multi-exon mRNA may vary in several ways, and is usually divided into SE, A5, A3, Mutually Exclusive Exon (MX), RI, AF, and Alternative Last Exon (AL), leading to multiple transcripts of some genes [42]. Therefore, AS markedly increases the complexity and flexibility of the transcriptome and proteome [43]. In addition, AS is involved in the regulation of growth, development, signal transduction, flowering, and responses to various abiotic stresses [44–47]. Although RNA-Seq can accurately quantify and annotate individual AS events, it is hard to deduce full-length splicing isoforms that contain a combination of these individual events [48,49]. SMRT sequencing enables the generation of full-length sequences and the identification of complex splice isoforms, which are difficult to detect and reconstruct by RNA-Seq [50]. For example, PacBio identified more AS events in strawberry (*Fragaria vesca*) (17,260) compared with Illumina (12,080) [42]. In cotton (*Gossypium* spp.), PacBio (133,229) retrieved eight-times more AS events than Illumina (16,437) [51]. In the present study, 182 AS events were identified by PacBio Sequel in *M. pasquieri*, which were classified into five types, including 42 A3, 33 A5, 18 AF, 82 RI, and seven SE (Figure 6b,c). The majority of AS events were RI (45.5%), similar to previous reports in other plant species, such as sorghum (*Sorghum bicolor* BTx623) [52], bread wheat (*Triticum aestivum* L.) [53], and cassava (*Manihot esculenta*) [54]. In our study, these AS events greatly enriched the transcriptional information of *M. pasquieri*. Studies have reported specific expression of AS events in different plant tissues. For example, the proportion of different AS

events varied among maize and sorghum tissues [55]. Dynamic changes in AS events occur during different development stages and tissues of strawberry; for example, anthers at floral stages 7 and 8 had more AS genes compared with anthers from other anther stages [42]. These studies also provide direction for further research on AS events in *M. pasquieri*.

4.3. Analysis of lncRNAs Detected by PacBio Sequel

In addition to protein-coding RNAs, non-coding RNAs constitute a major component of the transcriptome [56]. Generally, lncRNAs are more than 200 nt in length, possess no apparent CDS or ORF, and lack protein coding capability [57]. Based on their genomic location, lncRNAs can be classified as antisense, intronic, and long intergenic noncoding RNA [58]. In recent years, studies have found that lncRNAs play a significant role in the physiology and development of plants, especially in some key biological processes [59]. However, only a small number of lncRNA functions have been determined. For example, studies have confirmed that lncRNAs participate in abiotic stress responses and act as regulatory factors [60]. In a transcriptional study on soybean (*Glycine max*) roots under continuous salt stress, about 77% of identified lncRNAs were activated or up-regulated by more than two-fold, and functional analysis of proteins with binding and catalytic activities were major targets of these newly identified lncRNAs, indicating the regulatory role of lncRNAs in soybean roots resistant to salt stress [61]. RNA Seq short-read sequencing, which is a powerful tool used to describe gene expression, has been widely used; however, it cannot provide full-length sequences for each RNA, which also increases the difficulty of detecting lncRNAs. Nevertheless, SMRT-seq technology can effectively capture full-length sequences of the genome and transcriptome [50]. In a study investigating the maize transcriptome, SMRT-seq identified 867 novel high-confidence lncRNAs with a mean length of 1.1 kb, which were much longer than the lncRNAs identified by RNA-Seq short-read sequencing [32]. LncRNAs have not yet been identified in *M. pasquieri*. In the present study, 149 common lncRNAs were predicted by four programs (Figure 7a), which will contribute to the functional study of lncRNAs in *M. pasquieri*. Although lncRNAs were identified by PacBio Sequel in this study, they could not be classified nor further studied due to a lack of genome data for *M. pasquieri*. A previous study also detected 223 and 205 lncRNAs in the leaf and root of *Astragalus membranaceus*, respectively [62], which may be helpful for the further study of lncRNA expression in different tissues of *M. pasquieri*.

4.4. Analysis of Nr Annotation and Transcription Factors

Among 25,339 transcripts, a total of 24,405 transcripts were annotated using four databases (Nr, Swissprot, KOG, and KEGG), including 24,358 transcripts annotated in the Nr database, accounting for 96.13% of the total annotated transcripts (Figure 3a and Figure S3). Comparison of *M. pasquieri* transcripts with the Nr data revealed that *M. pasquieri* shares homology with *Vitis vinifera* (3484, 14.30%), *Theobroma cacao* (1432, 5.88%), *Sesamum indicum* (1182, 4.85%), *Juglans regia* (1182, 4.85%), and *Nelumbo nucifera* (1063, 4.36%) (Figure 8b). *Vitis vinifera* possesses the highest homology, which may be explained by its relatively extensive database and better annotation compared with that of other species; however, its homology ratio is relatively low compared with other species. For example, in coffee (*Coffea arabica*) bean, a Nr-annotated tobacco species was much larger than that of *Coffea canephora* (1,746,308 versus 142,656 hits; maximum 50 hits per sequence) [63]. This is not unexpected, since there is no available genomic and transcriptomic information for *M. pasquieri* or a comprehensive genomic resource for Sapotaceae, only the genome of *Argania spinosa* has been reported [64], so as the plastome sequence of *Pouteria campechiana* (Kunth) Baehni [65], *Manilkara zapota* (L.) P.Royen [66], and chloroplast genome of *Lucuma nervosa* [67], *Vitellaria paradoxa*, and *Sideroxylon wightianum* [68]. Since studies on *M. pasquieri* remain in their infancy, and information available from other plants is relatively limited, further research is needed.

TFs are important regulatory components for seed germination and plant development [69], and many TF families, including WRKY, MYB, NAC, and bHLH, have been studied extensively in model plants and crops [70], but fewer studied in non-model plants [71]. For example, members of the MYB

(HORVU0Hr1G018970, HORVU2Hr1G010450) and NAC (HORVU2Hr1G077320) family were found associated with regulating germination or root development in barley (*Hordeum vulgare*) [72]. *SPATULA*, a member of bHLH, mediates seed germination by affecting cell elongation in *Arabidopsis* [73]. Here, 1058 and 2048 TF genes were identified by PacBio and Illumina, and were classified into 51 and 57 TF families, respectively. Moreover, we found that they have the same abundant TF families, including ERF, WRKY, GRAS, NAC, bHLH, C3H, bZIP, C2H2, and MYB_related (Table 1). This indicated that these TF families were actively involved in the material synthesis and growth metabolism of *M. pasquieri* during all stages, which requires further studies.

4.5. Excavation of KEGG Annotation Pathways Gene Annotation Information in M. pasquieri

A large number of transcripts from *M. pasquieri* were associated with metabolic pathways (3795), biosynthesis of secondary metabolites (2189), biosynthesis of antibiotics (1229), microbial metabolism in diverse environments (1081), and carbon metabolism (910), indicating that the germination and growth of *M. pasquieri* requires varied metabolic supports. This also shows that there are multiple functional metabolites in *M. pasquieri*, many of which may be of potential value. Although some pathways were associated with fewer transcripts, they may still be worth noting.

Previous studies have indicated that most phytohormones, such as ABA, GA, auxin, ethylene, cytokinine, brassinosteroid and jasmonic acid are involved in seed germination and growth regulation [74]. In this study, 349 PacBio transcript isoforms have been involved in plant hormone signal transduction pathway (ko04075; Table S5). Studies have shown that GA promotes seed germination, whereas ABA is the most notorious GA antagonist for its inhibitory effect on seed germination [75,76]. It has been reported that GA mainly stimulates germination by promoting radicle elongation and penetration of the seed coat [71], and GA-GID1 complex induces the degradation of the plant growth inhibitor DELLA proteins to promote plant germination [77]. In the study, 22 transcripts were involved in GA pathway, and nine and ten transcripts were annotated as GID1 and DELLA, respectively. These results might suggest that specific members of the GID1 and DELLA genes of *M. pasquieri* are involved in the regulation of seed germination. Furthermore, PYR/PYL (17), PP2C (10), SnRK2 (19), and ABF (11), associated with ABA pathway, were identified in our study, which have been proven to be key components of ABA signaling in sheepgrass (*Leymus chinensis*) [78]. Auxin is present in the seedling radicle tip during and after germination, and cytokinine is activated during germination [79]. And, we found AUX1 (8), TIR1 (5), AUX/IAA (26), ARF (12), GH3 (2), and SAUR (6) were involved in auxin pathway; CRE1 (1), AHP (2), B-ARR (3), and A-ARR (3) in cytokinine pathway of *M. pasquieri*. Although, these results might indicate that these specific transcripts were associated with the regulation of seed germination and post-germination in *M. pasquieri*, we could not obtain more accurate information in specific time, and tissues.

Other pathways, like carbon fixation in photosynthetic organisms (ko00710), photosynthesis (ko00195) pathways were also important in *M. pasquieri*, especially in post-germination stages. Notably, during cultivation of *M. pasquieri*, the leaves changed from a distinct red to a dark red, and finally to green between the two to the nine-leaf stage, which may be associated with anthocyanin biosynthesis pathway (ko00942) and 20 annotated transcripts were involved in the study. Furthermore, flavonoid biosynthesis pathway (ko00941), isoflavonoid biosynthesis pathway (ko00943), flavone and flavonol biosynthesis pathway (ko00944), terpenoid backbone biosynthesis (ko00900), sesquiterpenoid and triterpenoid biosynthesis (ko00909), monoterpenoid biosynthesis (ko00902), and diterpenoid biosynthesis (ko00904) pathways were also found, providing support for development and utilization of *M. pasquieri*.

Interestingly, 1229 and 1081 PacBio transcript isoforms have been involved in biosynthesis of antibiotics (ko01130) and microbial metabolism in diverse environments (ko01120), respectively, while none of transcript unigenes involved in *de novo* assembly from Illumina. On the one hand, this might be the differences between PacBio and Illumina platforms. And the sample used in SMRT sequencing were mixed, however in NGS *de novo* assembly were individual samples, which may filter

some lowquality reads during assembly, resulting in different transcripts being obtained. On the other hand, previous studies have shown that the annotation rate of PacBio isoforms were much higher than that of the *de novo* unigenes [42,80]. And our results showed the same conclusion (96.31% versus 53.07%), suggesting that longer transcripts may be easier annotated. This may explain that transcript unigenes, involved in biosynthesis of antibiotics and microbial metabolism in diverse environments, were not annotated, which need further studies.

5. Conclusions

In conclusion, this was the first comprehensive transcriptome analysis of *M. pasquieri* combining SMRT and NGS sequencing. We identified 25,339 transcript isoforms by PacBio, including 24,492 CDSs, 9440 SSRs, and 149 lncRNAs. A total of 1058 transcripts were identified as TFs, which were classified into 51 TF families. Additionally, 182 AS events were detected across five types (A3, A5, AF, RI, and SE), among which a majority was IR. Although *de novo* assembly from Illumina obtained more unigenes (124,405) owing to its greater sequencing depth, PacBio Sequel recovered more FL transcripts, with a longer mean length and N50, longer CDSs, and higher expression level. Using four databases, 24,405 transcripts (96.31%) were annotated by PacBio, while 66,026 unigenes were annotated by *de novo* assembly, accounting for only 53.07% of the total, indicating that PacBio can more accurately annotate transcripts. And, we found that 8.2% of the *de novo* transcript unigenes exhibited similarity to 61.4% of the PacBio transcript isoforms, and that 91.8% unigenes and 38.6% isoforms were unique to the Illumina and PacBio database, respectively. Functional annotation revealed a role for the auxin, GA, ABA, and cytokinine metabolic pathways, which are associated with seed germination and post-germination. In addition, multiple flavonoid and terpenoid metabolic pathways have been identified, which may be related to the potential value of *M. pasquieri*. Moreover, we can combine the metabolomics and proteomics in the further research, so as to better understand the mechanism of germination and growth of *M. pasquieri*. Our work provides a comprehensive transcriptome resource for future studies on functional gene mining and utilization, genetic resource classification and evolution, molecular marker development, and endangered mechanism of *M. pasquieri*.

Supplementary Materials: The following are available online at http://www.mdpi.com/1999-4907/11/8/866/s1, Figure S1: Evaluation of PacBio and Illumina data by BUSCO software, Figure S2: Length distribution of unigenes obtained by de novo assembly, Figure S3: Functional annotations of unique transcripts in transcriptomes generated by Illumina and PacBio, Figure S4: The length distribution of Blast coding sequences (CDSs) in de novo assembly, Figure S5: The proportion of SSRs of different tandem repeat element types among the total SSR in de novo assembly, Figure S6: Annotated transcripts in 'plant hormone signal transduction' of KEGG pathways, Table S1: Statistics of the PacBio and de novo assembly data, Table S2: Statistics of 15 samples data filtering of RNA-Seq, Table S3: Base information statistics for 15 samples of RNA-Seq, Table S4: Statistics of simple sequence repeat (SSR) distribution in de novo assembly, Table S5: Statistics of KEGG pathways enriched of transcripts in *M. pasquieri*.

Author Contributions: Conceptualization, L.K.; methodology, L.K.; software, L.K.; validation, L.K. and Q.L.; formal analysis, L.K.; investigation, Q.L., Y.T. and S.W.; resources, L.Z.; data curation, Q.L.; writing—original draft preparation, L.K.; writing—review and editing, L.Z. and Z.S.; visualization, L.K.; supervision, L.Z.; project administration, L.Z.; funding acquisition, L.Z. All authors have read and agreed to the published version of the manuscript.

Funding: This research was funded by Guangdong Provincial Special Fund for Forestry Development and Protection (Forestry Science and Technology Innovation Project 2017KJCX037/2019KJCX007), Guangdong Strategy for Rural Revitalization of Finance Special Fund (forest resources cultivation, management and protection, development of forestry industry) (2130207-2) and Forestry Department of Guangdong Province, China, for non-commercial ecological forest research (2020STGYL001).

Acknowledgments: We thank the Guangzhou Gene Denovo Biotechnology Company for assisting with the sequencing analysis.

Conflicts of Interest: The authors declare no conflict of interest. Data Availability: Transcriptome datasets supporting the conclusions of this article are available in the NCBI SRA repository under the accession number SRP267710.

References

1. Conesa, A.; Madrigal, P.; Tarazona, S.; Gomez-Cabrero, D.; Cervera, A.; McPherson, A.; Szczesniak, M.W.; Gaffney, D.J.; Elo, L.L.; Zhang, X.; et al. A survey of best practices for RNA-seq data analysis. *Genome Biol.* **2016**, *17*, 13. [CrossRef] [PubMed]
2. Chao, Y.; Yuan, J.; Li, S.; Jia, S.; Han, L.; Xu, L. Analysis of transcripts and splice isoforms in red clover (*Trifolium pratense* L.) by single-molecule long-read sequencing. *BMC Plant Biol.* **2018**, *18*, 300. [CrossRef] [PubMed]
3. Liu, N.; Cheng, F.; Zhong, Y.; Guo, X. Comparative transcriptome and coexpression network analysis of carpel quantitative variation in *Paeonia rockii*. *BMC Genom.* **2019**, *20*, 683. [CrossRef] [PubMed]
4. Yang, L.; Jin, Y.; Huang, W.; Sun, Q.; Liu, F.; Huang, X. Full-length transcriptome sequences of ephemeral plant *Arabidopsis pumila* provides insight into gene expression dynamics during continuous salt stress. *BMC Genom.* **2018**, *19*, 717. [CrossRef] [PubMed]
5. Wang, Y.; Ju, D.; Yang, X.; Ma, D.; Wang, X. Comparative transcriptome analysis between resistant and susceptible rice cultivars responding to striped stem borer (SSB), *Chilo suppressalis* (Walker) infestation. *Front. Physiol.* **2018**, *9*, 1717. [CrossRef] [PubMed]
6. Piriyapongsa, J.; Kaewprommal, P.; Vaiwsri, S.; Anuntakarun, S.; Wirojsirasak, W.; Punpee, P.; Klomsa-Ard, P.; Shaw, P.J.; Pootakham, W.; Yoocha, T.; et al. Uncovering full-length transcript isoforms of sugarcane cultivar Khon Kaen 3 using single-molecule long-read sequencing. *PeerJ* **2018**, *6*, e5818. [CrossRef]
7. Rather, G.A.; Sharma, A.; Pandith, S.A.; Kaul, V.; Nandi, U.; Misra, P.; Lattoo, S.K. *De novo* transcriptome analyses reveals putative pathway genes involved in biosynthesis and regulation of camptothecin in *Nothapodytes nimmoniana* (Graham) Mabb. *Plant Mol. Biol.* **2018**, *96*, 197–215. [CrossRef]
8. Dharshini, S.; Chakravarthi, M.; Narayan, J.A.; Manoj, V.M.; Naveenarani, M.; Kumar, R.; Meena, M.; Ram, B.; Appunu, C. *De novo* sequencing and transcriptome analysis of a low temperature tolerant *Saccharum spontaneum* clone IND 00-1037. *J. Biotechnol.* **2016**, *231*, 280–294. [CrossRef]
9. Xu, Q.; Zhu, J.; Zhao, S.; Hou, Y.; Li, F.; Tai, Y.; Wan, X.; Wei, C. Transcriptome profiling using single-molecule direct RNA sequencing approach for in-depth understanding of genes in secondary metabolism pathways of *Camellia sinensis*. *Front. Plant Sci.* **2017**, *8*, 1205. [CrossRef]
10. Rhoads, A.; Au, K.F. PacBio sequencing and its applications. *Genom. Proteom. Bioinf.* **2015**, *13*, 278–289. [CrossRef]
11. Wang, L.; Jiang, X.; Wang, L.; Wang, W.; Fu, C.; Yan, X.; Geng, X. A survey of transcriptome complexity using PacBio single-molecule real-time analysis combined with Illumina RNA sequencing for a better understanding of ricinoleic acid biosynthesis in *Ricinus communis*. *BMC Genom.* **2019**, *20*, 456. [CrossRef] [PubMed]
12. Chao, Y.; Yuan, J.; Guo, T.; Xu, L.; Mu, Z.; Han, L. Analysis of transcripts and splice isoforms in *Medicago sativa* L. by single-molecule long-read sequencing. *Plant Mol. Biol.* **2019**, *99*, 219–235. [CrossRef] [PubMed]
13. Dong, L.; Liu, H.; Zhang, J.; Yang, S.; Kong, G.; Chu, J.S.; Chen, N.; Wang, D. Single-molecule real-time transcript sequencing facilitates common wheat genome annotation and grain transcriptome research. *BMC Genom.* **2015**, *16*, 1039. [CrossRef] [PubMed]
14. Wang, T.; Wang, H.; Cai, D.; Gao, Y.; Zhang, H.; Wang, Y.; Lin, C.; Ma, L.; Gu, L. Comprehensive profiling of rhizome-associated alternative splicing and alternative polyadenylation in moso bamboo (*Phyllostachys edulis*). *Plant J.* **2017**, *91*, 684–699. [CrossRef] [PubMed]
15. Ma, J.; Xiang, Y.; Xiong, Y.; Lin, Z.; Xue, Y.; Mao, M.; Sun, L.; Zhou, Y.; Li, X.; Huang, Z. SMRT sequencing analysis reveals the full-length transcripts and alternative splicing patterns in *Ananas comosus* var. *bracteatus*. *PeerJ* **2019**, *7*, e7062. [CrossRef] [PubMed]
16. Zuo, C.; Blow, M.; Sreedasyam, A.; Kuo, R.C.; Ramamoorthy, G.K.; Torres-Jerez, I.; Li, G.; Wang, M.; Dilworth, D.; Barry, K.; et al. Revealing the transcriptomic complexity of switchgrass by PacBio long-read sequencing. *Biotechnol. Biofuels* **2018**, *11*, 170. [CrossRef]
17. Wang, Y.; Zeng, Z.; Li, F.; Yang, X.; Gao, X.; Ma, Y.; Rao, J.; Wang, H.; Liu, T. A genomic resource derived from the integration of genome sequences, expressed transcripts and genetic markers in ramie. *BMC Genom.* **2019**, *20*, 476. [CrossRef]

18. Edger, P.P.; VanBuren, R.; Colle, M.; Poorten, T.J.; Wai, C.M.; Niederhuth, C.E.; Alger, E.I.; Ou, S.; Acharya, C.B.; Wang, J.; et al. Single-molecule sequencing and optical mapping yields an improved genome of woodland strawberry (*Fragaria vesca*) with chromosome-scale contiguity. *Gigascience* **2018**, *7*, 1–7. [CrossRef]
19. An, D.; Cao, H.X.; Li, C.; Humbeck, K.; Wang, W. Isoform sequencing and state-of-art applications for unravelling complexity of plant transcriptomes. *Genes* **2018**, *9*, 43. [CrossRef]
20. Hoang, N.V.; Furtado, A.; Mason, P.J.; Marquardt, A.; Kasirajan, L.; Thirugnanasambandam, P.P.; Botha, F.C.; Henry, R.J. A survey of the complex transcriptome from the highly polyploid sugarcane genome using full-length isoform sequencing and *de novo* assembly from short read sequencing. *BMC Genom.* **2017**, *18*, 395. [CrossRef]
21. Xu, Z.; Peters, R.J.; Weirather, J.; Luo, H.; Liao, B.; Zhang, X.; Zhu, Y.; Ji, A.; Zhang, B.; Hu, S.; et al. Full-length transcriptome sequences and splice variants obtained by a combination of sequencing platforms applied to different root tissues of *Salvia miltiorrhiza* and tanshinone biosynthesis. *Plant J.* **2015**, *82*, 951–961. [CrossRef] [PubMed]
22. Xu, C.Q.; Liu, H.; Zhou, S.S.; Zhang, D.X.; Zhao, W.; Wang, S.; Chen, F.; Sun, Y.Q.; Nie, S.; Jia, K.H.; et al. Genome sequence of *Malania oleifera*, a tree with great value for nervonic acid production. *Gigascience* **2019**, *8*, 1–14. [CrossRef] [PubMed]
23. Tan, C.; Liu, H.; Ren, J.; Ye, X.; Feng, H.; Liu, Z. Single-molecule real-time sequencing facilitates the analysis of transcripts and splice isoforms of anthers in Chinese cabbage (*Brassica rapa* L. ssp. *pekinensis*). *BMC Plant Biol.* **2019**, *19*, 517. [CrossRef] [PubMed]
24. Kuang, X.; Sun, S.; Wei, J.; Li, Y.; Sun, C. Iso-Seq analysis of the *Taxus cuspidata* transcriptome reveals the complexity of Taxol biosynthesis. *BMC Plant Biol.* **2019**, *19*, 210. [CrossRef]
25. Liu, B.; Lin, R.; Jiang, Y.; Jiang, S.; Xiong, Y.; Lian, H.; Zeng, Q.; Liu, X.; Liu, Z.J.; Chen, S. Transcriptome analysis and identification of genes associated with starch metabolism in *Castanea henryi* seed (Fagaceae). *Int. J. Mol. Sci.* **2020**, *21*, 1431. [CrossRef]
26. Iralu, V.; Barbhuyan, H.S.A.; Upadhaya, K. Ecology of seed germination in threatened trees: A review. *Energ. Ecol. Environ.* **2019**, *4*, 189–210. [CrossRef]
27. Zhou, T.; Li, Z.H.; Bai, G.Q.; Feng, L.; Chen, C.; Wei, Y.; Chang, Y.X.; Zhao, G.F. Transcriptome sequencing and development of genic SSR markers of an endangered Chinese endemic *Genus Dipteronia* Oliver (Aceraceae). *Molecules* **2016**, *21*, 166. [CrossRef]
28. Zhang, Y.; Zhang, X.; Wang, Y.H.; Shen, S.K. *De Novo* assembly of transcriptome and development of novel EST-SSR markers in *Rhododendron rex* Levl. through Illumina Sequencing. *Front. Plant Sci.* **2017**, *8*, 1664. [CrossRef]
29. Li, X.; Li, M.; Hou, L.; Zhang, Z.; Pang, X.; Li, Y. *De novo* transcriptome assembly and population genetic analyses for an endangered Chinese endemic *Acer miaotaiense* (Aceraceae). *Genes* **2018**, *9*, 378. [CrossRef]
30. Chen, S.; Dong, M.; Zhang, Y.; Qi, S.; Liu, X.; Zhang, J.; Zhao, J. Development and characterization of simple sequence repeat markers for, and genetic diversity analysis of *Liquidambar formosana*. *Forests* **2020**, *11*, 203. [CrossRef]
31. Chen, F.; Hu, Y.; Vannozzi, A.; Wu, K.; Cai, H.; Qin, Y.; Mullis, A.; Lin, Z.; Zhang, L. The WRKY transcription factor family in model plants and crops. *Crit. Rev. Plant Sci.* **2018**, *36*, 311–335. [CrossRef]
32. Wang, B.; Tseng, E.; Regulski, M.; Clark, T.A.; Hon, T.; Jiao, Y.; Lu, Z.; Olson, A.; Stein, J.C.; Ware, D. Unveiling the complexity of the maize transcriptome by single-molecule long-read sequencing. *Nat. Commun.* **2016**, *7*, 11708. [CrossRef] [PubMed]
33. Liu, X.; Mei, W.; Soltis, P.S.; Soltis, D.E.; Barbazuk, W.B. Detecting alternatively spliced transcript isoforms from single-molecule long-read sequences without a reference genome. *Mol. Ecol. Resour.* **2017**, *17*, 1243–1256. [CrossRef] [PubMed]
34. Ge, Y.; Cheng, Z.; Si, X.; Ma, W.; Tan, L.; Zang, X.; Wu, B.; Xu, Z.; Wang, N.; Zhou, Z.; et al. Transcriptome profiling provides insight into the genes in carotenoid biosynthesis during the mesocarp and seed developmental stages of avocado (*Persea americana*). *Int. J. Mol. Sci.* **2019**, *20*, 4117. [CrossRef] [PubMed]
35. Hu, H.; Yang, W.; Zheng, Z.; Niu, Z.; Yang, Y.; Wan, D.; Liu, J.; Ma, T. Analysis of alternative splicing and alternative polyadenylation in *Populus alba* var. *pyramidalis* by single-molecular long-read sequencing. *Front. Genet.* **2020**, *11*, 48. [CrossRef]

36. Luo, D.; Zhou, Q.; Wu, Y.; Chai, X.; Liu, W.; Wang, Y.; Yang, Q.; Wang, Z.; Liu, Z. Full-length transcript sequencing and comparative transcriptomic analysis to evaluate the contribution of osmotic and ionic stress components towards salinity tolerance in the roots of cultivated alfalfa (*Medicago sativa* L.). *BMC Plant Biol.* **2019**, *19*, 32. [CrossRef]
37. Deng, N.; Hou, C.; Ma, F.; Liu, C.; Tian, Y. Single-molecule long-read sequencing reveals the diversity of full-length transcripts in leaves of *Gnetum* (Gnetales). *Int. J. Mol. Sci.* **2019**, *20*, 6350. [CrossRef]
38. Kang, S.H.; Lee, J.Y.; Lee, T.H.; Park, S.Y.; Kim, C.K. *De novo* transcriptome assembly of the Chinese pearl barley, adlay, by full-length isoform and short-read RNA sequencing. *PLoS ONE* **2018**, *13*, e0208344. [CrossRef]
39. Hallegger, M.; Llorian, M.; Smith, C.W. Alternative splicing: Global insights. *FEBS J.* **2010**, *277*, 856–866. [CrossRef]
40. McManus, C.J.; Graveley, B.R. RNA structure and the mechanisms of alternative splicing. *Curr. Opin. Genet. Dev.* **2011**, *21*, 373–379. [CrossRef]
41. Reddy, A.S.; Marquez, Y.; Kalyna, M.; Barta, A. Complexity of the alternative splicing landscape in plants. *Plant Cell* **2013**, *25*, 3657–3683. [CrossRef] [PubMed]
42. Li, Y.; Dai, C.; Hu, C.; Liu, Z.; Kang, C. Global identification of alternative splicing via comparative analysis of SMRT- and Illumina-based RNA-seq in strawberry. *Plant J.* **2017**, *90*, 164–176. [CrossRef] [PubMed]
43. Chaudhary, S.; Jabre, I.; Reddy, A.S.N.; Staiger, D.; Syed, N.H. Perspective on alternative splicing and proteome complexity in plants. *Trends Plant Sci.* **2019**, *24*, 496–506. [CrossRef] [PubMed]
44. Zhang, Q.; Zhang, X.; Wang, S.; Tan, C.; Zhou, G.; Li, C. Involvement of alternative splicing in barley seed germination. *PLoS ONE* **2016**, *11*, e0152824. [CrossRef]
45. Chao, Q.; Gao, Z.; Zhang, D.; Zhao, B.; Dong, F.; Fu, C.; Liu, L.; Wang, B. The developmental dynamics of the *Populus stem* transcriptome. *Plant Biotechnol. J.* **2019**, *17*, 206–219. [CrossRef]
46. Qian, X.; Sun, Y.; Zhou, G.; Yuan, Y.; Li, J.; Huang, H.; Xu, L.; Li, L. Single-molecule real-time transcript sequencing identified flowering regulatory genes in *Crocus sativus*. *BMC Genom.* **2019**, *20*, 857. [CrossRef]
47. Li, Y.; Mi, X.; Zhao, S.; Zhu, J.; Guo, R.; Xia, X.; Liu, L.; Liu, S.; Wei, C. Comprehensive profiling of alternative splicing landscape during cold acclimation in tea plant. *BMC Genom.* **2020**, *21*, 65. [CrossRef]
48. Steijger, T.; Abril, J.F.; Engstrom, P.G.; Kokocinski, F.; Consortium, R.; Hubbard, T.J.; Guigo, R.; Harrow, J.; Bertone, P. Assessment of transcript reconstruction methods for RNA-seq. *Nat. Methods* **2013**, *10*, 1177–1184. [CrossRef]
49. Shang, X.; Cao, Y.; Ma, L. Alternative splicing in plant genes: A means of regulating the environmental fitness of plants. *Int. J. Mol. Sci.* **2017**, *18*, 432. [CrossRef]
50. Zhao, L.; Zhang, H.; Kohnen, M.V.; Prasad, K.; Gu, L.; Reddy, A.S.N. Analysis of transcriptome and epitranscriptome in plants using PacBio Iso-Seq and Nanopore-Based direct RNA sequencing. *Front. Genet.* **2019**, *10*, 253. [CrossRef]
51. Wang, M.; Wang, P.; Liang, F.; Ye, Z.; Li, J.; Shen, C.; Pei, L.; Wang, F.; Hu, J.; Tu, L.; et al. A global survey of alternative splicing in allopolyploid cotton: Landscape, complexity and regulation. *New Phytol.* **2018**, *217*, 163–178. [CrossRef] [PubMed]
52. Abdel-Ghany, S.E.; Hamilton, M.; Jacobi, J.L.; Ngam, P.; Devitt, N.; Schilkey, F.; Ben-Hur, A.; Reddy, A.S. A survey of the sorghum transcriptome using single-molecule long reads. *Nat. Commun.* **2016**, *7*, 11706. [CrossRef] [PubMed]
53. Wei, J.; Cao, H.; Liu, J.D.; Zuo, J.H.; Fang, Y.; Lin, C.T.; Sun, R.Z.; Li, W.L.; Liu, Y.X. Insights into transcriptional characteristics and homoeolog expression bias of embryo and de-embryonated kernels in developing grain through RNA-Seq and Iso-Seq. *Funct. Integr. Genom.* **2019**, *19*, 919–932. [CrossRef] [PubMed]
54. Li, S.; Yu, X.; Cheng, Z.; Zeng, C.; Li, W.; Zhang, L.; Peng, M. Large-scale analysis of the cassava transcriptome reveals the impact of cold stress on alternative splicing. *J. Exp. Bot.* **2020**, *71*, 422–434. [CrossRef]
55. Wang, B.; Regulski, M.; Tseng, E.; Olson, A.; Goodwin, S.; McCombie, W.R.; Ware, D. A comparative transcriptional landscape of maize and sorghum obtained by single-molecule sequencing. *Genome Res.* **2018**, *28*, 921–932. [CrossRef]
56. Long, Y.; Wang, X.; Youmans, D.T.; Cech, T.R. How do lncRNAs regulate transcription? *Sci. Adv.* **2017**, *3*, eaao2110. [CrossRef]

57. Cui, J.; Luan, Y.; Jiang, N.; Bao, H.; Meng, J. Comparative transcriptome analysis between resistant and susceptible tomato allows the identification of lncRNA16397 conferring resistance to *Phytophthora infestans* by co-expressing glutaredoxin. *Plant J.* **2017**, *89*, 577–589. [CrossRef]
58. Rai, M.I.; Alam, M.; Lightfoot, D.A.; Gurha, P.; Afzal, A.J. Classification and experimental identification of plant long non-coding RNAs. *Genomics* **2019**, *111*, 997–1005. [CrossRef]
59. Tian, J.; Feng, S.; Liu, Y.; Zhao, L.; Tian, L.; Hu, Y.; Yang, T.; Wei, A. Single-molecule long-read sequencing of *Zanthoxylum bungeanum* Maxim. transcriptome: Identification of aroma-related genes. *Forests* **2018**, *9*, 765. [CrossRef]
60. Deng, F.; Zhang, X.; Wang, W.; Yuan, R.; Shen, F. Identification of *Gossypium hirsutum* long non-coding RNAs (lncRNAs) under salt stress. *BMC Plant Biol.* **2018**, *18*, 23. [CrossRef]
61. Chen, R.; Li, M.; Zhang, H.; Duan, L.; Sun, X.; Jiang, Q.; Zhang, H.; Hu, Z. Continuous salt stress-induced long non-coding RNAs and DNA methylation patterns in soybean roots. *BMC Genom.* **2019**, *20*, 730. [CrossRef] [PubMed]
62. Li, J.; Harata-Lee, Y.; Denton, M.D.; Feng, Q.; Rathjen, J.R.; Qu, Z.; Adelson, D.L. Long read reference genome-free reconstruction of a full-length transcriptome from *Astragalus membranaceus* reveals transcript variants involved in bioactive compound biosynthesis. *Cell Discov.* **2017**, *3*, 17031. [CrossRef] [PubMed]
63. Cheng, B.; Furtado, A.; Henry, R.J. Long-read sequencing of the coffee bean transcriptome reveals the diversity of full-length transcripts. *Gigascience* **2017**, *6*, 1–13. [CrossRef] [PubMed]
64. El Bahloul, Y.; Dauchot, N.; Machtoun, I.; Gaboun, F.; Van Cutsem, P. Development and characterization of microsatellite loci for the Moroccan endemic endangered species *Argania spinosa* (Sapotaceae). *Appl. Plant Sci.* **2014**, *2*, 1300071. [CrossRef]
65. Jo, S.; Kim, H.-W.; Kim, Y.-K.; Cheon, S.-H.; Kim, K.-J. The first complete plastome sequence from the family Sapotaceae, *Pouteria campechiana*(Kunth) Baehni. *Mitochondrial DNA B* **2016**, *1*, 734–736. [CrossRef]
66. Li, S.; Zhang, X.; Wang, H.; Zhu, Z.; Wang, H. Complete plastome sequence of *Manilkara zapota* (L.) P.Royen (Sapotaceae). *Mitochondrial DNA B* **2019**, *4*, 3114–3115. [CrossRef]
67. Niu, Y.; Ni, S.; Liu, Z.; Zheng, C.; Mao, C.; Shi, C.; Liu, J. The complete chloroplast genome of tropical and sub-tropical fruit tree *Lucuma nervosa* (Sapotaceae). *Mitochondrial DNA B* **2018**, *3*, 440–441. [CrossRef]
68. Wang, Y.; Yuan, X.; Chen, Z.; Luo, T. The complete chloroplast genome sequence of *Vitellaria paradoxa*. *Mitochondrial DNA B* **2019**, *4*, 2403–2404. [CrossRef]
69. Han, Z.; Wang, B.; Tian, L.; Wang, S.; Zhang, J.; Guo, S.; Zhang, H.; Xu, L.; Chen, Y. Comprehensive dynamic transcriptome analysis at two seed germination stages in maize (*Zea mays* L.). *Physiol. Plant.* **2020**, *168*, 205–217. [CrossRef]
70. Kushwaha, S.K.; Grimberg, A.; Carlsson, A.S.; Hofvander, P. Charting oat (*Avena sativa*) embryo and endosperm transcription factor expression reveals differential expression of potential importance for seed development. *Mol. Genet. Genom.* **2019**, *294*, 1183–1197. [CrossRef]
71. Song, Q.; Cheng, S.; Chen, Z.; Nie, G.; Xu, F.; Zhang, J.; Zhou, M.; Zhang, W.; Liao, Y.; Ye, J. Comparative transcriptome analysis revealing the potential mechanism of seed germination stimulated by exogenous gibberellin in *Fraxinus hupehensis*. *BMC Plant Biol.* **2019**, *19*, 199. [CrossRef] [PubMed]
72. Liew, L.C.; Narsai, R.; Wang, Y.; Berkowitz, O.; Whelan, J.; Lewsey, M.G. Temporal tissue-specific regulation of transcriptomes during barley (*Hordeum vulgare*) seed germination. *Plant J.* **2020**, *101*, 700–715. [CrossRef] [PubMed]
73. Groszmann, M.; Bylstra, Y.; Lampugnani, E.R.; Smyth, D.R. Regulation of tissue-specific expression of *SPATULA*, a bHLH gene involved in carpel development, seedling germination, and lateral organ growth in *Arabidopsis*. *J. Exp. Bot.* **2010**, *61*, 1495–1508. [CrossRef] [PubMed]
74. Wu, Q.; Bai, X.; Wu, X.; Xiang, D.; Wan, Y.; Luo, Y.; Shi, X.; Li, Q.; Zhao, J.; Qin, P.; et al. Transcriptome profiling identifies transcription factors and key homologs involved in seed dormancy and germination regulation of *Chenopodium quinoa*. *Plant Physiol. Biochem.* **2020**, *151*, 443–456. [CrossRef] [PubMed]
75. Wang, Y.; Htwe, Y.M.; Li, J.; Shi, P.; Zhang, D.; Zhao, Z.; Ihase, L.O. Integrative omics analysis on phytohormones involved in oil palm seed germination. *BMC Plant Biol.* **2019**, *19*, 363. [CrossRef] [PubMed]
76. Kurita, M.; Mishima, K.; Tsubomura, M.; Takashima, Y.; Nose, M.; Hirao, T.; Takahashi, M. Transcriptome analysis in male strobilus induction by gibberellin treatment in *Cryptomeria japonica* D. Don. *Forests* **2020**, *11*, 633. [CrossRef]

77. Gazara, R.K.; de Oliveira, E.A.G.; Rodrigues, B.C.; Nunes da Fonseca, R.; Oliveira, A.E.A.; Venancio, T.M. Transcriptional landscape of soybean (*Glycine max*) embryonic axes during germination in the presence of paclobutrazol, a gibberellin biosynthesis inhibitor. *Sci. Rep.* **2019**, *9*, 9601. [CrossRef]
78. Li, X.; Liu, S.; Yuan, G.; Zhao, P.; Yang, W.; Jia, J.; Cheng, L.; Qi, D.; Chen, S.; Liu, G. Comparative transcriptome analysis provides insights into the distinct germination in sheepgrass (*Leymus chinensis*) during seed development. *Plant Physiol. Biochem.* **2019**, *139*, 446–458. [CrossRef]
79. Shen, Q.; Zhang, S.; Liu, S.; Chen, J.; Ma, H.; Cui, Z.; Zhang, X.; Ge, C.; Liu, R.; Li, Y.; et al. Comparative transcriptome analysis provides insights into the seed germination in cotton in response to chilling stress. *Int. J. Mol. Sci.* **2020**, *21*, 2067. [CrossRef]
80. Lin, J.; Shi, X.; Fang, S.; Zhang, Y.; You, C.; Ma, H.; Lin, F. Comparative transcriptome analysis combining SMRT and NGS sequencing provides novel insights into sex differentiation and development in mud crab (*Scylla paramamosain*). *Aquaculture* **2019**, *513*, 734447. [CrossRef]

forests

MDPI

Article

The Composition and Diversity of Soil Bacterial and Fungal Communities Along an Urban-To-Rural Gradient in South China

Xuelian Tan, Lei Kan, Zhiyao Su, Xiaodong Liu and Lu Zhang *

College of Forestry and Landscape Architecture, South China Agricultural University, Guangzhou 510642, China; xueliantan@stu.scau.edu.cn (X.T.); kanlei5523@stu.scau.edu.cn (L.K.); zysu@scau.edu.cn (Z.S.); liuxd@scau.edu.cn (X.L.)

* Correspondence: zhanglu@scau.edu.cn; Tel.: +86-020-8528-0263

Received: 23 July 2019; Accepted: 10 September 2019; Published: 12 September 2019

Abstract: Soil microbes are of great significance to driving the biogeochemical cycles and are affected by multiple factors, including urbanization. However, the response of soil microbes to urbanization remains unclear. Therefore, we designed an urban-to-rural gradient experiment to investigate the response of soil microbial composition and diversity to urbanization. Here, we used a high-throughput sequencing method to analyze the biotic and abiotic effects on soil microbial composition and diversity along the urban-to-rural gradient. Our results showed that soil bacterial diversity was the highest in urban areas, followed by suburban areas, and was the lowest in exurbs; however, fungal diversity did not vary significantly among the three areas. Plant traits, i.e., tree richness, shrub richness, the number of tree stems, diameter at breast height of trees, and soil properties, i.e., pH, soil organic carbon, soil exchangeable calcium and magnesium, and soil water content, were only significantly influenced bacterial diversity, but not fungal diversity. The effect of trees and shrubs was higher than that of herbs on microbial composition. Soil organic carbon, pH, soil available nitrogen, soil exchangeable calcium, and magnesium were the major soil factors influencing the soil bacterial and fungal composition. Soil properties had a greater influence on bacterial than on fungal composition at genus level, while plant traits contributed more to fungal than to bacterial composition at genus level. Our study suggests that the urban-to-rural gradient affect the composition and diversity of bacterial community as well as the fungal composition, but not the fungal diversity.

Keywords: urbanization; bacteria; fungi; plant traits; soil properties

1. Introduction

Acceleration of urbanization globally has led to an explosive increase in global urban population. In 2018, the global urban population of 4.2 billion accounted for 55% of the total population worldwide [1]. Despite rapid economic development, urbanization has resulted in a series of ecological challenges, such as urban heat islands [2], increased atmospheric CO_2 concentration [3], nitrogen deposition [4], and decreased biodiversity [5]. However, urban forests play a positive role under the enormous pressure of urbanization. Urban forests are associated with multiple ecological benefits such as absorption of carbon and release of oxygen, regulation of urban microclimate, and diminishing heat island effect, thus alleviating the impacts of urbanization [6].

As an essential component of urban forest ecosystem, soil microbes participate in many ecological processes and play an important role in urban forest ecosystem. Soil microbes drive biogeochemical cycles [7], via litter decomposition [8,9], catalyzing the turnover of soil carbon and nutrients [10] and alleviation of changes induced by urbanization. Therefore, subtle changes in soil microbes may reflect

significant changes in nutrient cycles of the plant-soil system [11]. However, the response of soil microbial composition and diversity to biotic (plant traits) and abiotic (soil physicochemical attributes) factors remains unclear.

Studies have shown that plant diversity is a determinant of soil microbial biomass. Increased plant diversity significantly increases microbial biomass [12,13], microbial diversity [14], and microbial activity [15], and enhances the rate of microbial use of rhizosphere carbon [16]. In addition, plant diversity can predict soil microbial beta diversity [17]. The various soil microbial groups and the diversity of different plant layers show varying levels of relationship. Soil bacterial diversity is significantly correlated with tree and shrub diversity [18,19], while the correlation between fungal and plant diversity is weak [18,20]. However, a strong correlation exists between the composition of fungal and plant communities [20]. Soil microbes are very sensitive to the soil microenvironment. Studies have shown that the soil physicochemical attributes (pH, C source, available nutrients, water content, and soil structure) [21] can significantly affect the diversity of the soil microbial community. Soil pH is currently recognized as a key factor affecting soil microbes [22,23]. However, Wang et al. [24] showed that the changes in the rate of soil nitrogen utilization and soil organic carbon following nitrogen addition significantly reduced soil microbial diversity; soil pH did not significantly affect the soil microbial diversity. To date, the differential impact of plant traits and soil properties on soil microbes remains understudied.

Recent studies investigating the role and the assembly mechanism of urban forests mainly focused on soil properties [25,26] and plant communities [5,27]. However, the response of soil microbial communities to urbanization and the impact of changes in plant traits and soil properties induced by urbanization on the soil microbes have yet to be investigated systematically. The Pearl River Delta in China has experienced rapid urbanization since the economic reform in 1978 and is one of the three major urban agglomerations in the country. It has surpassed Tokyo in Japan to become the world's largest urban agglomerate facilitating the study of the response of soil microbial communities to urbanization [28]. Therefore, we designed an urban-to-rural gradient experiment (urban-suburb-exurb) in Dongguan, one of the important cities in China's Pearl River Delta urban agglomeration to address this concern. The composition and diversity of soil microbial community and the related biotic (plant traits) and abiotic (soil properties) factors were systematically investigated along the urban-to-rural gradient. Based on previous studies investigating soil microbial community [18,29–32], we predicted that plant traits may have stronger effects on fungal rather than on bacterial community along the urban-to-rural gradient, while soil properties may affect bacteria more than the fungal community. The specific objectives of this investigation were to (1) test the responses of soil bacterial and fungal communities to urbanization based on their composition and diversity along the urban-to-rural gradient, respectively, and (2) analyze the relationships between soil microbial composition and diversity, and plant traits and soil properties.

2. Materials and Methods

2.1. Study Site

We conducted our study in Dongguan (113°31′–114°15′ E, 22°39′–23°09′ N), which is located in the Pearl River Delta, South China (Figure 1). The climate in Dongguan is warm and humid. The annual average temperature is 22.1 °C, and the average temperatures during the hottest (July) and the coldest (January) months are 28.2 °C and 13.4 °C, respectively. The annual average precipitation is 1796 mm. The rainfall during the rainy season (April to September) accounts for approximately 80% of the precipitation during the whole year. The soil type is red and the soil texture is sandy and loam. The evergreen broad-leaved zonal forest is well preserved in the south of Dongguan [33]. Therefore, we selected the research sites from the city center to the south, with an almost consistent longitude.

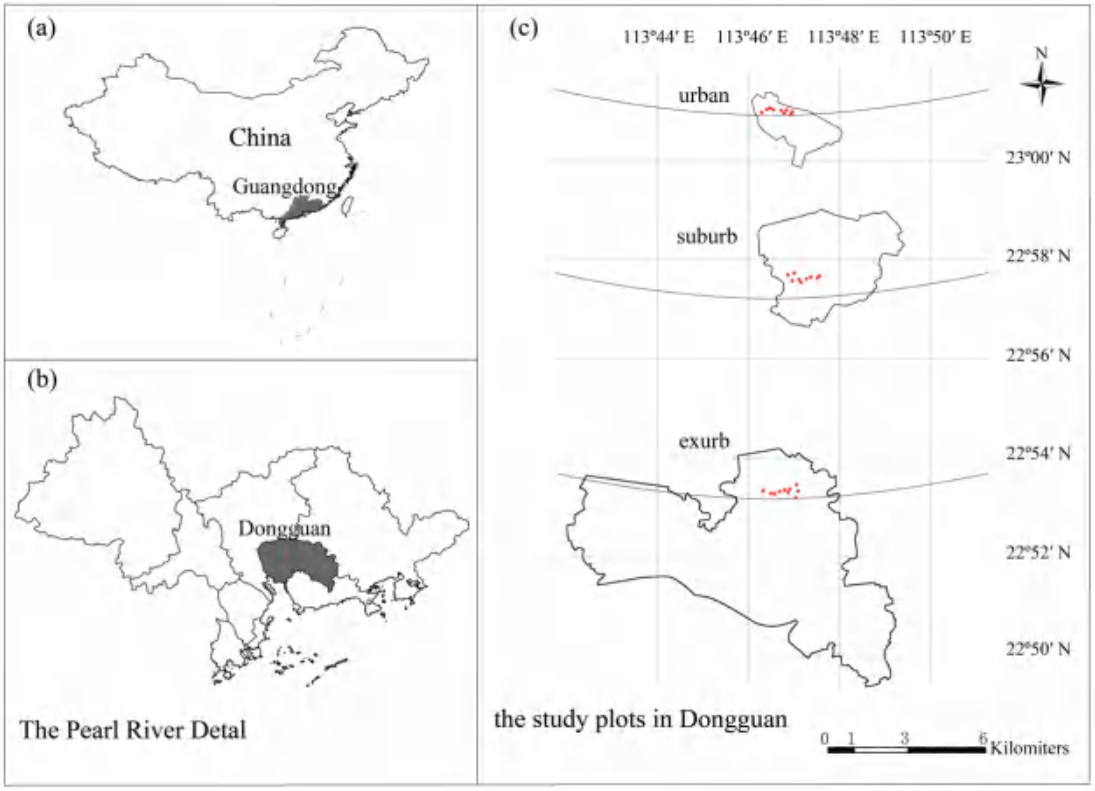

Figure 1. Locations of the three study sites and 27 plots in Dongguan, south China.

We selected the following study sites: Qifeng Park (113°45′50″–113°46′26″ E, 23°00′50″–23°01′04″ N) in the urban areas, the Tongsha Ecological park (113°45′54″–113°46′45″ E, 22°57′45″–23°58′25″ N) in the suburban areas about 6 km from the city center, and the Dalingshan Forest Park (113°45′56″–113°46′46″ E, 22°52′28″–22°53′09″ N) in the exurban areas about 16 km from the city center. The population densities of the three sites decreased from urban to exurban areas [33]. Qifeng Park is located in the center of Dongguan with a high degree of disturbance. Plantation is the main vegetation type. Tongsha Ecological Park is located in the suburb of Dongguan. The vegetation types include mainly plantations and natural secondary forests. The existing subtropical evergreen broad-leaved forests are mainly artificial, and the natural secondary forests are mainly composed of evergreen shrubs and small trees. Dalingshan Forest Park is located in the exurb of Dongguan. The vegetation types mainly include secondary forests and plantations. The secondary forest is well preserved due to effective long-term protection (Table 1).

Table 1. Stand characteristics of three sites along the urban-to-rural gradient in Dongguan, south China.

Site	DBH Mean ± S.E.	H Mean ± S.E.	Representative Species
urban	14.31 ± 0.41 cm	8.79 ± 0.19 m	*Cinnamomum burmanni*, *Ficus microcarpa* and *Albizia falcataria*
suburb	11.55 ± 0.27 cm	8.21 ± 0.14 m	*Eucalyptus urophylla*, *Elaeocarpus sylvestris* and *Spathodea campanulata*
exurb	7.71 ± 0.13 cm	6.70 ± 0.08 m	*Schefflera octophylla*, *Acronychia pedunculata* and *Acronychia pedunculata*

DBH and H indicated the diameter at breast height and average height of trees, respectively.

2.2. Experimental Design, Plant Census, and Soil Sampling

The experiment was carried out in Dongguan in January 2018. Nine independent plots with identical size (20 × 20 m) were randomly designated within each site for vegetation census and soil sampling. The space between each two plots was more than 20 m. In each plot, we recorded all trees (diameter at breast height (DBH) ≥ 3 cm) including the species name, DBH, and the number of stems. Four 25 m^2 (5 × 5 m) subplots and five 1 m^2 (1 × 1 m) subplots were selected in each plot for investigation of shrubs and herbs, respectively. In the shrub quadrats, the individual species name and their number were recorded. In the herb quadrats, the species name and cover were recorded. Plant traits used for analyses included diameter at breast height of trees (DBH), the number of tree stems (TS), tree richness (TR), shrub richness (SR), and herb richness (HR) (Table S1).

For soil sampling, after removing the litter layer, six samples were collected in an "S" shape (0–10 cm) and thoroughly mixed. Then, we removed impurities such as plant roots and stones to provide a composite soil sample in each plot. The composite soil sample was divided into two subsamples: one (>6 g) was immediately transferred into the portable ice box designed for microbial identification and another (>500 g) carried in a sealed bag for the determination of soil chemical properties. We also obtained soil samples from each plot using a cut ring (50 mm diameter) to measure the soil water content. All soil samples were collected within a single day.

2.3. Soil Physicochemical Properties

Soil water content (SWC) was calculated gravimetrically via oven drying to constant mass at 105 °C. Soil pH was measured via glass electrode method in a 1:2.5 (v/v) soil:water suspension. We determined soil organic carbon (SOC) using the $K_2Cr_2O_7$ oxidation method and soil available nitrogen (AvN) via alkaline hydrolysis diffusion method. Soil available potassium (AvK), soil exchangeable calcium (Ca^{2+}) and soil exchangeable magnesium (Mg^{2+}) were determined via flame atomic absorption spectrophotometry after extraction with 1 mol·L^{-1} ammonium acetate. Soil available phosphorus (AvP) was determined using the molybdenum-antimony colorimetric method after extraction with 0.03 mol·L^{-1} ammonium fluoride and 1 mol·L^{-1} hydrochloric acid [34] (Table S1).

2.4. Soil Microbial Communities

Soil microbial DNA was extracted from fresh soil using a MOBIO PowerSoil® DNA Isolation Kit (MOBIO laboratories, Carlsbad, CA, USA) for the corresponding sample according to the manufacturer's instructions. The concentration and purity of the extracted DNA were quantified using the NanoDrop One (Thermo Fisher Scientific, MA, USA). The 16S rRNA (for bacteria) and ITS3 (for fungi) genes of distinct regions were amplified using a specific primer with 12 bp barcode. Primers were synthesized by Invitrogen (Invitrogen, Carlsbad, CA, USA). PCR reactions, containing 25 µL 2x Premix Taq (Takara Biotechnology, Dalian Co. Ltd., China), 1 µL of each primer (10 mM) and 3 µL DNA (20 ng/µL) template in a volume of 50 µl, were amplified by thermocycling: 5 min at 94 °C for initialization; 30 cycles of 30 s each for denaturation at 94 °C, 30 s annealing at 52 °C, and 30 s extension at 72 °C; followed by a 10 min final elongation step at 72 °C.

PCR products were analyzed and purified by 1% agarose gel electrophoresis for further experiments. The selected PCR products were mixed in equidensity ratios according to the GeneTools Analysis Software (Version4.03.05.0, a division of Synoptics, Cambridge, England). The PCR product mixtures were purified with EZNA Gel Extraction Kit (Omega, USA). Sequencing libraries were finally generated using NEBNext® Ultra™ DNA Library Prep Kit for Illumina® (New England Biolabs, MA, USA), and sequenced on an IlluminaHiseq2500 platform to generate 250 bp paired-end reads (Guangdong Magigene Biotechnology Co.,Ltd. Guangzhou, China).

The paired-end raw reads were filtered to obtain the high-quality clean reads according to the Trimmomatic (V0.33, http://www.usadellab.org/cms/?page=Trimmomatic, Aachen, Germany). The paired-end clean reads were merged according to the degree of overlap between the paired-end

reads by FLASH (V1.2.11, https://ccb.jhu.edu/software/FLASH/, MD, USA), and the spliced sequences designated as Raw Tags. Using Mothur software (V1.35.1, http://www.mothur.org, MA, USA), the sequences were assigned to each sample based on their unique barcode and primer, after which the barcodes and primers were removed to obtain the effective Clean Tags. Usearch software (V10, http://www.drive5.com/usearch/, CA, USA) was used to select operational taxonomic units (OTU) by combining the reads of clustered OTUs with 97% similarity. Finally, the normalized (subsampled) OTU table was obtained according to the sample with the least sequences. The OTU table with annotations of fungal taxonomy was then used to analyze ecological groups of fungi with FUNGuild software (MN, USA) [35]. The OTU table with annotations of bacterial taxonomy was then used with FAPROTAX (Vancouver, Cananda) software to find the bacterial functional group for each OUT [36].

2.5. Statistical Analyses

The Chao1 index and Shannon index of bacteria ($Chao1_B$ and $Shannon_B$) and fungi ($Chao1_F$ and $Shannon_F$) were calculated with QIIME (V1.9.1, http://qiime.org, CA, USA) based on bacterial and fungal OTUs. The Chao1 index indicated the microbial species richness, and the Shannon index represented both the microbial species richness and evenness.

Kruskal–Wallis nonparametric test was conducted to analyze the differences in soil properties, plant traits, microbial diversity, and the relative abundance of the main bacterial and fungal phyla and genera along the urban-to-rural gradient. The differences of both bacterial and fungal composition (OTUs) along the urban-to-rural gradient and the differences of both bacterial and fungal functional groups along the urban-to-rural gradient were detected by permutational multivariate analysis of variance (PerMANOVA) with 999 permutations. Redundancy analysis (RDA) was used to determine the correlation between the composition of bacterial and fungal communities, and soil properties and plant traits. Also, we used the Spearman correlation analyses to determine the relationship of bacterial and fungal diversities, composition, and bacterial and fungal functional groups with soil properties and plant traits. Furthermore, the contribution of soil properties and plant traits to the composition of bacterial and fungal community was identified via variation partitioning analysis (VPA) [37]. All analyses were conducted in R (3.4.4, Vienna, Austria) software with 'agricolae', 'psych', and 'vegan' packages. p value < 0.05 was considered statistically significant.

3. Results

3.1. Changes in Plant and Soil Variables

Plant and soil properties greatly varied along the urban-to-rural gradient displaying different trends in these variations (Table 2). Among plant traits, TR, SR, and TS significantly increased along the urban-to-rural gradient ($p < 0.01$), whereas HR and DBH showed the opposite trend. All the soil properties varied significantly along the urban-to-rural gradient ($p < 0.05$) except AvK. The soil was acidic and the pH decreased along the urban-to-rural gradient. SOC, AvN, and SWC were the highest in exurban areas. However, Ca^{2+} and Mg^{2+} had the highest values in urban area soils. AvP in the suburban areas was significantly higher than in urban and exurban areas ($p < 0.01$).

Table 2. Characteristics of plant and soil along the urban-to-rural gradient.

Variables	Urban	Suburb	Exurb	*p* Value
pH	5.47 ± 0.26 a	4.66 ± 0.09 a	4.24 ± 0.04 b	<0.001
SWC ($g \cdot kg^{-1}$)	155.65 ± 13.19 b	187.43 ± 9.15 ab	208.97 ± 13.33 a	<0.05
SOC ($g \cdot kg^{-1}$)	15.95 ± 1.6 b	17.2 ± 0.9 b	32.72 ± 2.36 a	<0.001
AvN ($mg \cdot kg^{-1}$)	84.29 ± 6.37 b	84.58 ± 4.85 b	142.25 ± 10.07 a	<0.001
AvP ($mg \cdot kg^{-1}$)	3.98 ± 0.53 b	12.92 ± 3.76 a	2.44 ± 0.09 b	<0.01
AvK ($mg \cdot kg^{-1}$)	74.05 ± 5.06	57.01 ± 4.88	68.48 ± 3.57	0.074
Ca^{2+} ($mg \cdot kg^{-1}$)	660.53 ± 146.93 a	214.54 ± 73.14 b	72.81 ± 6.92 b	<0.01
Mg^{2+} ($mg \cdot kg^{-1}$)	33.13 ± 5.39 a	11.51 ± 2.17 b	11.17 ± 0.91 b	<0.01
DBH (cm)	14.71 ± 0.84 a	11.49 ± 1.09 b	7.76 ± 0.37 c	<0.001
TS	53.11 ± 4.31 c	82.89 ± 5.72 b	153.67 ± 5.06 a	<0.001
TR	7.67 ± 0.91 c	11.56 ± 1.18 b	17.67 ± 0.62 a	<0.001
SR	10.33 ± 1.52 b	14.67 ± 2.02 b	29.67 ± 1.09 a	<0.001
HR	10.11 ± 1.33 a	7.67 ± 1.26 ab	5.44 ± 0.38 b	<0.05

Abbreviations: SWC, soil water content; SOC, soil organic carbon; AvN, soil available nitrogen; AvK, Soil available potassium; AvP, soil available phosphorus; Ca^{2+}, soil exchangeable calcium; Mg^{2+}, soil exchangeable magnesium; DBH, diameter at breast height of trees; TS, the number of tree stems; TR, tree richness; SR, shrub richness; HR, herb richness. Values are means ± SE. Different lowercase letters indicate significant differences among three areas based on Kruskal–Wallis nonparametric test ($p < 0.05$).

3.2. Communities of Soil Bacteria and Fungi

A total of 82,683 bacteria OTUs and 27813 fungi OTUs were identified in soil samples. The main bacterial phyla (relative abundance > 1%) across all samples were Proteobacteria, Acidobacteria, Actinobacteria, Verrucomicrobia, WPS-2, Planctomycetes, Chloroflexi, Bacteroidetes, Gemmatimonadetes, and Latescibacteria. Proteobacteria and Acidobacteria were the most abundant bacterial phyla constituting 40.94% and 25.73%, respectively (Figure S1A, Table S2). Except for the Acidobacteria, Chloroflexi, Planctomycetes, and Verrucomicrobia, the relative abundance of other main bacterial phyla differed significantly along the urban-to-rural gradient ($p < 0.05$, Table S2). Additionally, the relative abundance of Actinobacteria, Proteobacteria, and WPS-2 increased significantly along the urban-to-rural gradient, whereas those of Bacteroidetes, Gemmatimonadetes, and Latescibacteria decreased along the gradient ($p < 0.05$, Table S2). At the genus level, there were 20 main bacterial genera (relative abundance > 1%, Figure 2A). The relative abundance of all the main bacterial genera, except for Occallatibacter, exhibited a significant difference along the urban-to-rural gradient ($p < 0.05$, Table S2). Nine genera with the most abundance showed different trends. Bryobacter, from Acidobacteria, exhibited the lowest abundance in the exurban areas; however, another genus belonging to Acidobacteria, Candidatus_Solibacter, showed the highest abundance in the suburban areas ($p < 0.05$, Table S2). Within the Proteobacteria, the abundance of three genera (Acidibacter, Bradyrhizobium, and Roseiarcus) significantly increased from urban to exurban areas. The abundance of other two genera (Burkholderia-Caballeronia-Paraburkholderia and Rhodoplanes) in the urban areas was significantly lower than in suburban and exurban areas ($p < 0.05$, Table S2). Acidothermus in Actinobacteria also increased in the abundance along the gradient, and ADurb.Bin063-1 in Verrucomicrobia was predominant in suburban areas ($p < 0.05$, Table S2). The PerMANOVA analyses of bacterial OTUs indicated that the composition of bacterial community significantly differed along the urban-to-rural gradient ($p < 0.001$, Table S4).

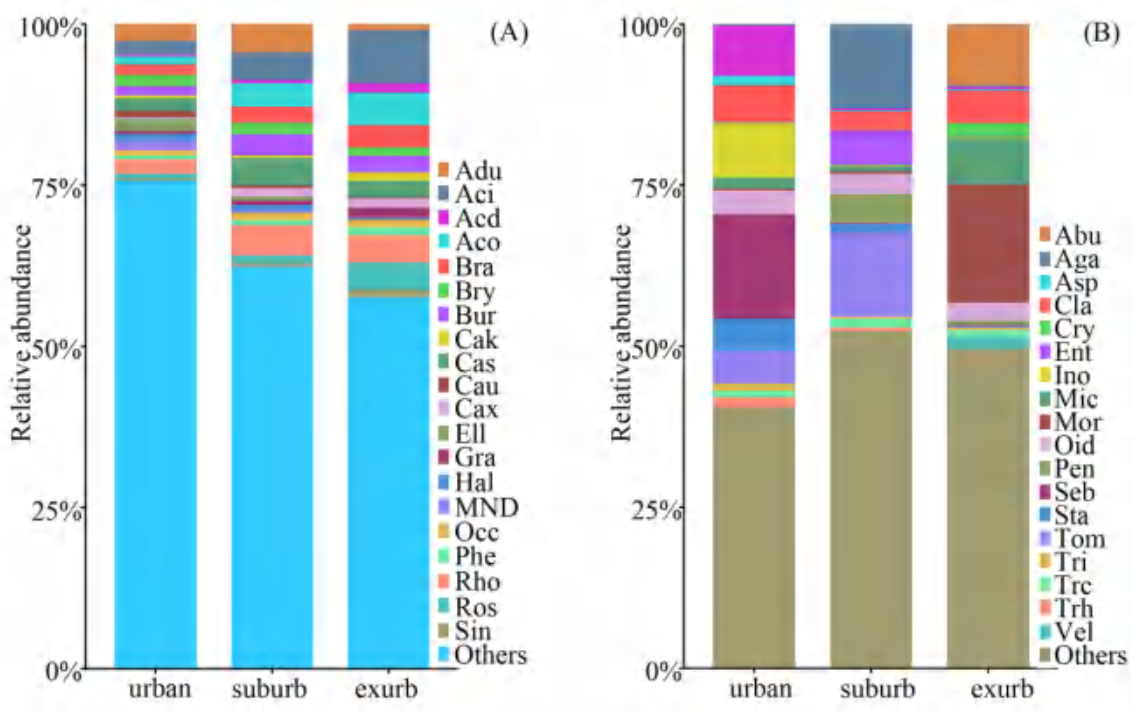

Figure 2. Relative abundance of bacterial genera (**A**) and fungal genera (**B**) along the urban-to-rural gradient at the Dongguan city, southern China. Abbreviations: Aci, *Acidibacter*; Acd, *Acidicaldus*; Aco, *Acidothermus*; Adu, *ADurb.Bin063-1*; Bra, *Bradyrhizobium*; Bry, *Bryobacter*; Bur, *Burkholderia-Caballeronia-Paraburkholderia*; Cak, *Candidatus_Koribacter*; Cas, *Candidatus_Solibacter*; Cau, *Candidatus_Udaeobacter*; Cax, *Candidatus_Xiphinematobacter*; Ell, *Ellin6067*; Hal, *Haliangium*; MND, *MND1*; Rho, *Rhodoplanes*; Phe, *Phenylobacterium*; Ros, *Roseiarcus*; Sin, *Singulisphaera*; Occ, *Occallatibacter*; Gra, *Granulicella*; Abu, *Abundisporus*; Aga, *Agaricus*; Asp, *Aspergillus*; Cla, *Cladosporium*; Cry, *Cryptococcus*; Ent, *Entoloma*; Ino, *Inocybe*; Mic, *Micropsalliota*; Mor, *Mortierella*; Oid, *Oidiodendron*; Pen, *Penicillium*; Scl, *Scleroderma*; Seb, *Sebacina*; Sta, *Staphylotrichum*; Tom, *Tomentella*; Tri, *Trichocladium*; Trc, *Trichoderma*; Trh, *Trichosporon*; Vel, *Veluticeps*.

Among the fungal communities, the main phyla (relative abundance > 1%) were Ascomycota (38.77%), Basidiomycota (50.71%), and Zygomycota (4.12%, Figure S1B, Table S3). Only the relative abundance of Zygomycota showed a significant difference along the urban-to-rural gradient ($p < 0.05$, Table S3). At the genus level, the fungal genera varied greatly along the urban-to-rural gradient (Figure 2B, Table S3). There were 19 main fungal genera (relative abundance > 1%), and the relative abundance of almost half of which significantly differed along the urban-to-rural gradient ($p < 0.05$, Table S3). The relative abundance of Aspergillus, Staphylotrichum, and Trichocladium belonging to Ascomycota, and Tomentella and Trichosporon included in Basidiomycota was significantly higher in the urban than in exurban areas. However, Oidiodendron, from Ascomycota, and Abundisporus, Entoloma, and Veluticeps from Basidiomycota had the highest abundance in exurban areas ($p < 0.05$, Table S3). The PerMANOVA analyses of fungal OTUs also indicated that the composition of fungal community significantly differed along the urban-to-rural gradient ($p < 0.001$, Table S4).

Both indices (Chao1 and Shannon) characterizing the diversity of bacterial communities decreased significantly along the urban-to-rural gradient (Figure 3A,B). At the same time, diversity of fungal communities did not vary significantly along the gradient (Figure 3C,D).

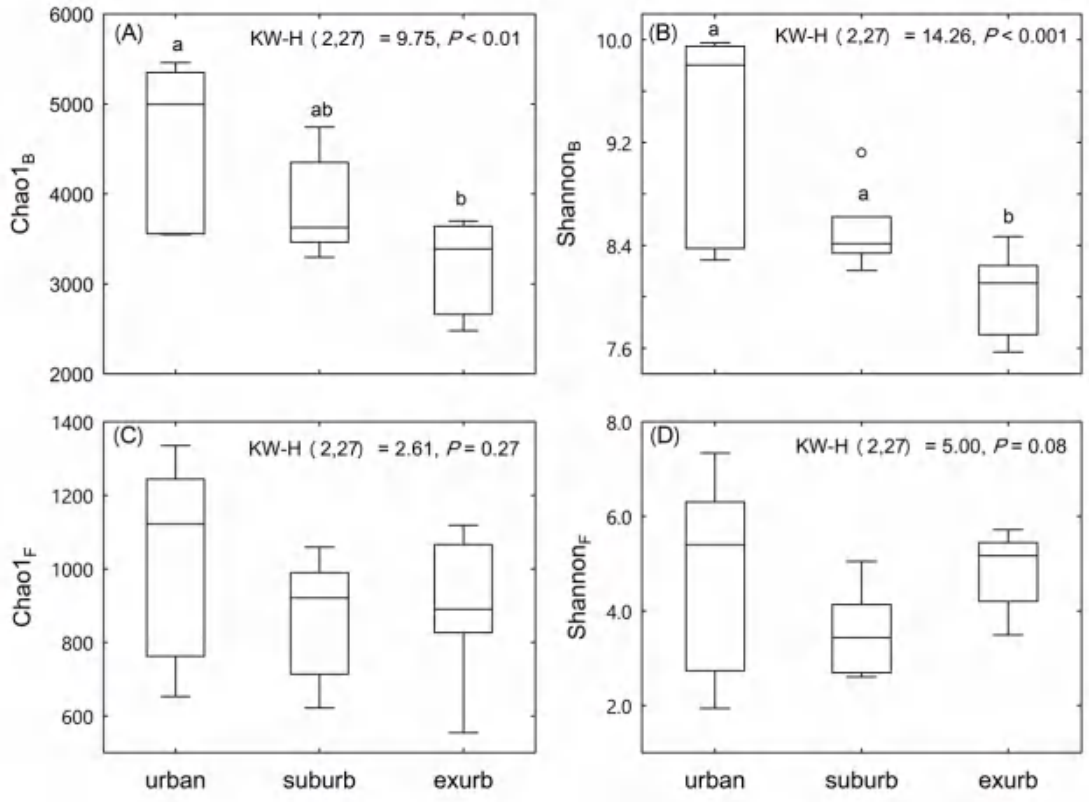

Figure 3. Diversity of soil bacterial community (**A**,**B**) and soil fungal community (**C**,**D**) along the urban-to-rural gradient at the Dongguan city, southern China. Different lowercase letters indicate significant differences among three areas based on Kruskal–Wallis nonparametric test ($p < 0.05$).

3.3. Bacterial and Fungal Functional Groups

FAPROTAX assigned 108,854, 128,508, and 153,970 squences to 62, 61, and 62 bacterial functional groups in urban, suburban, and exurban areas, respectively. The main six abundant groups were influenced by urban-to-rural gradient (Figure 4A). The relative abundance of chemoheterotrophy, aerobic_chemoheterotrophy, cellulolysis, and iron_respiration was higher in exurban areas than in suburban and urban areas. However, the relative abundance of predatory_or_exoparasitic increased in urban areas (Figure 4A). The PerMANOVA analyses indicated that the composition of bacterial functional groups significantly differed along the urban-to-rural gradient ($p < 0.01$, Table S5).

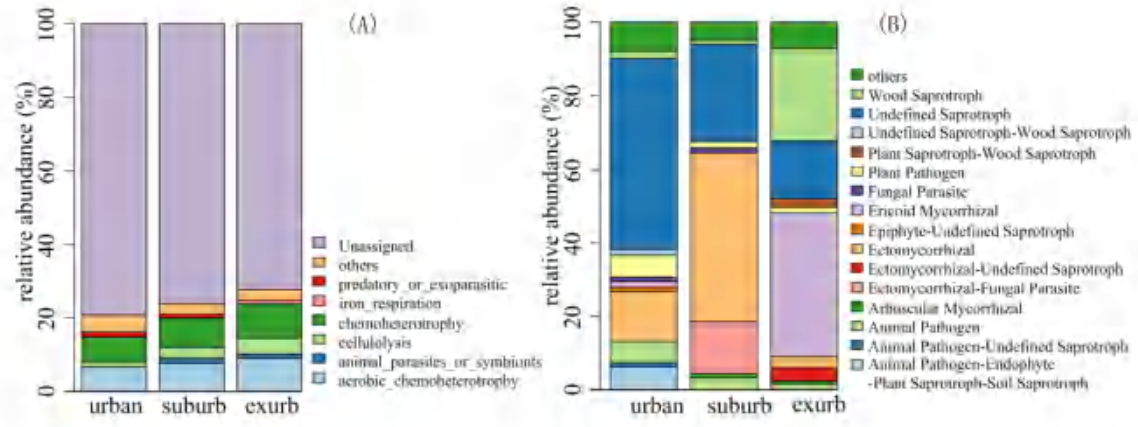

Figure 4. Relative abundance of bacterial (**A**) and fungal (**B**) functional groups along the urban-to-rural gradient at the Dongguan city, southern China.

FUNGuild assigned 32,878, 51,000, and 39,390 sequences to 59, 54, and 58 fungal functional guilds in urban, suburban, and exurban areas, respectively, with the "confidence ranking" of "highly probable" or "probable". There were 15 main guilds (Figure 4B). For example, the relative abundance of wood saprotroph and ericoid mycorrhizal fungi was the highest in exurban areas than in urban and suburban areas. The guilds of undefined saprotroph, plant pathogen, animal pathogen, and animal pathogen-endophyte-plant saprotroph-soil saprotroph were most abundant in urban areas (Figure 4B). The PerMANOVA analyses also indicated that the composition of fungal functional guilds were significantly influenced by the urban-to-rural gradient ($p < 0.01$, Table S5).

3.4. Correlation of Characteristics of Soil Bacterial and Fungal Communities with Plant and Soil Variables

According to Spearman correlation analyses, DBH, TS, TR, SR, HR, pH, SOC, Ca^{2+}, Mg^{2+}, and SWC significantly influenced six bacterial functional groups ($p < 0.05$, Table S6). For fungal functional groups, the abundance of wood saprotroph was negatively correlated with DBH and pH, while positively with TS, TR, SR, SOC, and AvN. The abundance of ericoid mycorrhizal fungi was correlated with plant traits and soil properties except for AvK. The abundance of animal pathogen and animal pathogen-endophyte-plant saprotroph-soil saprotroph was positively correlated with Ca^{2+} and Mg^{2+}. The abundance of plant pathogen was positively and significantly associated with pH, but negatively with TS, TR, SOC, and AvN ($p < 0.05$, Table S6).

According to Spearman correlation analyses, the diversity of bacterial communities ($Chao1_B$, $Shannon_B$) was strongly correlated with almost all plant and soil variables (Table 3). However, the fungal diversity was not influenced by plant and soil variables (Table 3).

Table 3. Spearman correlations of bacterial (B) and fungal (F) diversity with plant traits and soil properties.

Variables	$Chao1_B$	$Shannon_B$	$Chao1_F$	$Shannon_F$
DBH (cm)	0.63 ***	0.69 ***	0.20	−0.13
TS	−0.55 **	−0.67 ***	−0.29	−0.01
TR	−0.67 ***	−0.77 ***	−0.23	0.00
SR	−0.69 ***	−0.78 ***	−0.08	0.22
HR	0.43 *	0.48 *	0.02	−0.24
pH	0.78 ***	0.79 ***	0.26	−0.04
SOC ($g \cdot kg^{-1}$)	−0.71 ***	−0.82 ***	−0.22	−0.03
AvN ($mg \cdot kg^{-1}$)	−0.62 **	−0.68 **	−0.19	0.04
AvP ($mg \cdot kg^{-1}$)	0.38	0.45 *	0.29	−0.03
AcK ($mg \cdot kg^{-1}$)	0.34	0.24	0.29	0.14
Ca^{2+} ($mg \cdot kg^{-1}$)	0.74 ***	0.71 ***	0.28	0.04
Mg^{2+} ($mg \cdot kg^{-1}$)	0.65 ***	0.59 **	0.38	0.21
SWC ($g \cdot kg^{-1}$)	−0.60 **	−0.69 ***	−0.09	0.01

Abbreviations: SWC, soil water content; SOC, soil organic carbon; AvN, soil available nitrogen; AvK, Soil available potassium; AvP, soil available phosphorus; Ca^{2+}, soil exchangeable calcium; Mg^{2+}, soil exchangeable magnesium; DBH, diameter at breast height of trees; TS, the number of tree stems; TR, tree richness; SR, shrub richness; HR, herb richness. * $p < 0.05$; ** $p < 0.01$; *** $p < 0.001$.

The Redundancy analyses (RDA) and Spearman correlation analyses indicated that plant traits including TS, DBH, TR, SR, and HR significantly affected the bacterial composition. SR was the most important factor, while HR had the least effect (Figure 5B and Figure S2B, Tables S7, S8, and S11). Among soil properties, pH, SOC, Ca^{2+}, and Mg^{2+} were identified as the most important predictors of bacterial composition (Figure 5A and Figure S2A, Tables S7, S8, and S11). AvP did not influence the bacterial community significantly (Table S11). The changes in the abundance of Proteobacteria, Bacteroidetes, and WPS-2 were related to plant traits (SR, TR, TS, and DBH) and soil properties (pH, Ca^{2+}, Mg^{2+}, SOC, and SWC) (Figure S2A,B, Table S7). Moreover, the abundance of Acidibacter and Roseiarcus in Proteobacteria was positively associated with SWC, AvN, SOC, SR, TR, and TS, but

negatively correlated with pH, Ca^{2+}, Mg^{2+}, and DBH; however, the effect of the observed factors on the other three genera (Ellin6067, Haliangium, and MND1) belonging to Proteobacteria was opposite (Figure 5A,B, Table S8).

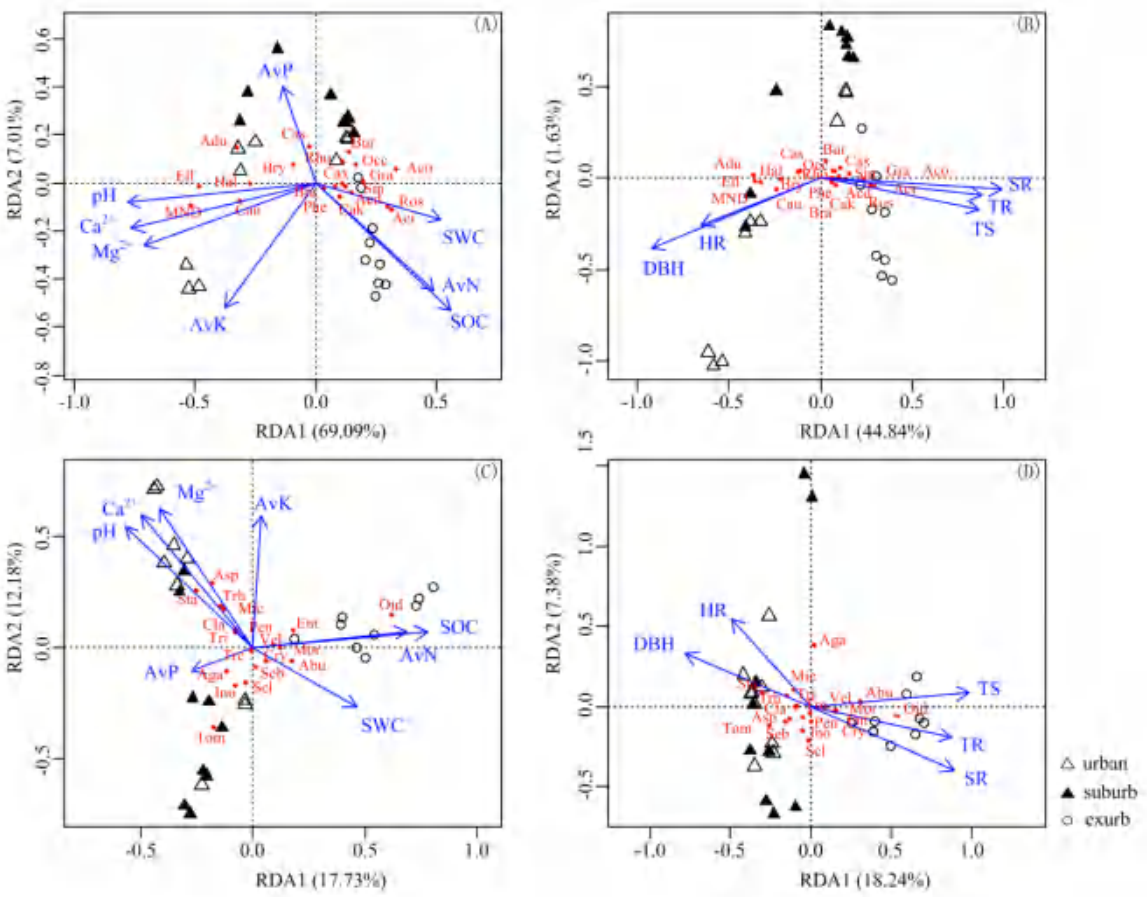

Figure 5. Redundancy analysis (RDA) plot showing influence of soil properties and plant traits on the distribution of main genera in soil bacterial (**A**,**B**) and fungal (**C**,**D**) communities. Abbreviations: SWC, soil water content; SOC, soil organic carbon; AvN, soil available nitrogen; AvK, Soil available potassium; AvP, soil available phosphorus; Ca^{2+}, soil exchangeable calcium; Mg^{2+}, soil exchangeable magnesium; DBH, diameter at breast height of trees; TS, the number of tree stems; TR, tree richness; SR, shrub richness; HR, herb richness; Aci, *Acidibacter*; Acd, *Acidicaldus*; Aco, *Acidothermus*; Adu, *ADurb.Bin063-1*; Bra, *Bradyrhizobium*; Bry, *Bryobacter*; Bur, *Burkholderia-Caballeronia-Paraburkholderia*; Cak, *Candidatus_Koribacter*; Cas, *Candidatus_Solibacter*; Cau, *Candidatus_Udaeobacter*; Cax, *Candidatus_Xiphinematobacter*; Ell, *Ellin6067*; Hal, *Haliangium*; MND, *MND1*; Rho, *Rhodoplanes*; Phe, *Phenylobacterium*; Ros, *Roseiarcus*; Sin, *Singulisphaera*; Occ, *Occallatibacter*; Gra, *Granulicella*; Abu, *Abundisporus*; Aga, *Agaricus*; Asp, *Aspergillus*; Cla, *Cladosporium*; Cry, *Cryptococcus*; Ent, *Entoloma*; Ino, *Inocybe*; Mic, *Micropsalliota*; Mor, *Mortierella*; Oid, *Oidiodendron*; Pen, *Penicillium*; Scl, *Scleroderma*; Seb, *Sebacina*; Sta, *Staphylotrichum*; Tom, *Tomentella*; Tri, *Trichocladium*; Trc, *Trichoderma*; Trh, *Trichosporon*; Vel, *Veluticeps*.

The plant and soil properties had no effect on fungal community at the phylum level ($p > 0.05$, Figure S2C,D). However, plant traits including TS, DBH, TR, SR, and HR significantly affected the fungal composition at the genus level. SR and TS influenced fungal composition the most at the genus level (Figure 5D, Tables S10 and S11). Among soil properties, SOC, pH, AvN, Ca^{2+}, and Mg^{2+} most significantly affected the fungal composition at the genus level (Figure 5C, Tables S10 and S11). Similarly, AvP did not influence the fungal community significantly (Table S11). In addition, only the abundance of Zygomycota was positively and significantly correlated with SOC, AvN, SWC, and SR,

but negatively with pH and DBH (Table S9). SOC, AvN, SWC, TS, TR, and SR positively influenced the aboundance of Oidiodendron, from Ascomycota, whereas pH, Ca^{2+}, Mg^{2+}, and DBH had negative influence. However, SOC, AvN, SWC, TS, TR, and SR negatively influenced the aboundance of Staphylotrichum in Ascomycota, pH, Ca^{2+}, Mg^{2+}, and DBH had positive influence (Figure 5C,D, Table S10).

Variation partitioning analysis (VPA) indicated that 76% of variation in bacterial community at the phylum level (Figure S3A), and 77% at the genus level were attributed to plant and soil variables (Figure 6A). Soil properties contributed to higher variation in bacterial community compared with plant traits (Figure 6 and Figure S3A). However, a large proportion of variation in fungal community could not be explained by plant and soil variables (Figure 6B and Figure S3B). More importantly, plant and soil variables did not significantly affect fungal community at the phylum level (Figure S3B), but significantly affected fungal community at the genus level (Figure 6B). The result showed that soil properties had a greater effect on bacterial than on fungal composition at genus level. By contrast, plant traits contributed more to fungal than to bacterial composition at genus level.

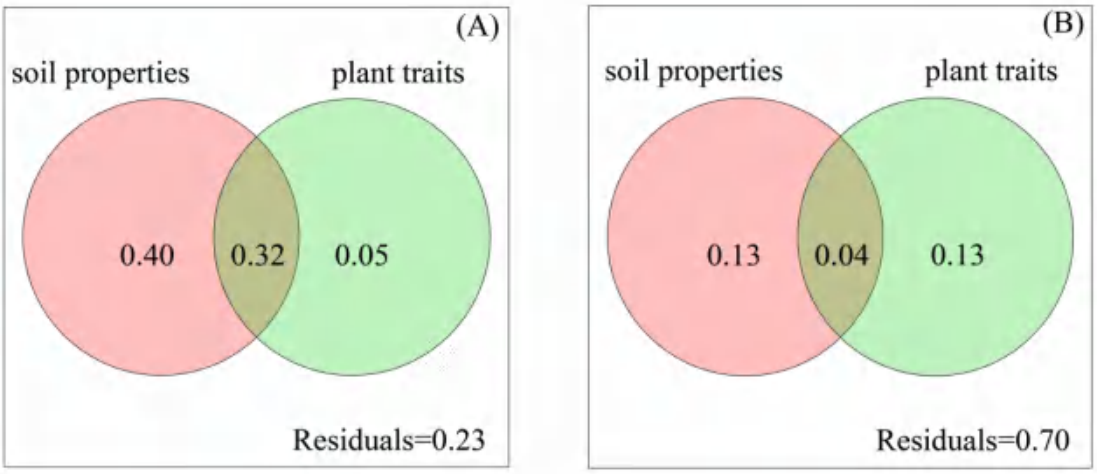

Figure 6. The proportions of variation at genus level in composition of soil bacterial community (**A**) and soil fungal community (**B**) composition explained by soil and plant variables.4. Discussion.

4. Discussion

4.1. The Composition and Diversity of Soil Microbial Community Varied Along the Urban-To-Rural Gradient

The composition and diversity of soil microbial communities are closely related to urbanization [38]. Our results confirmed that the urban-to-rural gradient affected the composition of soil microbial community, with varying degrees of influence on bacterial and fungal communities (Figure 2, Figure 3, and Figure S1, Tables S2 and S3). Along the urban-to-rural gradient, the relative abundance of the main bacterial phyla and genera differed significantly (Figure 2 and Figure S1, Tables S2). The relative abundance of main fungal genera differed significantly along the urban-to-rural gradient (Figure 2, Table S3). In addition, the PerMANOVA analyses showed that the composition of both bacterial and fungal OTUs had significant difference along the urban-to-rural gradient (Table S4). This result indicates that bacteria respond to urbanization via changes in relative abundance at the phylum and genus level, while fungi respond to urbanization via changes in relative abundance at the genus level. Further, we found that bacterial diversity decreased significantly along the urban-to-rural gradient, whereas the fungal diversity did not change significantly (Figure 3). Our results are similar to the studies of Barrico et al. [29]. With the intensity of urbanization, a few main bacteria OTUs are suppressed, while the survival of other OTUs were promoted in specific habitats. In addition, disturbances can increase environmental heterogeneity, creating more diverse niches for coexistence of other OTUs. Therefore, the diversity of bacteria is higher in urban areas with large disturbance.

Moreover, due to the high functional redundancy of bacteria community [39], higher bacterial diversity contributes to maintaining the ecosystems stability.

According to the bacterial and fungal functional groups analyses, our results indicated that the urban-to-rural gradient significantly impacted the composition of bacterial and fungal functional groups. The relative abundance of chemoheterotrophy, aerobic_chemoheterotrophy, cellulolysis, wood saprotroph, and ericoid mycorrhizal fungi was the highest in exurban areas. Chemoheterotrophic bacteria and aerobic_chemoheterotrophic bacteria utilize the soil organic carbon which is higher in exurban areas. Because the secondary forest is well preserved in exurban areas, there are more litter and coarse woody debris containing lignin, cellulose, and hemicellulose in exurban areas. Wood saprotroph can decompose lignin, cellulose, and hemicellulose; therefore, the relative abundance of wood saprotroph fungi was higher in exurban areas. In addition, the spearman correlation analyses showed wood saprotroph fungi was highly correlated with SR and TR, wich showed the highest value in exurban areas (Table S6). Ericoid mycorrhizal fungi, limited of Ericaceae [40], have a strong ability to take up phosphorus directly from organic matters [41]. Our study showed that ericoid mycorrhizal fungi were negatively correlated with available phosphorus (Table S6), and the available phosphorus was the lowest in exurbs (Table 1). Moreover, the Ericaceae plants are abundant in exurban areas, especially Rhododendron moulmainense. Therefore, the relative abundance of ericoid mycorrhizal fungi was the highest in exurban areas. Moreover, the higher relative abundance of plant and animal pathogens in urban areas indicates that urbanization can increase the potential risk of pathogen infection.

Our results indicated that the urban-to-rural gradient significantly affected the composition of soil bacterial communities at the level of phyla, genera, and OTUs and fungal communities at the level of genera and OTUs. The bacterial diversity was significantly influenced by the urban-to-rural gradient, while the fungal diversity was not.

4.2. Plant and Soil Variables Significantly Affect Soil Bacterial Diversity, but Not Fungal Diversity

Along the urban-to-rural gradient, differences in plant and soil variables explain changes in soil microbial communities [29]. Our results showed that soil bacterial diversity was the highest in urban areas and the lowest in exurban areas. However, fungal diversity did not vary significantly along the urban-to-rural gradient (Figure 3) because urbanization-induced changes in plant and soil variables (TR, SR, TS, DBH, pH, SOC, AvN, Ca^{2+}, Mg^{2+}, SWC) significantly affect bacterial diversity but not fungal diversity. Generally, soil microbes interact with plants, with synergistic as well as positive or negative feedback effects [42]. Therefore, we expect a significant correlation between microbial diversity and plant diversity. However, we found that only bacterial diversity was significantly related to TR, SR, TS, DBH, while fungal diversity was not correlated with plant traits. Hu et al. [20] also found that fungal diversity was weakly related to plant diversity in the forests of five climate regions in China; similarly, plant diversity did not determine fungal diversity at a global scale [43]. However, Hiiesalu et al. [44] found that plant diversity determined fungal diversity at a regional scale in temperate pine forests. This finding indicates that the relationship between fungal diversity and plant communities is very complex and depends on spatial scales.

4.3. Soil Properties Affect Bacterial Composition More Than Fungal Composition, While Plant Traits Affect Fungal Composition More Than Bacterial Composition

The changes in soil microbial communities along the urban-to-rural gradient and the relationship between soil microbial diversity and plant and soil variables are described above. However, the link between soil microbial composition and plant and soil variables remains unclear. In this study, we found that plant and soil variables explained large variation in the bacterial community composition, with 76% and 77% at the phylum and genus level, respectively (Figure 6A and Figure S3A). However, plant and soil variables did not significantly affect fungal community at the phylum level and explained 30% of variation in fungal community composition at the genus level (Figure 6B and Figure S3B).

Both RDA and VPA showed that explanatory variables contributed to significant variation in fungal composition at the genus level (Figure 5C,D and Figure 6B). Studies have shown that fungal community composition is mainly affected by climatic factors (rainfall and temperature) [18]. The heat island effect caused by urbanization raises the urban temperature significantly higher than that of suburban and exurban areas [2]. Therefore, temperature may be an important factor affecting the composition of fungal community in urban forest soils.

We found that TR and SR had a greater impact on soil bacterial and fungal composition, whereas HR had less impact (Tables S7–S10). Therefore, woody plants had a stronger effect than herbs on soil microbial community. The study of Hu et al. [20] reported similar results. We also found that the effect of plant diversity on soil fungal composition was stronger than on bacterial composition at genus level (Figure 6). Fungi are the major organisms that can decompose woody litter containing lignin, which accounts for 60–75% of woody litter affected by plant diversity [45]. Moreover, mycorrhizal fungi develop a symbiosis with plants [46]. Therefore, plant diversity explained more variations in fungal composition (13% of variation at genus level, Figure 6B) than in bacterial composition (5% of variation at genus level, Figure 6A). However, only a small proportion of variation in fungal composition was explained by plant diversity. Perhaps plant composition greatly influences fungal composition [17,20].

Moreover, soil pH and SOC largely affect soil bacterial community composition. Soil pH, SOC, and AvN were the important factors influencing soil fungal community composition (Table S11), which was similar to the results of other studies [21,23]. Notably, we found strong effects of Ca^{2+} and Mg^{2+} on soil bacterial and fungal composition (Table S11). Barrico et al. [29] also showed that Mg^{2+} was an important factor affecting the fungi community. Our research sites were located in urban parks and subjected to human disturbance, such as artificial fertilization. Since calcium and magnesium are essential trace elements in plants, $MgSO_4$ is often used by gardeners for the management of garden plants, releasing large amounts of magnesium within a short time [47]. Treatment of ornamental plants in urban parks with artificial fertilizers raises the soil content of magnesium and calcium. Soil microbes facilitate the absorption of trace elements by plants. Therefore, in urban forests, due to human disturbance (fertilizers, etc.), the content of soil Ca^{2+} and Mg^{2+} is changed, resulting in a strong correlation between soil microbial community and levels of Ca^{2+} and Mg^{2+}. Overall, these results support the hypothesis that plant and soil variables significantly affected the composition of soil bacterial and fungal composition. The influence of trees and shrubs on the composition of soil microbial community was larger than that of herbs. Soil properties exert larger effect on bacterial than on fungal composition at genus level, while plant variables had larger effect on fungal than on bacterial composition at genus level.

5. Conclusions

The results demonstrated that urbanization affected the composition and diversity of soil bacteria and fungi. The composition of soil bacterial communities at the level of phyla, genera, and OTUs and fungal communities at the level of genera and OTUs significantly varied along the urban-to-rural gradient. The bacterial diversity decreased significantly along the urban-to-rural gradient. However, fungal diversity did not significantly differ along the urban-to-rural gradient. Moreover, the composition of both soil bacterial and fungal communities varied in response to plant and soil variables. Soil properties had a greater effect on bacterial than on fungal composition at genus level. By contrast, plant traits contributed more to fungal than to bacterial composition at genus level. Trees and shrubs had a higher impact than herbs on the microbial community composition. Among soil properties, in addition to pH, SOC, and AvN, the changes in soil Ca^{2+} and Mg^{2+} caused by urbanization had a significant impact on soil bacterial and fungal communities.

Supplementary Materials: The following are available online at http://www.mdpi.com/1999-4907/10/9/797/s1, Figure S1: Relative abundance of bacterial phyla (A) and fungal phyla (B) along the urban-to-rural gradient at the Dongguan city, southern China, Figure S2: RDA plot showing influence of soil properties and plant traits on the distribution of main phyla in soil bacterial (A and B) and fungal (C and D) communities, Figure S3: The

proportions of variation at phylum level in composition of soil bacterial community (A) and soil fungal community (B) composition explained by soil and plant variables, Table S1: Abbreviations and corresponding full names of plant traits and soil properties in this paper, Table S2: Relative abundance of bacterial composition along the urban-to-rural gradient at phylum and genus level, Table S3: Relative abundance of fungal composition along the urban-to-rural gradient at phylum and genus level, Table S4. The PerMANOVA analyses of bacterial and fungal OTUs along the urban-to-rural gradient, Table S5: The PerMANOVA analyses of bacterial and fungal functional groups along the urban-to-rural gradient; Table S6. Spearman correlation of bacterial and fungal functional groups with plant and soil variables, Table S7: Spearman correlation of bacterial composition with plant and soil variables at phylum level, Table S8: Spearman correlation of bacterial composition with plant and soil variables at genus level, Table S9: Spearman correlation of fungal composition with plant and soil properties at phylum level, Table S10: Spearman correlation of fungal composition with plant traits and soil properties at genus level, Table S11: The results of RDA monte carlo tests of soil bacterial and fungal community compositions.

Author Contributions: L.Z. and X.T. conceived and designed the experiments. X.T. and L.K. performed field surveys and collected the data. X.T. analyzed the data, prepared the figures and tables, and wrote the first draft. Z.S., X.L. and L.Z. reviewed and edited the manuscript.

Funding: This research was funded by the Guangdong Provincial Special Fund for Forestry Development and Protection (Forestry Science and Technology Innovation Project 2017KJCX037/2019KJCX007), Guangdong Natural Science Foundation (2015A030313403) and State Forestry Administration (2130211).

Acknowledgments: We thank Linying Cai, Xingyuan Zhang for their assistance with plot establishment and field data collection, Qifeng Mo for his comments and discussions on the early version of the manuscript.

Conflicts of Interest: The authors declare no conflict of interest.

References

1. Department of Economic and Social Affairs. *2018 Revision of World Urbanization Prospects*; United Nations: New York, NY, USA, 2018.
2. Li, X.M.; Zhou, W.Q. Optimizing urban greenspace spatial pattern to mitigate urban heat island effects: Extending understanding from local to the city scale. *Urban For. Urban Green.* **2019**, *41*, 255–263. [CrossRef]
3. Yazdi, S.K.; Dariani, A.G. CO_2 emissions, urbanisation and economic growth: Evidence from Asian countries. *Econ. Res.-Ekon. Istraz.* **2019**, *32*, 510–530. [CrossRef]
4. Cui, Y.Z.; Zhang, W.S.; Bao, H.J.; Wang, C.; Cai, W.J.; Yu, J.; Streets, D.G. Spatiotemporal dynamics of nitrogen dioxide pollution and urban development: Satellite observations over China, 2005–2016. *Resour. Conserv. Recy.* **2019**, *142*, 59–68. [CrossRef]
5. Lopez, B.E.; Urban, D.; White, P.S. Testing the effects of four urbanization filters on forest plant taxonomic, functional, and phylogenetic diversity. *Ecol. Appl.* **2018**, *28*, 2197–2205. [CrossRef] [PubMed]
6. Ning, Z.H.; Chambers, R.; Abdollahi, K. Modeling air pollutant removal, carbon storage, and CO_2 sequestration potential of urban forests in Scotlandville, Louisiana, USA. *iForest* **2016**, *9*, 860–867. [CrossRef]
7. Veresoglou, S.D.; Halley, J.M.; Rillig, M.C. Extinction risk of soil biota. *Nat. Commun.* **2015**, *6*. [CrossRef]
8. Klimek, B.; Chodak, M.; Jazwa, M.; Niklinska, M. Functional diversity of soil microbial communities in boreal and temperate Scots pine forests. *Eur. J. For. Res.* **2016**, *135*, 731–742. [CrossRef]
9. Wardle, D.A.; Bardgett, R.D.; Klironomos, J.N.; Setala, H.; van der Putten, W.H.; Wall, D.H. Ecological linkages between aboveground and belowground biota. *Science* **2004**, *304*, 1629–1633. [CrossRef]
10. Li, J.; Li, Z.A.; Wang, F.M.; Zou, B.; Chen, Y.; Zhao, J.; Mo, Q.F.; Li, Y.W.; Li, X.B.; Xia, H.P. Effects of nitrogen and phosphorus addition on soil microbial community in a secondary tropical forest of China. *Biol. Fert. Soils* **2015**, *51*, 207–215. [CrossRef]
11. Deng, Q.; Cheng, X.L.; Hui, D.F.; Zhang, Q.; Li, M.; Zhang, Q.F. Soil microbial community and its interaction with soil carbon and nitrogen dynamics following afforestation in central China. *Sci. Total Environ.* **2016**, *541*, 230–237. [CrossRef]
12. Strecker, T.; Mace, O.G.; Scheu, S.; Eisenhauer, N. Functional composition of plant communities determines the spatial and temporal stability of soil microbial properties in a long-term plant diversity experiment. *Oikos* **2016**, *125*, 1743–1754. [CrossRef]
13. Thakur, M.P.; Milcu, A.; Manning, P.; Niklaus, P.A.; Roscher, C.; Power, S.; Reich, P.B.; Scheu, S.; Tilman, D.; Ai, F.X.; et al. Plant diversity drives soil microbial biomass carbon in grasslands irrespective of global environmental change factors. *Glob. Chang. Biol.* **2015**, *21*, 4076–4085. [CrossRef]

14. Thompson, G.L.; Kao-Kniffin, J. Diversity Enhances NPP, N Retention, and Soil Microbial Diversity in Experimental Urban Grassland Assemblages. *PLoS ONE* **2016**, *11*, e0155986. [CrossRef]
15. Lange, M.; Eisenhauer, N.; Sierra, C.A.; Bessler, H.; Engels, C.; Griffiths, R.I.; Mellado-Vazquez, P.G.; Malik, A.A.; Roy, J.; Scheu, S.; et al. Plant diversity increases soil microbial activity and soil carbon storage. *Nat. Commun.* **2015**, *6*. [CrossRef]
16. Mellado-Vazquez, P.G.; Lange, M.; Bachmann, D.; Gockele, A.; Karlowsky, S.; Milcu, A.; Piel, C.; Roscher, C.; Roy, J.; Gleixner, G. Plant diversity generates enhanced soil microbial access to recently photosynthesized carbon in the rhizosphere. *Soil Biol. Biochem.* **2016**, *94*, 122–132. [CrossRef]
17. Prober, S.M.; Leff, J.W.; Bates, S.T.; Borer, E.T.; Firn, J.; Harpole, W.S.; Lind, E.M.; Seabloom, E.W.; Adler, P.B.; Bakker, J.D.; et al. Plant diversity predicts beta but not alpha diversity of soil microbes across grasslands worldwide. *Ecol. Lett.* **2015**, *18*, 85–95. [CrossRef]
18. Ren, C.J.; Zhang, W.; Zhong, Z.K.; Han, X.H.; Yang, G.H.; Feng, Y.Z.; Ren, G.X. Differential responses of soil microbial biomass, diversity, and compositions to altitudinal gradients depend on plant and soil characteristics. *Sci. Total Environ.* **2018**, *610*, 750–758. [CrossRef]
19. Zhang, Y.G.; Cong, J.; Lu, H.; Li, G.L.; Xue, Y.D.; Deng, Y.; Li, H.; Zhou, J.Z.; Li, D.Q. Soil bacterial diversity patterns and drivers along an elevational gradient on Shennongjia Mountain, China. *Microb. Biotechnol.* **2015**, *8*, 739–746. [CrossRef]
20. Hu, Y.J.; Veresoglou, S.D.; Tedersoo, L.; Xu, T.L.; Ge, T.D.; Liu, L.; Chen, Y.L.; Hao, Z.P.; Su, Y.R.; Rillig, M.C.; et al. Contrasting latitudinal diversity and co-occurrence patterns of soil fungi and plants in forest ecosystems. *Soil Biol. Biochem.* **2019**, *131*, 100–110. [CrossRef]
21. Brant, J.B.; Myrold, D.D.; Sulzman, E.W. Root controls on soil microbial community structure in forest soils. *Oecologia* **2006**, *148*, 650–659. [CrossRef]
22. Shen, C.; Xiong, J.; Zhang, H.; Feng, Y.; Lin, X.; Li, X.; Liang, W.; Chu, H. Soil pH drives the spatial distribution of bacterial communities along elevation on Changbai Mountain. *Soil Biol. Biochem.* **2013**, *57*, 204–211. [CrossRef]
23. Zhou, X.Q.; Guo, Z.Y.; Chen, C.R.; Jia, Z.J. Soil microbial community structure and diversity are largely influenced by soil pH and nutrient quality in 78-year-old tree plantations. *Biogeosciences* **2017**, *14*, 2101–2111. [CrossRef]
24. Wang, C.; Liu, D.W.; Bai, E. Decreasing soil microbial diversity is associated with decreasing microbial biomass under nitrogen addition. *Soil Biol. Biochem.* **2018**, *120*, 126–133. [CrossRef]
25. Apeagyei, E.; Bank, M.S.; Spengler, J.D. Distribution of heavy metals in road dust along an urban-rural gradient in Massachusetts. *Atmos. Environ.* **2011**, *45*, 2310–2323. [CrossRef]
26. Fang, S.B.; Qiao, Y.J.; Yin, C.S.; Yang, X.Y.; Li, N. Characterizing the physical and demographic variables associated with heavy metal distribution along urban-rural gradient. *Environ. Monit. Assess.* **2015**, *187*, 570. [CrossRef]
27. Vakhlamova, T.; Rusterholz, H.P.; Kanibolotskaya, Y.; Baur, B. Changes in plant diversity along an urban-rural gradient in an expanding city in Kazakhstan, Western Siberia. *Landsc. Urban Plan.* **2014**, *132*, 111–120. [CrossRef]
28. Huang, J.; Liu, J.X.; Zhang, W.; Cai, X.A.; Liu, L.; Zheng, M.H.; Mo, J.M. Effects of urbanization on plant phosphorus availability in broadleaf and needleleaf subtropical forests. *Sci. Total Environ.* **2019**, *684*, 50–57. [CrossRef]
29. Barrico, L.; Castro, H.; Coutinho, A.P.; Goncalves, M.T.; Freitas, H.; Castro, P. Plant and microbial biodiversity in urban forests and public gardens: Insights for cities' sustainable development. *Urban For. Urban Green.* **2018**, *29*, 19–27. [CrossRef]
30. Kivlin, S.N.; Hawkes, C.V. Tree species, spatial heterogeneity, and seasonality drive soil fungal abundance, richness, and composition in Neotropical rainforests. *Environ. Microbiol.* **2016**, *18*, 4662–4673. [CrossRef]
31. Nguyen, N.H.; Williams, L.J.; Vincent, J.B.; Stefanski, A.; Cavender-Bares, J.; Messier, C.; Paquette, A.; Gravel, D.; Reich, P.B.; Kennedy, P.G. Ectomycorrhizal fungal diversity and saprotrophic fungal diversity are linked to different tree community attributes in a field-based tree experiment. *Mol. Ecol.* **2016**, *25*, 4032–4046. [CrossRef]

32. Ito, N.; Iwanaga, H.; Charles, S.; Diway, B.; Sabang, J.; Chong, L.; Nanami, S.; Kamiya, K.; Lum, S.; Siregar, U.J.; et al. Geographical variation in soil bacterial community structure in tropical forests in Southeast Asia and temperate forests in Japan based on pyrosequencing analysis of 16S rRNA. *Genes Genet. Syst.* **2017**, *92*, 1–20. [CrossRef]
33. Sun, J.; Li, Y.P.; Gao, P.P.; Suo, C.; Xia, B.C. Analyzing urban ecosystem variation in the City of Dongguan: A stepwise cluster modeling approach. *Environ. Res.* **2018**, *166*, 276–289. [CrossRef]
34. Lu, R.Q. *Methods of Soil Agricultural Chemical Analysis*; China Agricultural Science and Technology Press: Beijing, China, 1999.
35. Nguyen, N.H.; Song, Z.; Bates, S.T.; Branco, S.; Tedersoo, L.; Menke, J.; Schilling, J.S.; Kennedy, P.G. FUNGuild: An open annotation tool for parsing fungal community datasets by ecological guild. *Fungal. Ecol.* **2016**, *20*, 241–248. [CrossRef]
36. Louca, S.; Parfrey, L.W.; Doebeli, M. Decoupling function and taxonomy in the global ocean microbiome. *Science* **2016**, *353*, 1272–1277. [CrossRef]
37. Peres-Neto, P.R.; Legendre, P.; Dray, S.; Borcard, D. Variation partitioning of species data matrices: Estimation and comparison of fractions. *Ecology* **2006**, *87*, 2614–2625. [CrossRef]
38. Yan, B.; Li, J.S.; Xiao, N.W.; Qi, Y.; Fu, G.; Liu, G.H.; Qiao, M.P. Urban-development-induced Changes in the Diversity and Composition of the Soil Bacterial Community in Beijing. *Sci. Rep. UK* **2016**, *6*. [CrossRef]
39. Comte, J.; del Giorgio, P.A. Linking the patterns of change in composition and function in bacterioplankton successions along environmental gradients. *Ecology* **2010**, *91*, 1466–1476. [CrossRef]
40. Brundrett, M.C.; Tedersoo, L. Evolutionary history of mycorrhizal symbioses and global host plant diversity. *New Phytol.* **2018**, *220*, 1108–1115. [CrossRef]
41. Peay, K.G. The Mutualistic Niche: Mycorrhizal Symbiosis and Community Dynamics. *Annu. Rev. Ecol. Evol. Syst.* **2016**, *47*, 143–164. [CrossRef]
42. Sinha, S.; Masto, R.E.; Ram, L.C.; Selvi, V.A.; Srivastava, N.K.; Tripathi, R.C.; George, J. Rhizosphere soil microbial index of tree species in a coal mining ecosystem. *Soil. Biol. Biochem.* **2009**, *41*, 1824–1832. [CrossRef]
43. Tedersoo, L.; Bahram, M.; Polme, S.; Koljalg, U.; Yorou, N.S.; Wijesundera, R.; Ruiz, L.V.; Vasco-Palacios, A.M.; Thu, P.Q.; Suija, A.; et al. Global diversity and geography of soil fungi. *Science* **2014**, *346*, 125688. [CrossRef]
44. Hiiesalu, I.; Bahram, M.; Tedersoo, L. Plant species richness and productivity determine the diversity of soil fungal guilds in temperate coniferous forest and bog habitats. *Mol. Ecol.* **2017**, *26*, 4846–4858. [CrossRef]
45. Bardelli, T.; Ascher-Jenull, J.; Stocker, E.B.; Fornasier, F.; Arfaioli, P.; Fravolini, G.; Medeiros, L.R.A.; Egli, M.; Pietramellara, G.; Insam, H.; et al. Impact of slope exposure on chemical and microbiological properties of Norway spruce deadwood and underlying soil during early stages of decomposition in the Italian Alps. *Catena* **2018**, *167*, 100–115. [CrossRef]
46. Rineau, F.; Shah, F.; Smits, M.M.; Persson, P.; Johansson, T.; Carleer, R.; Troein, C.; Tunlid, A. Carbon availability triggers the decomposition of plant litter and assimilation of nitrogen by an ectomycorrhizal fungus. *ISME J.* **2013**, *7*, 2010–2022. [CrossRef]
47. Härdter, R.; Rex, M.; Orlovius, K. Effects of different Mg fertilizer sources on the magnesium availability in soils. *Nutr. Cycl. Agroecosyst.* **2004**, *70*, 249–259. [CrossRef]

Volume 38, Number 11 November 2019

ISSN 1000-4890
CODEN SZAZEC

生态学杂志

2019年11月
第38卷 第11期

Chinese Journal of Ecology

中国生态学学会
中国科学院沈阳应用生态研究所 主办

科学出版社出版

生态学杂志

SHENGTAIXUE ZAZHI

2019 年 11 月　　第 38 卷　第 11 期

目　次

本期执行编辑　张　敏

生态学杂志 Chinese Journal of Ecology 2019,38(11):3306-3312 DOI: 10.13292/j.1000-4890.201911.017

城市森林土壤微生物群落结构的季节变化

谭雪莲 阚 蕾 张 璐* 郑嘉仪
(华南农业大学林学与风景园林学院,广州 510642)

摘 要 土壤微生物在森林生态系统中扮演重要的角色,是森林生态系统中物质循环的驱动因素,但目前对于城市森林土壤微生物群落的季节变化及其影响因素研究较少。因此,本研究以东莞城市森林为对象,采用高通量测序方法研究城市森林土壤微生物的季节变化规律及其影响因素。结果表明:土壤微生物群落结构和多样性有显著的季节变化,湿季土壤微生物总数量显著低于干季,但湿季土壤微生物 Chao1 指数和 Shannon 指数显著高于干季,湿季细菌和真菌的多样性和菌群结构更为丰富,其中细菌主要通过数量改变适应季节的变化,真菌主要通过数量以及物种组成的改变适应季节变化。土壤有效硼是细菌群落结构的主要影响因子,pH 是真菌群落结构的主要影响因子,土壤中交换性钙和交换性镁亦是影响细菌和真菌群落的重要因子。

关键词 高通量测序; 城市森林; 真菌; 细菌; 干季; 湿季

Seasonal dynamics of soil microbial community structure in urban forest. TAN Xue-lian, KAN Lei, ZHANG Lu*, ZHENG Jia-yi (*College of Forestry and Landscape Architecture, South China Agricultural University, Guangzhou* 510642, *China*).

Abstract: Soil microbes play an important role in forest ecosystem and are the driving factor of material cycling. Few studies have been conducted on the seasonal changes and the influencing factors of soil microbial communities in urban forests. Using high-throughput sequencing methods, we investigated the seasonal changes of soil microbial community in the urban forest of Dongguan and analyzed their influencing factors. The results showed that the structure and diversity of soil microbial community significantly differed among seasons. The total abundance of soil microbes was significantly lower in wet season than in dry season. In contrast, both Chao1 index and Shannon index showed the opposite seasonal patterns compared with that of microbial abundance, with higher diversity and structure in the bacterial and fungal community in wet season. In adaptation to the seasonal change, bacteria mainly adjusted their total abundance, while fungi changed their total abundance and species composition. Soil available boron was the major factor influencing bacterial community structure, while soil pH was the major factor influencing fungal community structure. Exchangeable calcium and exchangeable magnesium in soil were the important factors influencing both bacterial and fungal communities.

Key words: high-throughput sequencing; urban forest; fungi; bacteria; dry season; wet season.

随着经济的发展,城市化和工业化加快。城市基础设施、工厂建设导致土地利用方式改变以及化石燃料燃烧的增加,从而带来了诸如城市热岛效应、土地退化、生物多样性降低等一系列生态环境问题(杨沅志等,2016; Lopez *et al.*,2018)。城市森林对城市可持续发展具有积极作用,能够汇碳释氧、调节城市小气候、减缓热岛效应等城市发展所带来的负面生态环境问题,给城市带来诸多生态、经济和社会效益(Ning *et al.*,2016; 姚鑫等,2017; 张英杰等,2018)。因此,城市森林在城市发展过程中具有十分重要的作用。

土壤微生物作为森林生态系统中的重要组成部分,参与了许多重要的生态过程。土壤微生物能够

广东省林业科技创新项目(2017KJCX037,2019KJCX007)和广东省自然科学基金自由申请项目(2015A030313403)资助。
收稿日期:2019-02-22 接受日期:2019-08-1
* 通讯作者 E-mail: zhanglu@scau.edu.cn

分解凋落物(Wardle,2004; Klimek *et al.*,2016),催化土壤碳和营养元素周转(Li *et al.*,2015; 丁国昌等,2017),是生物地球化学过程的重要驱动因素(Veresoglou *et al.*,2015)。土壤微生物对环境变化非常敏感,受多种环境因素影响。例如,土壤微生物对水分条件以及温度的变化非常敏感,水分的增加、持续的增温以及干旱时间的提前,都会使土壤微生物量碳和氮增加(Wu *et al.*,2015; 王宁等,2015; 高艳娜等,2018)。季节性降水变化会显著增加土壤中稀有细菌和土壤中的优势真菌(He *et al.*,2017; Zhao *et al.*,2017)。此外,土壤微生物与土壤有机碳、土壤 pH、全氮、土壤有机质等具有显著正相关性(刘旻霞等,2018; 罗蓉等,2018; 涂志华等,2018; 王璐璐等,2018)。然而,吴华清等(2016)研究发现,土壤微生物总磷脂脂肪酸(PLFAs)量与土壤 pH 呈极显著负相关性。水分、温度以及土壤的理化性状等均会随季节变化而改变,导致土壤微生物群落结构和多样性表现出明显的季节动态(王薪琪等,2017)。有研究表明,季节会改变氮沉降对土壤微生物群落结构的影响,导致土壤微生物对氮沉降有不同的响应(Yan *et al.*,2017; 郑裕雄等,2018);干季时,70 kg·hm^{-2}·a^{-1}的氮沉降对微生物的促进作用最显著,而湿季时 105 kg·hm^{-2}·a^{-1}的氮水平对微生物的促进作用最显著(倪壮等,2018)。但有研究发现,季节并不是影响土壤微生物群落结构的主要因子(Siles *et al.*,2016)。可见,季节变化对土壤微生物的群落结构和多样性的影响尚存在争议,且由季节变化而引起的多种环境因子变化对土壤微生物群落结构和多样性影响的相对重要性也未明确,有待进一步加强研究。

珠江三角洲城市群是我国三大城市群之一,人口众多,经济发展迅速。东莞市是珠江三角洲城市群的重要城市,有国家森林城市之称。然而,目前有关东莞城市森林的研究较少,相关研究主要报道了东莞城市森林碳储量(刘刚等,2010)和土壤性状(欧芷阳等,2013),而针对东莞城市森林土壤微生物群落结构和多样性的研究较少见报道,尤其是土壤微生物的干湿季节动态特征。因此,本研究以东莞城市森林为研究对象,以期探讨城市森林土壤微生物的季节变化规律及其影响因素,为保护和提高土壤微生物多样性,维持城市森林生态系统物质正常循环提供科学依据,同时为珠江三角洲国家森林城市群建设提供理论参考。

1 研究地区与研究方法

1.1 研究区概况

东莞市(113°31′E—114°15′E,22°39′N—23°09′N)位于华南地区,属于亚热带季风气候,温暖多雨。年平均气温 22.1 ℃,最热月平均气温 28.2 ℃(7 月),最冷月平均气温 13.4 ℃(1 月)。年平均降水量 1796 mm,每年 4—9 月为雨季,降雨量约占全年的 80%(欧芷阳等,2013)。地貌以丘陵、平原为主,土壤类型为赤红壤,土壤质地为沙土类和壤土类,自然土层较深厚。地带性森林植被类型为常绿阔叶林(刘刚等,2010)。

1.2 研究方法

1.2.1 样方设置与样品采集 为使取样更具代表性,分别在东莞市市区旗峰公园、近郊同沙生态公园和远郊大岭山森林公园选择地带性常绿阔叶林群落设置调查样地。旗峰公园(113°45′50″E—113°46′26″E,23°00′50″N—23°01′04″N)位于东莞市中心,受干扰强度大,植被类型以人工林为主,样地以阴香(*Cinnamomum burmanni*)和榕树(*Ficus microcarpa*)为优势种。同沙生态公园(113°45′54″E—113°46′45″E,22°57′45″N—23°58′25″N)位于东莞市近郊,植被类型主要是人工林和天然次生林,现存的亚热带常绿阔叶林主要是人工种植,而天然次生林则主要是由常绿灌木和小乔木组成,尾叶桉(*Eucalyptus urophylla*)和山杜英(*Elaeocarpus sylvestris*)占优势。大岭山森林公园(113°45′56″E—113°46′46″E,22°52′28″N—22°53′09″N)则位于东莞市远郊,植被类型主要包括次生林和人工林,由于长期的有效保护,次生林保存较好,鹅掌柴(*Schefflera octophylla*)和山油柑(*Acronychia pedunculata*)为其优势种。

每个样地分别设置 9 个 20 m×20 m 的样方(间隔 20 m),分别于 2018 年干季(1 月份)和湿季(9 月份)在每个样方采集 0~10 cm 的表层土混合样(S 形取样,6 个取样点),共获得 54 个混合土样。每份混合土样又分为 2 份,分别用于化学性状(每份不少于 500 g)、细菌和真菌多样性(每份不少于 6 g,冷藏带回实验室)测定。此外,用环刀取样用于测定土壤自然含水量。

1.2.2 土壤理化性质测定 土壤基本理化性状指标包括 pH 值、有机质(SOM)、碱解氮(AvN)、有效磷(AvP)、速效钾(AcK)、交换性钙(EvCa)、交换性镁(EvMg)、有效铜(AvCu)、有效锌(AvZn)、有效铁

(AvFe)、有效锰(AvMn)、有效硼(AvB)、土壤自然含水量(SW),测定方法参照《土壤农业化学分析方法》(鲁如坤,1999)。

1.2.3 土壤微生物群落多样性测定 使用 MOBIO PowerSoil© DNA Isolation Kit 试剂盒提取土壤样品 DNA,提取后的 DNA 用 0.8%的琼脂糖凝胶电泳检测其完整度、纯度和浓度。细菌和真菌分别选择 16S 的 V4 高变区和 ITS 的 ITS2 区进行 PCR 扩增,并基于 Illumina 平台进行测序,得到完整的 16S rDNA 基因 V4 区目的片段序列和 ITS 基因 ITS2 区目的片段序列。然后将高通量测序获得的 16S rDNA 和 ITS 基因序列按照 97%的序列相似性挑选 OTU,并对每个 OTU 的代表序列进行物种注释分类(使用 rdp 分类方法)。微生物多样性指数 Chao1 反应样品中群落的丰富度,仅考虑群落中物种的数量而不考虑每个物种的丰度,Shannon 指数则综合考虑物种的丰富度和均匀度,Chao1 指数和 Shannon 指数的计算公式如下:

$$Chao1 = S + \frac{n_1(n_1-1)}{2(n_2+1)} \quad (1)$$

$$Shannon = -\sum_{i=1}^{S} \frac{n_i}{N} \ln \frac{n_i}{N} \quad (2)$$

式中,S 为实际观测到的 OTU 数;n_1 为只含有一条序列的 OTU 数目;n_2 为含有两条序列的 OTU 数目,n_i 为含有 i 条序列的 OTU 数目;N 为所有的序列数。

1.3 数据分析

采用 Wilcox 非参数方差检验比较干湿季节土壤理化性状及土壤微生物多样性的差异。采用 PerManova 非参数多元方差分析比较干湿季细菌和真菌群落的组成差异。由于对细菌丰度排名前 30 的属的 DCA 排序第 1 轴长度小于 3,而真菌的 DCA 排序第 1 轴长度大于 4,因此分别对细菌和真菌采用 RDA、CCA 分析细菌和真菌群落多样性的影响因子。所有分析均在 R(3.4.4)软件中进行。

2 结果与分析

2.1 城市森林干湿季土壤理化性状

如表 1 所示,东莞城市森林土壤呈酸性。土壤 pH、有机质、速效钾、有效铁、有效硼的含量从干季到湿季表现为降低的趋势,而碱解氮、有效磷、交换性钙、交换性镁、有效铜、有效锰、土壤自然含水量的变化趋势则相反,表现为升高的趋势。进一步的 Wilcox 显著性检验结果表明,土壤自然含水量,有效硼在干湿季节间表现为极显著差异($P<0.001$),其他指标在干湿季均无显著差异。

2.2 城市森林干湿季土壤微生物群落结构和多样性

干季时细菌和真菌序列数显著高于湿季时的序列数,且不管干季还是湿季细菌序列数均高于真菌(表 2)。从门水平到属水平的注释分类结果发现,干季时细菌所检测出的门、纲、目、科、属以及 OTU 数均高于湿季,而真菌在干季时所检测出的各分类水平的个数低于湿季。从干季到湿季,细菌和真菌总的数量减少,且细菌的 OTU 数减少,但是真菌的 OTU 数增加了。

从干季到湿季,真菌属水平上菌群种类变化比细菌的主要菌群变化明显(图 1)。细菌在干季相对丰度大于 1%的有 10 属,湿季相对丰度大于 1%的有 12 属,干湿季共有属有 9 属。排名前 5 的属在干季和湿季间保持不变,其中 *Acidibacter* 在干季和湿季的相对丰度都是最大的,分别为干季 4.86%,湿季 4.46%,表明 *Acidibacter* 是土壤中的核心菌群。真菌在干季相对丰度大于1%的有14属,湿季相对丰度

表 1 干湿季土壤理化性状

Table 1 Physicochemical properties of soil in dry and wet seasons

土壤理化性状	干季	湿季
pH	4.79±0.13	4.75±0.17
土壤自然含水量 SW($g \cdot kg^{-1}$)	184.02±7.94 b	269.87±13.51 a
有机质 SOM($g \cdot kg^{-1}$)	21.96±1.78	21.21±2.10
碱解氮 AvN($mg \cdot kg^{-1}$)	103.71±6.75	111.40±8.50
有效磷 AvP($mg \cdot kg^{-1}$)	6.45±1.52	9.33±3.13
速效钾 AcK($mg \cdot kg^{-1}$)	66.52±2.88	56.76±3.98
交换性钙 EvCa($mg \cdot kg^{-1}$)	315.96±71.97	343.72±91.54
交换性镁 EvMg($mg \cdot kg^{-1}$)	18.60±2.76	22.27±3.51
有效铜 AvCu($mg \cdot kg^{-1}$)	1.17±0.10	1.32±0.09
有效锌 AvZn($mg \cdot kg^{-1}$)	3.05±0.23	3.05±0.21
有效铁 AvFe($mg \cdot kg^{-1}$)	96.23±7.80	91.29±6.16
有效锰 AvMn($mg \cdot kg^{-1}$)	7.84±0.99	7.95±1.13
有效硼 AvB($mg \cdot kg^{-1}$)	0.31±0.02 a	0.15±0.01 b

表中数值为平均值±标准差;表中数字后不同字母表示干湿季节间具有显著差异。

表 2 土壤微生物群落各分类单元的物种丰富度特征

Table 2 Species richness of community of soil microbes

微生物	季节	门	纲	目	科	属	OTU	序列数
细菌	干季	48	115	244	357	636	10307	1864402
	湿季	38	99	221	328	555	9821	716261
真菌	干季	6	32	112	256	644	4691	1256438
	湿季	8	36	121	274	686	5620	700446

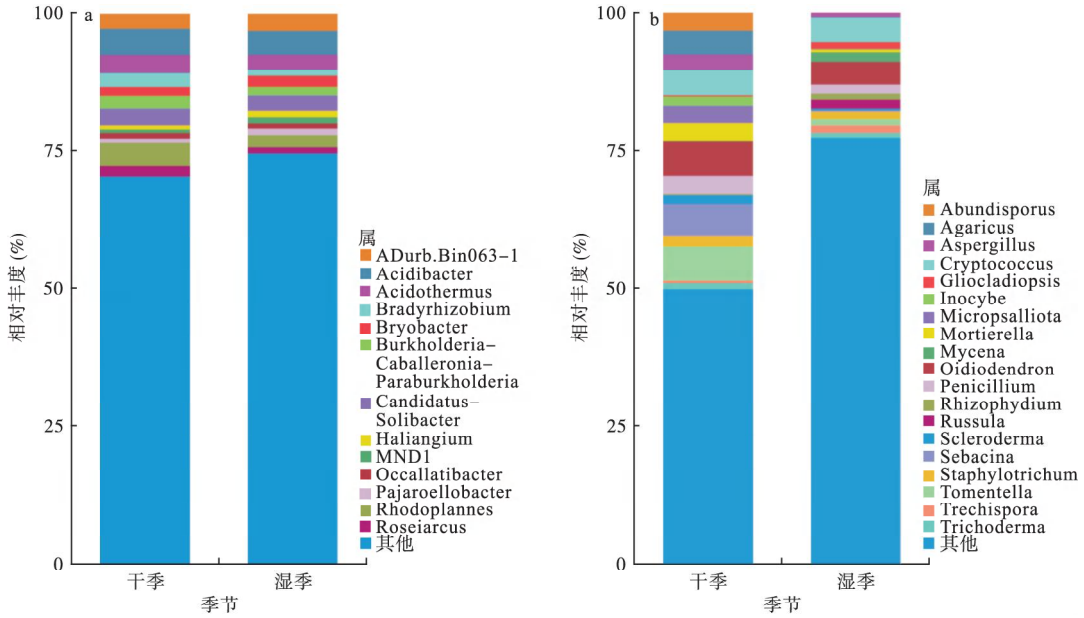

图 1 土壤细菌(a)和真菌(b)属水平相对丰度
Fig.1 Relative abundance of soil bacterial genera and fungal genera

大于 1%的有 11 属,干湿季共有 6 属。其中 *Oidiodendron*(树粉孢属)、*Tomentella*(革菌属)、*Cryptococcus*(隐球菌属)在干季的相对丰度较大,分别为 6.31%、6.19%、4.54%,而在湿季时,*Cryptococcus* 相对丰度基本不变(4.57%),但 *Oidiodendron* 和 *Tomentella* 分别降低了 33.71%和 82.87%,表明 *Cryptococcus* 适应干湿季节的变化,而 *Oidiodendron* 和 *Tomentella* 对干湿季节的变化比较敏感。湿季的细菌和真菌 Chao1 和 Shannon 多样性指数均显著高于干季($P<0.001$,图 2)。

2.3 土壤微生物群落结构的影响因子

土壤理化性状对细菌群落物种分布总的解释

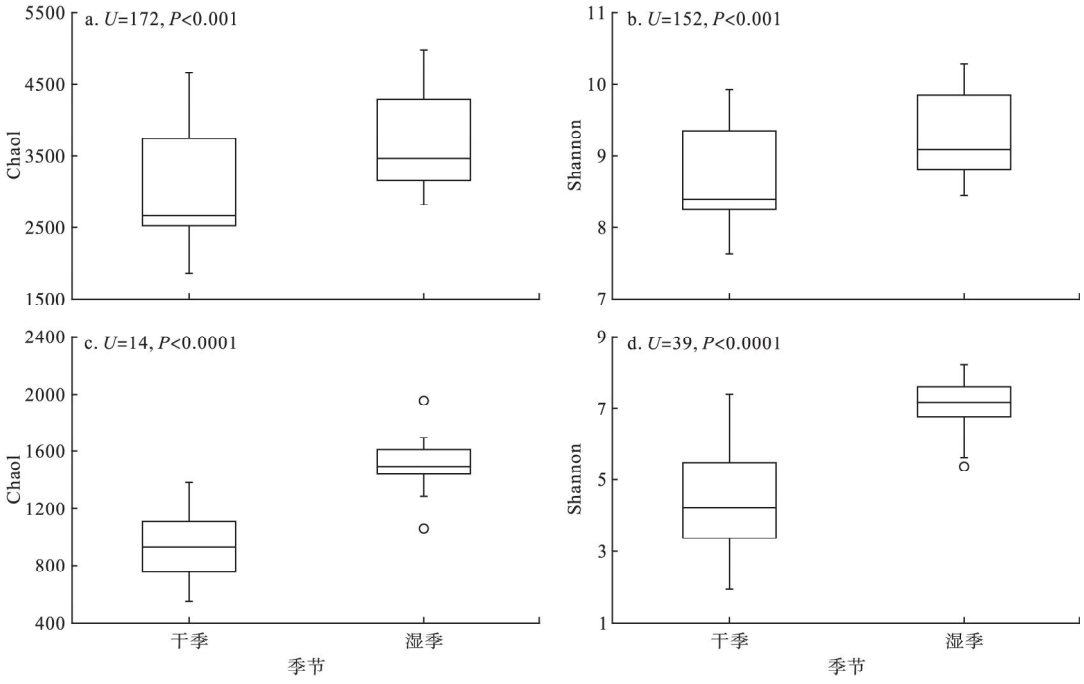

图 2 土壤微生物多样性指数干湿季差异分析
Fig.2 Analysis of soil microbial diversity index in dry and wet seasons
图 a 为细菌 Chao1 指数,图 b 为细菌 Shannon 指数,图 c 为真菌 Chao1 指数,图 d 为真菌 Shannon 指数。

量为 69.6%，达到极显著水平（$P<0.001$）。干季和湿季的分布界线明显，PerManova 分析结果发现，干湿季节相比细菌群落的物种组成有极显著差异（$P<0.001$，表 3），表明季节影响了细菌群落的物种组成。从图 3 可以看出，有效锰、有效磷、有效铜及有效锌与细菌群落物种分布相关性较小，而有效硼、pH、土壤自然含水量、交换性钙、交换性镁、有机质、有效铁、碱解氮及速效钾等对细菌群落的物种组成影响较大。蒙特卡罗检验进一步表明，有效硼、pH、土壤自然含水量、交换性钙、交换性镁、有机质、有效铁、碱解氮及速效钾对细菌群落物种分布具有极显著影响（$P<0.01$，表 4）。

土壤理化性状对真菌群落物种分布总的解释量为 38.4%，同样达到极显著水平（$P<0.001$）。干季和湿季的分布界线较明显，同样干湿季节相比真菌群落的物种组成发生极显著变化（$P<0.001$，表 3）。从图 4 可以看出，有效磷、有效锌对真菌群落物种组成影响较小，而其他土壤理化性状与真菌群落物种组成相关性较大。蒙特卡罗显著性检验结果进一步表明，有机质、碱解氮、pH、土壤自然含水量、交换性钙、交换性镁、有效铁、有效硼、有效铜、有效锰及速效钾对真菌群落结构有显著影响（表 4）。

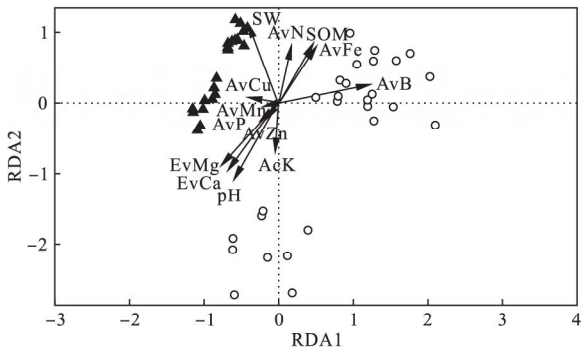

图 3 土壤细菌与土壤理化性状的 RDA 分析

Fig.3 RDA analysis of soil bacteria and soil physicochemical properties

圆形表示干季，三角形表示湿季，SOM（有机质）、AvN（碱解氮）、AvP（有效磷）、AcK（速效钾）、EvCa（交换性钙）、EvMg（交换性镁）、AvCu（有效铜）、AvZn（有效锌）、AvFe（有效铁）、AvMn（有效锰）、AvB（有效硼）、SW（土壤自然含水量）。

表 3 土壤微生物干湿季的 PerManova 分析结果

Table 3 PerManova analysis of soil microbes in dry and wet seasons

微生物	自由度	F	R^2	$Pr(>F)$
细菌	1	27.694	0.347	<0.001
真菌	1	8.299	0.137	<0.001

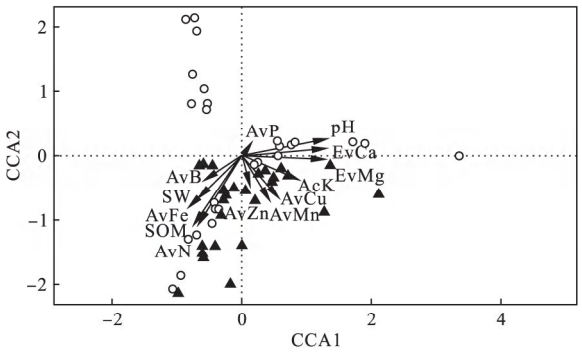

图 4 土壤真菌与土壤理化性状的 CCA 分析

Fig.4 CCA analysis of soil fungi and soil physicochemical properties

圆形表示干季，三角形表示湿季 SOM（有机质）、AvN（碱解氮）、AvP（有效磷）、AcK（速效钾）、EvCa（交换性钙）、EvMg（交换性镁）、AvCu（有效铜）、AvZn（有效锌）、AvFe（有效铁）、AvMn（有效锰）、AvB（有效硼）、SW（土壤自然含水量）。

表 4 土壤细菌和真菌的 RDA 及 CCA 蒙特卡罗检验

Table 4 RDA and CCA Monte Carlo tests of soil bacteria and fungi

土壤理化性状	细菌		真菌	
	r^2	$Pr(>r)$	r^2	$Pr(>r)$
pH	0.530	<0.001	0.749	<0.001
有机质 SOM（$g \cdot kg^{-1}$）	0.336	<0.001	0.655	<0.001
碱解氮 SOM（$g \cdot kg^{-1}$）	0.245	<0.01	0.609	<0.001
有效磷 AvP（$mg \cdot kg^{-1}$）	0.052	0.260	0.032	0.561
速效钾 AcK（$mg \cdot kg^{-1}$）	0.187	<0.010	0.359	<0.010
交换性钙 EvCa（$mg \cdot kg^{-1}$）	0.485	<0.001	0.709	<0.001
交换性镁 EvMg（$mg \cdot kg^{-1}$）	0.499	<0.001	0.675	<0.001
有效铜 AvCu（$mg \cdot kg^{-1}$）	0.081	0.109	0.281	<0.050
有效锌 AvZn（$mg \cdot kg^{-1}$）	0.038	0.356	0.085	0.388
有效铁 AvFe（$mg \cdot kg^{-1}$）	0.333	<0.001	0.534	<0.001
有效锰 AvMn（$mg \cdot kg^{-1}$）	0.010	0.757	0.245	<0.05
有效硼 AvB（$mg \cdot kg^{-1}$）	0.631	<0.001	0.227	<0.05
土壤自然含水量 SW（$g \cdot kg^{-1}$）	0.516	<0.001	0.369	<0.01

3 讨 论

土壤微生物群落在陆地生态系统中扮演着重要的角色，保证了整个陆地生态系统的稳定性，使得整个生态系统的物质循环和能量流动得以正常的运行（Zhang *et al.*，2013）。本研究结果表明，季节变化能够显著影响土壤微生物群落结构和多样性，湿季土壤中微生物的总数量显著低于干季。一方面，土壤微生物可通过分解植物凋落物等将有机物转化为无机养分以促进物质循环，在干季时植物处于凋落期，土壤表面存在大量的枯枝落叶，需要大量微生物参与分解，因此土壤微生物数量在干季时较高。另一方面，土壤微生物与植物共同竞争土壤中的养分，例

如 NH_4^+和 NO_3^-等,湿季时植物处于旺盛生长期,需要大量的营养物质,植物与微生物竞争养分以致土壤微生物所需养分减少,抑制了土壤微生物活动,因此土壤微生物数量在湿季时较低。武夷山不同海拔梯度土壤微生物量均表现为夏季最小(何容等,2009),鼎湖山常绿阔叶林不同施氮水平干季土壤微生物量始终显著高于湿季土壤微生物量(倪壮等,2018),这与本研究结果相似。但是,也有研究发现,黄土高原 8 年生、13 年生和 18 年生沙棘人工林的土壤微生物量雨季时显著高于旱季(罗蓉等,2018),兰州市南山土壤微生物类群总数表现为夏季最高(刘旻霞等,2018),这与本研究结果相反。这可能与研究地所处气候不同有关。黄土高原和兰州处于半干旱地区,土壤水分是其限制因子,夏季土壤湿度增加,有利于土壤微生物的生长,而鼎湖山和武夷山处于亚热带地区,气候温暖湿润,土壤水分之外的其他土壤理化性状成为土壤微生物的限制因素。

本研究还揭示,湿季土壤细菌和真菌的多样性和菌群结构更为丰富。细菌和真菌的 Chao1 指数和 Shannon 指数均表现为湿季显著高于干季,从干季到湿季,细菌总数量及真菌总数量都减少,但属分类水平上,相对丰度大于 1%的细菌种类基本保持不变,而真菌种类则变化明显,表明细菌主要是通过数量变化适应干湿季节变化,而真菌主要是通过数量和物种组成变化适应干湿季节变化。*Acidibacter* 是 Proteobacteria(变形菌门)中的一属,本研究还发现 *Acidibacter* 是土壤中的核心菌群,表明变形菌门是东莞城市森林土壤中最为丰富的菌群,这与他人的研究结果相一致(Zhang *et al.*,2014; 刘兴等,2015)。

本研究揭示,土壤微生物群落结构与土壤理化性状有密切关系,且土壤理化性状对细菌群落的影响高于对真菌群落的影响。其中细菌与有效硼相关系数最大,其次为 pH、土壤自然含水量、交换性镁、交换性钙,而真菌与 pH 相关系数最大,其次为交换性钙、交换性镁、有机质、碱解氮。但是,细菌和真菌与有效磷和有效锌均无显著相关性。有研究发现,土壤 pH 是 78 年生人工林土壤细菌和真菌群落的重要影响因子(Zhou *et al.*,2017)。同样,长白山土壤 pH 与细菌多样性呈显著正相关关系(Shen *et al.*,2013),这与本研究结果相似。然而,也有研究发现磷元素与真菌群落结构和多样性有密切的关系(He *et al.*,2017),这与本研究结果不一致。此外,大量研究表明,土壤有机碳、全氮、土壤含水量等是土壤微生物群落的重要影响因素(李巍等,2017; 倪壮等,2018; 涂志华等,2018)。本研究表明,土壤有效硼是影响细菌群落结构最主要的因子,交换性钙、交换性镁是影响细菌和真菌群落结构的重要因子。这可能是因为本研究样地位于城市公园,受人为影响较大,例如人工施肥。由于硼是植物生长的必须微量元素,为提高植物生长质量,可以在城市公园林木养护中人为施用硼肥。在湿季,由于雨量增加,水溶态硼容易淋失,导致湿季土壤有效硼显著低于干季。同时,钙和镁也是植物所必需的微量元素,钙和镁用于农业可提高产品质量(Santamaría *et al.*,2014),钙镁磷肥是常用的一种底肥,水溶液呈碱性,可改良酸性土壤,在城市公园中种植较多观赏价值较高的园林植物,人工施肥较多,从而使镁含量和钙含量较高。另有研究表明,$MgSO_4$常被园林工作者用于园林植物的管理,可在较短时间内释放大量镁元素(Härdter *et al.*,2004)。而土壤微生物能促进植物对微量元素的吸收,例如丛枝菌根,可通过其菌丝吸收土壤中的微量元素传送给植物。因此,在城市森林中,由于人为影响(施肥等)改变了土壤的有效硼、交换性钙和交换性镁的含量,导致土壤微生物与有效硼、交换性钙和交换性镁有较强的相关性。可见,土壤中除了大量元素 C、N、P 以及土壤湿度等对土壤微生物群落结构有影响外,土壤中其他一些关注较少的微量元素例如硼、钙、镁等对微生物群落结构亦有重要影响。

4 结 论

土壤微生物群落结构和多样性具有显著的季节特征。湿季土壤微生物总数量显著低于干季,而湿季土壤微生物 Chao1 指数和 Shannon 指数显著高于干季,且湿季细菌和真菌的多样性和菌群结构更为丰富。细菌主要通过数量改变适应季节的变化,真菌主要通过数量以及物种组成的改变适应季节变化。土壤有效硼是细菌群落结构的主要影响因子,pH 是真菌群落结构的主要影响因子,同时土壤中交换性钙和交换性镁亦是影响细菌和真菌群落的重要因子。

参考文献

丁国昌, 万晓华, 杨起帆, 等. 2017. 亚热带树种转换对林地土壤微生物群落结构和功能的影响. 应用生态学报, **28**(11): 3751-3758.

高艳娜，戚志伟，仲启铖，等. 2018. 长期模拟升温对崇明东滩湿地土壤微生物生物量的影响. 生态学报，38(2)：711-720.
何 容，王国兵，汪家社，等. 2009. 武夷山不同海拔植被土壤微生物量的季节动态及主要影响因子. 生态学杂志，28(3)：394-399.
李 巍，刘 洋，罗 钦，等. 2017. 武夷山常绿阔叶林土壤微生物多样性的季节动态. 热带亚热带植物学报，25(2)：115-126.
刘 刚，朱剑云，叶永昌，等. 2010. 东莞主要森林群落凋落物碳储量及其空间分布. 山地学报，28(1)：69-75.
刘 兴，王世杰，刘秀明，等. 2015. 贵州喀斯特地区土壤细菌群落结构特征及变化. 地球与环境，43(5)：490-497.
刘旻霞，李 瑞，张 灿，等. 2018. 兰州市南山季节性土壤微生物特征及影响因素. 中国环境科学，38(7)：2722-2730.
鲁如坤. 1999. 土壤农业化学分析方法. 北京：中国农业科技出版社.
罗 蓉，杨 苗，余 旋，等. 2018. 沙棘人工林土壤微生物群落结构及酶活性的季节变化. 应用生态学报，29(4)：1163-1169.
倪 壮，聂彦霞，欧阳胜男，等. 2018. 氮添加对南亚热带常绿阔叶林土壤微生物群落结构的影响. 生态学杂志，37(11)：3202-3209.
欧芷阳，苏志尧，朱剑云. 2013. 东莞主要森林群落的土壤基本性质和综合评价. 中南林业科技大学学报，33(8)：96-102.
涂志华，尉永键，范志平，等. 2018. 太子河源流域不同类型水源涵养林土壤微生物生物量碳、氮的季节动态. 生态学杂志，37(7)：2139-2147.
王 宁，王美菊，李世兰，等. 2015. 降水变化对红松阔叶林土壤微生物生物量生长季动态的影响. 应用生态学报，26(5)：1297-1305.
王璐璐，马大龙，李森森，等. 2018. 扎龙湿地土壤微生物群落结构的季节变化特征. 应用与环境生物学报，24(1)：166-171.
王薪琪，韩 轶，王传宽. 2017. 帽儿山不同林龄落叶阔叶林土壤微生物生物量及其季节动态. 植物生态学报，41(6)：597-609.
吴华清，陈小梅，林媚珍，等. 2016. 降水处理对南亚热带季风林土壤微生物群落结构的影响. 生态环境学报，25(4)：583-590.
杨沅志，薛冬冬，张 浩，等. 2016. 快速城市化地区城市森林景观破碎化的动态演变分析. 华南农业大学学报，37(4)：97-104.
姚 鑫，赵 敏. 2017. 城市化对城市森林组成和结构的影响——以上海“城-郊”样带为例. 自然资源学报，32(7)：1113-1124.
张英杰，李心斐，程宝栋. 2018. 国内森林城市研究进展评述. 林业经济，40(9)：92-96.
郑裕雄，曹际玲，杨智杰，等. 2018. 氮沉降对亚热带常绿阔叶天然林不同季节土壤微生物群落结构的影响. 土壤学报，55(6)：1534-1544.
Härdter R，Rex M，Orlovius K. 2004. Effects of different Mg fertilizer sources on the magnesium availability in soil. *Nutrient Cycling in Agroecosystems*，**70**：249-259.
He D，Shen WJ，Eberwein J，*et al*. 2017. Diversity and co-occurrence network of soil fungi are more responsive than those of bacteria to shifts in precipitation seasonality in a subtropical forest. *Soil Biology and Biochemistry*，**115**：499-510.
Klimek B，Chodak M，Jaźwa M，*et al*. 2016. Functional diversity of soil microbial communities in boreal and temperate Scots pine forests. *European Journal of Forest Research*，**135**：731-742.
Li J，Li ZA，Wang FM，*et al*. 2015. Effects of nitrogen and phosphorus addition on soil microbial community in a secondary tropical forest of China. *Biology and Fertility of Soils*，**51**：207-215.
Lopez BE，Urban D，White PS. 2018. Testing the effects of four urbanization filters on forest plant taxonomic，functional，and phylogenetic diversity. *Ecological Applications*，**28**：2197-2205.
Ning ZH，Chambers R，Abdollahi K. 2016. Modeling air pollutant removal，carbon storage，and CO_2 sequestration potential of urban forests in Scotlandville，Louisiana，USA. *iForest*：*Biogeosciences and Forestry*，**9**：860-867.
Santamaría O，Rodrigo S，Poblaciones MJ，*et al*. 2014. Fertilizer application (P，K，S，Ca and Mg) on pasture in calcareous dehesas：Effects on herbage yield，botanical composition and nutritive value. *Plant*，*Soil and Environment*，**60**：303-308.
Shen CC，Xiong JB，Zhang HY，*et al*. 2013. Soil pH drives the spatial distribution of bacterial communities along elevation on Changbai Mountain. *Soil Biology and Biochemistry*，**57**：204-211.
Siles JA，Cajthaml T，Minerbi S，*et al*. 2016. Effect of altitude and season on microbial activity，abundance and community structure in Alpine forest soils. *FEMS Microbiology Ecology*，**92**：fiw008.
Veresoglou SD，Halley JM，Rillig MC. 2015. Extinction risk of soil biota. *Nature Communications*，**6**：8862.
Wardle DA，Bardgett RD，Klironomos JN，*et al*. 2004. Ecological linkages between aboveground and belowground biota. *Science*，**304**：1629-1633.
Wu HP，Zeng GM，Liang J，*et al*. 2015. Effect of early dry season induced by the Three Gorges Dam on the soil microbial biomass and bacterial community structure in the Dongting Lake wetland. *Ecological Indicators*，**53**：129-136.
Yan GY，Xing YJ，Xu LJ，*et al*. 2017. Effects of different nitrogen additions on soil microbial communities in different seasons in a boreal forest. *Ecosphere*，**8**：e01879.
Zhang HF，Li G，Song XL，*et al*. 2013. Changes in soil microbial functional diversity under different vegetation restoration patterns for Hulunbeier Sandy Land. *Acta Ecologica Sinica*，**33**：38-44.
Zhang YG，Cong J，Lu H，*et al*. 2014. An integrated study to analyze soil microbial community structure and metabolic potential in two forest types. *PLoS ONE*，**9**：e93773.
Zhao Q，Jian SG，Nunan N，*et al*. 2017. Altered precipitation seasonality impacts the dominant fungal but rare bacterial taxa in subtropical forest soils. *Biology and Fertility of Soils*，**53**：231-245.
Zhou XQ，Guo ZY，Chen CR，*et al*. 2017. Soil microbial community structure and diversity are largely influenced by soil pH and nutrient quality in 78-year-old tree plantations. *Biogeosciences*，**14**：2101-2111.

作者简介 谭雪莲，女，1994年生，硕士研究生，研究方向为森林生态学，已发表论文2篇。E-mail：3380183587@qq.com
责任编辑 张 敏

《生态学杂志》第九届编辑委员会

生态学杂志

（月刊　1982 年创刊）

2019 年 11 月第 38 卷第 11 期（总第 316 期）

Chinese Journal of Ecology

（Monthly, Started in 1982）

Vol.38, No.11　November 2019

主　　管　中国科学技术协会

主　　办　中国生态学学会

中国科学院沈阳应用生态研究所

主　　编　贾永锋

编　　辑　生态学杂志　编辑部

（沈阳市文化路 72 号，邮编 110016）

电　话：（024）83970394

传　真：（024）83970394

E-mail：cje@iae.ac.cn

http://www.cje.net.cn

出　　版　科学出版社

（北京东黄城根北街 16 号，邮编 100717）

印　　刷　沈阳中科印刷有限责任公司

发　　行　辽宁省邮政公司报刊发行公司

中国国际图书贸易总公司

（北京 399 信箱，邮编 100044）

Superintended by China Association for Science & Technology

Sponsored by Ecological Society of China

Institute of Applied Ecology, Chinese Academy of Sciences

Editor-in-Chief: Jia Yongfeng

Edited by Editorial Board of Chinese Journal of Ecology

（72 Wenhua Road, Shenyang 110016, China）

Tel:（024）83970394　Fax:（024）83970394

E-mail: cje@iae.ac.cn　http://www.cje.net.cn

Published by Science Press（16 Donghuangchenggen North Street, Beijing 100717, China）

Printed by Shenyang Zhongke Printing Co, Ltd.

Distributed by Distribution Center of Newspapers and Journals, Liaoning Post Corporation（Domestic）;

China International Book Trading Corporation

（P.O. Box 399, Beijing 100044, China）（International）

ISSN 1000-4890　国内邮发代号：8-161

CN 21-1148/Q　国外发行代号：BM6077

国内外发行　定　价：50.00 元

ISSN 1000-4890

中文核心期刊
中国科技核心期刊
中国核心学术期刊

ISSN 2095-1914
CN 53-1218/S
CODEN XLXUEZ

西南林业大学学报

Journal of Southwest Forestry University

（自然科学）

（Natural Sciences）

西南林业大学 主办

2019 1

第39卷 第1期 Vol.39 No.1

西南林业大学学报（自然科学）

JOURNAL OF SOUTHWEST FORESTRY UNIVERSITY (Natural Sciences)

2019 年 1 月　第 39 卷　第 1 期　总第 149 期

Vol. 39　No. 1　Sum No. 149　Jan. 2019

目　　次　　CONTENTS

·研究简报　Research Bulletin·

[**期刊基本参数**] CN53-1218/S * 1981 * b * A4 * 192 * zh * P * ￥20.00 * 800 * 24 * 2019-01
英文编辑：徐写秋　冯　雪

DOI: 10.11929/j.swfu.201810020
引文格式：谭雪莲, 敬小丽, 阚蕾, 等. 亚热带常绿阔叶林锥和木荷枯立木点格局分析 [J]. 西南林业大学学报（自然科学）, 2019, 39(1): 132–138.

亚热带常绿阔叶林锥和木荷枯立木点格局分析

谭雪莲 敬小丽 阚 蕾 苏志尧 张 璐
(华南农业大学林学与风景园林学院，广东 广州 510642)

摘要： 在广东省康禾自然保护区 10 hm^2 常绿阔叶林样地中，设置 1 000 个样方调查枯立木，选取主要树种锥及木荷运用单变量成对相关函数 $g(r)$ 函数进行个体点格局分析，采用标记相关函数 $k_{mm}(r)$ 以枯立木胸高断面积为标记进行标记点格局分析，探究枯立木空间分布格局的形成原因。结果表明：锥和木荷枯立木个体径级结构均表现为“L”型，小径级个体死亡多，随着径级的增大，死亡个体数减少。锥枯立木个体空间分布格局在 0～50 m 尺度下表现为聚集分布，随着尺度的增大，聚集程度降低；木荷枯立木个体空间分布格局在 0～4.3 m 以及 8.7～14.0 m 时表现为聚集分布，4.4～8.6 m 以及 14.1 m 后均表现为随机分布。锥及木荷枯立木同种个体间无显著相关性，表明同种枯立木在死亡前个体间无竞争作用。枯立木个体在生长发育早期死亡较多，其空间分布格局的形成可能主要是受活立木种子的扩散限制、密度制约和生境过滤的多重影响，而大径级枯立木主要是由于自然衰老导致其死亡。

关键词： 自然保护区；标记相关函数；多度；断面积；锥；木荷
中图分类号： S718.5 **文献标志码：** A **文章编号：** 2095−1914(2019)01−0132−07

Spatial Point Patterns of Snags of *Castanopsis chinensis* and *Schima superba* in a Subtropic Evergreen Broad-leaved Forest

Tan Xuelian，Jing Xiaoli，Kan Lei，Su Zhiyao，Zhang Lu
(College of Forestry and Landescape Architecture, South China Agricultural University, Guangzhou Guangdong 510642, China)

Abstract: We established 1000 quadrats in 10 hm^2 subtropic evergreen broad-leaved forest located in the Guangdong Kanghe Provincial Natrue Reserve. Using spatial point pattern analysis and marked point pattern analysis with dominant species of *Castanopsis chinensis* and *Schima superba*, we determined the spatial point pattern of individual and basal area to explore the formation of spatial patterns of snags. The results showed that the most snags of *C. chinensis* and *S. superba* were those with small DBH, and the abundance of snags decreased with the DBH increased. The snags of *C. chinensis* showed an aggregated distribution at the scale of 0−50 m, and the aggregation declined as the scale enlarged; the snags of *S. superba* showed randomly distribution at the scale of 4.4−8.6 m and 14.1−50 m, and aggregated at local scale of 0−4.3 m and 8.7−14.0 m. The basal area of *C. chinensis* and *S. superba* showed that sangs were independent, which indicated no competition among snags. *C. chinensis* and *Schima superba* died more in their early stages. The formation of snags of these two species might be influenced by

收稿日期: 2018−10−11；**修回日期:** 2018−12−20
基金项目: 广东省省级林业发展及保护专项资金林业科技创新项目(2017KJCX037)资助；广东省自然科学基金自由申请项目(2015A030313403)资助。
第 1 作者: 谭雪莲（1994—），女，硕士研究生。研究方向：森林生态学。Email: 3380183587@qq.com。
通信作者: 张璐（1973—），女，博士，副教授。研究方向：森林生态学及保护生物学。Email: zhanglu@scau.edu.cn。

dispersal limitation of seeds and density dependence as well as environment filter, the lager trees might die because of intrinsic aging.

Key words: natrue reserve; mark correlation function; abundance; basal area; *Castanopsis chinensis*; *Schima superba*

枯立木作为森林生态系统中的重要组成部分[1]，是森林生态系统的重要碳库[2-3]，在碳循环[4]以及为其他有机体[5-6]提供生境等环节中发挥着不可忽视的作用。枯立木的形成是森林生态系统中的一个重要且复杂的生态学过程，其原因有很多，如竞争、衰老、生境过滤、自然灾害以及病虫害等[7]。近年来，随着对枯立木的深入认识，其独特的生态价值使生态学学者越来越重视对枯立木的研究[8]，研究内容主要集中在枯立木的基础特征（物种组成、多度、径级结构、储量、分布格局）[7, 9]，分解速率[10]以及生境关联[11-12]等方面。

种群的空间分布格局是种群的基本特征之一，其空间分布是一系列生态过程综合作用的结果，不仅反映了群落中种间和种内关系，也反映了种群和生境的关系[13]。由于种群的空间分布格局与尺度密切相关，因此可以用点格局分析将群落中的个体看成点，以个体的坐标值为基础，分析不同尺度下的空间分布格局[14]，揭示森林群落构建机制。目前对于枯立木空间分布格局的研究多数集中于枯立木个体的空间分布[9, 15]，然而种群的空间分布格局形成机制非常复杂，而枯立木个体数所反映的信息有限，因此将个体属性诸如树高、胸径、胸高断面积等作为标记进行标记点格局分析更能反映枯立木空间分布格局的形成机制[16]。本研究以广东省康禾自然保护区的 10 hm^2 亚热带常绿阔叶林固定样地中的主要树种锥（*Castanopsis chinensis*）和木荷（*Schima superba*）枯立木为研究对象，运用空间点格局分析成对相关函数研究主要树种枯立木个体空间分布格局，并将枯立木胸高断面积（BA）作为个体标记，运用标记点格局分析标记相关函数研究枯立木胸高断面积分布格局，以期揭示亚热带常绿阔叶林树木死亡机制，为森林群落更新提供参考。

1　研究区概况

康禾自然保护区（23°25′49″ ~ 23°31′39″N，116°30′3″ ~ 116°37′44″E）位于广东省河源市东源县，保护区总面积 6 494 hm^2，属于半山区半丘陵地区，成土母岩为花岗岩和砂岩，土壤以赤红壤为主。保护区地处中亚热带和南亚热带交界处，年平均气温 21.1 ℃，年平均无霜期 343.3 d，年平均日照时数 2 003.6 h，年平均降水量 1 912 mm[17]。地带性典型植被为亚热带常绿阔叶林，主要以壳斗科（Fagaceae）和山茶科（Theaceae）树种占优势。活立木中主要的乔木树种有锥、木荷、罗伞树（*Ardisia quinquegona*）、鼠刺（*Itea chinensis*）、多毛茜草树（*Aidia pycnantha*）。

2　研究方法

2.1　样地设置与调查

在康禾自然保护区内选择地带性典型植被群落亚热带常绿阔叶林设置 10 hm^2 固定样地，样地呈长方形，西北-东南方向长 500 m，西南-东北方向宽 200 m，利用全站仪将整个样地分为 250 个 20 m × 20 m 的大样方，每个大样方分为 4 个 10 m × 10 m 的小样方，共 1 000 个样方。在每个小样方内采用逆时针顺序调查胸径（DBH）不小于 2 cm 且树高（H）不小于 1.3 m 的木本植物（不含藤本）[18]，记录其种名、树高、胸径、分枝高并编号，同时标注其在样方中的位置。样地中活立木和枯立木基本数量特征统计结果见表 1。

表 1　样地中活立木和枯立木基本数量特征

Table 1　Quantitative characteristics of standing living trees and snags in the study site

	种名	属名	科名	多度	频度	平均胸径 ±S.E./cm	平均树高 ±S.E./m
活立木	锥（*Castanopsis chinensis*）	栲属（*Castanopsis*）	壳斗科（Fagaceae）	9 942	850	11.60±0.10	11.90±0.07
	木荷（*Schima superba*）	木荷属（*Schima*）	山茶科（Theaceae）	6 642	842	7.38±0.08	8.41±0.06

续表 1

	种名	属名	科名	多度	频度	平均胸径±SE/cm	平均树高±SE/m
枯立木	罗伞树（*Ardisia quinquegona*）	紫金牛属（*Ardisia*）	紫金牛科（Myrsinaceae）	4 942	513	1.58±0.01	3.02±0.01
	鼠刺（*Itea chinensis*）	鼠刺属（*Itea*）	鼠刺科（Escalloniaceae）	3 119	644	2.92±0.03	4.57±0.03
	多毛茜草树（*Aidia pycnantha*）	茜树属（*Aidia*）	茜草科（Rubiaceae）	1 803	234	2.93±0.06	4.45±0.05
	锥（*Castanopsis chinensis*）	栲属（*Castanopsis*）	壳斗科（Fagaceae）	277	195	8.78±0.43	5.78±0.24
	木荷（*Schima superba*）	木荷属（*Schima*）	山茶科（Theaceae）	71	58	7.72±0.97	4.44±0.31
	油茶（*Camellia oleifera*）	茶属（*Camellia*）	山茶科（Theaceae）	68	30	2.50±0.06	2.88±0.15
	黄樟（*Cinnamomum porrectum*）	樟属（*Cinnamomum*）	樟科（Lauraceae）	63	54	6.33±0.70	5.63±0.40
	华润楠（*Machilus chinensis*）	润楠属（*Machilus*）	樟科（Lauraceae）	53	41	5.16±0.48	4.57±0.32

研究区枯立木中常见的木本植物有锥、木荷、油茶（*Camellia oleifera*）、黄樟（*Cinnamomum porrectum*）、华润楠（*Machilus chinensis*）。本样地的枯立木中锥的数量占绝对优势，其次为木荷，在活立木中锥和木荷为优势种（表 1），因此本研究选择锥和木荷的枯立木进行分析。

2.2 枯立木径级划分

本研究参考 Sweeney 等[19] 的划分方法，根据样地枯立木胸径实测值，将枯立木胸径分为 4 级，幼苗（2 cm ≤ DBH ≤ 10 cm），小树（10 cm < DBH ≤ 20 cm），中树（20 cm < DBH ≤ 30 cm），大树（DBH > 30 cm）。

2.3 空间点格局分析

2.3.1 个体空间分布格局分析

个体空间分布格局分析采用完全随机模型（CSR），用 Monte-Carlo 模拟进行置信度检验，计算得出 99% 的置信区间并绘图。当在 r 距离时 $g(r)$ 实际观测值高于置信区间上限则为聚集分布，位于置信区间内则为随机分布，低于置信区间下限则为均匀分布。种群个体空间点格局选用单变量成对相关函数 $g(r)$ 进行分析[20]，表达式为：

$$g(r) = \mathrm{d}K(r) / (\mathrm{d}r \cdot 2\pi r) \quad (1)$$

$$K(r) = \frac{A}{n^2} \sum_{i-1}^{n} \sum_{j-1}^{n} \frac{1}{W_{ij}} I_r(u_{ij}) \quad (2)$$

式中：r 表示空间尺度，u_{ij} 表示 i 个体和 j 个体之间的距离，W_{ij} 是以为 i 圆心 u_{ij} 为半径的圆落在面积 A 中的比例，n 为样地中个体总数。

2.3.2 标记点格局分析

标记点格局分析采用随机标记模型（RLM）进行置信度检验并绘图。当在 r 距离时 $k_{mm}(r)$ 实际观测值高于置信区间上限则标记之间为正相关，位于置信区间内则标记之间无相关性，低于置信区间下限则标记之间为负相关。数据分析均在 R（3.4.4）spatstat 包中进行，$g(r)$ 和 $k_{mm}(r)$ 分别用 pcf 和 markcorr 函数计算[21]。胸高断面积标记点格局选用标记相关函数 $k_{mm}(r)$ 分析[22]，表达式为：

$$k_{mm}(r) = \frac{\sum_{o,u} M(o) M(u)}{\sum (M \times M')} \quad (3)$$

式中：o 和 u 代表距离 r 的 2 个植物个体，$M(o)$、$M(u)$ 分别表示 2 个植物个体的标记属性，M、M'是从标记的边际分布中独立抽取的随机标记，表示标记的均值。$k_{mm}(r)$ 是 $M(o)$、$M(u)$ 的非标准化均值。

3 结果与分析

3.1 主要树种枯立木径级分布

在康禾自然保护区亚热带常绿阔叶林固定样地中共记录到锥的枯立木个体数为 277 株，木荷的枯立木个体数为 71 株，锥和木荷枯立木径级分布见图 1。由图 1 可知，锥的枯立木种群中幼苗（2 cm ≤ DBH ≤ 10 cm）、小树（10 cm < DBH ≤ 20 cm）、中树（20 cm < DBH ≤ 30 cm）、大树（DBH > 30 cm）分别占 66.06%、24.91%、7.94%、1.08%，而木荷枯立木种群中幼苗、小树、中树、大树分别占 78.87%、11.27%、7.04%、2.82%。锥和木荷枯立木径级分布都呈“L”型分布。随径级的增大，锥和木荷枯立木个体数都减少，且二者枯立木中幼树和小树所占比例都较高，小径级枯立木个体数量在枯立木径级分布中优势显著，这表明锥和木荷在生长发育的早期死亡率较高。

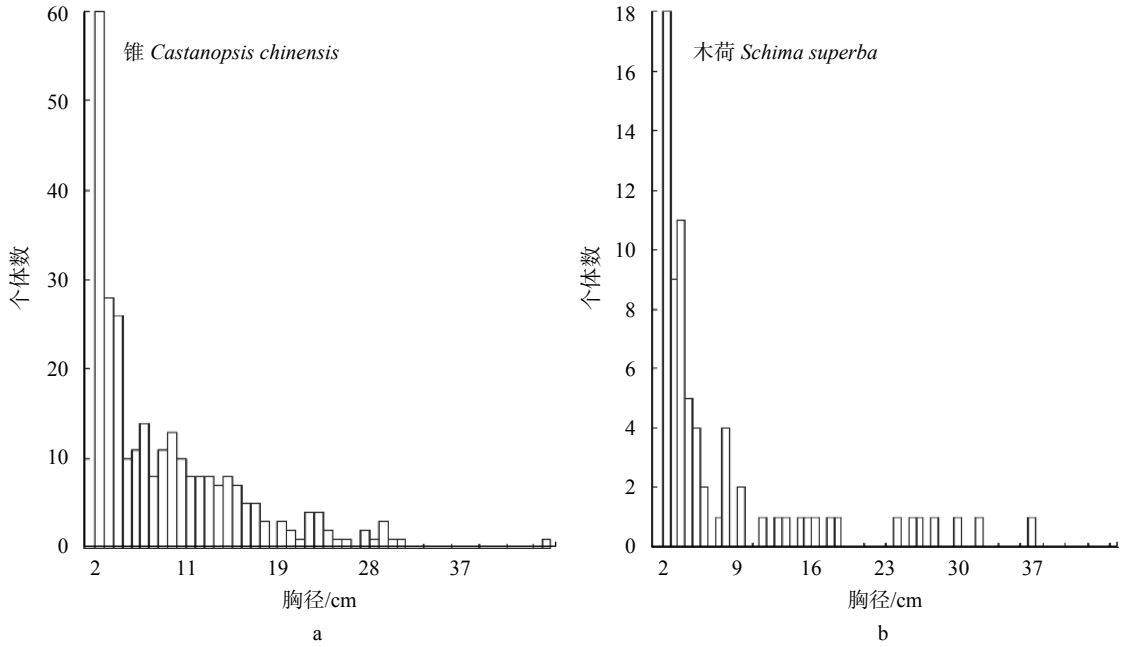

图 1　锥和木荷枯立木径级分布

Fig. 1　DBH class of snags of *C. chinensis* and *S. superba*

3.2　主要树种枯立木个体空间点格局

锥和木荷枯立木个体空间分布见图 2。由图 2 可知，锥的枯立木个体表现为聚集分布，符合自然群落中种群聚集分布的一般规律，并且胸高断面积小的个体数量占多数，随着胸高断面积增大，个体数减少。木荷的枯立木个体则表现为小尺度聚集分布，大尺度上随机分布，多数死亡个体为胸高断面积较小的个体，其枯立木数量特征与锥一致。

锥和木荷枯立木的空间分布格局分析结果见图 3。由图 3 可知，锥枯立木个体在 0 ~ 50 m 的空间尺度上均表现为聚集分布，且随着尺度的增大聚集强度减弱，当尺度增加到接近 50 m 时逐渐表现为随机分布；木荷的枯立木空间分布格局稍显复杂，在 0 ~ 4.3 m 以及 8.7 ~ 14.0 m 时表现为聚集分布，4.4 ~ 8.6 m 以及 14.1 m 后均表现为随机分布。总体来看，锥在 0 ~ 50 m 的尺度上为聚集分布，木荷在小尺度上聚集分布，尺度增大表现为随机分布，这与空间分布图（图 2）的直观表现一致。

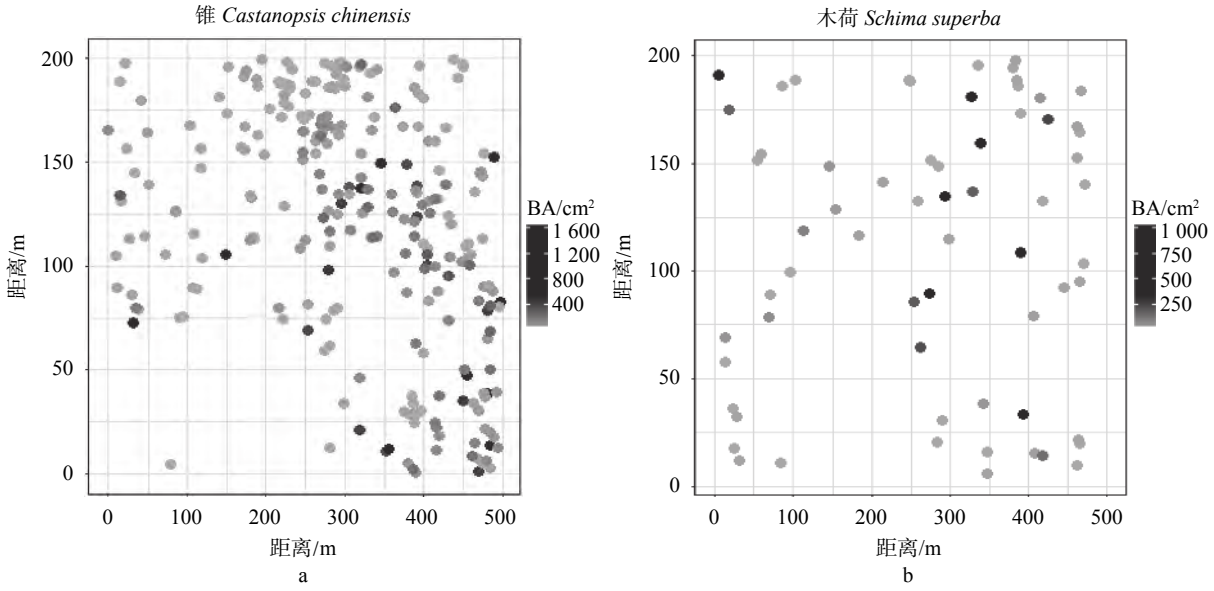

图 2　锥和木荷枯立木个体空间分布

Fig. 2　The scatter diagram of snags of *C.s chinensis* and *S. superba*

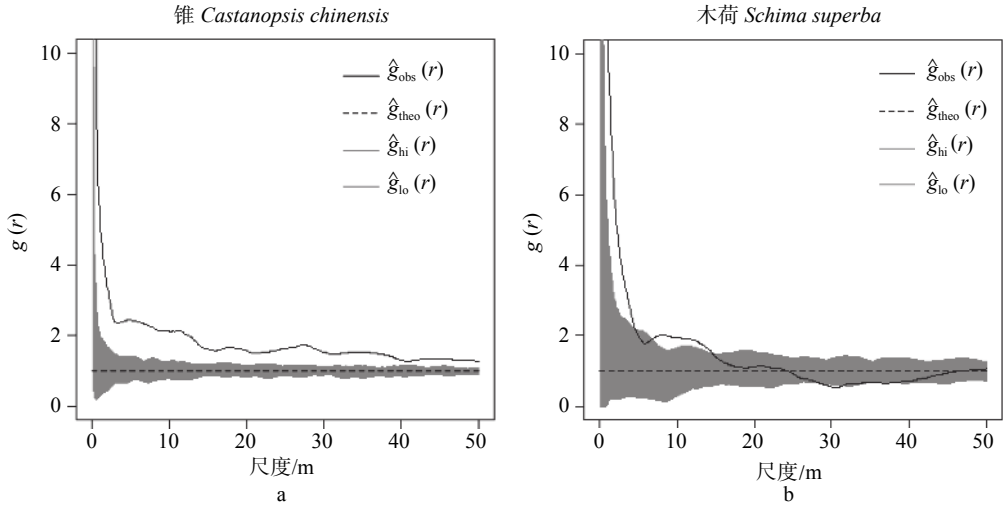

$\hat{g}_{obs}(r)$表示$g(r)$函数的观测值，$\hat{g}_{theo}(r)$表示理论值，$\hat{g}_{hi}(r)$表示模拟置信区间上限，$\hat{g}_{lo}(r)$表示模拟置信区间下限。

图 3 锥和木荷枯立木个体点格局分析尺度

Fig. 3 The spatial point pattern analysis of snags of *C. chinensis* and *S. superba*

3.3 主要树种枯立木胸高断面积标记点格局

锥和木荷枯立木胸高断面积空间分布格局结果如图 4。由图 4 可知，锥枯立木胸高断面积标记间在 0 ~ 50 m 的多数尺度表现为不相关，标记间相互独立，仅在 24.3 ~ 27.2 m 的尺度下表现为正相关；木荷枯立木胸高断面积标记间在 0 ~ 50 m 的尺度下多位于置信区间内，标记间不相关，只在 24.5 ~ 26.3 m 的尺度下表现为正相关。锥和木荷枯立木个体标记间均表现为不相关，这表明其死亡个体之间不存在竞争，个体死亡的原因可能与活立木的竞争有关，即活立木通过密度制约导致同种个体枯立木的形成。

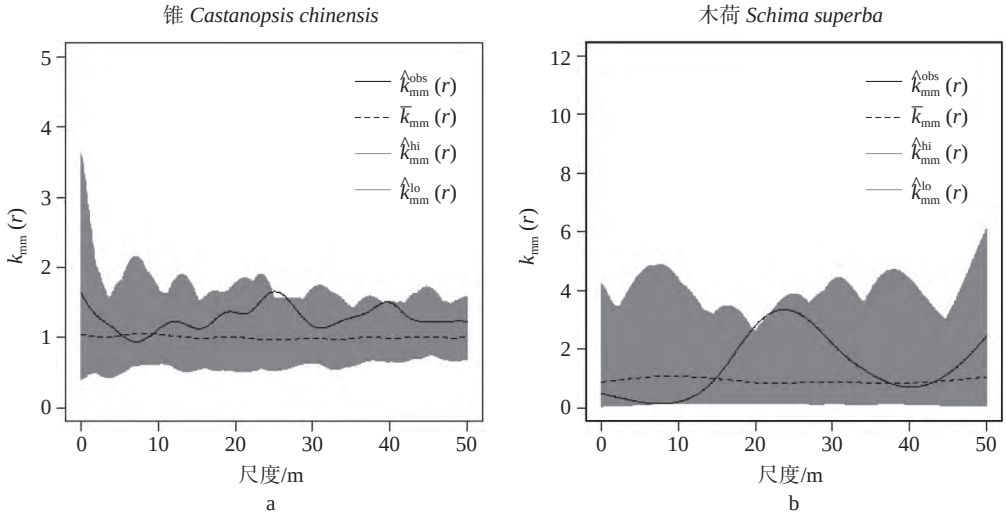

$\hat{k}^{obs}_{mm}(r)$表示$k_{mm}(r)$函数的观测值，$\bar{k}_{mm}(r)$表示理论值，$\hat{k}^{hi}_{mm}(r)$表示模拟置信区间上限，$\hat{k}^{lo}_{mm}(r)$表示模拟置信区间下限。

图 4 锥和木荷枯立木胸高断面积点格局分析

Fig. 4 The spatial point patterns analysis for basal area of *C. chinensis* and *S. superba*

4 结论与讨论

在森林生态系统中，树木死亡是很正常且重要的过程，发生在树木发育的各个阶段。锥是亚热带常绿阔叶林森林群落演替稳定阶段的优势中性树种，木荷是亚热带常绿阔叶林中典型的阳性先锋树种，在枯立木中锥和木荷也是数量最多的[23]，这可能是由于在森林群落演替过程中，木荷作为先锋树种，生长快，在其成林后为其他中性树种如锥创造了良好的环境，随着群落演替的进行，中性树种生长良好，使林下郁闭度增加，导致先锋树种不能自然更新，而使群落最后成为

以中性树种如锥为优势种的稳定群落。而锥个体之间又通过密度制约以及自疏作用等淘汰部分个体以维持森林群落的稳定，因此锥和木荷作为亚热带常绿阔叶林群落的优势种，其死亡的个体也是最多的。

研究发现样地内锥和木荷枯立木主要形成于幼苗阶段，枯立木的径级结构呈“L”型，径级组成较完整，小径级的枯立木占据优势。随着径级的增大，枯立木个体数逐渐减少。该结果与其他地方枯立木特征相同，如周小勇等[24] 等对鼎湖山针阔混交林 4 a 演替过程的分析发现幼树减少的最多，说明幼树在生长发育过程中死亡较多；弄岗喀斯特季节性雨林枯立木多度的研究也表明随径级的增大枯立木个体数减少[12]。小径级个体死亡多，大径级个体死亡较少，可能是由于小径级个体比较脆弱，易受环境因子的影响[11, 25]，如果光照、水分、营养得不到满足小径级个体将会容易死亡。而大径级的个体随着个体的生长发育，竞争能力增强，通过自疏作用淘汰其他同种个体，减小种内竞争，使自己获得足够的资源。此外大径级个体抵抗能力更强，不易受到环境变化的影响，因此大径级更多可能是由于自然衰老死亡。

聚集分布格局是自然界中常见的物种分布方式，本研究结果表明锥在 0 ~ 50 m 的尺度上均表现为聚集分布，随着尺度增加，聚集强度减弱；而木荷表现为在小尺度上聚集分布，大尺度上随机分布。郭屹立等[11] 对桂西南喀斯特季节性雨林枯立木空间分布的研究表明在小尺度上为聚集分布，而卢志军等[7] 对八公山落叶阔叶混交林枯立木的研究表明在 0 ~ 30 m 的尺度下为聚集分布，结果都与本研究不同。这可能是由于研究对象不同，本研究从种水平来分析，对象的个体数相对来说少一些，对结果有一定的影响。枯立木的空间分布格局与林木死亡前的空间分布格局有关，林木死亡前后的空间分布格局相近。本研究中，木荷的枯立木在小尺度呈聚集分布，而在大尺度呈随机分布，说明木荷枯立木的空间分布格局在小尺度主要受生境过滤等作用的影响，而在大尺度上主要受扩散限制等作用的影响。因为木荷蒴果成熟开裂后，其种子轻薄，其扩散受到风等随机因素的影响较大。锥的果实为坚果，果大而重，其传播距离较近，因此表现为聚集分布。此外，随着尺度的增大，锥越来越接近随机分布，木荷也表现为随机分布，这说明随着距离的增大，同种个体之间竞争减弱。

现有的枯立木点格局分析多从个体多度来分析，但是胸高断面积可以反映储量，更能反映种内的竞争关系。总体来看，锥及木荷枯立木同种个体间无显著相关性，表明同种枯立木在死亡前个体之间无竞争作用。这说明树木死亡不是由于同种个体之间的资源竞争导致共同死亡。此外研究地内部分区域地表被岩石覆盖，缺乏植物生长所需的土壤，不利于植物生长，因此也可能是由于环境恶劣，使植物无法生长发育而形成枯立木，即生境过滤可能也是枯立木空间分布格局形成的原因之一。枯立木的空间分布对于群落动态有重要影响，树木死亡可以改善群落内物种间的竞争关系，改变森林的光环境，其形成的腐殖质可以向土壤内释放有机物[12]，本研究仅分析了主要树种枯立木多度和胸高断面积的空间分布格局，未涉及主要树种枯立木的种间关系、枯立木与活立木之间的关系研究以及枯立木的空间分布格局的生境关联分析，因此将标记点格局用于枯立木种间竞争关系、枯立木与活立木关系以及枯立木与生境关联分析将有助于更深入地探索枯立木分布格局的形成机制。

锥和木荷在其个体生长发育早期死亡率较高，锥枯立木个体的空间分布格局在 0 ~ 50 m 尺度下表现为聚集分布，随着尺度增大，聚集程度减弱；木荷枯立木个体的空间分布格局在小尺度下表现为聚集分布，大尺度下为随机分布。锥及木荷枯立木同种个体间无显著相关性，表明同种枯立木在死亡前个体之间无竞争作用。锥和木荷枯立木个体空间分布格局的形成可能主要受活立木种子的扩散限制、密度制约和生境过滤的多重影响。

[参　考　文　献]

[1] Cousins S J M, Battles J J, Sanders J E, et al. Decay patterns and carbon density of standing dead trees in California mixed conifer forests [J]. Forest Ecology and Management, 2015, 353: 136−147.

[2] 赵嘉诚, 李海奎. 广东省森林死木碳库特征 [J]. 生态学报, 2018, 38(2): 550−559.

[3] 顾丽, 屈宏胜, 王广儒, 等. 黄土高原天然次生林木质残体的基础特征 [J]. 福建农林大学学报(自然科学版), 2016, 45(1): 30−34.

[4] Carmichael M J, Helton A M, White J C, et al. Stand-

ing Dead Trees are a Conduit for the Atmospheric Flux of CH4 and CO2 from Wetlands [J]. Wetlands, 2018, 38(1): 133−143.

[5] Riffell S, Verschuyl J, Miller D, et al. Biofuel harvests, coarse woody debris, and biodiversity: A meta-analysis [J]. Forest Ecology and Management, 2011, 261(4): 878−887.

[6] Pasanen H, Junninen K, Boberg J, et al. Life after tree death: Does restored dead wood host different fungal communities to natural woody substrates? [J]. Forest Ecology and Management, 2018, 409: 863−871.

[7] 卢志军, 刘福玲, 吴浩, 等. 八大公山常绿落叶阔叶混交林枯立木物种组成、大小级与分布格局 [J]. 生物多样性, 2015, 23(2): 167−173.

[8] Onodera K, Tokuda S. Do larger snags stand longer?: snag longevity in mixed conifer–hardwood forests in Hokkaido, Japan [J]. Annals of Forest Science, 2015, 72(5): 621−629.

[9] 安云, 丁国栋, 高广磊, 等. 华北土石山区天然次生林枯立木数量特征与分布格局 [J]. 水土保持通报, 2012, 32(4): 246−250.

[10] Oberle B, Ogle K, Zanne A E, et al. When a tree falls: Controls on wood decay predict standing dead tree fall and new risks in changing forests [J]. PLOS ONE, 2018, 13(5): e0196712.

[11] 郭屹立, 王斌, 向悟生, 等. 桂西南喀斯特季节性雨林枯立木的空间格局及生境关联性分析 [J]. 广西植物, 2016, 36(2): 154−161.

[12] 王斌, 向悟生, 丁涛, 等. 弄岗喀斯特季节性雨林枯立木多度的空间分布及影响因子 [J]. 科学通报, 2014, 59(35): 3479−3490.

[13] 梅军林, 庄枫红, 马姜明, 等. 桂林喀斯特地区克隆生长红背山麻杆种群的点格局分析 [J]. 生态学报, 2017, 37(9): 3164−3171.

[14] Baddeley A, Turner R. spatstat: An R Package for Analyzing Spatial Point Patterns [J]. Journal of Statistical Software, 2005, 12(12): 1−42.

[15] 玉宝, 张秋良, 王立明. 兴安落叶松过伐林枯立木分布格局特征分析 [J]. 林业科学研究, 2015, 28(1): 81−87.

[16] Grabarnik P, Myllymäki M, Stoyan D. Correct testing of mark independence for marked point patterns [J]. Ecological Modelling, 2011, 222(23/24): 3888−3894.

[17] 徐明锋, 胡砚秋, 李文斌, 等. 土壤养分对亚热带天然林物种分布的影响 [J]. 中南林业科技大学学报, 2014, 34(9): 91−97.

[18] Iwashita D K, Litton C M, Giardina C P. Coarse woody debris carbon storage across a mean annual temperature gradient in tropical montane wet forest [J]. Forest Ecology and Management, 2013, 291(2): 336−343.

[19] Sweeney O F M, Martin R D, Irwin S, et al. A lack of large-diameter logs and snags characterises dead wood patterns in Irish forests [J]. Forest Ecology and Management, 2010, 259(10): 2056−2064.

[20] 贾美玉, 张金屯, 梁钰, 等. 五台山林线过渡带华北落叶松格局过程和尺度分析 [J]. 生态学报, 2018, 38(20): 1−8.

[21] Gray L, He F. Spatial point-pattern analysis for detecting density-dependent competition in a boreal chronosequence of Alberta [J]. Forest Ecology and Management, 2009, 259(1): 98−106.

[22] 胡砚秋, 李文斌, 崔佳玉, 等. 亚热带常绿阔叶林优势种个体及生物量的点格局分析 [J]. 生态学报, 2016, 36(4): 1066−1072.

[23] 杨方方, 李跃林. 鼎湖山粗死木质残体生物量特征 [J]. 应用与环境生物学报, 2011, 17(5): 750−752.

[24] 周小勇, 黄忠良, 史军辉, 等. 鼎湖山针阔混交林演替过程中群落组成和结构短期动态研究 [J]. 热带亚热带植物学报, 2004, 12(4): 323−330.

[25] 张璐, 敬小丽, 苏志尧, 等. 亚热带常绿阔叶林枯立木与冠层结构的关系 [J]. 森林与环境学报, 2018, 38(1): 64−70.

(责任编辑 陆 驰)

- 2018 年、2016 年入选中国高校优秀科技期刊
- 2013 年《西南林业大学学报》编辑部获全国高等农业院校学报优秀团队奖
- 2009 年获全国高校科技期刊优秀编辑质量奖
- 2009 年获第三届云南期刊奖改革创新奖
- 本刊为中文核心期刊、中国科技核心期刊、中国核心学术期刊（RCCSE）
- 被美国《乌利希期刊指南》（Ulrich's Periodicals Directory）收录
- 被美国《化学文摘》（Chemical Abstracts，CA）收录
- 被波兰《哥白尼索引》（Index Copernicus，IC）收录
- 被英国《动物学记录》（Zoological Record，ZR）收录
- 被英国《国际农业与生物科学研究中心》（Centre for Agriculture and Bioscience International，CABI）收录
- 被中国学术期刊综合评价数据库（CAJCED）全文收录
- 被中国期刊全文数据库（CJFD）全文收录
- 被《中国知网》、《中国学术期刊（光盘版）》全文收录
- 被中国核心期刊（遴选）数据库收录
- 被中文科技期刊数据库收录
- 被 RCCSE 中国权威学术期刊数据库收录

西南林业大学学报
XINAN LINYE DAXUE XUEBAO
（自然科学　单月出版　1981 年创刊）
2019 年 1 月　第 39 卷　第 1 期

Journal of Southwest Forestry University
（Natural Sciences, Started in 1981）
Vol.39　No.1，2019 January

主管单位	云南省教育厅	**Administrated by**	Yunnan Provincial Education Department
主办单位	西南林业大学	**Sponsored by**	Southwest Forestry University
主　　编	郭辉军	**Editor-in-chief**	Guo Huijun
编辑出版	《西南林业大学学报》编辑部	**Edited & Published by**	Editorial Department of Journal of Southwest Forestry University 300 Bailongsi, Kunming, Yunnan 650224, P.R. China
	地址：云南昆明白龙寺300号		Tel: 0871-63863029　63862787
	邮编：650224		Website: http://xnldxb.swfu.edu.cn
	电话：0871-63863029　63862787		Email: swfcbjb@vip.163.com
	网址：http://xnldxb.swfu.edu.cn		
	Email：swfcbjb@vip.163.com		
印　　刷	昆明天欣彩印包装有限公司	**Printed by**	Kunming Tianxin Color Printing and Packaging Co.,Ltd.
发行订购	《西南林业大学学报》编辑部	**Distributed by**	Editorial Department of Journal of Southwest Forestry University
发行范围	公开发行	**Range of Distribution**	Openly Published and Distributed

刊号：ISSN 2095-1914 / CN 53 - 1218/S　　定价：20.00元　120.00元/年

ISSN 2095-1914

ISSN 1673-923X
CODEN ZLKDA5

中南林业科技大学学报

Journal of Central South University of Forestry & Technology

第38卷 Volume 38 | 第7期 Number 7

- 中国精品科技期刊
- 中国高校优秀科技期刊
- 全国中文核心期刊
- 中国科技核心期刊
- RCCSE中国权威学术期刊
- 中国科学引文数据库(CSCD)来源期刊
- 中国科技论文与引文数据库(CSTPCD)来源期刊
- 美国CA、日本JST等来源期刊

7

2018

目　次

林　学

生态学

[期刊基本参数]CN43—1470/S*m*A4*124*zh*P*￥20.00*1000*25*2014—05*n

第38卷 第7期
2018年7月
中南林业科技大学学报
Journal of Central South University of Forestry & Technology
Vol. 38 No. 7
Jul. 2018
Doi:10.14067/j.cnki.1673-923x.2018.07.007
http: //qks.csuft.edu.cn

不同冠层结构下的植物生长型与生活型特征

张星元，张　璐，马　丁，蔡琳颖
（华南农业大学 林学与风景园林学院，广东 广州 510642）

摘　要：为了探明森林群落冠层结构、光环境特性与林下植被生长型和生活型的关系，采用经典群落学调查方法和半球面影像技术，定量研究了在林下、林隙边缘和林隙中心这3种冠层结构下，植物生长型和生活型的数量特征及其对不同冠层结构参数的响应。结果表明：（1）不同冠层结构下，乔木和灌木的优势地位明显，草本与藤本在林下的生长优势最弱，而蕨类最适于在林隙边缘生长；不同冠层结构下的植物生活型均表现为先增后减，说明林隙边缘的生活环境更适合植物群落的生长。（2）Kruskal-Wallis分析表明，草本和灌木，以及小高位芽、矮高位芽和地上芽植物在不同冠层结构间存在显著差异（$P < 0.05$）。（3）CCA排序表明不同生长型和生活型植物对冠层结构参数的响应不一致。在林下和林隙中心，物种分布受到林冠开度、叶面积指数、林下直射光、散射光和总光照这5个冠层结构参数的影响；而在林隙边缘，物种分布只与林冠开度、叶面积指数和林下散射光有关。

关键词：生长型；生活型；物种分布；林下光环境；林冠层
中图分类号：S718.5　　**文献标志码**：A　　**文章编号**：1673-923X(2018)07-0037-08

Characteristic of plant growth forms and life forms of different canopy structures in subtropical mountainous forest

ZHANG Xingyuan, ZHANG Lu, MA Ding, CAI Linying

(College of Forestry and Landscape Architecture, South China Agricultural University, Guangzhou 510624, Guangdong, China)

Abstract: In order to study the relationship among canopy structure, understory light environment, plant growth forms and life forms, the quadrat method and hemispherical photography were used to quantify the plant growth forms and life forms of understory, gap-edge and gap-center and their response to different canopy structural parameters in a subtropical mountainous forest in South China. The results showed that: (1) Trees and shrubs were obviously dominant in different canopy structures. The growth of herbs and vines was the weakest under the forest, and the ferns were most suitable for the growth at the gap-edge. The plant life forms in different canopy structures increased first and then decreased, indicating that the habitat of the gap-edge was more suitable for plant growth. (2) Kruskal-Wallis analysis revealed that there was a significant difference between herbs and shrubs, as well as microphanerophytes, nanophanerophyte and chamaephytes in different canopy structures ($P < 0.05$). (3) Canonical Correspondence Analysis (CCA) showed that the responses of different ecotypic plants to canopy structural parameters were different. The species distribution of understory and gap-center were affected by five canopy structural parameters, i.e., canopy opening, leaf area index, transmitted direct light, transmitted diffused light and transmitted total light, respectively. However, the species distribution of gap-edge was affected by canopy openness, leaf area index and transmitted diffused light.

Keywords: growth forms; life forms; species distribution; understory light environment; canopy layer

森林冠层是影响森林生态系统特性最基本的因素[1]，是森林生态系统与外界环境作用最直接与最活跃的界面[2]。我国对森林冠层结构的研究起步较晚，随着林冠实测技术的发展，冠层研究从定性描述发展为更加严格的量化研究[3-4]。而国外学者对森林冠层结构、林下植被及光环境特征的研究已有30多年，目前已有大量的研究成果[5-6]。林木冠层通过对光照进行吸收、反射和投射，改变林下光照条件，从而对林下植被的物种组成与物种多度产生影响[7-8]。根据冠层结构在森林群落

收稿日期：2017-08-06
基金项目：广东省省级林业发展及保护专项资金（林业科技创新项目）（2017KJCX037）；广东省自然科学基金项目（2015A030313403）；国家林业局资助项目（2130211）
作者简介：张星元，硕士研究生　　通信作者：张　璐，副教授，博士；E-mail：zhanglu@scau.edu.cn
引文格式：张星元，张　璐，马　丁，等. 不同冠层结构下的植物生长型和生活型特征 [J]. 中南林业科技大学学报，2018,38(7):37-44.

中位置的不同，可将其分为林下、林隙边缘和林隙中心。研究森林群落不同冠层结构下植物生长型和生活型的特征，不仅可为森林生态系统小气候、群落演替及其进化史等提供关键信息[9]，也可加强对整个森林生态系统演替进程及其机制的理解[10]。

植物生长型和生活型深刻解析植物群落结构及其与环境的关系，对研究植物群落的发生、发展以及演替规律具有重要意义[11]。植物的生活型是植物对于综合生境条件长期适应而在外貌上反映出来的植物类型[12]。森林群落的外貌主要取决于生活型的组成，通过对植物群落生活型的研究既可以发现控制和影响群落的主要气候因素、植物群落与环境之间的关系，又可以了解群落组成种的外貌特征随着地理位置或生境的改变而发生的变化[13]。植物生长型是指根据植物的可见结构划分的类群，是表征群落外貌特征和垂直结构的重要指标[14]。植物的生长型反映植物生活的环境条件，相同的环境条件具有相似的生长型，是趋同适应的结果[15]。

该研究以南岭山地森林群落为研究对象，量化其冠层结构、光环境特性与林下植被生长型和生活型的关系，以期为亚热带森林群落更新和维持提供理论和数据支持。主要研究以下问题：南岭山地森林林下植被在林下、林隙边缘和林隙中心这3种冠层结构下的生长型和生活型表现特征是否都遵循同一模式？该地区森林群落的物种分布对不同冠层结构参数的响应是否一致？

1 材料与方法

1.1 研究区概况

研究试验地设在广东南岭国家级自然保护区内（112°41′～113°15′E，24°39′～28°08′N），总面积58 368.4 hm^2。保护区位于广东北部南岭山脉南坡中段，是广东省陆地森林面积最大的自然保护区，保存有较完整的中亚热带针叶林、针阔混交林、常绿阔叶林、山地矮林等[16]。该区位于中亚热带湿润性季风气候区，海拔500～600 m，年均气温17.4 ℃，最冷月（1月份）平均气温7.1 ℃，最热月（7月份）平均气温26.2 ℃，年均降雨量2 108.4 mm，年平均相对湿度84%，日照率40%。水平地带性土壤为红壤，地带性植被为亚热带常绿阔叶林，森林覆盖率达98%[17]。

1.2 样方设置与调查

在南岭国家级自然保护区，以亚热带山地森林群落为研究对象，采用样方法，以10 m×10 m为样方单元，在每个样方单元内进行每木调查，测定胸径（DBH）≥3 cm的所有活立木的种名、胸径、树高和冠幅，共计调查了100个样方（10 000 m^2）。同时，在每个样方单元的四角和对角线中心各设置1个2 m×2 m的小样方，记录每个小样方内林下植物的种名、多度与盖度。

1.3 半球面影像拍摄与分析

半球面影像技术是一种快捷、准确、高性价比的近距离遥感方法，近年来成功应用于森林生态监测和评价研究中。具体方法为：用三脚架将Nikon CoolPix 4500数码相机外接Nikkor FC-E8鱼眼镜头转换器水平放置于离地面1.65 m处，用指南针确定方向使记录的照片顶部与磁北方向重合，在每个10 m×10 m样方单元中心和对角线四分位处镜头朝上拍摄半球面林冠影像。采用Gap Light Analyzer 2.0（GLA）图像处理软件分析林冠影像，输出林冠开度（CO）、叶面积指数（LAI）、林下直射光（Transmitted direct light, Tdir）、散射光（Transmitted diffused light, Tdif）和总光照（Transmitted total light, Ttot）5个冠层结构参数，并进行冠层结构参数分组[18-20]。

1.4 数据分析

参照Whittaker[21]的群落分类系统，结合亚热带山地森林的植物类型，将森林群落维管束植物按生长型分为乔木、灌木、草本、藤本和蕨类五个层次。参照Raunkiaer[22]的分类系统，将群落按生活型分为地面芽、地上芽、高位芽3个类别。高位芽又进一步分为藤本高位芽、矮高位芽、小高位芽和中高位芽。同时，参照樊大勇等[23]的林冠划分依据，并结合实地观测，将林冠开度从0～7%定为林下，7%～14%定为林隙边缘，19%～21%定为林隙中心。运用Statistica 8.0统计软件对不同冠层结构下植被生长型和生活型的物种多度以及冠层的叶面积指数、林冠开度和林下散射光等5个结构参数分别进行Kruskal-Wallis（非参数ANOVA）分析，检验物种多度在各分组变量间是否存在差异。运用PC-ORD 6.0多元分析软件对山地森林群落冠层结构各参数典范对应分析（Canonical correspondence analysis, CCA），并采用蒙特卡罗检验来检验结果是否具有统计显著性。

2　结果与分析

2.1　不同冠层结构下的植物生长型和生活型

2.1.1　不同冠层结构下的植物生长型特征

在不同冠层结构下，森林群落乔木多度均显著大于草本、藤本和蕨类的多度，说明乔木在南岭山地森林不同冠层结构下均占据优势地位。灌木的优势地位也较明显，仅次于乔木，而草本、藤本以及蕨类的丰富度与多度表现不尽一致（见图1）。其中，林下草本与藤本的丰富度和多度均小于其在林隙边缘和林隙中心，蕨类在林隙边缘的多度最大，说明草本与藤本在林下的生长优势最弱，而蕨类最适于在林隙边缘生长。

2.1.2　不同冠层结构下的植物生活型特征

基于10 000 m^2样地的调查数据，共记录到高位芽植物297种、地面芽植物36种、地上芽植物13种。在不同冠层结构下，植物群落丰富度与多度的生活型数量特征表现基本一致（见图2），表明研究区植物群落的生活环境适宜而稳定。随着林冠开度的增加，地面芽、地上芽和高位芽植物的物种丰富度和多度均表现为先增后减，说明在该地区林隙边缘的生活环境更适合植物群落的生长。对群落高位芽植物进一步的分析得知，在林下、林隙边缘和林隙中心这3种不同的冠层结构下，各高位芽植物的丰富度与多度的特征表现一致，从小到大依次为藤本高位芽，矮高位芽，小高位芽，中高位芽。其中，中高位芽植物优势明显，而地上芽植物最少，在林下这一冠层结构下没有地上芽植物，藤本高位芽也较少，表明在中亚热带山地森林适宜中高位芽的生长，不适宜地上芽和藤本高位芽的生长。

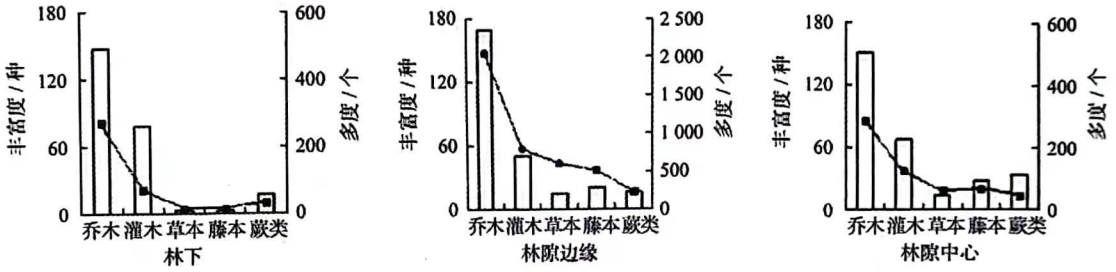

图1　不同冠层结构下的植物生长型数量特征

Fig. 1　Plant growth forms characteristics of different canopy structures in subtropical mountainous forest

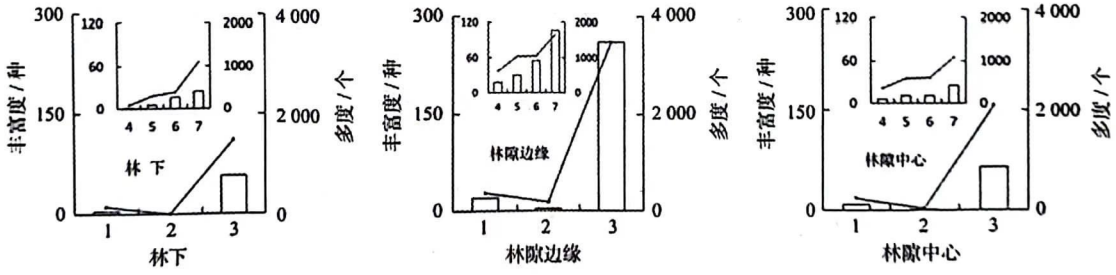

1. 地面芽；2. 地上芽；3. 高位芽；4. 藤本高位芽；5. 矮高位芽；6. 小高位芽；7. 中高位芽

图2　不同冠层结构下的植物生活型数量特征

Fig. 2　Characteristics of plant life forms of different canopy structures in subtropical mountainous forest

2.2　不同冠层结构下植物生长型和生活型的差异性分析

对不同冠层结构下各个生长型的多度进行的Kruskal-Wallis分析表明（见图3），灌木多度呈极显著差异（$P < 0.001$），草本植物表现为显著差异（$P < 0.05$），但乔木、藤本与蕨类植物的差异性水平并不显著（$P > 0.05$）。多重比较进一步表明，林下的草本多度与其他2个冠层结构差异显著，说明林下的生活环境不利于草本植物的生长；林下和林隙边缘的灌木多度差异显著，但林隙中心的灌木多度与林下和林隙边缘都没有达到显著性水平。

与生长型类似，3个冠层结构下的中高位芽、藤本高位芽与地面芽植物多度的差异性水平也不显著（$P > 0.05$）（见图4）。多重比较进一步发现，小高位芽在林下和林隙中心这2种冠层结构下差异显著（$P < 0.05$），但在林隙边缘差异不显

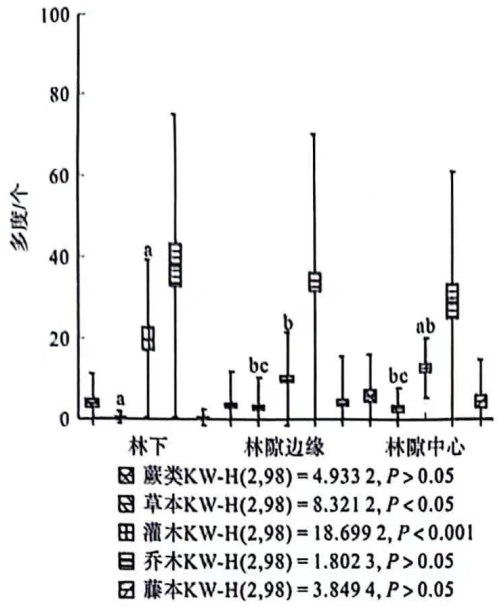

图 3 不同冠层结构下的植物生长型差异性分析

Fig. 3 Kruskal-Wallis analysis of growth forms of different canopy structures in subtropical mountainous forest

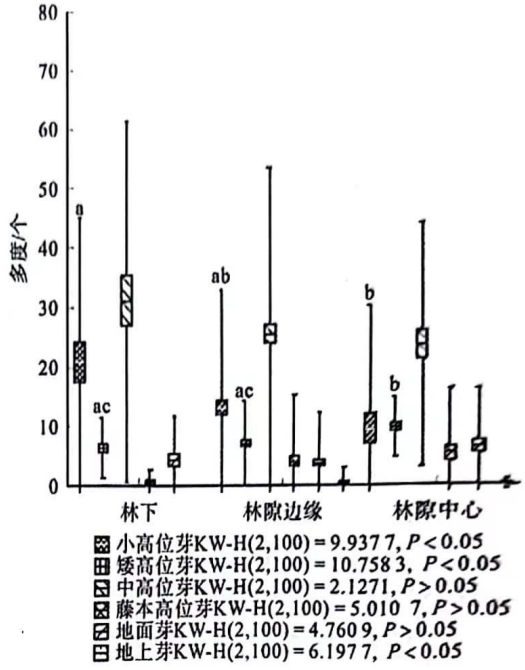

图 4 不同冠层结构下的植物生活型差异性分析

Fig. 4 Kruskal-Wallis analysis of life forms of different canopy structures in subtropical mountainous forest

著（$P > 0.05$）。矮高位芽只在林隙中心与林下和林隙边缘存在显著差异（$P < 0.05$）。

2.3 不同生长型和生活型植物分布对冠层结构的响应

冠层结构参数与环境轴的相关系数以及不同冠层结构下的 CCA 特征根如表 1 所示，在林下，CO 和 LAI 与环境轴 2 相关性最大，而 Tdir、Tdif 和 Ttot 与环境轴 1 相关性最大；在林隙边缘，CO、LAI、Tdif 和 Ttot 均与环境轴 3 最具相关性，而 Tdir 与环境轴 1 相关性最大；在林隙中心，五种冠层结构参数均与环境轴 1 最具相关性。同时，蒙特卡罗检验特征值以及物种与环境因子的相关系数 P 值皆小于 0.05，说明排序效果理想。

表 1 不同冠层结构下各参数与环境轴的相关系数以及特征根

Table 1 The correlation coefficient and characteristic roots of parameters and environmental axis under different canopy structures

	林下			林隙边缘			林隙中心		
	第 1 轴	第 2 轴	第 3 轴	第 1 轴	第 2 轴	第 3 轴	第 1 轴	第 2 轴	第 3 轴
CO /%	-0.141	0.720	0.121	0.359	-0.309	-0.741	-0.997	-0.025	0.045
LAI	0.463	-0.644	0.504	0.137	0.226	0.900	0.854	0.084	-0.101
Tdir /(mol·m^{-2}d^{-1})	-0.642	0.367	-0.049	0.337	-0.190	-0.184	-0.706	0.021	0.672
Tdif /(mol·m^{-2}d^{-1})	-0.575	0.513	-0.108	-0.116	-0.187	-0.585	-0.943	0.208	0.200
Ttot /(mol·m^{-2}d^{-1})	-0.648	0.443	-0.072	0.193	-0.175	-0.366	-0.847	0.105	0.498
特征值	0.562	0.133	0.076	0.372	0.260	0.179	0.597	0.313	0.197
物种环境相关系数	0.960	0.932	0.758	0.751	0.898	0.631	0.924	0.839	0.737

CCA 排序结果显示（见图 5 和表 2），在林下和林隙中心，不同生长型和生活型植物受到 5 个冠层结构参数的影响，而在林隙边缘，物种分布只与叶面积指数、林冠开度和林下散射光有关。在林下，腺萼马银花 *Rhododendron bachii*、杨桐 *Adinandra millettii* 和黄丹木姜子 *Litsea elongata* 等集中分布在 CCA 排序图中林冠开度较小或叶面积指数较大的区域，表明这些物种较喜欢阴蔽的环境或具备耐阴性。在林隙边缘，华山姜 *Alpinia oblongifolia*、石斑木 *Raphiolepis indica* 和乐东拟单性木兰 *Parakmeria lotungensis* 等分布在林冠开度较大的区域，表明这些物种适合生长在林冠光照较强的区域。在林隙中心，假地枫皮 *Illicium jiadifengpi* 和青冈 *Cyclobalanopsis glauca* 等分布在林冠开度较大的区域，而檵木 *Loropetalum chinense* 分布在林下直射光较大的区域，说明

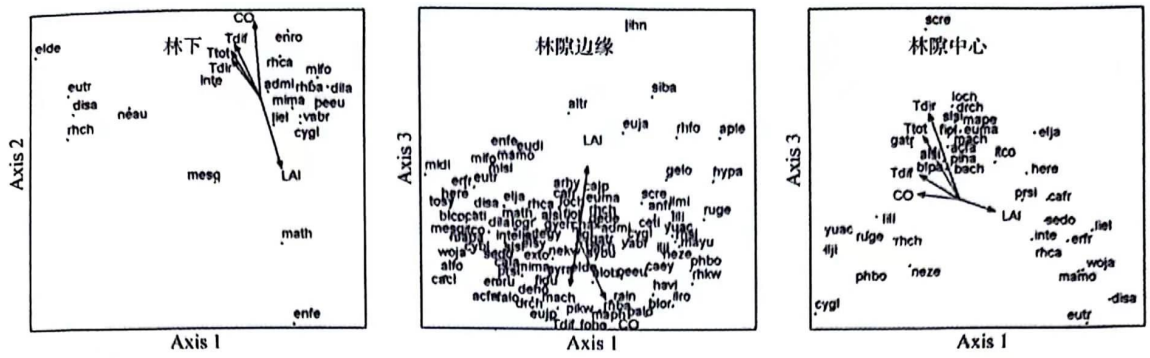

图 5　不同冠层结构下的优势种与环境因子的 CCA 分析

Fig. 5　CCA analysis of dominant tree species and environmental factors in different canopy strutures in subtropical mountainous forest

表 2　CCA排序图物种名称及代码

Table 2　The species and species code of CCA

种名	代码	种名	代码	种名	代码
五列木 *Pentaphylax euryoides*	*peeu*	圆锥绣球 *Hydrangea paniculata*	*hypa*	山鸡血藤 *Millettia dielsiana*	*midi*
多花杜鹃 *Rhododendron cavaleriei*	*rhca*	龙须藤 *Bauhinia championii*	*bach*	广东杜鹃 *Rhododendron kwangtungense*	*rhkw*
腺萼马银花 *Rhododendron bachii*	*rhba*	凤凰润楠 *Machilus phoenicis*	*maph*	杜英 *Elaeocarpus decipiens*	*elde*
箬竹 *Indocalamus tessellatus*	*inte*	华南五针松 *Pinus kwangtungensis*	*pikw*	薜荔 *Ficus Dumila*	*fidu*
黄丹木姜子 *Litsea elongata*	*liel*	闽楠 *Phoebe bournei*	*phbo*	赤楠 *Syzygium buxifolium*	*sybu*
毛果柃 *Eurya trichocarpa*	*eutr*	链珠藤 *Alyxia sinensis*	*alsi*	南酸枣 *Choerospondias axillaris*	*chax*
杨桐 *Adinandra millettii*	*admi*	网脉酸藤子 *Embelia rudis*	*emru*	刨花润楠 *Machilus pauhoi*	*mapa*
青冈 *Cyclobalanopsis glauca*	*cygl*	单叶新月蕨 *Pronephrium simplex*	*prsi*	野漆树 *Toxicodendron sylvestris*	*tosy*
南烛 *Vaccinium bracteatum*	*vabr*	猴欢喜 *Sloanea sinensis*	*slsi*	细叶芹 *Apium leptophyllum*	*aple*
金叶含笑 *Michelia foveolata*	*mifo*	多花山矾 *Symplocos ramosissima*	*syra*	石斑木 *Raphiolepis indica*	*rain*
深山含笑 *Michelia maudiae*	*mima*	深山含笑 *Michelia maudiae*	*mima*	树参 *Dendropanax dentiger*	*dede*
光里白 *Diplopterygium laevissima*	*dila*	野鸦椿 *Euscaphis japonica*	*euja*	水青冈 *Fagus longipetiolata*	*falo*
戟叶圣蕨 *Dictyocline sagittifolia*	*disa*	柃木 *Euyra japonica*	*eujp*	华南龙胆 *Gentiana loureirii*	*gelo*
黄杞 *Engelhardtia roxburghiana*	*enro*	柯 *Lithocarpus glabra*	*ligl*	山杜英 *Elaeocarpus sylvestris*	*elsy*
红楠 *Machilus thunbergii*	*math*	深绿卷柏 *Selaginella doederleinii*	*sedo*	贴毛折柄茶 *Hartia villosa*	*havi*
粘毛杜鹃 *Rhododendron championae*	*rhch*	南岭箭竹 *Sinarundinaria basihirsuta*	*siba*	箬竹 *Indocalamus tessellatus*	*inte*
杜英 *Elaeocarpus decipiens*	*elde*	铁冬青 *Ilex rotunda*	*ilro*	檵木 *Loropetalum chinense*	*loch*
少叶黄杞 *Engelhardtia fenzelii*	*enfe*	戟叶圣蕨 *Dictyocline sagittifolia*	*disa*	假地枫皮 *Illicium jiadifengpi*	*ilji*
新木姜子 *Neolitsea aurata*	*neau*	米锥 *Castanopsis carlesii*	*cacl*	青冈 *Cyclobalanopsis glauca*	*cygl*
樟叶泡花树 *Meliosma squamulata*	*mesq*	香花枇杷 *Eriobotrya fragrans*	*erfr*	疏齿木荷 *Schima remotiserrata*	*scre*
猴头杜鹃 *Rhododendron simiarum*	*rhsi*	淡竹叶 *Lophatherum gracile*	*logr*	粘毛杜鹃 *Rhododendron championae*	*rhch*
五列木 *Pentaphylax euryoides*	*peeu*	乌毛蕨 *Blechnum orientale*	*blor*	阔鳞毛蕨 *Dryopteris championii*	*drch*
青冈 *Cyclobalanopsis glauca*	*cygl*	阔鳞毛蕨 *Dryopteris championii*	*drch*	罗浮槭 *Acer fabri*	*acfa*
箬竹 *Indocalamus tessellatus*	*inte*	毛桃木莲 *Manglietia moto*	*mamo*	网脉山龙眼 *Helicia reticulata*	*here*
木姜子柯 *Lithocarpus litseifolius*	*lili*	茶梨 *Anneslea fragrans*	*anfr*	抱秆黄竹 *Yushania actinoseta*	*yuac*
抱秆黄竹 *Yushania actinoseta*	*yuac*	钩锥 *Castanopsis tibetana*	*cati*	南亚新木姜 *Neolitsea zeylanica*	*neze*
疏齿木荷 *Schima remotiserrata*	*scre*	香港四照花 *Dendrobenthamia hongkongensis*	*deho*	单叶新月蕨 *Pronephrium simplex*	*prsi*
杨桐 *Adinandra millettii*	*admi*	白桂木 *Artocarpus hypargyreus*	*arhy*	深绿卷柏 *Selaginella doederleinii*	*sedo*
多花杜鹃 *Rhododendron cavaleriei*	*rhca*	二列叶柃 *Eurya distichaophylla*	*eudi*	闽楠 *Phoebe bournei*	*phbo*
檵木 *Loropetalum chinense*	*loch*	肥皂荚 *Gymnocladus chinensis*	*gych*	毛果柃 *Eurya trichocarpa*	*eutr*
赤杨叶 *Alniphyllum fortunei*	*alfo*	福建柏 *Fokienia hodginsii*	*foho*	木姜子柯 *Lithocarpus litseifolius*	*lili*
粘毛杜鹃 *Rhododendron championae*	*rhch*	广西新木姜子 *Neolitsea kwangsiensis*	*nekw*	日本杜英 *Elaeocarpus japonicus*	*elja*
假玉桂 *Celtis timorensis*	*ceti*	厚皮香 *Ternstroemia gymnanthera*	*tegy*	猴欢喜 *Sloanea sinensis*	*slsi*
腺萼马银花 *Rhododendron bachii*	*rhba*	乳源木莲 *Manglietia yuyanensis*	*mayu*	厚叶鼠刺 *Itea coriacea*	*itco*
南亚新木姜 *Neolitsea zeylanica*	*neze*	云锦杜鹃 *Rhododendron fortunei*	*rhfo*	山蒟 *Piper hancei*	*piha*

续表 2
Continuation of table 2

种名	代码	种名	代码	种名	代码
南亚新木姜 *Neolitsea zeylanica*	*neze*	云锦杜鹃 *Rhododendron fortunei*	*rhfo*	山蒟 *Piper hancei*	*piha*
光里白 *Diplopterygium laevissima*	*dila*	芒 *Miscanthus sinensis*	*misi*	狗脊 *Woodwardia japonica*	*woja*
黄丹木姜子 *Litsea elongata*	*liel*	乌泡子 *Rubus gentillanus*	*ruge*	戟叶圣蕨 *Dictyocline sagittifolia*	*dist*
栲 *Castanopsis fargesii*	*cafr*	黑柃 *Eurya macartneyi*	*euma*	栲 *Castanopsis fargesii*	*cafr*
瓜馥木 *Fissistigma oldhamii*	*fiol*	硬壳柯 *Lithocarpus hancei*	*lihn*	瓜馥木 *Fissistigma oldhamii*	*fiol*
乌蔹莓 *Cayratia japonica*	*cajp*	华山姜 *Alpinia oblongifolia*	*alob*	龙须藤 *Bauhinia championii*	*bach*
黑莎草 *Gahnia tristis*	*gatr*	华润楠 *Machilus chinensis*	*mach*	多花杜鹃 *Rhododendron cavaleriei*	*rhca*
日本杜英 *Elaeocarpus japonicus*	*elja*	金叶含笑 *Michelia foveolata*	*mifo*	黑莎草 *Gahnia tristis*	*gatr*
甜槠 *Castanopsis eyrei*	*caey*	罗浮槭 *Acer fabri*	*acfa*	鲫鱼胆 *Maesa perlarius*	*mape*
狗脊 *Woodwardia japonica*	*woja*	少叶黄杞 *Engelhardtia fenzelii*	*enfe*	少花柏拉木 *Blastus pauciflorus*	*blpa*
南烛 *Vaccinium bracteatum*	*vabr*	柏拉木 *Blastus cochinchinensis*	*blco*	乌泡子 *Rubus gentilianus*	*ruge*
网脉山龙眼 *Helicia reticulata*	*here*	镰羽贯众 *Cyrtomium balansae*	*cybl*	黑柃 *Eurya macartneyi*	*euma*
大果马蹄荷 *Exbucklandia tonkinensis*	*exto*	红楠 *Machilus thunbergii*	*math*	华润楠 *Machilus chinensis*	*mach*
鹿角栲 *Castanopsis lamontii*	*cala*	江南桤木 *Alnus trabeculosa*	*altr*	黄丹木姜子 *Litsea elongata*	*liel*
假地枫皮 *Illicium jiadifengpi*	*ilji*	乐东拟单性木兰 *Parakmeria lotungensis*	*palo*	毛桃木莲 *Manglietia moto*	*mamo*
厚叶鼠刺 *Itea coriacea*	*itco*	小果冬青 *Ilex micrococca*	*ilmi*	香花枇杷 *Eriobotrya fragrans*	*erfr*
毛果柃 *Eurya trichocarpa*	*eutr*	樟叶泡花树 *Meliosma squamulata*	*mesq*	链珠藤 *Alyxia sinensis*	*alsi*

这几种植物都具喜阳特性。藤本植物山蒟 *Piper hancei*、龙须藤 *Bauhinia championii* 和瓜馥木 *Fissistigma oldhamii* 等均分布在光照参数周围，受光照影响较大，且藤本植物对林下直射光的依赖性较强。在林隙中心的大多数蕨类，如阔鳞毛蕨 *Dryopteris championii*、单叶新月蕨 *Pronephrium simplex* 和深绿卷柏 *Selaginella doederleinii* 等均分布在叶面积指数较大的区域，说明多数蕨类植物尽管生长在林冠开度较大的环境中，却仍属耐阴性植物。

3 结论与讨论

3.1 森林群落冠层结构与植物生长型和生活型的关系

相对于密集的冠层结构，草本植物在稀疏冠层结构下的生物量会更多[24]。在林隙光照强的地方，林下植物的多度相对较高[25]。Gálhidy 等[26]认为草本植物在大林隙中的平均覆盖度和丰富度均比小林隙中的大。王永强等[27]认为，在林冠开度为 10%～30% 时，林下植物的多样性随林冠开度的增加略有增加，表现为不显著相关。该研究表明，不同冠层结构下乔木和灌木的多度均显著大于草本、藤本和蕨类。其中，乔木、藤本和蕨类植物没有显著性差异，而灌木和草本则差异显著，说明冠层结构对灌木和草本植物的生长影响较大。同时，不同冠层结构下，矮高位芽、小高位芽和地上芽均表现为显著差异，说明不同的冠层结构对植物的生活型有不同的影响。而地上芽在林下的多度为零，可能是由于地上芽对光有较大需求，不适合在郁闭度较大的林下生长。

3.2 森林群落冠层结构与物种分布的关系

冠层通过影响林下小气候、改变植被生长条件[28]，从而对林下植被的生长、更新与物种组成产生影响[29-30]。该研究表明，不同冠层结构下植物的物种组成与分布表现不一。林冠开度与林下光照条件直接相关，可通过影响林下光照进而影响植被生长[17]。其中，红楠 *Machilus thunbergii* 和少叶黄杞 *Engelhardtia fenzelii* 等均分布在林冠开度较小的阴蔽环境，这与房震等[31]研究中指出红楠喜湿耐阴林隙边缘的结论一致。而华山姜、石斑木和乐东拟单性木兰等物种则分布在林冠开度较大的区域。山蒟、龙须藤和瓜馥木等藤本高位芽植物均分布在直射光较大的强光区，阔鳞毛蕨、单叶新月蕨和深绿卷柏等蕨类植物则分布在叶面积指数较大的区域，说明藤本植物比蕨类植物更具喜光性。毛果柃 *Eurya trichocarpa* Korth、箬竹 *Indocalamus tessellatus*、粘毛杜鹃 *Rhododendron championae* 与黄丹木姜子这四种植物在不同冠层结构下均有分布，表明这 4 种植物具较强适应性并在群落中占据优势地位。同时，冠层结构参数与植物分布也具相关关系，林冠开度（CO）和叶面积指数（LAI）均与环境轴的夹角较小，表明与

植物分布的相关性较强，且CO和光照因子均与LAI成负相关，这与崔佳玉等[32]的研究一致。

研究中发现，一些珍稀濒危植物如金毛狗*Cibotium barometz*、白豆杉*Pseudotaxus chienii*和白桂木*Artocarpus hypargyreus*等仅生长于林隙边缘或林隙中心，乐东拟单性木兰、华南五针松*Pinus kwangtungensis*和福建柏*Fokienia hodginsii*等仅在林下和林隙边缘有分布。还有一些具有观赏价值或者药用价值的植物如檵木*Loropetalum chinense*和假地枫皮*Illicium jiadifengpi*等在林隙中心生长较好，戟叶圣蕨*Dictyocline sagittifolia*和光里白*Diplopterygium laevissima*等则分布在林下叶面积指数较大的区域。探究各冠层结构下不同功能性植物的分布特征，可明确其生长习性，并采取适当保护措施。

该研究还表明，林隙边缘的生活环境更适合植物群落的生长。相对于林冠开度较小的林下和林冠开度较大的林隙中心，林冠开度中等的林隙边缘的地面芽、地上芽和高位芽植物的物种丰富度和多度均较大。这与Connell[33]的“中等干扰假说”相符，即物种丰富度在受到中等强度干扰的环境中最大，在未受干扰和受到高强度干扰的环境中则相对较小。由于在未受干扰时，存在大量的先锋种，不利于其它物种的生长，有的甚至被排挤掉；相反，在受高强度干扰的环境中，大量物种因无法承受干扰而消失，只有少量的耐受性较高的物种还存在；而在中等强度干扰的环境中，先锋种受到一定的限制，同时又不至使一些物种因干扰而消失，因此大量的物种可以共存，物种丰富度最高。臧润国等[34]研究的南亚热带常绿阔叶林不同大小和发育阶段林隙的树种多样性，结果也显示物种丰富度和多样性指数随林隙大小的变化呈现单峰型趋势。

该研究采用间接梯度分析的方法，分析各物种的生活型和生长型特征及其与林下不同生境的关系，探讨了山地森林中优势种对光环境的选择，明确其耐阴或喜光特性，不但为研究亚热带山地森林生态系统更新和维持其生物多样性提供理论和数据支持，还可为城市园林及药用植物物种驯化和植物选择提供科学参考，并为亚热带森林生态系统多样性保护和珍稀濒危物种保育提供科学依据。但由于森林冠层结构的复杂性，对于林冠结构的形成过程、林冠成熟及达到顶级时期的动态变化和不同时期冠层结构形成的光环境条件对林下植被的影响，还没有做到很系统的研究。而叶面积指数和林冠开度应该可以指示这种时间和空间上的动态变化，但要确定其关系，还有待进一步的研究。

参考文献：

[1] Hansen A J, Phillips L B, Dubayah R, *et al.* Regional-scale application of lidar: Variation in forest canopy structure across the southeastern US[J]. Forest Ecology and Management,2014, 329: 214-226.

[2] 敬小丽，张 璐，杜伟静，等．南岭山地森林群落冠层结构对林下野生花卉的影响[J]. 西南农业学报，2015,28(2):833-838.

[3] 任 海，彭少麟．鼎湖山森林群落的几种叶面积指数测定方法的比较[J]. 生态学报，1997, 17(2):110-113.

[4] 李德志，臧润国．森林冠层结构与功能及其时空变化研究进展[J]. 世界林业研究，2004, 17(3):12-16.

[5] Ediriweera S, Singhakumara B M P, Ashton M S. Variation in canopy structure, light and soil nutrition across elevation of a Sri Lankan tropical rain forest[J].Forest Ecology and Management,2008, 256(6): 1339-1349.

[6] Gillespie T W, de Goede J, Aguilar L, *et al.* Predicting tree species richness in urban forests[J]. Urban Ecosystems,2017, 20(4): 839-849.

[7] Brunet J R, Valtinat K, Mayr M L, *et al.* Understory succession in post-agricultural oak forests: Habitat fragmentation affects forest specialists and generalists differently[J]. Forest Ecology and Management. 2011, 262(9): 1863-1871.

[8] Yu M, Sun O J. Effects of forest patch type and site on herb-layer vegetation in a temperate forest ecosystem[J]. Forest Ecology and Management,2013, 300(300): 14-20.

[9] Leibold J M C A. Ecological Niches: Linking Classical and Contemporary Approaches[J]. Biodiversity and Conservation, 2004, 13(9): 1791-1793.

[10] Steenberg J W N, Millward A A, Nowak D J, *et al.* Forecasting Urban Forest Ecosystem Structure, Function, and Vulnerability[J]. Environmental Management,2017,59(3):373-392.

[11] 侯志勇，谢永宏，陈心胜，等．洞庭湖湿地植物生活型与生态型[J]. 湖泊科学，2016,28(5): 1095-1102.

[12] 黎燕琼，郑绍伟，龚固堂，等．米仓山巴山水青冈群落结构特征及更新状况分析[J]. 四川林业科技，2014,35(2):44-46.

[13] 薛 睿，张继强，王三英，等．甘肃陇南地震扰动区植被群落特征[J]. 草业科学，2015,32(11): 1774-1780.

[14] Rowe N S T. Plant growth forms: An ecological and evolutionary perspective[J].New Phytologist,2005, 166(1): 61-72.

[15] 周会萍，职丽娟，蔡祖国，等．江西吉安退化湿地松群落外貌特征分析[J]. 江西农业大学学报，2009,31(4):690-694.

[16] 程 真，周光益，吴仲民，等．南岭南坡中段不同群落林下幼树的生物多样性及分布[J]. 林业科学研究，2015,28(4):543-550.

[17] 敬小丽，杜伟静，张 璐，等．南岭山地森林群落冠层结构与立木多度的关系 [J]. 中南林业科技大学学报，2014,34(5):59-65.

[18] Soudani K, Trautmann J, *et al.* Leaf area index and canopy stratification in Scots pine (*Pinus sylvestris* L.) stands[J]. International Journal of Remote Sensing,2002,23(18):3605-3618.

[19] Lertzman KP, Sutherland GD, Inselberg A, *et al.* Canopy gaps and the landscape mosaic in a coastal temperate rain forest[J]. Ecology,1996,77(4):1254-1270.

[20] 苏志尧，贾小容，解丹丹，等．用半球面影像技术测定城市林分的冠层结构参数 [J]. 华南农业大学学报，2007,28(2):65-68.

[21] Whittaker R H. Communities and ecosystems(2nd Revised edition)[M]. Prentice Hall (a Pearson Education Company): New Jersey, 1975:1-352.

[22] Raunkiaer C. The life-forms of plants and statistical geography[M]. Oxford:The Clarendon Press: 1934:1-359.

[23] 樊大勇，张旺峰，陈志刚，等．沿林冠开度梯度的银杉幼树对光的适应性 [J]. 植物生态学报，2005,29(5):713-723.

[24] Shirima D D, Pfeifer M, Platts P J, *et al.* Interactions between Canopy Structure and Herbaceous Biomass along Environmental Gradients in Moist Forest and Dry Miombo Woodland of Tanzania[J]. PLOS ONE,2015,10(11): e142784.

[25] 孙 东，朱 纯，熊咏梅，等．林隙光照对广州市风景林林下植物分布的影响 [J]. 华南农业大学学报，2011,32(4):63-66.

[26] Lhidy L S, Mih K B, Hagy A, *et al.* Effects of gap size and associated changes in light and soil moisture on the understorey vegetation of a Hungarian beech forest[J]. Plant Ecology, 2006, 183(1): 133-145.

[27] 王永强，蔡燕茹，曾焕忱，等．不同林冠开度下亚热带林下植物的组成和多样性 [J]. 西北农林科技大学学报（自然科学版），2016,44(5):64-72.

[28] Dumais D, Prévost M. Physiology and growth of advance Picea rubens and Abies balsamea regeneration following different canopy openings[J]. Tree Physiology,2014,34(2):194-204.

[29] Mori A S, Fukasawa Y, Takeda H. Tree mortality and habitat shifts in the regeneration trajectory underneath canopy of an old-growth subalpine forest[J].Forest Ecology and Management, 2008, 255(11): 3758-3767.

[30] Vizoso-Arribe O, Díaz-Maroto I, Vila-Lameiro P, *et al.* Influence of the canopy in the natural regeneration of Quercus robur in NW Spain[J]. Biologia,2014,69(12):1678-1684.

[31] 房 震．红楠的特征特性及育苗技术 [J]. 现代农业科技，2012(6):220-221.

[32] 崔佳玉，曾焕忱，王永强，等．银瓶山自然保护区阔叶林冠层结构与辐射消减效应 [J]. 西北林学院学报，2015,30(4):45-49.

[33] Connell J H.Diversity in tropical rain forest and coral reefs[J]. Science,1978,199: 1302-1310.

[34] 臧润国，王伯荪，刘静艳．南亚热带常绿阔叶林不同大小和发育阶段林隙的树种多样性研究 [J]. 应用生态学报，2000, 11(4):485-488.

[本文编校：吴 毅]

（上接第36页）

[8] 李 欢，李建贵．果园微气候及土壤养分对灰枣果实矿物元素含量的影响 [J]. 经济林研究，2016,34(3):8-15.

[9] 董敏慧，张良成，文 丽，等．松树-樟树混交林、纯林土壤微生物量碳、氮及多样性特征研究 [J]. 中南林业科技大学学报，2017,37(11):146-153.

[10] 王年金，张盛剿，钱小娟，等．樟树地理种源幼林期生长性状差异分析及优良种源初步选择 [J]. 浙江林业科技，2009, 29(4): 69-72.

[11] 盖钧镒．试验统计方法 [M]. 北京：中国农业出版社，2000.

[12] 张志杰．樟树人工林经营效果分析 [J]. 绿色科技，2014(7):87-88.

[13] 朱有章．培育樟树速生良材的好途径——杉、樟混交 [J]. 江西林业科技，1982(2):19-20.

[14] 刘德良，王楚正．几种樟树育苗及幼苗生长特性观察 [J]. 经济林研究，2003,21(1):25-28

[15] 田大伦，陈书军．樟树人工林土壤水文-物理性质特征分析 [J]. 中南林学院学报，2005,25(2):1-6.

[本文编校：吴 毅]

中南林业科技大学学报
ZHONGNAN LINYE KEJI DAXUE XUEBAO

（月刊，1981年创刊）
第38卷第7期（总第205期） 2018年7月出版

主管单位 湖南省教育厅
主办单位 中南林业科技大学
主　　编 吴义强
社　　长 伍　谦
编辑出版《中南林业科技大学学报》编辑部
湖南长沙市韶山南路498号 邮政编码：410004
电话：0731-85623395
http://qks.csuft.edu.cn
印　　刷 长沙市雅捷印务有限公司
国外总发行 中国出版对外贸易总公司
（北京782信箱，邮编：100011）
国内发行 中南林业科技大学期刊社

JOURNAL OF CENTRAL SOUTH UNIVERSITY OF FORESTRY & TECHNOLOGY

(Monthly, Started in 1981)
Vol. 38 No. 7 (Sum 205) Jul. 2018

Administered by Education Department of Hunan Province

Sponsored by Central South University of Forestry & Technology

Chief Editor WU Yiqiang

Periodicals Press Director WU Qian

Edited & Published by Ed.Dept.of Journ.of CSUFT
(Changsha 410004, Hunan, China)
http://qks.csuft.edu.cn

Printed by Changsha Yajie Color Printing Co. Ltd.

Distributed abroad by China National Publishing Industry Trading Corporation
(P.O.BOX 782, Beijing,100011, China)

Distributed domestically by Periodicals Press of CSUFT

刊　　号：ISSN 1673-923X
CN43-1470/S
订阅网址：www.kankan.com.cn
国内定价：20.00元/本

中国中文核心期刊
中国科技核心期刊
中国科学引文数据库来源期刊
广西十强期刊

ISSN 1000-3142
CODEN GUZHEI

广西植物

GUIHAIA

第38卷 第7期 Vol. 38 No. 7

广西壮族自治区中国科学院广西植物研究所 广西植物学会 主办
Guangxi Institute of Botany, Guangxi Zhuang Autonomous Region and Chinese Academy of Sciences
Guangxi Society of Botany

科学出版社 Science Press 出版

7
2018

广西植物
GUANGXI ZHIWU

2018 年 7 月　第 38 卷 第 7 期
（月刊）

目　　次

期刊基本参数：CN 45-1134/Q * 1981 * m * A4 * 144 * zh+en * P * ￥45.00 * 1200 * 16 * 2018-07

封面说明：秋海棠属（*Begonia* L.）系秋海棠科（Begoniaceae）多年生草本植物，全球约有1 800余种，广布热带和亚热带地区，温带也有分布。中国是秋海棠属植物种类自然分布较为丰富的国家之一，现已知并发表的种类224 种，其中 197 种为中国特有的分布种类，约占中国分布种类的87.9%。秋海棠属植物花朵艳丽，叶形千差万别，几乎包含了植物界所有的叶形，叶片斑纹丰富多样、色彩华丽，具有很高的观赏价值，是一种极为优良的草本观赏花卉。照片示：部分代表性秋海棠属植物。1. 马关秋海棠-雄花；2. 球根秋海棠品种；3. 橙花秋海棠-雌花；4. 广西秋海棠-花序；5. 马山秋海棠-花序；6. 皮尔斯秋海棠-雄花；7. 玻利维亚秋海棠-雌雄花。（相关内容详见本期正文 851~858 页李景秀等的文章）

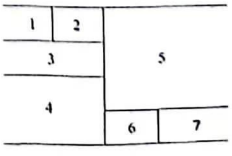

广西植物 Guihaia Jul. 2018, 38(7): 866-875
http://journal.gxzw.gxib.cn
http://www.guihaia-journal.com

DOI: 10.11931/guihaia.gxzw201705024
引文格式：蔡琳颖, 张星元, 张璐, 等. 珍稀濒危植物紫荆木生态学研究进展 [J]. 广西植物, 2018, 38(7): 866-875
CAI LY, ZHANG XY, ZHANG L, et al. Research advances on ecological characteristics of a rare and endangered plant *Madhuca pasquieri* [J]. Guihaia, 2018, 38(7): 866-875

珍稀濒危植物紫荆木生态学研究进展

蔡琳颖, 张星元, 张 璐*, 马 丁

(华南农业大学 林学与风景园林学院, 广州 510642)

摘 要: 珍稀濒危植物作为生物多样性的重要组成部分,是保护生物学研究的核心内容之一。紫荆木(*Madhuca pasquieri*)为现状稀有种,IUCN名录中濒危等级为VU易危,在中国被列为国家重点保护野生植物(Ⅱ级)和极小种群野生植物,是稀有的油料树种和珍贵的用材树种,具有极高的药用价值。在全球气候变化和生境破碎化的大背景下,紫荆木的现状研究和保护策略的制定显得尤为重要。该文介绍了紫荆木自然地理分布、群落生态学特征,归纳总结了国内外的保护应用及研究现状。目前针对紫荆木就地保护、迁地保护、化学成分、人工培育技术等方面已开展了一些研究工作,但研究仍处于初级阶段。下一步可完善紫荆木分布信息,并结合野外调查和长期实验,系统研究其生物及生态学特性。同时,将就地保护、迁地保护和回归有机结合,应用分子生物学技术加强紫荆木育种、繁殖和栽培技术的研究,建立繁殖培育基地,并积极开发其经济价值,在园林绿化中推广应用。

关键词: 地理分布, 群落特征, 生境, 物种保护, 紫荆木

中图分类号: Q948 **文献标识码**: A **文章编号**: 1000-3142(2018)07-0866-10

Research advances on ecological characteristics of a rare and endangered plant *Madhuca pasquieri*

CAI Linying, ZHANG Xingyuan, ZHANG Lu*, MA Ding

(*College of Forestry and Landscape Architecture, South China Agricultural University*, Guangzhou 510642, China)

Abstract: As an important component of biodiversity, rare and endangered plants are one of the core contents of conservation biology. *Madhuca pasquieri*, a rare species currently, is regarded as VU (vulnerable) species in the IUCN Red List and listed as a kind of national key protected wild plants (Ⅱ) and wild plants of extremely small population. It is also a kind of rare oil tree species and precious timber species with high medicinal value. Due to the global climate change and the habitat fragmentation, it is rather important to study the current situation of *M. pasquieri* and formulate relevant conservation strategies. Based on the data of specimen records of herbariums, this paper mainly introduced the

收稿日期: 2017-08-14
基金项目: 国家林业局资助项目(2130211); 广东省省级林业发展及保护专项项目(林业科技创新项目 2017KJCX037); 广东省自然科学基金自由申请项目(2015A030313403) [Supported by the State Forestry Administration (2130211); Guangdong Provincial Special Fund for Forestry Development and Protection (Forestry Science and Technology Innovation Program, 2017KJCX037); Guangdong Natural Science Foundation (2015A030313403)]。
作者简介: 蔡琳颖(1993-),女,广东汕头人,硕士研究生,主要从事森林生态学的研究,(E-mail)296575369@qq.com。
通信作者: 张璐,博士,副教授,硕士研究生导师,主要研究方向为森林生态学和保护生物学,(E-mail)zhanglu@scau.edu.cn。

natural geographical distribution of *M. pasquieri*, compared population and community characteristics of the main distribution sites of *M. pasquieri* and systematically analyzed the current research and protection at domestic and overseas. The results are as follows: (1) With a wide range of vertical distribution from 200 to 1 400 m above, wild populations of *M. pasquieri* are mainly distributed in North Vietnam, South Guangxi, Southwest Guangdong and Southeast Yunnan. (2) The community of *M. pasquieri* forest has abundant species in tree layer, shrub layer, herb layer and vine layer. *M. pasquieri* is the dominant species in the main forest layer or important companion species in acid rain forest in Guangxi. (3) Mainly scattered in the warm and humid habitat, *M. pasquieri* is tolerant of drought and barren environments with krasnozem and laterite soil. It is concluded that the research of *in situ* and *ex situ* conservations, chemical composition and artificial cultivation of *M. pasquieri* have been carried out. However, these researches are still in primary stages. The following are hoped to be strengthened in the future: The supplement of the distribution information, field investigations with long-term experiment and the reintroduce of *M. pasquieri* based on *in situ* and *ex situ* conservations. Furthermore, molecular biology techniques are needed to strengthen the breeding, propagation and cultivation techniques of *M. pasquieri*, and can be actively developed for economic value and can be applied in landscaping.

Key words: geographical distribution, community characteristics, habitat, species conservation, *Madhuca pasquieri*

近年来，随着全球气候变化和人类对自然资源的滥用及对植物生境的破坏，生物多样性丧失已成为全球最严重的环境问题之一（Cardinale et al, 2012; Chapin et al, 2000）。珍稀濒危野生植物作为生物多样性的重要组成部分，如何对它们进行有效的保护是生态学家和保护生物学家亟待解决的问题之一（张殷波和马克平，2008）。目前，对珍稀濒危植物的保护研究主要集中在其地理分布和繁殖培育技术方面。在地理分布上，应用地理信息技术（Geo-Information）获得濒危植物分布热点（hotspots）（Huang et al, 2012）及生境特点（Varghese & Murthy, 2006），明确重点植物保护区域（priority protected areas）（Wang et al, 2015）。物种分布模型（species distribution modeling）（Rovzar et al, 2016），生态位模型（ecological niche modeling）也被广泛应用到濒危植物研究中（Araujo & Peterson, 2012）。在繁殖培育技术上，国内外研究集中于生物技术（biotechnology）（Engelmann, 2011; Khan et al, 2012; Slazak et al, 2015; Gushi et al, 2015）、回归（reintroduction）（Griffith et al, 1989; Godefroid et al, 2011; Bullock & Hodder, 1997; Ren et al, 2012）、生态恢复（restoration）（Liu et al, 2014）等方面。

紫荆木（*Madhuca pasquieri*），又名滇紫荆木、滇木花生、出奶木（云南），铁色、木花生（广西），马胡卡、海胡卡（广东），与海南紫荆木（*Madhuca hainanensis*）同属于紫荆木属（*Madhuca*）山榄科（Sapotaceae）。紫荆木为常绿乔木，高可达 30 m，胸径可达 60 cm，观花、观果，果可食（Fan et al, 2011），具有药用价值（Hoang et al, 2015, 2016）。紫荆木含丰富的乳汁，可提取硬橡胶。紫荆木还是稀有的油料树种（Franzke et al, 1971）。紫荆木与格木（*Erythrophleum fordii*）、铁力木（*Mesua ferrea*）、铁木（*Ostrya japonica*）并称广西“四大硬木”，是珍贵的用材树种。在越南北部富寿省、河静省等地区，紫荆木被广泛应用于家具制造和单板制造，在家庭使用中被用做锯材、薪柴（Kien & Harwood, 2016）。紫荆木在越南已被用作治疗细菌感染和糖尿病（Hoang et al, 2015, 2016）。紫荆木为现状稀有种，IUCN 名录中濒危等级为 VU 易危，在中国被列为国家重点保护野生植物（Ⅱ级）（中华人民共和国国务院正式批准公布中国植物学会，1999）、极小种群野生植物、全国重点植物保护对象、广西重点保护植物。然而，自然状态存活的紫荆木种群规模小，种群数量仍在缩减。

本研究广泛调查和收集紫荆木野生种群各分布点的保护管理和监测数据资料，并查阅中国数字植物标本馆（http://www.cvh.org.cn）、中国科学院华南植物园标本馆（http://herbarium.scbg.cas.cn/）以及中国自然植物标本馆（http://

www.cfh.ac.cn/)标本记录,在对紫荆木的地理分布资料进行了梳理,构建地理分布数据库的基础上,综述了紫荆木的自然地理分布、群落生态学特征、保护应用及研究现状,从生态学角度剖析紫荆木面临的问题,并指出未来可能的发展方向。

1 紫荆木的地理分布

1.1 紫荆木的水平地理分布

从水平分布的纬向来看,紫荆木大致分布在北回归线上,属热带性植物。紫荆木野生种群自然分布区域主要集中在越南北部以及我国的广西南部、广东西南部和云南东南部,贵州荔波石灰岩山地和山顶偶有分布。在越南北部,紫荆木野生种群广泛分布于富寿省、东京郎昂村细黄毛山、凉山温州、河静省,西北部的奠边、莱州、山萝省,中部顺化西南部均有分布(Dung & Webb, 2008;Tran et al, 2005)。在中国广西,紫荆木野生种群分布区主要为北热带季风区,包括梧州、防城、东兴、玉林、上思、武鸣、宁明、龙州、靖西、钦县等地(吴庆初,1990;王双玲等,2011)。在中国广东,紫荆木野生种群主要分布于封开、广宁、信宜、阳春、乐东等地(陈里娥等,1997;缪绅裕等,2008)。在中国云南,紫荆木野生种群分布于南热带季风区,主要分布点有绿春县黄连山,屏边县玉屏乡新农,麻栗坡县八布乡等地(西部林业科学编辑部,1979;施莹和杨斌,2009)。

1.2 紫荆木的垂直地理分布

紫荆木野生种群的垂直分布范围较广,从200 m到1 400 m均有分布(表1)。在广西和广东,紫荆木野生种群多集中在海拔200~600 m的低山或丘陵(吴庆初,1990)。在云南,紫荆木野生种群在海拔1 000 m以上保持较好(李玉媛等,2003)。广西多山地丘陵,广东地形以低山、丘陵为主,云南地处低纬度高原。

紫荆木生境分布范围较广。其野生种群在山顶、山谷、土山、石山,石上、石缝、石边,水旁、河边、路边、沟谷旁,灌木林边缘山地、密林、疏林、疏林灌丛,山谷疏林、林缘、林中均有分布(西部林业科学编辑部,1979)。

2 紫荆木的群落生态学特征

2.1 紫荆木的群落特征

在广西低山丘陵常绿季雨林中,常见的天然植被类型有毛果石栎(*Lithocarpus pseudovestitus*)+紫荆木林,紫荆木+南岭山矾(*Symplocos confusa*)+黄果厚壳桂(*Cryptocarya concinna*)林,紫荆木+格木林(温远光等,2014)。在广西十万大山、大青山和六万大山一带的酸性土地季雨林中,紫荆木是主林层优势种或重要的伴生种(王献溥和胡舜士,1982;向悟生等,2015)。已确定的群丛包括紫荆木+厚壳桂(*Cryptocarya chinensis*)—肾形果(*Pygeum topengii*)—九节木(*Psychotria rubra*)—华山姜(*Alpinia chinensis*)群丛以及紫荆木—岭南山竹子(*Garcinia oblongifolia*)—罗伞树(*Ardisia quinquegona*)+九节木—金狗毛(*Cibotium barometz*)群丛。以紫荆木为主的季节性雨林,乔木层、灌木层、草本层、藤本层物种组成丰富(图1)(王献溥等,2001)。

而以大果马蹄荷(*Exbucklandia tonkinensis*)、小叶红光树(*Knema guangxiensis*)、风吹楠(*Horsfieldia amydalina*)、红鳞蒲桃(*Syzygium hancei*)为主的季节性雨林,主林层包括紫荆木在内的种类较多(王献溥等,2001)。从整个乔木层来分析,紫荆木是重要的伴生种。在云南河口、屏边大围山、紫荆木林分布有明显的垂直分带(西部林业科学编辑部,1979)(图2)。

在海拔1 000 m以下时,紫荆木分布在准热带沟谷雨林,而分布在海拔1 000~1 400 m的热带山地雨林群落,紫荆木可在林中成为优势树种、主要伴生树种分为3层。群落外貌浓密、林相整齐、郁闭度在0.7以上,林分蓄积量高、林内空旷、通视良好。地面及树干上都有很丰富的地衣,形成一种比较典型的热带山地雨林。当海拔升高在1 400 m以上时,紫荆木零星分布,逐渐过渡到栎类苔鲜林。

2.2 紫荆木的生境及生长特征

紫荆木主要分布区气候温暖潮湿,土壤多为由花岗岩、砂岩和页岩发育而成的红壤和砖红壤

表 1　不同海拔高度紫荆木的生境特征

Table 1　Habitat characteristics of *Madhuca pasquieri* at different altitudes

海拔 Altitude (m)	生境 Habitat		
	广西 Guangxi	广东 Guangdong	云南 Yunnan
200～600	山顶、疏林、石山、山谷、密林、石上、水旁、路边、沟谷旁，灌木林边缘山地、石缝、山地(土山) Top of mountain, woodland, stone mountain, valley, dense forest, on the stone, top water side, road side, beside valley, shrub edge mountain, alcove, hill (earth piled hill)	疏林、林缘、山地、山顶 Woodland, forest margin, mountain, mountain top	少见 Seldom
600～1 000	山地、灌丛 Mountain, brushwood	少见 Seldom	山地、密林、灌丛 Mountain, dense forest, brushwood
1 000～1 400	山谷、疏林 Valley, sparse forest	林中、石边、疏林、河边 Forest, stone edge, woodland, riverbank	林中、疏林 Forest, woodland

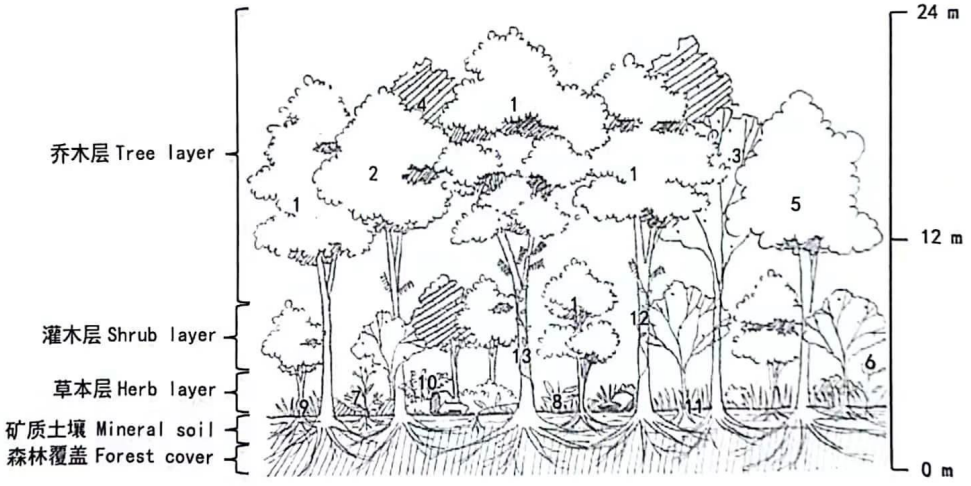

图 1　广西酸性土以紫荆木为主的季节性雨林结构剖面图

Fig. 1　Structure section of seasonal rain forests dominated by *Madhuca pasquieri* in acid soil regions of Guangxi

性红壤，pH 值 4.5～6.2(吴庆初，1990)，土层深厚，质地粘重。作为阳性树种，紫荆木能耐干旱瘠薄的环境，在石灰岩山地和土山上也能生长。植被类型常为石灰岩季雨林、常绿阔叶林、混交林和山地雨林。

越南清化省自然保护区分布有紫荆木纯林、紫荆木格木混交林、紫荆木印度苦槠(*Castanopsis indica*)混交林(Pham, 2011)。紫荆木在密林中生长缓慢，寿命很长。在密林林冠下，紫荆木天然更新良好，林下幼苗生长良好，大部分由种子萌发，高度小于 1 m。格木林下的紫荆木生长受到限制，为获取林下有限的光资源，树冠偏离中心。紫荆木幼苗和种子呈集群分布。紫荆木密度较高，多由成熟树组成。紫荆木更新速率高，但苗木的成活率低。在郁闭度 0.65～0.75 的林中，紫荆木生长速率和成活率最高。

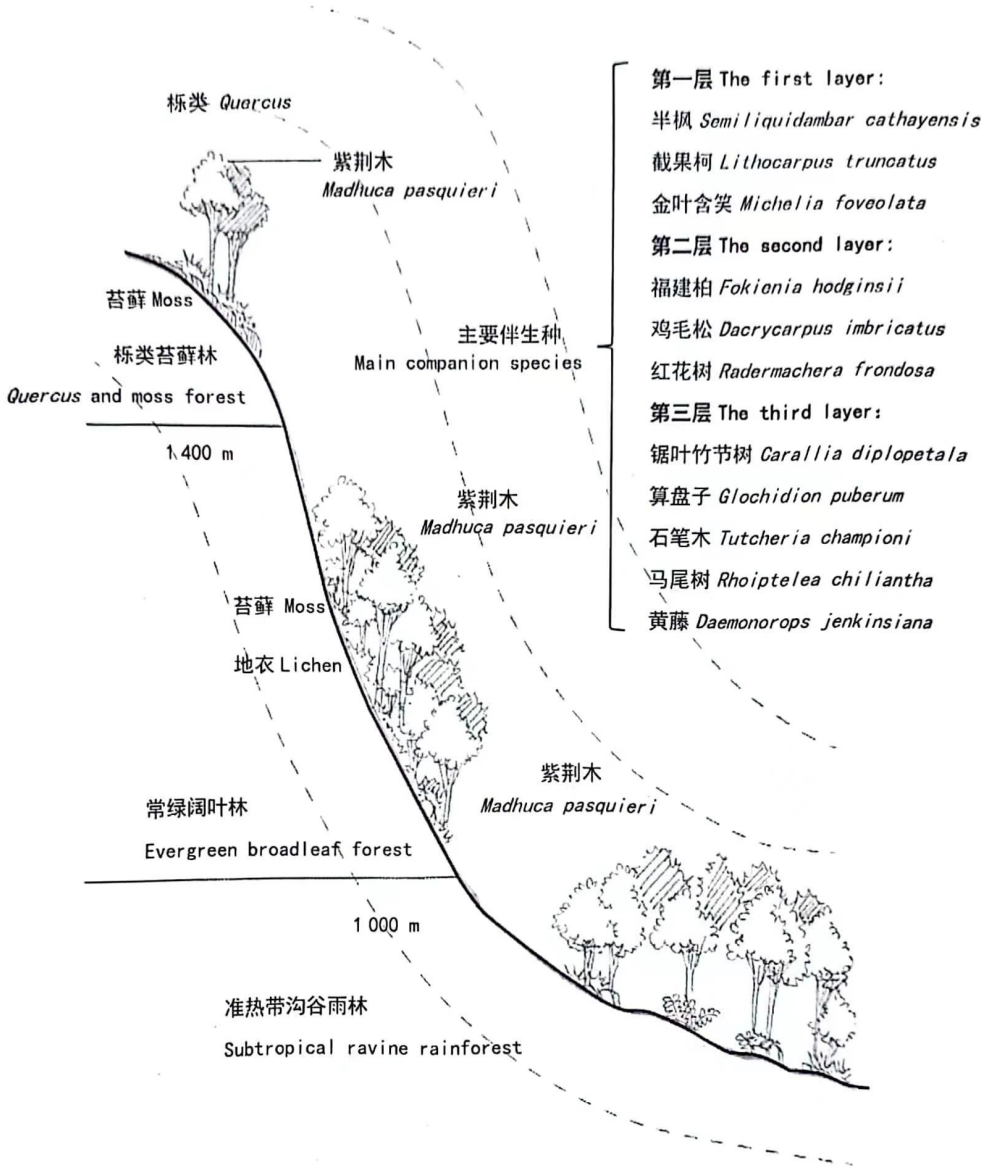

图 2 云南河口、屏边大围山紫荆木群落特征

Fig. 2 Community characteristics of *Madhuca pasquieri* at Hekou and Pingbian Mountain in Yunnan

在广西红鳞蒲桃季雨林中，紫荆木高温胁迫半致死温度为 53.7 ℃，低温胁迫半致死温度为 -4.0 ℃（莫竹承等，2013a），能适应广西海岸的极端温度，因此不影响其在广西海岸的分布与生长。紫荆木的物候特征受降水量和日照时数的影响（莫竹承等，2013b）。新梢期、展叶期分别出现在日照时数多和降水量大的 5 月和 6 月，在 6—9 月的雨季开花，9 月到次年 4 月结果。

3 紫荆木保护应用及研究现状

目前，国内外针对紫荆木就地保护、迁地保护、化学成分、人工培育等开展了研究，但仍处于初级阶段，尤其缺乏长期的跟踪观测（表2）。在

表 2　紫荆木研究现状

Table 2　Research overview on *Madhuca pasquieri*

内容 Content	发现 Main result	国家 Country	来源 Reference
就地保护 *In situ* conservation	在广西弄岗自然保护区，广东罗浮山自然保护区、鼎湖山自然保护区，英德石门台自然保护区，连州田心保护区等开展。Nonggang Nature Reserve in Guangxi, Guangdong Luofu Mountain Nature Reserve, Dinghu Mountain Nature Reserve, Yingde Shimentai Nature Reserve, Lianzhou Tianxin Reserve.	中国 China	王俊浩，1994；邓华格等，2010；缪绅裕等，2013
迁地保护 *Ex situ* conservation	广东树木公园、华南农业大学树木园、云南西双版纳植物园、华南植物园、越南清化省紫荆木保护区开展。Guangdong Trees Park, Arboretum of South China Agricultural University, Yunnan Xishuangbanna Botanical Garden, South China Botanical Garden, Tam Qui Natural Madhuca Reserve.	中国 China	温小莹等，2006；吴水彬和冯志坚，2006（http://herbarium.scbg.cas.cn/）
化学成分 Chemical content	从紫荆木树叶中提取出吡咯里西啶生物碱，进行分离和鉴定，研究其抗炎和细胞毒性的活动；提取出的一种新的高单萜苷，并研究分离化合物对 NO 合成的影响。Pyrrolizidine alkaloid and madhumidine A were isolated and identified from leaves of *Madhuca pasquieri*, and their anti-inflammatory and cytotoxic activities were studied. A new high-monoterpenoid glycoside was extracted and the effect of isolated compounds on NO production were studied.	韩国 Korea	Hoang et al, 2015, 2016
培育技术 Cultivating technology	根据紫荆木种子发芽快的特点，应推广采用容器育苗。Container seedling can be promoted, according to the characteristics of fast germination of the seeds.	中国 China	吴庆初，1990
种子育苗 Seed seedling	紫荆木的芽苗切根处理保留胚根长 2～4 cm，成活率最高，根系及植株的生长量也最大。Keep the radicle 2–4 cm with the highest survival rate and the biggest root and plant growth of *M. pasquieri*.	中国 China	宾耀梅等，2015
温度胁迫 Temperature stress	紫荆木高温胁迫半致死温度为 53.7 ℃，低温胁迫半致死温度为−4.0 ℃。Semilethal temperature（LT50）is 53.7 ℃, the cold LT50 is −4.0 ℃.	中国 China	莫竹承等，2013a
移栽胁迫 Transplanting stress	移栽胁迫对紫荆木的影响较小。Transplanting stress has little effect on *M. pasquieri*.	中国 China	曾聪等，2014
NaCl 胁迫 Nacl stress	NaCl 浓度越高，紫荆木开始发芽时间和最大发芽量时间越往后推迟。Higher NaCl concentration means later germination beginning time, later occurring time of maximum germination amount, shorter interval and lower maximum germination amount.	中国 China	李建凡等，2014

韩国，学者对紫荆木的化学成分和生物活性进行研究。越南清化省已建立保护区作为紫荆木培育基地，研究其生长情况，开展保护和引种栽培（Pham, 2011）。

当前人工培育的紫荆木既有实生苗（施莹等，2009），也有扦插育苗。紫荆木种子发芽快，建议推广采用容器育苗（吴庆初，1990）。芽苗切根能抑制根系的顶端优势，促进须根和侧根的生长。紫荆木的芽苗切根处理保留胚根长 2～4 cm，成活率最高，根系及植株的生长量也最大（宾耀梅等，2015）。

种子的萌发直接影响着种群的生存和发展，因此研究影响种子的萌发因素，对提高紫荆木幼苗的生长有着至关重要的作用。紫荆木种子萌发受 NaCl 胁迫影响极其显著，无浓度（0 mmol · L^{-1}）和低浓度（50 mmol · L^{-1}）条件下最适合种子萌发。在低浓度的 NaCl 胁迫下紫荆木种子各生长指标较高，高浓度时则具有明显的抑制作用。

移栽是植被恢复和重建的主要组成部分，研究苗木忍耐移栽胁迫的能力，对其移栽成活及生长非常重要。在红鳞蒲桃季雨林树种中，紫荆木的最佳移栽时间为起苗后 16 h 内，移栽胁迫对紫荆木的影响较小（曾聪等，2014）。

紫荆木目前零星分布于各自然保护区内，数量较少。就地保护是保护紫荆木的主要方式，主要通过保护紫荆木的种质资源及它们藉以生存的

自然生态系统实施保护(严岳鸿等,2004;邓华格等,2010;缪绅裕等,2013;王俊浩,1994)。迁地保护在云南西双版纳植物园、华南植物园、鼎湖山树木园有一定进展(吴永彬和冯志坚,2006;温小莹等,2006;王俊浩,1994),紫荆木在华南农业大学树木园、鼎湖山自然保护区生长良好。目前国内外了开展大量的珍稀濒危植物回归工作,其中研究比较系统的有报春苣苔(*Primulina tabacum*)、虎颜花(*Tigridiopalma magnifica*)、滇瑞木(*Acer yangbiense*)等(任海等,2014),但目前国内外尚未对紫荆木开展回归研究。

4 研究展望

4.1 完善物种分布信息

研究表明,紫荆木野生种群自然分布区域主要集中在越南北部以及我国的广西南部、广东西南部和云南东南部。但是,物种分布信息不全面,部分植物标本缺乏海拔记录。因此,在地理分布基础上,开展紫荆木资源与分布区现状调查,分析地理分布规律、区系特征,完善标本记录,建立 GIS 信息管理系统档案。同时根据全球气候预测模型,将气候对紫荆木地理分布的可能影响进行预测,可为今后紫荆木的科学管理和进一步深入研究提供信息支撑。

4.2 开展野外群落学调查

紫荆木群落的物种组成丰富,垂直分布范围较广,在云南河口、屏边大围山的分布有明显的垂直分带。然而,在全球气候变化的条件下,受热量和水分影响的紫荆木分布格局变化还有待进一步研究。并且,目前仅对广西、云南的紫荆木野生种群有进行过群落调查,缺乏对其种群结构特征和动态演替规律的全面研究,譬如水平生态位、垂直生态位。可进一步在紫荆木主要分布点展开调查,对比研究其种群结构、空间分布格局动态、种间关联及环境因子尤其是海拔梯度对其种群分布的影响等,以探讨紫荆木分布格局及其形成机制,不仅对保护、恢复与扩大紫荆木的种群,发展其植物资源具有十分重要的意义,还可为分析亚热带、热带山地雨林多物种共存机制提供参考。

4.3 就地保护、迁地保护和回归有机结合

通过就地保护、迁地保护、回归三位一体的方式实现对珍稀濒危植物的保护(任海等,2014)。紫荆木野生种群地理分布研究揭示,紫荆木多分布在海拔较低的低山或丘陵。再加上人们无限制采收,其原有的生态环境受到毁林开荒等一系列人类活动的破坏,造成种群面积缩小和生境破碎化。因此加强就地保护,即在现有自然保护区和国家公园体系原生境保护的基础上,在紫荆木分布相对集中的区域,建立就地保护点位和长期固定监测样地,对低山、丘陵等被破坏的生境进行生态恢复,适时监测各地紫荆木的种群,建立物种就地保护点档案,为开展珍稀濒危植物的生态学与生物学特性研究以及探索其致濒原因提供宝贵的材料和基地(Ren et al, 2010)。

与此同时,通过植物园及其它引种设施对紫荆木进行迁地保护。进行合理的紫荆木种子保存工作和离体保存植物的器官和组织(吴小巧等,2004),深入研究人工培育技术,建立紫荆木的繁殖基地,扩大种群数量,为紫荆木种群恢复提供后备资源,使物种得以保存和繁衍进一步成为普通树种和园林绿化树种,促进城市绿化物种多样化。

对紫荆木实行野外回归工作应以就地保护和迁地保护为支撑,通过人工繁殖把植物引入到其原来分布的自然或半自然的生境中,以建立具有足够的遗传资源来适应进化改变、可自然维持和更新的新种群(Griffith et al, 1989)。在充分了解紫荆木生态学和生物学特性、繁育性状、遗传多样性水平等基础上(Wang et al, 2013),选择与紫荆木相同或相似的生境。利用生境分布模型预测适宜的回归地点(Adhikari et al, 2012),开展野外回归工作。这三类保护措施相辅相成、有助于实现对紫荆木的有效保护。

5 结论

紫荆木为现状稀有种,IUCN 名录中濒危等级为 VU 易危,在中国被列为国家重点保护野生植物(Ⅱ级)和极小种群野生植物,是稀有的油料树种和珍贵的用材树种,具有极高的药用价值。在全

球气候变化和生境破碎化的大背景下，很有必要开展紫荆木的现状研究和制定保护策略。目前国内外在紫荆木的就地保护、迁地保护、人工培育技术等方面已开展了一些研究工作，但仍处于初级阶段。基于前人的研究经验，下一步建议完善野生紫荆木分布信息，开展野外群落学调查，并将就地保护、迁地保护和回归有机结合，并应用分子生物学技术加强紫荆木育种、繁殖和栽培技术的研究，以期实现对紫荆木的有效保护。

参考文献：

ADHIKARI D, BARIK SK, UPADHAYA K, 2012. Habitat distribution modelling for reintroduction of *Ilex khasiana* Purk. a critically endangered tree species of northeastern India [J]. Ecol Eng, 40(3): 37-43.

ARAUJO MB, PETERSON AT, 2012. Uses and misuses of bioclimatic envelope modeling [J]. Ecology, 93(7): 1527-1539.

BIN YM, SUN X, LI L, et al, 2015. The effect of taproot-cutting treatments on seedling growth of *Madhuca pasquieri* [J]. Guangxi For Sci, 25(1): 63-66. [宾耀梅，孙熹，李璐，等，2015. 不同芽苗切根育苗处理对紫荆木苗木生长的影响 [J]. 广西林业科学，25(1)：63-66.]

BULLOCK JM, HODDER KH, 1997. Reintroduction: challenges and lessons for basic ecol [J]. Trends Ecol Evol, 12(2): 68-69.

CARDINALE BJ, DUFFY JE, GONZALEZ A, et al, 2012. Biodiversity loss and its impact on humanity [J]. Nature, 486(7401): 59-67.

CHAPIN FR, ZAVALETA ES, EVINER VT, et al, 2000. Consequences of changing biodiversity [J]. Nature, 405(6783): 234-242.

CHEN LE, YU SX, MIAO RH, 1997. Rare and endangered plants and their distribution in Guangdong [J]. J Trop Subtrop Bot, 5(4): 1-7. [陈里娥，余世孝，缪汝槐，1997. 广东省国家级珍稀濒危保护植物及其分布 [J]. 热带亚热带植物学报，5(4)：1-7.]

DENG HG, WEN ZT, MIAO SY, et al, 2010. Species diversity of wild rare and endangered plants and characteristics of *Erythrophleum fordii* community on Luofushan [J]. For Sci Technol Guangdong, 26(3): 35-41. [邓华格，温志滔，缪绅裕，等，2010. 广东罗浮山珍稀濒危植物多样性及格木群落特征 [J]. 广东林业科技，26(3)：35-41.]

DUNG NT, WEBB EL, 2008. Combining local ecological knowledge and quantitative forest surveys to select indicator species for forest condition monitoring in central Vietnam [J]. Ecol Ind, 8(5): 767-770.

ENGELMANN F, 2011. Use of biotechnologies for the conservation of plant biodiversity [J]. In Vitro Cell Dev Biol-Plant, 47(1SI): 5-16.

FAN P, FEI H, SCOTT MB, et al, 2011. Habitat and food choice of the critically endangered cao vit gibbon (*Nomascus nasutus*) in China: Implications for conservation [J]. Biol Conserv, 144(9): 2247-2254.

FRANZKE C, DUONGUONG TP, HOLLSTEIN E, 1971. Fatty acid composition of wild seeds of wildly growing oil-bearing plants of Vietnam [J]. Fette Seifen Anstrichm, 73(10): 639-642.

GASHI B, ABDULLAI K, SOTA V, et al, 2015. Micropropagation and *in vitro* conservation of the rare and threatened plants *Ramonda serbica* and *Ramonda nathaliae* [J]. Physiol Mol Biol Plant, 21(1): 123-136.

GODEFROID S, PIAZZA C, ROSSI G, et al, 2011. How successful are plant species reintroductions? [J]. Biol Conserv, 144(2): 672-682.

GRIFFITH B, SCOTT JM, CARPENTER JW, et al, 1989. Translocation as a species conservation tool: status and strategy [J]. Science (New York), 245(4917): 477-480.

HOANG LS, TRAN MH, LEE JS, et al, 2015. Anti-inflammatory activity of pyrrolizidine alkaloids from the leaves of *Madhuca pasquieri* (Dubard) [J]. Chem Pharm Bull (Tokyo), 63(6): 481-484.

HOANG LS, TRAN MH, NGUYEN VT, et al, 2016. Isolation of a new homomonoterpene from *Madhuca pasquieri* and effect of isolated compounds on NO production [J]. Nat Prod Comm, 11(6): 729-732.

HUANG J, CHEN B, LIU C, et al, 2012. Identifying hotspots of endemic woody seed plant diversity in China [J]. Divers Distrib, 18(7): 673-688.

Journal West China Forestry Science, 1979. *Madhuca pasquieri* (Dubard) Lam [J]. J W Chin For Sci, 1: 1-5. [西部林业科学编辑部，1979. 滇木花生 [J]. 西部林业科学，1：1-5.]

KHAN S, AL-QURAINY F, MADEE M, 2012. Biotechnological approaches for conservation and improvement of rare and endangered plants of *Saudi arabia* [J]. Saud J Biol Sci, 19(1): 1-11.

KIEN N D, HARWOOD C, 2016. Timber demand and supply in Northwest Vietnam: The roles of natural forests and planted trees [J]. Small-Scale For, 16: 65-82.

LI JF, LI RF, YAN RB, et al, 2014. NaCl stress' impact on seed germination of *Madhuca pasquieri* [J]. J Guangxi Agric, 29(4): 27-29. [李建凡，李日飞，严荣斌，等，2014. NaCl 胁迫对紫荆木种子萌发的影响 [J]. 广西农学报，29(4)：27-29.]

LIU N, ZHU W, SUN Z, et al, 2014. Canopy size dependent facilitations from the native shrub rhodomyrtus tomentosa to the early establishment of native trees *Castanopsis fissa* and *Syzygium hancei* in Tropical China [J]. Restor Ecol, 22 (4): 509-516.

LI YY, SIMA YK, FANG B, et al, 2003. Current situation and evaluation of the national key protected wild plant resources in Yunnan Province [J]. Acta Bot Yunnan, 25(2): 181-191. [李玉媛,司马永康,方波,等,2003. 云南省国家重点保护野生植物资源的现状与评价 [J]. 云南植物研究,25 (2):181-191.]

MIAO SY, HUANG JL, TANG ZX, et al, 2013. Studies on the rare, endangered and national key protected plants at Tianxin Natrual Reserves of Lianzhou [J]. J Guangzhou Univ (Nat Sci Ed), 12(5): 29-34. [缪绅裕,黄金玲,唐志信,等,2013. 广东连州田心保护区珍稀濒危保护植物研究 [J]. 广州大学学报(自然科学版),12(5):29-34.]

MIAO SY, WANG HL, HUANG JL, et al, 2008. Population characteristics of some wild rare and endangered plants in North and Northeast of Guangdong Province, China [J] J Trop Subtrop Bot, 16(05): 397-406. [缪绅裕,王厚麟,黄金玲,等,2008. 粤北和粤东北若干珍稀濒危野生植物的种群特征 [J]. 热带亚热带植物学报,16(05):397-406.]

MO ZC, JIANG H, ZHANG XG, 2013a. Extreme temperateure stress on dominant trees of *Syzygium hancei* forest along Guangxi coast [J]. Guangxi Sci, 20(1): 48-51. [莫竹承,姜恒,张秀国,2013a. 广西海岸红鳞蒲桃林主要树种的温度胁迫 [J]. 广西科学,20(1):48-51.]

MO ZC, XU JQ, CHEN SY, 2013b. Phenological characters of dominant trees in *Syzygium hancei* monsoon forest [J]. Guangxi Sci, 20(3): 193-198. [莫竹承,徐剑强,陈树宇,2013b. 红鳞蒲桃季雨林重要树种的物候特征 [J]. 广西科学,20(3):193-198.]

The State Forestry / The Ministry of Agriculture Administration, 1999. National key protected wild plants list (first batch) [J]. Bull State Council People's Repub Chin, 5: 4-11. [国家林业局/农业局,1999. 国家重点保护野生植物名录(第一批) [J]. 中华人民共和国国务院公报,5:4-11.]

PHAM QV, 2011. Research on silvicultural properties of *Madhuca pasquieri* H. J. lam species in Tam Qui Natural Madhuca Reserve, Ha Trung District, Thanh Hoa Province [J]. Nong Nghiep Phat Trien Nong Thon, 7: 86.

REN H, JIAN SG, LIU HX, et al, 2014. Advances in the reintroduction of rare and endangered rild plant species [J]. Sci Sin (Vit), 57(6): 603-609. [任海,简曙光,刘红晓,等,2014. 珍稀濒危植物的野外回归研究进展 [J]. 中国科学:生命科学,57(6):603-609.]

REN H, ZHANG Q, WANG Z, et al, 2010. Conservation and possible reintroduction of an endangered plant based on an analysis of community ecology: A case study of *Primulina tabacum* Hance in China [J]. Plant Spec Biol, 25(1): 43-50.

REN H, ZHANG Q, LU H, et al, 2012. Wild plant species with extremely small populations require conservation and reintroduction in China [J]. Ambio, 41(8): 913-917.

ROVZAR C, GILLESPIE TW, KAWELO K, 2016. Landscape to site variations in species distribution models for endangered plants [J]. For Ecol Manag, 369: 20-28.

SHI Y, YANG B, 2009. Seedling cultivation techniques [J]. For Sci Technol, 11:31 [施莹,杨斌,2009. 滇木花生实生苗培育技术 [J]. 林业科技通讯,11:31.]

SLAZAK B, SLIWINSKA E, SALUGA M, et al, 2015. Micropropagation of *Viola uliginosa* (Violaceae) for endangered species conservation and for somaclonal variation-enhanced cyclotide biosynthesis [J]. Plant Cell Tiss Org, 120(1): 179-19.

TRAN H, IIDA S, INOUE S, 2005. Species composition, diversity and structure of secondary tropical forests following selective logging in Huong Son, Ha Tinh Province, Vietnam [J]. J Fac Agric Kyushu Univ, 50(2): 551-571.

VARGHESE AO, MURTHY Y, 2006. Application of geoinformatics for conservation and management of rare and threatened plant species [J]. Curr Sci, 91(6): 762-769.

WANG C, WAN J, MU X, et al, 2015. Management planning for endangered plant species in priority protected areas [J]. Biodivers Conserv, 24(10): 2383-2397.

WANG JH, 1994. *Ex* and *in situ* conservation of the rare and endangered plants in Dinghushan Biospere Reserve [C]. Beijing: The first National Biodiversity Conservation and Sustainable Use Conference:5. [王俊浩,1994. 鼎湖山自然保护区珍稀濒危植物的迁地、就地保护 [C]. 北京:首届全国生物多样性保护与持续利用研讨会:5.]

WANG SL, TAN WF, PENG DR, et al, 2011. Analysis on *in situ* conservation of important species in Guangxi [J]. J Beijing For Univ, 33 (S2): 72-78. [王双玲,谭伟福,彭定人,等,2011. 广西重点物种就地保护现状分析 [J]. 北京林业大学学报,33(S2):72-78.]

WANG XP, LI JQ, LI XX, 2001. The study of seasonal rain forest classification in acid soil region of Guangxi [J]. Bull Bot Res, 4: 456-469. [王献溥,李俊清,李信贤,2001. 广西酸性土地区季节性雨林的分类研究 [J]. 植物研究,4:456-469.]

WANG XP, HU SS, 1982. Community characteristics of seasonal rain forests in acid soil region of Guangxi [J]. Acta Bot Boreal-Occident Sin, 2(2): 69-82. [王献溥,胡舜士,1982. 广西酸性土地区季节性雨林的群落学特点 [J]. 西北植物学报,2(2):69-82.]

WANG ZF, REN H, LI ZC, et al, 2013. Local genetic structure in the critically endangered, cave-associated peren-

nial herb *Primulina tabacum* (Gesneriaceae) [J]. Biol J Linn Soc, 109(4): 747-756.

WEN XY, CHEN JX, WANG MH, et al, 2006. Rare and endangered plants and national key protected plants in Guangdong Tree Park [J]. Guangdong For Sci Technol, 22(4): 26-30. [温小莹,陈建新,王明怀,等,2006. 广东树木公园珍稀植物资源现状及保护对策 [J]. 广东林业科技,22(4):26-30.]

WEN YG, LI ZJ, LI XX, et al, 2014. Types of vegetation and their classified systems in Guangxi [J]. Guangxi Sci, 21(5): 484-513. [温远光,李治基,李信贤,等,2014. 广西植被类型及其分类系统 [J]. 广西科学,21(5):484-513.]

WU QC, 1990. Analysis and study on the trunks of *Madhuca pasquieri* [J]. Guangxi For Sci Technol, 3: 29-32. [吴庆初,1990. 紫荆木的树干解析及其研究 [J]. 广西林业科技,3:29-32.]

WU XQ, HUANG BL, DING YL, 2004. The advance on the study of protection of rare and endangered plants in China [J]. J Nanjing For Univ (Nat Sci Ed), 28(2): 72-76. [吴小巧,黄宝龙,丁雨龙,2004. 中国珍稀濒危植物保护研究现状与进展 [J]. 南京林业大学学报(自然科学版),28(2):72-76.]

WU YB, FENG ZJ, 2006. Rare and endangered plants and national key protected plants for *ex situ* conservation in South China Agricultural University Arboretum [J]. J S Chin Agric Univ,27(3):118-121. [吴永彬,冯志坚,2006. 华南农业大学树木园稀有濒危植物和国家重点保护植物的迁地保护 [J]. 华南农业大学学报,27(3):118-121.]

XIANG WS, LU SH, WEN SJ, et al, 2015. Sample effects on species-area relationships of typical forests in karst and non-karst mixing distribution areas [J]. Guihaia, 35(3): 309-316. [向悟生,陆树华,文淑均,等,2015. 取样方式对喀斯特和非喀斯特混合分布区森林种—面积关系的影响 [J]. 广西植物,35(3):309-316.]

YAN YH, HE ZX, CHEN HF, et al, 2004. The survey and conservation on the rare and endangered plants in Shimentai Nature Reserve, Guangdong [J]. Guihaia,24(1): 1-6. [严岳鸿,何祖霞,陈红锋,等,2004. 广东石门台自然保护区珍稀濒危植物及其保护 [J]. 广西植物,24(1):1-6.]

ZENG C, SHI XF, QIU GL, et al, 2014. The influence of transplanting stress on seedlings physiological characteristic of five dominant species in *Syzygium hancei* communities [J]. J Guangxi Acad Sci, 4, 263-268. [曾聪,史小芳,邱广龙,等,2014. 移栽胁迫对红鳞蒲桃群落 5 种优势植物苗木生理特征的影响 [J]. 广西科学院学报,4:263-268.]

ZHANG YB, MA KP, 2008. Geographic distribution characteristics of the nationa key protected wild plants in China [J]. Chin J Appl Ecol,19(8): 1670-1675. [张殷波,马克平,2008. 中国国家重点保护野生植物的地理分布特征 [J]. 应用生态学报,19(8):1670-1675.]

广西植物被国际和国内重要数据库收录：

☆ 俄罗斯《文摘杂志》(AJ，VINITI，Abstract Journal)
☆ 美国《化学文摘》(CA，Chemical Abstracts)
☆ 美国《史蒂芬斯全文数据库》(EBSCOhost)
☆ 英国《农业与生物科学研究中心文摘》(CAB Abstracts)
☆ 英国《全球健康》(Global Health)
☆ 美国《剑桥科学文摘》(CSA)
☆《日本科学技术振兴机构数据库》(JST，Japan Science and Technology Agency)
☆ 美国《乌利希期刊指南》(Ulrich's PD，Ulrich's Periodicals Directory)
☆ 英国《邱园索引》(Index Kewensis)
☆ 美国《柯尔比科学文化信息中心》(CICSC)
☆ 波兰《哥白尼索引》(IC，Index of Copernicus)
☆ 台湾华艺中文电子期刊服务资料库--思博网 (CEPS) (http://www.ceps.com.tw)
☆ 中国生命科学文献数据库(http://www.cba.ac.cn)
☆ 中国科技论文统计与分析数据库 (CSTPCD)
☆ 中国科学引文数据库 (CSCD)
☆ 科学引文数据库 (SCD)
☆ 中国学术期刊综合评价数据库 (CAJCED)
☆ 中国生物学文献数据库 (CBAD)、中国生物学文摘 (CBA)
☆ 中国生物医学文献服务系统 (SinoMed) (http://www.sinomed.ac.cn)
☆ 中国学术期刊文摘数据库 (CSAD)
☆ 中国化学化工文摘
☆ 博看网（http://www.bookan.com.cn）、龙源期刊网（http://www.qikan.com.cn）收录期刊
☆ 中国知网《中国学术期刊（网络版）》（CAJ-N）首批收录期刊（http://navi.cnki.net/knavi/JournalDetail?pcode=CJFD&pykm=GXZW）
☆ 中国学术期刊网络出版总库(http://epub.cnki.net)
☆ 中国数字化期刊群(http://www.periodicals.net.cn)
☆ 中文科技期刊数据库 (http://www.cqvip.com)
☆ 万方数据知识服务平台(http://c.wanfangdata.com.cn)
☆ 中国科学院科技期刊开放获取平台(CAS-OAJ)收录期刊 (http://www.oaj.cas.cn)
☆ 中国科学院科技论文预发布平台（ChinaXiv）收录期刊（http://chinaxiv.org）

广西植物

月刊，1981年创刊
第38卷 第7期 2018年7月

GUIHAIA

Monthly，Started in 1981
Vol. 38 No. 7 Jul. 2018

主管单位：广西科学院
主办单位：广西壮族自治区中国科学院广西植物研究所
广西植物学会
名誉主编：马克平
主　　编：李先琨
常务副主编/编辑部主任：蒋巧媛
编辑单位：《广西植物》编辑部
地　　址：桂林市雁山　邮编：541006
电话/传真：（0773）3550074
电子信箱：guihaia@gxib.cn
网　　址：http://www.guihaia-journal.com
出版单位：科学出版社
（北京东黄城根北街16号　邮编：100717）
印刷装订：桂林日报印刷厂
订 购 处：全国各地邮局
总 发 行：科学出版社
国内发行：桂林市邮局
国外发行：中国国际图书贸易集团有限公司
（北京市海淀区车公庄西路35号　邮编：100048
电子信箱：bk@mail.cibtc.com.cn）

Supervised by Guangxi Academy of Sciences
Sponsored by Guangxi Institute of Botany, Guangxi Zhuang Autonomous Region and Chinese Academy of Sciences
Guangxi Society of Botany
Honorary Editor-in-Chief: MA Keping
Editor-in-Chief: LI Xiankun
Deputy Editor-in-Chief: JIANG Qiaoyuan
Edited by Editorial Office of *GUIHAIA*
Addr.: Yanshan, Guilin 541006, Guangxi, China
Tel. / Fax: 86-773-3550074
E-mail: guihaia@gxib.cn
http://www.guihaia-journal.com
Published by Science Press
(16 Donghuangchenggen North Street, Beijing 100717, China)
Printed by Guilin Daily Printer (China)
Distributed by Science Press
Domestic Subscription: All Local Post Offices in China
Foreign Subscription: China International Book Trading Corporation
(35 Chegongzhuang West Road, Haidian District, Beijing 100048, China
E-mail: bk@mail.cibtc.com.cn)

ISSN 1000-3142
CN 45-1134/Q
国内邮发代号：48-43　国内定价：45.00元　国外发行代号：MO-5054

国内外公开发行
ISSN 1000-3142

ISSN 1001-4829
CN51-1213/S
CODEN XNXUEF

中文核心期刊
中国科技核心期刊
中国农业核心期刊
RCCSE中国核心学术期刊
中国科学引文数据库库源期刊

西南农业学报

SOUTHWEST CHINA JOURNAL OF AGRICULTURAL SCIENCES

第28卷 第2期
Vol.28 No.2

2015

ISSN 1001-4829
04
001482157

《西南农业学报》编辑委员会

农业气象·烟草科学·农业信息

畜牧·兽医·水产·资源昆虫

简 报

文章编号:1001-4829(2015)02-0833-06
DOI:10.16213/j.cnki.scjas.2015.02.072

南岭山地森林群落冠层结构对林下野生花卉的影响

敬小丽,张 璐*,杜伟静,苏志尧

(华南农业大学林学院,广东 广州 510642)

摘 要:为探讨冠层结构与林下野生花卉的关系,采用典型群落调查法,以南岭山地森林群落林下野生花卉为研究对象,研究林下野生花卉物种数量特征及冠层结构对其的影响,以期为野生花卉的园林应用提供理论参考。结果显示,南岭山地森林群落 1 hm^2 林下植被中共有野生花卉 104 种,分属 55 科 92 属,其中箬竹、瓜馥木和南岭箭竹为优势种;方差分析与回归分析表明,叶面积指数、林冠开度和林下散射光对林下野生花卉多度的影响较其他冠层结构参数大;冠层结构各参数对 3 种色调(冷、暖、中性)林下野生花卉物种密度的影响均未达到显著性差异($P>0.05$),但 3 种色调的野生花卉物种密度均随叶面积指数与林下总光照先减少后增加;多响应置换过程分析和指示种分析揭示棱果花和巴戟天同为林冠开度与叶面积指数的指示种,对冠层结构变化有较强的响应。

关键词:野生花卉;花卉颜色;冠层结构;指示种;南岭
中图分类号:Q948 **文献标识码**:A

Effect of Canopy Structure on Understory Wild Flower in Nanling Mountain Forest Community of South China

JING Xiao-li, ZHANG Lu*, DU Wei-jing, SU Zhi-yao
(College of Forestry, South China Agricultural University, Guangdong Guangzhou 510642, China)

Abstract: To investigate the relationship between canopy structure and understory wild flower, the typical method of plant community was applied to research the effect of canopy structure on wild flower in Nanling mountain forest and provide theoretical reference for the garden application of wild flower. The result showed that there were 104 species/hm^2 in investigated area, which belonged to 55 families and 92 genuses, in which *Indocalamus tessellates*, *Fissistigma oldhamii* and *Sinarundinaria basihirsuta* were dominant species; Kruskal-Wallis analysis and regression analysis indicated that leaf area index (*LAI*), canopy openness (*CO*) and transmitted diffused light (*Tdif*) had larger effects on understory wild flower than other canopy structure parameters; The effects of each canopy parameters on wild flower species density of three hues (cold, warm and neutral) had no significant differences, while the species density of three hues decreased at first and increased later with *LAI* and transmitted total light changing; Multi-Response Permulation Procedure (*MRPP*) and Indicator Species Analysis (*ISA*) revealed that *Morinda officinalis* and *Barthea barthei* were the indicative species of both *CO* and *LAI* which had stronger responses to change of canopy structures.

Key words: Wild flower; Flower color; Canopy structure; Indicator species; Nanling

森林冠层(Forest canopy)是森林生态系统中与外界环境作用最直接与最活跃的界面。林冠通过截留降水,影响林内水文循环[1];通过对光照进行吸收、反射和投射,改变林下光照条件[2],从而对林下植被的物种组成[3]与物种多度[4]产生影响。树木死亡形成林隙破坏了冠层结构,使林冠开度增大,影响着周围植物的生长。在林隙边缘,树木的死亡率较大,从林隙边缘到森林内部,死亡率逐渐降低[5]。野生花卉作为林下植被的组成部分,必然会受到冠层结构的影响。

花卉是城市园林造景中常用的素材,花坛、花境、花台、花池等花卉植物造景,为园林增添了一层美感。野生花卉是指目前还在原产地处于野生或半野生状态,没有被人工栽培应用的观赏树木和花卉[6]。我国野生花卉资源丰富,据统计,我国野生

收稿日期:2014-05-23
基金项目:广东省科技计划农业领域项目:珠三角近自然城市森林群落构建关键技术研究(2013B020305009);广东省林业科技创新专项资金项目(2011KJCX031-02)
作者简介:敬小丽(1989-),女,在读硕士研究生,研究方向为森林生态学,E-mail:jingxiaoli0930@163.com,*为通讯作者。

表1 冠层结构参数分组

Table 1 Groups of canopy structures parameters

组号	林冠开度 (%)	叶面积指数 (mol/m²/s/d)	林下直射光 (MJ/m²/d)	林下散射光 (MJ/m²/d)	林下总光照 (MJ/m²/d)
1	≤10.0(39)	≤2.30(18)	≤2.00(23)	≤2.00(20)	≤3.60(14)
2	10.1~15.5(51)	2.31~3.22(72)	2.01~4.00(64)	2.01~3.00(46)	3.61~7.20(69)
3	≥15.6(10)	≥3.23(10)	≥4.01(13)	≥3.01(34)	≥7.21(17)

注:括号内为样方数。

Note: The data in the bracket means the number of plot.

花卉大概有7000余种,有1000种以上能直接进行观赏应用,有开发潜力的也有数千种[7]。我国自20世纪70年代起,开展了对野生花卉资源的调查研究,引种筛选出了大批有应用前景的园林绿化植物[8]。目前对花卉的研究多集中在生物量[9]、物种多样性[10]、耐旱性[11]、抗寒性[12]以及资源调查统计方面,对野生花卉与冠层的关系研究还未见报道。本文通过量化冠层结构与林下野生花卉植物的关系,探讨适合野生花卉生长的冠层结构,为野生花卉的引种栽培及园林应用提供理论参考。

1 材料与方法

1.1 研究区概况

南岭国家级自然保护区位于广东省北部(24°37′~24°57′ N,112°30′~113°04′ E),总面积58 368.4 hm²,为目前广东省陆地面积最大的保护区。该区属于中亚热带湿润性季风气候,年均气温17.4 ℃,年均降雨量2108.4 mm,年相对湿度84 %,日照率40 %。水平地带性土壤为红壤,地带性植被为常绿阔叶林,森林覆盖率达98 %[13]。主体岩石为花岗岩,最高峰为海拔1902 m的石坑崆。该区地理条件优越,植物资源丰富,有维管束植物227科1048属3115种,其中蕨类植物47科110属358种,裸子植物7科13属19种,被子植物173科925属2748种。

1.2 研究方法

1.2.1 林下植被调查 在线路勘察的基础上,选择典型群落,采用样方法设置样地,以10 m×10 m为样方单元,在每个样方单元的四角和对角线中心各设置1个2 m×2 m的小样方,共调查了10 000 m²。测定每个小样方内林下植物的种名、株数、盖度,筛选出其中的花卉植物作为研究对象。

1.2.2 冠层照片拍摄与分析 用三脚架将Nikon CoolPix 4500数码相机外接Nikkor FC-E8鱼眼镜头转换器水平放置于离地面1.65 m处,用指南针确定方向使记录的照片顶部与磁北方向重合,在每个10 m×10 m样方单元中心和对角线四分位处镜头朝上拍摄半球面林冠影像。采用Gap Light Analyzer 2.0(GLA)图像处理软件分析林冠影像(图1),输出林冠开度(CO)、叶面积指数(LAI)、林下直射光(Transmitted Direct Light, Tdir)、散射光(Transmitted Diffused Light, Tdif)和总光照(Transmitted Total Light, Ttot)5个冠层结构参数,并按照表1进行冠层结构参数分组。

1.3 数据分析

采用公式:$IV = A_R + F_R + P_R$[23]计算每个物种的重要值,式中,A_R为相对多度,F_R为相对频度,P_R为相对优势度。采用Statistica 8.0统计软件对花

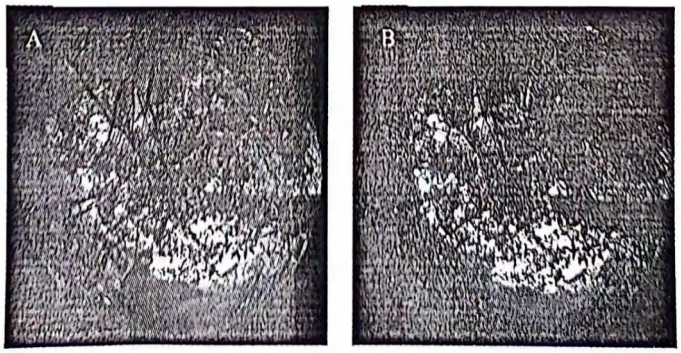

A为原林冠影像;B为预处理后的林冠影像

A stands for origin canopy image; B stands for preprocessed

图1 林冠影像处理

Fig. 1 Process of canopy image

表2　南岭山地森林常见林下野生花卉物种

Table 2　Common species of understory wild flower in Nanling mountain

种名	科名	多度(株)	出现的样方数(个)	盖度(%)	重要值
箬竹 *Indocalamus tessellatus*	禾本科 Gramineae	7619	48	78.56	128.92
瓜馥木 *Fissistigma oldhamii*	番荔枝 Annonaceae	128	22	20.04	18.53
南岭箭竹 *Sinarundinaria basihirsuta*	禾本科 Gramineae	652	5	15.0	17.20
黑莎草 *Gahnia tristis*	莎草科 Cyperaceae	208	36	2.24	10.22
链珠藤 *Alyxia sinensis*	夹竹桃 Apocynaceae	240	24	2.61	8.54
龙须藤 *Bauhinia championii*	豆科 Leguminosae	91	22	3.37	7.21
网脉酸藤子 *Embelia rudis*	紫金牛 Myrsinaceae	56	21	4.09	7.15
乌蔹莓 *Cayratia japonica*	葡萄科 Vitaceae	109	15	4.42	6.77

卉植物多度与5个冠层结构参数分别进行Kruskal-Wallis检验,检验花卉植物多度在各分组变量(表1)间是否存在差异。同时对花卉植物多度与冠层结构各参数进行回归分析(Regression Analysis, RA),分析花卉植物多度随冠层结构各参数变化的趋势。

采用PC-ORD 6.0多元分析软件对冠层结构各参数进行多响应置换过程分析(Multi-response Permulation Procedure, MRPP)和指示种分析(Indicator Species Analysis, ISA),并采用蒙特卡罗检验来检验结果是否具有统计显著性。

2　结果与分析

2.1　南岭山地林下野生花卉数量特征

基于10 000 m^2 的样方调查数据,南岭山地森林群落林下植被共计有野生花卉植物104种,分属于55科92属(表2)。其中草本18科24属25种,占野生花卉总数的24.04%;灌木30科44属50种,占总数的48.08%;藤本14科23属25种,占总数的24.04%;竹类1科4属4种,占总数的3.85%。禾本科的箬竹(*Indocalamus tessellatus*)重要值最大,数量最多。且在重要值≥3.00的物种中,禾本科居多,除箬竹外,还有南岭箭竹(*Sinarundinaria basihirsuta*)和淡竹叶(*Lophatherum gracile*)。

2.2　冠层结构与林下野生花卉多度的关系

Kruskal-Wallis检验结果显示,野生花卉多度在冠层结构各参数分组变量间的差异性均达到极显著($P < 0.01$)。其中,在林冠开度与林下散射光分组变量间的差异性最显著(图2)。花卉多度随林冠开度、林下散射光和林下直射光的增加而减少,随叶面积指数的增加而增加。说明林冠开度增加与叶面积指数减小有利于林下花卉植物生长,也许是由于二者的变化导致林下光照强度增加,间接利于花卉的生长。

冠层结构与林下野生花卉多度的回归分析结果显示,冠层结构与花卉植物多度呈极显著线性相关($P < 0.01$)(表3)。除叶面积指数外,林冠开度、林下直射光、散射光与总光照均与花卉植物多度呈正相关,且叶面积指数与花卉植物多度的相关性最大最显著,说明叶面积指数对林下花卉植物数量影响最大。林下散射光与花卉植物多度的相关性较直射光大,说明林下散射光对林下花卉植物的影响作用更大。可能是因为生长在林下的花卉植物对光照的要求不强,散射光即可满足其生长,而直射光由于透过冠层直接照射植物,强度相对于散射光较大,不利于花卉植物的生长。

表3　冠层结构参数与林下野生花卉多度的回归模型

Table 3　Regression models between canopy structure parameters and understory wild flower abundance

参数	回归模型	R^2	P
林冠开度(*CO*)	$A = 271.4462 - 15.074 \times CO$	0.1360	0.0002
叶面积指数(*LAI*)	$A = -245.4967 + 131.1326 \times LAI$	0.1571	0.00004
林下散射光(*Tdif*)	$A = 276.3679 - 64.1844 \times Tdif$	0.1277	0.0003
林下直射光(*Tdir*)	$A = 208.9094 - 38.0575 \times Tdir$	0.1089	0.0008
林下总光照(*Ttot*)	$A = 243.7322 - 25.6542 \times Ttot$	0.1244	0.0003

注:A 为野生花卉多度;R^2 为决定系数。

Note: A represents the abundance of wild flowers and R^2 represents the coefficient of determination.

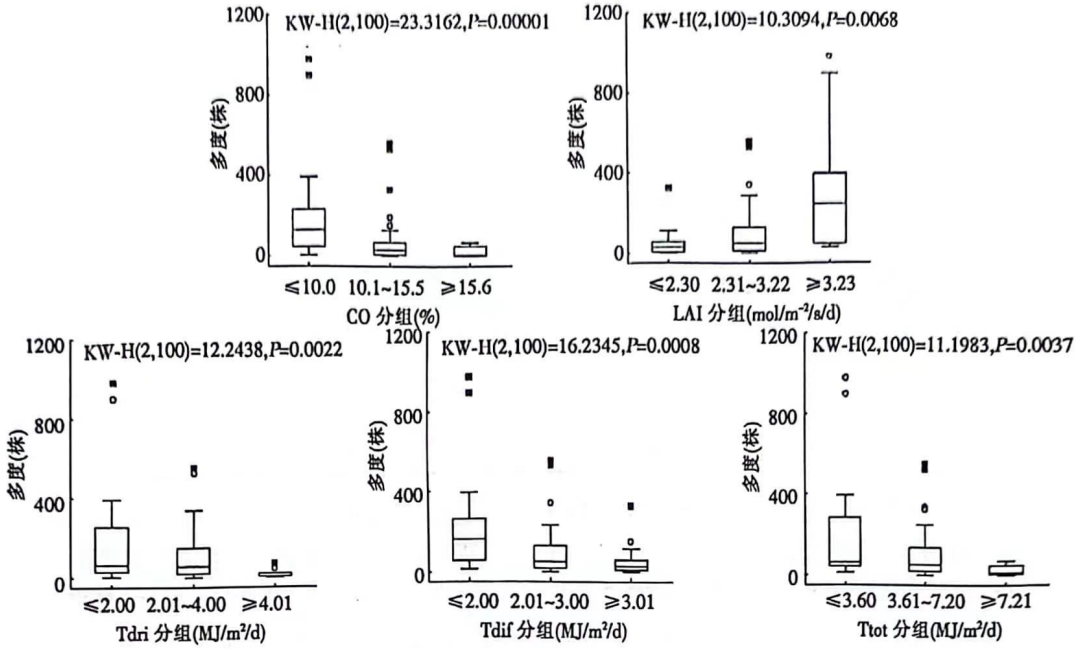

图2 花卉多度与冠层结构参数的 Kruskal-Wallis 检验

Fig. 2 Kruskal-Wallis test between flower abundance and canopy structure parameters

2.3 林下野生花卉颜色对冠层结构的响应

根据调查数据，将花卉颜色分为冷色调、暖色调和中性色3个色调，其中冷色调包括黄绿色、绿色、蓝色、紫色，暖色调包括红色、黄色、橙色，中性色只包括白色[14]。分别统计出在冠层结构各参数分组变量中3个色调花卉的物种数及物种密度（单位面积物种数）。基于1 hm^2 样方调查数据，南岭山地森林群落林下野生花卉中，冷色调、暖色调及中性色调的花卉分别有38、32和34种。3个色调林下野生花卉的物种密度随叶面积指数和林下总光照的变化为先减少后增加，而在林冠开度、林下直射光和散射光分组变量间未表现出明显的变化趋势。非参数方差分析结果表明，各冠层结构参数对3种色调花卉物种密度的影响均未达到显著性差异（$P > 0.05$）（图3）。

2.4 林下野生花卉对冠层结构的指示作用

先采用 MRPP 分析野生花卉在冠层结构参数各组间的差异，T 是描述组间分离的检验统计量，A 是

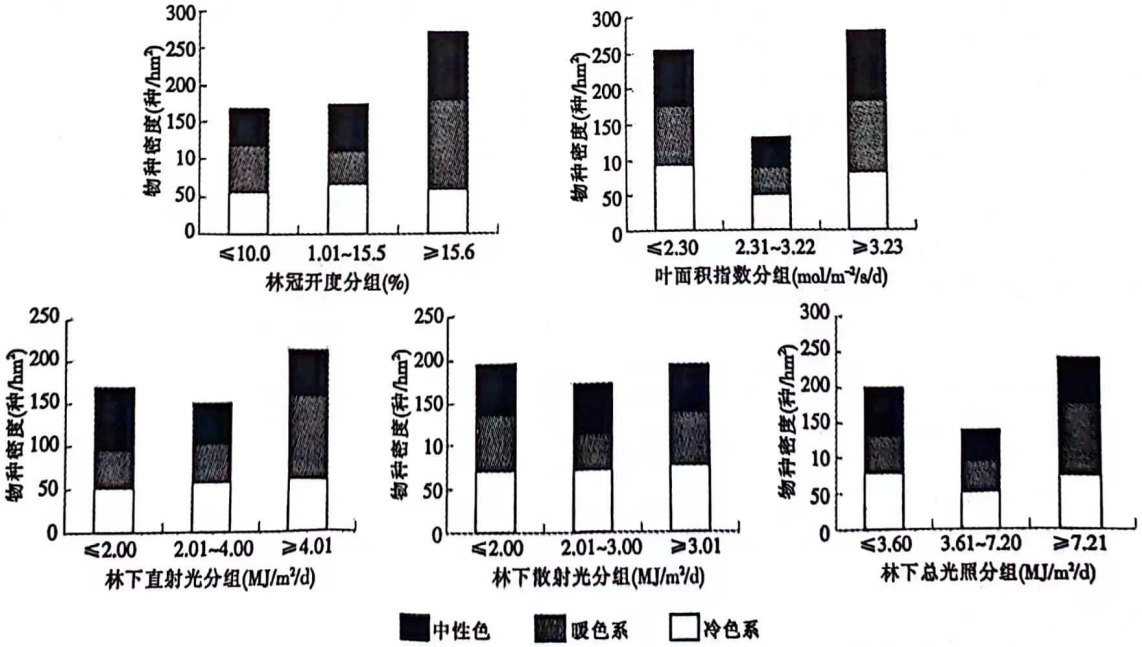

图3 花卉颜色对冠层结构的响应

Fig. 3 Response of flower color to canopy structure

表4　多响应置换过程分析(MRPP)的统计值

Table 4　Summary statistics for multi-response permulation procedures

分组变量	观测 Delta	预测 Delta	*T* 值	*A* 值	*P* 值
CO	0.4588	0.4988	-2.9980	0.0801	0.0039
LAI	0.4730	0.4989	-3.8595	0.0518	0.0012
Tdif	0.4583	0.4989	-4.9387	0.0813	0.0001
Tdir	0.4704	0.4988	-4.0592	0.0569	0.0010
Ttot	0.4655	0.4988	-3.2356	0.0668	0.0027

表5　林下光照的指示种分析

Table 5　Indicator species analysis of transmitted light

林下光照	指示种	多度	指示值	*P* 值
散射光(*Tdif*)	南蛇藤	1	50.0	0.0450
直射光(*Tdir*)	暗色菝葜	7	29.9	0.0110
	东南长蒴苣苔	43	34.2	0.0045
	锐尖山香圆	2	40.0	0.0026
	唐竹	42	23.4	0.0310
总光照(*Ttot*)	常春藤	10	40.9	0.0460
	少花柏拉木	73	39.7	0.0410
	棱果花	5	50.0	0.0373
	异形南五味子	7	46.6	0.0163

描述组内同质性的一致性统计量。结果显示,南岭山地森林群落林下野生花卉在冠层结构各参数组间差异显著,尤其在林下散射光组间差异最显著;在林下散射光与直射光的组间分离性较强,在林冠开度与林下散射光的组内一致性较强(表4)。进一步采用指示种分析,分析花卉对冠层结构的指示作用。将指示值(IV)≥23,$P < 0.05$ 的种视为潜在的指示种。结果表明,林冠开度与叶面积指数的指示种相同,均为棱果花(*Barthea barthei*)和巴戟天(*Morinda officinalis*),其中棱果花对林冠开度与叶面积指数的指示值均为50.0,巴戟天的指示值分别为31.0和43.0(表5)。棱果花属为我国特有属,仅包含棱果花一个种,喜欢生长在山坡和山谷疏林中;巴戟天具有耐荫的特性,喜欢生长在疏林下,为乔灌木所荫蔽。林冠开度和叶面积指数与林下的光照条件密切相关,说明棱果花与巴戟天对林冠开度与叶面积指数的变化较敏感。

林下散射光的指示种为南蛇藤,落叶藤本植物,多生长于山坡灌丛中。林下直射光的指示种有4种,分别为暗色菝葜(*Smilax lanceifolia*)、东南长蒴苣苔(*Didymocarpus hancei*)、锐尖山香圆(*Turpinia arguta*)和唐竹(*Sinobambusa tootsik*),林下总光照的指示种有4种,分别为常春藤(*Hedera nepalensis*)、少花柏拉木(*Blastus pauciflorus*)、棱果花和异形南五味子(*Kadsura heteroclita*)(表5)。林下直射光和总光照的指示种多喜欢生长在山谷、林下等弱光照的环境中,对光照的变化敏感。

3　讨　论

3.1　林下野生花卉对冠层结构的不同响应

冠层结构影响着林下的光照条件和水分条件,从而影响林下植物的生长,但冠层结构各项参数对林下花卉植物的生长影响大小不同。本研究表明,林下野生花卉植物多度在林冠开度与林下散射光分组变量间的差异性最显著,光照对野生花卉的影响大于其他冠层结构参数。李烨与张秀峰[15]对4种林下植物研究表明,不同物种适应不同的光照,但适应林下散射光的3物种:移山参(*Radix ginseng*)、穿龙薯蓣(*Dioscorea nipponica*)和细辛(*Asarum sieboldii*)均为草本植物,林下散射光对林下草本植物的生长影响更大。野生花卉多度与冠层结构各参数均呈线性关系,除叶面积指数外,均呈负相关,且与叶面积指数的相关性最显著,表明叶面积指数对林下植物的影响最大。但 Jelaska 等[16]的研究表明,在38种草本植物中只有6种与叶面积指数的相关性较大,叶面积指数对不同植物的影响不同。

本研究揭示了对南岭山地森林群落冠层结构具有潜在指示作用的林下野生花卉植物共10种,除东

南长蒴苣苔、唐竹和少花柏拉木之外其他种的重要值均 < 1。欧芷阳等[17]对东莞森林土壤的指示种研究显示,23 种指示种中包括 8 种草本植物,4 种蕨类植物和 3 种藤本植物,林下植物对环境具有较强的指示作用。蔡永立与宋永昌[18]对藤本植物叶片研究表明,短梗南蛇藤(*Celastrus rosthornianus*)表现出对较强光照的适应,但本研究显示南蛇藤是林下散射光唯一的潜在指示种,适应较弱的光照条件,也许是由于同属物种间的差异。

3.2 不同冠层结构下林下野生花卉的园林应用潜力

棱果花和巴戟天作为林冠开度与叶面积指数的指示种,表明它们对冠层结构的变化有较强的响应。棱果花开白色至粉红色或紫红色花,兰思仁[19]运用公式计算福建省观花植物的观赏及开发价值,结果表明,棱果花具有较高的开发价值,适宜作园林中的地被植物。而巴戟天作为药用植物,应用在园林中,即使被人误食,也不会对人体有害。本研究还发现,南岭山地森林群落林下野生花卉植物中,灌木花卉物种数居多,但从总体上来看,禾本科物种居多,包括箬竹、南岭箭竹、淡竹叶和芒(*Miscanthus sinensis*),其中,南岭箭竹为该地的乡土物种,开紫绿色的花,可作为园林植物色彩搭配中一个新的选择。淡竹叶在虞山群落类型中属于草本层植物的优势种,适应林下生长环境,可作为园林植物造景中良好的林下物种。唐竹不仅形态挺拔秀气,是优良的传统观赏竹种,而且是适应当前生态型绿化的优良竹种,具有较高的滞尘量[20],既可在园林中作观赏,也可在道路旁作绿化。南蛇藤形态优美,开黄色花。茎、蔓、叶、果均具有较高的观赏价值,是城市优良的垂直绿化材料之一,还可培育作整形灌木[21]。

我国野生花卉资源丰富,很多种类尚待开发研究利用。探讨适合野生花卉生长的冠层结构,重点考虑叶面积指数和散射光对林下花卉的影响,可为野生花卉的引种栽培及园林应用提供新思路。

参考文献:

[1] Siles P, Vaast P, Dreyer E, et al. Rainfall partitioning into through fall, stem flow and interception loss in a coffee (*Coffea arabica* L.) monoculture compared to an agroforestry system with Inga densiflora[J]. Journal of Hydrology, 2010, 395(1 - 2):39 - 48.

[2] Beaudet M, Harvey B D, Messier C, et al. Managing understory light conditions in boreal mixedwoods through variation in the intensity and spatial pattern of harvest: A modelling approach[J]. Forest Ecology and Management, 2011, 261(1):84 - 94.

[3] Yu M, Sun O J. Effects of forest patch type and site on herb-layer vegetation in a temperate forest ecosystem[J]. Forest Ecology and Management, 2013, 300:14 - 20.

[4] Brunet J, Valtinat K, Mayr M L, et al. Understory succession in post-agricultural oak forests: Habitat fragmentation affects forest specialists and generalists differently[J]. Forest Ecology and Management, 2011, 262(9):1863 - 1871.

[5] Gray A N, Spies T A, Pabst R J. Canopy gaps affect long-term patterns of tree growth and mortality in mature and old-growth forests in the Pacific Northwest[J]. Forest Ecology and Management, 2012, 281:111 - 120.

[6] 杨晓盆, 王跃进. 山西珍稀野生花卉种质资源与利用[J]. 中国野生植物资源, 2004, 23(3):21 - 23.

[7] 张启翔, 潘会堂. 中国新花卉作物与城市园林绿化建设[J]. 中国园林, 2009(1):71 - 74.

[8] 潘会堂, 张启翔. 花卉种质资源与遗传育种研究进展[J]. 北京林业大学学报, 2000, 22(1):81 - 86.

[9] 蔡 蕾, 刘兴良, 何 飞, 等. 巴郎山高山及亚高山草甸花卉植物生物量海拔梯度格局[J]. 应用生态学报, 2011, 22(11):2822 - 2828.

[10] Frank T, Kehrli P, Germann C. Density and nutritional condition of carabid beetles in wildflower areas of different age[J]. Agriculture, Ecosystems & Environment, 2007, 120(2 - 4):377 - 383.

[11] 徐兴友, 杜金友, 龙 茹, 等. 干旱胁迫下 6 种野生耐旱花卉苗木蒸腾耗水与耐旱性的关系[J]. 经济林研究, 2010, 28(1):9 - 13.

[12] 涛 郑, 陈振东, 林秀香, 等. 野牡丹科、金粟兰科野生花卉抗寒性研究[J]. 西南林学院学报, 2010, 30(1):29 - 33.

[13] 张 璐, 贺立静, 区余端, 等. 南岭自然保护区常绿阔叶林枯立木数量特征分析[J]. 福建林学院学报, 2012, 32(1):64 - 69.

[14] 黄银秀. 色彩在园林中的应用初探[J]. 中国园艺文摘, 2011(10):110 - 111.

[15] 李 焯, 张秀峰. 冠层结构对林下经济植物的影响[J]. 山东林业科技, 2010(3):15 - 17.

[16] Jelaska S D, Antonic O, Bozic M, et al. Responses of forest herbs to available understory light measured with hemispherical photographs in silver fir-beech forest in Croatia[J]. Ecological Modelling, 2006, 194(1 - 3):209 - 218.

[17] 欧芷阳, 苏志尧, 叶永昌, 等. 东莞地表植被对表层土壤化学特性的指示作用[J]. 生态学报, 2009, 29(2):984 - 992.

[18] 蔡永立, 宋永昌. 浙江天童常绿阔叶林藤本植物的适应生态学叶片解剖特征的比较[J]. 植物生态学报, 2001, 25(1):90 - 98.

[19] 任斌斌, 李树华, 殷丽峰, 等. 模拟常熟地区自然群落的植物景观设计[J]. 林业科学, 2009, 45(12):139 - 145.

[20] 兰思仁. 福建省野生观赏植物资源调查与观花植物的观赏特性评价[J]. 中国园林, 2010:63 - 67.

[21] 徐学敏. 垂直绿化植物_南蛇藤的园林用途及培育[J]. 中国林副特产, 2011(4):62 - 63.

(责任编辑 陈 虹)

西南农业学报（双月刊）
Xinan Nongye Xuebao
2015年4月出版（公开发行）
2015年第28卷第2期

Southwest China Journal of Agricultural Sciences(Bimonthly)
Vol. 28 No. 2 2015
Published on Apr. 28, 2015

协　办：四川省农作物育种攻关领导小组办公室
联系人：何希德
电　话：（028）84504004

主　　管：四川省农业厅
主　　办：四川、云南、贵州、广西、西藏及重庆省（区、市)农科院
编辑出版：《西南农业学报》编辑部
编辑部地址：成都市锦江区净居寺路20号附101号（邮码：610066)
照　　排：锦江区海林印务部
印　　刷：成都市锦慧彩印有限公司
国内订阅发行：四川省报刊发行局
国外订阅发行：中国出版对外贸易总公司（北京782信箱)
中国标准刊号：CN51-1213/S　ISSN 1001-4829　CODEN XNXUEF

Sponsored by Sichuan,Yunnan,Guizhou,Guang Tibet and Chongqing Academies of Agri.Sci.
Edited and Published by Editorial Department of Southwest China Journal of Agri.Sci.
Address:20-101, Jingjusi Road, Jinjiang Distri Chengdu,Sichuan 610066

Distributed by China Publish Foreign Trading Corporation(P.O.Box 782,Beijing,China)
E-mail: Jxuebao@sina.com
http://xnnyxb.periodicals.net.cn/default.html

2015
第28卷 第2期
Vol.28 No.2

公开发行　　邮发代号：62-152　　国内订价：30.00

ISSN 1673-923X
CODEN ZLKDA5

中南林业科技大学学报

Journal of Central South University of Forestry & Technology

第34卷 Volume 34 | 第5期 Number 5

- ◆全国中文核心期刊
- ◆全国高校优秀科技期刊
- ◆全国优秀高校自然科学学报
- ◆中国科技核心期刊
- ◆RCCSE中国核心学术期刊
- ◆中国科学引文数据库(CSCD)来源期刊
- ◆中国科技论文与引文数据库(CSTPCD)来源期刊
- ◆美国CA、日本JST等来源期刊

5
2014
中国·长沙

目　次

林　　学

生态学

[期刊基本参数]CN43—1470/S*m*A4*124*zh*P* ￥20.00*1000*25*2014—05*n

南岭山地森林群落冠层结构与立木多度的关系

敬小丽，杜伟静，张 璐，苏志尧
（华南农业大学 林学院，广东 广州 510642）

摘 要：林冠是森林与外部环境相互作用最直接与最活跃的界面层，影响着森林的物理环境和生物环境。采用半球面摄影技术（Hemispherical Photography）、典范对应分析（Canonical Correspondence Analysis, CCA）和 Kruskal-Wallis 分析定量研究了森林群落冠层结构与立木分布及多度的关系。结果表明：（1）基于 10 000 m^2 调查样地，南岭山地森林群落共有立木 47 科 81 属 143 种，枯立木多来源于林冠上层大树；（2）CCA 排序结果显示，冠层结构各参数与立木分布均有一定相关性，叶面积指数、林冠开度与立木分布的关系尤为密切；（3）立木多度与活立木多度在林下散射光分组变量间差异显著（$P < 0.05$），枯立木多度在林冠开度分组变量间的差异性显著（$P < 0.05$），立木多度随林下直射光增强而减少。叶面积指数和林冠开度通过影响林下光照条件进而影响立木，尤其是枯立木的形成和多度。

关键词：山地森林群落；冠层结构；立木多度；活立木；枯立木；叶面积指数；林冠开度
中图分类号：S718.5 **文献标志码**：A **文章编号**：1673-923X(2014)05-0059-07

Relationship between canopy structure factors and abundance of standing trees in Nanling mountain forest communities

JING Xiao-li, DU Wei-jing, ZHANG Lu, SU Zhi-yao
(College of Forestry, South China Agricultural University, Guangzhou 510642, Guangdong, China)

Abstract: Canopy is the most direct and active interface layer between forest and external environment, which affects physical and biotic environment of forest. By using Hemispherical Photography, Canonical Correspondence Analysis (CCA) and Kruskal-Wallis methods, the relations among the distribution and abundance of standing trees and forest canopy structure were quantitatively studied. The results indicated that (1) There were 47 families, 81 genera and 143 species based on the 10 000 m^2 sampling investigations and most of the dead standing trees derived from over-story big old-aged trees; (2) the results of CCA ordination indicated that all of the canopy structure parameters had a certain correlation with distribution of standing trees, and the leaf area index (LAI) and canopy openness (CO) had a significant correlation with distribution of standing trees; (3) The abundance of standing trees and abundance of living standing trees had a significant difference among Transmitted Diffused Light (TDif) groups ($P < 0.05$) and abundance of snags had a significant difference among canopy openness groups ($P < 0.05$), besides, the abundance of standing trees decreased with the enhancement of Transmitted Direct Light (TDir). Moreover, LAI and CO affected under-story light conditions, thereby to the stumpage, especially the formation and abundance degrees of the withered tree.

Key words: mountain forest communities; canopy structure; stumpage abundance; standing tree; dead standing tree; leaf area index (LAI); canopy openness (CO)

林冠（Canopy）是由森林上部郁闭的枝叶和层内空气所组成的，是某一范围内所有树冠 (包括枝叶) 的集合体 [1]。林冠通过截留降水影响森林水文循环 [2-3]，通过对光的吸收、反射和折射影响林下光照条件 [4-5]，还为某些节肢动物提供了栖息场所 [6]，从而有利于维持生物多样性。物理环境和生物环境的异质性影响森林环境及其生物进程 [7]。在全球变化的大背景下，人们越来越深刻地认识到森林是气候变化的良好指示器 [8]。林冠开度（Canopy Openness, CO）与叶面积指数（Leaf Area Index, LAI）是冠层结构的基本参数。同一树冠内的光照强度存在上下和内外的差异 [9]，森林冠层结构也强烈影响着林下光照条件 [10]，通过控制太阳能的截获量来调节林下直射光 (Transmitted Direct Light,

收稿日期：2013-08-10
基金项目：广东省林业科技创新专项资金项目（2011KJCX031-02）
作者简介：敬小丽（1989-），女，四川遂宁人，硕士研究生，研究方向：森林生态学；E-mail：jingxiaoli0930@163.com
通讯作者：张 璐（1973-），女，贵州习水人，副教授，博士，研究方向：森林生态学；E-mail：zhanglu@scau.edu.cn

TDir)、散射光 (Transmitted Diffused Light, TDif) 和总光照 (Transmitted Total Light, TTot) 等 [4]。运用半球面影像技术 (hemispherical photography) 可以快速、方便地测定冠层结构参数，该技术现已广泛应用于生态学领域的研究，如特定树种在不同区域的冠幅差异 [11]、估算林冠属性 [12-13]、估算冠层孔隙度 [14] 以及干扰对冠层结构的影响 [4]。为了探讨森林群落冠层结构与立木多度的关系，以及冠层结构对枯立木形成的影响，本研究以南岭山地森林群落的立木（活立木与枯立木）为研究对象，定量研究了冠层结构参数与立木多度之间的相关性及其大小，为种间与种内竞争分析提供研究思路和参考依据。

1 研究地概况

研究样地位于广东省南岭国家级自然保护区（24º37′ ～ 24º57′ N，112º30′ ～ 113º04′ E），东邻乳源县，南接阳山岭背镇，西靠连州市，北部与湖南省宜章县莽山森林公园接壤，总面积 58 368.4 hm^2，是目前广东省陆地面积最大的保护区。该区属于亚热带季风气候区，年平均温度 17.4 ℃，最冷月（1 月）平均气温 7.1 ℃，最热月（7 月）平均气温 26.2 ℃，年均降水量 1 705 mm，多集中于 8 月。年相对湿度 84%，冬季偶有降雪，日照率 40%。水平地带性土壤多为红壤，分布的土壤类型随海拔高度的不同而不同。该区树种组成丰富，乔木层主要以金缕梅科 Hamamelidaceae、松科 Pinaceae、山茶科 Theaceae、杜鹃花科 Ericaceae 及壳斗科 Fagaceae 占优势，优势种主要有檵木 *Loropetalum chinensis*、华南五针松 *Pinus kwangtungensis*、五列木 *Pentaphylax euryoides*、猴头杜鹃 *Rhododendron simiarum*、疏齿木荷 *Schima remotiserrata*[15]。

2 研究方法

2.1 林分调查

在线路勘察的基础上，采用样方法设置样地，以 10 m×10 m 为样方单元，共计调查了 100 个样方（10 000 m^2）。在每个样方单元内进行每木调查，测定胸径（DBH）≥ 3 cm 的所有活立木的种名、胸径、树高和冠幅。同时根据与枯立木丛生的个体、根部萌枝、树形或木质等特征，记录 DBH ≥ 5 cm 且高度不低于 2 m 的枯立木种名、胸径和树高。

2.2 半球面林冠影像拍摄与分析

选择阴天或无风的天气，在日出或日落的时间 [16]，用三脚架将 Nikon CoolPix 4500 数码相机外接 Nikkor FC-E8 鱼眼镜头转换器水平放置于离地面 1. 65 m 处，用指南针确定方向使记录的照片顶部与磁北方向重合，在每个 10 m×10 m 样方单元中心和对角线四分位处镜头朝上拍摄半球面林冠影像。采用 Gap Light Analyzer 2.0（GLA）图像处理软件分析林冠影像，以输出的林冠开度（CO）、叶面积指数（LAI）、林下直射光（Transmitted Direct Light, TDir）、散射光（Transmitted Diffused Light, TDif）和总光照（Transmitted Total Light, TTot）等 5 个指标作为冠层结构参数。

2.3 数据分析

在 CANOCO 4.5 中采用典范对应分析（Canonical Correspondence Analysis, CCA）方法分析活立木和枯立木在样地中的分布状况及其与林冠开度、叶面积指数、林下直射光、散射光和总光照 5 个冠层结构参数之间的关系。对数据进行蒙特卡罗检验（Monte Carlo Test），并计算冠层结构参数之间的相关系数及其与立木排序轴之间的相关系数。

采用 Statistica 8.0 统计软件对活力木和枯立木的多度与 5 个冠层结构参数分别进行 Kruskal-Wallis（非参数 ANOVA）分析，检验立木多度在各分组变量（见表 1）间是否存在差异，并对其中差异性显著的进行多重比较。

表 1 冠层结构参数分组†

Table 1 Groups of canopy structure parameters

组号	林冠开度 /%	叶面积指数	林下总光照	林下直射光	林下散射光
1	≤ 10.0（39）	≤ 2.00（7）	≤ 5.0（44）	≤ 3.00（63）	≤ 2.00（21）
2	10.1 ～ 15.5（54）	2.01 ～ 3.00（73）	5.1 ～ 10.0（43）	3.01 ～ 5.00（34）	2.01 ～ 3.00（46）
3	15.6 ～ 21.5（12）	≥ 3.01（20）	≥ 10.1（3）	≥ 5.01（3）	3.01 ～ 4.00（29）
4	≥ 21.6（2）				≥ 4.01（5）

† 括号内为样方数。

3　结果与分析

3.1　立木组成与数量特征

基于 10 000 m^2 的样方调查数据，南岭山地森林共计有立木 47 科 81 属 143 种，其中活立木 47 科 81 属 143 种，枯立木 12 科 17 属 17 种。在 143 种活立木中，以五列木科 Pentaphylacaceae 的五列木 *Pentaphylax euryoides* 和甜茶椆 *Lithocarpus polystachyus*、壳斗科的青冈 *Cyclobalanopsis glauca* 以及杜鹃花科的猴头杜鹃和羊角杜鹃 *Rhododendron cavaleriei* 为优势种（见表 2），此外还有金缕梅科的大果马蹄荷 *Exbucklandia tonkinensis* 和檫木、茶科的疏齿木荷和杨桐 *Adinandra millettii* 以及杜鹃花科的石壁杜鹃 *Rhododendron bachii*。

表 2　南岭山地森林群落优势立木数量特征†

Table 2　Quantitative characteristics of dominant standing trees in Nanling mountain forests

立木类型	物种	多度 / 株	频度 / %	平均胸径 /cm	最大胸径 / cm	平均树高 /m	最大树高 / m
活立木	五列木 *Pentaphylax euryoides*	238	29	8.5±4.02	23	8.9±5.93	28.9
	青冈 *Cyclobalanopsis glauca*	162	45	6.2±3.91	21	9.5±8.00	62.5
	猴头杜鹃 *Rhododendron simiarum*	161	15	3.8±0.94	7	6.9±3.54	20.0
	羊角杜鹃 *Rhododendron cavaleriei*	109	18	6.7±2.16	12	6.4±2.81	20.1
	甜茶椆 *Lithocarpus polystachyus*	101	18	4.4±1.22	8	6.1±2.90	15.8
枯立木	赤杨叶 *Alniphyllum fortunei*	4	3	6.8±2.35	9.5	9.5±2.89	13.0
	毒八角 *Illicium toxicum*	3	2	10.3±9.07	20.6	10.0±2.65	12.0
	罗浮锥 *Castanopsis fabri*	3	3	7.7±0.96	8.7	8.8±1.61	10.0
	小果冬青 *Ilex micrococca*	3	1	4.6±0.67	5.2	5.8±0.53	6.2
	青冈 *Cyclobalanopsis glauca*	2	2	19.2±19.5	33	9.5±0.71	10.0

†　表中所列为多度排名前5的活立木和枯立木。

在 17 种枯立木中，以安息香科的赤杨叶 *Alniphyllum fortunei*、八角科 Illiciaceae 的毒八角 *Illicium toxicum*、壳斗科的罗浮锥 *Castanopsis fabri*、青冈以及冬青科 Aquifoliaceae 的小果冬青 *Ilex micrococca* 为优势种，其他枯立木种类还有檫木 *Sassafras tsumu*、长苞铁杉 *Tsuga longibracteata*、檫木、金叶含笑 *Michelia foveolata*、柃木 *Euyra japonica* 等。赤杨叶、毒八角、檫木、罗浮锥、南亚新木姜 *Neolitsea zeylanica*、青冈和五列木是活立木和枯立木的共同优势木。从胸径上看，赤杨叶、檫木、罗浮锥的枯立木胸径比活立木小，而毒八角和青冈的枯立木胸径比活立木大，南亚新木姜和五列木枯立木的平均胸径与活立木相近；从树高上看，仅赤杨叶和五列木枯立木的树高明显比活立木小，其它树种的树高均比活立木大或与之相近。表明林冠上层大树枯死较多，成为枯立木的重要来源。

3.2　冠层结构与立木分布的关系

排除多度≤ 5 的物种，对 84 种常见立木进行多度与冠层结构的典范对应（CCA）分析，结果显示，四个排序轴的特征值分别为 0.381、0.207、0.115 和 0.110，特征值与第一轴和全部轴均通过蒙特卡罗检验（$P < 0.05$），说明排序结果可信（见表 3）。

表 3　各排序轴的加权相关矩阵

Table 3　Weighted correlation matrix of canonical correspondence analysis

特征值	排序轴			
	1	2	3	4
物种 - 环境关系	0.381	0.207	0.115	0.110
变量累积百分比	0.739	0.671	0.596	0.684
物种数据	3.4	5.2	6.2	7.2
物种 - 环境关系	43.9	67.7	80.9	93.6
所有特征值之和	11.267			
所有典范特征值之和	0.869			
第一典范轴 *P* 值	0.021 5			
所有典范轴 *P* 值	0.010 7			

立木冠层结构参数与排序轴之间的相关分析揭示，冠层结构与环境轴 1 和环境轴 2 的相关性较强（见表 4），其中林冠开度与环境轴 1 的相关性最大 ($r = 0.685\ 1$)，叶面积指数与环境轴 2 的相关性最大 ($r = 0.891\ 8$)。

表 4　立木冠层结构参数与环境轴的相关系数

Table 4　Correlation coefficients of canopy structure parameters and environmental axis

环境轴	林冠开度	叶面积指数	林下直射光	林下散射光	林下总光照
环境轴 1	0.685 1	-0.393 3	0.502 9	0.395 7	0.477 1
环境轴 2	-0.661 5	0.891 8	-0.604 1	-0.840 8	-0.721 9
环境轴 3	0.085 7	0.201 1	0.245 2	0.137 6	0.207 6
环境轴 4	-0.289 2	0.001 0	0.023 7	-0.266 8	-0.096 5

冠层结构与立木的 CCA 二维排序图进一步表明立木分布与冠层结构各参数均有一定相关性（见图 1）。图 1 中实心圆点代表立木种类，不同字母组成代表不同树种，带有箭头的连线代表冠层结构参数，箭头所指的方向代表该冠层结构参数的变化趋势，箭头长度代表相关性的大小，箭头连线与排序轴的夹角表示冠层结构参数与排序轴的相关性的大小，夹角越大说明相关性越大，物种点与冠层结构参数的箭头共同反映立木种类沿每一参数梯度方向的变化特征。从图 1 还可看出，立木在二、三象限分布相对较多且密集，对应叶面积指数较小、林冠开度较大的冠层结构以及林下光照较强的光照环境，而在一、四象限的分布较少且较稀疏，尤其在一象限分布最少最稀疏，对应叶面积指数较大、林冠开度较小的冠层结构以及林下光照较弱的光照环境。结合表 4 分析可知，叶面积指数和林冠开度与立木分布的关系较为密切。

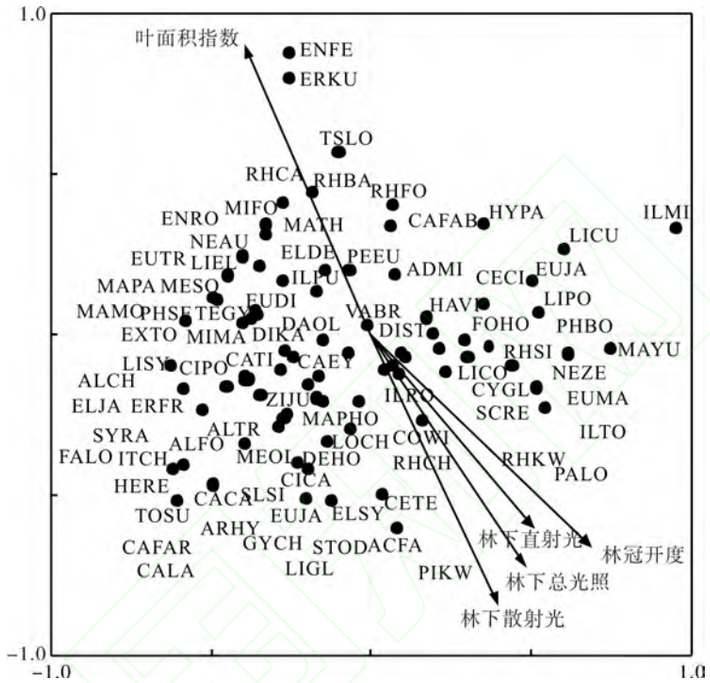

ALCH，阿丁枫；ARHY，白桂木；ALFO，赤杨叶；RHCH，刺毛杜鹃；EXTO，大果马蹄荷；ERKU，东方古柯；ILPU，冬青；ILTO，毒八角；ELDE，杜英；SYRA，多花山矾；EUDI，二列叶柃；GYCH，肥皂荚；GYCH，芬芳安息香；FOHO，福建柏；CATI，钩栲；COWI，光皮树；RHKW，广东杜鹃；PIKW，广东松；HAVI，广东舟柄茶；EUMA，黑柃；CAFAR，红背栲；MATH，红楠；MEOL，红枝柴；SLSI，猴欢喜；RHSI，猴头杜鹃；TEGY，厚皮香；DAOL，虎皮楠；ENRO，黄杞；CIPO，黄樟；LOCH，榄木；CECI，假肉桂；ALTR，江南楂木；MIFO，金叶含笑；PALO，乐东拟单性木兰；EUJA，柃木；CALA，鹿角栲；ACFA，罗浮槭；CAFAB，罗浮锥；DIST，马蹄参；EUTR，毛果柃；MAMO，毛桃木莲；CACA，米锥；PHBO，闽楠；NEZE，南亚新木姜；MAPA，刨花润楠；CETE，朴树；CYGL，青冈；ELJA，日本杜英；MAYU，乳源木莲；LICU，山苍子；ELSY，山杜英；ENFE，少叶黄杞；MIMA，深山含笑；RHBA，石壁杜鹃；LIGL，石栎；SCRE，疏齿木荷；ITCH，鼠刺；FALO，水青冈；ZIJU，酸枣；LIPO，甜茶稠；CAEY，甜槠；ILRO，铁冬青；HERE，网脉山龙眼；VABR，乌饭树；PEEU，五列木；DEHO，香港四照花；ERFR，香花枇杷；ILMI，小果冬青；NEAU，新木姜；LICO，烟斗柯；RHCA，羊角杜鹃；ADMI，杨桐；TOSU，野漆树；DIKA，野柿；EUJA，野鸦椿；LISY，硬叶稠；MAPHO，硬叶楠；HYPA，圆锥绣球；RHFO，云锦杜鹃；PHSE，凿木；CICA，樟树；MESQ，樟叶泡花树；TSLO，长苞铁杉；LIEL，长叶木姜

图 1　冠层结构与立木的典范对应分析

Fig.1　Canonical correspondence analysis between canopy structure factors and common standing trees

3.3　冠层结构与立木多度的关系

3.3.1　林冠开度与立木多度的关系

总的立木多度与活立木多度在林冠开度分组变量间的差异不显著（$P > 0.05$），但枯立木多度在林冠开度分组变量间的差异显著（$P < 0.05$）（见表 5）。活立木多度在林冠开度 10.1 ～ 15.5 的范围内达到最大，此后逐渐减少，说明该范围内的光照、水分、温度等条件最适合该样地林木生长。枯立木多度在不同分组间的变化趋势跟活立木相似，在林冠开度 10.1 ～ 15.5 时多度最大，此后逐渐减少（见图 2 A）。

3.3.2　叶面积指数与立木多度的关系

立木多度在叶面积指数分组变量间的差异不显著（$P > 0.05$）（见表 5），在叶面积指数为 2.01 ～ 3.00 的范围内达到峰值（见图 2 B），在两端的范围内明显减少，说明此范围内的叶面积指数最适合林木生长，可能是该范围内的叶面积指数有最适合林木生长的光照强度和水分条件。在叶面积指数再增大的过程中，林下光照减弱，影响植物的光合作用，进而影响植物生长。

表 5　冠层结构与立木的Kruskal-Wallis分析
Table 5　Kruskal-Wallis analysis of standing trees with canopy structure parameters

项目	立木		活立木		枯立木	
	H 值	P 值	H 值	P 值	H 值	P 值
林冠开度	2.292 3	0.514 0	2.828 9	0.418 8	7.760 0	0.020 7
叶面积指数	2.661 5	0.264 3	2.867 0	0.238 5	0.967 1	0.616 6
林下直射光	1.305 5	0.520 6	1.461 4	0.481 6	0.512 0	0.774 1
林下散射光	9.771 4	0.020 6	10.388 8	0.015 5	2.688 0	0.442 3
林下总光照	1.435 7	0.487 8	1.600 5	0.448 2	0.668 4	0.715 9

3.3.3　林下光照与立木多度的关系

从 Kruskal-Wallis 分析的结果看，总的立木多度与活立木多度均在林下散射光的分组变量间差异显著（$P < 0.05$），枯立木多度在林下光照分组变量间差异均不显著（$P > 0.05$）（见表 5）。由图 2（D）可知，立木多度随着林下直射光的增强呈现明显的减少趋势。活立木与枯立木多度均在林下散射光 2.01 ～ 3.00 的范围内和在林下直射光 ≤ 3 的范围内达到最大，枯立木多度变化趋势与活立木和总的立木多度变化趋势相同。活立木多度在林下总光照≤ 5 和 5.01 ～ 10.00 的范围内均很大，在≥ 10.01 的范围内明显减少（见图 2 C, D, E），枯立木则在林下总光照 5.01 ～ 10.00 的范围内达到峰值，两端减少。

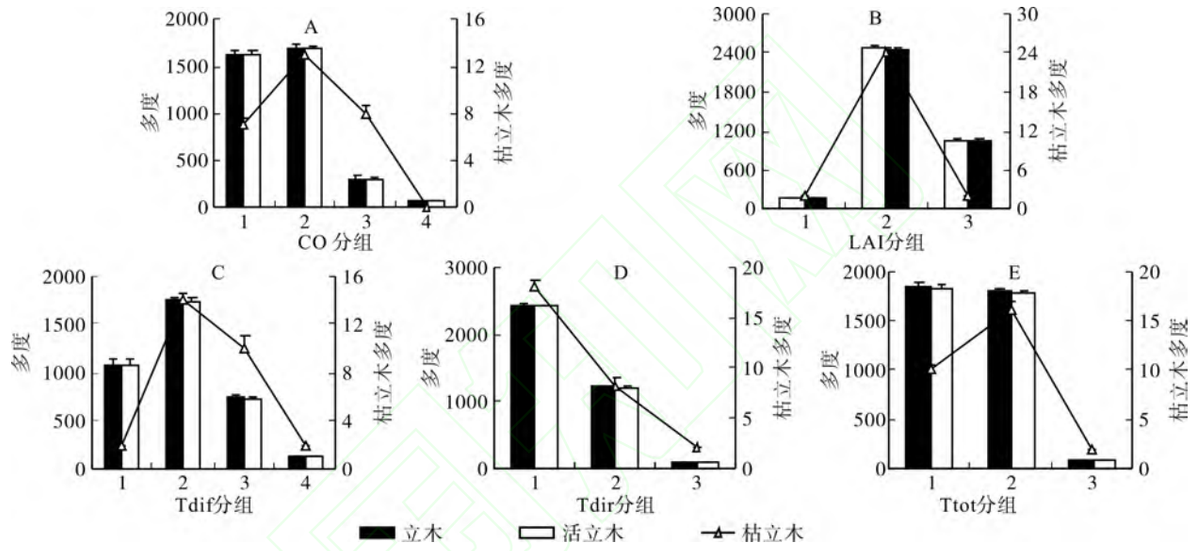

图 2　立木多度对冠层结构分组变量的响应
Fig.2　Responses of standing trees to canopy grouping variables

4　结论与讨论

4.1　叶面积指数通过改变林下光照条件进而影响立木分布

叶片是植物重要的光合作用器官，冠层叶面积指数对群落的生物量有显著影响 [17]，而且与光合有效辐射（Photosynthetically Active Radiation, PAR）的关系密切 [18]，光合有效辐射影响着阳性植物和耐阴植物的分布。杨慧等 [19] 的研究结果表明，生物因素和环境因素是影响白桦 *Betula platyphylla* 种群空间分布格局的两个主要原因，在种间竞争不强的地区呈集群分布，在种间竞争激烈的地区呈随机分布。本研究表明，叶面积指数与典范对应分析环境轴 2 呈正相关，且相关性最大，说明叶面积指数对立木的分布影响较大。同时，叶面积指数与林下直射光、林下散射光呈显著负相关，叶面积指数越大，林下光照条件越差 [19]，说明叶面积指数主要通过影响林下光照条件影响植物分布。

4.2　林冠开度影响枯立木形成及多度

枯立木形成的原因包括对环境因子的竞争 [21]、自然灾害 [22]、地形因子 [23] 等。Sprintsin 等 [24] 的研究表明，林冠开度和立地密度（单位样方内的林木数量）呈显著的线性正相关 ($R^2 = 0.96$)。在林冠开度为 53% 时，立木密度达到最大值。营建母树林时，也需要伐除病虫危害株等扩大林冠开度 [25]，促进植株生长，说明林冠开度对林木的生长有一定影响。本研究结果也揭示，枯立木多度在林冠开度分组变量间的差异显著（$P < 0.05$），说明林冠开度对枯立木形成及多度有影响。林冠开度与林下光照条件直接相关，可能通过影响林下光照进而影响林木生长。

4.3 林下光照条件对立木多度影响显著

光照是影响植物生长的重要生态因子，本研究结果表明林下直射光和林下散射光对立木多度影响显著。立木多度随林下直射光的增强而减少，总的立木多度与活立木多度在林下散射光的分组间差异显著。有研究表明，提高散射光的比率能增加植物光能利用率 [26]，而植物通过调整光能利用率比改变生理结构更能促进光合生产 [27]，进一步说明散射光可以影响立木多度。林下直射光是通过林冠空隙直接入射到森林内部的太阳光线，是植物进行光合作用的重要光照来源，对植物的生长影响最大。本研究结果中，立木多度随着林下直射光增强而减少也证明了这一点。而且林下直射光强度与林冠开度直接相关，林冠开度越大，林下直射光越强，对植物生长越有利，本研究结果也表明立木多度随林冠开度和林下直射光的变化趋势大致相同。

综上所述，森林群落冠层结构与立木关系密切，叶面积指数和林冠开度通过影响林下光照条件进而影响立木，尤其是枯立木的形成和多度。林下直射光与林下散射光均对立木多度有影响，其中立木多度随林下直射光的变化趋势最明显，随着林下直射光增强而减少。不同的林冠开度有不同的林下光照条件和水分条件，从而影响不同种植物间或同种植物内部对光照、水分等生态因子的竞争作用，在研究森林群落种内种间竞争关系的过程中可将冠层结构作为影响因子纳入研究范围，作为一个研究竞争关系的新方向，探讨不同冠层结构条件下种内种间的竞争作用及强度。

参考文献：

[1] 陈 厦 , 桑卫国 . 暖温带地区 3 种森林群落叶面积指数和林冠开阔度的季节动态 [J]. 植物生态学报 , 2007, 31(3): 431-436.

[2] 李汉强 , 邱治军 , 张宁南 , 等 . 马占相思人工林的林冠截留效应 [J]. 中南林业科技大学学报 , 2013, 33(2): 86-90.

[3] Siles P, Vaast P, Dreyer E, *et al*. Rainfall partitioning into throughfall, stemflow and interception loss in a coffee (*Coffea arabica* L.) monoculture compared to an agroforestry system with Inga densiflora[J]. Journal of Hydrology,2010,395(1-2):39-48.

[4] 区余端 , 苏志尧 . 粤北山地常绿阔叶林自然干扰后冠层结构与林下光照动态 [J]. 生态学报 , 2012, 32(18): 5637-5645.

[5] Beaudet M, Harvey B D, Messier C, *et al*. Managing understory light conditions in boreal mixedwoods through variation in the intensity and spatial pattern of harvest: A modelling approach[J]. Forest Ecology and Management, 2011, 261(1): 84-94.

[6] 郑 国 , 李枢强 . 森林冠层节肢动物多样性研究进展 [J]. 动物分类学报 , 2013, 38(1): 178-182.

[7] Ediriweera S, Singhakumara B M P, Ashton M S. Variation in canopy structure, light and soil nutrition across elevation of a Sri Lankan tropical rain forest[J]. Forest Ecology and Management, 2008, 256: 1339-1349.

[8] Iglesias M R , Barchuk A, Grilli M P. Carbon storage, community structure and canopy cover: A comparison along a precipitation gradient[J]. Forest Ecology and Management, 2012, 265: 218-229.

[9] 刘 娟 , 廖 康 , 安晓芹 , 等 . 不同主枝开张角度杏树冠层微气候特征的差异 [J]. 经济林研究 ,2012, 30(4): 82-86.

[10] Lhotka J M, Loewenstein E F. Indirect measures for characterizing light along a gradient of mixed-hardwood riparian forest canopy structures[J]. Forest Ecology and Management, 2006, 226(1-3): 310-318.

[11] Astrup R, Larson B C. Regional variability of species-specific crown openness for aspen and spruce in western boreal Canada [J]. Forest Ecology and Management, 2006, 228(1-3): 241-250.

[12] Ohsawa M, Shimokawa T. Extending the rotation period in larch plantations increases canopy heterogeneity and promotes species richness and abundance of native beetles: Implications for the conservation of biodiversity [J]. Biological Conservation, 2011, 144(12): 3106-3116.

[13] Chianucci F, Cutini A. Estimation of canopy properties in deciduous forests with digital hemispherical and cover photography [J]. Agricultural and Forest Meteorology, 2013, 168: 130-139.

[14] Lang M, Kuusk A, Mõttus M, *et al*. Canopy gap fraction estimation from digital hemispherical images using sky radiance models and a linear conversion method[J]. Agricultural and Forest Meteorology, 2010, 150(1): 20-29.

[15] 张 璐 , 苏志尧 , 陈北光 , 等 . 广东石坑崆森林群落优势种群生态位宽度沿海拔梯度的变化 [J]. 林业科学研究 , 2007, 20(5): 598-603.

[16] Beaudet M, Messier C. Variation in canopy openness and light transmission following selection cutting in northern hardwood stands: an assessment based on hemispherical photographs[J]. Agricultural and Forest Meteorology, 2002, 110(3): 217-228.

[17] 莫丽芬 , 唐建维 , 刀祥生 , 等 . 林分密度对小桐子生物量及其产量的影响 [J]. 中南林业科技大学学报 ,2010, 30(4): 61-68.

[18] 蚁伟民 , 张祝平 , 丁明懋 , 等 . 鼎湖山格木群落的生物量和光能利用效率 [J]. 生态学报 ,2000, 20(2): 397-403.

[19] 杨 慧 , 娄安如 , 高益军 , 等 . 北京东灵山地区白桦种群生活史特征与空间分布格局 [J]. 植物生态学报 ,2007,31(2):272-282.

[20] 贾小容 , 苏志尧 , 区余端 , 等 . 三种人工林分的冠层结构参数

与林下光照条件 [J]. 广西植物 ,2011, 31 (4): 473-478.

[21] 张笑菁 , 赵秀海 , 康峰峰 , 等 . 太岳山油松天然林林木的空间格局 [J]. 生态学报 , 2010, 30(18): 4821-4827.

[22] 沈泽昊 , 王功芳 , 李道兴 . 三峡大老岭山地常绿落叶阔叶混交林林隙干扰研究Ⅱ . 林隙干扰的地形格局 [J]. 植物生态学报 , 2001, 26(2): 149-156.

[23] 刘妍妍 , 金光泽 . 地形对小兴安岭阔叶红松 (*Pinus koraiensis*) 林粗木质残体分布的影响 [J]. 生态学报 ,2009,29(3):1398-1407.

[24] Sprintsin M, Karnieli A, Sprintsin S, *et al*. Relationships between stand density and canopy structure in a dryland forest as estimated by ground-based measurements and multi-spectral spaceborne images[J]. Journal of Arid Environments, 2009, 73(10): 955-962.

[25] 余远国 , 谈建文 , 李万德 . 阳新县吴茱萸母树林营建技术 [J]. 经济林研究， 2005, 23 (3): 62-64.

[26] Jenkins J P, Richardson A D, Braswell B H, *et al*. Refining light use efficiency calculations for a deciduous forest canopy using simultaneous tower-based carbon flux and radio-metric measurements[J]. Agricultural and Forest Meteorology, 2007, 143: 64-79.

[27] Niinemets B. Photosynthesis and resource distribution through plant canopies[J]. Plant, Cell and Environment, 2007, 30: 1052-1071.

[本文编校：谢荣秀]

（上接第 58 页）

参考文献：

[1] 李志辉 , 李柏海 , 祁承经 , 等 . 我国南方珍贵用材树种资源的重要性及其发展策略 [J]. 中南林业科技大学学报 ,2012, 32(11): 1-8.

[2] 方精云 , 王襄平 , 沈泽昊 , 等 . 植物群落清查的主要内容、方法和技术规范 [J]. 生物多样性 ,2009,17(6):533-548.

[3] 古丽努尔·沙比尔哈孜 , 潘伯荣 , 段士民 . 塔里木盆地塔里木沙拐枣群落特征 [J]. 生态学报 ,2012,32(10):3288-3295.

[4] Loreau M, Naeem S,Inchausti P, *et al.* Biodiversity and ecosystem functioning: Current knowledge and future challenges[J]. Science, 2001,294: 804-808.

[5] 吴丽君 , 李志辉 , 邹　峰 . 水分胁迫对珍贵树种赤皮青冈幼苗生理特性的影响 [J]. 中南林业科技大学学报 ,2012,32(7):10-13.

[6] 吴　毅 , 曹基武 , 周国英 , 等 . 湖南衡山优势种群金钱松群落研究 [J]. 中南林业科技大学学报 ,2012,32(11):85-88.

[7] 赵嫦妮 , 徐德禄 , 李志辉 . 配方施肥对赤皮青冈容器苗生长的影响 [J]. 中南林业科技大学学报 ,2013,33(5):22-25.

[8] 钱迎倩 , 马克平 . 生物多样性研究的原理与方法 [M]. 北京 : 中国科学技术出版社 ,1994:141-165.

[9] 吴　毅 . 太行山南麓森林群落景观特征与优良观赏植物遴选 [D]. 长沙 : 中南林业科技大学 ,2008.

[10] 祁承经 , 汤庚国 . 树木学 (南方本) [M]. 第 2 版 . 北京 : 中国林业出版社 , 2005.

[11] 张文辉 , 卢志军 , 李景侠 , 等 . 秦岭北坡栓皮栎种群动态的研究 [J]. 应用生态学报 ,2003,14(9):1427-1432.

[12] 张文辉 , 卢彦昌 , 周建云 , 等 . 巴山北坡不同干扰条件下栓皮栎种群结构与动态 [J]. 林业科学 ,2008,44(7):11-16.

[13] 邱汉周 . 淮南潘集煤矿区植被恢复模式及其土壤修复效应研究 [D]. 长沙 : 中南林业科技大学 ,2012.

[本文编校：吴　毅]

中南林业科技大学学报

ZHONGNAN LINYE KEJI DAXUE XUEBAO

（月刊，1981年创刊）
第34卷第5期（总第155期） 2014年5月出版

主管单位 湖南省教育厅
主办单位 中南林业科技大学
主　　编 吴晓芙
社　　长 伍　谦
编辑出版 《中南林业科技大学学报》编辑部
湖南长沙市韶山南路498号 邮政编码：410004
电话：0731-85623395
Http://qks.csuft.edu.cn
印　　刷 长沙市雅捷印务有限公司
国外总发行 中国出版对外贸易总公司
（北京782信箱，邮编：100011）
国内发行 中南林业科技大学期刊社

JOURNAL OF CENTRAL SOUTH UNIVERSITY OF FORESTRY & TECHNOLOGY

(Monthly, Started in 1981)
Vol. 34 No. 5 (Sum 155) May 2014

Administered by Education Department of Hunan Province
Central South University of Forestry & Technology

Chief Editor WU Xiao-fu

Periodicals Press Director WU Qian

Edited & Published by Ed.Dept.of Journ.of CSUFT
(Changsha 410004, Hunan, China)
Http://qks.csuft.edu.cn

Printed by Changsha Yajie Color Printing Co.Ltd.

Distributed abroad by China National Publishing Industry Trading Corporation
(P.O.BOX 782, Beijing,100011, China)

Distributed domestically by Periodicals Press of CSUFT

刊　　号：ISSN 1673-923X
CN43-1470/S

订阅网址：www.kankan.com.cn

国内定价：20.00元/本

⊙平面设计：周基东设计工作室

中文核心期刊

ISSN 1671-5470
CN 35-1255/S

福建农林大学学报

JOURNAL OF FUJIAN AGRICULTURE AND FORESTRY UNIVERSITY

自然科学版
NATURAL SCIENCE EDITION

ISSN 1671-5470

第42卷 第6期 Vol.42 No.6
中国·福州 Fuzhou,China
2013年11月 Nov., 2013

福建农林大学学报(自然科学版)

Fujian Nonglin Daxue Xuebao (Ziran Kexue Ban) **2013 年 11 月 18 日 第 42 卷第 6 期**

目 次

期刊基本参数：CN 35－1255/S＊1953＊b＊A4＊112＊zh＋en＊P＊￥8.00＊1200＊21＊2013-11 **第 42 卷卷终**

南岭国家级自然保护区森林群落枯立木分布与地形因子的相关性

杜伟静, 苏志尧, 张　璐
(华南农业大学林学院,广东 广州 510642)

摘要: 应用典范对应分析(canonical correspondence analysis, CCA)方法和Kruskal-Wallis(非参数ANOVA)分析方法研究了南岭国家级自然保护区山地森林群落枯立木分布与地形因子的关系. 结果表明:(1)调查枯立木77株,分属17科25属32种;(2)海拔、坡度、坡向、坡位和坡形等5个地形因子的综合作用对枯立木的分布格局具有显著影响($P<0.01$),地形因子与3个排序轴均有较强的相关性,地形因子在第1排和第2排序轴的位置明显反映其生态特点;(3)海拔对枯立木多度的影响显著,海拔是影响枯立木分布的首要控制因子.

关键词: 枯立木; 地形因子; 海拔; 典范对应分析
中图分类号: Q948　　**文献标识码**: A　　**文章编号**:1671-5470(2013)06-0603-07

Correlation of snags with topographical factors in montane forests in Nanling National Nature Reserve

DU Wei-jing, SU Zhi-yao, ZHANG Lu
(College of Forestry, South China Agriculture University, Guangzhou, Guangdong 510642, China)

Abstract: By using canonical correspondence analysis (CCA) and Kruskal-Wallis (nonparametric ANOVA) analysis method, the relationship between distribution of snags and topographical factors in montane forests in Nanling National Nature Reserve was researched. The results were as follows. (1) 77 stems, 32 species in 25 genera and 17 families of snags were found in the plot. (2) Elevation, slope grade, slope aspect, slope position and slope shape had significantly integrative effects on distribution of snags ($P<0.01$). Topographical factors had significant correlations with the three axes in CCA plot, and the environmental factors in the first and second axes reflected the ecological conditions of the community. (3) In the five topographic factors, elevation had significant effects on the distribution of snags which was the primary control factor affecting the distribution of snags.

Key words: snags; topographical factor; elevation; canonical correspondence analysis (CCA)

在全球气候变化和生物多样性保护研究广泛开展的背景下,森林生态系统中的粗木质物残体(coarse woody debris, CWD)越来越受到生态学家的关注[1]. 枯立木是森林生态系统中CWD的重要组成部分,在生态系统碳贮量和碳循环过程中发挥不可替代的作用[2],而且是野生动物筑巢、栖居、造穴、休息、觅食、避难和繁殖后代[3,4]的重要场所. 地形因子是为植物群落提供生境多样性的最重要的环境梯度之一,而且植被格局与地形格局密切相关[5]. 地形通过地貌过程影响土壤的水、热及养分的再分配,进而对植被产生直接的空间再分配,是影响林分发展和演替的重要因子. 而林分的生长和死亡是森林生态系统动态过程的重要特征.

国外对枯立木的研究主要集中在欧洲和美洲北部的温带森林,其次为热带雨林,北回归线附近的森林较少. 对枯立木的储量、分解率、呼吸量的测定,以及对森林生态系统的功能和枯立木在森林经营等方面都有较多的研究报道[2-4]. 我国学者对长白山[6]、大兴安岭[7]、小兴安岭[8]、武夷山[9]、秦岭[10]、哀牢山[11]、西双版纳[12]、鼎湖山[13]等地枯立木进行了研究,主要对暗针叶林、阔叶红松林、红松针阔混交林、冷杉林等温带森林,以及寒温带落叶松林、西南湿性常绿阔叶林、季风常绿阔叶林和武夷山甜槠林等热带亚热带森林的储量、分布、组成及其分解等进行了研究[14-16],但是对地形因子与枯立木分布的关系方面的研究还

收稿日期:2013-01-16　　**修回日期**:2013-06-11
基金项目:广东省林业科技创新专项资金资助项目(2011KJCX031-02).
作者简介:杜伟静(1987-),女,硕士研究生. 研究方向:森林生态. Email:gdduweijing@163.com. 通讯作者张璐(1973-),女,副教授,博士. 研究方向:森林生态学. Email:zhanglu@scau.edu.cn.

比较缺乏[8]. 南岭山地是广东北部的天然屏障,是我国生物多样性保护的关键性地区和开展生态系统就地保护的重要基地,至今仍保存着大面积原生性较强的天然常绿阔叶林. 但对南岭国家级自然保护区常绿阔叶林枯立木分布与地形因子关系的研究尚未见报道.

1 研究地概况

研究试验地设在广东南岭国家级自然保护区内(112°41 -′113°15′ E, 24°39′ -28°08′ N). 总面积 5.63 万 hm^2,是广东省目前陆地森林面积最大的国家级自然保护区. 保护区最低处海拔 200 m,最高峰(石坑崆峰)海拔 1902 m,属中山地貌,山地坡度一般为 25° -50°,局部可达 60°以上. 山脉多为西北—东南走向,平地多为红壤,分布的土壤类型随海拔高度的不同而异,年平均气温 18 -21 ℃,最冷月(1 月份) 平均气温为 5 -10 ℃,最热月(7 月份) 平均气温 22 -29 ℃,降水量充沛,年平均降水量 1400 -2000 mm,降雨量多集中在 3 -8 月份,年相对湿度 84%,冬季偶或降雪,日照率 40%[16]. 该区森林覆盖率达 98%以上,植被主要被划分为 7 个类型、29 个群系和 73 个群从. 该区植被类型复杂而多样,树种组成丰富[17],组成种类主要有青冈(*Cyclobalanopsis glauca*)、罗浮锥(*Castanopsis fabri*)、甜槠(*Castanopsis eyrei*)等壳斗科(Fagaceae)常绿树种以及松科(Pinaceae)华南五针松(*Pinus kwangtungensis*)、茶科(Theaceae)疏齿木荷(*Schima remotiserrata*)、五列木科(Pentaphylacaceae)五列木(*Pentaphylax euryoides*)、杜鹃花科(Ericaceae)南华杜鹃(*Rhododendron simiarum*)、金缕梅科(Hamamelidaceae)大果马蹄荷(*Exbucklandia tonkinensis*)和檵木(*Loropetalum chinensis*)、安息香科(Styraceae)赤杨叶(*Alniphyllum fortunei*)等.

2 研究方法

2.1 取样方法

在线路勘察的基础上,采用连续样带取样法,海拔 300 -1800 m 以样带形式设置样地. 海拔每升高 100 m 设置 1 条水平样带,共 16 条样带,样地面积共计 19200 m^2. 运用邻接格子样方法,每条样带设置 12 个 10 m ×10 m 的样方单元. 在每个 10 m ×10 m 样方内进行每木调查,测定胸径(*DBH*) ≥ 3 cm[11]的所有立木的胸径、树高、冠幅和林分郁闭度. 枯立木要求 *DBH*≥ 5 cm,高度不低于 2 m. 根据与枯立木丛生的个体、根部萌枝、树形或木质等特征确定枯立木的种名.

2.2 地形因子

采用手持式 GPS、气压式海拔表、坡度计等实测样方的地理坐标、海拔、坡度、坡向等地形因子. 同时目测坡位和坡形. 样地海拔高度为 300 -1800 m,样地坡度为 2.5° -58.1°,分为 4 组,分别赋值 1 -4. 以北为起点(0°)顺时针方向旋转,坡向可划分为北坡(338° -22°) 、东北坡(23° -67°)、东坡(68° -112°)、东南坡(113° -157°) 、南坡(158° -202°)、西南坡(203° -247°)、西坡(248° -292°)和西北坡(293° -337°). 坡位从山谷到山脊,包括下坡位、中坡位、上坡位,坡形分凸、平、凹 3 级,分别赋值 1 -3[18](表 1).

表 1 地形因子分组

Table 1 Group of topographical factors

	海拔/m	坡度/(°)	坡向	坡位	坡形
1	300 -600(6)	2.5 -14.9 平缓坡(2)	东坡和东南坡(10)	下坡(6)	凹(7)
2	700 -1000(6)	15.0 -34.9 斜陡坡(9)	南坡和西南坡(14)	中坡(20)	平(12)
3	1100 -1400(14)	35.0 -44.9 急坡(20)	西坡和西北坡(6)	上坡(15)	凸(22)
4	1500 -1800(15)	45.0 -58.1 险坡(10)	北坡和东北坡(11)		

2.3 数据处理

采用典范对应分析(canonical correspondence analysis, CCA) 方法在 PC-ORD(6.0)中分析枯立木 32 个种群在 41 个样地中的分布状况及其与海拔高度、坡度、坡向、坡位、坡形等 5 个地形因子的相互关系. 在进行 CCA 排序前用对数转化法对数据集的环境变量进行标准化,选择变量最优的方式排序,并进行蒙特卡罗检验,同时计算地形变量之间的相关性和地形变量与枯立木种类排序轴之间的相关系数.

采用 Statistica 8.0 软件对枯立木多度和丰富度与 5 个地形因子的相关性分别进行 Kruskal-Wallis(非参数 ANOVA)分析,检验枯立木多度和丰富度在各分组变量间是否存在差异,并对其差异显著进行多重

比较.

3　结果与分析

3.1　枯立木的物种组成

南岭国家级自然保护区 1.92 hm^2 的调查样地共调查到有枯立木 77 株,分属于 17 科 25 属 32 种(表 2). 枯立木数量分配以壳斗科、五列木科、冬青科(Aquifoliaceae)、樟科(Lauraceae)为优势科. 壳斗科作为南岭自然保护区中常绿阔叶林枯立木的最为优势的科成分,3 属 6 种. 枯立木分布从属的层次上看,以五列木属(*Pentaphylax*)为首,多度为 11,出现在 7 个样方中,其次是栲属(*Castanopsis*). 而从枯立木的种层次上看,以五列木科的五列木、壳斗科的罗浮锥、安息香科的赤杨叶、柏科(Cupressaceae)的福建柏(*Fokienia hodginsii*)、冬青科的铁冬青(*Ilex rotunda*)、樟科的粗壮润楠(*Machilus robusta*)为主. 组成种类以五列木和罗浮锥占优势.

表 2　南岭山地森林群落枯立木的物种组成

Table 2　Species composition of standing dead trees of the montane forests in Nanling

科名	属名	种名	物种代码	多度	样方数
壳斗科 Fagaceae	栲属 *Castanopsis*	罗浮锥 *Castanopsis fabri*	CAFA	7	6
		甜槠 *Castanopsis eyrei*	CAEY	2	1
		藜蒴 *Castanopsis fissa*	CAFI	1	1
	青冈属 *Cyclobalanopsis*	青冈 *Cyclobalanopsis glauca*	CYGL	2	2
	柯属 *Lithocarpus*	胡氏青冈 *Cyclobalanopsis hui*	CYHU	1	1
		烟斗柯 *Lithocarpus corneus*	LICO	2	1
五列木科 Pentaphylacaceae	五列木属 *Pentaphylax*	五列木 *Pentaphylax euryoides*	PEEU	11	7
冬青科 Aquifoliaceae	冬青属 *Ilex*	铁冬青 *Ilex rotunda*	ILRO	4	1
		小果冬青 *Ilex micrococca*	ILMI	3	1
樟科 Lauraceae	润楠属 *Machilus*	粗壮润楠 *Machilus robusta*	MARO	4	2
	檫木属 *Sassafras*	檫木 *Sassafras tsumu*	SATS	1	1
	新木姜属 *Neolitsea*	南亚新木姜 *Neolitsea zeylanica*	NEZE	1	1
		新木姜 *Neolitsea aurata*	NEAU	1	1
杜鹃花科 Ericaceae	杜鹃花属 *Rhododendron*	石壁杜鹃 *Rhododendron bachii*	RHBA	3	1
		羊角杜鹃 *Rhododendron cavaleriei*	RHCA	2	2
		南华杜鹃 *Rhododendron simiarum*	RHSI	1	1
松科 Pinaceae	松属 *Pinus*	华南五针松 *Pinus kwangtungensis*	PIKW	3	2
	油杉属 *Tsuga*	长苞铁杉 *Tsuga longibracteata*	TSLO	3	3
安息香科 Styraceae	赤杨叶属 *Alniphyllum*	赤杨叶 *Alniphyllum fortunei*	ALFO	4	3
柏科 Cupressaceae	福建柏属 *Fokienia*	福建柏 *Fokienia hodginsii*	FOHO	4	3
八角科 Illiciaceae	八角属 *Illicium*	毒八角 *Illicium toxicum*	ILTO	3	2
桃金娘科 Myrtaceae	蒲桃属 *Syzygium*	赤楠蒲桃 *Syzygium buxifolium*	SYBU	3	1
杜英科 Elaeocarpaceae	杜英属 *Elaeocarpus*	日本杜英 *Elaeocarpus japonicus*	ELJA	2	2
茶科 Theaceae	柃属 *Euyra*	柃木 *Euyra japonica*	EUJA	1	1
	木荷属 *Schima*	疏齿木荷 *Schima remotiserrata*	SCRE	1	1
木兰科 Magnoliaceae	含笑属 *Michelia*	金叶含笑 *Michelia foveolata*	MIFO	1	1
	木莲属 *Manglietia*	乳源木莲 *Manglietia yuyanensis*	MAYU	1	1
鼠李科 Rhamnaceae	枣属 *Ziziphus*	酸枣 *Ziziphus jujuba*	ZIJU	1	1
	枳椇属 *Hovenia*	拐枣 *Hovenia acerba*	HOAC	1	1
金缕梅科 Hamamelidaceae	檵木属 *Loropetalum*	檵木 *Loropetalum chinensis*	LOCH	1	1
槭树科 Aceraceae	槭属 *Acer*	青榨槭 *Acer davidii*	ACDA	1	1
蔷薇科 Rosaceae	石楠属 *Photinia*	桃叶石楠 *Photinia prunifolia*	PHPR	1	1

3.2　地形因子对枯立木分布的影响

采用 CCA 方法能够在同一排序图上展示植物种类与环境因子的关系,是当今生态学应用最广泛的直接梯度排序方法. 南岭山地森林群落枯立木与地形因子的 CCA 方法中 3 个排序轴的特征根值分别为 0.952、0.909 和 0.800,群落枯立木与环境因子 3 个排序轴的相关系数分别为 0.981、0.968 和 0.912,且特征值和枯立木种群与环境因子的相关系数都通过蒙特卡罗检验,P 值皆为 0.01,说明排序效果理想. 5 个环境因子与 3 个排序轴均有不同程度的相关性(表 3). 海拔高度与第 1 排序轴的正相关性最大,坡位次

之,坡形、坡向最小. 坡度与第 1 排序轴的相关性最小,相关系数仅为 -0.094. 坡度、坡向与第 2 排序轴呈负相关,坡位、坡形与第 2 排序轴呈正相关. 与第 1 排序轴和第 2 排序轴相比,除了坡度与第 3 排序轴有较强的负相关性外,其余地形因子与第 3 排序轴的相关性较弱. 说明第 1 排和第 2 排序轴与环境因子的关系比第 3 排序轴与环境因子的关系显著,地形因子在第 1 排、第 2 排序轴的位置明显反映其生态特点.

表 3 环境因子与排序轴以及环境因子之间的相关系数

Table 3 Correlation coefficients of topographic factors and axes

	第 1 轴	第 2 轴	第 3 轴	海拔	坡度	坡向	坡位	坡形
海拔	0.896	0.148	0.184	1				
坡度	-0.094	-0.619	-0.517	0.039	1			
坡向	0.405	-0.391	-0.260	0.205	0.307	1		
坡位	0.721	0.524	-0.275	0.648	0.031	-0.044	1	
坡形	0.409	0.487	-0.016	0.553	-0.009	0.077	0.791	1

在 5 个环境因子中,海拔与坡位、坡形都存在着较强的正相关性,坡度与坡向呈正相关性,而坡位与坡形也有较强的正相关性. 南岭山地森林群落枯立木与地形因子的 CCA 二维排序图较好解释了 32 个枯立木种类的生态分布与 5 个环境因子的相关性. 图 1 中实心圆点代表枯立木种类(物种代码见表 2),实线长度表示地形因子与枯立木种类的相关性,实心圆点与实线的相对位置表示枯立木种类与地形因子的相关性. 32 个枯立木种类沿第 1 排序轴可以大致分为两大类,一类分布于第 1 排序轴的左侧,另一类主要集中于排序轴的右侧,表现出与物种性状相关的特征. 第 1 排序轴左侧的拐枣(*Hovenia acerba*)、酸枣(*Ziziphus jujube*)、櫸木、胡氏青冈(*Cyclobalanopsis hui*)等枯立木多为落叶树种,多分布在低海拔山地,而且频度较小. 而右侧的物种多为常绿树种,除了赤扬叶、小果冬青(*Ilex micrococca*)与其它种相隔较远外,其余的种群都集中于第 1 排序轴周围. 小果冬青和赤扬叶是分布于第 1 排序轴右侧的落叶物种,二者适应生境的能力与其它物种相比差异较大,负相关性较强.

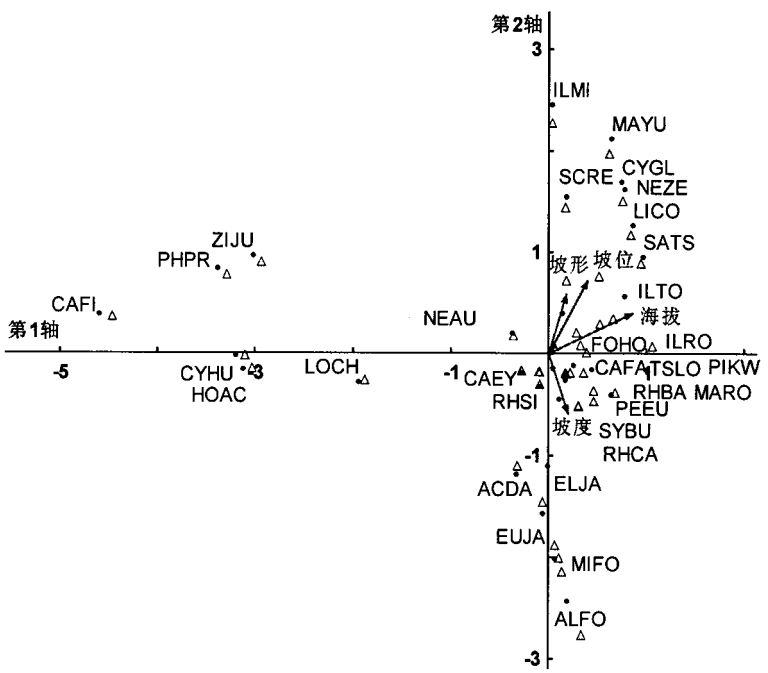

图 1 枯立木与地形因子的典范对应分析

Fig. 1 Canonical correspondence analyses between snags and topographic factors

3.3　枯立木分布对地形因子的响应

3.3.1　枯立木分布对海拔因子的响应　枯立木多度在海拔分组变量间差异极显著($P < 0.01$)(表 4),多重比较进一步表明,300 – 600 m 海拔段的枯立木个体分布与 1100 – 1400 m 海拔段的存在显著差异($P < 0.05$),而其余海拔段两两之间枯立木分布没有显著差异($P > 0.05$). 枯立木的多度随着海拔的升高而增大,1100 – 1400 m 处达到最大值(图 2A). 枯立木丰富度在海拔变量间没有显著性差异($P > 0.05$),在 1100 – 1400 m 海拔段出现最大值(图 2A),这与枯立木多度发展趋势相对应. 由此可见,海拔对枯立木多度分布的影响较大,对枯立木丰富度影响较小.

表 4　枯立木与地形因子的 Kruskal-Wallis 分析

Table 4　Kruskal-Wallis analysis of snags and topographic factor

	多度		丰富度	
	H 值	*P* 值	*H* 值	*P* 值
海拔	11.4399	0.0096	6.2228	0.1013
坡度	4.0289	0.2584	2.0577	0.5605
坡向	6.3181	0.0971	5.2298	0.1557
坡位	2.3396	0.3104	0.8549	0.6522
坡形	1.6393	0.4406	4.5210	0.1043

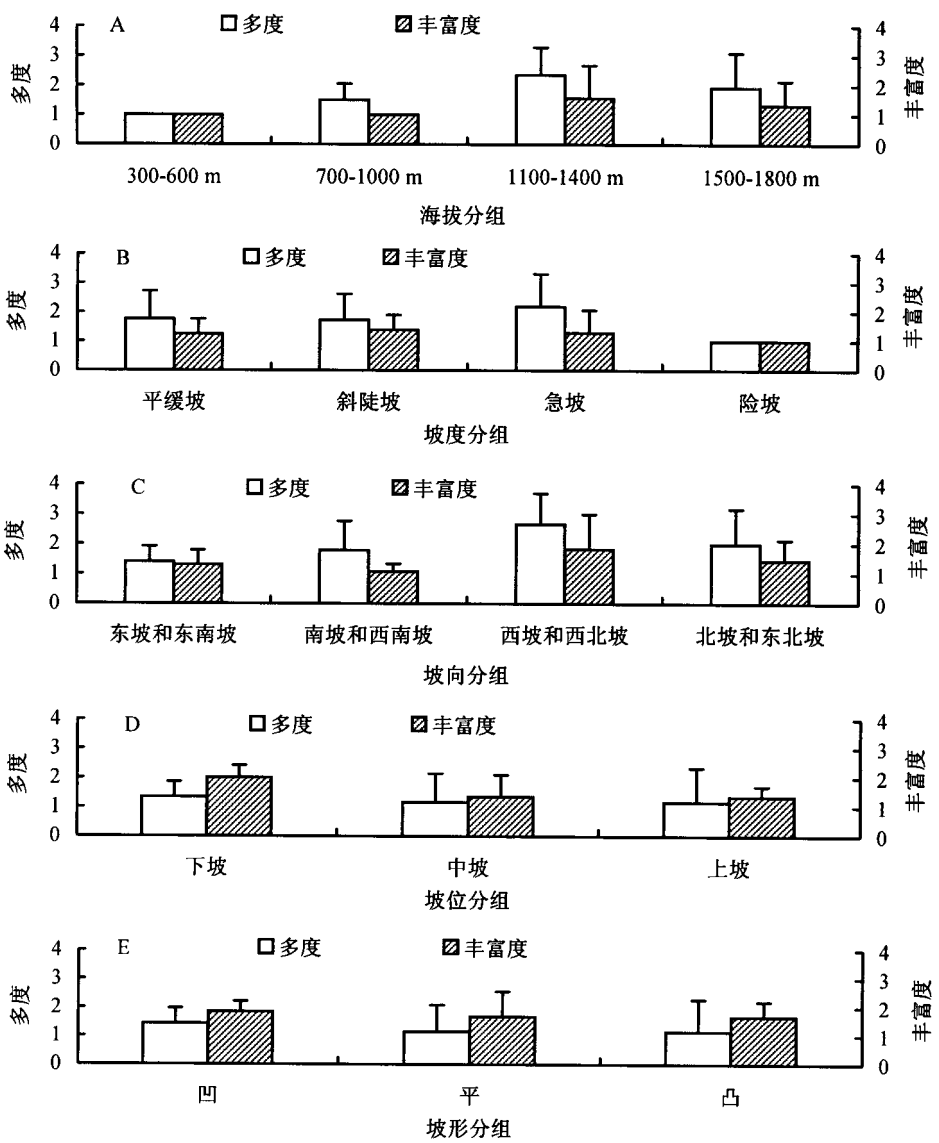

A. 枯立木对海拔分组变量的响应;B. 枯立木对坡度分组变量的响应;C. 枯立木对坡向分组变量的响应;D. 枯立木对坡位分组变量的响应;E. 枯立木对坡形分组变量的响应.

图 2　枯立木对地形因子分组变量的响应

Fig. 2　Response of snags to topography grouping variables

3.3.2　枯立木分布对坡度因子的响应　枯立木多度、丰富度在坡度分组变量间有一定的差异,但差异不显著($P > 0.05$)(表 4). 多度和丰富度的平均值都在急坡处达到最大值(图 2B),这可能是由于急坡坡度

大,水分流失较严重,林木间竞争较强.

3.3.3 枯立木分布对坡向因子的响应 随着坡向的变化,枯立木的多度和丰富度也有一定差异,但枯立木多度、丰富度在坡向分组变量间差异不显著($P>0.05$)(表 4). 枯立木多度和丰富度的平均值均在西坡和西北坡达到最大值(图 2C). 随着坡向从东坡向北坡的变化,枯立木的多度逐渐增加,在西坡达到最大,这可能与不同坡向的光、热、水和土壤条件的差异有关.

3.3.4 枯立木分布对坡位因子的响应 随着坡位的上升,枯立木的多度增大,但枯立木多度、丰富度在坡位分组变量间差异不显著($P>0.05$)(表 4). 枯立木多度和丰富度均在中坡位达到最大值(图 2D).

3.3.5 枯立木分布对坡形因子的响应 枯立木多度随坡形的变化而增大,但枯立木多度、丰富度在坡形分组变量间差异不显著($P>0.05$)(表 3). 枯立木多度最大值出现在凸坡,而丰富度最大值出现在平坡(图 2E).

4 小结与讨论

4.1 枯立木分布与海拔梯度的关系

海拔是影响物种丰富度格局的决定性因素之一[19]. 研究[20]表明海拔拥有最高的物种丰富度. 但也有研究指出物种丰富度与海拔梯度呈负相关或者物种丰富度随海拔的升高没有明显变化[21]. 文献[8,22,23]研究结果表明枯立木的分布与海拔梯度有关,本研究也发现枯立木多度随着海拔的上升而增加(图 2A),枯立木多度在海拔分组变量间差异显著($P<0.01$),此结果与刘妍妍等[8]和游惠明等[21]的研究结果相符,但枯立木丰富度在海拔分组变量间差异不显著($P>0.05$). 随海拔的上升,不仅温度、降雨等气象因子发生显著的变化,土壤理化性质、植被性质、土壤微生物群落等生物、非生物因子也发生变化,CWD 也表现出一定的变化趋势. 群落结构,植物地上、地下生物量等有可能也是导致 CWD 沿海拔梯度变化的重要因子.

4.2 枯立木分布与地形因子的关系

研究认为,枯立木的分布受地形因子的影响显著[8,12,23]. 邓云等[12]认为 CWD 分布受坡度、坡向的影响,多数大径级的 CWD 分布于 15° – 25°的坡地上,样地中 CWD 的分布也主要集中于东南、西北及其邻近坡向. 本研究结果表明枯立木与坡度相关性较小,与邓云等[12]的研究不一致,但与刘妍妍等[8]和 Rubino et al[23]研究结果相符. 地形因子通过地貌过程影响土壤的水、热及养分的再分配,地形因子可能对 CWD 腐烂等级的影响较大,而对 CWD 数量分布的影响较小. 因此,地形因子对枯立木腐烂程度的影响有待进一步研究.

综上所述,影响枯立木分布的因素包括地形因子、植被类型、土壤理化性质、物种组成、植被性质,土壤微生物群落等生物和非生物因子. 本研究结果表明海拔梯度是枯立木分布的首要控制因子,而地形因子(坡度、坡位、坡向、坡形)对枯立木分布的影响较小,这可能与该研究地的物种组成、植被性质以及外界干扰有关,有待进一步研究.

参考文献

[1] 陈华,徐振邦. 粗木质物残体生态研究历史、现状和趋势[J]. 生态学杂志,1991,10(1):45 – 50.

[2] TEODOSIU M, BOURIAUD O B. Deadwood specific density and its influential factors: a case study from a pure Norway spruce old-growth forest in the Eastern Carpathians[J]. Forest Ecology and Management, 2012,283:77 – 85.

[3] KEBLI H, BRAIS S, KERNAGHAN G, et al. Impact of harvesting intensity on wood-inhabiting fungi in boreal aspen forests of Eastern Canada[J]. Forest Ecology and Management, 2012,279:45 – 54.

[4] 袁杰,侯琳,张硕新. 森林粗木质残体研究进展[J]. 西北林学院学报,2011(4):90 – 98.

[5] OU Y D, SU Z Y, KE X D, et al. Vascular ground flora in relation to topography, canopy structure and gap light regimes in subtropical broadleaved forest (South China)[J]. Polish Journal of Ecology, 2012,60:463 – 478.

[6] 陈华,徐振邦. 长白山红松针阔混交林林木死亡的初步研究[J]. 应用生态学报,1991,2(1):89 – 91.

[7] 王文娟,常禹,刘志华,等. 大兴安岭呼中林区粗木质残体贮量及其环境梯度[J]. 应用生态学报,2009,20(4):773 – 778.

[8] 刘妍妍,金光泽. 地形对小兴安岭阔叶红松(*Pinus koraiensis*)林粗木质残体分布的影响[J]. 生态学报,2009,29(3):1398 – 1407.

[9] 凌浩,邢雪荣,黄大明,等. 武夷山甜槠林粗死木质残体的贮量、动态及其功能评述[J]. 植物生态学报,1996,20(2):132 – 143.

[10] 李凌浩,党高弟,汪铁军,等. 秦岭巴山冷杉林粗死木质残体研究[J]. 植物生态学报,1998,22(5):51 – 57.

[11] 张树斌,郑征. 哀牢山中山湿性常绿阔叶林枯立木数量及分配规律[J]. 东北林业大学学报,2009,37(2):3 – 5,13.

[12] 邓云,张文富,邓晓保,等. 西双版纳热带季节雨林粗木质物残体储量及其空间分布[J]. 生态学杂志,2012,31(2):261 – 270.

[13] YANG F F, LI Y L, ZHOU G Y, et al. Dynamics of coarse woody debris and decomposition rates in an old-growth forest in lower tropical China[J]. Forest Ecology and Management, 2010,259(8):1666 – 1672.

[14] 唐旭利,周国逸. 南亚热带典型森林演替类型粗死木质残体贮量及其对碳循环的潜在影响[J]. 植物生态学报,2005,29(4):559 – 568.

[15] 张利敏,王传宽,唐艳. 11 种温带树种粗木质残体分解初期结构性成分和呼吸速率的变化[J]. 生态学报,2011,31(17):5017 – 5024.

[16] 张璐,贺立静,区余端,等. 南岭自然保护区常绿阔叶林枯立木数量特征分析[J]. 福建林学院学报,2012,32(1):64 – 69.

[17] 陈北光,苏志尧,谢正生,等. 广东南岭国家级自然保护区主要森林植被类型及其结构特征[A]//庞雄飞. 广东南岭国家级自然保护区生物多样性研究[C]. 广州:广东科技出版社,2003:14 – 27.

[18] 张璐,李镇魁,苏志尧,等. 南岭国家级自然保护区森林群落的数量分类与排序[J]. 华南农业大学学报,2007,28(3):71 – 75.

[19] LIEBERMAN D, LIEBERMAN M, PERALTA R, et al. Tropical forest structure and composition on a large scale altitudinal gradient in Costa Rica[J]. Journal of Ecology, 1996,84:137 – 152.

[20] LOMOLINO M V. Elevational gradients of species density: historical and prospective views[J]. Global Ecology & Biogeography, 2001,10:3 – 13.

[21] OHSAWA M. Latitudinal comparison of altitudinal changes in forest structure, leaf-type, and species richness in humid monsoon Asia[J]. Vegetatio, 1995,121:3 – 10.

[22] 游惠明,何东进,洪伟,等. 海拔对天宝岩长苞铁杉林粗死木质残体分布的影响[J]. 福建农林大学学报:自然科学版,2011,40(4):365 – 369.

[23] RUBINO D L, MCCARTHY B C. Evaluation of coarse woody debris and forest vegetation across topographic gradients in a southern Ohio forest[J]. Forest Ecology and Management, 2003,183(1 – 3):221 – 238.

(责任编辑:叶济蓉)

本刊为中文核心期刊、中国期刊方阵“双效”期刊、中国高校精品科技期刊

○ 1999年获全国高校自然科学学报及教育部优秀科技期刊二等奖、福建省高校优秀自然科学学报一等奖
○ 2000年获全国优秀农业期刊一等奖
○ 2004年获全国高校科技期刊一等奖
○ 2006年获中国高校优秀科技期刊奖、福建省高校精品学报奖
○ 2008年获中国高校精品科技期刊奖、福建省十佳期刊提名奖
○ 2009年获华东地区优秀期刊奖
○ 2010年获中国高校精品科技期刊奖
○ 2012年获华东地区优秀期刊奖

本刊被下列数据库和检索刊物固定收录：

○ 中国科学引文数据库
○ 中国学术期刊综合评价数据库
○ 国际农业与生物科学中心数据库（CAB）
○ 联合国粮食与农业组织国际农业科技情报系统数据库（AGRIS）
○ 俄罗斯《文摘杂志》
○ 中国知网、中国学术期刊（光盘版）（全文收录）
○ 万方数字化期刊群（全文收录）
○ 中文科技期刊数据库（全文收录）

福建农林大学学报（自然科学版）
Fujian Nonglin Daxue Xuebao(Ziran Kexue Ban)
（双月刊 1953年创刊）
第42卷 第6期 2013年11月18日

Journal of Fujian Agriculture and Forestry University
(Natural Science Edition)
(Bimonthly, Started in 1953)
Vol. 42 No. 6 November 18, 2013

主办单位 福建农林大学
主管单位 福建农林大学
编辑出版 福建农林大学学报编辑部
（福州金山，邮政编码 350002）
Email: jfau@fafu.edu.cn
主　　编 兰思仁
副 主 编 尤民生 林国栋（常务）
印　　刷 福建农林大学印刷厂
（福州金山，邮政编码 350002）
发行范围 公开发行
国内发行 福州市邮政局
订　　阅 全国各地邮局（所）
国外发行 中国国际图书贸易总公司
（北京399信箱，邮政编码100044）

Sponsored by Fujian Agriculture and Forestry University
Edited and Published by Editorial Department of Journal of Fujian Agriculture and Forestry University
(Jinshan, Fuzhou, Fujian 350002, China)
Email: jfau@fafu.edu.cn
Chief Editor: Lan Siren
Deputy Chief Editors: You Minsheng, Lin Guodong
Issued in Public
Distributed abroad by China International Book Trading Corporation (P. O. Box 399, Beijing 100044, China)

ISSN 1671-5470
CN 35-1255/S
国外代号: **BM 675**　　报刊代号: **34-16**　　国内定价: **8.00**元

4. 学术著作

极小种群野生植物 科普丛书

虫创纪 绘

不再孤独的紫荆木

张璐 著

中国林业出版社
China Forestry Publishing House

图书在版编目（CIP）数据

不再孤独的紫荆木 / 张璐等著 ; 虫创纪绘. -- 北京 : 中国林业出版社, 2023.11
（极小种群野生植物科普丛书）
ISBN 978-7-5219-2424-4

Ⅰ. ①不… Ⅱ. ①张… ②虫… Ⅲ. ①乔木－普及读物 Ⅳ. ①S718.4-49

中国国家版本馆CIP数据核字(2023)第223349号

审图号：GS京（2024）0089号

策划编辑：袁丽莉
责任编辑：袁丽莉
装帧设计：北京八度出版服务机构
宣传营销：张　东

出版发行：中国林业出版社
（100009，北京市西城区刘海胡同 7 号，电话 83143633）
电子邮箱：cfphzbs@163.com
网址：www.forestry.gov.cn/lycb.html
印刷：河北京平诚乾印刷有限公司
版次：2023 年 11 月第 1 版
印次：2023 年 11 月第 1 次
开本：889mm×1194mm　1/16
印张：2.75
字数：10 千字
定价：29.80 元

编委会

张　璐　　焦正利　　陈芷鹏　　马艺菲

林浩有　　汪书钰　　叶水云　　刘效东

指导单位

广东省林业局

写在前面

小朋友们，大家好！我是你们的新朋友——紫荆木美美。

你们可能没有听说过我的名字，但是我相信你们会慢慢地认识我、熟悉我、理解我，并最终和我一起守护我们的家园，共建地球生命共同体。

《不再孤独的紫荆木》是第一本专为儿童打造的知识性和趣味性兼具的紫荆木科普读物。书中通过生动有趣的成长故事，以图文并茂的形式讲述我从种子萌发露头—胚根长出—胚芽长出—二叶期—幼苗—幼树—成树—开花结实的生活史，展现我在不同生长期的形态特征、生境特点、生存状况，以及就地保护和迁地保护等措施。

现在，请翻开下一页，看看我的成长故事吧！

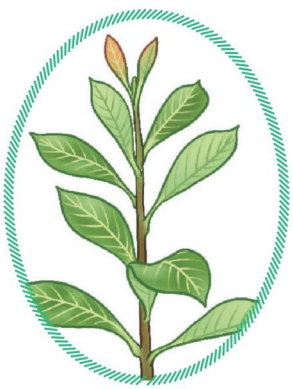

壹自然
ONE NATURE

ISBN 978-7-5219-2424-4
9 787521 924244 >
定价：29.80元

出版证明

《不再孤独的紫荆木》由张璐等著、虫创纪绘，编委会成员包括：张璐、焦正利、陈芷鹏、马艺菲、林浩有、汪书钰、叶水云、刘效东。该书是“极小种群野生植物科普丛书”的第一本，由中国林业出版社于2023年11月公开出版发行，书号978-7-5219-2424-4，定价29.80元。

特此证明。

中国林业出版社有限公司总编辑办公室

2024年3月12日

叶永昌　苏志尧　主编

DONGGUAN FOREST ECOLOGICAL CONSTRUCTION MODE AND EVALUATION

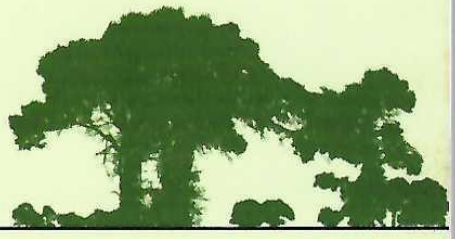

东莞森林生态建设模式与评价

东莞市林业科学研究所
华南农业大学林学院

中国林业出版社

目　录

第一部分　总　论

第二部分　森林植被及土壤

第三部分　自然保护与森林重建

第四部分　林分改造

第五部分　森林生态建设及效益评价

《东莞森林生态建设模式与评价》编委会

主　任　罗松茂

副主任　陈　坚　胡炽海　詹惠航

主　编　叶永昌　苏志尧

副主编　朱剑云　刘颂颂　张　璐　周　庆

编　委（以姓氏笔画为序）

叶永昌　叶耀雄　刘颂颂　吕浩荣
朱　嵬　朱剑云　吴学扬　张　璐
李年生　李镇魁　苏志尧　陈　坚
周　庆　周永东　罗松茂　柯娴氡
胡炽海　赵晓勤　徐正球　秦新生
莫罗坚　黄敏怡　詹惠航　戴朝晖

图书在版编目（CIP）数据

东莞森林生态建设模式与评价/叶永昌，苏志尧主编．
北京：中国林业出版社，2008.11

ISBN 978-7-5038-5372-2

Ⅰ．东…　Ⅱ．①叶…②苏…　Ⅲ．森林-生态环境-建设-研究-东莞市
Ⅳ．S732.653

中国版本图书馆 CIP 数据核字（2008）第 179425 号

出　版：中国林业出版社（100009　北京西城区德内大街刘海胡同 7 号）
网　址：www.cfph.com.cn
E-mail：cfphz@public.bta.net.cn　　电话：（010）66184477
发　行：新华书店北京发行所
印　刷：中国农业出版社印刷厂
版　次：2008 年 11 月第 1 版
印　次：2008 年 11 月第 1 次
开　本：787mm×1092mm　1/16
印　张：17
彩　插：8P
字　数：425 千字
印　数：1～1000 册
定　价：60.00 元

四、科研成果

1. 标准

广东省地方标准
批准发布公告

2017 第 1 号（总第 175 号）

广东省质量技术监督局批准发布以下 32 项地方标准，现予以公告。

广东省质监局

2017 年 3 月 10 日

序号	标准编号	标准名称	发布日期	实施日期
1	DB44/T 1959-2017	地理标志产品 新兴话梅	2017-03-10	2017-06-10
2	DB44/T 1960-2017	地理标志产品 马图绿茶	2017-03-10	2017-06-10
3	DB44/T 1961-2017	地理标志产品 西岩乌龙茶	2017-03-10	2017-06-10
4	DB44/T 1962-2017	沙栏鸡种鸡饲养管理技术规程	2017-03-10	2017-06-10
5	DB44/T 1963-2017	地理标志产品 连平鹰嘴蜜桃	2017-03-10	2017-06-10
6	DB44/T 1964-2017	主要乡土阔叶树种良种选育技术规程	2017-03-10	2017-06-10
7	DB44/T 1965-2017	桉树人工林测土配方施肥技术规程	2017-03-10	2017-06-10
8	DB44/T 1966-2017	黄蝉和软枝黄蝉苗木培育与栽培技术规程	2017-03-10	2017-06-10
9	DB44/T 1967-2017	红背桂苗木培育与栽培技术规程	2017-03-10	2017-06-10
10	DB44/T 1968-2017	桉树优树选择与优良无性系选育技术规程	2017-03-10	2017-06-10
11	DB44/T 1969-2017	米老排种实采收及处理技术规程	2017-03-10	2017-06-10
12	DB44/T 1970-2017	林下种植经营管理规范	2017-03-10	2017-06-10
13	DB44/T 1971-2017	地理标志产品 封开油栗	2017-03-10	2017-06-10

ICS 65.020.20
B 05
备案号：54299—2017

DB44

广　东　省　地　方　标　准

DB44/T 1967—2017

红背桂苗木培育与栽培技术规程

Technical regulations on cultivation of *Excoecaria cochinchinensis*

2017-03-10 发布　　2017-06-10 实施

广东省质量技术监督局　发布

前　言

本标准按 GB/T 1.1－2009 的规定编写。

本标准由广东省林业厅科技与交流合作处提出。

本标准由广东省林业厅归口。

本标准起草单位：华南农业大学。

本标准主要起草人：张璐、苏志尧、李镇魁、敬小丽、薛蛟、马丁、崔佳玉。

本标准首次发布。

红背桂苗木培育与栽培技术规程

1 范围

本标准规定了红背桂（*Excoecaria cochinchinensis* Lour.）苗木培育、苗木出圃、栽培及档案管理等技术要求。

本标准适用于红背桂的苗木生产与园林绿化栽培。

2 规范性引用文件

下列文件对于本文件的应用是必不可少的。凡是注日期的引用文件，仅所注日期的版本适用于本文件。凡是不注日期的引用文件，其最新版本（包括所有的修改单）适用于本文件。

CJ/T 23 城市园林苗圃育苗技术规程

LY/T 1000 容器育苗技术

3 苗木培育

3.1 容器扦插育苗

3.1.1 育苗容器

常用的有：无纺布育苗袋、塑料薄膜容器、硬塑料杯和育苗穴盘。容器多为圆筒状。具体容器种类及技术要求按 LY/T 1000 执行。

3.1.2 基质

用黄心土或黄心土外加 3%～5%经沤制过的过磷酸钙作基质，过筛装袋。在扦插前一天用 0.5%的高锰酸钾水溶液进行基质消毒。

3.1.3 插穗

选用生长良好的母株当年生木质化健壮枝条，截成 8 cm～10 cm 作为插穗；插穗切口上平下斜，上下两端留节眼，剪去下部叶片，上端留 1 片～2 片叶。

3.1.4 扦插

插前先用 0.05%浓度的 ABT 生根粉、0.1%浓度的吲哚乙酸或 0.2%浓度的萘乙酸等植物激素将插穗基部（约 2 cm 长）浸泡 6 h 以上，然后用清水冲洗并插于容器育苗袋中。扦插深度 3 cm～5 cm。

3.2 苗床扦插育苗

3.2.1 苗床

选择向阳地段，作床长 8 m～10 m、宽 0.8 m～1.0 m，上面铺一层 15 cm～20 cm 的河沙或河沙混蛭石、珍珠岩作为苗床，其间留 30 cm～40 cm 宽的工作步道。

3.2.2 扦插

插穗和扦插要求按 3.1.3、3.1.4 执行，其中，苗床扦插的株行距 5 cm×10 cm。

3.2.3 插后管理

插后浇透水，罩上高度约 80 cm 的拱形塑料薄膜棚。保持棚内温度 20℃～25℃，相对湿度 80%～85%。遇到暴雨天气要及时清沟排涝。扦插后可结合喷水喷洒 1 次～2 次 1000 倍液的多菌灵。苗生根后，可逐步揭去塑料薄膜以延长光照，每 10 d～15 d 喷施 0.1%的尿素和磷酸二氢钾叶面肥。

3.2.4 移苗

苗高 15 cm 左右时，苗床扦插苗可移苗上袋。育苗袋采用 3.1.1 的规格，基质按 3.1.2 配制。晴天移植应在早、晚进行；移苗前将苗床和营养袋中的营养土淋透水，移植后淋一次定根水；移苗时按苗木粗壮程度分级分批选择壮苗，使用竹签小心起苗，保持根系完整，每袋种植 1 株，移植于容器中央，使泥土覆盖根部，略高于根颈即可（浇水及压实营养土后，根颈应与土面平齐）。移入容器时防止弯根、浅植或深植，移后随时检查，及时补苗。

3.3 苗期管理

3.3.1 水分管理

苗床扦插苗移植于容器或插穗在容器中直接扦插后，及时在大棚或拱棚上覆盖塑料薄膜，一周内需每天早、晚浇水。其后，晴天时每天浇水一次，阴天时 2 d～3 d 浇水一次。有条件的苗圃可采用自动喷灌或滴灌。

3.3.2 追肥管理

小苗移植生长稳定或容器内扦插生根，长出新叶后宜每月喷施 1 次～2 次 1%～2%的复合肥。

3.3.3 其他管理

每隔一段时间，袋苗宜稍微移动，以避免过多根系长出袋子而影响日后苗木的出圃。

3.4 苗木出圃

3.4.1 质量要求

3.4.1.1 直观综合指标

植株生长正常，苗木各部分结构完整，色泽正常，健壮，无检疫对象病虫害，无机械损伤，容器完整。

3.4.1.2 质量分级

以苗龄、地径、苗高和叶片数作为苗木分级指标，将红背桂容器苗分为 2 个等级，具体指标见表 1。

3.4.2 出圃

苗木达到Ⅱ级苗以上质量要求即可出圃。起苗时要注意保持容器内根团完整，防止容器破碎。切断穿出容器的根系，不能硬拔，严禁用手提苗。出圃苗木应做到土壤湿润、包装结实、不裂不散。苗木应带有标志牌，标注内容包括：苗木名称、拉丁名、起苗日期、苗龄、等级、数量和发苗单位等。

表1 苗木质量等级

苗龄	苗木等级	地径(mm)	苗高(cm)	叶片数（片）
半年生	Ⅰ级苗	> 45.5	> 21.5	> 35
	Ⅱ级苗	33.6～45.5	14.0～21.5	16～35
一年生	Ⅰ级苗	> 75.0	> 32.0	> 60
	Ⅱ级苗	36.0～75.0	19.0～32.0	30～60

4 栽培

4.1 整地

选择半阴的种植地，清除砾石杂草杂物，填入一层 10 cm 左右厚的有机肥，深翻 20 cm～30 cm，将肥与土充分混匀，使土壤疏松、通气良好。

4.2 移植

一年四季均可栽植，深浅与原种植线一致；随填土随踏实，使根部与土紧密结合。自然式栽植、规则式栽植和混合式栽植的方式皆可。绿篱和花坛种植分别采用不同的种植密度：

——绿篱：栽成单行或双行，株距可采用 20 cm～40 cm，行距为 30 cm～50 cm，双行式绿篱成三角形叉排列。

——花坛：半年生红背桂种植密度 45 株/m^2～50 株/m^2，一年生红背桂种植密度 25 株/m^2～35 株/m^2。

4.3 抚育管理

栽植后，淋定根水，保持土壤湿透。淋水时应注意地面的排水效果是否良好，以防止积水泡坏植物根系。对绿篱状红背桂，对阴生枝及部分嫩枝进行轻度修剪成型。对于花坛状的红背桂，只需对部分嫩枝进行轻修剪成型即可。

4.4 病虫害防治

4.4.1 预防

随时对苗木和栽后植株进行病虫害监测，建立植保档案；外地调入的苗木，严加检疫；加强水肥管理，增强植株抗性；可喷洒 50%多菌灵可湿性粉剂 1000 倍液喷洒等预防。

4.4.2 除治

红背桂的常见病害炭疽病、叶枯病和根结线虫病。炭疽病、叶枯病可用 65%代森锌可湿性粉剂 500 倍液喷洒处理；根结线虫病发病后可用克线磷（1 g/m^2～1.3 g/m^2）和丙线磷(3 g/m^2～4.5 g/m^2)处理。

5 档案管理

按 CJ/T 23 执行。

广东省地方标准

红背桂苗木培育与栽培技术规程

DB44/T 1967—2017

*

广东省标准化研究院组织印刷

广州市海珠区南田路563号1104室

邮政编码：510220

网址：www.bz360.org

电话：020-84250337

广东省农垦总局印刷厂

2017-03-10 发布　　2017-06-10 实施

ICS 65.020.99
B 65
国家质量监督检验检疫总局备案号

DB44

广　东　省　地　方　标　准

DB 44/T 1389—2014

生态公益林样地调查技术规程

Technical Regulations for Plot Sampling of Non-commercial Ecological Forest

2014-08-18 发布　　2014-11-18 实施

广东省质量技术监督局　发布

目　　次

前　言

本标准按 GB/T 1.1-2009 的规定编写。

本标准由广东省林业厅科技与交流合作处提出。

本标准由广东省林业厅归口。

本标准起草单位：华南农业大学。

本标准主要起草人：苏志尧、张璐、欧芷阳、周庆、贾小容、陈北光。

本标准首次发布。

生态公益林样地调查技术规程

1 范围

本标准规定了生态公益林样地设置、样地调查、数据整理及数据归档等技术要求。

本标准适用于生态公益林样地调查。

2 规范性引用文件

下列文件对于本规程的应用是必不可少的。凡是注日期的引用文件，仅所注日期的版本适用于本文件。凡是不注日期的引用文件，其最新版本（包括所有的修改单）适用于本文件。

DB44/T 552 林业生态术语

DB44/T 553 森林资源管理

3 术语和定义

DB44/T 552和DB44/T 553确立的及下列术语和定义适用于本文件。

3.1 天然次生林 secondary forest

原始林或人工林，经人为的或自然的因素破坏之后，未经人工干预或经营，借助自然力量恢复起来的一种天然林。

3.2 林相 forest physiognomy

森林的外貌，主要指林冠层次垂直配置的情况，是划分林分依据的主要森林结构特征。

3.3 混交林 mixed forest

由两个或两个以上树种组成的林分。任一树种在林内所占的比例均不足65%，且能够较长时间形成稳定群体的林分。

3.4 优势种 dominant species

指群落中占优势的种类，包括群落每层中在数量、体积上最大、对生境影响最大的种类。群落的不同层次可以有各自的优势种。

3.5 建群种 constructive species

1

优势层中的优势种，在个体数量上不一定占绝对优势，但决定着群落内部的结构和特殊环境条件。

3.6 **伴生种** accompanying species

指有些植物虽然在群落中出现，但属于对群落的作用和影响不大的非优势种。

3.7 **重要值** importance value

研究某个种在群落中的地位和作用的综合数量指标。是相对密度、相对频度、相对优势度的总和。其值一般介于0～300之间。

3.8 **林分密度** stand density

单位面积林地上活立木的株数。

3.9 **植被盖度** vegetation coverage

地面上所有植冠（含乔木、灌木、草本）覆盖面积与地面总面积之比，用10分法表示，最大为10。

3.10 **多度** abundance

指物种的个体数目。调查区所有物种的个体总数称为总多度。

3.11 **多度级** abundance class

对个体数量进行定性的群落测度等级，一般分为7级，见附录A的表A.1。

3.12 **群落层次结构** community stratum structure

对环境有不同需求的植物，由于生态幅度和适应特点的差异，各自占据一定的空间，分层次排列在群落中。

3.13 **群落垂直结构** vertical community structure

群落在空间中的垂直分化或成层现象。

3.14 **群落水平结构** horizontal community structure

指群落的水平配置状况或水平格局，其主要表现特征是镶嵌性。

3.15 **乔木层** tree layer

森林中由乔木树冠构成的最上面一层，具有多年生的大型木质树干，高在3 m以上。

3.16 **灌木层** shrub layer

位于乔木层之下，由灌木树种和一些未长到乔木层高度的幼年乔木共同构成的中间层植被。

3.17 **草本层** herbaceous layer

不具有多年生地上茎的植物构成的林下层。

3.18 **层间植物层** inter-stratum plant layer

森林中的附生植物和藤本植物，附着或攀缘在直立植株的不同部位，构成林内一个独特层次。

3.19 **苔藓地衣层** mosses and lichens layer

分布于森林内的地面、粗糙的树皮或裸露的岩石上，由苔藓、地衣等非维管束植物组成。

3.20 **生态交错区** ecotone

生态交错区又称群落交错区或生态过渡带，是两个或多个生态地带之间（或群落之间）的过渡区域。如森林和草原之间有一森林草原地带，两个不同森林类型之间或两个草本群落之间也都存在交错区。

3.21 **起测直径** measurable diameter

在林分或伐区调查时，规定每木检尺的最小胸径（或地径）或用材材种起测（商用材界限）的最小胸径（或地径）的下限值。

3.22 **胸高断面积** basal area, cross-sectional area at breast height

根据立木胸径算出的胸高处的横断面积。

3.23 **树高** tree height

树木全高，即立木的根颈至树梢端点间的距离。

3.24 **枝下高** branching height

林木第一活枝距地面的高度。

3.25 **每木调查** tree tally, tree census

按照一定的起测直径对全林分或标准地内的林木进行逐株调查测量，测定树木的胸径、树高、冠幅、枝下高，并记载树种、年龄和林层等因子。调查因子可根据调查目的不同而做适当调整。

3.26 **冠层植物** canopy plants

居于森林群落林冠层（或上层）的乔木和高大灌木。

3.27 **林下植物** understory plant

居于森林群落林冠层之下的所有木本和草本植物的统称。

3.28 **群落更新** community regeneration

指当某种群的个体死亡后，能由同一种群或相同性质的种群的新个体所替代的过程，群落的总体宏观结构和性质不发生改变。群落更新是群落发生演替的内源性因素。

3.29 群落演替 community succession

指一定地段内的植物群落由一个群落类型转变为另一个群落类型的过程。

3.30 主林层 canopy tree layer

优势树种林冠顶端至林冠下沿。

3.31 演替层 succession layer

林冠下沿至距地面1 m高处，主要分布着未成熟的小树和幼树。

3.32 更新层 regeneration layer

林内距地面1 m高处至地面的范围，主要分布着树木的幼苗。

3.33 线路调查

指在拟调查的目标林分中沿一定路线踏查，并记录林分概况和植物类型。线路调查可为样地选址和设置提供有用信息，同时，线路调查的数据也可用于对生态公益林进行定性和半定量的分析和评价。

4 样地设置

4.1 样地选择

在线路调查的基础上，选择具有代表性、典型性、均一性的地段作样地，尽可能避开河流、道路、林缘，回避人为干扰。

4.2 取样面积

以管理评价为目标的样地调查最小取样面积宜达到：人工林0.27 hm^2，单个样地面积900 m^2; 天然林0.36 hm^2, 单个样地面积1200 m^2。以研究和探索为目标的单个样地调查最小取样面积宜达到：人工林0.5 hm^2，天然林1 hm^2。

4.3 样地形状和样方设置

样地设置为正方形或长方形，边长为10 m的倍数。将样地划分为10 m×10 m的相邻格子样方进行每木调查。在每个10 m×10 m的样方中设4个1 m×1 m的小样方，进行林下植物调查和更新演替调查。

5 样地调查

5.1 每木调查

5.1.1 胸径测量

使用围尺测量树干离上坡地面1.3 m高度处的树干直径。胸径 < 5 cm的幼苗和幼树，使用游标卡尺测量。测量值精确到0.1 cm，记入每木调查表（附录A的表A.2）。

5.1.2 冠幅测量

以树冠垂直投影确定冠幅宽度，分“上下坡”和“水平”两个方向量测，精确到0.1 m，记入每木调查表（附录A的表A.2）。

5.1.3 树高测量

用测高器或米尺实测，精确到0.5 m，记入每木调查表（附录A的表A.2）。

5.1.4 枝下高测量

用测高器或米尺实测，精确到0.5 m，记入每木调查表（附录A的表A.2）。

5.2 林下植物调查

在每个 1 m × 1 m 的小样方内，分别记录林下灌木的种类、株数和盖度；并记录草本和蕨类植物的种类、丛数和盖度，记入小样方调查表（附录 A 的表 A.3）。

5.3 更新演替调查

5.3.1 分层

分为主林层、演替层、更新层3层。

5.3.2 调查及计算

在每个 1 m×1 m 的小样方内，分层记录树种名称及株数，记入森林更新及演替调查表（附录 A 的表 A.4）。统计小样方内各树种更新幼苗和幼树的株数，计算出更新幼苗和幼树的更新密度和更新频度。更新组成按下列计算式计算：

$$\text{更新密度}\ (N/hm^2)=\frac{\text{株数合计}}{\text{样方面积}\times\text{样方数}}\times 10000$$

$$\text{某个种的更新频度}(\%)=\frac{\text{该种幼苗(树)出现的样方数}}{\text{样方总数}}\times 100$$

$$\text{更新总频度}(\%)=\frac{\text{出现幼苗(树)的样方数}}{\text{样方总数}}\times 100$$

5.4 样地环境因子调查

5.4.1 地理坐标

在每个样方中心点位置利用GPS仪实测。

5.4.2 地貌

按中山、低山、丘陵和平原 4 种类型记录。

5.4.3 海拔

利用海拔仪实测，记至小数点后1位。

5.4.4 坡向

用罗盘仪实测，记录度数，以正北为0°。

5.4.5 坡位

按照脊、上、中、下、谷、平地6个坡位进行记录。

5.4.6 坡度

用坡度计实测，记录度数。若有样地地形图，可根据样地高差与垂直投影距离来计算。

6 数据整理

6.1 数据录入

6.1.1 植物调查数据录入

将外业线路调查、样地调查及更新演替调查中现场记录的数据录入数据库。

6.1.2 环境因子数据录入

将外业调查获取的地理坐标、海拔高度、地貌、坡度、坡向、坡位等环境要素录入数据库。

6.2 数据核查

6.2.1 交叉核查

数据录入后，由2人通过电脑屏幕或打印稿进行核查；或由2人分别录入数据，通过比对录入结果进行核查。

6.2.2 实地核查

数据录入后，对其中有疑问或明显错漏的数据进行实地查证。

7 数据归档

7.1 纸质档案

将外业调查所记录的生态公益林线路调查记录表、每木调查表、小样方调查表和更新演替调查表等原始纸质表整理后，分类保管。

7.2 电子档案

通过计算机磁盘等设备存储已录入数据库的生态公益林线路调查记录表、每木调查表、小样方调查表和更新演替调查表等文件信息。

附 录 A
（规范性附录）
生态公益林样地调查记录表

表A.1 线路调查记录表

调查者：_____时间：_____地点：_____
生境：_____

序号	种名	层次	多度级	序号	种名	层次	多度级
…	…	…	…	…	…	…	…

层次及多度级记录说明：
层次又分为乔木层(T1、T2、T3) 、灌木层（S）和草本层(H)；
多度级共分 7 级：
——第一级记作 SOC，指植株覆盖满或几乎满样方，盖度 76%～100%；
——第二级记作 COP3，指植株很多，但连接不完全，盖度 51%～75%；
——第三级记作 COP2，指植株较多，盖度 26%～50%；
——第四级记作 COP1，指植株尚多，盖度 6%～25%；
——第五级记作 SP，指植株少量散生，盖度 1%～5%；
——第六级记作 SOI，指仅有个别植株，盖度＜1%；
——第七级记作 Un，指样方中偶有 1 株～2 株。

表A.2　每木调查表

样方面积：_____m^2　样方号：_____　日期：_____地点：_____
坡度：_____　坡向：_____　坡位：_____母岩：_____
起测径阶:_____　测定人:_____　记录人：_____
样地海拔高：_____m　经度：_____　纬度：_____
公里网格：东西_____，南北_____

序号	种名	树高	胸径	冠幅（上下坡）	冠幅（水平）	枝下高	备注
…	…	…	…	…	…	…	…

备注：DBH 精确到 0.1 cm，树高、枝下高、冠幅精确到 0.5 m。
样地环境概况：

表A.3　小样方调查表

时间：_____地点：_____　记录人：_____

样方号	小样方号	种名	多度（株数）	盖度	备注
…	…	…	…	…	…

表 A.4 更新演替调查表

时间：_____地点:_____记录人:_____

样方号	小样方号	种名	主林层	演替层	更新层	备注
…	…	…	…	…	…	…

DB44/T 1398—2014

广东省地方标准
生态公益林样地调查技术规程
DB44/T 1398—2014
*
广东省标准化研究院组织印刷
广州市海珠区南田路563号1104室
邮政编码：510220
网址：www.bz360.org
电话：020-84250337
南方医科大学广州广卫印刷厂

ICS65.020.01
B04
国家质量监督检验检疫总局备案号：23366-2008

DB44

广　东　省　地　方　标　准

DB44/T 552—2008

林业生态　术语

Basic Nomenclature of Forestry Ecology

2008-07-11 发布　　2008-10-01 实施

广东省质量技术监督局 发布

目　　录

前　言

本标准的附录 A、附录 B 为规范性附录。

本标准由广东省林业局科技与对外合作处提出。

本标准由广东省林业局归口。

本标准起草单位：华南农业大学林学院。

本标准主要起草人：苏志尧、周庆、张璐、贾小容、陈北光、黎彩敏。

林业生态　术语

1　范围

本标准统一和规范了林业生态建设与管理的有关术语和定义。

本标准适用于林业生态建设、管理、经营、科研及其他相关领域。

2　通用术语

2.1　全国荒山造林绿化第一省 the Number One Province in National Mountain Afforestation

1985年，广东省委、省人民政府作出了《关于加快造林步伐，尽快绿化全省的决定》，提出了“五年消灭荒山，十年绿化广东”的号召，全省掀起了植树造林高潮；至1990年，全省386.7万hm^{2}宜林荒山披上绿装，1991年被党中央、国务院授予“全国荒山造林绿化第一省”的光荣称号，并于1993年提前两年实现了绿化广东大地的目标。

2.2　林业生态省　Forestry Ecological Province

2004 年，《广东林业生态省建设规划》经广东省政府正式批准实施；2005 年，广东省委、省人民政府作出了《关于加快建设林业生态省的决定》，确立了以生态建设为主体的林业可持续发展道路，建设以森林植被为主体的国土生态安全保障体系，构建以生态经济为特色的林业产业体系，基本形成山川秀美、生态良好、人与自然和谐相处的生态文明社会。到 2020 年，全面建成林业生态省，森林覆盖率达到 60%，森林资源综合效益总值比 2003 年翻两番，达到 18800 亿元，建成完备的国土生态安全体系和发达的林业产业体系，实现生态良好、生活富裕、人与自然和谐相处的目标。

2.3　林业生态县　Forestry Ecological County

2003年，广东省人民政府办公厅印发了《广东省创建林业生态县实施方案》，正式启动了创建林业生态县工作。通过加强森林资源的培育与保护，促进我省完成宜林荒山、荒地、荒滩造林绿化，构建稳定的生态公益林体系，建立起与国民经济和社会可持续发展相适应的森林生态系统，实现青山绿水蓝天和山川秀美的宏伟目标。到2005年，全省20％左右的县达到林业生态县标准；到2010年，争取50％的县达到林业生态县标准；到2015年，力争全省各县基本达到林业生态县标准。

2.4　植树造林　afforestation

指新造或更新森林的生产活动，是培育森林的一个基本环节。如果面积很小，将来不能形成森林和森林环境的，则称为植树。种植面积较大而且将来能形成森林和森林环境的，则称为造林。

2.5　退耕还林　converting farmland to forestland

将水土流失严重的耕地，沙化、盐碱化、石漠化严重的耕地以及粮食产量低而不稳的耕地，有计划、有步骤地停止耕种，因地制宜地造林种草，恢复植被。

2.6　生态学　ecology

研究生物有机体与其周围环境相互关系的科学。按生物学组织水平可分为个体、种群、群落及生态系统生态学。

2.7　森林生态学　forest ecology

研究森林中乔木树种之间、乔木树种与其他生物之间，以及与所处的外界环境之间相互关系的学科。包括个体生态、种群生态、群落生态和森林生态系统等内容。

2.8 林业生态 forestry ecology

与林业生产和环境建设相关的生态过程、机制、管理和政策。

2.9 现代林业 modern forestry

就是科学发展的林业，以人为本、全面协调可持续发展的林业；是体现现代社会主要特征，具有较高生产力发展水平，能够最大限度拓展林业多种功能，满足社会多样化需求的林业。现代林业建设的目标是构建完善的林业生态体系、发达的林业产业体系和繁荣的生态文化体系。

2.10 生态林业 eco-forestry; ecological forestry

是一种以生态学、经济学原理为指导的可持续林业发展模式。其特征是把自然生态系统的原理与林业经营管理相结合，寻求生态、经济、社会效益的高度统一和综合效益的最大化，建设可持续发展的高功能的林业生态经济系统。

2.11 城市林业 urban forestry

现代林业的一个分支，以服务城市、保护环境为目的，对城市范围内森林生态系统、森林景观系统及其附属工程的经营与管理。

2.12 生态公益林 non-commercial ecological forest

为维护和改善生态环境，保持生态平衡，保护生物多样性及满足人类社会生态、社会需求和可持续发展为主体功能，主要提供公益性、社会性产品或服务的森林。

2.13 乡村林业 rural forestry

以发展乡村经济为主要目的，并改善乡村生态环境和农民生活条件的林业经营活动。

2.14 农田林网 farmland forest network

为保护农作物不受风沙灾害，防御其它农业自然灾害的威胁，使农作物得以正常生长发育，获得稳定高产而营造的呈片状、带状的防护林。

2.15 林分改造 stand improvement

以森林生态学、森林培育学的理论和方法为指导，遵循森林植物群落演替规律，根据树种的生物学特征和仿生学原理，用人工措施构成或人工促进恢复的方法建立起生态功能显著、抗逆性强、生长稳定的森林。

2.16 地带性植被 zonal vegetation

又称“显域植被”，指由水平或垂直的生物气候带决定或随其变化的有规律分布的植物群落。

2.17 林业生态工程 forestry ecological engineering

根据生态学、生态经济学、系统科学与生态工程原理，针对自然资源环境特征和社会经济发展现状所进行的以木本植物为主体，并将相应的植物、动物、微生物等生物种群人工匹配结合而形成的稳定且高效的人工复合生态系统的过程。

2.18 林业生态体系 forestry ecological system

在保护现有的森林生态系统的基础上，运用生态经济原理，从国土整治的全局和可持续发展的需要出发，以维护和再造良性生态以及维护生物多样性和具代表性的自然景观为目的，在全国范围内，由自然力和人力共同作用保护和建立起的不同层次、不同水平、不同规模的森林生态系统，组成一个完整的体系。

2.19 林业生态建设 forestry ecological construction

从国土整治的全局和国家可持续发展的需要出发，以维护和再造良性生态环境及维护生物多样性和具有代表性的自然景观为目的，根据生态学、林学及生态控制论，设计、建造与调控以木本植物为主的优质、高效、稳定的人工复合生态系统。

2.20 **生态文明** ecological civilization

指人类遵循人、自然、社会和谐发展这一客观规律而取得的物质与精神成果的总和；它是指人与自然、人与人、人与社会和谐共生、良性循环、全面发展、持续繁荣为基本宗旨的文化伦理形态。生态文明是对现有文明的超越，它将引领人类放弃工业文明时期形成的重功利、重物欲的享乐主义，形成生态与社会协调和谐发展的局面。

2.21 **生态因子** ecological factor

环境对生物的生长、发育、生殖、行为和分布有直接和间接影响的环境要素。分为非生物因子和生物因子。

2.22 **生态安全** ecological security

指一个国家或地区的生态环境资源状况能持续满足社会经济发展需要，社会经济发展不受或少受来自于资源和生态环境的制约与威胁的状态。

2.23 **生态系统** ecosystem

在一定空间中共同栖息着的所有生物（即生物群落）与其环境之间由于不断地进行物质循环和能量流动过程而形成的统一整体。生态系统是生物与环境之间进行能量转换和物质循环的基本功能单位。

2.24 **生态恶化** ecological deterioration

生境生态脆弱度的加剧和环境的急剧恶化。通常表现为森林资源贫乏，草地退化严重，耕地质量下降，荒漠化现象严重，以及生物物种减少等。

2.25 **林业可持续发展** sustainable forestry development; sustainable forestry

是对森林生态系统在确保其生产力和可更新能力，以及森林生态系统的物种和生态多样性不受到损害前提下的林业实践活动，它是通过综合开发培育和利用森林，以发挥其多种功能，并且保护土壤、空气和水的质量，以及森林动植物的生存环境，既满足当前社会经济发展的需要，又不损害未来满足其需求能力的林业。

2.26 **林分结构** stand structure

指一个林分或整个森林经营单位的树种、株数、年龄、径级及林层等构成的类型。它是森林经营和分析中的一个重要因子，是对林分发展过程如更新、竞争、自稀疏和经历的干扰活动的综合反映。

2.27 **人工林** artificial forest

用植苗、播种、扦插和其他各种人工方法培育的森林。

2.28 **天然林** natural forest

未经人为措施而自然起源的原始林和天然次生林。

2.29 **用材林** timber forest

以生产木材为主要目的的森林和林木，包括以生产竹材为主要目的的竹林。

2.30 **亚热带季风常绿阔叶林** subtropical monsoon evergreen broadleaved forest

南亚热带季风气候区典型的地带性森林类型，主要由樟科、山茶科、木兰科、五味子科、八角科、金缕梅科、番荔枝科、壳斗科的常绿树种组成，植物区系成分丰富，群落结构复杂。

2.31 **亚热带山顶矮林** montane elfin woodland

分布于温暖潮湿区域高海拔山地或山顶的以低矮树木为特征的森林。我省南岭国家级自然保护区、石门台自然保护区等地均有分布。

2.32 **经济林** economic forest; cash crop forest

以生产果品、食用油料、饮料、调料、工业原料和药材等为主要目的的林分。

2.33 **乡土树种** indigenous tree species; native tree species

地带性植被中的优势种或建群种，广义的乡土树种应该是地带性植被或者说是本地植物区系成分中所有的乔木种类。

2.34 薪炭林 fuelwood forest

以生产薪炭材和提供燃料为主要目的的乔木林和灌木林。

2.35 水土流失 soil and water erosion

在水流作用下，土壤被侵蚀、搬运和沉淀的整个过程。在自然状态下，纯粹由自然因素引起的地表侵蚀过程非常缓慢，常与土壤形成过程处于相对平衡状态。

2.36 生态系统服务 ecosystem services

生态系统与生态过程所形成及所维持的人类赖以生存的自然环境条件与效用。不仅为人类提供了食品、医药及其他生产生活资料，还创造与维持了地球生命支持系统，形成了人类生存所必需的环境条件。

2.37 外来物种 alien species

在该物种自然分布范围之外，经直接或间接途径进入生态系统中的物种。

2.38 外来入侵种 alien invasive species

借助于人类活动越过不能自然逾越的空间障碍进入生态系统中的物种，在当地自然或人工生态系统中定居，并可自行繁殖和扩散，而且对当地的生态系统和景观造成了明显改变的物种。

2.39 农林复合经营；复合农林业；农用林业 agroforestry

在同一土地管理单元上，人为地把多年生木本植物（如乔木、灌木、棕榈、竹类等）与其它栽培植物（如农作物、药用植物、经济植物以及真菌等）和（或）动物在空间上或按一定的时序安排在一起而进行管理的土地利用和技术系统的综合。

2.40 社区林业 community forestry; social forestry

林学和社会学的新型交叉科学。是以社区农民为主体，按照“自下而上”的原则，以积极参与为核心，以社区现有的组织形式、传统的生产方式和知识水平为基础，以林业及相关部门或外界机构协调配合的多种有效支持为手段的一种新的理论和方法。

2.41 参与式林业 participatory forestry

参与式发展理论和方法运用到森林资源管理中，是让生产者直接参与林业活动的规划、执行和管理等过程。

2.42 森林分类经营 classified forest management

按林种、按土地生产潜力科学组织森林经营，按各林种的功能定向培育森林。即以发挥某一林种某一效益为主，兼顾其它方面效益的经营模式。现在一般将森林分为生态公益林、商品林两种经营模式。

2.43 森林火灾 forest fire

失去人为控制，在森林中自由蔓延和扩展，达到一定的面积，对森林生态环境和人类生命财产带来一定危害和损失的森林燃烧。

2.44 森林生物种质资源 forest germplasm resource

以森林生物为对象的遗传多样性资源，特指种内继代繁殖不受瓶颈效应制约的种质样本库。

2.45 森林经营管理 forest management

以生态学的等级理论与尺度理论为基础，对森林资源的保护、利用、更新实行管理和监督。

2.46 森林健康 forest health

森林保持自身良性存在和更新，实现最佳的多种服务功能的状态。

2.47 森林覆盖率 forest coverage

一定区域内森林面积与土地总面积的百分比。森林面积包括郁闭度0.2以上的乔木林地面积和竹林地面积，国家特别规定的灌木林地面积、农田林网以及“四旁”(村旁、路旁、

水旁、宅旁)林木的覆盖面积。森林覆盖率是反映森林资源的丰富程度和生态平衡状况的重要指标。计算公式为：森林覆盖率(%)=森林面积/土地总面积×100%。

2.48 植物群落 plant community

在特定时空条件下，具有一定的植物种类组成及其与环境之间彼此影响、相互作用，具有一定的外貌及结构，包括一定形态结构与营养结构，并具特定的功能的植物集合体。

2.49 演替 succession

一个群落为另一个群落所取代的过程，是群落动态的一个最重要的特征。

2.50 碳汇 carbon sink

从大气中清除二氧化碳的过程、活动或机制，反映生态系统从大气中清除二氧化碳的能力。

2.51 碳源 carbon source

任何向大气净排放二氧化碳的场所或人类活动过程。

2.52 森林固碳 carbon sequestration by forest

森林对二氧化碳(CO_2)的吸收和固定作用。是减缓温室效应，维持全球碳氧平衡的重要途径。

2.53 热带雨林 tropical rain forest

热带终年高温多雨地区的常绿森林群落。群落结构复杂，组成种类极为丰富。是拥有全球最大生物量的陆地生态系统。

2.54 常绿阔叶林 evergreen broadleaved forest

亚热带地区的地带性植被，立木以常绿双子叶树种为主。

2.55 森林小气候 forest microclimate

在森林植被影响下形成的特殊小气候。森林中水、气、热等各种气象要素的综合表现，森林的结构、郁闭度、林木种类、林龄、林下植被状况等对它的形成起着很大的作用。

2.56 顶极群落 climax community

生物群落经过一系列演替，最后所产生的保持相对稳定的群落。

2.57 蓄积量 stand volume

林分中所有活立木材积的总和称作林分蓄积量，简称蓄积。林分蓄积量是重要的林分调查因子。

2.58 森林生物多样性 forest biodiversity

森林生态系统中各种活有机体及其遗传变异的有规律组合。主要包括森林生态系统多样性、物种多样性和遗传多样性等三方面的含义。

2.59 珍稀树种 rare and precious tree species

通常指列入国际自然保护联盟（IUCN）或国家重点保护野生植物名录且有重要经济价值的树种。

2.60 自然保护区 nature reserve

对有代表性的自然生态系统、珍稀濒危野生动植物物种的天然集中分布区、有特殊意义的自然遗迹等保护对象所在的陆地、陆地水体或者海域，依法划出一定面积予以特殊保护和管理的区域。

2.61 自然保护小区 small protected area

自然保护区的延伸和补充，自然保护小区是在群众自发性基础上建立的，采取分散、小型、单位或群众自办自管的办法，以保护原始森林、原始次生林、水源涵养林、风景林、风水林、拯救珍稀濒危物种，保护生态系统的完整性和生物多样性为目的的保护区域。

2.62 湿地生态系统 wetland ecosystem

在一定时空范围内依赖于湿地而生存的生物与非生物因子通过物质循环和能量流动相

互作用、相互依存而构成的一个生态学功能单位。

2.63 湿地公园 wetland park

以具有显著或特殊生态、文化、美学和生物多样性价值的湿地景观为主体，以保护湿地生态系统完整性、维护湿地生态过程和生态服务功能并在此基础上以充分发挥湿地的多种功能效益、开展湿地合理利用为宗旨，可供公众浏览、休闲或进行科学、文化和教育活动的特定湿地区域。

2.64 野生动物 wildlife

凡生存在天然自由状态下，或来源于天然自由状态的虽然已经短期驯养但还没有产生进化变异的各种动物，均可称为野生动物。野生动物根据不同的标准，有着不同的分类。《野生动物保护法》第三条规定，野生动物资源属国家所有。

2.65 野生动植物 wildlife and forest plants

在自然状态下生长、栖息的一切动物和植物的总称。

3 森林生态系统

3.1 森林生态系统 forest ecosystem

以乔木树种为主体的生物群落（包括动物、植物、微生物），是随时间和空间不断进行能量交换、物质循环和能量传递的有生命及再生能力的功能单位。

3.2 森林生态环境监测 forest environmental monitoring

对特定区域范围内森林生态系统的类型、结构和功能及其组合要素等进行系统测定和观察的过程，监测的结果用于评价和预测人类活动对生态系统的影响，为合理利用资源、改善生态环境和自然保护提供决策依据。

3.3 森林生态环境效益评价 appraisal of forest ecological and environmental benefits

对森林为人类提供服务的能力进行定性或定量的评估，主要有涵养水源效益、保育土壤效益、固碳释氧效益、保护生物多样性效益和游憩效益等5种类型。

3.4 长期生态学研究 Longterm Ecological Research (LTER)

在一个或者若干个生态站对某些生态现象或过程进行较长时间的连续观测和研究。

3.5 森林景观 forest landscape

以各种类型或不同演替阶段的森林生态系统为主体构成的一类景观。

3.6 定位研究站 permanent research station

为开展长期生态学研究而设置的站点。

3.7 半定位研究站 semi-permanent research station

结合当地的自然条件和生产实际开展专项半定位的观测站点。

3.8 物质循环 matter cycle; matter cycling

无机化合物和单质通过生态系统的循环运动。生态系统的物质循环可分为三大类型，即水循环(water cycle)，气体型循环(gaseous cycle)和沉积型循环(sedimentary cycle)。

3.9 养分循环 nutrient cycle; nutrient cycling

化学元素及其组成的各种化合物在自然界中的迁移和转化的过程。

3.10 能量流动 energy flow

生态系统的基本功能之一，第一次能量固定始于绿色植物光合作用对太阳能的固定。

3.11 地球化学循环 geochemical cycle

化学元素在不同生态系统之间进行的迁移与交换。

3.12 生物地球化学循环 biogeochemical cycle

生态系统内各组分之间化学元素的交换。

3.13 **生物化学循环** biochemical cycle

养分在生物体内的再分配。

3.14 **全球碳循环** global carbon cycle

碳通过大气圈、生物圈、土壤圈、岩石圈和水圈的变化和传输的总过程。

3.15 **碳储量** carbon stock; carbon storage

生态系统及其组分所储存碳的现存量。

3.16 **初级生产** primary production

绿色植物光合作用固定太阳能并制造有机物质的过程。

3.17 **次级生产** secondary production

除生产者外的其它有机体的生产。

3.18 **生产者** producer

构成生态系统的三大功能类群之一，指能利用简单无机物制造有机物的自养生物。

3.19 **分解者** decomposer

构成生态系统的三大功能类群之一，是异养生物，其作用是把动植物体的复杂有机物分解为生产者能重新利用的简单的化合物，并释放出能量。

3.20 **消费者** consumer

构成生态系统的3大功能类群之一，直接或间接地依赖于生产者所制造的有机物质而生活的异养生物。

3.21 **生态金字塔** ecological pyramid

生物量或能量，按营养级顺序排列并绘制成图，其形似金字塔，故称生态金字塔。

3.22 **分解作用** decomposition

生态系统中死有机物质的逐步降解过程。

3.23 **食物链** food chain

各种生物按其取食和被取食的关系而排列的链状顺序。

3.24 **食物网** food web

生态系统中的食物链彼此交错连接形成的一个网状结构。

3.25 **营养级** trophic level

物种在食物链中所处的位置。生态系统中的生物形成复杂的营养关系，即构成食物链和食物网，而营养级是食物链中的一个环节。

3.26 **种间关系** interspecific relation

生活于同一生境中的异种种群之间的相互关系。

3.27 **种内关系** intraspecific relation

同一种群内不同个体间的相互关系。

3.28 **植物种群** plant population

植物群落中，同一物种占有一定空间和一定时间的个体集合体。

3.29 **乔木** tree，arbor

有一个直立主干、且高达5 m以上的木本植物。

3.30 **灌木** shrub

没有明显的主干、呈丛生状态的木本植物。

3.31 **草本** herb

植物体木质部较不发达至不发达，茎多汁，较柔软的一类植物。

3.32 **藤本植物** liana

需要其他植物或岩石或特殊地上物支撑的攀援植物。

3.33 **凋落物** litter

掉落地面的植物器官，包括枯枝落叶、落果等。凋落物在森林生态系统养分循环中起着重要作用。

3.34 温室效应 greenhouse effect

太阳短波辐射可以透过大气射入地面，而地面增暖后放出的长波辐射却被大气中的二氧化碳等物质所吸收，从而产生大气变暖的效应。

3.35 吸碳放氧 carbon sequestration and oxygen production

绿色植物通过光合作用，吸收CO_2和释放O_2的功能。

3.36 非生物环境 abiotic environment

包括参加物质循环的无机元素和化合物，联系生物和非生物成分的有机物质和气候或其他物理条件。

3.37 生物环境 biotic environment

生物群落，包括生产者、消费者、分解者等三大基本成分。

3.38 生态恢复 ecological restoration; rehabilitation

生态退化的逆转过程，指恢复系统的合理结构、高效的功能和协调的关系。

3.39 气候变化 climate change

气候要素在连续几十年或者更长的时间长期统计结果的任何系统性变化。气候变化的原因可能是自然界的外源强迫，也可能是气候系统固有的内部过程，还可能是人类活动的强迫。

3.40 景观动态 landscape dynamics

景观遭受干扰时发生的现象，是一个复杂的多尺度过程，对绝大多数生物体具有极为重要的意义。

3.41 景观格局 landscape pattern

景观异质性的一种表现，指当景观异质性表现为某种相对稳定或普遍的规律性时，有规律的空间分布模式。

3.42 景观功能 landscape function

景观与周围环境进行的物质、能量和信息交换以及这种交换影响下景观内部发生的变化和所表现出来的性能。

3.43 景观过程 landscape process

强调事件或现象的发生、发展的动态特征，通常包括获取（输入）、生产、循环、贮存和输出5类主要过程。

3.44 景观结构 landscape structure

景观内部的形态结构，属于景观形态学的研究范畴。

3.45 景观要素 landscape element

景观的基本单元，其最一般的数量特征是面积、周长、形状。

3.46 外业调查 field survey

室外作业或野外取样。

3.47 生活型 lifeform

植物对于综合环境条件的长期适应，在外貌上表现相似的植物类型。

3.48 生态型 ecotype

同一物种内因适应不同生境而表现出具有一定结构或功能差异的不同类群。

3.49 生长型 growth form

生物体的生长习性。

4 营林生态

4.1 林分 stand

在林木起源、林相、树种组成、年龄、地位级、疏密度、林型等内部特征相同的一个群落，并与相邻群落有明显区别的一片森林。

4.2 营林规划 silvicultural planning

在科学的森林经营理论指导下，定性分析与定量分析相结合的森林资源规划设计。

4.3 森林培育 silviculture

按既定培育目标和客观自然规律，从采种育苗开始，包括整地、造林、抚育、间伐、改造直至成熟的营林全过程。

4.4 宜林荒山 barren hills suitable for afforestation

适宜于营造森林的疏林草地和荒山荒地。

4.5 义务植树 obligatory tree planting

公民为国土绿化无报酬地完成规定劳动量的植树、整地、抚育和管护等绿化任务。

4.6 造林技术 silvicultural technique

指人工造林中造林地选择、整地、栽植、补植等造林的各个环节所采用的方法与措施。

4.7 飞播造林 aerial seeding

又叫飞播。是用飞机撒播林木种子的播种造林法。

4.8 封山育林 closing the hill for reforestation

对具有天然下种或萌蘖能力的疏林，无立木林地、宜林地、灌丛实施封禁，保护植物的自然繁殖生长，并辅以人工促进手段，促使恢复形成森林或灌草植被；以及对低质、低效有林地、灌木林地进行封禁，并辅以人工促进经营改造措施，以提高森林质量的一项技术措施。

4.9 抚育管理 tending

为了某种利用目的对森林进行培育而实行的各种人工作业。

4.10 疏伐 thinning

在幼龄林郁闭以后至成熟龄前的一个龄级的林分内，为调节目的树种个体间的矛盾而进行的森林抚育采伐。

4.11 有林地 forested land

连续面积大于 0.067 hm^2、附着的植被郁闭度在 0.2 以上(含 0.2)或成林幼林达到一定保存密度要求的林地。根据附着植被的差异，有林地包括乔木林和竹林两种类型。

4.12 无林地 nonforested land

宜林地中的一个类别，由于采伐或其它原因所造成的空旷而暂时又没有生长出树林的土地。

4.13 灌木林地 scrubland

以灌木的经济效益或防护功能为经营目的，植被为灌木树种或为因生境恶劣而矮化成灌木型的乔木树种以及为胸径小于 2 cm 的小杂竹丛，连续面积在 0.067 hm^2 以上(含 0.067 hm^2)、覆盖度在 30%以上(含 30%)的林地。灌木林地包括国家特别规定的灌木林地（简称国灌）和其它灌木林地（简称其灌）两种类型。

4.14 皆伐 clear cutting

在划定的森林面积上，把林分中的林木，一次采完或基本采完（保留木蓄积小于伐前全林蓄积的 20%）的一种采伐方式。

4.15 择伐 selective cutting

在一定的森林面积上，分期选择一部分合乎一定经济要求的成熟林木和应当采伐的林木所进行的采伐。择伐后借助于母树的天然下种更新或人工补植，能使林地始终保持不同年龄的有林状态。

4.16 立地 site

林地上影响林木生长发育的自然环境因子的综合。

4.17 生境 habitat

生物生活的空间和其中全部生态因子的总和。包括光照、温度、水分、空气、无机盐类等非生物因子和食物、天敌等生物因子。

4.18 枯立木 snag

因外界原因而死亡或自然枯死但未倒下的死树。

4.19 低效林 low-function forest

受人为因素的直接作用或诱导自然因素的影响，林分结构和稳定性失调，林木生长发育衰竭，系统功能退化或丧失，导致森林生态功能、林产品产量或生物量显著低于同类立地条件下相同林分平均水平的林分总称。根据起源的不同，低效林可分为低效次生林和低效人工林；根据经营目标的不同，低效林可分为低效防护林和低质低产林。

4.20 优势木 dominant tree

树冠处于主林层之上，几乎不被挤压的树木。

4.21 林班 compartment

为了便于调查设计和长期的经营管理，在基层林业单位（如林场）内，把土地分成大致相等的基本单位。林班具有永久性质，其境界线必须明确标明。林班面积的大小，因经营强度而不同。划分林班的方法有人工区划、自然区划和综合区划三种。林班的编号用大写正体的罗马数字，以便与小班编号相区别。

4.22 小班 subcompartment

是开展森林经理工作的基本单位，其林分的立地条件和经营特征都比较相同，为便于森林资源统计计算和经营管理，将林班土地划分为多个范围比较固定的基本单位。

4.23 林窗，林隙 forest gap

林冠中出现的较大空隙，其宽度约相当于树高的1/4。

4.24 自然稀疏 natural thinning; self-thinning

林分内的个体由于竞争有限的资源而引起的一部分个体死亡的现象。

4.25 郁闭度 rate of canopy closure; canopy closure

林分中树冠彼此连接的程度，是反映林分质量的指标。

4.26 速生丰产林 fast-growing and high-yield plantation

通过使用良种壮苗和实施集约经营，缩短培育周期，获取最佳经济效益，森林生长指标可以或已达到相应树种速生丰产林国家（行业）标准的森林、林木和林地。

4.27 母树林 seed production area

优良天然林或种源清楚的优良人工林，通过留优去劣疏伐，或用优良种苗以造林方法营建的，用以生产遗传品质较好的林木种子的林分。

4.28 林地退化 forest land degradation

由于树种布局、栽培制度、群落结构、粗放经营和连作等原因而导致的森林地力衰退。

5 林业生态经济

5.1 林业生态经济 forestry eco-economics

由林业生态和经济相互渗透、有机结合而形成复合体。

5.2 林业产业结构 forestry industrial structure

组成林业的各产业各部门间的比例关系。

5.3 生态经济效益 eco-economic benefit

经济效益、生态效益产出的综合和劳动投入的对比关系。生态经济效益是现代生态经济发展的必然产物和客观要求。

5.4 人工生态系统 artificial ecosystem

以人类活动为生态环境中心，按照人类的理想要求建立的生态系统。如城市生态系统，农业生态系统等。

5.5 自然生态系统 natural ecosystem

一定的空间和时间内生物资源与自然环境通过能量流动和物质循环而相互作用依存，呈现动态平衡的自然生命支持系统。

5.6 林地生产力 forestland productivity

单位时间（一般为一年）单位面积林地范围内所生产的生物产量总和。

5.7 绿色产业 green industry

泛指对环境友好的产业。

5.8 非木材效益 non-timber benefit

林业非木材产品创造的效益。

5.9 采伐限额 cut quota

通过编制各采伐类型和消耗结构的森林采伐指标，确定一定时期内的合理采伐量。

5.10 森工企业 forest enterprise

以经营林地和林木资源为主的企业。

5.11 森林旅游业 forest tour industry

利用森林自然景观及其附属的人文景观资源，地形地貌资源等为人们提供旅游、休憩、疗养、科学考察、探险等活动的产业，是“生态旅游”的主体。

5.12 商品林 commercial forest

以生产木材、薪炭、干鲜果品及其他工业原料等为主要经营目标的森林和灌木林。商品林涉及用材林、薪炭林和经济林三个林种，相应包括一般用材林、短轮伐期用材林、薪炭林、油料林、特种经济林、果树林、其他经济林等7个二级林种。

5.13 营林费 silvicultural cost

在营林生产过程中发生的各种费用，包括营林直接费用以及因营林活动而产生的管理费用。

5.14 使用价值 use value

通过直接或间接利用环境资源而获得的效益。

5.15 间接使用价值 indirect use value

体现在人们对自然资源的间接利用上。如森林不仅能提供木材，还具有净化空气、涵养水源、调节气候等生态。

5.16 直接使用价值 direct use value

生物资源可供人类消费的特性，如作为食物、药材和工业原料等。

5.17 非使用价值 non-use value

环境和自然资源所拥有的并非通过人类有形使用而产生的经济价值，包括存在价值、遗产价值、选择价值等。

6 林业生态工程

6.1 生态建设 ecological construction

生态系统的建设，包括新的生态系统的建立和原有生态系统的结构和功能的加强、改善或改进。

6.2 林网建设 forest network construction

建设集经济、生态、社会三大效益为一体的农林复合生态体系，是把林业可持续发展与农业产业结构调整相互联结的一种模式，是改善农村生态环境、增强农业发展后劲的基础生态工程。

6.3 “四江”流域 the Xijiang, Beijiang, Dongjiang, and Hanjiang Watersheds

指广东省境内的西江、北江、东江、韩江流域。

6.4 防护林体系 shelterbelt system

在一个自然景观地带内，依据不同的防护目的和地貌类型而将各种人工防护林和原有的天然林，按总体规划有机地结合起来，具有防灾减灾功能的森林植物群体系统。

6.5 农田防护林 farmland protection forest

为了改善气候、土壤、水文条件，防止自然灾害，特别是灾害性天气对农业生产的危害，创造有利于农作物生长发育的环境条件，以保障农业稳产高产，在农田中或沿农田边缘营造的带状或网状林分，是一种能够提供多种效用的人工林生态系统。

6.6 沿海防护林 coastal protection forest

具有防风固沙、保持水土、涵养水源、抵御海啸和风暴潮危害、护卫滨海国土、美化人居环境等作用的防护林。

6.7 护岸林 riverbank protection forest

为了护岸护堤，保护江河两岸大坝安全而营建的防护林。

6.8 庭院经济 garden economy

一种特殊的微域经济系统，指农户充分利用家庭院落的空间和各种资源,从事高度集约化商品生产的一种经营形式,主要有种植业、养殖业、加工业。林果种植是庭院经济的一种重要形式

6.9 生态脆弱区 ecologically fragile area

生态稳定性差、生物组成和生产力波动大，对人类活动及突发性灾害反应敏感，自然环境易向不利于人类利用方向演变的一种自然环境类型。

6.10 小流域综合治理 integrated watershed management

又称流域管理、集水区经营等。以小流域为单元，在全面规划的基础上，合理安排农、林、牧等各业用地，因地制宜地布设综合治理措施，治理与开发相结合，对流域水土等自然资源进行保护、改良与合理利用。

7 生态公益林

7.1 生态公益林补偿 value compensation for non-commercial ecological forest

由国家、社会、集体、个人等多多渠道、多层次对公益林的经营主体按价值规律进行资金、技术等多方面的补偿。

7.2 生态公益林管理 management of non-commercial ecological forest

对生态公益林实行统一规划、分步实施、依法保护、严格管理、权责一致、分级负责的措施。

7.3 生态公益林价值核算 valuation of non-commercial ecological forest

对包括森林环境价值在内的生态公益林价值进行的核算。

7.4 生态作用 ecological effect

在生态系统内通过生态功能的实现而显现出来的作用或效果。

7.5 植被恢复 vegetation restoration

运用生态学原理，通过保护现有植被、封山育林或营造人工林、灌、草植被，修复或重建被毁坏或被破坏的森林和其他自然生态系统，恢复其生物多样性及其生态系统功能。

7.6 植被型 vegetation type

以群落外貌特征为基础划分植被类型，是植被分类的一级单位，如常绿阔叶林。

7.7 风水林 *Fengshui* woods; sacred woods

人工培植或天然生长且因宗教、文化或风俗等原因而得到保护并具有一定规模的林分。

7.8 **生态功能** ecological function

生态系统及其生态过程所形成的有利于人类生存与发展的生态环境条件与效用。

7.9 **生态美学** ecological aesthetics

是生态学与美学的有机结合，从生态学的角度研究美学问题，将生态学的重要观点运用到美学之中，从而形成一种崭新的美学理论形态。生态美学体现出一种人与自然的和谐的生态审美关系。

7.10 **生态平衡** ecological balance; ecological equilibrium

生态系统各组成部分的内部或相互之间，在长期的发展演化过程中，通过相互制约、转化、补偿、交换及适应而建立起来的一种相互协调的动态平衡关系。

7.11 **生态效益** ecological benefit

生态系统产生的对环境及人类生产、生活有益的作用或效果。如水土保持效益、碳汇效益等。

7.12 **生态效益补偿** compensation for ecological benefit

对提供生态系统服务功能的单位或个人进行资金的补偿，解决由于市场机制失灵造成的生态效益的外部性并保持社会发展的公平性，达到保护生态与环境效益的目标。

7.13 **生态效益评价** valuation of ecological benefits

对生态效益进行评估和价值量化。

7.14 **生态学原则** ecological principle

指生态学的基本原理、准则及重要理论。是进行林业生态建设、土地资源管理、森林资源保护和利用时应遵循的基本准则。

7.15 **适地适树** matching tree species to site

在选择造林树种时，注意使造林树种的生物学和生态学特性与造林地的立地条件相适应，以充分发挥生产潜力，达到该立地在当前技术经济条件下可能达到的高产水平。

7.16 **水土保持林** soil and water conservation forest

以调节地表径流、涵养水源、防止土壤侵蚀，改善生态条件和农业生产条件为目的的天然或人工林分。

7.17 **水源涵养林** water conservation forest

也称水源林，是具有特殊意义的水土防护林种之一，泛指河川、水库、湖泊的上游集水区内大面积的天然林和人工林。

7.18 **特种用途林** special-purpose forest; forest for special purpose

以国防、环境保护、科学实验等为主要目的的森林和林木。

7.19 **物种多样性** species diversity

生物多样性在物种水平上的表现形式，一般以丰富度、多度、物种多样性指数等指标来描述。

7.20 **休憩林** recreational forest; forest for recreation

特种用途林之一，主要提供休憩的功能。

7.21 **防风固沙林** windbreak and sand-fixation forest

控制和固定流沙，防止风沙危害, 改良沙地性质的一种防护林种。

7.22 **防护林** shelterbelt forest; protection forest

以防护为主要目的的森林、林木和灌木丛。

7.23 **风景观赏林** amenity forest

特种用途林之一，主要提供美学和观赏游览的功能。

7.24 **红树林** mangrove

生长在热带、亚热带海洋潮间带及海岸边的植物群落，是具有维护海岸带生态平衡功能

的湿地生态系统。

7.25 实验林 experimental forest

特种用途林之一，主要提供科学研究的功能。

7.26 森林公园 forest park

森林景观优美，自然景观和人文景物集中，具有一定规模，可供人们游览、休憩或进行科学、文化、教育活动，并经法定程序申报设立的场所。

7.27 森林生态效能 forest ecological effect and function

森林环境具有的生态效能，包括涵养水源、保持水土、防止土地沙化、防止土壤退化等。

7.28 稀有濒危物种 rare and endangered species

指列入国际或某个国家红皮书的受威胁物种。一般包括稀有、渐危、濒危等级别。

7.29 环境效益 environmental benefit

自然环境本身所提供的生态系统服务功能和效用或人类活动引起的环境影响，有正效益和负效益之分。

7.30 低效林改造 low-valued forest stand improvement

为改善低效林的林分结构，开发林地生产潜力，提高林分质量和效益水平，而采取的结构调整、树种更新、补植套种、封山育林、林分抚育、嫁接复壮等营林措施。

7.31 生物防火林带 biological firebreak forest belts

以耐火、抗火的树种营造不同结构的林带，分隔一定面积的森林。若发生林火，可达到阻止其蔓延的作用。

8 生态管理

8.1 森林生态系统管理 forest ecosystem management

应用生态学、经济学、管理学等多学科的原理和方法，在景观水平上对森林进行科学的规划和经营，以达到维持森林生态系统的完整性，实现可持续经营的目标。

8.2 森林资源连续清查 continuous forest inventory

简称一类清查。以省（区、市）为单位，利用固定样地为主进行定期复查的森林资源调查方法，每5年复查一次。国家森林资源连续清查是全国森林资源与生态综合监测体系的重要组成部分，是掌握宏观森林资源现状及其消长动态，制定和调整林业方针政策、规划、计划，监督检查领导干部实行森林资源消长任期目标责任制的重要依据。

8.3 森林资源数据库 forest resource database

汇集森林资源调查数据，提供检索、查询、打印等多种利用功能的森林资源数据系统。

8.4 森林区划 forest regionalization

根据特定要求，对一定范围内的森林资源划分为不同的森林地段或单元的森林经理工作，是合理组织林业生产、科学经营管理森林资源的基础。

8.5 森林认证 forest certification

森林可持续经营认证的简称，是一种运用市场机制来促进森林可持续经营，实现生态、社会和经济目标的工具。也就是指通过独立的第三方对某一森林经营单位或区域的森林进行可持续经营的总体评价，以验证该单位或区域的森林经营是否经营良好，是否符合可持续发展原则和标准的要求，并颁发证书的过程。

8.6 有害生物生态管理 ecological management of hazardous organism

在人类与自然协同发展的思想指导下，以生态学原理为理论基础，维持森林生态系统的格局、过程和生物多样性，从而达到害虫的长期持续控制。

8.7 森林文化 forest culture

是指人与森林、人与自然之间建立的相互依存、相互作用、相互融合的关系，是人类在

社会实践中创造的森林物质财富和精神财富的总和，包括与森林有关的社会意识形态，以及与之相适应的制度和组织机构、风俗习惯及行为模式。

8.8 生态文化 eco-culture

生态文明的主流文化形式，是各民族为适应特定的生态环境而创造的生态智慧和生态知识，是反映人与自然、社会与自然、人与社会之间和睦相处、和谐发展的一种社会文化。

8.9 生态旅游 ecotourism

是一种以自然生境为目的地的旅游。是具有保护自然环境和维护当地人民生活双重责任的旅游活动。生态旅游的内涵更强调的是对自然景观的保护，是可持续发展的旅游。

附 录 A
（规范性附录）
汉语拼音术语条目索引

G

H

J

K

L

M

N

Q

R

S

T

W

X

Y

Z

附 录 B
（规范性附录）
英文术语条目索引

A

B

C

D

E

F

G

H

I

L

M

N

O

P

R

S

T

U

V

W

Z

五、其他业绩

1.指导学生学科竞赛

2.个人荣誉

3.其他

荣誉证书

HONORARY CREDENTIAL

阚蕾：

您在第七届全国种群生态学前沿论坛做的报告荣获“第七届全国种群生态学前沿论坛·北京力科惠泽优秀青年报告奖”二等奖。感谢您为中国种群生态学研究的发展做出的贡献。

特发此证，谨表谢忱。

中国生态学学会种群生态专业委员会

江苏大学

2020 年 11 月 15 日

荣誉证书

林浩有 同学：

您的报告《单细胞分辨率下的紫荆木幼苗生长与防御基因及代谢通路的研究》

在第三届全国林木基因组与现代种业学术研讨会研究生报告评选中荣获

二等奖

特发此证，以资鼓励！

林木遗传育种全国重点实验室

2024 年 12 月 8 日

证 书

张璐 同志

被评为《中国林业教育》2009年度优秀作者。特颁此证。

《中国林业教育》编辑部

2010年3月31日

第九届中国林业经济论坛闭幕 我校多篇论文获奖

撰写时间: 2011-12-12 作者: 来源: 校报学生记者社

12月11日下午，第九届中国林业经济论坛在经管学院大楼圆满闭幕。本次大会对提交的120余篇论文进行了评选，我校高岚、张自强提交的论文《产权管制、要素投入与林业经济增长关系的实证分析》获优秀论文一等奖；张璐、徐正春提交的论文《基于聚类和排序的广东省自然保护区管理策略研究》获优秀论文二等奖；杜国明提交的论文《是否“均山”：集体山林经营方式选择——暨广东林改新路探析》获优秀论文三等奖。（文/校报学生记者 关凤湾 图/校报学生记者 叶凌风）

（责任编辑：方玮）

证书

张璐、徐正春 同志：

您的论文《基于聚类和排序的广东省自然保护区管理策略研究》获第九届中国林业经济论坛论文二等奖。

中国林业经济论坛

二〇一一年十二月

3.2.社会服务

近两年，申请人课题组围绕国家专项拯救的极小种群野生植物紫荆木开展了就地保护、迁地保护、野外回归和科普宣传等社会服务工作。

3.2.1. 2023 年度社会服务

2023 年度在广东云开山国家级自然保护区、华南农业大学、广州市动物园、广东省高州市深镇镇耀新村、广东惠东海龟国家级自然保护区等地开展极小种群野生植物紫荆木拯救科普宣传活动。极小种群野生植物社会服务案例获广东省林业局官网和茂名网报道。

（1）广东省林业局门户网站

http://lyj.gd.gov.cn/gkmlpt/content/4/4207/post_4207566.html#2441

（2）茂名网

https://www.mm111.net/2023/06/23/991330486.html

云开山国家级自然保护区联合华南农业大学研究团队开展紫荆木拯救保护科普宣传活动

广东省云开山国家级自然保护区紫荆木科普宣传活动

华南农业大学林学与风景园林学院紫荆木科普宣传活动

华南农业大学树木园科普宣传活动

广州市动物园科普宣传活动

3.2.2. 2024 年度社会服务

2024 年度以服务省委“百千万工程”和绿美广东生态建设为契机，实现了国内首次极小种群野生植物紫荆木野外回归云开山国家级自然保护区。申请人课题组还针对幼儿园小朋友、中学生、大学生、基层林业一线技术人员以及紫荆木原生境居民开展紫荆木科普宣传活动和紫荆木就地保护。极小种群野生植物社会服务案例被广东省林业局门户网站、茂名市人民政府门户网站报道、茂名日报、信宜共青团公众号、信宜发布、广东林业公众号、南岭探秘公众号等多家媒体报道和转载。

（1）广东省林业局门户网站

http://lyj.gd.gov.cn/news/forestry/content/post_4399268.html

（2）茂名市人民政府门户网站

http://www.maoming.gov.cn/xxgkml/lyj/fdzdgknr/gzdt/content/post_1324672.html

（3）茂名日报

https://www.mm111.net/mpaper/2024-04/08/content_991401821.html

（4）信宜共青团公众号

https://mp.weixin.qq.com/s/URlE0bKOPTtpOe8aHuoOog

（5）信宜发布

https://mp.weixin.qq.com/s/76Pny1Rax8QuD0bhZbFycw

（6）信宜市融媒体中心

https://w.xytv.cc/h-nd-17369.html

（7）广东林业公众号

https://mp.weixin.qq.com/s/RlgJOoZ-ds2YkLcY8be92A

（8）南岭探秘公众号

https://mp.weixin.qq.com/s/GEO5XZvkuNOJpepbbco68A

（9）关注森林网

http://www.isenlin.cn/sf_B0D4263919174209AA6C78E08FB3BD7A_209_gdly.html

（10）搜狐网

https://www.sohu.com/a/768744689_121124004

（11）腾讯新闻

https://new.qq.com/rain/a/20240403A03Q8100

（12）网易报道

https://www.163.com/dy/article/IUS63GCE0534S1WJ.html

（13）SCAU 林风青年公众号

https://mp.weixin.qq.com/s/mUiAnli_e2ECsHGJoPbWWQ

（14）中国林业出版社公众号

https://mp.weixin.qq.com/s/F0Vm8pdoaqY1cL9U2GpJuQ

（15）高州市人民政府公众网

http://www.gaozhou.gov.cn/zwgk/content/mpost_1364171.html

（二）活动现场照片

<table>
<tr><td>  </td><td>  </td></tr>
<tr><td colspan="2">针对幼儿园小朋友开展紫荆木拯救科普活动</td></tr>
</table>

针对中学生开展紫荆木拯救科普活动

针对大学生开展紫荆木拯救科普活动

针对林业基层一线工作人员开展紫荆木拯救科普宣传活动

针对紫荆木原生境村民开展极小种群野生植物拯救科普宣传活动

高州市人民政府
www.gaozhou.gov.cn

关怀版

请输入关键字

首页 政务公开 新闻动态 政务服务

政民互动 高州概况

政务公开

高州市深镇镇耀新村：保护紫荆木，我们在行动——极小种群野生植物紫荆木就地保护

来源：本网 时间：2024-07-22 08:45:46

紫荆木（Madhuca pasquieri （Dubard） H. J. Lam）是山榄科（Sapotaceae）紫荆木属（Madhuca）的常绿高大乔木，国家重点保护野生植物（Ⅱ级），国家林业和草原局“十四五”规划保护的50种极小种群野生植物之一。紫荆木野生种群天然更新能力弱、规模小且数量仍在持续减少，加强紫荆木野生种群拯救刻不容缓。

而在广东省高州市深镇镇耀新村桥头垌路边就有这样一棵1株树龄120年以上的紫荆木。由于距主干路旁护栏不足2米，车流量十分大，严重影响到紫荆木的生长安全。为了更好地保护这一极小种群树木，耀新村党员干部主动担责，积极作为，邀请华南农业大学张璐课题组到本地，双方就紫荆木的保护工作开展实地调研，根据紫荆木根系情况、周遭环境影响等诸多影响因素，

紫荆木野生植株就地保护及科普宣传活动

紫荆木野外回归及科普宣传活动